



Hashemite Kingdom of Jordan



Jordan Journal of



Biological Sciences

An International Peer-Reviewed Scientific Journal

Financed by the Scientific Research and Innovation Support Fund



<http://jjbs.hu.edu.jo/>

المجلة الأردنية للعلوم الحياتية
Jordan Journal of Biological Sciences (JJBS)

<http://jjbs.hu.edu.jo>

Jordan Journal of Biological Sciences (JJBS) (ISSN: 1995–6673 (Print); 2307-7166 (Online)): An International Peer- Reviewed Open Access Research Journal financed by the Scientific Research and Innovation Support Fund, Ministry of Higher Education and Scientific Research, Jordan and published quarterly by the Deanship of Scientific Research , The Hashemite University, Jordan.

Editor-in-Chief

Professor Atoum, Manar F.

Molecular Biology and Genetics,
The Hashemite University

Assistant Editor

Dr. Muhannad, Massadeh I.

Microbial Biotechnology,
The Hashemite University

Editorial Board (Arranged alphabetically)

Professor Amr, Zuhair S.

Animal Ecology and Biodiversity
Jordan University of Science and Technology

Professor Hunaiti, Abdulrahim A.

Biochemistry
The University of Jordan

Professor Khleifat, Khaled M.

Microbiology and Biotechnology
Mutah University

Professor Lahham, Jamil N.

Plant Taxonomy
Yarmouk University

Professor Malkawi, Hanan I.

Microbiology and Molecular Biology
Yarmouk University

Associate Editorial Board

Professor Al-Hindi, Adnan I.

Parasitology
The Islamic University of Gaza, Faculty of Health
Sciences, Palestine

Dr Gammoh, Noor

Tumor Virology
Cancer Research UK Edinburgh Centre, University of
Edinburgh, U.K.

Professor Kasperek, Max

Natural Sciences
Editor-in-Chief, Journal Zoology in the Middle East,
Germany

Professor Krystufek, Boris

Conservation Biology
Slovenian Museum of Natural History,
Slovenia

Dr Rabei, Sami H.

Plant Ecology and Taxonomy
Botany and Microbiology Department,
Faculty of Science, Damietta University, Egypt

Professor Simerly, Calvin R.

Reproductive Biology
Department of Obstetrics/Gynecology and
Reproductive Sciences, University of
Pittsburgh, USA

Editorial Board Support Team

Language Editor

Dr. Shadi Neimneh

Publishing Layout

Eng.Mohannad Oqdeh

Submission Address

Professor Atoum, Manar F

The Hashemite University
P.O. Box 330127, Zarqa, 13115, Jordan
Phone: +962-5-3903333 ext.4147
E-Mail: jjbs@hu.edu.jo

International Advisory Board (Arranged alphabetically)

Professor Ahmad M. Khalil

Department of Biological Sciences, Faculty of Science,
Yarmouk University, Jordan

Professor Anilava Kaviraj

Department of Zoology, University of Kalyani, India

Professor Bipul Kumar Das

Faculty of Fishery Sciences W. B. University of Animal &
Fishery Sciences, India

Professor Elias Baydoun

Department of Biology, American University of Beirut
Lebanon

Professor Hala Gali-Muhtasib

Department of Biology, American University of Beirut
Lebanon

Professor Ibrahim M. AlRawashdeh

Department of Biological Sciences, Faculty of Science, Al-
Hussein Bin Talal University, Jordan

Professor João Ramalho-Santos

Department of Life Sciences, University of Coimbra, Portugal

Professor Khaled M. Al-Qaoud

Department of Biological sciences, Faculty of Science,
Yarmouk University, Jordan

Professor Mahmoud A. Ghannoum

Center for Medical Mycology and Mycology Reference
Laboratory, Department of Dermatology, Case Western
Reserve University and University Hospitals Case Medical
Center, USA

Professor Mawieh Hamad

Department of Medical Lab Sciences, College of Health
Sciences , University of Sharjah, UAE

Professor Michael D Garrick

Department of Biochemistry, State University of New York at
Buffalo, USA

Professor Nabil. A. Bashir

Department of Physiology and Biochemistry, Faculty of
Medicine, Jordan University of Science and Technology,
Jordan

Professor Nizar M. Abuharfeil

Department of Biotechnology and Genetic Engineering, Jordan
University of Science and Technology, Jordan

Professor Samih M. Tamimi

Department of Biological Sciences, Faculty of Science, The
University of Jordan, Jordan

Professor Ulrich Joger

State Museum of Natural History Braunschweig, Germany

Professor Aida I. El Makawy

Division of Genetic Engineering and Biotechnology, National
Research Center. Giza, Egypt

Professor Bechan Sharma

Department of Biochemistry, Faculty of Science University of
Allahabad, India

Professor Boguslaw Buszewski

Chair of Environmental Chemistry and Bioanalytics, Faculty of
Chemistry, Nicolaus Copernicus University Poland

Professor Gerald Schatten

Pittsburgh Development Center, Division of Developmental
and Regenerative Medicine, University of Pittsburgh, School
of Medicine, USA

Professor Hala Khyami-Horani

Department of Biological Sciences, Faculty of Science, The
University of Jordan, Jordan

Professor James R. Bamburg

Department of Biochemistry and Molecular Biology, Colorado
State University, USA

Professor Jumah M. Shakhaneh

Department of Biological Sciences, Faculty of Science, Mutah
University, Jordan

Dr. Lukmanul Hakkim Faruck

Department of Mathematics and Sciences College of Arts and
Applied Sciences, Dhofar, Oman

Professor Md. Yeamin Hossain

Department of Fisheries, Faculty of Fisheries , University of
Rajshahi, Bangladesh

Professor Mazin B. Qumsiyeh

Palestine Museum of Natural History and Palestine Institute for
Biodiversity and Sustainability, Bethlehem University,
Palestine

Professor Mohamad S. Hamada

Genetics Department, Faculty of Agriculture, Damietta
University, Egypt

Professor Nawroz Abdul-razzak Tahir

Plant Molecular Biology and Phytochemistry, University of
Sulaimani, College of Agricultural Sciences, Iraq

Professor Ratib M. AL- Ouran

Department of Biological Sciences, Faculty of Science, Mutah
University, Jordan

Professor Shtaywy S. Abdalla Abbadi

Department of Biological Sciences, Faculty of Science, The
University of Jordan, Jordan

Professor Zihad Bouslama

Department of Biology, Faculty of Science Badji Mokhtar
University, Algeria

Instructions to Authors

Scopes

Study areas include cell biology, genomics, microbiology, immunology, molecular biology, biochemistry, embryology, immunogenetics, cell and tissue culture, molecular ecology, genetic engineering and biological engineering, bioremediation and biodegradation, bioinformatics, biotechnology regulations, gene therapy, organismal biology, microbial and environmental biotechnology, marine sciences. The JJBS welcomes the submission of manuscript that meets the general criteria of significance and academic excellence. All articles published in JJBS are peer-reviewed. Papers will be published approximately one to two months after acceptance.

Type of Papers

The journal publishes high-quality original scientific papers, short communications, correspondence and case studies. Review articles are usually by invitation only. However, Review articles of current interest and high standard will be considered.

Submission of Manuscript

Manuscript, or the essence of their content, must be previously unpublished and should not be under simultaneous consideration by another journal. The authors should also declare if any similar work has been submitted to or published by another journal. They should also declare that it has not been submitted/ published elsewhere in the same form, in English or in any other language, without the written consent of the Publisher. The authors should also declare that the paper is the original work of the author(s) and not copied (in whole or in part) from any other work. All papers will be automatically checked for duplicate publication and plagiarism. If detected, appropriate action will be taken in accordance with International Ethical Guideline. By virtue of the submitted manuscript, the corresponding author acknowledges that all the co-authors have seen and approved the final version of the manuscript. The corresponding author should provide all co-authors with information regarding the manuscript, and obtain their approval before submitting any revisions. Electronic submission of manuscripts is strongly recommended, provided that the text, tables and figures are included in a single Microsoft Word file. Submit manuscript as e-mail attachment to the Editorial Office at: JJBS@hu.edu.jo. After submission, a manuscript number will be communicated to the corresponding author within 48 hours.

Peer-review Process

It is requested to submit, with the manuscript, the names, addresses and e-mail addresses of at least 4 potential reviewers. It is the sole right of the editor to decide whether or not the suggested reviewers to be used. The reviewers' comments will be sent to authors within 6-8 weeks after submission. Manuscripts and figures for review will not be returned to authors whether the editorial decision is to accept, revise, or reject. All Case Reports and Short Communication must include at least one table and/ or one figure.

Preparation of Manuscript

The manuscript should be written in English with simple lay out. The text should be prepared in single column format. Bold face, italics, subscripts, superscripts etc. can be used. Pages should be numbered consecutively, beginning with the title page and continuing through the last page of typewritten material.

The text can be divided into numbered sections with brief headings. Starting from introduction with section 1. Subsections should be numbered (for example 2.1 (then 2.1.1, 2.1.2, 2.2, etc.), up to three levels. Manuscripts in general should be organized in the following manner:

Title Page

The title page should contain a brief title, correct first name, middle initial and family name of each author and name and address of the department(s) and institution(s) from where the research was carried out for each author. The title should be without any abbreviations and it should enlighten the contents of the paper. All affiliations should be provided with a lower-case superscript number just after the author's name and in front of the appropriate address.

The name of the corresponding author should be indicated along with telephone and fax numbers (with country and area code) along with full postal address and e-mail address.

Abstract

The abstract should be concise and informative. It should not exceed **350 words** in length for full manuscript and Review article and **150 words** in case of Case Report and/ or Short Communication. It should briefly describe the purpose of the work, techniques and methods used, major findings with important data and conclusions. No references should be cited in this part. Generally non-standard abbreviations should not be used, if necessary they should be clearly defined in the abstract, at first use.

Keywords

Immediately after the abstract, **about 4-8 keywords** should be given. Use of abbreviations should be avoided, only standard abbreviations, well known in the established area may be used, if appropriate. These keywords will be used for indexing.

Abbreviations

Non-standard abbreviations should be listed and full form of each abbreviation should be given in parentheses at first use in the text.

Introduction

Provide a factual background, clearly defined problem, proposed solution, a brief literature survey and the scope and justification of the work done.

Materials and Methods

Give adequate information to allow the experiment to be reproduced. Already published methods should be mentioned with references. Significant modifications of published methods and new methods should be described in detail. Capitalize trade names and include the manufacturer's name and address. Subheading should be used.

Results

Results should be clearly described in a concise manner. Results for different parameters should be described under subheadings or in separate paragraph. Results should be explained, but largely without referring to the literature. Table or figure numbers should be mentioned in parentheses for better understanding.

Discussion

The discussion should not repeat the results, but provide detailed interpretation of data. This should interpret the significance of the findings of the work. Citations should be given in support of the findings. The results and discussion part can also be described as separate, if appropriate. The Results and Discussion sections can include subheadings, and when appropriate, both sections can be combined

Conclusions

This should briefly state the major findings of the study.

Acknowledgment

A brief acknowledgment section may be given after the conclusion section just before the references. The acknowledgment of people who provided assistance in manuscript preparation, funding for research, etc. should be listed in this section.

Tables and Figures

Tables and figures should be presented as per their appearance in the text. It is suggested that the discussion about the tables and figures should appear in the text before the appearance of the respective tables and figures. No tables or figures should be given without discussion or reference inside the text.

Tables should be explanatory enough to be understandable without any text reference. Double spacing should be maintained throughout the table, including table headings and footnotes. Table headings should be placed above the table. Footnotes should be placed below the table with superscript lowercase letters. Each table should be on a separate page, numbered consecutively in Arabic numerals.

Each figure should have a caption. The caption should be concise and typed separately, not on the figure area. Figures should be self-explanatory. Information presented in the figure should not be repeated in the table. All symbols and abbreviations used in the illustrations should be defined clearly. Figure legends should be given below the figures.

References

References should be listed alphabetically at the end of the manuscript. Every reference referred in the text must be also present in the reference list and vice versa. In the text, a reference identified by means of an author's name should be followed by the year of publication in parentheses (e.g.(Brown,2009)). For two authors, both authors' names followed by the year of publication (e.g.(Nelson and Brown, 2007)). When there are more than two authors, only the first author's name followed by "*et al.*" and the year of publication (e.g. (Abu-Elteen *et al.*, 2010)). When two or more works of an author has been published during the same year, the reference should be identified by the letters "a", "b", "c", etc., placed after the year of publication. This should be followed both in the text and reference list. e.g., Hilly, (2002a, 2002b); Hilly, and Nelson, (2004). Articles in preparation or submitted for publication, unpublished observations, personal communications, etc. should not be included in the reference list but should only be mentioned in the article text (e.g., Shtyawy,A., University of Jordan, personal communication). Journal titles should be abbreviated according to the system adopted in Biological Abstract and Index Medicus, if not included in Biological Abstract or Index Medicus journal title should be given in full. The author is responsible for the scuracy and completeness of the references and for their correct textual citation. Failure to do so may result in the paper being withdraw from the evaluation process. Example of correct reference form is given as follows:-

Reference to a journal publication:

Bloch BK. 2002. Econazole nitrate in the treatment of *Candida vaginitis*. *S Afr Med J.* , **58**:314-323.

Ogunseitan OA and Ndoye IL. 2006. Protein method for investigating mercuric reductase gene expression in aquatic environments. *Appl Environ Microbiol.*, **64**: 695-702.

Hilly MO, Adams MN and Nelson SC. 2009. Potential fly-ash utilization in agriculture. *Progress in Natural Sci.*, **19**: 1173-1186.

Reference to a book:

Brown WY and White SR.1985. **The Elements of Style**, third ed. MacMillan, New York.

Reference to a chapter in an edited book:

Mettam GR and Adams LB. 2010. How to prepare an electronic version of your article. In: Jones BS and Smith RZ (Eds.), **Introduction to the Electronic Age**. Kluwer Academic Publishers, Netherlands, pp. 281–304.

Conferences and Meetings:

Embabi NS. 1990. Environmental aspects of distribution of mangrove in the United Arab Emirates. Proceedings of the First ASWAS Conference. University of the United Arab Emirates. Al-Ain, United Arab Emirates.

Theses and Dissertations:

El-Labadi SN. 2002. Intestinal digenetic trematodes of some marine fishes from the Gulf of Aqaba. MSc dissertation, The Hashemite University, Zarqa, Jordan.

Nomenclature and Units

Internationally accepted rules and the international system of units (SI) should be used. If other units are mentioned, please give their equivalent in SI.

For biological nomenclature, the conventions of the *International Code of Botanical Nomenclature*, the *International Code of Nomenclature of Bacteria*, and the *International Code of Zoological Nomenclature* should be followed.

Scientific names of all biological creatures (crops, plants, insects, birds, mammals, etc.) should be mentioned in parentheses at first use of their English term.

Chemical nomenclature, as laid down in the *International Union of Pure and Applied Chemistry* and the official recommendations of the *IUPAC-IUB Combined Commission on Biochemical Nomenclature* should be followed. All biocides and other organic compounds must be identified by their Geneva names when first used in the text. Active ingredients of all formulations should be likewise identified.

Math formulae

All equations referred to in the text should be numbered serially at the right-hand side in parentheses. Meaning of all symbols should be given immediately after the equation at first use. Instead of root signs fractional powers should be used. Subscripts and superscripts should be presented clearly. Variables should be presented in italics. Greek letters and non-Roman symbols should be described in the margin at their first use.

To avoid any misunderstanding zero (0) and the letter O, and one (1) and the letter l should be clearly differentiated. For simple fractions use of the solidus (/) instead of a horizontal line is recommended. Levels of statistical significance such as: * $P < 0.05$, ** $P < 0.01$ and *** $P < 0.001$ do not require any further explanation.

Copyright

Submission of a manuscript clearly indicates that: the study has not been published before or is not under consideration for publication elsewhere (except as an abstract or as part of a published lecture or academic thesis); its publication is permitted by all authors and after accepted for publication it will not be submitted for publication anywhere else, in English or in any other language, without the written approval of the copyright-holder. The journal may consider manuscripts that are translations of articles originally published in another language. In this case, the consent of the journal in which the article was originally published must be obtained and the fact that the article has already been published must be made clear on submission and stated in the abstract. It is compulsory for the authors to ensure that no material submitted as part of a manuscript infringes existing copyrights, or the rights of a third party.

Ethical Consent

All manuscripts reporting the results of experimental investigation involving human subjects should include a statement confirming that each subject or subject's guardian obtains an informed consent, after the approval of the experimental protocol by a local human ethics committee or IRB. When reporting experiments on animals, authors should indicate whether the institutional and national guide for the care and use of laboratory animals was followed.

Plagiarism

The JJBS hold no responsibility for plagiarism. If a published paper is found later to be extensively plagiarized and is found to be a duplicate or redundant publication, a note of retraction will be published, and copies of the correspondence will be sent to the authors' head of institute.

Galley Proofs

The Editorial Office will send proofs of the manuscript to the corresponding author as an e-mail attachment for final proof reading and it will be the responsibility of the corresponding author to return the galley proof materials appropriately corrected within the stipulated time. Authors will be asked to check any typographical or minor clerical errors in the manuscript at this stage. No other major alteration in the manuscript is allowed. After publication authors can freely access the full text of the article as well as can download and print the PDF file.

Publication Charges

There are no page charges for publication in Jordan Journal of Biological Sciences, except for color illustrations,

Reprints

Ten (10) reprints are provided to corresponding author free of charge within two weeks after the printed journal date. For orders of more reprints, a reprint order form and prices will be sent with article proofs, which should be returned directly to the Editor for processing.

Disclaimer

Articles, communication, or editorials published by JJBS represent the sole opinions of the authors. The publisher shoulders no responsibility or liability what so ever for the use or misuse of the information published by JJBS.

Indexing

JJBS is indexed and abstracted by:

DOAJ (Directory of Open Access Journals)

Google Scholar

Journal Seek

HINARI

Index Copernicus

NDL Japanese Periodicals Index

SCIRUS

OAJSE

ISC (Islamic World Science Citation Center)

Directory of Research Journal Indexing
(DRJI)

Ulrich's

CABI

EBSCO

CAS (Chemical Abstract Service)

ETH- Citations

Open J-Gat

SCImago

Clarivate Analytics (Zoological Abstract)

Scopus

AGORA (United Nation's FAO database)

SHERPA/RoMEO (UK)

المجلة الأردنية للعلوم الحياتية
Jordan Journal of Biological Sciences (JJBS)
ISSN 1995- 6673 (Print), 2307- 7166 (Online)

<http://jjbs.hu.edu.jo>

The Hashemite University
Deanship of Scientific Research
TRANSFER OF COPYRIGHT AGREEMENT

Journal publishers and authors share a common interest in the protection of copyright: authors principally because they want their creative works to be protected from plagiarism and other unlawful uses, publishers because they need to protect their work and investment in the production, marketing and distribution of the published version of the article. In order to do so effectively, publishers request a formal written transfer of copyright from the author(s) for each article published. Publishers and authors are also concerned that the integrity of the official record of publication of an article (once refereed and published) be maintained, and in order to protect that reference value and validation process, we ask that authors recognize that distribution (including through the Internet/WWW or other on-line means) of the authoritative version of the article as published is best administered by the Publisher.

To avoid any delay in the publication of your article, please read the terms of this agreement, sign in the space provided and return the complete form to us at the address below as quickly as possible.

Article entitled:-----

Corresponding author: -----

To be published in the journal: Jordan Journal of Biological Sciences (JJBS)

I hereby assign to the Hashemite University the copyright in the manuscript identified above and any supplemental tables, illustrations or other information submitted therewith (the "article") in all forms and media (whether now known or hereafter developed), throughout the world, in all languages, for the full term of copyright and all extensions and renewals thereof, effective when and if the article is accepted for publication. This transfer includes the right to adapt the presentation of the article for use in conjunction with computer systems and programs, including reproduction or publication in machine-readable form and incorporation in electronic retrieval systems.

Authors retain or are hereby granted (without the need to obtain further permission) rights to use the article for traditional scholarship communications, for teaching, and for distribution within their institution.

- I am the sole author of the manuscript
- I am signing on behalf of all co-authors of the manuscript
- The article is a 'work made for hire' and I am signing as an authorized representative of the employing company/institution

Please mark one or more of the above boxes (as appropriate) and then sign and date the document in black ink.

Signed: _____ Name printed: _____
Title and Company (if employer representative) : _____
Date: _____

Data Protection: By submitting this form you are consenting that the personal information provided herein may be used by the Hashemite University and its affiliated institutions worldwide to contact you concerning the publishing of your article.

Please return the completed and signed original of this form by mail or fax, or a scanned copy of the signed original by e-mail, retaining a copy for your files, to:

Hashemite University
Jordan Journal of Biological Sciences
Zarqa 13115 Jordan
Fax: +962 5 3903338
Email: jjbs@hu.edu.jo

EDITORIAL PREFACE

Jordan Journal of Biological Sciences (JJBS) is a refereed, quarterly international journal financed by the Scientific Research and Innovation Support Fund, Ministry of Higher Education and Scientific Research in cooperation with the Hashemite University, Jordan. JJBS celebrated its 12th commencement this past January, 2020. JJBS was founded in 2008 to create a peer-reviewed journal that publishes high-quality research articles, reviews and short communications on novel and innovative aspects of a wide variety of biological sciences such as cell biology, developmental biology, structural biology, microbiology, entomology, molecular biology, biochemistry, medical biotechnology, biodiversity, ecology, marine biology, plant and animal biology, plant and animal physiology, genomics and bioinformatics.

We have watched the growth and success of JJBS over the years. JJBS has published 11 volumes, 45 issues and 479 articles. JJBS has been indexed by SCOPUS, CABI's Full-Text Repository, EBSCO, Clarivate Analytics- Zoological Record and recently has been included in the UGC India approved journals. JJBS Cite Score has improved from 0.18 in 2015 to 0.7 in 2019 (Last updated on 1 March, 2021) and with Scimago Institution Ranking (SJR) 0.18 (Q3) in 2019.

A group of highly valuable scholars have agreed to serve on the editorial board and this places JJBS in a position of most authoritative on biological sciences. I am honored to have six eminent associate editors from various countries. I am also delighted with our group of international advisory board members coming from 15 countries worldwide for their continuous support of JJBS. With our editorial board's cumulative experience in various fields of biological sciences, this journal brings a substantial representation of biological sciences in different disciplines. Without the service and dedication of our editorial; associate editorial and international advisory board members, JJBS would have never existed.

In the coming year, we hope that JJBS will be indexed in Clarivate Analytics and MEDLINE (the U.S. National Library of Medicine database) and others. As you read throughout this volume of JJBS, I would like to remind you that the success of our journal depends on the number of quality articles submitted for review. Accordingly, I would like to request your participation and colleagues by submitting quality manuscripts for review. One of the great benefits we can provide to our prospective authors, regardless of acceptance of their manuscripts or not, is the feedback of our review process. JJBS provides authors with high quality, helpful reviews to improve their manuscripts.

Finally, JJBS would not have succeeded without the collaboration of authors and referees. Their work is greatly appreciated. Furthermore, my thanks are also extended to The Hashemite University and the Scientific Research and Innovation Support Fund, Ministry of Higher Education and Scientific Research for their continuous financial and administrative support to JJBS.

Professor Atoum, Manar F.
March, 2021

CONTENTS

Original Articles

- 621 - 628 Supplementation of Nucleotides to Enhance Performance and Immune Responses of Asian Seabass
Sri Dwi Hastuti , James Munro, Stephen Pyecroft, Mary Barton, Maurizio Costabile and Brett Glencross
- 629 - 635 Purification and Characterization of a Detergent Compatible Alkaline Protease Produced by *Bacillus raris* Isolated from Vegetable Oil Factory Effluent in Owo, Ondo State, Nigeria
Adebayo Olawande OSESUSI , Victor Olusegun OYETAYO and Daniel Juwon AROTUPIN
- 637 - 645 Wound healing activities of *Moringa oleifera* leaves extract cultivated in Kurdistan region-Iraq
Shang A. Tofiq, Hoshayr A. Azeez and Hemn Hassan Othman
- 647 - 661 An Assessment of Proximate Composition, Antioxidant Activities and LC/MS Based Phytochemical Profiling of Some Lichen Species Collected From Western Ghats of Southern Part of India
Shenbagam Muthu, Mariraj Murugan, Kalidoss Rajendran, and Ponmurugan Ponnusamy
- 663 - 669 Metabolites profiling of *Limonium tubiflorum* (Delile) Kuntze var *tubiflorum* via UPLC-qTOF-MS technique in relation to its cytotoxic activity
Salah M. El-Kousy, Shalabia S. Emam, Ahmed R. Hassan, Ibrahim M. Sanad
- 671 - 676 Expression levels of heat shock proteins through western blot and real-time polymerase chain reaction in maize
Mohamed Abdel-Salam Rashed, Mahmoud Hussien Abou-Deif , Kamal Mohamed Khalil and Fatma El-Sayed Mahmoud
- 677 - 685 Isolation of the Astacin-like metalloprotease coding gene (*astI*) and assessment of its insecticidal activity towards *Spodoptera littoralis* and *Sitophilus oryzae*
Mervat R. Diab, Mahmoud M. Ahmed , Ebtissam H.A. Hussein and Ahmed M. A. Mohammed
- 687 - 692 Embryonic development of the striped spiny eel, *Mastacembelus pancalus* (Hamilton, 1822) in captive condition
Md. Sherazul Islam and Tandra Rani
- 693 - 697 Oxidative Toxic Stress and DNA Damage as a Promising Strategy for Identifying Patients with Nonalcoholic Fatty Liver Disease
Mahshid Abdolmaleki, Maryam Mehrpooya , Bahram Sifizarei, Masoud Saidijam, Ali Reza Soltanian, Maziar Ganji, and Akram Ranjbar
- 699 - 707 The Potential Impact of Different Types of Yogurt Fortified with Inulin and/or Microencapsulated Probiotic Bacteria on Diabetic Rats
Abdel-moniem Naguib, Abdel-kader Morsy Abdel- Samad, Osama M. Sharaf, Ibrahim M. Hamed, Shaimaa I. Soltan , Mona M. Hussein
- 709 - 717 Molecular Characterization and Expression Analysis of *aflR*, *aflS*, and *aflD* in Non-Aflatoxigenic and Aflatoxigenic *Aspergillus flavus* Treated with Gallic Acid.
Ghada M. El-Sayed, Rasha G. Salim, Soher E-S. Aly and Nivien A. Abosereh
- 719 - 726 Mycobiota and Fungal Metabolites in Improved Groundnut Varieties in Nigeria
Toba S. Anjorin, Alhassan Usman, Stephen O. Fapohunda, Adobe Kwanashie, Michael Sulyok and Rudolf Krska
- 727 - 732 Homology modeling of apoprotein Opsin and covalent docking of 11-cis retinal and 11-cis 3, 4-didehyretinal to obtain structures of Rhodopsin and Porphyropsin from Zebra danio, *Danio rerio* (Hamilton, 1822)
Susmita Dey, Gitartha Kaushik, Saurav Mahanta and Arijit Chakraborty
- 733 - 741 A preliminary study of Aminoglycoside Modifying Enzymes (AMEs) of Multiple Antibiotic Resistance of Methicillin-resistant *Staphylococcus aureus* (MRSA) isolated from clinical specimens in Al-Diwaniya/Iraq
Firas Srhan Abd Al- Mayahi

- 743 - 753 Isolation and evaluation of culture media for mycelia growth of an emerging faba bean (*Vicia faba* L.) gall-forming disease causal agent in Ethiopia
Alemayehu Dugassa , Tesfaye Alemu and Yitbarek Woldehawariat
- 755 - 761 The Agar Production, Pigment and Nutrient Content in *Gracilaria* sp. Grown in Two Habitats with Varying Salinity and Nutrient Levels
Ervia Yudiati , Annisa Afifah Nugroho, Sri Sedjati, Zaenal Arifin, Ali Ridlo
- 763 - 767 Biochemical changes in the liver, kidney and serum of rats exposed to ethanolic leaf extract of *Ziziphus spina-christi*
Sabah M. Khaleel, Rana A. Almuher, Taghleab M.F. Al-Deeb and Adnan S. Jaran
- 769 - 773 Morphological and Phylogenetic Characteristics of *Ditylenchus dipsaci* among Garlic Plants
Miftahul Ajri , Siwi Indarti , Alan Soffan and Nguyen Ngoc Huu
- 775 - 789 Genetic Diversity of Local Cowpea (*Vigna spp.* (L.) Walp.) Accessions Cultivated in Some Regions of Egypt
Ehab M.B. Mahdy , Hossam F.A. El-Shaer, Abd El-Hadi I.H. Sayed and Abeer El-Halwagi
- 791 - 797 Isolation and Identification of Dibenzothiophene Desulfurizing Bacteria Occurring in Oil Contaminated Soils of Mechanical Workshops
Praveen Reddy P and UmaMaheswara Rao V
- 799 - 804 Quantitative Probiotic Analysis of Various Kefir Samples
Aylin USKUDAR GUCLU , Esen YESIL, Aylin ALTAY KOCAK, Mendane SAKA, Hasan Cenk MIRZA, Bedia DINC And Ahmet BASUSTA OGLU
- 805 - 812 Bacterial strain *Pseudomonas avellanae* 6CH2 with anti-Fusarium activity in mitigation of herbicidal stress in wheat plants
Sergey Chetverikov, Danil Sharipov, Margarita Bakaeva, Daria Chetverikova, Maksim Timergalin and Timur Rameev
- 813 - 817 Evaluation of Quorum-Sensing, Antibiotics Resistance, and Biofilm Formation in Pathogenic Bacteria from the Hospital Environments
Fadhl A. S. Al Gashaa, Laith B. Alhusseini, Shayma M. A. Al Baker , Mohammed F. AL Marjani, Zahraa A. Khadam, Dunya J. Ridha and Aws H. Al Rahhal
- 819 - 823 Antioxidant and Apoptotic Effect of *Muscari muscarimi*, an Endemic Geophyte Species from Turkey
Cennet Ozay , Ege Riza Karagur, Ramazan Mammadov and Hakan Akca
- 825 - 846 Fauna of the Ladybird Beetles (Coleoptera: Coccinellidae) and their Associated Host Plants from Southern Syria
Nazir Khalil, Abdoulrahman Mourad, Mahmoud Karoum, Mohammad Abu Baker and Zuhair Amr
- 847 - 852 Larvicidal Potentials of Three Indigenous Plants Against Malaria Vector, *Anopheles Gambiae* L.
Sulaimon Adebisi Aina , Ismail Babatunde Onajobi, Ajoke Saidat Sanusi and Oluwatobi Shakirat Kolejo
- 853 - 858 Examination of Microplastic Particles in Reef Fish Food in Ternate Island Waters, Indonesia
Mimien Henie Irawati Al Muhdhar, I Wayan Sumberartha, Zainudin Hassan ,Muhammad Shalahuddin Rahmansyah and M. Nasir Tamalene
- 859 - 865 Genetic improvement of *Pseudomonas aeruginosa* and *Bacillus cereus* for controlling root knot nematode and two weeds under laboratory conditions.
Shereen AH. Mohamed , Hoda H. Ameen, Usama S. Elkelany , Mona A. El-Wakeel, Mostafa MA. Hammam and Gaziea M. Soliman
- 867 – 871 Smoking increases the premature associated senescence phenotype of circulating Endothelial Progenitor Cells
Kumboyono Kumboyono , Wiwit Nurwidyaningtyas, Indah Nur Chomsy, Fibe Yulinda Cesa and Titin Andri Wihastuti
- 873- 880 Light Microscopic Changes in The Epididymis of Different Age Groups of The African Greater Cane Rat (*Thryonomys swinderianus*, Temminck 1827)
Omirinde Jamiu Oyewole , Olukole Samuel Gbadebo and Oke Bankole Olusiji

Supplementation of Nucleotides to Enhance Performance and Immune Responses of Asian Seabass

Sri Dwi Hastuti^{1,2,*}, James Munro¹, Stephen Pyecroft¹, Mary Barton³, Maurizio Costabile^{3,4} and Brett Glencross⁵

¹School of Animal and Veterinary Sciences, The University of Adelaide, Australia, Mudla Wirra Road, Roseworthy South Australia 5371; ²Department of Aquaculture, University of Muhammadiyah Malang, Indonesia, Jl. Raya Tlogomas 246 Malang 65144; ³School of Pharmacy and Medical Sciences, University of South Australia, Australia; ⁴Centre for Cancer Biology, University of South Australia and SA Pathology, Frome Road, Adelaide, South Australia 5000; ⁵Institute of Aquaculture, University of Stirling, FK9 4LA United Kingdom

Abstract

Supplementation of nucleotides into fish diets can be an alternative method to manage disease problems in aquaculture, since it was reported could improve the growth rate and immunity of some aquaculture species. The present study assessed the growth and immune performance of Asian seabass (*Lates calcarifer* Bloch 1790) after being fed diets containing different levels of a commercial nucleotide (Optimun®) and a purified mixture of nucleotides containing AMP (Adenosine monophosphate), IMP (Inosine monophosphate), UMP (Uridine monophosphate), GMP (Guanidine monophosphate) and CMP (Cytidine monophosphate) in equal amounts. Six nucleotide supplemented diets and a control diet were used in this study, namely O1 (Optimun® 0.25 %), O2 (Optimun® 0.5 %), O3 (Optimun® 0.75 %), P1 (0.25 % mixed pure nucleotides), P2 (0.5 % mixed pure nucleotides), P3 (0.75 % mixed pure nucleotide) and C (control/diet without nucleotide supplementation). The treatment diets were fed to juvenile Asian seabass (average initial weight of 13.19 g ± 0.58 g) at 3 % body weight per day for six weeks. The results showed that weight gain, total serum protein and globulin were significantly higher in fish fed diet P2 (0.5 % of a mix pure nucleotides) compared to the control group ($P < 0.05$). In comparison, leucocrit level and respiratory burst activity were increased significantly ($P < 0.05$) in fish fed diet O1 (0.25 % of Optimun®) and the highest hematocrit level ($P < 0.05$) occurred in diet P3 (0.75 % of mixed pure nucleotides). Nevertheless, specific growth rate, feed conversion ratio, lysozyme activity, albumin serum and survival rate were not affected by dietary nucleotides ($P > 0.05$). In conclusion, supplementation of nucleotides in Asian seabass diet may have positive effect on growth performance and immune response of the fish, while diet containing 0.5% of mixed pure nucleotides tend to have a better result compared to other diet groups.

Keywords: Dietary nucleotides, Disease control, Growth rate, Fish immunity

1. Introduction

Asian seabass (*Lates calcarifer* Bloch, 1790) is an important species for aquaculture, especially in the Asia Pacific region. The production of Asian seabass globally according to the Food and Agriculture Organisation was 71 581 t year⁻¹ (FAO 2018). Intensive farming with high stocking densities and over feeding has been developed to increase the production of this species. However, it usually leads to physiological stress in the target animal, which increases the possibility of disease occurrence (Lieke *et al.*, 2019; Mehana *et al.*, 2015). The economic losses due to an outbreaks of diseases in the aquaculture industries have been estimated to reach of several billion USD per year (Assefa and Abunna 2018).

Commonly, antibiotics are used as a strategy to control diseases in aquaculture. However, some consequences can arise from this strategy, for instance the accumulation of antibiotic residues in the environment which can impact the non-target bacterial communities, the possible risk of antibiotic residues in aquaculture products or the emergence of bacterial strains which are resistant to

antibiotics (Miranda *et al.*, 2018). Therefore, alternative methods to combat disease in aquaculture should be considered, for example by increasing the immune responses of the animal to protect themselves from the variety of diseases caused by infectious organisms or environmental stressors. This protection can be gained through supplementation of the diet with immunostimulants or nucleotides (Wang *et al.*, 2017).

Nucleotides are intracellular biological compounds with low molecular weight, which have significant roles in the formation of nucleic acids (Guo *et al.*, 2017). Nucleotides could be synthesized through de novo and the salvage pathways and from the diet. However, de novo synthesis and the salvage pathway are metabolically costly processes in terms of time and energy (Hossain *et al.*, 2016a). In addition, during specific life periods, such as diseases, fast growth, the presence of environmental stressors or limited nutritional support, *de novo* synthesis is probably not adequate to cover the needs of the animal. Therefore, it is believed that adding supplementary exogenous nucleotides into fish diet can optimise the function of tissue division during rapid growth and improve the health performance of an organism (Roige,

* Corresponding author e-mail: sri.hastuti@adelaide.edu.au / hastuti@umm.ac.id.

2017). Hence, it can be considered that nucleotides are semi-essential nutrients, especially at the early infancy stages of life and under stressful conditions (Arshadi *et al.*, 2018).

Research comparing the benefit of nucleotide supplemented diets on the growth and immune responses has been conducted on number of aquaculture species, with positive results such as an increase in growth performance, the capacity of the animal to deal with stressors, and also the modulation of the intrinsic and acquired immune systems. There are some studies on using commercial dietary nucleotides on fish such as Optimun® and Ascogen for promoting growth and fish immunity (Tahmasebi-Kohyani *et al.*, 2012; Yousefi *et al.*, 2012). However, some studies attempted to add pure nucleotides into the fish diet (Hossain *et al.*, 2017, Huu *et al.*, 2013, Lin *et al.* 2009, Welker *et al.*, 2011).

Currently, there are limited studies on the use of dietary nucleotides in Asian seabass. Only two studies have been found, first is a study by Glencross and Rutherford (2010) which used Optimun® (the commercial nucleotides) at 0.2 % and the other is a study by Hastuti *et al.*, (2016) who studied the supplementation of nucleotides into the diet at 0.25 %. Therefore, this study aimed to investigate the effect of supplementation nucleotides (commercial or mixed pure nucleotides) at different levels on the growth and immune responses of Asian seabass.

2. Materials and Methods

2.1. . Experimental conditions

A total of 105 juvenile Asian seabass with the initial weight of 13.19 ± 0.58 g (mean \pm SD) from a local hatchery (Robbara Broodstock and Sanctuary, South

Australia) were used in this experiment. Fish which were used in this research have been approved by Adelaide University Animal Ethics Committee with approval number S-2015-104. Prior to the experiment, fish were acclimated to laboratory condition for 2 wk (week). Following the acclimation period, fish were randomly allocated in a 65 L tank, at the stocking density of five fish tank⁻¹. Each tank was equipped with a recirculation filter. Water temperature ranged from 27 °C to 30 °C, pH was between 6.8 and 7.7, and ammonia between 0.25 mg L⁻¹ and 8 mg L⁻¹. Fish were hand fed to 3 % BW (body weight) day⁻¹ for 6 wk.

2.2. Diet Preparation

Optimun®, a commercial nucleotide supplement (Chemoforma, Switzerland) or mixed pure nucleotides containing AMP, IMP, UMP, GMP and CMP (Sigma Aldrich, Australia) with the ratios (1:1:1:1:1) were incorporated into the fish feed at the following doses : (0.25, 0.5 and 0.75) % kg⁻¹ of feed and the basal diet was used as a control (no added nucleotides). The diets were named in abbreviation as follows: O1 (Optimun® 0.25 %), O2 (Optimun® 0.5 %), O3 (Optimun® 0.75 %), P1 (0.25 % mixed pure nucleotides), P2 (0.5 % mixed pure nucleotides), P3 (0.75 % mixed pure nucleotide) and C (control/diet without nucleotide supplementation). All ingredients were carefully mixed with water to make a dough. The dough was processed into pellets using a New Flora domestic meat grinder mincer (Flora Livings, Australia), then oven dried at 55 °C. The pellets were placed in plastic bags and stored at 4 °C. The basal dietary formulation is presented in Table 1, with the composition from proximate analysis in Table 2.

Table 1. Composition of basal and experimental diets for Asian seabass

Ingredients (percent in diet)	Diet groups						
	C	O1	O2	O3	P1	P2	P3
Fish meal	70	70	70	70	70	70	70
Fish oil	15	15	15	15	15	15	15
Wheat flour	14.4	14.15	13.9	13.65	14.15	13.9	13.65
Vitamin and mineral premix	0.5	0.5	0.5	0.5	0.5	0.5	0.5
Yttrium oxide	0.1	0.1	0.1	0.1	0.1	0.1	0.1
Optimun® (O)	0	0.25	0.5	0.75	0	0	0
Mixed pure nucleotide (P)	0	0	0	0	0.25	0.5	0.75

Vitamin and mineral premix includes (IU kg⁻¹ or g kg⁻¹ of premix): vitamin A, 2.5MIU; vitamin D3, 0.25 MIU; vitamin E, 16.7 g; vitamin K3, 1.7 g; vitamin B1, 2.5 g; vitamin B2, 4.2 g; vitamin B3, 25 g; vitamin B5, 8.3 g; vitamin B6, 2.0 g; vitamin B9, 0.8 g; vitamin B12, 0.005 g; biotin, 0.17 g; vitamin C, 75 g; choline, 166.7 g; inositol, 58.3 g; ethoxyquin, 20.8 g; copper, 2.5 g; ferrous iron, 10.0 g; magnesium, 16.6 g; manganese, 15.0 g; zinc, 25.0 g

Table 2. Proximate analysis of the experimental diets

Parameters (% in diet)	Diet groups						
	C	O1	O2	O3	P1	P2	P3
Dry matter content	93.28	94.77	94.8	94.36	94.53	94.51	93.56
Ash	9.91	9.89	9.91	9.94	9.89	10.02	10.02
Crude protein	50.46	48.31	50.06	47.57	47.99	48.47	49.42
Crude lipid	18.91	18.45	18.59	18.89	18.88	18.12	18.48
Fibre	0.82	1.92	1.77	1.15	1.85	1.18	1.43

Noted: C (control/no supplemented nucleotides); O1 (Optimun® at 0.25 %), O2 (Optimun® at 0.5 %), O3 (Optimun® at 0.75 %), P1 (0.25 % of mixed pure nucleotides), P2 (0.5 % of mixed pure nucleotides), P3 (0.75 % of mixed pure nucleotide).

2.3. Sampling and calculations

After completion of the feeding trial, all fish in each tank were counted and weighed to calculate the weight gain (W), specific growth rate (SGR), feed conversion ratio (FCR) and survival rate (SR) using following formulae (1 to 4).

$$W (g) = \text{Final weight (g)} - \text{Initial weight (g)} \quad (1)$$

$$SGR (\% \text{ day}^{-1}) = 100 \times \frac{\ln \text{final weight (g)} - \ln \text{initial weight (g)}}{\text{time (days)}} \quad (2)$$

$$FCR = \frac{\text{Weight of food supplied to the fish (g)}}{\text{Final weight (g)} - \text{Initial weight (g)}} \quad (3)$$

$$SR (\%) = 100 \times \frac{\text{final weight (g)}}{\text{initial weight (g)}} \quad (4)$$

A blood sample was obtained from three fish per tank. Blood was taken from the caudal vein of the fish using 1 ml syringe, centrifuged at 3 000 x g for 15 min, and then serum was collected, pooled and stored at -80 °C for further haematological and immunological assays.

2.4. Hematocrit and leucocrit measurements

Hematocrit and leucocrit levels were performed as described by Siwicki *et al.* (1994). Briefly, sample was placed in a micro hematocrit capillary tube to two thirds of the tube volume, one end of the tube was sealed with clay. The sample was centrifuged for 5 min at 15 000 g, and the hematocrit level measured by calculating the ratio of the red blood cell layer to the total blood sample in the capillary tube and the leucocrit level by calculating the ratio of the white blood cell layer to the total blood volume in the capillary tube. The values of hematocrit and leucocrit were expressed in % of total sample.

2.5. Serum lysozyme assay

Serum lysozyme activity was measured using a method by Milla *et al.* (2010). Ten microlitres of Asian seabass serum was placed into Corning 96 well plate flat bottom (Adelab Scientific, Australia) and mixed with 10 µL of 0.05 M sodium phosphate buffer (Na₂HPO₄ dodecahydrate (12 H₂O)) (Sigma Aldrich, Australia) at pH 6.2. As much as 130 µL of lyophilized *Micrococcus lysodeikticus* (Sigma Aldrich, Australia) suspension at a concentration of 0.6 mg mL⁻¹ in phosphate buffer, pH = 6.2 was added to the wells. Absorbance was monitored at 450 nm at 0 min and 10 min using a Benchmark Plus microplate spectrophotometer, Bio-Rad version 5.2.1. One unit of lysozyme activity was defined as the quantity of serum which caused a 0.001 min⁻¹ decrease in absorbance. The serum lysozyme activity was expressed in unit mL⁻¹ serum.

2.6. Respiratory burst activity assay

Kidney macrophage burst activity was measured following a method from Ulvestad *et al.* (2018) with a slight modification. Briefly, the head kidney was aseptically removed. The tissue was homogenized in L-15 (Leibovitz) medium containing 100 µL mL⁻¹ penicillin/streptomycin, 10 µL mL⁻¹ heparin and 2 % (v/v) Fetal Bovine Serum (FBS), then gently filtered through nylon (mesh size 100 µm). The cell suspensions were layered onto a 34 % to 51 % Percoll density gradient, then

centrifuged at 450 × g for 30 min at 4 °C. After centrifugation, the macrophage enriched interfaces were collected, washed, and adjusted to 1 × 10⁶ cells mL⁻¹ using a haemocytometer. Following adjustment, 100 µL of the cell suspension were placed in the Corning 96 well tissue culture plate flat bottom (Adelab Scientific, Australia) and incubated at 20 °C for 2 h. Then the non-adherent cells were removed by gently washing the wells with L-15 medium. Amount 100 µL of 0.2 % nitroblue tetrazolium (NBT, Sigma) and 0.2 µL of phorbol 12-myristate 13-acetate (1 mg mL⁻¹) solution were added to each well and the plate was incubated for 1 h at room temperature. The medium was carefully removed from the plate and the cells were fixed by the addition of 100 % methanol and incubated for 10 min. Subsequently, the cells were washed with 70 % methanol to remove unreduced NBT, and then were air-dried. The formazan was dissolved in 120 µL of 2M KOH and 140 µL DMSO, and the optical density was measured by using a Benchmark Plus microplate spectrophotometer, Bio-Rad version 5.2.1 at 630 nm using KOH and DMSO as blanks.

2.7. Total protein, albumin and globulin

Blood samples were taken from the caudal vein of the fish and placed into 1.5 mL microtubes. The blood was centrifuged at 3 000 × g for 15 min at 4 °C, and serum was collected and transferred to new tubes. 200 µL of pooled serum from each treatment was used to measure total protein, albumin and globulin of the serum using an auto-analyser AU480 (Beckman-Coulter) machine by following the standard protocols provided in the machine user guide.

2.8. Statistical analysis

Results were analysed by one-way analysis of variance (ANOVA) using IBM SPSS version 22.0 statistical software, followed by Duncan's test to compare the means between individual treatments. Significance was set at $P < 0.05$.

3. Results

The growth and survival rates of the fish after six weeks of feeding trial are shown in Table 3. It was found that nucleotide supplemented diets did not significantly improve the specific growth rate (SGR), feed conversion ratio (FCR) or survival rate (SR) of Asian seabass ($P > 0.05$). However, there is a significant impact ($P < 0.05$) of diet supplemented with 0.5 % of mixed pure nucleotide (diet P2) on fish weight gain (WG), with value was 47.73 g ± 9.15 g (mean ± SD), total protein serum, with value was 50.33 ± 0.666 (mean ± SD) and globulin serum, with value was 36.33 ± 0.577 (mean ± SD). Although statistically there was no significant difference in SGR and FCR between the diet groups, P2 diet gave the highest SGR and FCR with the value of 3.56 % ± 0.37 % BW d⁻¹ (mean ± SD) and 1.85 ± 0.34 (mean ± SD) respectively. In terms of survival rate, there were also no significant differences among the groups. The SR ranged from 66.67 % to 93.33 %. Mortality occurred due to cannibalism in some tanks.

Hematocrit and leucocrit levels of Asian seabass showed in Table 4. Hematocrit levels were significantly higher ($P < 0.05$) in fish fed diet P3 (0.75 % of mixed pure nucleotides) compared to those fed diets without supplementation of nucleotides (C), with the value of

45.68 % \pm 4.16 % (mean \pm SD). In addition, it was found that fish fed diet P3 experienced a significant decrease in the level of leucocrit ($P < 0.05$), with the value of 0.246 % \pm 0.1 % (mean \pm SD) compared to other groups. In comparison, diet O1 showed the highest level of leucocrit with the value of 1.397 % \pm 0.45 % (mean \pm SD).

Supplementation of nucleotide in fish diet had no significant influence ($P > 0.05$) on lysozyme activity (Table 4). However, it is noted that P1 diet group had the highest lysozyme activity compared to others with the activity of 560 \pm 309.6 unit mL⁻¹ (mean \pm SD). Respiratory burst activity of Asian seabass fed nucleotides diet was presented in Table 4. Respiratory burst activity on the fish fed O1 diet group was significantly higher ($P < 0.05$) compared to other diet groups with the respiratory burst reading value of 0.177 \pm 0.04 (mean \pm SD). At the same time, it is noted that fish fed diet containing 0.75 % of mixed pure nucleotide (P3) showed a significant decrease on the respiratory burst activity reaching 0.122 \pm 0.004 (mean \pm SD).

Table 3. Growth and survival rate of Asian seabass after 6 wk of feeding trial

Diet Groups	Initial weight (g)	Final weight (g)	Weight gain (WG, g)	Specific Growth Rate (SGR, %BW d ⁻¹)	Feed Conversion Ratio (FCR)	Survival Rate (SR, %)
C	13.33 \pm 0.61	43.37 \pm 5.02	30.03 \pm 4.88 ^a	2.80 \pm 0.28 ^a	2.85 \pm 0.5 ^a	86.67 \pm 11.55 ^a
O1	12.67 \pm 0.12	38.86 \pm 11.64	26.19 \pm 11.56 ^a	2.59 \pm 0.78 ^a	3.66 \pm 2.10 ^a	66.67 \pm 11.55 ^a
O2	13.27 \pm 0.31	37.60 \pm 12.97	24.33 \pm 13.24 ^a	2.39 \pm 0.84 ^a	4.15 \pm 2.06 ^a	93.33 \pm 11.55 ^a
O3	13.07 \pm 0.61	45.53 \pm 5.90	32.47 \pm 5.37 ^{ab}	2.96 \pm 0.23 ^a	2.57 \pm 0.35 ^a	93.33 \pm 11.55 ^a
P1	13.27 \pm 0.31	39.95 \pm 12.70	26.68 \pm 12.94 ^a	2.55 \pm 0.75 ^a	3.59 \pm 1.43 ^a	86.67 \pm 11.55 ^a
P2	13.67 \pm 0.46	61.40 \pm 9.01	47.73 \pm 9.15 ^b	3.56 \pm 0.37 ^a	1.85 \pm 0.34 ^a	73.33 \pm 30.55 ^a
P3	13.07 \pm 1.15	39.73 \pm 11.12	26.67 \pm 12.23 ^a	2.58 \pm 0.93 ^a	3.89 \pm 2.68 ^a	86.67 \pm 23.09 ^a

Noted: Data presented as means of triplicates \pm SD. Different superscripts in the column indicate significant (< 0.05) difference between different diet groups. C (control/no supplemented nucleotides); O1 (Optimun® at 0.25 %), O2 (Optimun® at 0.5 %), O3 (Optimun® at 0.75 %), P1 (0.25 % of mixed pure nucleotides), P2 (0.5 % of mixed pure nucleotides), P3 (0.75 % of mixed pure nucleotide).

Table 4. Effect of nucleotide supplemented diet on Asian seabass immunity after 6 wk of feeding trial

Immune parameters	Diet groups						
	C	O1	O2	O3	P1	P2	P3
Hematocrit level (%)	27.1 \pm 6.44 ^a	34.28 \pm 8.87 ^{ab}	36.35 \pm 8.95 ^{ab}	37.07 \pm 1.22 ^{ab}	25.55 \pm 12.84 ^a	33.92 \pm 7.97 ^{ab}	45.68 \pm 4.16 ^b
Leucocrit level (%)	1.327 \pm 0.53 ^{ab}	1.397 \pm 0.45 ^b	1.05 \pm 0.84 ^{ab}	0.945 \pm 0.12 ^{ab}	0.83 \pm 0.82 ^{ab}	0.56 \pm 0.25 ^{ab}	0.246 \pm 0.10 ^a
Lysozyme (unit mL ⁻¹)	404.8 \pm 51.95 ^a	436.7 \pm 65.15 ^a	265.6 \pm 148.9 ^a	324 \pm 166.5 ^a	560 \pm 309.6 ^a	347.4 \pm 12.07 ^a	372.9 \pm 143.4 ^a
Resburst (OD630)	0.136 \pm 0.02 ^{ab}	0.177 \pm 0.04 ^b	0.145 \pm 0.04 ^{ab}	0.137 \pm 0.01 ^{ab}	0.147 \pm 0.02 ^{ab}	0.149 \pm 0.007 ^{ab}	0.122 \pm 0.004 ^a
Total serum protein (g L ⁻¹)	42.5 \pm 3.14 ^a	48.27 \pm 2.875 ^{ab}	45.27 \pm 0.513 ^{ab}	44.6 \pm 7.15 ^{ab}	45.9 \pm 2.6 ^{ab}	50.33 \pm 0.666 ^b	43.8 \pm 1.4 ^a
Total albumin (g L ⁻¹)	12.1 \pm 0.3 ^a	13.47 \pm 0.802 ^a	13.07 \pm 0.757 ^a	12.6 \pm 2.13 ^a	13.33 \pm 0.61 ^a	13.83 \pm 0.057 ^a	12.6 \pm 0.3 ^a
Total globulin (g L ⁻¹)	30.33 \pm 2.89 ^a	34.67 \pm 2.082 ^{ab}	32.33 \pm 0.577 ^{ab}	32.33 \pm 5.03 ^{ab}	32.67 \pm 2.08 ^{ab}	36.33 \pm 0.577 ^b	31.33 \pm 1.155 ^a
A : G ratio	0.4 \pm 0.03 ^a	0.39 \pm 0.01 ^a	0.41 \pm 0.03 ^a	0.39 \pm 0.01 ^a	0.41 \pm 0.02 ^a	0.38 \pm 0.01 ^a	0.4 \pm 0.01 ^a

Noted: Data presented as means of triplicates \pm SD. Different superscripts indicate significant (< 0.05) difference between different diet groups. Resburst = Respiratory burst activity, A : G = ratio of albumin to globulin. C (control/no supplemented nucleotides); O1 (Optimun® at 0.25 %), O2 (Optimun® at 0.5 %), O3 (Optimun® at 0.75 %), P1 (0.25 % of mixed pure nucleotides), P2 (0.5 % of mixed pure nucleotides), P3 (0.75 % of mixed pure nucleotide)

4. Discussion

Adequate nutrition given to the animal could determine its health status and growth performance. Since Asian seabass are carnivorous animals and require high protein content mainly from fish meal (usually provided by fish meal for farmed fish), in this study we used a basal diet which contained greater than 45 % crude protein and approximately 18 % of lipids. The basal diet we used for this study fulfilled the nutrient requirements for Asian seabass growth. Glencross (2006) reported that diets

The fish serum contains protein compounds, including albumin and globulin. The level of albumin and globulin reflect the health status of the animal since they are important components of the fish innate immune system (Syed *et al.*, 2018). Our study found significant differences in the total protein and globulin serum of Asian seabass after 6 wk of the feeding trial, except for the albumin serum of the fish. Moreover, fish fed diet with 0.5 % supplementation of mixed pure nucleotides showed significantly higher in total protein and globulin serum ($P < 0.05$), accounting for 50.33 g L⁻¹ \pm 0.666 g L⁻¹ and 36.33 g L⁻¹ \pm 0.577 g L⁻¹ (mean \pm SD) respectively. Although total albumin was not significantly different between the treatment groups, it was found that diet P2 resulted in higher albumin serum compared to other diet groups with the values of 13.83 g g L⁻¹ \pm 0.057 g L⁻¹ (mean \pm SD.)

containing 45 % to 50 % crude protein and 15 % to 18 % lipid gave the best growth rates for Asian seabass in several studies.

Numerous studies on supplementation of nucleotides in diets have been conducted for aquatic species including fish. The supplementation of nucleotides into fish diets could improve growth and survival rate of the fish as well as enhance their immune responses (Hossain *et al.*, 2016a, 2016b; Kader *et al.*, 2018; Lin *et al.*, 2009). Our study found that weight gain of Asian seabass increased significantly in the fish fed a mix pure nucleotide

supplemented diet at 0.5 % (P2). This finding is similar to a study by Huu *et al.* (2013) in which supplementation with pure nucleotide GMP at 0.5 % or combination between two pure nucleotides GMP + AMP/IMP (0.4 % + 0.1 %) into the diet gave a higher growth rate in Black tiger shrimp (*Penaeus monodon*) compared to control diet and diet supplemented with GMP 0.4 %. In another study, Hossain *et al.* (2017) found the optimal dose of IMP supplementation which gave the best growth performance for juvenile amberjack (*Seriola dumerili* Risso, 1810) diet was 0.54 %. Specific growth rate and feed conversion ratio in our study was not affected by a diet supplemented with nucleotides. However, there was a trend that diet P2 (0.5 % supplementation of a mix pure nucleotide) demonstrated better SGR and FCR compared to other diet groups. In a previous study, Asian seabass fed with mixed pure nucleotides at 0.25 % for 4 wk showed no significant differences in their growth performance (Hastuti *et al.*, 2016). In contrast, this present study revealed that Asian seabass fed a mix pure nucleotide diet at 0.5 % for 6 wk showed a significantly higher growth performance. Hence, supplementation of mixed pure nucleotides at a concentration of 0.5 % might effectively improve the growth performance of Asian seabass.

Many studies suggested supplementation of nucleotides at around 0.2 % kg⁻¹ of feed for aquatic animals (Hossain *et al.*, 2016a; Kenari *et al.*, 2013; Lin *et al.*, 2009), whereas some studies found that fish need higher levels of nucleotides supplementation. For example, Xu *et al.* (2015) reported the optimum level of nucleotide supplementation in the diet of hybrid tilapia (*Oreochromis niloticus* ♀ x *Oreochromis aureus* ♂) to give better performance was 0.63 %, while a study by (Hossain *et al.*, 2017) suggested the optimal dose of nucleotide supplementation for increasing growth and immunity of amberjack were 0.54 % and 0.67 % respectively. In contrast, some studies found that fish only need a lower level of nucleotide supplementation to obtain a better performance, for example the addition of 0.1 % of mixed pure nucleotide to the zebra fish (*Danio rerio* F. Hamilton, 1822) diet, increased weight gain of the fish significantly (Guo *et al.*, 2017).

Hematological parameters could reflect the physiological and general health status of fish (Hossain *et al.*, 2016a, 2016b). This present study found that supplementation of the diet with mixed pure nucleotides at 0.75 % (diet P3) significantly increased the hematocrit levels of Asian seabass. The increase of hematocrit levels as an impact of dietary nucleotides also occurred in a study by Hossain *et al.* (2016b) who reported that feeding red sea bream (*Pagrus major* Temminck and Schlegel, 1843) with nucleotide enriched product for 60 d increased hematocrit levels of the fish. Similarly, Rachmawati *et al.* (2021) reported that feeding Java barb (*Barbonymus gonionotus* Bleeker, 1850) with a diet containing nucleotides from *Sacharomyces cereviceae*, increased the hematocrit levels of the fish significantly. The present study found that supplementation of Optimun® into the fish diet 0.25 % to 0.75 % resulted in rising hematocrit levels compared to the fish fed control diet. This finding was similar to a study by Yousefi *et al.*, 2012 who reported that hematocrit of Beluga sturgeon (*Huso huso* Linnaeus, 1758) increased significantly in fish fed Optimun® supplementation diet for 62 d. It indicated that the

inclusion of both commercial nucleotide product (Optimun®) or a mix of pure nucleotides into the Asian seabass diet might significantly affect the hematocrit level of Asian seabass. In terms of leucocrit levels, we found that diet contains 0.25 % of Optimun® showed a significant higher leucocrit levels, whereas diet containing 0.75 % of mixed pure nucleotides demonstrated a significant lower of leucocrit level compared to other diet groups. The excessive dose of nucleotide supplementation might impair the immune responses of the fish, as reported in a study of channel catfish (*Ictalurus punctatus* Rafinesque, 1818) (Welker *et al.*, 2011).

Respiratory burst activity is a non-specific immune parameter which is usually used to determine health status of the fish. Lin *et al.* (2009) found that respiratory burst activity of grouper (*Epinephelus malabaricus* Bloch and Schneider, 1801) head kidney increased significantly in response to enrichment of the diet with nucleotide. Another study also reported that feeding tilapia with a nucleotide supplemented diet increase the fish respiratory burst activity (Shiau *et al.*, 2015). This present study found a significant increase in the respiratory burst activity of Asian seabass fed diet containing Optimun® at 0.25 % (O1). Similar findings occurred in a study by Andriano *et al.* (2012), in which Optimun® at the level of 0.2 % was supplemented into Pacific white shrimp (*Litopenaeus vannamei* Boone, 1931) diet resulted in a significant enhanced of respiratory burst activity. The positive effect of dietary nucleotides on respiratory burst activity was also reported by Cheng *et al.* (2011) in red drum (*Sciaenops ocellatus* Linnaeus, 1766), Baidya *et al.* (2015) in *Labeo rohita* F. Hamilton, 1822 and Jha *et al.* (2007) in *Catla catla* F. Hamilton, 1822. On the contrary, this study revealed that feeding a mixed pure nucleotide diet at 0.75 % was decreased respiratory burst activity in Asian seabass. Thus, the high concentration of nucleotides inclusion into the diet might harm the fish immune system. Furthermore, Welker *et al.* (2011) reported that channel catfish (*Ictalurus punctatus* Rafinesque, 1818) fed a high dose of mixed pure nucleotide diet at 0.9 % and 2.7 % for eight weeks demonstrated immune responses decline and reduced resistance of the fish against bacterial infection. Therefore, the excessive concentration implemented should be concerned in the application of dietary nucleotides for aquaculture animals.

Lysozyme protects the animal from microbial invasion, since it has lytic activity against both Gram-negative and Gram-positive bacteria (Saurabh and Sahoo, 2008). Studies on rainbow trout (*Onchorynchus mykiss* Walbaum, 1792) (Hunt *et al.*, 2016), Caspian brown trout (*Salmo trutta* Linnaeus, 1758) (Kenari *et al.*, (2013) and hybrid tilapia (Shiau *et al.*, 2015) showed that feeding fish with a nucleotide supplemented diet could significantly increase their serum lysozyme activity. In contrast, our study found that supplementation of Asian seabass diet with nucleotides did not considerably impact lysozyme activity ($P > 0.05$) in all diet groups. Previous experiments on rainbow trout fed nucleotide supplemented diet at 0.2 % for 45 d also resulted in no significant effect on fish lysozyme activity (Yousefi *et al.*, 2016). Similarly, red drum (*Sciaenops ocellatus* Linnaeus, 1766) fed 0.5 and 1 % nucleotide diets for 42 d had no significant differences in their serum lysozyme activity compared to those fed control diet (Cheng *et al.*, 2011). Although in this present

study dietary nucleotides did not significantly affect the lysozyme activity of Asian seabass, fish fed diet supplemented with 0.25 % of mixed pure nucleotides (P1) tend to have a higher lysozyme activity compared to other diet groups.

Reda *et al.* (2018) reported, total protein, albumin and serum globulin of Nile tilapia (*Oreochromis niloticus* Linnaeus, 1758) increased significantly in fish fed diet supplemented with 0.25 % nucleotides. They also found an increase in the IgM levels of the fish and a decrease in the ratio of albumin/globulin (A:G ratio). This present study found that concentrations of total protein and globulin serum in Asian seabass fed diet supplemented with a mix pure nucleotide at 0.5 % were significantly higher than those without nucleotides supplementation. This finding is consistent with a study by Jha *et al.* (2007), which reported that serum total protein and globulin concentrations were significantly higher in *C. catla* fed dietary nucleotides. In addition, a study by Tahmasebi-Kohyani *et al.* (2011) reported a significant increase of Immunoglobulin levels of rainbow trout fed nucleotide diet. In contrast, our study failed to demonstrate the considerable effect of nucleotide diets on the albumin serum and A:G ratio ($P > 0.05$). However, it was noted that fish fed 0.5 % of mixed pure nucleotides diet experienced higher albumin serum level and lower A:G ratio compared to those fed other diet groups. Higher globulin concentrations and a lower A:G ratio indicates an increase in antibody response since gamma globulins play an important role in the fish immune system (Kumar *et al.*, 2005).

Information about the standard administration dose of nucleotide supplemented into fish diets is still not clear since there are inconsistent results regarding the effect of nucleotide supplemented diets, even when using the same fish species. Optimun® as a commercial product of nucleotide has been extensively used in many studies for different kind of aquatic animals. It has been reported Optimun® increased health and growth performance of rainbow trout (Tahmasebi-Kohyani *et al.*, 2011, 2012), and striped bass (Li *et al.*, 2015) at low dose administration around 0.15 % to 0.2 % in diet, while the use of higher doses was found to be effective in Black tiger shrimp (*Penaeus monodon* Fabricius, 1798) with the optimal dose at 0.56 % (Huu *et al.*, 2012). The optimal dose of Optimun® for beluga sturgeon (*H. huso*) was found around 0.25 % to 0.35 % (Yousefi *et al.*, 2012), while the best dose for striped catfish (*Pangasianodon hypophthalmus* Sauvage, 1878) was 0.25 % to 0.5 % (Yaghobi *et al.*, 2015). The size of fish could influence the effect of dietary nucleotides. Tahmasebi-Kohyani *et al.* (2012) reported that rainbow trout with an average weight of 23 g demonstrated the best growth performance and health status when they were fed 0.2 % Optimun® supplementation diet for 8 wk. In contrast, feeding the same source of nucleotide (Optimun®) at the same level (0.2 %) for the same fish species (rainbow trout) resulted in no significant growth improvement and even caused immunological and metabolic problems in smaller fish with an average weight of 3.79 g (Yousefi *et al.*, 2016). In this present study, feeding Asian seabass with Optimun® supplemented diet at 0.75 % showed a higher weight gain compared to the fish fed diet supplemented with 0.25 % and 0.5 % Optimun®. Hastuti *et al.* (2016) reported that supplementation of Optimun® at 0.25 % did not affect

growth performance and immune responses of the fish. Thus, Asian seabass might need higher concentration of Optimun® supplementation to improve its performance and health.

The type of nucleotide becoming one factor which should be considered, since the results obtained could be different when a different type of nucleotides are used. For example, a study in Tilapia found that using a commercial nucleotide (AccelerAid™, FormilVet Brazil) at different levels for 60 d did not significantly increase growth performance and immune responses of fingerling Tilapia (Barros *et al.*, 2015). Similarly, the inclusion of 0.15 % and 0.3 % Laltide® into European seabass (*Dicentrarchus labrax* Linnaeus, 1758) diet for 42 d resulted in no significant differences on growth performance and feed conversion ratio of the fish (Bowyer *et al.*, 2019). On the other hand, significant improvements in growth performance and immune responses occurred when the fish were fed a commercial nucleotide (Rovimax NX™, Switzerland) supplemented diet for 70 d, with the optimal application dose was 0.024 % (Shiau *et al.*, 2015). Positive effects of a nucleotide-enriched diet in tilapia was obtained with a *Saccharomyces cerevisiae*-derived nucleotide mixture from Biotgether (Nanjing China) for 8 wk, with the optimal dose of around 0.6 % (Xu *et al.*, 2015). Additionally, Hunt *et al.* (2016) found that supplementation of rainbow trout diet with another commercial nucleotide (Nu-Pro™, Alltech Inc, USA) at 20 % to 60 % for 60 d, significantly increased immune parameters of the fish. A study of grouper by Lin *et al.* (2009) showed that fish growth, feed efficiency, respiratory burst and fish survival were significantly enhanced with the supplementation with a purified mixture of nucleotides. In addition, turbot fed a diet containing a mixture of purified nucleotides showed improvement in fish respiratory burst and lysozyme activity, and intestinal micromorphology (Peng *et al.*, 2013).

The exact mechanism of the immune enhancing effects of dietary nucleotide is still unclear. In terms of the selected doses of nucleotides used, it has been reported that some fish species require a lower dose of nucleotide supplementation of around less than 0.25 % to boost the immune parameters or growth performance of the animal (Lin *et al.*, 2009; Shiau *et al.*, 2015; Yousefi *et al.*, 2012), while some studies also reported that some fish need a higher dose of nucleotide supplementation at ≥ 0.5 % in the diet to promote immune responses (Hunt *et al.*, 2016; Xu *et al.*, 2015). In terms of the feeding regime implemented, both short and long periods of dietary nucleotides administrations have been reported to have positive effect on fish growth and immunity. Some experiments were conducted over short periods of time, such as 4 wk or less (Guo *et al.*, 2017; Reda *et al.*, 2018), but others, fed the fish with nucleotide diets for 10 wk or more (Shiau *et al.*, 2015; Yaghobi *et al.*, 2015). However, some researchers reported that prolonged administration of nucleotide-supplemented diets led to immune response suppression which negatively impacted the health of the fish. Li *et al.* (2007) reported that juvenile red drum fed pure nucleotide supplementation diet for one week showed a significant increase in weight gain and feed efficiency, but when the feeding trial was extended for three additional weeks, less significant weight gain was found. In addition, tilapia fed yeast nucleotide supplemented diet

for 15 d, experienced an increase in some innate immune parameters compared to the fish which fed the same type of nucleotides for 30 d (Reda *et al.*, 2018). A previous study by Hastuti *et al.* (2016) in Asian seabass fed diet supplemented with Optimun® or mixed pure nucleotides at 0.25 % for 4 wk showed no significant differences in all the parameter tested. However, our present study revealed that feeding Asian seabass with 0.5 % of mixed pure nucleotide diet for 6 wk demonstrated positive results on fish growth and some immune parameters. The response of the fish to a nucleotide-supplemented diet for enhancing growth and immune function is still not well studied in Asian seabass, so it is not clear whether the response will be immediate or delayed after initial feeding. Future studies which compare different feeding periods from two weeks to 16 wk might be warranted to give better understanding on the kinetic effects of nucleotide supplemented diet on Asian seabass.

5. Conclusion

Based on the present finding, dietary nucleotides in Asian seabass could be a promising method to improve growth performance and health status of the fish. Diet supplemented with 0.5 % mixed pure nucleotide seems to have the best result compared to control and Optimun® supplementation diet, since it significantly increased fish growth and some immune parameters. Thus, supplementation of 0.5 % mixed pure nucleotides could be recommended in Asian seabass diet. A study for investigating the effect of single pure nucleotide supplementation in Asian seabass growth and immune responses is recommended to determine which type of single nucleotide could enhance better fish performance. Factors such as administration dose, feeding regime, type and source of nucleotide, fish species and size, initial immune status of individual fish, and basal diet nutrition content might influence the response to diets supplemented with nucleotides. Hence, further studies are warranted in this area.

Acknowledgement

The authors would like to thank Prof Brett Glencross for providing Optimun® in this study and giving valuable comments in this manuscript. The authors also would like to thank Directorate General for Higher Education, Ministry of Research Technology and Higher Education, Republic of Indonesia, and University of Muhammadiyah Indonesia, for supporting the first author in her PhD (No. 1633/E.4.4/2014) at the School of Animal and Veterinary Sciences, University of Adelaide, Australia.

References

Andrino KGS, Serrano Jr AE, Corre Jr VL. 2012. Effects of dietary nucleotides on the immune response and growth of juvenile Pacific white shrimp *Litopenaeus vannamei* (Boone, 1931). *Asian Fish. Sci* **25**: 180-192

Arshadi A, Yavari V, Oujifard A, Mousavi SM, Gisbert E and Mozanadeh MT. 2018. Dietary nucleotide mixture effects on reproductive and performance, ovary fatty acid profile and biochemical parameters of female Pacific shrimp *Litopenaeus vannamei*. *Aquac Nutr.*, **24**: 515-523.

Assefa A and Abunna F. 2018. Maintenance of fish health in aquaculture: Review of epidemiological approaches for

prevention and control of infectious disease of fish. *Vet Med Int. ID* **5432497**.

Baidya S, Shivananda MH, Jagadeesh TD, Sonowal S. 2015. Effect of nucleotide on growth, immune responses and resistance of *Labeo Rohita* to *Aeromonas hydrophila* infection. *J Aquac Mar Biol* **2(4)**: 00037.

Barros MM, Guimaraes IG, Pezzato LE, Orsi RO, Junior, ACF, Teixeira CP, Fleuri LF and Padovani CR. 2015. The effects of dietary nucleotide mixture on growth performance, haematological and immunological parameters of Nile tilapia. *Aquac Res.*, **46(4)**: 987-993.

Bowyer PH, El-Haroun ER, Hassan M, Salim H and Davies SJ. 2019. Dietary nucleotides enhance growth performance, feed efficiency and intestinal functional topography in European Seabass (*Dicentrarchus labrax*). *Aquac Res.*, **50(7)**:1921-1930.

Cheng Z, Buentello A and Gatlin III DM. 2011. Dietary nucleotide influence immune responses and intestinal morphology of red drum *Sciaenops ocellatus*. *Fish Shellfish Immunol.*, **30**:143-147.

FAO. 2018. The State of World Fisheries and Aquaculture 2018 - Meeting the sustainable development goals. Rome. Licence: CC BY-NC-SA 3.0 IGO. <http://www.fao.org/3/ca9229en/ca9229en.pdf>.

Glencross B. 2006. The nutritional management of barramundi, *Lates calcarifer* – a review. *Aquac Nutr.*, **12**:291-309.

Glencross B and Rutherford N. 2010. Dietary strategies to improve the growth and feed utilization of barramundi, *Lates calcarifer* under high water temperature conditions. *Aquac Nutr.*, **16**:343-350.

Guo X, Ran C, Zhang Z, He S, Jin M and Zhou Z. 2017. The growth-promoting effect of dietary nucleotides in fish is associated with an intestinal microbiota-mediated reduction in energy expenditure. *J Nutr* **147(5)**:781-788

Hastuti SD, Munro J and Pycroft S. 2016. Growth and non-specific immune responses of Asian Seabass (*Lates calcarifer*) fed on commercial and mixed pure nucleotides diet. *Indones. Aquac. J* **17**:69-74.

Hossain MS, Koshio S, Ishikawa M, Yokoyama S and Sony NM. 2016a. Dietary nucleotide administration influences growth, immune responses and oxidative stress resistance of juvenile red sea bream (*Pagrus major*). *Aquaculture*, **455**:41-49.

Hossain MS, Koshio S, Ishikawa M, Yokoyama S, Sony NM, Dawood MAO, Kader MA, Bulbul M and Fujieda T. 2016b. Efficacy of nucleotide related products on growth, blood chemistry, oxidative stress and growth factor gene expression of juvenile red sea bream, *Pagrus major*. *Aquaculture*, **464**:8-16.

Hossain MS, Koshio S, Ishikawa M, Yokoyama S, Sony NM, Kader MA, Maekawa M and Fujieda T. 2017. Effects of dietary administration of inosine on growth, immune response, oxidative stress and gut morphology of juvenile amberjack, *Seriola dumerili*. *Aquaculture*, **468**:534-544.

Hunt AO, Yilmaz FO, Berkoz M, Engin K, Gunduz SG and Yalin S. 2016. Effects of dietary nucleotide yeast on immune responses and antioxidant enzyme activities of rainbow trout juveniles (*Oncorhynchus mykiss*). *Isr J Aquacult Bamid.*, **68**:1-12.

Huu HD, Tabrett S, Hoffman K, Koppel P, Lucas J and Barnes AC. 2012. Dietary nucleotides are semi-essential nutrients for optimal growth of black tiger shrimp (*Penaeus monodon*). *Aquaculture*, **366-367**:115-121.

Huu HD, Tabrett S, Hoffman K, Koppel P and Barnes AC. 2013. The purine nucleotides guanine, adenine and inosine are a dietary requirement for optimal growth of black tiger prawn, *P. monodon*. *Aquaculture*, **408-409**:100-105.

- Jha AK, Pal AK, Sahu NP, Kumar S and Mukherjee SC. 2007. Haemato-immunological responses to dietary yeast RNA, ω -3 fatty acid and β -carotene in *Catla catla* juveniles. *Fish Shellfish Immunol.*, **23**(5): 917-927.
- Kader MA, Bulbul M, Abol-Munafi AB, Asaduzzaman M, Mian S, Bt. Mat Noordin N, Ali ME, Hossain MS and Koshio S. 2018. Modulation of growth performance, immunological responses and disease resistance of juvenile Nile tilapia (*Oreochromis niloticus*) (Linnaeus, 1758) by supplementing dietary inosine monophosphate. *Aquac Rep.*, **10**:23-31.
- Kenari AA, Mahmoudi N, Soltani M, and Kenari SA. 2013. Dietary nucleotide supplements influence the growth, haemato-immunological parameters and stress responses in endangered Caspian brown trout (*Salmo trutta caspius* Kessler, 1887). *Aquaculture Nutrition*, **19**:54-63.
- Kumar S, Sahu NP, Pal AK, Choudhury D, Yengkokpam S and Mukherjee SC. 2005. Effect of dietary carbohydrate on haematology, respiratory burst activity and histological changes in *L. rohita* juveniles. *Fish Shellfish Immunol.*, **19**:331-344.
- Li P, Gatlin III DM and Neill WH. 2007. Dietary supplementation of a purified nucleotide mixture transiently enhanced growth and feed utilization of juvenile red drum, *Sciaenops ocellatus*. *J World Aquac Soc.*, **38**:281-286.
- Li P, Zhao J and Gatlin III DM. 2015. Nucleotides. In: Lee C-S, Lim C, Gatlin III DM and Webster, C (Eds.), **Dietary Nutrients, Additives and Fish Health**. John Wiley and Sons Ltd, Wiley-Blackwell, United States, pp. 249-269.
- Lieke T, Meinelt T, Hoseinifar SH, Pan B, Straus DL and Steinberg CEW. 2020. Sustainable aquaculture requires environmental-friendly treatment strategies for fish diseases. *Rev Aquac.*, **12** (2):1-23.
- Lin YH, Wang H and Shiau SY. 2009. Dietary nucleotide supplementation enhances growth and immune responses of grouper, *Epinephelus malabaricus*. *Aquac Nutr.*, **15**:117-122.
- Mehana EE, Rahmani AH and Aly SM. 2015. Immunostimulant and Fish Culture: An Overview. *Annu Res Rev Biol.*, **5**(4):477 - 489.
- Milla S, Mathieu C, Wang N, Lambert S, Nadzialek S, Massart S, Henrotte E, Douxfils J, Melard C, Mandiki SN and Kestemont P. 2010. Spleen immune status is affected after acute handling stress but not regulated by cortisol in Eurasian perch, *Perca fluviatilis*. *Fish Shellfish Immunol.*, **28**(5-6):931-941.
- Miranda CD, Godoy FA and Lee MR. 2018. Current status of the use of antibiotics and the antimicrobial resistance in the Chilean Salmon Farms. *Front. Microbiol.*, **9**(1284):1-14.
- Peng M, Xu W, Ai Q, Mai K, Liufu Z, and Zhang K. 2013. Effects of nucleotide supplementation on growth, immune responses and intestinal morphology in juvenile turbot fed diets with graded levels of soybean meal (*Scophthalmus maximus* L.). *Aquaculture*, **392-395**:51-58.
- Rachmawati D, Setyobudi RH, Burlakovs J, Elfitasari T and Purnomo AH. 2021. Impacts of immunostimulant yeast (*Saccharomyces cerevisiae*) supplemented feed on growth and blood profile of Java barb (*Barbonymus gonionotus*). *Jordan J. Biol. Sci.* **14**(2):297-302
- Reda RM, Selim KM, Mahmoud R and El-Araby IE. 2018. Effect of dietary yeast nucleotide on antioxidant activity, non-specific immunity, intestinal cytokines, and disease resistance in Nile Tilapia. *Fish Shellfish Immunol.*, **80**:281-290.
- Roige O. 2017. Nucleotides in fish nutrition: The best strategy to enhance immunity and intestinal health. *Aquafeed Advances in Processing and Formulation*, **9**(2): 38-41.
- Saurabh S and Sahoo PK. 2008. Lysozyme: An important defence molecule of fish innate immune system. *Aquac Res.*, **39**(3):223-239.
- Shiau SY, Gabaudan J and Lin YH. 2015. Dietary nucleotide supplementation enhances immune responses and survival to *Streptococcus iniae* in hybrid tilapia fed diet containing low fish meal. *Aquac Rep.*, **2**:77-81.
- Siwicki A, Anderson D and Rumsey G. 1994. Dietary intake of immunostimulants by rainbow trout affects non-specific immunity and protection against furunculosis. *Vet Immunol Immunopathol.*, **41**(1-2):125-139.
- Syed F, Sawant PB, Asimi OA, Chadha NK and Balkhi MH. 2018. Effect of *Trigonella foenum graecum* seed as feed additive on growth, haematological responses and resistance to *Aeromonas hydrophila* in *Cyprinus carpio* fingerlings. *J. Pharmacogn. Phytochem.*, **7**(2):2889-2894.
- Tahmasebi-Kohyani A, Keyvanshokoo S, Nematollahi A, Mahmoudi N and Pasha-Zanoosi H. 2011. Dietary administration of nucleotides to enhance growth, humoral immune responses, and disease resistance of the rainbow trout (*Oncorhynchus mykiss*) fingerlings. *Fish & Shellfish Immunol.*, **30**(1):189-193.
- Tahmasebi-Kohyani A, Keyvanshokoo S, Nematollahi A, Mahmoudi N and Pasha-Zanoosi H. 2012. Effects of dietary nucleotides supplementation on rainbow trout (*Oncorhynchus mykiss*) performance and acute stress response. *Fish Physiol Biochem.*, **38**(2):431-440.
- Ulvestad JS, Kumari J, Seternes T, Chi H and Dalmo RA. 2018. Studies on the effects of LPS, β -glucan and metabolic inhibitors on the respiratory burst and gene expression in Atlantic salmon macrophages. *J. Fish Dis.*, **41**(7):1117-1127.
- Wang W, Sun J, Liu C and Xue Z. 2017. Application of immunostimulants in aquaculture: current knowledge and future perspectives. *Aquac Res.*, **48**(1):1-23.
- Welker TL, Lim C, Yildirim-Aksoy M and Klesius PH. 2011. Effects of dietary supplementation of a purified nucleotide mixture on immune function and disease and stress resistance in channel catfish, *Ictalurus punctatus*. *Aquac Res.*, **42**:1878-1889.
- Xu L, Ran C, He S, Zhang J, Hu J, Yang Y, Du Z, Yang Y, Zhou Z. 2015. Effects of dietary yeast nucleotides on growth, non-specific immunity, intestine growth and intestinal microbiota of juvenile hybrid tilapia *Oreochromis niloticus* ♀ x *Oreochromis aureus* ♂. *Anim Nutr.*, **1**(3):244-251.
- Yaghobi M, Dorafshan S, Akhlagi M, Heyrati FP and Mahmoudi N. 2015. Immune responses and intestinal morphology of striped catfish, *Pangasianodon hypophthalmus* (Sauvage, 1878), fed dietary nucleotides. *J. Appl. Ichthyol.*, **31**(1):83-87.
- Yousefi M, Abtahi B and Kenari AA. 2012. Hematological, serum biochemical parameters, and physiological responses to acute stress of Beluga sturgeon (*Huso huso*, Linnaeus 1785) juveniles fed dietary nucleotide. *Comp Clin Pathol.*, **21**:1043-1048.
- Yousefi M, Paktinat M, Mahmoudi N, Perez-Jimenez A and Hoseini SM. 2016. Serum biochemical and non-specific immune responses of rainbow trout (*Oncorhynchus mykiss*) to dietary nucleotide and chronic stress. *Fish Physiol Biochem.*, **42**:1417-1425.

Purification and Characterization of a Detergent Compatible Alkaline Protease Produced by *Bacillus raris* Isolated from Vegetable Oil Factory Effluent in Owo, Ondo State, Nigeria

Adebayo Olawande OSESUSI^{*}, Victor Olusegun OYETAYO and Daniel Juwon AROTUPIN

Department of Microbiology, Federal University of Technology Akure, P.M.B. 704. Akure. Nigeria.

Received: March 19, 2020; Revised: September 7, 2020; Accepted: Oct 2, 2020

Abstract

A thermostable alkaline protease was produced by *Bacillus raris* isolated from vegetable oil factory effluent in Owo, Ondo State, Nigeria. Detergents containing enzymes have been reported to possess more effective washing capabilities. The protease was purified and characterized. Biochemical characterization and 16S rRNA sequencing showed the strain was closely related to *Bacillus raris* with accession number NR_042161.1. The protease was purified with a 0.516 purification fold and 19% recovery with a Sephadex G-100 column fraction. The protease was relatively stable at alkaline pH retaining activity at pH 9.0 (100%). The protease was also thermally stable with the highest activity observed at 55 °C. *Bacillus raris* protease activity was stimulated by Ba²⁺, Ca²⁺, Cu²⁺ and Mn²⁺, while enzyme activity was inhibited by Zn²⁺ and Pb²⁺. Protease activity increased with an increase in substrate concentration. The Lineweaver-burk plot revealed Km = 0.14. Protease activity was influenced by the tested surfactants and inhibitors. The protease enzyme showed relative stability to some commercial detergents. Thus, the protease enzyme appears to possess properties desired for detergent formulation and inclusion in other biotechnological applications.

Keywords: Protease, enzyme activity, detergents, alkaline, *Bacillus raris*, purification.

1. Introduction

Enzymes have been used in fermentation processes from ancient times. Earlier reports of their use were reported by the ancient Greeks who used enzymes for baking, brewing, alcohol fermentation and cheese manufacture (Sharma *et al.*, 2017). Literature has also shown that enzymes can perform numerous roles, for example the selective manipulation of protein and lysis of fibroin clusters with advancements in analytical techniques (Sharma *et al.*, 2017).

Proteases are universal enzymes in nature, catalyzing the hydrolysis of protein molecules into peptides and amino acids (Matkawala *et al.*, 2019; Sumantha *et al.*, 2006). Proteases have attracted interests over the years, mainly because of the important roles they play in cellular metabolism and the biotechnology industry (Fatema *et al.*, 2019; Gupta *et al.*, 2002). Proteases are widely used in the food, laundry detergents, leather treatment, bioremediation processes and pharmaceutical industries where they mediate several changes in products taste, texture, appearance, quality and in waste recovery (Mamo & Assefa, 2018; Saha *et al.*, 2011; Sandhya *et al.*, 2005; Vadlamani and Parcha, 2011). In detergency, the combined action of surfactants and enzymes aids in the removal of difficult proteinous stains from fabrics (Olsen and Falholt, 1998). Proteases can be grouped based on

their sites of action as exopeptidases and endopeptidases. Proteases that cleave the peptide bond at the center of the amino or carboxyl termini of the polypeptide chain are referred to as exopeptidases, whereas endopeptidases cleave peptide bonds distant from the termini of the substrate (cut at the internal peptide bonds) (Mamo & Assefa, 2018; Rao *et al.*, 1998; Yegin and Dekker, 2013). Proteases are also grouped based on their acid-base behavior viz. acid, neutral and alkaline proteases (Sandhya *et al.*, 2005). Alkaline proteases are optically active in a neutral to basic pH (Sharma *et al.*, 2017). They either possess a serine center or a metallo-type, and are the most researched group of enzymes and are widely used in detergents and allied industries. The high specificity of enzymatic reactions also prevents damage to fabrics and surfaces, which is a matter of concern in chemical detergents (Singh *et al.*, 2016).

Proteases, amylases, lipases and cellulases are used in the starch, textile, detergent and baking industries, representing the second-biggest group, while proteases are the predominant enzyme type, owing to their extensive use in the cleansing and dairy industries (Nguyen *et al.*, 2015; Kirk *et al.*, 2002). Proteases are also used in the modification of proteins to reduce the allergenicity of cow milk for infant formula products in dairy industries (Kirk *et al.*, 2004).

The different products in the detergent industry contain proteases as a fundamental component or ingredient and

^{*} Corresponding author e-mail: osesusibayo@gmail.com.

are used for cleaning household laundries, false teeth, or contact focal lenses (Razzaq *et al.*, 2019). Successful deployment of enzymes is an integral part of the design and production of economical and environmental (biodegradable) friendly detergents (Dewan, 2017). Microbial alkaline sources have attracted increased demand from industries owing to their cost-adequacy, ready susceptibility to genetic manipulation and relative ease of cultivation (Razzaq *et al.*, 2019). Also, proteases intended for use in detergent formulation need not be in the purest state, unlike those for use in pharmaceutical, medical areas that require a higher degree of purity as a necessity.

The suitability of an enzyme for detergent formulation will depend on its ability to retain its function alongside other detergent constituents such as surfactants and oxidizers under quite harsh operating conditions (Boran, 2018). It should also possess the ability to perform over a range of pH and temperature (Griffin *et al.*, 1992). Certain procedures are also put in place to prevent the denaturation of the detergent enzymes (Boran, 2018). Scientists have also tried to isolate from natural environments, microbial enzymes possessing more tolerance against alkaline pH and chemicals in detergents (Boran, 2018), hence the need for isolation of more detergent-compatible microbial proteases.

This study investigated the production, purification and characterization of a detergent compatible protease using bacteria isolated from vegetable oil effluent soil in Owo, Ondo State, Nigeria.

2. Materials

2.1. Isolation and screening of proteolytic bacteria

Soil samples were collected from vegetable oil factory effluent dump in Owo, Ondo State, Nigeria. Isolation was done by serial dilution on a prepared nutrient agar plate (Oxoid). Single colonies were picked and purified by continuous streaking. Preliminary screening for protease production was done by subjecting the isolates to skimmed milk agar plate (SKMA) containing (% w/v); skimmed milk powder (1.0), peptone (0.1), NaCl (0.5) and agar (2.0) at pH 10, the plates were incubated at 37°C for 48 h. The occurrence of clear halo zones around distinct colonies is indicative of protease production by the bacteria (Bajaj and Jamwal, 2013). Isolate that showed higher protease production potential were selected for further production and assay (Arulmani *et al.*, 2007). Bacterial identification was carried out using morphological, biochemical characterization by 16S rDNA sequencing.

2.2. Protease production

Bacteria selected from SKMA screening were selected for protease production. Protease production media (PPM) consisted of: CaCl₂ (0.01 g/l), K₂HPO₄ (0.05 g/l), peptone (1.00 g/l), MgSO₄ (0.01 g/l), glucose (0.1 g/l), at pH 7.0 and was incubated on a shaker incubator at 37 °C for 48 hours. The cell-free supernatant was then obtained by centrifuging at 10,000 rpm for 10 minutes at 4 °C. The supernatant obtained was used as a crude protease for further studies (Guleria *et al.*, 2016).

2.3. Protease assay

Protease assay was carried out using the casein-pholine method by Cupp-Enyard (2008). Casein (1 % w/v) was dissolved in 0.1 M phosphate buffer at pH 7.0 and was used as the substrate, 1 mL of the enzyme was added to the substrate and incubated at 50 °C in a water bath for one hour. The reaction was then terminated by adding 3 mL of the tricarboxylic acid (TCA). The reaction cocktail was centrifuged at 5000 rpm for 15 minutes. Then 0.5 mL of the supernatant was drawn into a test-tube, 2.5 mL of 0.5 M sodium carbonate was added, vortexed well and incubated for 20 minutes. The reaction was terminated by the addition of 0.5 mL of 2.0 N Folin-phenol reagent and the absorbance was read at 660 nm using a UV-Spectrophotometer (752Pro15041, Spectrum Lab England). Protease produced was estimated and expressed in a microgram of tyrosine liberated by 1 mL of the protease in 30 minutes at 30 °C in tyrosine equivalent (Akhavan and Jabalameli, 2011; Joo *et al.*, 2002). One unit of protease activity was defined as the amount of enzyme required to liberate 1 µg of tyrosine/min under standard assay conditions based on a tyrosine calibration curve (Bhagwan *et al.*, 2015).

2.4. Protein assay

Total protein content was estimated following Lowry *et al.* (1951) using bovine serum albumin (BSA) as reference (Mothe and Sultanpuram, 2016).

2.5. Purification of the protease enzyme

The crude enzyme was subjected to precipitation in a salting-out process (Dixon and Webb, 1971). The precipitated fractions were dialyzed and separated using Sephadex G100 column chromatography (Ding *et al.*, 2012; Wakil and Osesusi, 2017). The fractions obtained were pooled together and their protease activity and protein content determined. These fractions were also used for further characterization.

3. Characterization of the purified protease enzyme

3.1. Effect of pH

The effect of pH on protease stability was assessed by incubating the protease-substrate mixture in appropriate buffers at intervals of 0.5 pH (Citrate-phosphate for pH 4 - 7 and Tris-HCl for pH 8 - 11) for one hour. Protease activity was determined using the standard assay method. Protease stability was expressed as relative activity (Niyonzima and More, 2014; Priya *et al.*, 2014).

3.2. Effect of temperature

The effect of temperature on the stability of protease was assessed by incubating the protease-substrate mixtures at varying temperatures (20 - 70 °C) at 5 °C intervals in a water bath for one hour. Protease activity was determined using the standard assay method. Protease stability was expressed as relative activity (Niyonzima and More, 2014; Priya *et al.*, 2014).

3.3. Effect of metal ions

The protease stability in the presence of metals was determined by pre-incubating the protease-substrate mixtures with metal (Ca²⁺, Cu²⁺, Mn²⁺, Mg²⁺, Ba²⁺, Zn²⁺, K⁺, Na⁺) for one hour. Metal salt concentrations of 5 mM

were used. Protease activity was determined using the standard assay method. Protease stability was expressed as relative activity (Priya *et al.*, 2014).

3.4. Effect of substrate concentration

The effect of varying substrate concentrations on the protease activity was determined by incubating different substrate concentrations (casein) from 0.2 to 1.2 mg/ml with protease for one hour under standard conditions. Protease activity was determined according to standard methods as previously described. The enzyme kinetics were also determined (Priya *et al.*, 2014). The Michaelis–Menten enzyme kinetic constants K_m and V_{max} were extrapolated from the Lineweaver–Burk plot (Priya *et al.*, 2014).

3.5. Effect of inhibitors and surfactants

Protease stability to surfactants and inhibitors; tween 20, triton X, sodium lauryl sulfate (SLS), sodium dodecyl sulfate (SDS), 2-mercaptoethanol (BME), dithiothreitol (DTT), and ethylenediaminetetraacetic acid (EDTA), were determined by pre-incubating the enzyme substrate mixtures with the surfactants and inhibitors at various concentrations for one hour at a concentration of 1 mM (Gohel and Singh, 2018). Protease activity was carried out according to standard methods as described earlier (Matkawala *et al.*, 2019).

3.6. Effect of detergents

The effect of commercial detergents (Ariel, Klin, Sunlight, Good mama, Canoe and Omo) on protease stability was evaluated by incubating detergents with the protease for one hour at 35 °C. The detergent solutions (0.1 % w/v) were prepared with double-distilled water, the detergent solutions were boiled at 100 °C to inactivate any enzymes already present, then cooled to room temperature. The solutions were then incubated with purified protease at 50 °C for one hour (Lam *et al.*, 2018; Matkawala *et al.*, 2019). Protease activity was determined using the standard assay method.

4. Results and Discussions

4.1. Isolation of proteolytic bacteria

The bacterial isolates that showed appreciable zone of hydrolysis on skimmed milk agar plates were subjected to protease production, and the bacteria with the highest protease production was selected for further study. Quantitative screening for protease production showed that OWO1 had the best protease activity (2.039 U/mL) while AKK1 had the lowest protease activity (0.072 U/mL) as shown in Figure 1. OWO1 was used for further study.

Vegetable oil factory effluents contain an immensely high volume of degradable organic matter. It is rich in nutrients and possesses fertilizing properties even in its raw state (Kamyab *et al.*, 2016). The nutrient-rich nature of the effluents may thus provide a good source of nutrients for proteolytic organisms to flourish.

Microscopic identification showed the isolate as spore-forming, Gram-positive rods, having flat elevation. Further identification showed the bacteria was catalase-positive and utilized citrate, it also utilized a range of hexose sugars, and disaccharide sugars (sucrose, maltose). 16S rDNA showed the isolate to have a 95.75 % homology with *Bacillus raris* NR_042161.1 upon submission of the sequence to the gene data bank of National Center for Biotechnology Information (NCBI). Naidu (2011) reported *Bacillus* species as being excellent protease producers. Sharma *et al.* (2017b) highlighted microbial enzyme activity as a function of several factors including nutritional and cultural variables viz. pH, temperature, carbon and nitrogen sources and duration of incubation of the microorganisms.

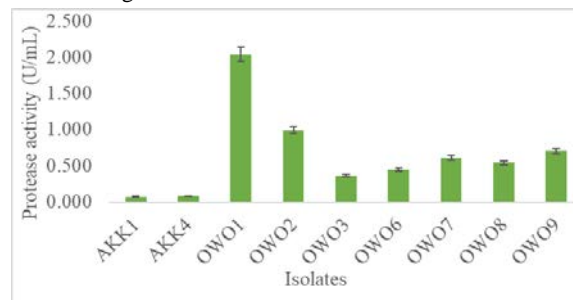


Figure 1. Screening for protease activity

The purification profile (Table I) of *Bacillus raris* protease showed that the total protease activity and total protein content were reduced significantly across the purification steps with the crude fraction having the highest values. The protease purification was found to decrease from 1 to 0.516 purification fold using Sephadex G-100 column chromatography. This is similar to reports by Josephine *et al.* (2012) and Jayashree *et al.* (2014) who reported a rise in the purification fold of *Bacillus* spp protease (Guleria *et al.*, 2016). This disagrees with reports by Naidu (2011) and Bajaj and Jamwal (2013) who reported increased protein content when purification was carried out to obtain the pure protease enzyme.

Bacillus raris protease was relatively stable across varying pH, maintaining relative stability at alkaline conditions up to pH 9.0, after which further rise in pH resulted in reduced protease activity (Figure 2). It was a good candidate for alkaline protease production, which is similar to findings by (Chu, 2007). These findings align with findings by Naidu (2011) who reported high *Bacillus subtilis* protease activity at pH 9.0. Niyonzima and More (2014) also reported that *Bacillus* spp. alkaline protease maintained stability within pH 8.0 – 12.0. Jayashree *et al.* (2014) reported a *Methylobacterium* sp. protease which retained over 50% activity at pH 7.0 - 11.0 but decreased to 30% beyond pH 12.0. Takami *et al.* (1990) attributed the increase in protease activity around the alkaline range to the binding that occurs in the enzyme-substrate complex, because pH greatly influences enzyme-substrate binding (Niyonzima and More, 2014).

Table I. Purification profile of *Bacillus raris* protease

Purification steps	Total protease activity (U/mL)	Total protein (U/mL)	Specific activity (U/mg)	Purification fold	Recovery yield %
Crude extract	1432.27	26.88	53.284	1	100
80% Ammonium sulphate precipitation	935.21	19.25	48.582	0.912	65
Dialysis	657.32	14.13	46.519	0.873	46
Gel chromatography	278.32	10.12	27.502	0.516	19

The results showed that the protease enzyme maintained relative stability after one hour when pre-incubated at varying temperatures between 20 - 70 °C as shown in figure 3, although activity decreased with increasing temperatures. *Bacillus raris* protease had its highest activity at 50 °C (100%), while further temperature rise resulted in reduced protease activity decreasing to 77.042 % at 70 °C. This result agrees with reports by (Adinarayana *et al.*, 2003; Giri *et al.*, 2011; Jayashree *et al.*, 2014; Niyonzima and More, 2014; Ramkumar *et al.*, 2018) who reported protease stability at 50 °C. This contrasts with Naidu (2011) who reported a reduction in protease activity beyond 35 °C. This inherent activity of the protease at alkaline and wide temperature regimes implies its potential for use across a range of washing temperatures (Niyonzima and More, 2014).

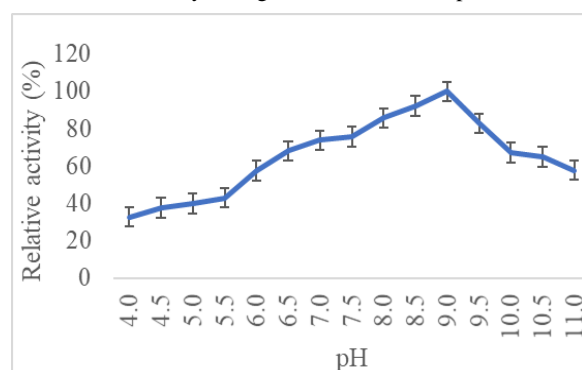
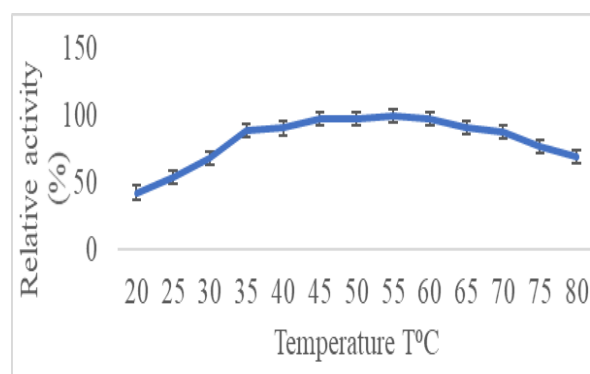
These findings show that *Bacillus raris* protease activity was stimulated by Ba²⁺, Zn²⁺, Cu²⁺, Ca²⁺, Mg²⁺, and Mn²⁺ with K⁺ (Figure 4) supporting the least protease activity, this highlights the protease stability in the presence of metals. This result is similar to reports by (Niyonzima and More, 2015) who reported that Ca²⁺ and Mg²⁺ stimulated protease production. Anandan *et al.* (2007); Niyonzima and More (2015); Sharma *et al.* (2005); Dubey *et al.* (2010) and Kalpana devi *et al.* (2008) positioned the importance of cations in maintaining the enzyme active sites, thus, improving protease thermostability. Also, Lobedanz *et al.* (2016) suggested that the actions of metal ions are dependent on their ability to bind specific sites in the enzyme molecule, ensuring the stability of the active enzyme conformation.

The findings show that increased substrate concentration also resulted in increased protease activity with the highest protease activity obtained at 1.5 mg/ml, while further increase in substrate concentration resulted in reduced protease activity (Figure 5). This corresponds to reports by Devanadera *et al.* (2016); Ramkumar *et al.* (2018); El-Safey and Abdul-Raouf (2004); Sumantha *et al.* (2006) who reported appreciable affinity for an increase in substrate concentration by protease enzyme after which further increase resulted in reduced protease production. The apparent K_m value of protease hydrolysis indicated the higher affinity and efficient catalytic role of *Bacillus* species protease towards their substrates to concentrate the active sites of an enzyme Ramkumar *et al.* (2018), as shown in Figure 6. It is also a measure of the enzyme-substrate (ES) complex. Singh *et al.* (2014) and Singh and Bajaj (2017) highlighted that proteases being designed for biotechnological applications should be robust and possess the structural and kinetic adaptations essential for extremes of industrial microenvironments, such as extreme temperature, pH and presence of inhibitors.

Findings from this study showed that surfactants such as tween 20, triton X, (SLS), (SDS), enhanced the protease activity of *Bacillus raris*, while inhibitors such as 2-

mercaptoethanol (BME), dithiothreitol (DTT), and ethylenediaminetetraacetic acid (EDTA) had varying inhibitory effects on *Bacillus raris* protease as shown in Figure 7. This result is similar to reports obtained by Jayashree *et al.* (2014) who reported improvement of protease activity by tween 20 and triton X and minimal effects of the oxidizing agents on protease enzyme. Further studies on enzyme inhibition could offer more insights regarding the nature of the proteases, its cofactor requirements and its active center (Jayashree *et al.*, 2014). The role of DTT in decreasing protease activity could be due to the excision of the intramolecular disulfide bonds essential for maintaining protease activity and stability (Jayashree *et al.*, 2014; Satyanarayana *et al.*, 2013 and Rai *et al.*, 2010).

The protease maintained relative stability in the presence of some commercial detergents (Figure 8), which is similar to reports by Adinarayana *et al.* (2003) and Ramkumar *et al.* (2018) who reported enzyme addition in detergents. Bajaj and Jamwal (2013) also reported a protease from *Bacillus pumilus* which showed significant stability and compatibility with surfactants and commercial laundry detergents at ambient temperature.

**Figure 2.** Effect of pH on activity of protease enzyme**Figure 3.** Effect of temperature on the activity of protease

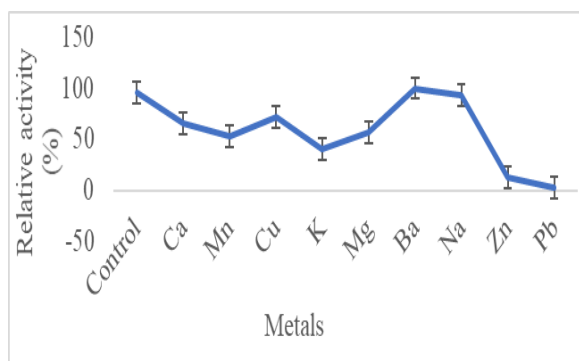


Figure 4. Effect of metal ions on protease activity

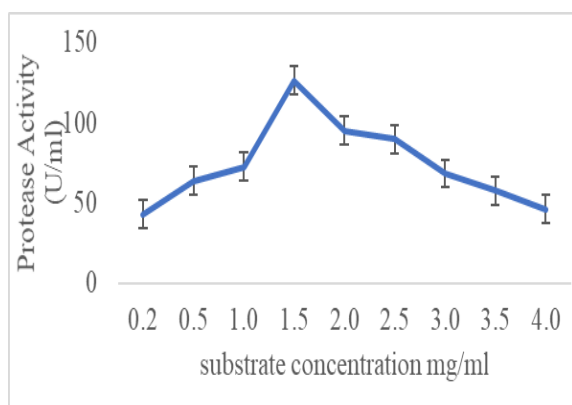


Figure 5. Effect of substrate concentration on protease activity

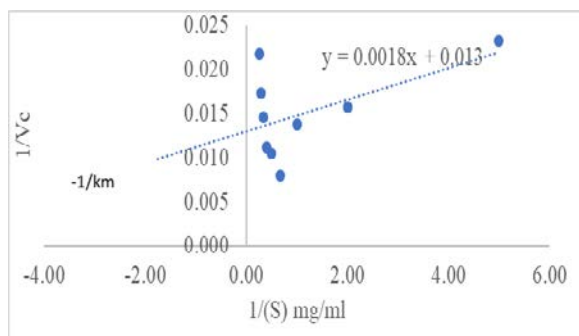


Figure 6. Lineweaver-burk plot for the hydrolysis of casein by the purified protease of *Bacillus raris*

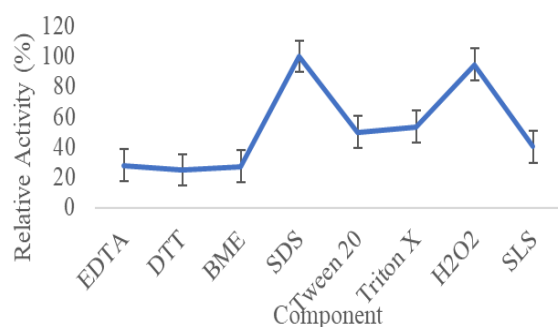


Figure 7. Effects of surfactants, inhibitors and oxidizing agents on protease activity

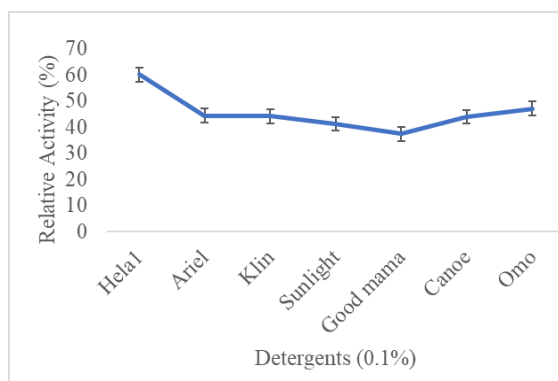


Figure 8. Protease activity in the presence of commercial detergents

5. Conclusion

In this study, an alkaline and thermostable protease was produced using *Bacillus raris* isolated from vegetable oil effluents in submerged fermentation. The protease maintained relative stability to inhibitors and commercial detergents. Protease remains one of the most important groups of industrial enzymes with numerous biotechnological applications. This suggests its potential for inclusion in a detergent formulation as well as other biotechnological uses. Further study on the protein interactions is necessary to tailor the protease appropriately for use.

Acknowledgements

The Authors wish to acknowledge and thank Dr. Femi Bamidele of the Department of Biochemistry, Federal University of Technology, Akure.

References

- Adinarayana K, Ellaiah P. and Prasad DS. 2003. Purification and partial characterization of thermostable serine alkaline protease from a newly isolated *Bacillus subtilis* PE-11. *J. Appl. Pharm. Sci.* **4(4)**: 1–9. doi: 10.1208/pt040456.
- Akhavan Sepahy A and Jabalameli L. 2011. Effect of culture conditions on the production of an extracellular protease by bacillus sp. isolated from soil sample of lavizan jungle park. *Enzyme Res.* 1-7. doi: 10.4061/2011/219628.
- Anandan D, Marmer WN and Dudley RL. 2007. Isolation, characterization and optimization of culture parameters for production of an alkaline protease isolated from *Aspergillus tamarii*. *J. Microbiol Biotechnol.* **34(5)**: 339–347. doi: 10.1007/s10295-006-0201-5.
- Arulmani M, Aparanjini K, Vasanthi K, Arumugam P. 2007. Purification and partial characterization of serine protease from thermostable alkalophilic *Bacillus laterosporus*-AK1. *World J. Microbiol. Biotechnol.* **23(4)**: 475–481. doi: 10.1007/s11274-006-9249-7.
- Bhagwan N and Rekadwad LVG. 2015. Isolation, Identification and Oil Resistance of Protease Producing *Bacillus Subtilis* from Automobile Repair Centre Soil, Nanded (India). *EC Bacteriol. Res.* **1(1)**: 17–23.

- Boran R. 2018. Detergent Compatible Extracellular Lipase from *Streptomyces cellulosa* AU-10: A Green Alternative for the Detergent Industry. *J. Surfactants Deterg.* **21(4)**: 565–573. doi: 10.1002/jsde.12049.
- Chu WH. 2007. Optimization of extracellular alkaline protease production from species of *Bacillus*. *J. Microbiol. Biotech.* **34(3)**: 241–245. doi: 10.1007/s10295-006-0192-2.
- Devanadera M, Mark KP. 2016. Optimization, Production, Partial Purification and Characterization of Neutral and Alkaline Proteases Produced By *Bacillus Subtilis*. *J. Microbiol. Biotech.* **6(2)**: 832–838. doi: 10.15414/jmbfs.2016.6.2.832-838.
- Dewan SS. 2017. Global Markets for Enzymes in Industrial Applications. *BCC Research: Wellesly, MA, USA*.
- Ding Z, Peng L, Chen Y, Zhang L, Gu Z, Shi G, and Zhang K. 2012. Production and characterization of thermostable laccase from the mushroom, *Ganoderma lucidum*, using submerged fermentation. *Afr. J. Microbiol. Res.* **6(6)**: 1147–1157.
- Dixon M, and Webb EC. 1971. Enzymes, in *Enzymes*. 2nd Edition. London: Academic press. 222-234.
- Dubey R, Adhikary S, Kumar J and Sinha N. 2010. Isolation, production, purification, assay and characterization of alkaline protease enzyme from *Aspergillus niger* and its compatibility with commercial detergent. *DMMB.* **1(1)**: 75–94.
- Matkawala F, Nighojkar NA and Kumar AN. 2019. Enhanced production of alkaline protease by *Neocosmospora* sp. N1 using custard apple seed powder as inducer and its application for stain removal and dehairing. *Biocatal. Agric. Biotechnol.* **21(1)**: 243-247.
- Garg G, Singh A, Kaur A, Singh R, Kaur J and Mahajan R. 2016. Microbial pectinases: an ecofriendly tool of nature for industries. *3 Biotech*, **6(1)**: 1–13. doi: 10.1007/s13205-016-0371-4.
- Giri, SS, Giri SS, Sukumaran V, Sen SS, Oviya M, Banu BN and Jena PK. 2011. Purification and partial characterization of a detergent and oxidizing agent stable alkaline protease from a newly isolated *Bacillus subtilis* VSG-4 of tropical soil. *J. Microbiol.* **49(3)**: 455–461. doi: 10.1007/s12275-011-0427-4.
- Gohel SD and Singh SP. 2018. Thermodynamics of a Ca²⁺ dependent, highly thermostable and detergent compatible purified alkaline serine protease from *Nocardioopsis xinjiangensis* strain OM-6. *Int. J. Biol. Macromol.* **211**: 4-7.
- Guleria S, Walia A, Chauhan A, Shirkot CK. 2016. Purification and characterization of detergent stable alkaline protease from *Bacillus amyloliquefaciens* SP1 isolated from apple rhizosphere', *J. Basic Microbio.* **56(2)**: 138–152. doi: 10.1002/jobm.201500341.
- Gupta R, Beg Q and Lorenz P. 2002. Bacterial alkaline proteases: Molecular approaches and industrial applications. *Appl. Microbiol. Biotechnol.* **59(1)**: 15–32. doi: 10.1007/s00253-002-0975-y.
- Joo HS, Kumar CG, Park GC, Kim KT and Chang,CS. 2002. Optimization of the production of an extracellular alkaline protease from *Bacillus horikoshii*. *Process Biochem.* **38(2)**: 155–159.
- Griffin HL, Greene RV and Cotta MA. 1992. Isolation and characterization of an alkaline protease from the marine shipworm bacterium. *Curr Microbiol.* **24(8)**: 111-117.
- Priya JDA, Divakar K, Prabha MS, Selvam GP and Gautam P. 2014. Isolation, Purification and Characterisation of an Organic Solvent-Tolerant Ca²⁺-Dependent Protease from *Bacillus megaterium* AU02. *Appl Biochem Biotechnol.* **172**: 910-932.
- Jayashree S, Annapurna B, Jayakumar R, Sa T and Seshadri S. 2014. Screening and characterization of alkaline protease produced by a pink pigmented facultative methylotrophic (PPFM) strain, MSF 46. *J. Genet. Eng. Biotechnol.* **12(2)**: 111–120. doi: 10.1016/j.jgeb.2014.11.002.
- Kalpna devi M, Banu AR, Gnanaprabhal GR, Pradeep BV and Palaniswamy M. 2008. Purification, characterization of alkaline protease enzyme from native isolate *Aspergillus niger* and its compatibility with commercial detergents. *Indian J Sci Tech.* **1(7)**: 1–6.
- Kamyab H, Din MFM, Hosseini SE, Ghoshal SK, Ashokkumar V and Keyvanfar A. 2016. Optimum lipid production using agro-industrial wastewater treated microalgae as biofuel substrate. *Clean Technol. Environ. Policy*, **18(8)**: 2513–2523.
- Kirk O, Borchert TV and Fuglsang CC. 2002. Industrial Enzyme Applications. *Curr. Opin. Biotechnol.* **4(1)**: 2-8
- Kirk O, Ture D, Torben V, Fuglsang, CC, Olsen T and Tage LKN. 2004. Enzyme Applications, Industrial. In *Kirk-Othmer Encyclopedia of Chemical Technology*. 10th edn. Hoboken, NJ: John Wiley & Son.
- Kumar BB and Jamwal G. 2013. Thermostable alkaline protease production from *Bacillus pumilus* D-6 by using agro-residues as substrates. *Adv. Enzyme Res.* **01(02)**: 30–36. doi: 10.4236/aer.2013.12003.
- Lam MQ, Nik Mut NN, Thevarajoo S, Chen SJ, Selvaratnam C, Hussin H, Jamaluddin H and Chong CS. 2018. Characterization of detergent compatible protease from halophilic *Virgibacillus* sp. CD6. *3 Biotech.* **8(2)**: 1–9. doi: 10.1007/s13205-018-1133-2.
- Lobedanz M, Sune TD, Torben V, Borchert TT, Hansen HL and Weijian LM. 2016. Enzymes in Industrial Biotechnology. *Curr. Opin. Biotechnol.*
- Lowry OH, Rosebrough NJ, Farr AL and Randall RJ. 1951 Protein measurement with Folin phenol reagent. *J. Biol. Chem.* **193(1)**: 265--275.
- Rao MB, Tanksale AM, Ghatge MS and Verna VD. 1998. Molecular and biotechnological aspects of microbial proteases. *Microbiol. Mol. Biol. Rev.* **62(3)**: 597–635.
- Mamo J and Assefa F. 2018. The Role of Microbial Aspartic Protease Enzyme in Food and Beverage Industries. *J. Food Qual.* **(20)1**: 8-9. doi: 10.1155/2018/7957269.
- Matkawala F, Nighojkar S, Kumar A, Nighojkar A. 2019. A novel thiol-dependent serine protease from *Neocosmospora* sp. N1. *Heliyon.* **5(8)**: p. e02246. doi: 10.1016/j.heliyon.2019.e02246.
- Mothe T and Sultanpuram VR. 2016. Production, purification and characterization of a thermotolerant alkaline serine protease from a novel species *Bacillus caseinilyticus*. *3 Biotech*, **6(1)**: 1–10. doi: 10.1007/s13205-016-0377-y.

- Nguyen QD, Erika BG, Styevkó, JM, Rezessy-Szabó A, and Hoschke Á. 2015. Fungal biomolecules for the food industry *Fungal Biomolecules*. 11-38.
- Niyonzima, FN and More S. 2014. Detergent-compatible proteases: Microbial production, properties, and stain removal analysis. *Prep. Biochem. Biotechnol.* **45(3)**: 233–258. doi: 10.1080/10826068.2014.907183.
- Niyonzima, FN and More SS. 2014. Purification and characterization of detergent-compatible protease from *Aspergillus terreus* gr. 3 *Biotech*, **5(1)**: 61–70. doi: 10.1007/s13205-014-0200-6.
- Olsen HS and Falholt P. 1998. The role of enzymes in modern detergency. *J. Surfactants Deterg.* **1(4)**: 555–567. doi: 10.1007/s11743-998-0058-7.
- Orhan E, Omay D and Güvenilir Y. 2005. Partial purification and characterization of protease enzyme from *Bacillus subtilis* and *Bacillus cereus*. Part A Enzyme Engineering and Biotechnology. *Appl. Biochem. Biotechnol.* **121(1–3)**: 183–194. doi: 10.1007/978-1-59259-991-2_16.
- Priya JDA, Divakar KK, Prabha MS, Selvam GP and Gautam P. 2014. Isolation, purification and characterisation of an organic solvent-tolerant Ca²⁺-dependent protease from *Bacillus megaterium* AU02. *Appl. Biochem. Biotechnol.* **172(2)**: 910–932. doi: 10.1007/s12010-013-0589-0.
- Rai, SK, Roy JK and Mukherjee AK. 2010. Characterization of a detergent-stable alkaline protease from a novel thermophilic strain *Paenibacillus tezpurensis* sp. nov. AS-S24-II. *Appl. Microbiol. Biotechnol.* **2(85)**: 1437–1450. doi: 10.1007/s00253-009-2145-y.
- Ramkumar A, Sivakumar N, Gujarathi A and Victor R. 2018. Production of thermotolerant, detergent stable alkaline protease using the gut waste of *Sardinella longiceps* as a substrate: Optimization and characterization. *Sci. Rep.*, **8(1)**: 1–15. doi: 10.1038/s41598-018-30155-9.
- Razzaq A, Razzaq A, Shamsi S, Ali A, Ali Q, Sajjad M, Malik A and Ashraf M. 2019. Microbial proteases applications. *Front. Bioeng. Biotechnol.*, **7(6)**: 1–20. doi: 10.3389/fbioe.2019.00110.
- Yegin S and Dekker P. 2013. Progress in the field of aspartic proteinases in cheese manufacturing: structures, functions, catalytic mechanism, inhibition, and engineering. *Dairy Sci. Technol.* **93(6)**: 565–594.
- Saha ML, Begum KJM, Khan MR and Gomes DJ. 2011. Bacterial Protease Enzyme: Safe and Good Alternative for Industrial and Commercial Use. *Plant Tissue Cult. Biotechnol.* **21**: 53–61.
- Sandhya C, Nampoothiri KM and Pandey A. 2005. Microbial protease in: *Microbial Enzyme and Biotransformation*. 1st Edition.
- Satyanarayana T, Kawarabayasi Y and Littlechild J. 2013. Thermophilic microbes in environmental and industrial biotechnology: *Biotechnology of thermophiles*, Springer Netherlands. doi: 10.1007/978-94-007-5899-5.
- Shanti NK. 2011. Characterization and purification of protease enzyme. *J. Appl. Pharm. Sci.* **1(3)**: 107–112.
- Sharma J, Singh A, Kumar R and Mittal A. 2012. Partial Purification Of An Alkaline Protease From A New Strain Of *Aspergillus Oryzae* AWT 20 And Its Enhanced Stabilization In Entrapped Ca-Alginate Beads. *The Internet J. Microbiol.* **2(2)**: 1-9. doi: 10.5580/b6f.
- Sharma KM, Mageswari A, Karthikeyan S, Anbalagan M, Sivakumar A and Gothandam KM. 2017. Microbial alkaline proteases: Optimization of production parameters and their properties. *J. Gen. Eng. Biotechnol.* **15(1)**: 115–126. doi: 10.1016/j.jgeb.2017.02.001.
- Singh S, Gupta P, Sharma V, Koul S, Kour K, Bajaj B and Kumar J. 2014. Multifarious potential applications of keratinase of *Bacillus subtilis* K-5. *Biocatal. Biotransformation*, **32(5–6)**: 333–342. doi: 10.3109/10242422.2014.978306.
- Singh S and Bajaj BK. 2017. Potential application spectrum of microbial proteases for clean and green industrial production *Energy, Ecology and Environment*, **2(6)**: 370–386. doi: 10.1007/s40974-017-0076-5.
- Josephine SF, Ramya SV, Neelam D, Ganapa B, Suresh G and Siddalingeshwara K. 2012. Isolation, production and characterization of protease from *Bacillus* sp isolated from soil sample. *J. Microbiol. Biotech. Res.* **2(1)**: 163–168.
- Sumantha A, Deepa P, Sandhya C, Szakacs G, Soccol CR and Pandey A. 2006. Rice bran as a substrate for proteolytic enzyme production. *Braz. Arch. Biol. Technol.* **49(5)**: 843–851. doi: 10.1590/S1516-89132006000600019.
- Sumantha A, Larroche C and Pandey A. 2006. Microbiology and industrial biotechnology of food-grade proteases: A perspective', *Food Technol. Biotechnol.* **44(2)**: 211–220.
- Takami H, Akiba T. and Horikoshai K. 1990. Characterization of an alkaline protease from *Bacillus* sp. no. AH-101. *Appl. Microbiol. Biotechnol.* **33(5)**: 519–523.
- Lowry OH, Rosebrough NJ, Farr AL and Randall RJ. 1951. Protein Determination. Modified Lowry Method **193**: 7–9.
- Vadlamani S and Parcha SR. 2011. Studies on industrially important alkaline protease production from locally isolated superior microbial strain from soil microorganisms. *Int. J. Biotechnol. Appl.* **3**: 102–105.
- Wakil SM and Osesusi AO 2017. Production, Characterization And Purification Of Lipase By Bacteria Isolated From Palm Oil Mill Effluent And Its Dumpsites Soil. *NJM*, **31(1)**: 3691–3703.

Wound healing activities of *Moringa oleifera* leaves extract cultivated in Kurdistan region-Iraq

Shang A. Tofiq¹, Hoshayr A. Azeez^{2,*} and Hemn Hassan Othman²

¹Department of Biology, College of Science, University of Sulaimani, Sulaimania-Iraq; ²College of Pharmacy, University of Sulaimani, Sulaimania -Iraq

Received: June 14, 2020; Revised: September 7, 2020; Accepted: Oct 13, 2020

Abstract

Medicinal plants have been used for many years as an ancient curative method for treating and healing wounds in different cultures. Therefore, and accordingly this work has been conducted to study wound healing activity of *Moringa oleifera* leaves extract cultivated in the Kurdistan region in the northern Iraq (KRG). In the current investigation, experimentally-induced wounds in rats have been infected with strains of *Staphylococcus aureus* and *Pseudomonas aeruginosa* clinically isolated from the wound site in hospitalized patients. High Performance Liquid Chromatography (HPLC) is used to determine some bioactive compounds within the extract. Plant leaf was extracted by using the maceration method and 70% ethanol as solvent. The HPLC results were dependent on comparison between the extract with standards. Two lacerated wounds were made on each animal at either side of the thoracolumbar spine and inoculated by a 0.4 ml bacterial suspension. The treatment regimen was for 14 days with different formulation of *ethanolic leaves* extract, and gentamicin ointment as a control positive. At the end point of the experimental trial, animals were euthanized humanly at day 15. Samples from healed-wounded skin was prepared for histological evaluation. Generally speaking, our findings indicated that alcoholic leaf extract showed potential wound healing property in different concentration as a dose-dependent manner of the extracted ointment 3.5%, 5%, 10% particularly 10% of the extract formulation which showed better results in comparison to gentamicin ointment. The presented essential constituents for *Moringa* leaf derivatives were gallic acid (3461 ppm), catechin (1201 ppm), rutin (286 ppm) and quercetin (88 ppm). Last but not least, the extract was able to provide promising evidence to possess a drug formulation material.

Keywords: *Moringa oleifera*, leaves extract, Bioactive compounds, HPLC, Wound healing.

1. Introduction

The largest organ of the body is skin which acts as a barrier against external means. The loss of skin tissue integrity, as in the development of wound, can cause lesions or illnesses (Sussman and Bates, 2007). Disturbance of the cellular and anatomic progression of a tissue defined as the wound with or without microbial infection is happening due to cut with sharp-edged things or any accident (Sabale *et al.*, 2012). It may occur due to chemical, immunological, physical and microbiological attacks to the tissue, leading to cellular disruption of tissue is occurring. Healing of wound is a procedure in which tissue regeneration occurs (Alam *et al.*, 2012). Wound healing is a natural circumstance by which the body itself replacing normal structure functions and gets over the damage to the tissue. The skin wound healing process includes progress in different phases such as hemostasis, inflammatory, proliferative and remodeling (Eming *et al.*, 2014). Natural sources of biologically active compounds were medicinal plants (Ji *et al.*, 2009; Zhang and Ma, 2018). Some of these biologically active compounds have advantageous effects, which can be used to enhance human health (Mohammed and Manan, 2015). The usage

of medicinal plants as an alternative to chemically synthesized drugs within the treatment of diseases has been accepted worldwide (Liew and Yong, 2016; Khdir *et al.*, 2019). Many medicinal plants are monitored for powerful, newer and low-cost wound-healing agents (Boakye *et al.*, 2018). Any plants characterized and proved to be antioxidant, antimicrobial and antiproliferative can be used in the wound treatment as an ointment delivery system (Arun *et al.*, 2016). Plants were used for this purpose, such as *Aloe vera*, *M. oleifera*, and *Kigelia Africana*, green tea, Echinacea, grapevine, ginseng, chamomile, rosemary (Pazyar *et al.*, 2014). *M. oleifera* is a plant that belongs to the family Moringaceae. It is commonly known as the drumstick tree or horseradish tree and is native to India but grown in different parts of the world. *M. oleifera* can be characterized by its nutritional values and medical uses. The plant of *Moringa* includes various components, which are quercetin, kaempferol, vitamins, carotenoids, B-sitosterol, caffeoylquinic acid, zeatin, tannin, flavonoids, alkaloids, polyphenol, phenolic acid, oxalates, isothiocyanates saponins, glucosinolates and phytates (Anwar *et al.*, 2007; Tahir *et al.*, 2020). Different methods to separation of these bioactive compounds such as high-performance liquid chromatography (HPLC) is a tool to determine qualitative

* Corresponding author e-mail: hoshayar.azeez@univsul.edu.iq.

and quantitative analysis of bioactive constituents such as phenol and flavonoids in the different plant parts (Nouman *et al.*, 2016, Maqsood *et al.*, 2017). Traditionally, leaf-paste of *M. oleifera* has been applied to infected wounds and treatment of sore eyes by traditional healers and has been shown to be successful (Rathi *et al.*, 2006). Many studies have shown that the leaf, flower, bark, root, seed, and nearly all of *M. oleifera* plants exhibit antimicrobial activity including antibacterial, antifungal, antiviral and antiparasitic activity. Many medicinal uses were also reported, which include anti-inflammatory, anti-hypertensive, antioxidant, hepatoprotective, anti-diabetic, anticancer, analgesic activity, cholesterol-lowering activity, cardiac and circulatory stimulant (Nweze and Nawfor, 2014; Mboosso *et al.*, 2014; Rani *et al.*, 2018).

M. oleifera leaves cultivated in Kurdistan region (KRG) of Iraq have never been screened for wound healing activity in Kurdistan region. Therefore, the objectives of this study are to determine the healing properties of *M. oleifera* extract on an infected wound in male wistar albino rats and to identify some bioactive compounds present in leaves using HPLC method.

2. Materials and Methods

2.1. Plant collection and identification

Leaves of *M. oleifera* were collected from Baranan mountain when cultivated for the first time in KRG-Iraq. The Baranan mountain has rocky slopes and valleys. The *Moringa* plantations are situated [latitude: 35.18279°N, longitude: 45.65111°E and altitude: 879.1 masl. Annual rainfall: 450-700 mm, temperatures ranged from -5° C to 45°C] (Tahir *et al.*, 2018). The plant was authenticated by the plant taxonomist Assistant Prof. Dr. Karzan O. Qadir at Biology Dept., College of Science /University of Sulaimani. The collected aerial parts were air-dried then ground into powder using a mechanical grinder (GEEPAS) and packed into an ice-packed plastic container for further use.

2.1.1. Plant extraction

Fifty grams of collected powdered form of leaves weighed and extracted with 1000 ml of 70% ethanol by maceration, using shaker incubator (Daihan LABTECH) for 72 hrs at 40°C. The extract solution was filtered by using filter paper (Whatman No.1) and the filtrate concentrated at 45°C by rotary evaporator (Heidolph); finally, the resulting extracts were freeze-dried by lyophilizer (Alpha 1-2 4Dplus) and the resultant crude powder was kept at -20 until use (Vongsak *et al.*, 2013).

2.2. Phytochemical analysis with the HPLC method

An amount of 0.5 g of plant powder was extracted with 10 ml of methanol (HPLC grade) for 1 h on a magnetic stirrer. The extract was achieved at room temperature and kept from light. After filtering the extract, the residue was re-extracted with the same volume of methanol, then both of the filtrates were mixed and evaporated to dryness. After that, it was dissolved in 5ml methanol (HPLC grade) to a final 1% concentration. Next, it was filtered using 0.45 µm membrane filters. Finally, the samples were stored at 4 °C, aiming bioactive compound identification (Azeez *et al.*, 2017). Different

concentrations of standards were used, 15ppm of gallic acid, rutin, catechin and 10ppm of quercetin.

2.3. Isolation and identification of bacterial isolates

Clinical isolates of *S. aureus* and *P. aeruginosa* were isolated from swab samples from wound infection in patients attending Shar Hospital. The isolates were identified using Gram staining, microbiological analysis using differential media (Mannitol Salt Agar, Cetrimide Agar) and Biochemical tests (VITEC2).

2.4. Experimental design

The healthy adult male Wistar albino rats of about 200-300g body weight were used; Animals were attained from Department of Biology, College of Education, University of Sulaimani; they were housed in a controlled environment that was a 12 hours' light/dark cycle, with a temperature of (23±5°C), and the rats were supplied with tap water and food *ad libitum*. The handling of animals and all of the experiments were carried out following the institutional guidelines and the Ethical Committee for Animal Research of Sulaimani University. The rats were housed individually in individual polyethylene cages kept one week before the experiment for adaptation. The rats were fasted overnight and then anesthetized as described by (Eyaref and Amid, 2010), with an intraperitoneal injection of 5% ketamine (35.0 mg/kg) and 2% xylazine (5.0 mg/kg). Two laceration wounds (3 cm long, 1cm deep) made on either side of the thoracolumbar spine of each rat were discussed by (Moscati *et al.*, 1998). The dorsal hair of rats was shaved by an electric shaver and the surface was cleaned with antiseptic. Bleeding was restricted by using sterile gauze pressure. Following laceration, wounds were inoculated with (0.4 ml of inoculum for each *S. aureus* and *p. aeruginosa*) standardized inoculum by spectrophotometer (10⁸ CFU/mL), let to not spread for 30 min.

The experimental rats were randomly divided into 7 groups with 6 animals per each group:

G1: wound without infection and treatment.

G2: infected wound without treatment.

G3: infected wound treated with Vaseline.

G4: infected wound treated with Gentamicin ointment.

G5: infected wound treated with *M. oleifera* leaf ethanolic extract in 3.5% ointment base.

G6: infected wound treated with *M. oleifera* leaf ethanolic extract in 5% ointment base.

G7: infected wound treated with *M. oleifera* leaf ethanolic extract in 10% ointment base.

2.5. Ointment preparation

For preparing extract formulations, 1.75g (3.5%), 2.5g (5%), 5g (10%) of the extract mixed with 48.25g, 47.5g, 45g white Vaseline, respectively. All ingredients of leaves extract ointment were mixed in the mortar and stirring constantly until homogenous and form an ointment preparation, and put in a clean container for topical application during the experiment (Laut *et al.*, 2019).

2.5.1. Treatment schedule

An amount of each of extract ointment, Gentamicin ointment as standard ointment and Vaseline was put in wounds once per day to treat different groups of animals for 14 days.

2.6. Histopathological Assessment

At day 15 of the experiment, the rats were slaughtered, tissue sections were taken from healed wounded skin for all rats, placed in 10% neutral buffered formalin solution for optimum fixation at the minimum 24hrs, at room temperature. Following fixation, the specimens were gradually dehydrated by using the ascending percentage of ethanol solution (60, 80, 90, and 98%, v/v), then cleared in xylene and embedded in paraffin. Histopathological tissue sections of 5 μm thickness were obtained and standard Hematoxylin and Eosin techniques were used for staining, and finally mounted on a glass slide then visualized under the light microscope (Prisacaru *et al.*, 2013).

2.6.1. Semi-quantitative histopathological evaluation

As a quantitative measure, histological sections of skin wounds from each animal were estimated and measured in μm and statistically evaluated as a mean percentage. While inflammatory cells were counted in a randomly chosen 10 fields tissue sections under high power magnification (100X), then the mean average was calculated statistically in percentage. Moreover, the area of granulation tissue formation, proliferated collagen fibers and epidermal thickness was measured in μm , and semi quantitatively evaluated in the same manner as inflammatory cells. Tissue samples were analyzed under the light microscope by the mean of image analyzer software (AmScope Ver. 3.7) using a digital microscope camera (MU300). The mean percentage of calculated values were estimated as following lesion scores (score >75% as mild lesion; score 50-75% as moderate lesion; score <50% as a severe lesion) (Aziz *et al.*, 2020).

2.7. Statistical analysis

Statistical analyses were conducted with SPSS20 (USA) software. Differences between groups were evaluated by ANOVA followed by Tukey post hoc test.

3. Results

3.1. Phytochemical analysis with the HPLC method

The results of qualitative and quantitative estimation of some bioactive compounds in the crude ethanolic extract of *M. oleifera* leaves by using HPLC assay “which is for the first time estimated in Kurdistan Region” indicated the presence of gallic acid, rutin, quercetin and catechin based on the retention time of the extract with different standards as represented in (Table 1); different concentrations of the compounds were used.

(Figure 1, 2, 3, 4) HPLC analysis of different standards: gallic acids, rutin, quercetin and catechin respectively, with (Figure 5) HPLC chromatogram of the ethanolic extract of *M. oleifera*.

Quantity of each compound was shown in (Figure 6): gallic acid (3461 ppm), rutin (286 ppm) and quercetin (88 ppm) and catechin (1201 ppm).

Table 1. Retention time, area and concentration of standards.

Compounds	Retention time (Min.)	Peak area	Concentration of the standard compound (ppm)
Gallic acid	3.06	100.314	15
Rutin	9.55	259.897	15
Quercetin	10.50	848.785	10
Catechin	11.90	916.878	15

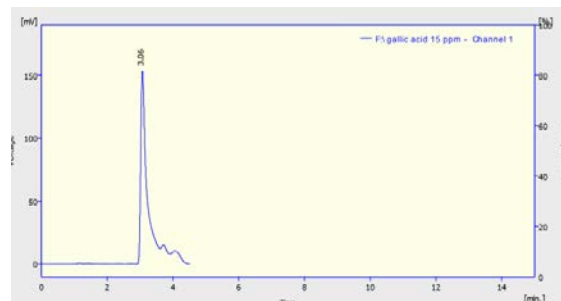


Figure 1. HPLC analysis for gallic acid standard.

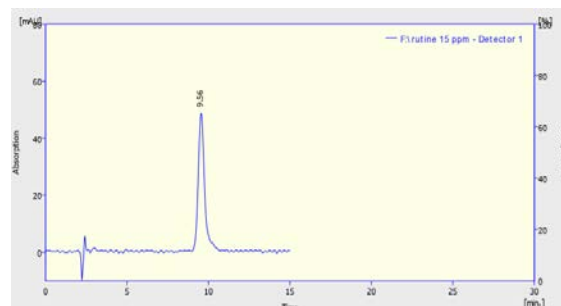


Figure 2. HPLC analysis for rutin standard.

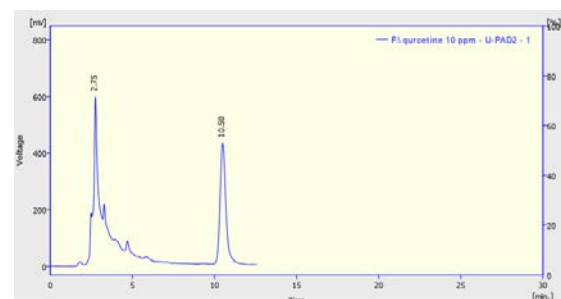


Figure 3. HPLC analysis for quercetin standard.

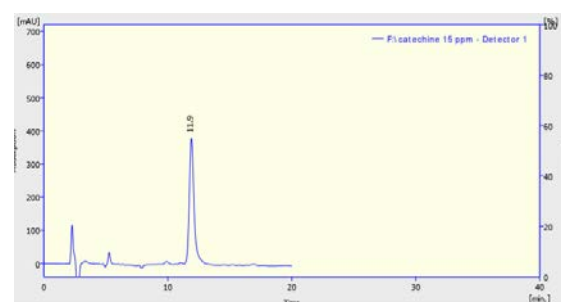


Figure 4. HPLC analysis for catechin standard.

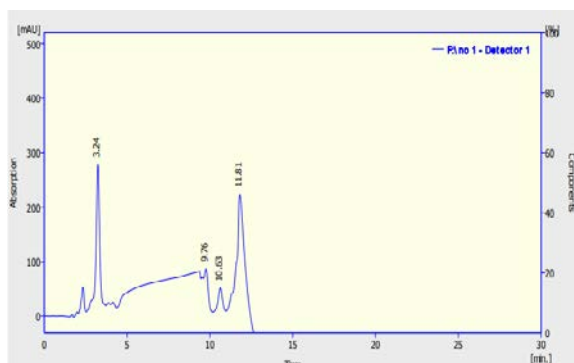


Figure 5. HPLC chromatogram of *M. oleifera* leaf extract.

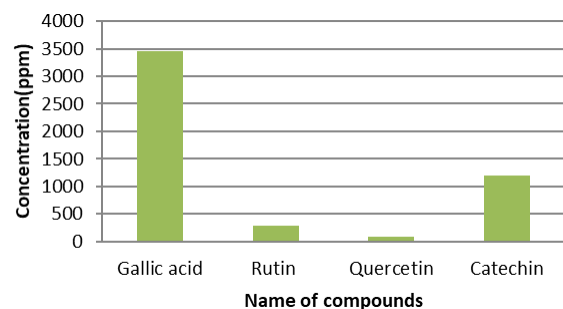


Figure 6. Concentration of some bioactive compounds accumulated in leaves of *M. oleifera*.

3.2. Wound healing property of *M. oleifera*

Histopathological features of lacerated animal skin were represented in (Figure 7) group1; after 14 days of laceration, the untreated wound showed individual variation. This figure shows diffuse dissemination of losing granulation tissue (GT), which is interlaced with newly formed blood vessels (BV). The section (upper left) shows necrotic debris at the skin surface mixed with inflammatory cells and dispersion of pink amorphous ground substances. While the upper right section displays vast proliferation of thicker granulation tissue (GT) perpendicular to the newly formed blood vessels and re-epithelialization of the epidermis (EP). This variation in healing may be due to the different immune response amongst the individuals and/or the animals may be already were infected. Group2a, which represents the infection by gram-positive bacteria *S. aureus* without treatment, indicates the formation of a significant amount of granulation tissue (GT) at the dermal layer with the presence of some giant cells, and newly formed blood vessels can also be seen. The section shows a considerable amount of necrotic debris at the epidermal layer. When compared with group2b (which represents infection by gram-negative bacteria *p. aeruginosa* without treatment), it shows a remarkable amount of fibrinous inflammatory exudate (IE) mixed with many inflammatory cells and bacterial colonies. Besides, the section reveals the deposition of a significant amount of proteinous ground substances in the dermis (GS). The section also shows the presence of many hair follicles (HF). Examination of (Figure 8) group3a, gram-positive, vaseline treated group reveal a significant loss (GT) formation, with an obvious longitudinal section of newly formed blood vessels and some (HF). The section (group3a) shows extended collagen bundles (CB), in addition the section showed epidermal tissue (ET) which were thicker than group3b.

Whereas, the group3b (gram-negative vaseline treated group) showed substantial proliferation of thick collagenous (GT). The area displays pinkish randomly running collagen fibers (CF). In addition, the section shows many (HF) and sebaceous glands. It may occur because of contraction of elastic fibers, more collagen fibers and elastic fibers were formed; it causes wound contract, nearing the wound edge, pulls hair follicles and sebaceous gland from surrounding wound skin into near the wounded area. Whereas group4a, gram-positive, gentamicin 0.1% ointment shows the considerable formation of (GT) together with perpendicular newly formed (BV). The section (group4a) shows some area of (HF) and significant regeneration of epidermal layer which is more than in group4b. The group4b (gram-negative, gentamicin 0.1% group) reveal significant development of (GT) at the wound area, assorted with clear deposition of pinkish (GS), together with the apparent formation of new blood vessels with proliferated (CF). Gentamicin ointment accelerates or stimulates wound healing through the formation of perpendicular blood vessels, regeneration of hair follicles and epidermal layer. Groups in (Figure 9) group5a, group6a and group7a, gram-positive, 3.5%, 5%, 10% plant extract formulation treated group respectively, appeared to heal better than the controls based on gross examination and histopathological evaluation. The wounds in all extract-treated groups showed significant formation and distribution of (GT), newly regenerated sebaceous gland and (HF) and excessive amount of collagen fibers and mature epidermis with a well-formed keratin layer, there was no noticeable necrosis or inflammation. (Figure 9) group5b, group6b and group7b which represent infected lacerated wound with gram-negative bacteria *P. aeruginosa* treated by 3.5%, 5%, 10% plant extract formulation, respectively. These sections demonstrate diffuse and proliferation of (GT) together with the proliferation of (CF) and significant amount of (GS) as well as many regenerated (HF). Excellent re-epithelialization indicated by re-establishment of the epithelial continuity in the form of a mature epidermis with a well-formed keratin layer were also shown. From this preliminary study, it can be illustrated that the rats infected by gram positive bacteria and treated with different formulation of plant extract possess better and moderate wound healing comparing to the vaseline and gentamicin treated group. Moreover, among plant extract treated groups, 10% extract treated group show better wound healing represented by less scarring, brighter skin, many regenerated hair follicles and sebaceous gland in comparison to those treated with 5% and 3.5% of plant extract and gentamicin treated groups. However, it is important to acknowledge that these observations were only based on the microscopic level to the changes occurred inside the wound which treated during fourteen days.

Table 2 represents the semi-quantitative measurement of wound healing properties of *M. oleifera* leaves. Since wound healing histological biomarkers show a significant increase in G1 control wound and other treatment groups including G3a, G4a and G7a which comprise vaseline, gentamicin and 10% plant extract formulation treatment group respectively, these treatment groups have been infected with gram-positive bacteria showing significant $P < 0.05$ increment in (GT) and (CF) proliferation as well as

proper re-epithelialization. While wounds infected with both gram-positive (G2a) and gram-negative (G2b) bacteria and didn't receive any treatment (untreated infected wounds) shows unfortunate healing behavior in comparison with the rest treatment groups. On the other hand, other treatment groups for both gram-positive and gram-negative bacterial infection express moderate healing properties in comparison with G3a, G4a and G7a, which

display significant healing performance among other groups. Thus, in conclusion, and according to lesion scoring shown in (Table 2), plant extract treatment groups show healing properties in all infected wounds, particularly in gram-positive groups in comparison to chemically synthesized ointment as positive control. However, it is in a dose-dependent manner.

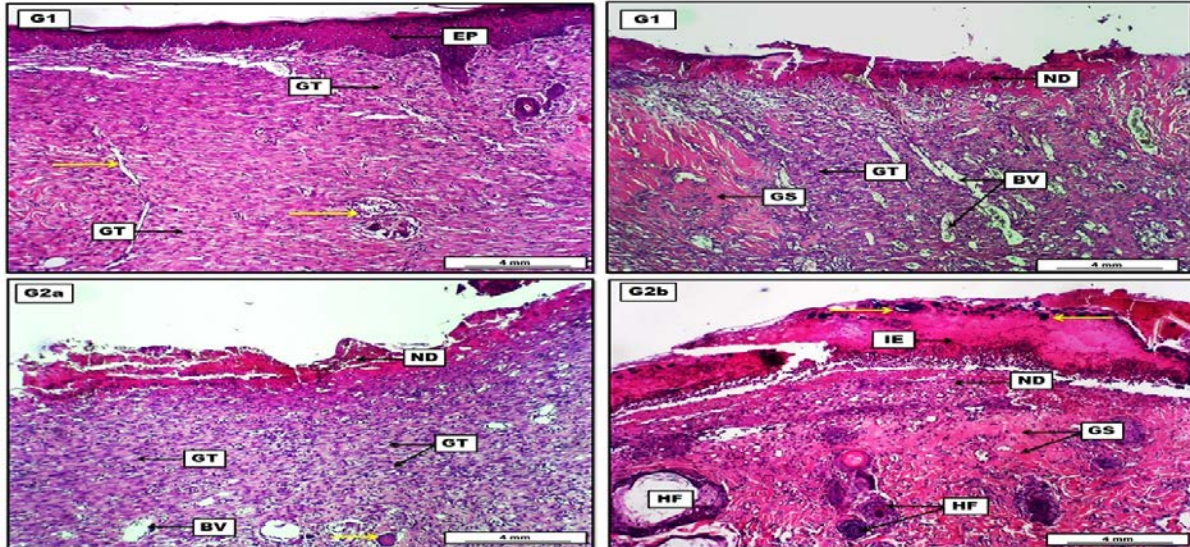


Figure 7. Photomicrograph of skin from groups; (G1) wound untreated group shows diffuse dissemination of loose (GT), which is interlaced with newly formed (BV) and (yellow arrows). The section shows deep pink necrotic debris at the skin surface mixed with inflammatory cells (ND). Dispersion of pink amorphous ground substances (GS). The upper right section shows apparent epidermal regeneration (EP). (G2a) gram-positive, untreated group indicates the formation of (GT) at the dermal layer with the presence of some giant cells (yellow arrow). Newly formed (BV) can also be seen. The section shows a considerable amount of necrotic debris (ND). (G2b) gram-negative, untreated group demonstrates deposition of fibrinous inflammatory exudate (IE) mixed with many inflammatory cells and bacterial colonies (yellow arrows). In addition, the section reveals the deposition of pinkish pretentious (GS) in the dermis together with the presence of (ND). The section also shows the presence of many (HF). H&E. Scale bars: 4 mm

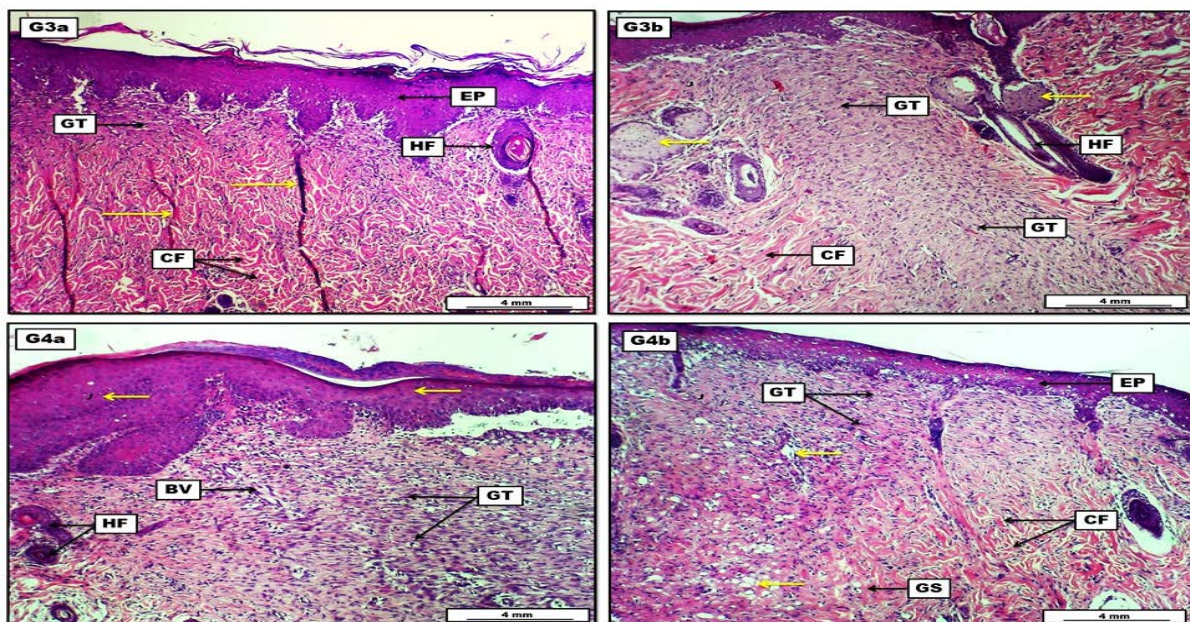


Figure 8. Photomicrograph of skin from groups; (G3a) gram-positive, vaseline group, reveals a significant loose (GT) formation, with an obvious longitudinal section of newly formed (BV)(yellow arrows). The section shows proliferated (CF), nearly thick epidermal layer (EP) and some (HF). (G3b) gram-negative, vaseline group, show proliferation of dense collagenous (GT). The area displays pinkish randomly running (CF). In addition, the section shows many (HF) and sebaceous glands (yellow arrows). (G4a) gram-positive, gentamicin treatment group, show formation of (GT) together with perpendicular newly formed (BV). Yellow arrows indicate significant regeneration of the epidermal layer. The area also shows some sections of (HF). (G4b) gram-negative, gentamicin treatment group, reveal the development of (GT) at the wound area, assorted with clear deposition of pinkish (GS), together with the apparent formation of new (BV) (yellow arrows) and proliferated (CF) along with the regenerative epithelial layer (EP). H&E. Scale bars: 4 mm.

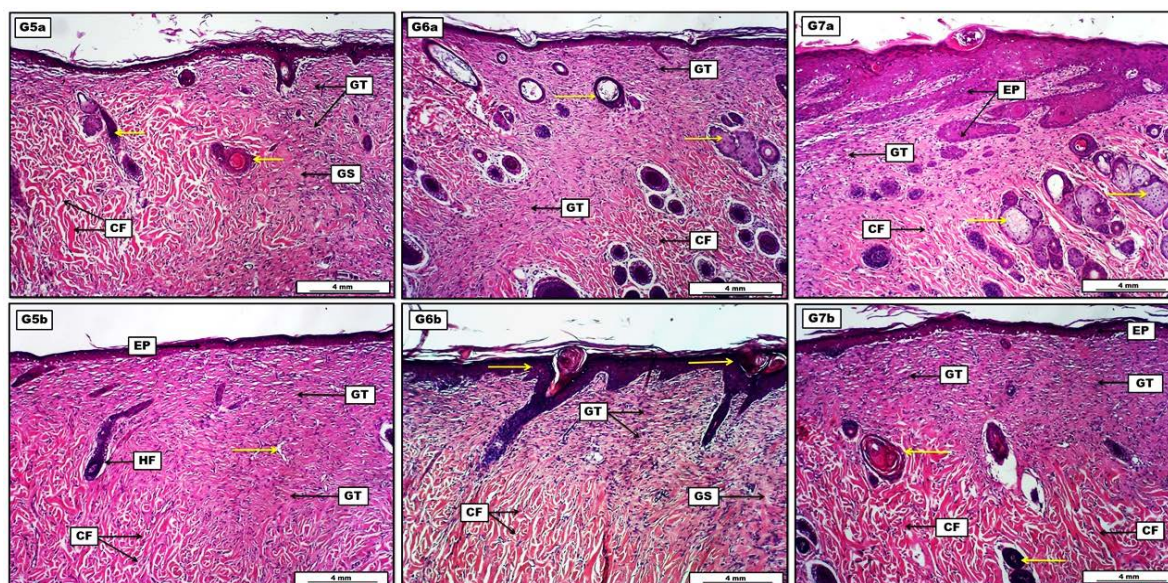


Figure 9. Photomicrograph of skin from groups; (G5a) gram-positive, 3.5% plant extract treatment group, reveals prominent fibrous connective tissue proliferation and (GT) formation, Indicated by bundles of proliferated (CF). Marked deposition of eosinophilic (GS) in the dermis. The section shows the reformation of many (HF) (yellow arrows). (G5b) gram-negative, 3.5% plant extract treatment group, displays formation and proliferation of (GT), in which extended and interlaced newly formed (BV) (yellow arrow). The proliferation of (CF) within the dermal layer, regeneration of some (HF) and the epidermis (EP) can also be seen. (G6a) gram-positive, 5% plant extract treatment group, shows significant formation and distribution of (GT) extended deeply into the dermis, together with newly regenerated sebaceous glands and (HF) (yellow arrows). The section shows an excessive amount of proliferated (CF). (G6b) gram-negative, 5% plant extract treatment group, demonstrates prominent (GT) formation together with the deposition of pinkish (GS). The section reveals the regenerative proliferation of (CF) and epidermal layers (yellow arrows). (G7a) gram-positive, 10% plant extract treatment group, show distinct proliferation of (CF) interlacing with (GT) formation. Presence of many newly formed sebaceous glands and (HF)(yellow arrows). The section also shows excessive regeneration of epithelial tissue leading to the formation of many epidermal papillae (EP). (G7b) gram-negative, 10% plant extract treatment group, display significant (GT) formation together with the proliferation of large bundles of pinkish (CF) within the dermis. The section shows many regenerated (HF) distributed within the dermal layer (yellow arrows) along with the regenerative epidermal layer (EP). H&E. Scale bars: 4 mm.

Table 2. Histological quantitative evaluation of skin wound with different treatment values

Experimental Groups N=6	Granulation Tissue Formation* (Mean%)**	Inflammatory Cells Infiltration (Mean %)**	Collagen Fibers Proliferation* (Mean %)**	Skin Epidermal regeneration* (Mean %)**	Lesion Scoring (0 -100%)	Lesion Grading
(G1) CWG†	78.9 ^{A#}	64.1 ^C	73.7 ^B	61.7 ^C	60-100	Mild
(G2a) G+ve WUG	57.4 ^C	74.3 ^B	58.5 ^C	44.8 ^E	40-75	Severe
(G2b) G-ve WUG	24.2 ^E	87.9 ^A	21.2 ^E	28.2 ^E	20-75	Severe
(G3a) G+ve + VTG	84.6 ^A	77.5 ^A	85.1 ^A	71.4 ^B	70-100	Mild
(G3b) G-ve + VTG	65.4 ^C	73.6 ^B	68.2 ^B	64.9 ^C	60-75	Moderate
(G4a) G+ve + GTG	79.2 ^A	70.6 ^B	84.8 ^A	63.8 ^C	60-85	Mild
(G4b) G-ve + GTG	61.6 ^C	69.2 ^B	59.7 ^C	60.5 ^C	60-75	Moderate
(G5a) G+ve + 3.5%PETG	60.7 ^C	64.8 ^C	61.8 ^C	68.3 ^B	60-75	Moderate
(G5b) G-ve + 3.5%PETG	54.2 ^D	69.4 ^B	53.9 ^D	59.4 ^C	50-75	Moderate
(G6a) G+ve + 5%PETG	62.4 ^C	60.6 ^C	68.6 ^B	67.8 ^B	60-75	Moderate
(G6b) G-ve + 5%PETG	60.7 ^C	67.9 ^B	61.3 ^C	62.6 ^C	60-75	Moderate
(G7a) G+ve + 10%PETG	74.3 ^B	54.6 ^D	80.8 ^A	73.6 ^B	50-85	Mild
(G7b) G-ve + 10%PETG	65.7 ^B	60.3 ^C	72.6 ^B	68.4 ^B	60-75	Moderate

Notes: *Area of granulation tissue formation, collagen fibers proliferation and skin epidermal regeneration were estimated in (μm). **Each value represents the mean percentage of (n=6). #Statistical comparison among groups: Mean values with different capital letters have significant differences at ($P < 0.05$). †G1: Control wound group; G2a: Gram-positive and wound untreated group; G2b: Gram-negative and wound untreated group; G3a: Gram-positive and vaseline treatment group; G3b: Gram-negative and vaseline treatment group; G4a: Gram-positive and gentamicin treatment group; G4b: Gram-negative and gentamicin treatment group; G5a: Gram-positive and 3.5%plant extract treatment group; G5b: Gram-negative and 3.5%plant extract treatment group; G6a: Gram-positive and 5%plant extract treatment group; G6b: Gram-negative and 5%plant extract treatment group; G7a: Gram-positive and 10%plant extract treatment group; G7b: Gram-negative and 10%plant extract treatment group.

4. Discussion

Owing to the occurrence of various secondary metabolites as alkaloids, tannins, glycosides and flavonoids, medicinal plants were lauded for their various pharmacological actions (Ali et al., 2008) (Pham et al., 2008). The current study determines the quality and quantity of some bioactive compounds in *M. oleifera* leaf by using HPLC method for the first time estimated in Kurdistan region. Determining of these compounds is correlated with the previous study which detected quercetin and rutin in methanolic extract of *M. oleifera* leaf (Khudaer et al., 2016). The presence of different phenolic acids such as Vanillic, Caffeic, Chlorogenic, Cinnamic, Coumaric, Ferulic, Syringic in the methanolic extract is inconsistent with our study in ethanolic extract; also, this study confirmed the presence of quercetin and rutin as our result (Al-shamma, 2014). Detection of gallic acid and quercetin is correlated with our study by (Nirajan et al., 2017). The presence of different phenolic compounds such as catechin, gallic acid, rutin and quercetin was detected by (Oboh et al., 2015). *Moringa* is a medicinal plant rich in phenols (gallic acid, p-coumaric acid and ferulic acid) flavonoids (Catechin, quercetin, kaempferol and niazimicin) (Tahir et al., 2020). Analysis of bioactive compounds by HPLC is affected by several factors, including purification of the sample, mobile phase, detectors and sorts of column (Katsube et al., 2004).

There are a number of wound contaminants which invade wound after occurring when it is exposed to external environments such as *Escherichia coli*, *S. aureus* and *P. aeruginosa* (Bowler et al., 2001). Wound healing is a complex and dynamic process in which the structure of cells and tissue layer of injured tissue are restoring into its natural state as carefully as possible. The healing process can be classified as a natural body mechanism to re-generating of epidermal and dermal tissues. It is clear that the rapidity of healing is directly related to providing suitable conditions of the damaged area to overcome the wound and the damage (Periyannayagam and Karthikeyan, 2013). Eventual agents to wound healing are plant products and mostly preferred due to their broad accessibility, non-toxicity, efficacy as crude preparations and little or lack of undesirable side effects (Kodati et al., 2011). The present investigation describes the wound healing activity of *M. oleifera* leaves; the crude extracts exhibited higher potency in infected rats with *S. aureus* and *P. aeruginosa* than the infected rats with no treatment and those treated by Vaseline and gentamicin ointment. Phytochemical analysis of *M. oleifera* indicated important classes of secondary metabolites that play an active role in wound healing and inhibition of microbial growth. Phytochemicals in *M. oleifera* which may speed up wound healing in rabbits (Kasolo et al., 2010). Topical application of *M. oleifera* leaves ethanolic extract in 3.5%, 5% and 10% ointment base stimulated wound healing in 14 days may due to the presence of flavonoids and phenols that may enhance vascularity, collagen synthesis promotes collagen cross linked (Kirubanadan and Bharathi, 2016). The result of this study is in agreement with the previous study which showed leaf ethyl acetate of *M. oleifera* extract had a potential therapeutic agent for healing wound through

increasing wound closure rate and promote fibroblast proliferation examined histologically (Gothai et al., 2016). Topical use of ointment with 3.5% and 5% of the extract influenced rapid wound closure rate, leading to faster epithelialization, granulation tissue resolution, and maturation at histology (Coker et al., 2018). Other studies reported that *M. oleifera* leaves contain nitrogen containing naturally occurring compounds which are called alkaloids which make them capable to intercalate with microorganism's DNA, hence they have antimicrobial properties. Tannins and flavonoids have been investigated and had shown antioxidant activity that enhance wound healing. Therefore, the high antioxidant activity of *Moringa* genus mostly because of its higher concentration of flavonoids (Wang et al., 2017). Presence of high phenolic content in the extracts of different plants may be responsible for the free radical scavenging activity of the extracts (Devika et al., 2016). Phenolic compounds, specifically tannins, and flavonoids are familiar to antimicrobial effects and facilitate faster skin replacement. Quality of phenolic compounds, the interaction of these metabolites, and their quantities in an extract sometimes give a connection with activity since the bioactivity of the secondary metabolites, including phenolic compounds. In tissue healing processes and skin burns, phenolic protein complexes produce a film that prevent chemical damage and microbial infection as this film prevents dehydration and make a physical barrier to damaged tissue (Luseba et al., 2007). Daily application of antibiotic ointments, besides the antibacterial activity provides moisture to the scar to help boost scar products by rapid epithelialization. This explains better scar results in our gentamicin ointment treated group that shows more re-epithelialization, fibrous granulation tissue consisting of fibrous connective tissue and newly formed blood vessels, mature collagen bundles in the dermal connective tissue and healthy hair follicles. Ointment formulation containing ethanol leaf extract of cultivated *M. oleifera* demonstrated better wound healing activity through reduced contraction rate and epithelialization period. Ethyl acetate fraction of *M. oleifera* was assessed in scratch assay and showed important constituents which effective in promoting cell proliferation and migration to close wound area (Gothai et al., 2016). Many polyphenolic compounds are able to reduce the expression of different pro-inflammatory cytokines, such as monocyte chemo attractant protein MCP-1, tumor necrosis factor TNF- α , interleukin IL-1 β , IL-6, in many cell types (Comalada et al., 2006). Quercetin is one of the bioactive compounds analysed through HPLC method in the present study. It has anti-inflammatory mechanism by inhibition of the expression of pro-inflammatory cytokines in the mast cell and suppression of TNF- α , thus, effect the wound healing (Pan et al., 2009). The use of the extract in ointment is more affective due to prolonged contact between extract with the wound area and it enhances the delivery of the extract to the wound site (Coker et al., 2018).

Finally, the present study suggested that ethanolic extract of *M. oleifera* leaves in different formulations promotes wound healing activity as the extract contains several bioactive compounds that possess an anti-inflammatory effect improving effective wound healing.

5. Conclusion

The current study confirms that leaves of *M. oleifera* cultivated in the Kurdistan region, Iraq, potentially exert wound healing activity in rats. It may be due to the presence of diverse bioactive compounds in different concentration such as gallic acid, rutin, quercetin and catechin. All these mixes are effective anti-inflammatory compounds which promote wound healing. Further studies to isolate and purified active compounds are needed to find the exact mechanism of *M. oleifera* leaves on wound healing.

Acknowledgment

The authors would like to express their utmost appreciation to the Department of Biology, College of Education, and the College of Pharmacy, University of Sulaimani for their support in providing many facilities such as laboratory animals, cages and animal house utilities with many other consumables to complete this project.

Disclosure

The authors report no conflicts of interest in this work.

References

- Alam G, Singh M.P. and Singh A. 2011. Wound healing potential of some medicinal plants. *Int. J. Pharm. Sci.*, **9(1)**:136-145.
- Ali S.S, Kasoju N, Luthra A, Singh A, Sharanabasava H, Sahu A and Bora U. 2008. Indian medicinal herbs as sources of antioxidants. *Int. Food Res. J.*, **41(1)**:1-15.
- Al-Shammaa D.A.S. 2014. Phytochemical Investigation of the most important phenolic compounds in *Moringa oleifera* L. cultivated in Iraq. *TJ'S Journal of Science & IT Management RJSITM.*, **3(8)**: 30-36.
- Anwar F, Latif S, Ashraf M and Gilani A.H. 2007. *Moringa oleifera*: a food plant with multiple medicinal uses. *Phytotherapy Research: Phytother Res [dnlm.]*, **21(1)**:17-25.
- Arun M, Satish S and Anima P. 2016. Evaluation of wound healing, antioxidant and antimicrobial efficacy of *Jasminum auriculatum* Vahl. leaves. *Avicenna J. Phytomed.*, **6(3)**:295.
- Azeez H, Ibrahim K, Pop R, Pamfil D, Hârța M and Bobiș O. 2017. Changes induced by gamma ray irradiation on biomass production and secondary metabolites accumulation in *Hypericum triquetrifolium* Turra callus cultures. *Ind Crops Prod.*, **108**:183-189.
- Aziz TA, Kareem AA, Othman HH and Ahmed ZA. 2020. The Anti-Inflammatory Effect of Different Doses of Aliskiren in Rat Models of Inflammation. *Drug Des Devel Ther.*, **14**: 2841.
- Boakye YD, Agyare C, Ayande GP, Titiloye N, Asiamah EA and Danquah KO. 2018. Assessment of Wound-Healing Properties of Medicinal Plants: The Case of *Phyllanthus muellerianus*. *Front Pharmacol.*, **9**:945.
- Bowler PG, Duerden BI and Armstrong DG. 2001. Wound microbiology and associated approaches to wound management. *Clin. Microbiol. Rev.*, **14(2)**:244-269.
- Coker M, Adejo G, Emikpe B and Oyeibanji V. 2018. Evaluation of the wound healing potential of ointment preparation of ethyl-acetate extract of *Moringa Oleifera* (Lam) in rats. *Afr J Tradit Complement Altern Med.*, **15(3)**:64-71.
- Comalada M, Ballester I, Bailon E, Sierra S, Xaus J, Gálvez J, de Medina FS and Zarzuelo A. 2006. Inhibition of pro-inflammatory markers in primary bone marrow-derived mouse macrophages by naturally occurring flavonoids: analysis of the structure-activity relationship. *Biochem. Pharmacol.*, **72(8)**: 1010-1021.
- Devika, M., Joshi, H. and Nalini, M.S., 2016. Phytochemicals, Antioxidative and in vivo Hepatoprotective Potentials of *Litsea floribunda* (BL.) Gamble (Lauraceae)-An Endemic Tree Species of the Southern Western Ghats, India. *JJBS.*, **9(3)**:163-171.
- Eming SA, Martin P and Tomic-Canic M. 2014. Wound repair and regeneration: mechanisms, signaling, and translation. *Sci. Transl. Med.*, **6(265)**:265sr6.
- Eyarefe OD and Amid SA. 2010. Small bowel wall response to enterotomy closure with polypropylene and polyglactin 910 using simple interrupted suture pattern in rats. *J Anim Vet Adv.*, **2(3)**:72-75.
- Gothai S, Arulselvan P, Tan WS and Fakurazi S. 2016. Wound healing properties of ethyl acetate fraction of *Moringa oleifera* in normal human dermal fibro blasts. *J. Intercult Ethnopharmacol.*, **5(1)**:1-6.
- Ji HF, Li XJ and Zhang HY. 2009. Natural products and drug discovery. Can thousands of years of ancient medical knowledge lead us to new and powerful drug combinations in the fight against cancer and dementia? *EMBO reports*, **10(3)**:194-200.
- Kasolo JN, Bimenya GS, Ojok L, Ochieng J and Ogwal-Okeng JW. 2010. Phytochemicals and uses of *Moringa oleifera* leaves in Ugandan rural communities. *J. Med. Plant Res.*, **4(9)**: 753-757.
- Katsube T, Tabata H, Ohta Y, Yamasaki Y, Anuurad E, Shiwaku K and Yamane Y, 2004. Screening for antioxidant activity in edible plant products: comparison of low-density lipoprotein oxidation assay, DPPH radical scavenging assay, and Folin-Ciocalteu assay. *J. Agric. Food Chem.*, **52(8)**: 2391-2396
- Khdhir JC, Ridha HH, and Azeez HA. 2019. Effect of Cherry Extract and Almond Oil on Oxonic cid-Induced Hyperuricemia in Male Albino Rats. *ANJS.*, **22(4)**: 59-67.
- Khudaer NB, Hassn ZYM, AL-Sammarrae KW and Ibrahim NK. 2016. Purification and Identification of Total Flavonoids Extracted from *Moringa oleifera* Leaves in Iraq. *Res. J. Biotechnol.*, **10(2)**:73-80.
- Kirubanadan S and Bharathi R. 2016. Histological and biochemical evaluation of wound regeneration potential of *Terminalia chebula* fruits. *Asian J. Pharm. Clin. Res.*, **9**:228-233.
- Kodati DR, Burra S and Kumar GP. 2011. Evaluation of wound healing activity of methanolic root extract of *Plumbago zeylanica* L. in wistar albino rats. *Asian J. Plant Sci.*, **1(2)**:26-34.
- Laut M, Ndaong NA and Utami T. 2019. Cutaneous wound healing activity of herbal ointment containing the leaf extract of *Acalypha indica* L. on mice (*Mus musculus*). *J. Phys. Conf. Ser.*, 1146: 012025.
- Liew PM and Yong YK. 2016. *Stachytarpheta jamaicensis* (L.) Vahl: from traditional usage to pharmacological evidence. *Evid Based Complement Alternat Med.*, Volume 2016, Article ID 7842340, 7 pages.
- Luseba D, Elgorashi EE, Ntloedibe DT and Van Staden J. 2007. Antibacterial, anti-inflammatory and mutagenic effects of some medicinal plants used in South Africa for the treatment of wounds and retained placenta in livestock. *S. Afr. J. Bot.*, **73(3)**:378-383.
- Maqsood I, Tayyaba B, Najmi MH, Mazhar W, Bader Z, Janjua A and Sabah S. 2017. Pharmacokinetic study of atorvastatin after single dose administration among pakistani population. *Pak Armed Forces Med.*, **67(4)**: 656-662.
- Mbosso EJT, Ngouela S, Nguedia JCA, Beng VP, Rohmer M and Tsamo E. 2010. In vitro antimicrobial activity of extracts and compounds of some selected medicinal plants from Cameroon. *J. Ethnopharmacol.*, **128(2)**:476-481.

- Mohammed S and Manan FA. 2015. Analysis of total phenolics, tannins and flavonoids from *Moringa oleifera* seed extract. *J. Chem. Pharm. Res.*, **7(1)**: 135-7.
- Moscatti R, Mayrose J, Fincher L and Jehle D. 1998. Comparison of normal saline with tap water for wound irrigation. *Am. J. Emerg. Med.*, **16(4)**:379-381.
- Niranjan A, Ngpoore NK, Anis N, Kumar A, Lehri A, Shirke PA and Tewari SK. 2017. Simultaneous quantification of six phenolic compounds in various parts of *Moringa oleifera* Lam. using high-performance thin-layer chromatography. *J. Planar Chromatogr.-Mod.TLC.*, **30(6)**:502-509.
- Nouman W, Anwar F, Gull T, Newton A, Rosa E and Domínguez-Perles R. 2016. Profiling of polyphenolics, nutrients and antioxidant potential of germplasm's leaves from seven cultivars of *Moringa oleifera* Lam. *Ind Crops Prod.*, **83**: 166-176.
- Nweze NO and Nwafor FI. 2014. Phytochemical, proximate and mineral composition of leaf extracts of *Moringa oleifera* Lam. from Nsukka, South-Eastern Nigeria: *JPBS.*, **9(1)**:99-103.
- Oboh G, Ademiluyi AO, Ademosun AO, Olasehinde TA, Oyeleye SI, Boligon AA and Athayde ML. 2015. Phenolic extract from *Moringa oleifera* leaves inhibits key enzymes linked to erectile dysfunction and oxidative stress in rats' penile tissues *Biochem. Res. Int.*, Volume 2015, Article ID 175950, 8 pages.
- Pazyar N, Yaghoobi R, Rafiee E, Mehrabian A and Feily A. 2014. Skin wound healing and phytomedicine: a review. *Skin Pharmacol Physiol.*, **27(6)**:303-310.
- Pan MH, Lai CS, Dushenkov S and Ho CT. 2009. Modulation of inflammatory genes by natural dietary bioactive compounds. *J. Agric. Food Chem.*, **57(11)**: 4467-4477..
- Periyannayagam K and Karthikeyan V. 2013. Wound healing activity of the leaves of *Artocarpus heterophyllus* Lam. (Mora ceae) on ex-vivo porcine skin wound healing model. *Innovare J. Life Sci.*, **1(1)**:28-33.
- Pham-Huy LA, He H and Pham-Huy C. 2008. Free radicals, antioxidants in disease and health: *Int J Biomed Sci.*, **4(2)**:89.
- Prisacaru AI, Andritoiu CV, Andriescu C, Havarneanu EC, Popa M, Motoc AG and Sava A. 2013. Evaluation of the wound-healing effect of a novel *Hypericum perforatum* ointment in skin injury *Rom J Morphol Embryol.*, **54(4)**: 1053-1059.
- Rani A, Zahirah N, Husain K and Kumolosasi E. 2018. *Moringa* genus: a review of phytochemistry and pharmacology. *Front. Pharmacol.*, **9**:108.
- Rathi BS, Bodhankar SL and Baheti AM. 2006. Evaluation of aqueous leaves extract of *Moringa oleifera* Linn for wound healing in albino rats. *Indian J. Exp. Biol.*, **44(11)**, 898-901.
- Sabale P, Bhimani B, Prajapati C and Sabale V. 2012. An overview of medicinal plants as wound healers. *J App Pharm Sci.*, **2(11)**:143-150.
- Sussman C and Bates-Jensen BM. 2007. *Wound care: a collaborative practice manual*, third ed. Lippincott Williams & Wilkins, Philadelphia.
- Tahir NA, Qader KO, Azeez HA and Rashid JS. 2018. Inhibitory allelopathic effects of *Moringa oleifera* Lam plant extracts on wheat and *Sinapis arvensis* L. *Allelopathy J.*, **44(1)**:35-48.
- Tahir NA, Majeed HO, Azeez HA, Omer DA, Faraj JM and Palani WRM. 2020. Allelopathic Plants: 27. *Moringa* species. *Allelopathy J.*, **50(1)**:35-46.
- Vongsak B, Sithisarn P, Mangmool S, Thongpraditchote S, Wongkrajang Y and Gritsanapan W. 2013. Maximizing total phenolics, total flavonoids contents and antioxidant activity of *Moringa oleifera* leaf extract by the appropriate extraction method. *Ind Crops Prod.*, **44**:566-571.
- Wang Y, Gao Y, Ding H, Liu S, Han X, Gui J and Liu D. 2017. Subcritical ethanol extraction of flavonoids from *Moringa oleifera* leaf and evaluation of antioxidant activity. *Food chem.*, **218**:152-158.
- Zhang H and Ma ZF. 2018. Phytochemical and pharmacological properties of *Capparis spinosa* as a medicinal plant. *Nutrients.*, **10(2)**:116.

An Assessment of Proximate Composition, Antioxidant Activities and LC/MS Based Phytochemical Profiling of Some Lichen Species Collected From Western Ghats of Southern Part of India

Shenbagam Muthu¹, Mariraj Murugan¹, Kalidoss Rajendran¹ and Ponnusamy^{2,*}

¹ Research Scholar, Biomedical Research Lab, Department of Botany, Bharathiar University, Coimbatore – 641 046, Tamil Nadu, India;

² Associate professor, Biomedical Research Lab, Department of Botany, Bharathiar University, Coimbatore – 641 046, Tamil Nadu, India.

Received: June 7, 2020; Revised: September 26, 2020; Accepted: Oct 13, 2020

Abstract

The lichen samples of *Parmotrema tinctorum*, *Pseudocyphellaria aurata*, *Ramalina taitensis*, *Usnea bismolliuscula* are being used as nutraceutical agents in indigenous system of medicine. The main objectives of this study were assessing the proximate composition in lichen samples of the extracts and their antioxidant properties. Using Liquid Chromatography Mass Spectrophotometric analysis with chemoprofiling of the studied lichen compositions were also done. The petroleum ether, acetone, methanol and water extracts of test samples obtained from Soxhlet apparatus were assessed for *in vitro* antioxidant activities using 1,1-diphenyl-2-picrylhydrazine, Superoxide anion radical, 2, 2'-Azino-Bis-3-Ethylbenzothiazoline-6-Sulfonic Acid scavenging and Phosphomolybdenum reduction assays. The methanol extract of test samples revealed higher content of phytochemical constituents. The acetone extract of *P. aurata* showed strong DPPH radical scavenging activity with IC₅₀ value of 93.339 µg/mL. Similarly, the methanol extract of *U. bismolliuscula* and *R. taitensis* showed maximum ABTS scavenging potency and phosphomolybdenum reduction activity and with the highest values of 85.6 ± 0.5 TE/g and 150.68 ± 1.15 mg AA/g respectively. LCMS analysis of lichen extracts exhibited the secondary metabolites containing atranorin, sekikaic acid and usnic acid. It is concluded that these lichen species might be a valuable nutraceutical agent. Thus, the lichen extracts may further be assessed to toxic assays on experimental animals to confirm their biological activities.

Keywords: Lichens, Nutritional, Phytochemicals, Antioxidants, LC/MS

1. Introduction

Lichens contain mycobiont that has a defensive role and photobiont that supplies food. They have historically been used as spices in food, dyes in textile, odorant in perfume industry (Kosanic *et al.*, 2014). In our human body, singlet oxygen, hydroxyl (OH[•]) radicals, super oxide (O²⁻) anions and hydrogen peroxide (H₂O₂) are biological Reactive Oxygen species (ROS) that induce oxidative stress and trigger degenerative diseases such as cancer, premature aging, diabetes, metabolism disorders and heart disorders (Kosanić & Ranković 2010). The lethal effect of radiation and pollutants and other exogenous factors are attributed to the formation of free radicals in biological systems. Lichen secondary metabolites such as depsides dibenzofuran-heterocyclic aromatic compound, depsidones-ester and pulvinic acid are all natural phenolic compounds were described to have antioxidant activities, and hence attracted considerable attention (Nguyen *et al.*, 2019).

Proximate elements of carbohydrates, proteins, fats and antioxidant properties of secondary metabolites of phenols are naturally found in lichens. Synthetic agents mostly

used as conventional chemical antioxidants have been pronounced to pose side effects such as inflammation and cell damage. Therefore, there has been the global interest in finding promising alternative antioxidant compound from natural sources. Conventionally, following solvents with different polarities such as petroleum ether, chloroform, acetone and methanol have commonly been employed to extract compounds from lichen thallus (Biney *et al.*, 2020) which deliver the dissolved compounds to diffuse into the cell through membrane pores and help to trigger its action. They have the property of low viscosity and high diffusivity (Biney *et al.*, 2020).

Although intensive and extensive assessment on the nutraceutical properties of most plants have been documented, little is known about the lichens in all over the World. Two such lichens include *Parmotrema tinctorum* and *Pseudocyphellaria aurata*, which are temperate foliose lichen. The relation of *Parmotrema tinctorum* with other spices in cooking is interesting and the use of this species may often add flavour in many dishes such as vegetables and meat by indigenous groups in Nepal and India (Upreti *et al.*, 2005). *Pseudocyphellaria aurata*, also known as specklebelly, belonged to the family Lobariaceae, while members of genus *Parmotrema* called

* Corresponding author e-mail: ponnusamy@buc.edu.in.

as “ruffle lichens” belonged to Parmeliaceae. The tea prepared from *Pseudocyphellaria aurata* is considered to be beneficial for the health, particularly for the intestinal tract in curing indigestion. This has been used in Madagascar. The *Ramalina taitensis*, used to synthesize chemical compounds such as tannins, alkaloids, and saponins that are for biological functions, including antioxidant role and defence against microbial agents (Chowdhery 2014). The lichen substances of *Usnea bismolliuscula* play a great role in inhibition of tyrosine activity in medicine (Rajeswari *et al.*, 2019). Two of these species include which are fruticose lichens in the family Ramalinaceae and Parmeliaceae respectively. The members of the genus *Usnea* are called old man’s beard lichens and *Ramalina* are called strap lichens. These lichens have shown many health beneficial properties, such as possessing antibiotic, antioxidant, antiviral, antitumour, anti-allergenic and anti-inflammatory properties (Shrestha & St. Clair 2013). This has aroused further interest in the study of these lichens. Therefore, in the present study, the proximate chemicals, antioxidant property, and LC/MS analysis of methanol and acetone-water extracts of *Parmotrema tinctorum*, *Pseudocyphellaria aurata*, *Ramalina taitensis*, *Usnea bismolliuscula* were investigated to document the potential biological activities of these lichens. The results indicated that these lichen possess very high antioxidant potentiality, which gave immense scope for further exploration in nutritional and phytochemical studies.

2. Materials and methods

2.1. Collection and identification of lichen samples

Fresh thalli of *Parmotrema tinctorum*, *Pseudocyphellaria aurata*, *Ramalina taitensis*,

Usnea bismolliuscula were collected from Kodaikanal hills of Western Ghats, Southern India, during the winter season (January 2019). The elevation of hills was measured about 2130 meters. Identification of lichen was carried out at Biomedical Research lab, Bharathiar University, Coimbatore, Tamil Nadu, India. Voucher specimens were deposited at lichen herbarium centres, Bharathiar University, Coimbatore, India and CSIR-National botanical research Institute NBRI, Lucknow, India. The lichen specimens were identified by matching with the identification keys documented in Awasthi’s identification key manual (Awasthi 2007). The species were chemically identified with the help of conventional spot tests (K, C, I, KC) (Orange *et al.*, 2001). Lichen thalli were rinsed under flowing tap water to wash away soil particles. The samples were air-dried and left under sun shade to remove moisture. The air dried samples were blended into powder using a mixer and used for further analysis.

2.2. Nutritional studies

2.2.1. Proximate chemical composition

Standard procedure was followed for the proximate chemical composition analysis of phytochemicals such as proteins, carbohydrates, total phenolics, amino acids, and total flavonoids (Lowry & Rosebrough 1951) lipids and fibre contents (AOAC 1990).

2.2.2. Amino acids analysis

Amino acid content in the lichen extract was quantified according to the procedure described by Mohapatra *et al.* (2019). Briefly, a known amount of 100 mg of blended sample was acid treated with 10 mL 6 N HCl. The reaction mixture was digested in an oven at 120°C for 24 h. The aliquots were filtered out using the filter paper Whatman No. 1. The content was subjected to a vacuum flash evaporator. The amino acid concentrate was acid treated using 0.05 N Hydrochloric acid and filtered again using a 0.45 µM membrane filter and a volume of 20 µL was passed by injection into an amino acid analyzer (Shimadzu LC-10AS HPLC, McKinley Scientific, Sparta, NJ, USA) fitted with an ion exchange resin (styrene divinyl benzene co-polymer with sulphonic group) in column. The reference amino acid was injected to measure the amount of amino acid in the test sample. Amino acid standard was also run to calculate the concentration of amino acids in the samples.

2.2.3. Mineral analysis by ICP-MS (Liu *et al.*, 2020)

During the last decades, ICP-MS (Inductively Coupled Plasma Mass Spectrometry) has emerged as the most promising technique for the analysis of trace elements of biological or environmental samples, and it is routinely used for the determination of up to eighteen elements in ionic research studies. The mineral analysis of lichen samples was done by the ICP – MS instrument of (Nex Ion 300 X, Perkin Elmer, USA). The powdered lichen material (200mg) was digested at 80°C with 10 mL of tri-acid (Nitric acid, Sulphuric acid and per chloric acid, 9:2:1) This test was performed by following the method of Lie *et al.* (2020). After digestion, all the samples were made up to 100 mL and aspirated into ICP – MS (Nex Ion 300 X, Perkin Elmer, USA).

2.3. Preparation of solvent extract

The extraction of lichen sample was done using the Soxhlet apparatus. The powdered lichen samples were loaded in pockets of thimbles and introduced in the extractor. Then, extraction was done separately using 250 mL solvents in an increasing polarity such as petroleum ether, acetone, methanol and water and heated up to 80°C for 8 h. Then, the extracts were concentrated using rotary vacuum evaporator (Superfit make, India). The concentrate thus obtained was weighed and stored in refrigeration at 4°C. Three samples from each solvent extract were examined for phytochemical and biological activities to assess variations in the test analysis. The presence of different lichen substances in each extract justifies the use of different solvents in an increasing polarity for extraction.

2.4. Quantitative analysis of phytochemicals.

2.4.1. Estimation of total phenolic content (TPC)

The procedure is based on the method given by Ng and See (2019); Gaafar *et al.* (2019). Each sample was tested by adding 100 µL of extract (1 mg/mL) in 500 µL of 10% Folin–Ciocalteu reagent solution and incubating for 5 min at room temperature. This was followed by adding 2.5 mL of 7.5% sodium carbonate solution and incubating in dark for 45 min. The colour changes in test tubes were measured in spectrophotometer at 760 nm. The concentration ranges between 0–100 µg/mL of the

suggested Gallic acid standard were analysed to obtain the calibration curve. The mean \pm standard deviation of readings was calculated, and the results of TPC were represented in milligrams of gallic acid equivalents (\pm sd) per g of the lichen extract.

2.4.2. Estimation of total flavonoid content (TFC)

The TFC procedure is based on Abdel-Mawgoud et al. (2019); Ng and See (2019) technique. About 500 μ L of the extracts were mixed with 300 μ L of 5% sodium nitrate solution followed by 300 μ L of 10% Aluminium chloride and incubated at room temperature. The content of the tube was added with 4% sodium hydroxide. As standard, a test tube containing Rutin was used to obtain calibration curve. From each extracts, triplicate samples were examined separately to find out any variations in the assessment of TFC and the mean value was calculated. The results were represented as Rutin Equivalents (\pm sd).

2.5. In vitro antioxidant assays

2.5.1. DPPH radical scavenging activity

The 1,1-diphenyl-2-picrylhydrazine (DPPH) radical scavenging activity was determined bestowing to the procedure of Ng and Rosman (2019); Sedjati et al. (2020). Stable 1,1-diphenyl-2-picrylhydrazyl (DPPH) was assessed to examine the free radical capturing ability of H⁺ ions. DPPH has the potency to donate H⁺ ions to atoms that can give rise to free radicals of hydrogen. Reduction in the amount of DPPH molecule determines the free radical scavenging ability. It was analysed by detecting the absorbance readings at 570 nm. Reading in the absorbance decreases as the free radicals scavenged by the active substances of the lichen extracts increases. The percentage of inhibition for lichen extract was compared with the commercial ascorbic acid standard. The reaction mixture contained 100 μ L of aliquots with different concentrations of extracts. The positive control has different concentrations of ascorbic acid standard added with 3.0 mL of DPPH solution. The mixture was left in dark for 30 min at room temperature. The absorbance of the sample was read at 517 nm against a blank (methanol). The average of three readings was calculated. The following formula determines the results of half the inhibition concentration value (IC₅₀) for DPPH radical scavenging ability of test samples:

$$X = [(A_0 - A_1) / A_0] \times 100$$

Where X= % Inhibition, A₀ is the absorbance of the control and A₁ is the absorbance of the sample extracts/standard.

2.5.2. Superoxide anion radical scavenging activity

The principle of this assay is based on the ability of lichen extracts to inhibit the formation of formazan by scavenging the superoxide radicals present in riboflavin–light–NBT system according to the procedure described by (Thangaraj, 2016). About 3 mL reaction mixture contained 50mM Sodium phosphate buffer pH (7.6), riboflavin 20 μ g, EDTA (12mM), NBT (0.1 mg) and 100 μ L sample of lichen extract. The absorbance of the sample was measured at 590 nm against a blank (methanol). The mean value of triplicate readings was recorded. The percentage of half the inhibition concentration value (IC₅₀) of superoxide anion generation was calculated by following equation:

$$X = [(A_0 - A_1) / A_0] \times 100$$

Where X= Superoxide anion scavenging activity, A₀ is the absorbance of the control and A₁ is the absorbance of the sample extracts/standard

2.5.3. ABTS⁺ (2, 2'-Azino-Bis-3-Ethylbenzothiazoline-6-Sulfonic Acid) radical scavenging activity

The principle of ABTS scavenging assay is based on the ability of lichen extract to reduce ABTS and lead to the decolouration of a green color complex to colourless. About 1 mL of diluted ABTS solution was transferred to the tube containing an aliquot of lichen extract (Rutin as standard) followed by adding 2.4 mM of potassium per sulphate and left in the dark. Triplicate determinations were calculated and the results of ABTS scavenging activity were read at 734 nm against a blank ethanol. The result was represented in mM of Trolox equivalents per g of the lichen extract (Makawy et al., 2019).

2.5.4. Phosphomolybdenum reduction assay

The antioxidant potency of the lichen extracts was assessed by the phosphomolybdenum reduction assay (Zengin et al., 2015). The assay was based on the ability of a substance in lichen extract to reduce phosphomolybdic acid to blue complex phosphomolybdenum. A reagent solution was prepared containing ammonium molybdate (4 mM/L) and sodium phosphate (0.6 mM/L). Exactly, 250 μ l of the extracts was added with 3 mL of the reagent solution. The tubes with reaction mixture were incubated at 95°C for 90 min. The absorbance of the reaction mixture was measured at 695 nm using spectrophotometer against blank (0.3 mL methanol and 3 mL reagent). The ascorbic acid was used as standard (1mmol/L ascorbic acid in DMSO). The assay was done in triplicates.

2.6. Liquid Chromatography coupled to Mass Spectrometry (LC/MS) analysis

For studying LC/MS method followed by Zhang et al. (2019), the lichen substances obtained from the methanol extract of lichen samples were identified using Linear Trap Mass Spectrometer (Thermo Scientific). The extracts containing 5 μ l were injected into a UPLC(R)BEH C18 1.7 μ m-(2.1x100mm) on a Water Xevo TQD 2000 C18 column which consists of 3000 nano system. The flow rate was followed at an interval of time 0.3 ml/min with the gradient elution program. The solvent mixture containing 70%-Acetonitrile : 30% Formic acid in water served as mobile phase and total run over time was automated to flow in 10.0 min. The compounds were identified using peaks and collected by scanning at wide wavelengths ranges between 100 and 1000 atomic mass units over the mass/charge number (m/z) (Xcalibur version 4.0). The LC/MS profile of the prevailing lichen compounds were compared with the standard Chemindex lichen data base. The mass spectral data for each compound was standardized to ensure the most favourable ion transfer conditions, ionization and obtained optimum peak of both the precursor and fragment ions. The source peak was compared for its identity for all the lichen samples.

2.7. Statistical analysis

All tests were prepared in triplicates. Data are documented as mean \pm standard error. The result was analysed statistically. The SPSS version 20.0 was used for this purpose. The one way ANOVA approach by Duncan's

test was followed. Mean values at $p < 0.05$ were found statistically significant. For the graphical representation, R software version 3.5.1 was employed.

3. Results

3.1. Proximate composition of samples.

3.1.1. Moisture and ash contents of samples.

The moisture and ash contents of *P. tinctorum*, *P. aurata*, *R. taiensis* and *U. bismolliuscula* were investigated and results are presented in Table 1. The availability of moisture content was found to be significant in lichen

Table 1. Proximate chemical composition of Lichen samples

Parameters	Total carbohydrates (mg glucose equivalents/g sample)	Total proteins (mg BSA equivalents/g sample)	Total starch (mg glucose equivalents/g sample)	Energy (%)	Moisture content (%)	Ash content (%)
<i>P. tinctorum</i>	64.6 ± 0.01	25.78 ± 0.03	0.17 ± 0.03	82.85	10.5	13.93
<i>P. aurata</i>	31.63 ± 0.3	11.65 ± 0.11	0.14 ± 0.09	54.75	9.3	1.93
<i>R. taiensis</i>	50.12 ± 0.1	14.10 ± 0.5	0.12 ± 0.06	74.89	10	4.41
<i>U. bismolliuscula</i>	58.52 ± 0.02	24.95 ± 0.03	0.13 ± 0.05	60.05	9.8	2.43

3.1.2. Determination of nutrient contents

The proximal composition of the lichen extracts such as *P. tinctorum*, *P. aurata*, *R. taiensis* and *U. bismolliuscula* are shown in Table 1. The total carbohydrates content was found highest in *P. tinctorum* (64.6 ± 0.01 mg GE/g sample), whereas *P. aurata* (31.63 ± 0.3 mg GE/g sample) registered lower carbohydrate content. The *P. tinctorum* had a maximal amount of total protein content (25.78±0.03mg BSAE/g sample) when compared to other lichens. Moreover, the lichen species, *R. taiensis* exhibited highest starch content. The *P. tinctorum* yielded a high energy level (82.85%) in the analyzed lichen extracts. The differences between the activity of standard used in each antioxidant assay was compared with previous published papers. Comparison of standard values with previous paper's standard values for the same assay validated moisture content results in this study. The present study has shown that the protein content of lichens is considerably low (foliose 1.87% and fruticose 1.9%) compared to the protein content of *P. pseudotinctorum* (16.2%) (Vinayaka *et al.*, 2010).

3.1.3. Mineral composition of lichen samples

Mineral composition of the *P. tinctorum*, *P. aurata*, *R. taiensis* and *U. bismolliuscula* were analysed and presented in Table 2. Among all minerals tested, calcium

extract at any stage of nutritive analysis. The lichen moisture content was carried out in triplicates. It was found that the *P. aurata* showed lichen with lowest moisture content (9.3%) as compared to other lichen extracts. The *U. bismolliuscula* showed moderate moisture content (9.8 %). The result findings of *P. tinctorum* showed maximum moisture content of 10.5 % followed by *R. taiensis* with 10%. Similarly, the ash content was calculated and the results indicated positive effect with the lichens. *Parmotrema tinctorum* extracts were compared with the values of other lichen samples which showed highest level of total ash content which was up to 13.93%.

was found to be the highest in all lichen extracts followed by potassium. The third highest element was magnesium in *R. taiensis* (710 ppm) and *U. bismolliuscula* (530 ppm), whereas the extract of *P. tinctorum* (710 ppm) and *P. aurata* (660 ppm) showed aluminium as the third highest element. Therefore, the mineral content of *R. taiensis* and *U. bismolliuscula* was found to be in the order of calcium > potassium > magnesium and aluminium but the extract of *P. tinctorum* was in the order of calcium > potassium > magnesium and *P. aurata* was in the order of aluminium > calcium > potassium > phosphorous. The extract of *R. taiensis* was found to possess more amount of calcium content (3800 ppm). The extract of *P. tinctorum* was found to have the highest potassium content. The aluminium content was high in the extract of *P. tinctorum* with the value of 710 ppm. In the case of *P. aurata*, the iron and magnesium and zinc contents showed higher concentrations than other lichen sample extracts. The mineral content of cobalt and cadmium were the least quantity of all lichen extracts.

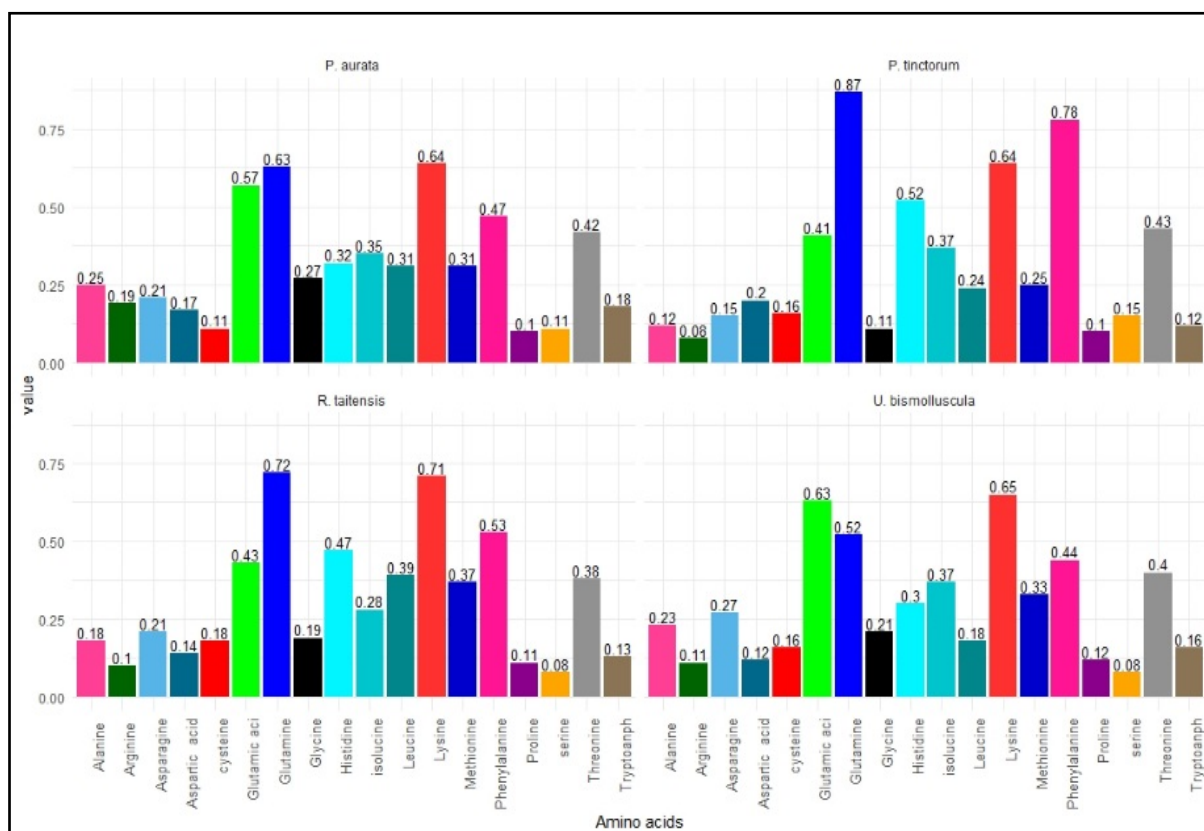
Vital minerals such as calcium (3800 ppm) and magnesium (710 ppm) were abundant in *R. taiensis*, and Sodium (200 ppm) and phosphorous were maximum in *P. tinctorum* compared to other lichens. Trace elements like Sr, Fe, B, Zn, Al, Si, Mn, and Cu also detected in all the analyzed lichens.

Table 2. Quantitative mineral element content of phytochemicals in lichen extracts

	<i>P. tinctorum</i> (ppm)	<i>P. aurata</i> (ppm)	<i>R. taitensis</i> (ppm)	<i>U. bismolluscula</i> (ppm)
Ca	1500	2500	3800	2000
Mg	510	420	710	530
Na	200	180	140	80
Sr	19	15	25	10
K	2000	1500	1600	1000
Fe	239	390	290	150
B	45	30	23	37
Zn	15	25	13	10
Al	710	660	340	460
Si	230	260	320	290
P	460	430	180	110
Mn	90	82	74	56
Cu	3.5	4.6	1.5	1
Co	0.1	0.4	0.5	0.2
Cr	0.2	0.7	1.2	1
Ni	1	1.2	1.4	1.2
Pb	40	28	30	17
Cd	0.1	0.3	0.5	0.2

3.1.4. Amino acids profiling of lichen samples

The amino acid composition of the lichen sample is shown in Figure 1. It was found that the proteins of the lichen contained adequate levels of amino acids. A total number of eighteen amino acids were identified from the studied samples. The estimated value of eight essential amino acids were found to be detected in all the four lichens. The amino acid glycine (0.27mg/g) was a dominant in *P. aurata* followed by alanine (0.25mg/g), arginine (0.19mg/g), tryptophan (0.18mg/g), aspartic acid (0.17mg/g). Glutamine (0.87mg/g), histidine (0.52mg/g), isoleucine 0.37mg/g, serine (0.15mg/g) and threonine (0.43mg/g) were higher in *P. tinctorum*. *R. taitensis* had its dominant amino acids of cystine (0.18mg/g), isoleucine (0.37mg/g), leucine (0.39mg/g), lysine (0.71mg/g), methionine (0.37mg/g) and phenylalanine (0.53mg/g). The amino acids of asparagine (0.27mg/g), glutamic acid (90.63mg/g) were more abundant in *U. bismolluscula*.

**Figure 1.** Amino acid profile of lichen extracts

3.1.5. Total phenolic content of lichen samples

Phenol plays an important role in scavenging free radicals present in the body. The TPC in *P. tinctorum*, *P. aurata*, *R. taitensis* and *U. bismolluscula* extracts were compared with the linear gallic acid standard curve. The phenolic amounts found in test samples of different lichen extracts were statistically evaluated and findings are shown in Table 3. The methanol extract of all the four lichen species showed a high amount of phenolic compound. In *R. taitensis*, it was 86.14 ± 1.42 mg GAE/g extract while *U. bismolluscula* had 55.60 ± 1.11 mg

GAE/g followed by *P. aurata* with the value of 40.4 ± 1.07 mg GAE/g extract and *P. tinctorum* had 39.5 ± 1.29 mg GAE/g extract. The aqueous extracts of *U. bismolluscula* showed the lowest phenolic content with the concentrations of 4.9 ± 1.31 mg GAE/g extract. The study was carried out following the method of Ng et al. (2020b) and Lapido et al. (2011). The considerable variation in total phenolic content was observed in our present study with the highest concentration of 86.14 ± 1.42 mg GAE / g extract in the methanol extract of *R. taitensis*.

Table 3. Estimation of total phenolics, flavonoids and ABTS radical scavenging activities, phosphomolybdenum, of lichen samples

Samples	Extracts	Total phenolics mg GAE / g extract	Total flavonoids mg RE / g extract	ABTS (mM TE/g extract)	Phosphomolybdenum (mg AAE/ g extract)
<i>P. tinctorum</i>	Petroleum ether	7.38 ± 0.10 ^j	8.63 ± 0.06 ^l	29.11 ± 1.06 ⁿ	27.78 ± 1.18 ⁱ
	Acetone	39.5 ± 1.29 ^c	17.6 ± 1.08 ^e	50.2 ± 4.9 ^f	37.00 ± 0.53 ^h
	Methanol	26.4 ± 1.15 ^d	25.8 ± 1.10 ^d	73.7 ± 5.2 ^b	42.56 ± 1.35 ^g
	Water	9.15 ± 1.21 ^l	5.9 ± 1.07 ⁿ	35.62 ± 0.03 ⁱ	31.62 ± 0.29 ^j
<i>P. aurata</i>	Petroleum ether	11.26 ± 0.03 ^h	7.73 ± 0.05 ^m	17.6 ± 6.10 ^o	27.35 ± 1.74 ⁱ
	Acetone	16.3 ± 2.04 ^f	10.6 ± 1.07 ^c	42.7 ± 5.11 ^g	50.68 ± 1.15 ^f
	Methanol	40.4 ± 1.07 ^b	26.9 ± 1.14 ^j	62.3 ± 15.1 ^c	68.54 ± 1.64 ^d
	Water	13.8 ± 0.01 ^g	3.6 ± 1.03 ^o	37.15 ± 0.04 ^h	59.74 ± 2.03 ^e
<i>R. taiensis</i>	Petroleum ether	12.01 ± 1.02 ^h	14.4 ± 1.088 ^g	29.5 ± 5.06 ^m	55.81 ± 0.08 ^f
	Acetone	22.87 ± 0.12 ^e	11.7 ± 1.10 ^f	30.4 ± 1.9 ^l	87.26 ± 0.39 ^b
	Methanol	86.14 ± 1.42 ^a	17.04 ± 0.04 ^h	53.12 ± 6.5 ^e	150.68 ± 1.15 ^a
	Water	6.3 ± 1.06 ^k	9.5 ± 1.08 ^k	14.2 ± 7.4 ^p	63.24 ± 0.391 ^e
<i>U. bismolluscula</i>	Petroleum ether	12.58 ± 0.082 ^h	11.36 ± 0.05 ⁱ	35.1 ± 6.1 ^j	72.47 ± 2.15 ^c
	Acetone	14.7 ± 1.04 ^e	30.05 ± 1.17 ^b	60.3 ± 14.2 ^d	51.196 ± 0.78 ^f
	Methanol	55.60 ± 1.11 ^a	31.2 ± 1.10 ^a	85.6 ± 0.5 ^a	87.78 ± 0.48 ^b
	Water	4.9 ± 1.31 ^k	10.4 ± 1.01 ^j	32.3 ± 2.19 ^k	71.93 ± 0.25 ^c

Values are mean of triplicate determination (n=3) ± standard deviation, % - % of Inhibition.

GAE-Gallic Acid Equivalents, RE- Rutin, TE- Trolox Equivalents. AAE- Ascorbic Acid Equivalents.

Statistically significant at $p < 0.05$ where ^a > ^b > ^c > ^d > ^e > ^f > ^g > ^h > ⁱ > ^k > ^m > ⁿ > ^o > ^p, in each column.

The results of the present study are strongly supportive in agreement to the findings of Rice-evans *et al.* (1995) and Singleton *et al.* (1999) that the TPC content of lichen extracts are responsible for antioxidant and biological activities of lichen extracts. Ganesan *et al.* (2015). Observed that the TPC value was significantly higher in the extract of benzene (154.2 mg GAE/g) than in other *P. tinctorum* extracts and reported that the availability of phenolic content sources could trigger the activity of lichen metabolites which probably play a subtle role in antimicrobial and antioxidant activities. The results are not in agreement with the report given by Ganesan *et al.*, (2015). The relative TPC values of lichen or tested plants may be varied due to age of the plant, methods of extraction procedure, choice of solvents, number of replicates used for investigation etc. Singleton *et al.* (1999) observed the number of phenolic groups in their native structure and reported that this may have the major reason for difference found between biological activities of lichen extracts. Rice-Evans *et al.* (1995) reasoned phenolic compound has the high potency of antioxidants because it acts as the single oxygen quenchers and oxygen donors. As reported, the acetone extracts of *P. austrosinense* and *P. tinctorum* exhibited high TPC corresponding to its high free radical scavenging activities (Kalidoss *et al.*, 2019).

3.1.6. Total flavonoid content of lichen samples

The TFC was determined in *P. tinctorum*, *P. aurata*, *R. taiensis* and *U. bismolluscula* and the results are presented in the Table 3. The highest TFC was observed in methanol extracts of *U. bismolluscula* (31.2 ± 1.10 mg RE/g extract) followed by *P. aurata* (26.9 ± 1.14 mg RE/g extract) and *P. tinctorum* (25.8 ± 1.10 mg RE/g extract) and *R. taiensis* (17.04 ± 0.04 mg RE/g extract). The aqueous extracts of *P. aurata* was found to be lower (3.6 ± 1.03 mg RE/g

extract). The results reported by Ng, Koick and Yong (2020a) are strongly supportive in agreement to the present investigation that the flavonoid and phenolic constituents of plant extracts are considered to be beneficial for health particularly for the antioxidant action. Thus, the use of lichen extracts for health benefits particularly for nutraceutical applications can be justified on the basis that these lichens were once thought to be medicinal is really due to their TPC, TFC and other chemical constituents.

3.2. In vitro antioxidant assays

3.2.1. DPPH radical scavenging activity

The DPPH radical scavenging activities of different lichen extracts of *P. tinctorum*, *P. aurata*, *R. taiensis* and *U. bismolluscula* are shown in the Figure 2. The IC₅₀ values (concentration of sample required to scavenging 50% of free radicals) were calculated from the regression equation prepared from the concentration of the extracts versus percentage inhibition of free radical formation. A lower IC₅₀ value indicates the greater DPPH radical scavenging activity. Among the all the lichens analysed the acetone extract of *P. aurata* shows lower IC₅₀ value of 93.339 µg/mL than the acetone extract of *U. bismolluscula* (106.786 µg/mL), petroleum ether extract of *R. taiensis* 146.9266 µg/mL and acetone extract of *P. tinctorum* (162.488 µg/mL). The petroleum ether extract of *P. tinctorum* shows minimal antioxidant activity with the highest IC₅₀ value of 372.825 µg/mL. The IC₅₀ value for ascorbic acid (20.32 µg/mL) standard employed in DPPH assay of the present study is closer to the value given by Ng *et al.* (2020c). The present study showed significant half the inhibition concentration of ascorbic acid standard with the IC₅₀ value of 20.32 µg/mL as compared to 23.45 mmol/L showed by Ng *et al.* (2019).

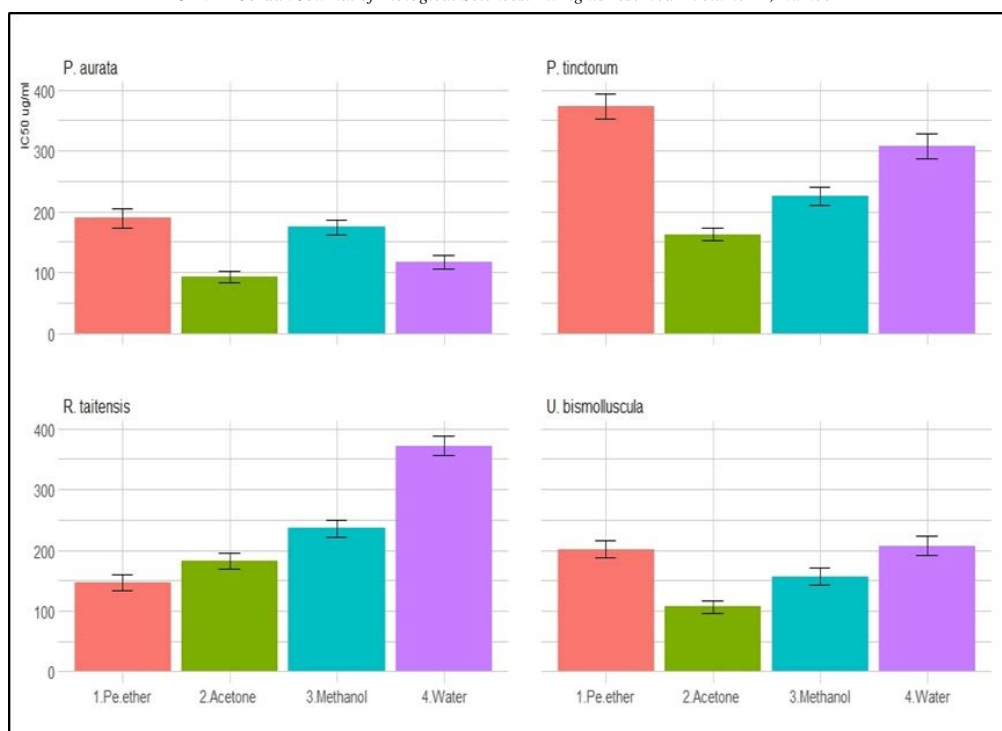


Figure 2. DPPH radical scavenging activity of lichen extracts

3.2.2. Superoxide anion radical scavenging activity

Superoxide anion radical scavenging activities of *P. tinctorum*, *P. aurata*, *R. taiensis* and *U. bismolluscula* were analysed, and the results are shown in Figure 3. The extracts were found to be containing high scavenging potential of superoxide radicals generated in riboflavin-NBT- light system. The water extract of *P. tinctorum*, was

showing higher (83 %) scavenging potential than the other extracts. The minimum activity with the IC₅₀ value was found in acetone extract of *P. aurata* (0.78%). The result proves that the percentage of inhibition is based on the concentration of the bioactive phenolic compounds present in solvent extract.

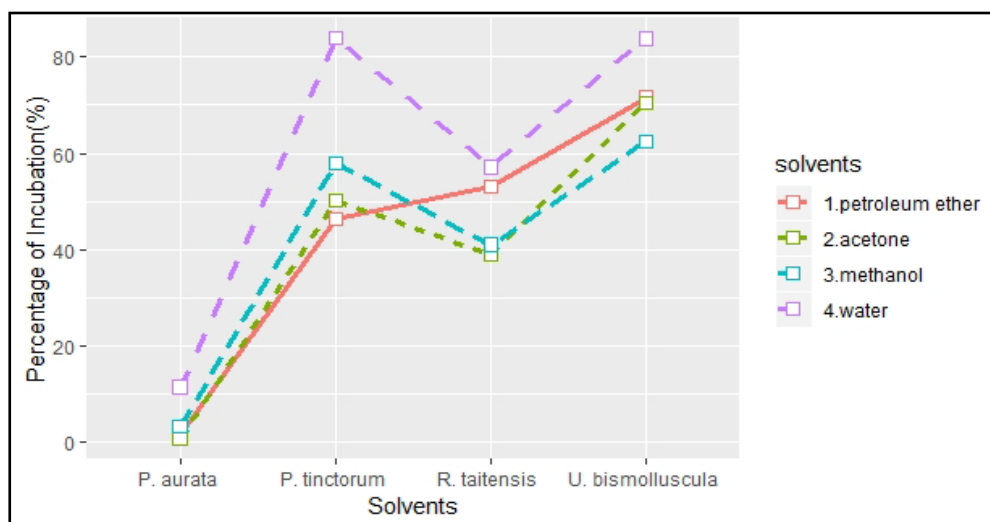


Figure 3. Superoxide radical scavenging activity of lichen extracts

3.2.3. ABTS⁺ radical scavenging activity

The extracts of *P. tinctorum*, *P. aurata*, *R. taiensis* and *U. bismolluscula* showed their antioxidant activities with regard to ABTS scavenging abilities (Table 3). The methanol extracts of *U. bismolluscula* showed highest ABTS scavenging activity with the value of 85.6 ± 0.5 mM TE/g extract. The methanol extract of *P. tinctorum* and *P. aurata* showed moderate activity with the values of 73.7 ± 5.2 and $62.3 \pm$

15.3 mM TE/g extract respectively. However, the methanol extracts of *R. taiensis* showed minimal scavenging values (53.12 ± 6.5 mM TE/g extract). The values of the various extracts of lichens for the ABTS scavenging activity falls in the order of *U. bismolluscula* > *P. tinctorum* > *P. aurata* > *R. taiensis* respectively. The standard rutin showed strong ABTS scavenging activity (111.3 ± 0.52 mM TE/g extract). Compared to that of standard rutin, moderate ABTS scavenging activity was observed in the methanol extract of *U. bismolluscula* (highest value of 85.6 ± 0.5 mM TE/g extract) in the

present study. Similar study conducted by Ng *et al.* (2020a) showed 0.01 mg/mL for trolox standard as compared to 111.3 ± 0.52 mM TE/g extract for rutin in the present study. Variations in the values are due to variations in the test standard.

3.2.4. Phosphomolybdenum reduction assay

The phosphomolybdenum assay was mostly used to measure the total antioxidant activity of substances and the results are presented in the Table 3. Among the different extracts *P. tinctorum*, *P. aurata*, *R. taiensis* and *U. bismolliuscula*, methanol extracts of *R. taiensis* showed highest value of reducing ability compared with other extracts (150.68 ± 1.15 mg AAE/ g extract). The methanol extracts of *P. tinctorum*, *P. aurata* and *U. bismolliuscula* were found to have moderate level of antioxidant activity with the concentrations of 42.56 ± 1.35 , 68.54 ± 1.64 and 87.78 ± 0.48 mg AAE/ g extract respectively. The rutin standard showed maximum activity (158.39 ± 1.79 mg AAE/ g extract) compared with lichen extracts in phosphomolybdenum reduction assay. The study carried out in methanol extracts of four lichen thalli showed maximum phosphomolybdenum activity when compared to the other solvent extracts. The phosphomolybdenum reduction value in methanol extract of *R. taiensis* is closer to the rutin standard.

4. Discussion

The nutritional constituents of two foliose and two fruticose forms of lichen species were documented as described by Hu *et al.* (2020); Rahman *et al.* (2018); Kekuda, *et al.* (2011); Joubert *et al.* (1982). The previous literature asserted that the nutritional contents of lichens such as tannins, flavonoids and phenolics are being used as medicine and can be useful to fortify them in human foods. Lichens and plants differ considerably in phytochemical constituents. Since many wild animals and mammals eat lichen as diets, it is vital to measure the nutritional content of lichens. The nutrient content of foliose lichen was comparable with fruticose lichen in all macro element parameters except ash content. The moisture content of the four different lichens was found to be in the order of *P. tinctorum* > *R. taiensis* > *U. bismolliuscula* > *P. aurata*. This may be the reason to suggest that the *P. tinctorum* weighs heavier than other lichens.

Compared with foliose forms, fruticose lichens were deficient in starch and ash content. Fruticose were also lower in energy than foliose lichen. Many lichen species are also shown to be eaten by many mammals such as red-backed voles, deer and squirrels and thereby may play an important role in economic botany as nutritional benefits to plants and animals.

Previous literatures have shown that organic solvents are generally used for extraction of lichen metabolites because lichen substances are either insoluble or partial soluble in water. Most organic solvent-soluble antioxidants are either bound to cortex or medulla in lichen thalli. Solvent extracts from test samples of four different lichen thalli responded effectively to various biological assays in the present investigation. The extract of a particular lichen substance influences the efficiency of biological assays and is based on the polarity of solvent.

According to Sarker *et al.* (2006), the use of organic solvent, methanol for extraction of metabolites to winged been seeds has been successful because these affected easy extraction process in many ways and that the methanol penetrated the thick seed coat structure and promoted fast recovery of plant nutrients. The mechanism behind the effect of solvent property may also depend on the electron-transfer kinetic mechanism and physiochemical properties (lipophilic and hydrophilic properties) of the phytochemical compounds. Previous records have shown that the ideal solvent examined for extracting the antioxidant compounds of *P. tetragonolobus* was methanol in antioxidant assays (Ng *et al.*, 2020b). This is in agreement with our findings that the methanol extract of all the four lichens had the highest radical scavenging activity and the values are comparable to the standard.

The use of petroleum ether and water had found negative effects in the present study on ABTS, DPPH, superoxide scavenging and phosphomolybdenum reduction assays by showing the weak activity (the highest IC₅₀ or low mM TE/mg values) with minimal antioxidants to scavenge radicals inhibiting cellular damage. The primary reason for lowest antioxidant activity may be attributed to the relative total antioxidant contents possessed in solvent extracts. Similarly, the considerable variation in types of substances or antioxidants has also been observed in the present investigation, thus they reacted differently to the range of solvents on the basis of their polarity. The radical scavenging activity suggested a contrast between the electron transfer kinetic mechanism of substances in solvent extracts. The DPPH radical scavenging power is attributed to the lipophilic antioxidants while, the ABTS antioxidant assay detects lipophilic and hydrophilic substances (Ng & See 2019) in the extracts indicating the differences in the antioxidant activity between these two scavenging assays.

The antioxidant activity may also be affected by enzymatic antioxidants. Previous literature indicated that the metabolite accumulation in plant part infers the induction of defence mechanism. Therefore, under abiotic stress, enzymatic antioxidants like, Superoxide dismutase and Quinone oxidoreductase are induced for scavenging reactive oxygen species (ROS). Superoxide dismutase play a significant role in the catalytic conversion of highly reactive superoxide anions to oxygen molecule while the quinone oxidoreductase enzymatic antioxidant involves in the conversion of highly reactive quinone to less reactive hydroxy quinones. This process of conversion of ROS is termed redox homeostasis defence mechanism (Ng *et al.*, 2014). The same reason may also be applicable to the present investigation that the level of enzymatic antioxidants in different solvent extracts might influence radical scavenging activities in antioxidant assays.

4.1. Proximate composition of samples

All the macro and micro nutrients estimated were found to be higher in fruticose form than in foliose form of lichen (Table 1). The results showed that the former had the profuse development and growth when compared to the latter. The mean average total carbohydrate and protein contents were higher in fruticose (54.32 and 19.525 mg glucose equivalent respectively) than in foliose (48.115 and 18.715 % respectively) but there was no significant difference drawn between foliose and fruticose forms of

lichen in the amount of macronutrient. Kirkpatrick (1996) found that *Bryoria* spp., contained considerable quantities of soluble carbohydrates and pointed out that it had low fiber and phenolic contents. Robbins (Robbins 1987) found that the crude protein content of *Alectoria sarmentosa* lichen was just 2% and an outcome was nitrogen losses in feces of mule deer.

Starch content was found to be 0.17 ± 0.03 mg glucose equivalents/g of samples in foliose followed by 0.13 ± 0.05 mg in fruticose lichens. Similar to that of macro-elements, the mean average ash content was more pronounced in foliose lichen (7.93%) followed by fruticose (3.42%) lichens. Moreover, such differences are determined experimentally, and the results were affected by environmental conditions such as air, pH of the substrata, temperature ...etc. There were no correlations between moisture and macro nutrient content in lichen growth forms (Table 1).

Thallus of *P. tinctorum* had a greater amount of ash content at 13.93% when compared to *R. taiensis* at 4.41%. The ash content of *U. bismolliuscula* thallus was found to be 2.43 % higher than 1.93% of *P. aurata*. The nutritional studies (Table 1) with thallus of foliose and fruticose lichen showed differences in starch, protein and total carbohydrate. This shows the significance of incorporating ash content in the analysis as majority of the nutritional content is included in the ash.

It follows from the results that foliose and fruticose lichen significantly differ in their nutritional values. Such differences are determined experimentally and may also be influenced by the nature of thallus.

4.2. Mineral composition of lichen samples

Carbohydrates, proteins, fats and vitamin constituents are more common in all plants determining the nutritional quality of any forage. This macro nutrient together with micro elements form a fodder for reindeer, caribou, squirrels. These micronutrients have been described to have many physiological functions such as anti-oxidant defence activity, electrolytic activity, components of enzymes, gas transport, regulate cellular energy transduction and regulate physico-chemical processes. Therefore, these microelements play a vital role on all living matter. The result of the present study is in accordance with Vinayaka *et al.* (2013) reported the content of calcium was highest among all other elements in *U. pictoides*. Similar result was obtained by Kekuda *et al.* (2011) for the lichen extracts of *Everniastrum cirrhatum* where the content of calcium was highest among all micronutrients. The reason for the difference in microelements is probably due to variation in abiotic and biotic factors viz., habitats, age of lichen, solvent used for extraction procedure and origin of plant materials.

4.3. Amino acids profiling of lichen samples

It was found that the lichen extracts contained sufficient amount of amino acids as compared to reports from WHO/ FAO 2007. The comprehensive outcome of this research culminates in the assumption that glutamine has a higher volume relative to all other amino acids in *P. tinctorum* in the present study. Supportive finding was recorded from Jäger and Weigel (1978) who reported that a conceivable intention for this similarity is that glutamine seems to play important role in nitrogen fixation and

Pseudevernia furfuracea (L.) Zopf was possessing high amounts of glutamic acid, aspartic acid, alanine, arginine, and taurine etc. Shelukheeva and Nikolaeva (2015) reported that amino acid content of *Cetraria islandica* and *C. laevigata* was found to possess 16 different amino acids, of which seven were essential. The present study detected 18 different amino acids from four different lichen samples.

4.4. Estimation of total phenolic content (TPC)

Singleton *et al.* (1999) observed the number of phenolic groups in their native structure and reported that this may have the major reason for variation in biological activities of lichen extracts. Rice-Evans *et al.* (1995) reasoned phenolic compound has the high potency of antioxidants because it acts as the single oxygen quenchers and oxygen donors. As reported, the acetone extracts of *P. tinctorum* exhibited high phenolic content corresponding to its strong free radical scavenging activity.

4.5. 4.1.5. Estimation of total flavonoid content (TFC)

In the present study, highest TFC was observed in the methanol extract of *U. bismolliuscula* 31.2 ± 1.10 mg RE /g while the least was in the aqueous extract of *P. aurata* 3.6 ± 1.03 mg RE /g. But, Ganesan *et al.* (2015) observed that the TFC of lichen extracts ranged from 20.16 to 50.72 mg RE/g, and the higher content was found in aqueous extract 50.72 ± 0.13 and lower in ethanolic extract 20.16 ± 0.11 mg RE/g. The results of the present study are in line with the Raj *et al.* (2014) reported that the total flavonoid and phenolic contents of *Parmotrema tinctorum* extracts were found to be 5.82 ± 0.96 mg quercetin equivalents/g and 9.67 ± 0.73 mg gallic acid equivalents/g of extract respectively.

4.6. DPPH radical scavenging activity

DPPH scavenging assay was conducted to identify substantial antioxidant activity. DPPH is a free radical used to measure the scavenging potential of any phytochemical compounds. Among all four lichen extracts, the IC₅₀ value of acetone extract of *P. aurata* (93.339 µg/ml) is comparable to that of ascorbic acid (20.32 µg/ml). The DPPH scavenging results are supportive in agreement to Ristic *et al.* (2016) where lecanoric acid showed weak activity with the highest IC₅₀ value of 424.51 µg/mL. Thus, this suggested that the polarity of solvent extract that determines the DPPH radical scavenging activity of phytochemical compounds.

4.7. Superoxide anion radical scavenging activity

The biological enzyme XO (xanthine oxidase) has significance in catalysing the bioconversion of hypoxanthine to xanthine and to uric acid while the SOD (superoxide dismutase) in superoxide into hydrogen peroxide and oxygen in biological tissues. The superoxide radical scavenging activity of the present analysis is in accordance with the Behera *et al.* (2016) who reported that the methanol extract of *U. ghattensis* exhibited strong activity with the value of 56%. The secondary metabolite of *U. ghattensis* contains usnic acid. The known standards BHA, BHT and quercetin showed scavenging activity with the value of 59, 68 and 47 % respectively. Kosanić *et al.* (2014) found that highest super oxide anion scavenging activity (67.37%) was observed in the acetone extracts of the lichen *Lasallia pustulata*. Aqueous extract of lichen

Parmelia sulcata showed the least scavenging activity (12.74%). The *P. tinctorum* aqueous extract of the present study showed the strong scavenging activity with the 87% while the weak activity was observed in acetone extracts of *P. aurata* with the lowest value of 0.78%.

4.8. ABTS⁺ radical scavenging activity

The comparison of the secondary metabolites of the tested lichen extracts and their free radical scavenging ability revealed a strong correlation with the previous study conducted by Raj *et al.* (2014). The solvent of choice greatly influenced the ABTS scavenging activity in extracts of all the four different lichen samples. This ethyl acetate extract of *P. tinctorum* exhibited significant antioxidant potential against ABTS with half the inhibitory concentrations of 151.34 ± 1.79 mg/mL and the results are supportive in agreement to the previous literature depicted that the antidiabetic nutraceutical properties have been identified from *P. tinctorum* samples. In the present study, petroleum ether and aqueous extract of *P. tinctorum* showed less activity when compared with acetone and methanol extracts. The highest activity was shown in methanol extract (85.6 ± 0.5 mM TE/g extract) of *U. bismolliuscula* followed by the *P. tinctorum* extract (73.7 ± 5.2 mM TE/g extract). The results of ethyl acetate extract of *P. tinctorum* are supportive in agreement to the report given by Raj *et al.* (2014). Ganesan *et al.* (2017) found that methanol extract of *Ramalina inflata* (80 µg/ml) was significantly lower than benzene extract (100 µg/ml) of those recorded in the fruticose lichen. The results of the present study are consistent with the report of Ganesan *et al.* (2017), in that the antioxidant activity in the petroleum ether extract was lower than that of the other extracts. The results of ethanol extract of *U. longissima* are in accordance with the findings of Aydin *et al.* (2018) who reported that ABTS radical scavenging assay for *U. longissima* ethanol extract and ethyl acetate were found as $73.31 \pm 0.007\%$ at 4000 µg/mL and $54.92 \pm 0.010\%$ at 4000 µg/ml respectively. Compared with standard control, in the present study, ABTS radical scavenging activity of acetone extract of *U. bismolliuscula* was found to be high (60.3 ± 14.2 mM TE/g extract) while the petroleum ether and aqueous extracts exhibited weak activity. The disparity in ABTS scavenging activity of lichen extracts may be due to variation in environment, lichen species, assessment methods and types of solvents used by researchers (Kazazic *et al.*, 2016).

4.9. Phosphomolybdenum reduction assay

In the present study, strong antioxidant activity was amounted to 150.68 ± 1.15 mg AAE/ g for methanol extracts of *Ramalina taitensis*. Previous literature has

reported the antioxidant properties of solvent extracts of many species of lichen, but the present study is the first attempt to document the phosphomolybdenum reduction assay of four different lichen extracts of commonly available lichen species such as *P. tinctorum*, *P. aurata*, *R. taitensis* and *U. bismolliuscula*. The results showed that the methanol extract had a higher phenolic content (except *P. tinctorum*), which in turn exhibited strong antioxidant potency than the other extracts. The present result is in agreement with Dandapat and Paul (2019) who opined that methanol is an ideal solvent for extraction of lichen bioactive compounds for antioxidant activities. It is suggested that the increase in phenolic groups in chemical structure of lichen compounds can have corresponding increase in antioxidant activity. This is in conformity with the reports of Tomović *et al.* (2016).

The results of Manojlovic *et al.* (2012) are in accordance to the present study that the redox properties of phenolic content in methanol extract activated the neutralizing free radicals activity which play a subtle role in quenching triplet and singlet oxygen. They have shown that a significant difference in TPC was observed between chloroform (71.32 ± 0.89) and methanol extracts (79.2 ± 0.59 mg GA/g) of *Umblicaria cylindrica*, and it was correlated with their antioxidant activity of 68.35 ± 0.15 µg AA/g and 74.65 ± 0.75 µg AA/g respectively. Similarly, Tomović *et al.* (2016) reported the supportive results for total antioxidant capacity with the concentrations of 91.52 ± 0.34 µg AA/g and 71.5 ± 0.29 µg AA/g, for methanol and ethyl acetate extracts of *Cetraria aculeata*, respectively.

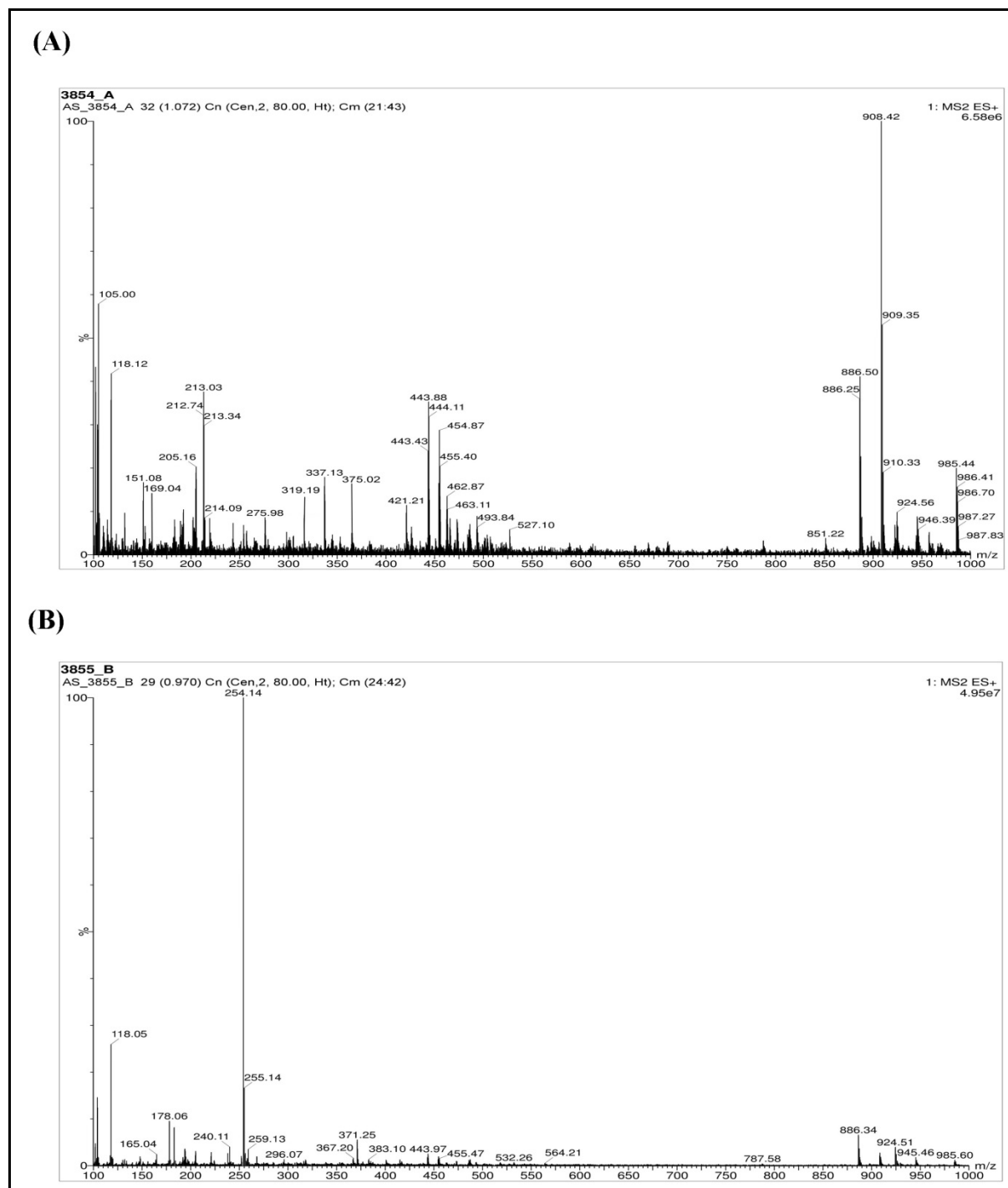
4.10. Compound identification by Liquid

Chromatography Mass Spectrometry (LC/MS)

The results obtained from the studies indicated that methanol extract showed higher activity than other solvents. The Liquid Chromatography Mass Spectrometry study was conducted to find out the active lichen compounds in test samples and the chromatogram are shown in the Figure 4 & 5. Major peaks with relative Mass spectral data were observed from chromatogram. The lichen compounds were detected based on their (Chemindex) library data base. The major lichen substances like atranorin, sekikaic acid, usnic acid, and other compounds identified are presented in Table 4. The findings are in line with the previous literature (Musharraf *et al.*, 2015). Biologically important phytochemicals are present in *P. tinctorum*, *P. aurata*, *R. taitensis* and *U. bismolliuscula*. It can be suggested that the antioxidant activity is determined by their biologically active compounds in the solvent extract.

Table 4. Compound Identification of lichen extract by LCMS method

S.No	Compound Name	Exact mass (m/z)	Observed mass (m/z)	Precursor m/z	Molecular formula
<i>Parmotrema tinctorum</i>					
1.	Diethanolamine	105.14	105.00	117.01 -ve	C ₄ H ₁₁ NO ₂
2.	Succinic acid	118.09	118.12	119.03 +ve	C ₄ H ₆ O ₄
3.	D-Carvone	150.22	151.08		C ₁₀ H ₁₄ O
4.	Orsellinic acid	168.15	169.04	167.03 -ve 167.10 -ve	C ₈ H ₈ O ₄
5.	Eugenitol	206.19	205.16	205.04 -ve 207.06 +ve	C ₁₁ H ₁₀ O ₄
6.	Volemitol	212.2	213.03	211.08 -ve	C ₇ H ₁₆ O ₇
7.	Lecanoric acid	318.28	319.19	317.06 -ve 317.06 -ve	C ₁₆ H ₁₄ O ₇
8.	Methyl protolichesterinate	338.5	337.24		C ₂₀ H ₃₄ O ₄
9.	Atranorin	374.3	375.02	373.09 -ve	C ₁₉ H ₁₈ O ₈
10.	Thamnolic acid	420.3	421.21	419.06 -ve	C ₁₉ H ₁₆ O ₁₁
11.	Perlatolic acid	444.5	443.88	443.2 -ve	C ₂₅ H ₃₂ O ₇
12.	Lobaric acid	456.5	455.4	457.18 ive	C ₂₅ H ₂₈ O ₈
13.	Leucotylin	460.7	462.87		C ₃₀ H ₅₂ O ₃
<i>Pseudocephalaria aurata</i>					
14.	Succinic acid	118.09	118.05	117.01 -ve 119.03 +ve	C ₄ H ₆ O ₄
15.	5,7Dihydroxy-6-methylphthalide	180.04	178.06		C ₉ H ₈ O ₄
16.	Chrysophanol	254.24	254.14	255.06 +ve	C ₁₅ H ₁₀ O ₄
17.	Conorlobaridone	370.14	371.25		C ₂₁ H ₂₂ O ₆
<i>Ramalina taiensis</i>					
18.	Fumaric acid	116.07	118.05	115.00 -ve	C ₄ H ₄ O ₄
19.	D-Arabinose	150.13	151.04	149.04 -ve	C ₅ H ₁₀ O ₅
20.	Methyl orsellinate	182.17	183.06	181.05 -ve	C ₉ H ₁₀ O ₄
21.	Cholin sulphate	183.05	184.12		C ₅ H ₁₃ NO ₄ S
22.	Methyl β-ornicolcarboxylate	196.2	197.08	195.06 -ve	C ₁₀ H ₁₂ O ₄
23.	Fukinanolide	234.33	236.14		C ₁₅ H ₂₂ O ₂
24.	Methyl porphyrilate	328.13	330.12		C ₁₇ H ₁₂ O ₇
25.	Usnic acid	344.3	345.08	343.08 -ve	C ₁₈ H ₁₆ O ₇
26.	3'-Dechlorolecideoidin	364.03	367.23		C ₁₇ H ₁₃ ClO ₇
27.	Sekikaic acid	418.4	419.35	417.14 -ve	C ₂₂ H ₂₆ O ₈
<i>Usnea bismolliuscula</i>					
28.	Diethanolamine	105.14	104.07		C ₄ H ₁₁ NO ₂
29.	Indolyl-3-acetic acid	175.18	175.04	176.06 +ve	C ₁₀ H ₉ NO ₂
30.	Olivetolmonomethylether	194.13	193.09		C ₁₂ H ₁₈ O ₂
31.	Ethyl everninate	210.23	211.11		C ₁₁ H ₁₄ O ₄
32.	Olivetolcarboxylic acid	224.25	225.17	223.09 -ve	C ₁₂ H ₁₆ O ₄
33.	Fukinanolide	234.33	236.14		C ₁₅ H ₂₂ O ₂
34.	Linoleic acid	280.4	279.27	279.23 -ve	C ₁₈ H ₃₂ O ₂
35.	Usnic acid	344.3	345.08	343.08 -ve	C ₁₈ H ₁₆ O ₇
36.	4-O-Methyl-5-dechlorovicanicin	362.09	363.10		C ₁₉ H ₁₉ ClO ₅



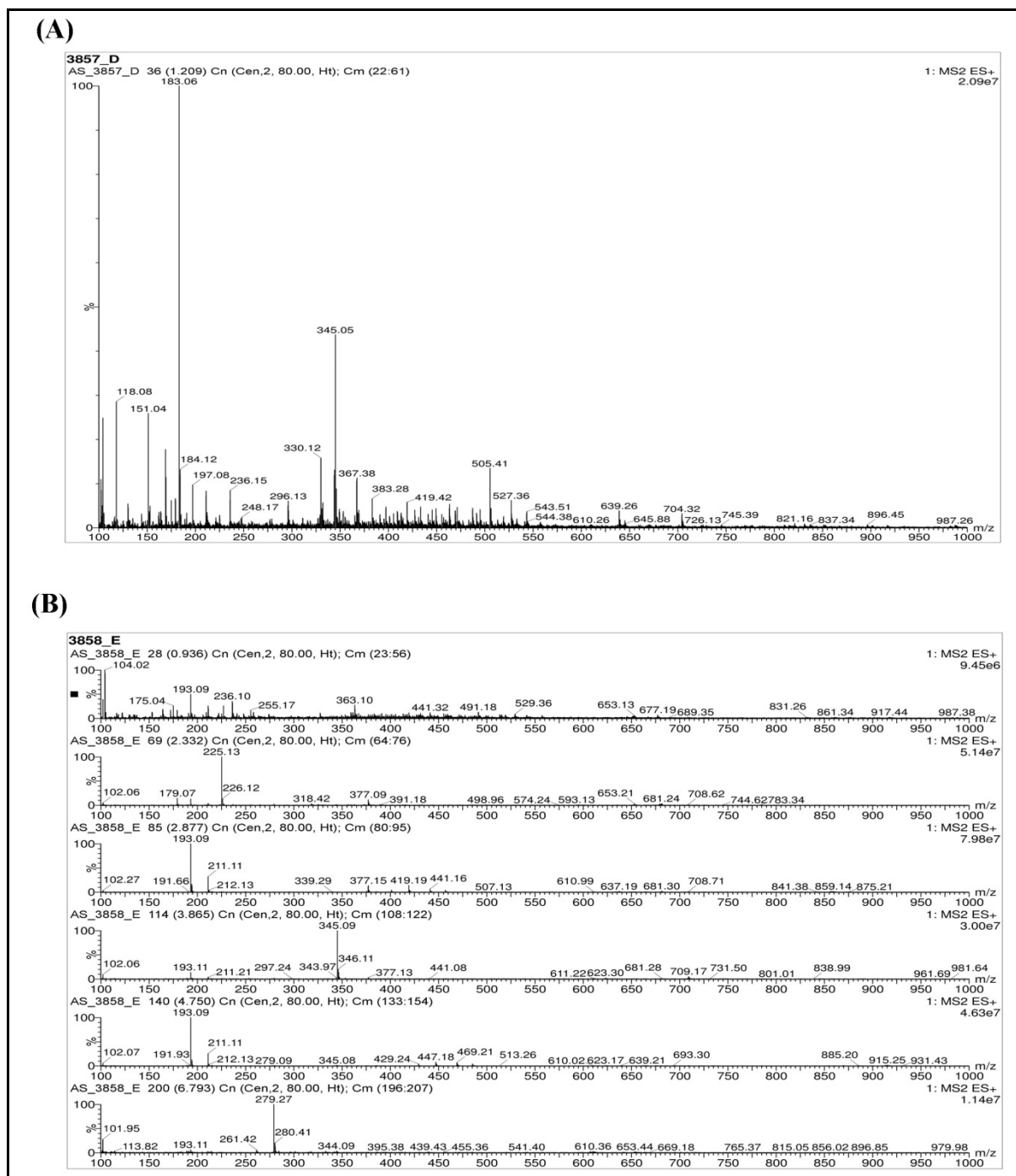


Figure 5. LC MS Chromatogram of A) *Ramalina taitensis* B) *Usnea bismolliuscula* extracts

5. Conclusion

The present research concluded that the extracts of *Parmotrema tinctorum*, *Pseudocyphellaria aurata*, *Ramalina taitensis*, *Usnea bismolliuscula* exhibited a variety of phytochemical constituents in solvent extracts. The moderate antioxidant activities of methanol extract depicted the possible application of these lichens in pharmacology. These can be a promising alternative to synthetic antioxidants. Additionally, it is suggested that the lichen substances such as atranorin, sekikaic acid, usnic acid detected in solvent extracts using LC/MS are responsible for radical scavenging activity. Further animal

studies are underway to assess the cytotoxicity effects of these lichen extracts.

Acknowledgement

Authors express their gratitude to Dr. A. Rajendran, Professor and Head, Department of Botany, Bharathiar University, Coimbatore, Tamil Nadu, India for providing excellent help throughout this research work. The authors wish to acknowledge the UGC-SAP and DST- FIST, Government of India for their funding towards this study.

Conflict of interest

The authors have no conflict of interest.

References

- Abdel-Mawgoud M, Khedr FG, Mohammed EI. 2019. Phenolic Compounds, Antioxidant and Antibacterial Activities of *Rhus flexicaulis* Baker. *Jordan J Biol Sci*, **12**:17–21.
- AOAC AA of OA. 1990. **Official methods of analysis** 15th ed. Method 991.43. Association of Official Analytical Chemists, Arlington, VA, USA.
- Awasthi DD. 2007. **Compendium of the Macrolichens from India, Nepal and Sri Lanka**. Bishen Singh Mahendra Pal Singh, Dehradun, India.
- Aydin S, Kinalioğlu K, Sökmen BB. 2018. Antioxidant, anti-urease and anti-elastase activities of *Usnea longissima* Ach. *Bangladesh J Bot*, **47**:429–435.
- Behera BC, Mangesh V. Morey, Subhash B. Gaikwad. 2016. Anti-lipoxygenase, Radical Scavenging and Antimicrobial Activities of Lichen Species of Genus *Heterodermia* (Physciaceae). *Bot Pacifica J Plant Sci Conserv*, **5**:79–85.
- Biney EE, Nkoom M, Darkwah WK, Puplampu JB. 2020. High-performance liquid chromatography analysis and antioxidant activities of extract of *Azadirachta indica* (Neem) leaves. *Pharmacogn Res*, **12**:29.
- Chowdhery HJ. 2014. Studies on the Subfamily Apostasioideae (Orchidaceae) in India. *Nelumbo*, **56**:1–13.
- Dandapat M and Paul S. 2019. Secondary metabolites from lichen *Usnea longissima* and its pharmacological relevance. *Pharmacogn Res*, **11**:103.
- Gaafar AA, Asker MS, MA A, Salama ZA. 2019. The Effectiveness of the Functional Components of Grape (*Vitis vinifera*) Pomace as Antioxidant, Antimicrobial, and Antiviral Agents. *Jordan J Biol Sci*, **12**:625–635.
- Ganesan A, Purushothaman D, Muralitharan U, Subbaiyan R. 2017. Metabolite profiling and in vitro assessment of antimicrobial and antioxidant activities of lichen *Ramalina inflata*. *Int Res J Pharm*, **7**:132–138.
- Ganesan A, Thangapandian M, Ponnusamy P, Sundararaj JP, Nayaka S. 2015. Antioxidant and antibacterial activity of parmelioid lichens from Shevaroy hills of Eastern Ghats, India. *Int J Pharm Tech Res*, **8**:13–23.
- Hu Q, Liu J, Li J, Liu H, Dong N, Geng Y, Lu Y, Wang Y. 2020. Phenolic composition and nutritional attributes of diaphragma *juglandis fructus* and shell of walnut (*Juglans regia* L.). *Food Sci Biotechnol*, **29**:187–196.
- Jäger H-J, Weigel H-J. 1978. Amino acid metabolism in lichens. *Bryologist*, 107–113.
- Joubert JJ, Steyn PL, Britz TJ, Wessels DCJ. 1982. Chemical composition of some lichen species occurring in the Namib Desert, South West Africa. *Dinteria*, **16**:33–43.
- Kazacic M, Djapo M, Ademovic E. 2016. Antioxidant activity of water extracts of some medicinal plants from Herzegovina region. *Int J Pure App Biosci*, **4**:85–90.
- Kalidoss. R, Merlin. J, Charumathy. M, Surekha. S, Arun Prasath. K, Mariraj. M, Shenbagam. M, Rajaprabu. N, and Ponmurugan. P. 2019. Lichen collections from Nilgiris of Western Ghats in Tamil Nadu and screening for antimicrobial, antioxidant efficacy of some selected species. *Pramana research journal*. **9(6)**: 1364–1386.
- Kekuda TRP, Vinayaka KS, Swathi D, Suchitha Y, Venugopal TM, Mallikarjun N. 2011. Mineral Composition, Total Phenol Content and Antioxidant Activity of a Macrolichen *Everniastrum cirrhatum* (Fr.) Hale (Parmeliaceae). *E-J Chem*, **8**:1886–1894.
- Kirkpatrick RC. 1996. Ecology and behavior of the yunnan Snub-Nosed langur (*Rhinopithecus bieti*, Colobinae) [Ph. D. dissertation]. University of California.
- Kosanić M, Ranković B. 2010. Screening of antimicrobial activity of some lichen species in vitro. *Kragujevac J Sci*, **32**:65–72.
- Kosanic M, Rankovic B, Stanojkovic T, Vasiljevic P, Manojlovic N. 2014. Biological activities and chemical composition of lichens from Serbia. *EXCLI j*, **13**:1226.
- Ladipo MK, Doherty VF, Kanife UC. 2011. Heavy metal analysis and phytochemical screening of two indigenous species (*Zingiber officinale* and *Centrosema pubescens*) from Nigeria. *Int J Curr Res*, **33**:95–99.
- Liu Y, Xue D, Li W, Li C, Wan B. 2020. A simple method for the precise determination of multi-elements in pyrite and magnetite by ICP-MS and ICP-OES with matrix removal. *Microchem J*, **158**:105221.
- Lowry OH, Rosebrough NJ. 1951. AL farr and RJ Randall. *J Biol Chem*, **193**:6.
- Makawy AI, Ibrahim FM, Abdel-Aziem SH. 2019. Assessment of *Satureja montana* L. and *Mentha piperita* L. Antioxidant Activity, Cytotoxicity and Pattern of Apoptotic Gene Expression in Hepatoma Cells. *Jordan J Biol Sci*, **12**:251–258.
- Manojlovic NT, Vasiljevic PJ, Maskovic PZ, Juskovic M, Bogdanovic-Dusanovic G. 2012. Chemical Composition, Antioxidant, and Antimicrobial Activities of Lichen *Umbilicaria cylindrica* (L.) Delise (Umbilicariaceae). *Evid Based Complement Alternat Med*, <https://doi.org/10.1155/2012/452431>.
- Mohapatra D, Patel AS, Kar A, Deshpande SS, Tripathi MK. 2019. Effect of different processing conditions on proximate composition, anti-oxidants, anti-nutrients and amino acid profile of grain sorghum. *Food Chem*, **271**:129–135.
- Musharraf SG, Kanwal N, Thadhani VM, Choudhary MI. 2015. Rapid identification of lichen compounds based on the structure-fragmentation relationship using ESI-MS/MS analysis. *Anal Methods*, **7**:6066–6076.
- Ng Z, Koick Y, Yong P. 2020a. Comparative analyses on radical scavenging and cytotoxic activity of phenolic and flavonoid content from selected medicinal plants. *Nat Prod Res*, 1–6.
- Ng ZX, Chua KH, Kuppusamy UR. 2014. Proteomic analysis of heat treated bitter melon (*Momordica charantia* L. var. *Hong Kong Green*) using 2D-DIGE. *Food Chem*, **148**:155–161.
- Ng ZX, Kuppusamy UR, Ng ZX, Kuppusamy UR. 2019. Effects of different heat treatments on the antioxidant activity and ascorbic acid content of bitter melon, *Momordica charantia*. *Braz J Food Technol*, 22 doi:10.1590/1981-6723.28318.
- Ng ZX, Rosman NF. 2019. In vitro digestion and domestic cooking improved the total antioxidant activity and carbohydrate-digestive enzymes inhibitory potential of selected edible mushrooms. *J Food Sci Technol*, **56**:865–877.
- Ng ZX, Samsuri SN, Yong PH. 2020b. The antioxidant index and chemometric analysis of tannin, flavonoid, and total phenolic extracted from medicinal plant foods with the solvents of different polarities. *J Food Process Preserv*, e14680.
- Ng ZX, See AN. 2019. Effect of in vitro digestion on the total polyphenol and flavonoid, antioxidant activity and carbohydrate hydrolyzing enzymes inhibitory potential of selected functional plant-based foods. *J Food Process Preserv*, **43**:e13903.
- Ng ZX, Yong PH, Lim SY. 2020c. Customized drying treatments increased the extraction of phytochemicals and antioxidant activity from economically viable medicinal plants. *Ind Crops Prod*, **155**:112815.
- Nguyen TTH, Dinh MH, Chi HT, Wang S-L, Nguyen Q, Tran TD, Nguyen AD. 2019. Antioxidant and cytotoxic activity of lichens collected from Bidoup Nui Ba National Park, Vietnam. *Res Chem Intermed*, **45**:33–49.

- Orange A, James PW, White FJ. 2001. **Microchemical methods for the identification of lichens**. Twayne Publishers, USA.
- Rahman E, Momin A, Zhao L, Guo X, Xu D, Zhou F, Ji B. 2018. Bioactive, nutritional composition, heavy metal and pesticide residue of four Chinese jujube cultivars. *Food Sci Biotechnol*, **27**:323–331.
- Raj PS, Prathapan A, Sebastian J, Antony AK, Riya MP, Rani MRP, Biju H, Priya S, Raghu KG. 2014. Parmotrema tinctorum exhibits antioxidant, antiglycation and inhibitory activities against aldose reductase and carbohydrate digestive enzymes: an in vitro study. *Nat Prod Res*, **28**:1480–1484.
- Rajeswari N, Mesta AR, Kanivebagilu VS, Babu HR. 2019. Medicinal importance of Usneoid lichens in Western Ghats, Southern India. *Plant Arch*, **19**:2540–2542.
- Rice-evans CA, Miller NJ, Bolwell PG, Bramley PM, Pridham JB. 1995. The Relative Antioxidant Activities of Plant-Derived Polyphenolic Flavonoids. *Free Radic Res*, **22**:375–383.
- Ristić S, Ranković B, Kosanić M, Stanojković T, Stamenković S, Vasiljević P, Manojlović I, Manojlović N. 2016. Phytochemical study and antioxidant, antimicrobial and anticancer activities of Melanelia subaurifera and Melanelia fuliginosa lichens. *J Food Sci Technol*, **53**:2804–2816.
- Robbins CT. 1987. Digestibility of an arboreal lichen by mule deer. *Rangel Ecol Manag Range Manag Arch*, **40**:491–492.
- Sarker S, Latif Z, Gray A. 2006. Natural product isolation: an overview. *Methods in Biotechnology* <https://pubs.acs.org/doi/10.1021/np078142v>
- Sedjati S, Pringgenies D, Fajri M. 2020. Determination of the Pigment Content and Antioxidant Activity of the Marine Microalga Tetraselmis suecica. *Jordan J Biol Sci*, **13**:55–58.
- Shelukheeva MG, Nikolaeva IG. 2015. Amino Acids from Lichens of the Genera Cladonia and Cladonia. *Chem Nat Compd*, **51**:397–398.
- Shrestha G, St. Clair LL. 2013. Lichens: a promising source of antibiotic and anticancer drugs. *Phytochem Rev*, **12**:229–244.
- Singleton VL, Orthofer R, Lamuela-Raventós RM. 1999. **Analysis of total phenols and other oxidation substrates and antioxidants by means of folin-ciocalteu reagent**. *Methods in Enzymology*. Academic Press. **299**: 152–178.
- Thangaraj P. 2016. **Pharmacological assays of plant-based natural products**. Springer.
- Tomović J, Rančić A, Vasiljević P, Mašković P, Živanović S, Manojlović N, Sovrlić M. 2016. Antioxidant activity of lichen Cetraria aculeata. *Prax medica*, **45**:93–99.
- Upreti DK, Divakar PK, Nayaka S. 2005. Commercial and ethnic use of lichens in India. *Eco Bot*, **59**:269.
- Vinayaka KS, Kekuda TRP, Kumar K a. R, Pavithra GM, Junaid S, Rakesh KN, Dileep N. 2013. Analysis of mineral elements of the lichen Usnea pictoides G. Awasthi by ICP-OES. *Int J Chem Sci*, **11**:1589–1594.
- Vinayaka KS, Kumar SP, Mallikarjun N, Kekuda PTR. 2010. Studies on insecticidal activity and nutritive composition of a macrolichen Parmotrema pseudotinctorum (des. Abb.) Hale (Parmeliaceae). *Drug Invent Today*, **2**:102–105.
- Zengin G, Sarikurkcü C, Gunes E, Uysal A, Ceylan R, Uysal S, Gungor H, Aktumsek A. 2015. Two Ganoderma species: profiling of phenolic compounds by HPLC–DAD, antioxidant, antimicrobial and inhibitory activities on key enzymes linked to diabetes mellitus, Alzheimer’s disease and skin disorders. *Food Funct*, **6**:2794–2802.
- Zhang L, Wang S, Yang R, Mao J, Jiang J, Wang X, Zhang W, Zhang Q, Li P. 2019. Simultaneous determination of tocopherols, carotenoids and phytosterols in edible vegetable oil by ultrasound-assisted saponification, LLE and LC-MS/MS. *Food Chem*, **289**:313–319.

Metabolites profiling of *Limonium tubiflorum* (Delile) Kuntze var *tubiflorum* via UPLC-qTOF-MS technique in relation to its cytotoxic activity

Salah M. El-Kousy¹, Shalabia S. Emam², Ahmed R. Hassan², Ibrahim M. Sanad^{2,*}

¹ Chemistry Department, Menoufia University, Shebin El-Kom 32861, El-Menoufia, Egypt; ² Medicinal and Aromatic Plants Department, Desert Research Center, El-Matariya 11753, Cairo, Egypt

Received: May 5, 2020; Revised: October 2, 2020; Accepted: October 16, 2020

Abstract

Ultra performance liquid chromatography coupled with quadrupole time-of-flight mass spectrometry (UPLC-qTOF-MS) technique led to the detection of 55 metabolites in *Limonium tubiflorum* (Delile) Kuntze var *tubiflorum* flowers extract for the first time including 38 flavonoids, 7 phenolic acids and 10 anthocyanins. The total phenolic content was (231.225 mg GAE g DW⁻¹) and the total flavonoid content was (136.66 mg rutin g DW⁻¹) in *L. tubiflorum* (Delile) Kuntze var *tubiflorum*. The flower plant powder has been prepared by successive fractionation. The successive extracts have been tested for *in vitro* cytotoxic activity against MCF7, HEPG2, and HCT116 and exhibited moderate to weak cytotoxic activities compared to Doxorubicin (positive control) which showed *in vitro* cytotoxic effect with IC₅₀ values of 2.97 ± 0.9, 4.57 ± 0.5 and 3.73 ± 0.6 µg/mL, respectively. The results also showed that the 95% ethanolic successive extract exhibited the strongest cytotoxic activity among all the tested extracts against HEPG2 and HCT116 cell lines with IC₅₀ values of 21 ± 0.5 and 21 ± 0.8 µg/mL, respectively, while 70% ethanolic successive extract showed the highest cytotoxic activity against MCF7 cell line with IC₅₀ value (26.6 ± 0.7 µg/mL). The hydro-ethanolic plant flower extracts are enriched in phenolic compounds (flavonoids, phenolic acids and anthocyanins) which are likely to mediate for cytotoxic activity.

Keywords: *Limonium tubiflorum* (Delile) Kuntze var *tubiflorum*, UPLC-qTOF-MS, flavonoids, anthocyanins, cytotoxicity

1. Introduction

Plumbaginaceae is a family of flowering plants cosmopolitan in distribution. It is sometimes referred to as the leadwort family or the plumbago. It consists of about 30 genera and 725 species (Christenhusz and Byng, 2016). *Limonium* genus, also known as (Statice or Sea-lavender), is one of the largest genus of this family comprising about 180 species of halophytic plants as perennial shrubs, subshrubs spread in Africa, Europe, America and Asia (Ksouri *et al.*, 2011).

The salt-tolerant halophyte *Limonium* genus has many potentially useful plants. It has traditionally been used to treat a wide range of diseases and ageing symptoms, and continues to be used for such medical purposes in rural areas (Ksouri *et al.* 2011). For examples, *Limonium brasiliense* Kuntze exhibits anti-inflammatory and antibacterial properties (Murray *et al.* 2004), *L. wrightii* (Hance) Kuntze is used to treat arthritis and fever (Aniya *et al.* 2002), *L. sinense* (Girard) Kuntze has been reported to possess antiviral properties (Yuh-Chi *et al.* 2002), and *L. axillare* (Forssk.) Kuntze and *L. californicum* (Boiss.) A. Heller have been shown cytotoxic and antibacterial effects (Kandil *et al.* 2000). *Limonium*

is reported to have a wide range of chemical diversity (Medini *et al.* 2014).

L. tubiflorum (Delile) Kuntze var *tubiflorum* is a perennial subshrub 10–35 cm, woody at the base, densely covered with scale-like tubercles; stems 1–5 cm, simple to richly branched, leafy; leaves restricted to basal part of the short stems, 0.5–2 x 0.2–0.5 cm, flowering stems branched, brittle; flowers 1 cm diam, the margin membranous; outer bracts 1.5–3.5 x 2 mm, unequal, broadly ovate, acute, the inner 7–9 x 2.5 mm; calyx-teeth ending in a reddish-brown awn 2–3 mm; petals . 1.5 cm vivid rose, fruit not seen. The plant has been recorded to grow in Egypt (South of Mersa Matruh region) in calcareous ridges (Boulos, 2000).

To the best of our knowledge, there are no previous studies regarding the chemical constituents of *L. tubiflorum* (Delile) Kuntze var *tubiflorum*. Therefore, this study targets the chemical profile of the flower extract of the plant and investigates *in vitro* cytotoxic activity of the successive extracts of the flower plant powder against MCF7, HEPG2 and HCT116 in order to evaluate its potential medicinal uses.

* Corresponding author e-mail: hemachemist52@yahoo.com.

2. Materials and Methods

2.1. Plant collection and Preparation

The aerial parts of *L. tubiflorum* (Delile) Kuntze var *tubiflorum* were collected in April 2017 from Wadi Habis at Mersa matrouh governorate, Northwestern coast, Egypt. The plant sample was identified by Prof. Dr. Azza El Hadidy, Professor of plant taxonomy and flora, Botany Department, Faculty of Science, Cairo University, Egypt. A voucher specimen of the plant (18/4/2017-H) was deposited at the Herbarium of Faculty of Science, Cairo University, Egypt. The flowers were separated then stored in plastic bags under dark, chilled conditions during transportation to the laboratory, then washed under tap water and air dried at Laboratory temperature till constant weight. The flowers were ground to fine powder to be used for chemical analysis.

2.2. Human tumor cell lines for the cytotoxic activity

Human tumor cell lines [HEPG2 (liver carcinoma cell line), MCF7 (breast carcinoma cell line) and HCT116 (colon carcinoma cell line)] were obtained in frozen state under liquid nitrogen (-180 °C) from the American Type Culture Collection. The cancer cell lines were maintained by serial sub-culturing in the National Cancer Institute, Cairo, Egypt. The cells were suspended in RPMI 1640 medium (Sigma-Aldrich, USA) supplemented with 10% fetal bovine serum (Sigma-Aldrich, USA) in presence of 1% antibiotic antimycotic mixture (10,000 U/mL K-penicillin, 10,000 U/mL streptomycin sulphate and 25 µg/mL amphotericin B) and 1% L-glutamine (all purchased from Lonza, Belgium).

2.3. Extraction procedure for *L. tubiflorum* (Delile) Kuntze var *tubiflorum* flowers

For chemical profile of *L. tubiflorum* (Delile) Kuntze var *tubiflorum* via high resolution UPLC-qTOF-MS analysis, 20 mg of the flowers plant powder was homogenized with 4 mL 70% MeOH using an ultrasonic bath for 30 min. Extract was then vortexed and centrifuged at 10,000g for 10 min to remove plant debris and filtered through 22 µm millipore filter. For cytotoxic assay, other quantity (25 g) of the air-dried powder of *L. tubiflorum* (Delile) Kuntze var *tubiflorum* flowers was subjected to successive extraction with gradient organic solvents in polarity (petroleum ether, chloroform, ethyl acetate, 95% ethanol and 70% ethanol) using soxhlet apparatus. The obtained residue from each solvent was dried and weighed.

2.4. Determination of Total Phenolic Content

The total phenol content was analyzed using a colorimetric measurement at 630 nm (Attard, 2013). A standard series of gallic acid (GA) was used for quantification. Each sample was measured as technical triplicate. Results were given as GA equivalents (GAE)/g dry weight. Gallic acid stock solution of 1mg/mL in methanol was prepared, and seven serial dilutions were prepared in the concentrations of 500, 250, 125, 62.5, 31.2, 15.6, and 7.8 µg/mL. Solution of flower sample was prepared in concentration of 5mg/mL in methanol. Then the results were recorded using microplate reader FluoStar Omega. Each of the 7 standards and the sample were pipetted in the plate wells in 6 replicates. Measurement was performed at 630 nm.

2.5. Determination of Total Flavonoid Content

The amount of total Flavonoid content was determined by aluminum chloride assay through colorimetric method at 510 nm (Herald *et al.* 2012). Distilled water (100 µL) was added to each of the 96 wells, followed by 10 µL of 50 g/L NaNO₂ and 25 µL of standard or flower sample solution. After 5 min, 15 µL of 100 g/L AlCl₃ was added to the mixture; 6 min later, 50 µL of 1 mol/L NaOH and 50 µL of distilled water were added. The plate was shaken for 30 seconds in the plate reader prior to absorbance measurement at 510 nm. Rutin was used as a standard, its stock solution of 1mg/mL in methanol was prepared, and 6 standards were prepared in the concentrations of 1000, 500, 250, 150, 100, and 50 µg/mL generate a calibration curve. Then, the results were recorded using microplate reader FluoStar Omega. Each of the 6 standards and the sample were pipetted in the plate wells in 6 replicates. Measurement was performed at 510 nm.

2.6. Metabolites analysis via high-resolution UPLC-qTOF-MS analysis

Chromatographic separations were performed on Sciex ExionLC chromatographic separation coupled with TripleTOF 5600+ equipped with a Xbridge C18 column (3.5 µm, 2.1x50 mm; Waters) applying the following elution binary gradient at a flow rate of 0.3 mL min⁻¹: 0–1 min, isocratic 90% A (5 mM ammonium formate buffer pH=8 containing 1% methanol [v/v]), 10% B (100 % acetonitrile); 1–21 min, linear from 10–90% B; 21–25 min, isocratic 90% B; 25–28 min, isocratic 10% B. The injection volume was 10µL. Eluted compounds from UPLC were detected from *m/z* 100 to 1000 using a MicroTOFQ hybrid quadrupole time-of-flight mass spectrometer (Bruker Daltonics) equipped with an Apollo-II electrospray ion source in negative ion modes using the following instrument settings: nebulizer gas, nitrogen, 1.6 bar; dry gas, nitrogen, 190 °C; capillary, 5500 V (+4000 V); end plate offset, 500 V; funnel 1 RF, 200 Vpp; funnel 2 RF, 200 Vpp. MicroTOF-Q: Precursor ions were selected in Q1 with an isolation width of ±2 D and fragmented in the collision cell applying collision energies in the range of 10–30 eV. Argon was used as collision gas. Product ions were detected using the following parameter settings: collision RF 150/400 Vpp (timing 50/50); transfer time, 70 ls; pre pulse storage, 5 ls; pulser frequency, 10 kHz; spectra rate, 1.5 Hz. The MSn spectra were recorded by using the following conditions: MS/MS analysis with starting collision-induced dissociation energy of 30 eV and an isolation width of ±2 D in a data dependent, negative ionization mode. UPLC-MS files were converted to netCDF file format using the File Converter tool in Bruker Daltonics software and further processed using AMDIS software to assist in adjacent peak deconvolution and background subtraction (Halket *et al.* 1999). Metabolites were characterized by their retention times, mass spectra and phytochemical dictionary of natural products database.

2.7. Cytotoxicity assay

Cytotoxicity assay of the successive extracts of the flowers of *L. tubiflorum* (Delile) Kuntze var *tubiflorum* was tested using the method of Skehan *et al.* 1990. Cells were plated in 96-multiwell plate (10⁴ cells /well) for 24 hours before treatment with the extracts. Different concentrations of each extract under test (0, 5, 12.5, 25 and

50 µg/mL) were added to the cell monolayer. Triplicate wells were prepared for each individual dose. Monolayer cells were incubated with the extracts for 48 hours at 37 °C and atmosphere of 5% CO₂. After 48 hours cells were fixed, washed and stained with sulforhodamine B stain (SRB). Excess stain was washed with acetic acid and attached stain was recovered. Tris-EDTA buffer Color intensity was measured in an ELISA reader. The relation between surviving fraction and extract concentration is plotted to get the survival curve of each tumor cell line after the specified extract under investigation was added. The IC₅₀ value was defined as the concentration of the tested extract (µg/mL) that decreased the number of viable cells by 50%. Results are expressed as the mean value of triplicate data points ± SD.

3. Results

3.1. Determination of Total Phenolic Content

Total phenolic content of *L. tubiflorum* (Delile) Kuntze var *tubiflorum* flowers was calculated and represented as gallic acid equivalent (mg GAE g DW⁻¹), where the total phenolic content was 231.225 ± 14.899 mg GAE g DW⁻¹.

3.2. Determination of Total Flavonoid Content

The total flavonoid content of *L. tubiflorum* (Delile) Kuntze var *tubiflorum* was expressed as rutin equivalents in [mg g DW⁻¹] and its value equal 136.66 ± 11.168 mg Rutin g DW⁻¹.

3.3. Metabolites profiling via UPLC-qTOF-MS

Chemical composition of *L. tubiflorum* (Delile) Kuntze var *tubiflorum* was performed via UPLC/qTOF-MS in negative ionization mode to provide a comprehensive coverage of metabolites composition. The metabolites profile of *L. tubiflorum* (Delile) Kuntze var *tubiflorum*

flower extract led to the identification of 55 metabolites belonging to phenolic compounds including flavonoids, phenolic acids, and anthocyanins (Table 1). These compounds include 38 flavonoids, namely Luteolin (1), Luteolin-7-*O*-glucoside (2), Kaempferol-7-*O*-neohesperidoside (3), Hesperidin (4), Quercetin-4'-*O*-glucoside (5), Quercetin (6), Luteolin-3', 7-di-*O*-glucoside (7), 3, 5, 7-trihydroxy-4'-methoxyflavone (8), Isorhamnetin-3-*O*-glucoside (9), Isorhamnetin-3-*O*-rutinoside (10), Kaempferol-3-*O*- α -L-rhamnoside (11), Apigenin 8-*C*-glucoside (12), Syringetin-3-*O*-glucoside (13), Apigenin (14), 3'-methoxy-4',5,7-trihydroxyflavonol (15), Kaempferol-3-*O*-glucuronide (16), Naringenin (17), Syringetin-3-*O*-galactoside (18), Rhoifolin (19), Formononetin (20), Acacetin-7-*O*-rutinoside (21), Quercetin-3-*O*-arabinoglucoside (22), Quercetin-3-*D*-xyloside (23), Catechin (24), Hesperetin (25), Myricitrin (26), Myricetin (27), Quercetin-3-*O*-glucuronide (28), Naringenin-7-*O*-glucoside (29), Apigenin-7-*O*-glucoside (30), Quercetin-3,4'-*O*-di-glucopyranoside (31), Quercetin-3-arabinoside (32), Acacetin (33), Kaempferol-3-*O*- α -L-arabinoside (34), Kaempferol-3-*O*-rabinoside-7-*O*-rhamnoside (35) Luteolin-6-*C*-glucoside (36), Isoquercitrin (37), Baicalein-7-*O*-glucuronide (38) and 7 phenolic acids namely D-(-)-Quinic acid (39), Chlorogenic acid (40), 3,4-dihydroxybenzoic acid (41), Homogenetic acid (42), Caffeic acid (43), Rosmarinic acid (44), *p*-hydroxybenzoic acid (45), and 10 anthocyanins namely Delphinidin-3-*O*- β -glucopyranoside (46), Pelargonidin-3-*O*-glucoside (47), Cyanidin-3,5-di-*O*-glucoside (48), Peonidin (49), Cyaniding-3-*O*-glucoside (50), Cyanidin-3-*O*-(2''-*O*- β -xylopyranosyl)- β -glucopyranoside (51), Petunidin-3-*O*- β -glucopyranoside (52), Malvidin-3,5-di-*O*-glucoside chloride (53), Peonidin-3-*O*-glucoside chloride (54), Malvidin-3-*O*-galactoside (55). The total ion chromatogram is shown in Fig. 1.

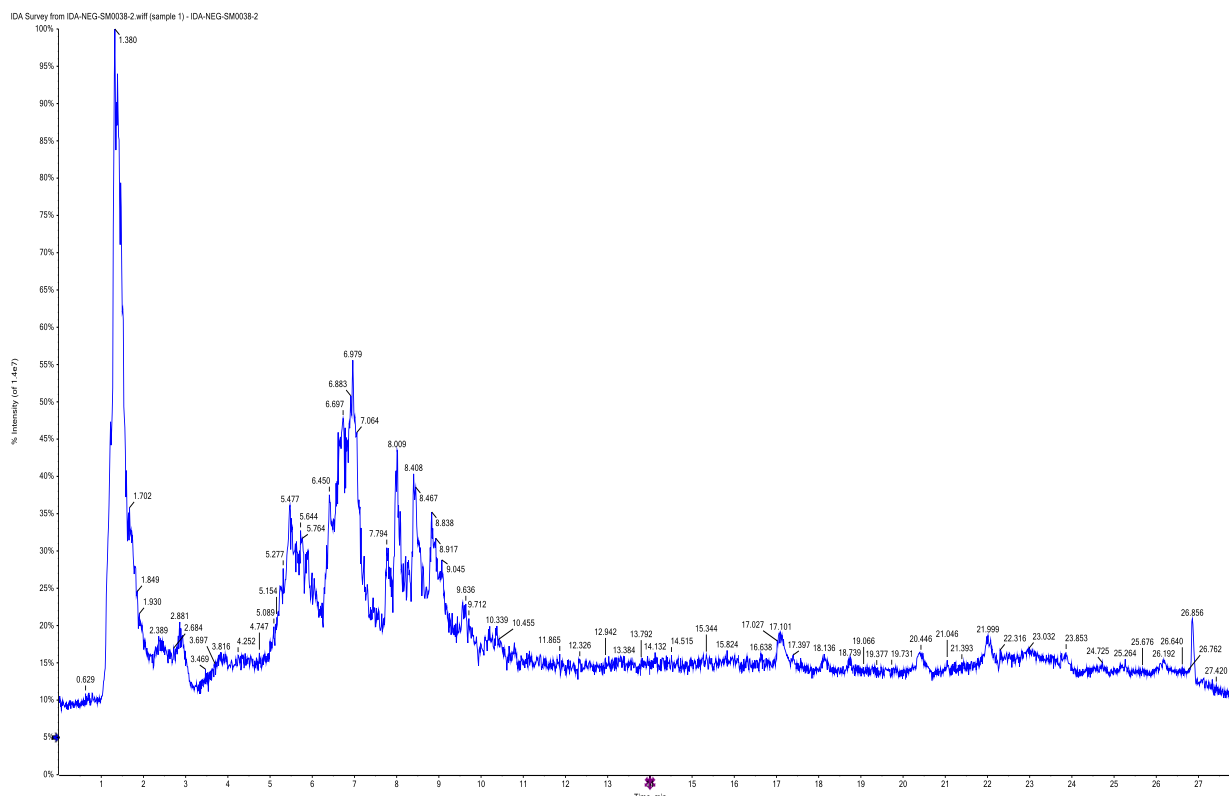


Figure 1. Total ion chromatogram of metabolites of *L. tubiflorum* (Delile) Kuntze var *tubiflorum* flowers

Table 1. Metabolites identified in 70% methanol flowers extract of *L. tubiflorum* (Delile) Kuntze var *tubiflorum* via UPLC-qTOF-MS in negative ionization mode.

Peak	R _t (min)	[M-H] ⁻ m/z	Formula	MS/MS	Identification
1	6.9611	477.1048	C ₂₂ H ₂₂ O ₁₂	317,316,286	Petunidin-3- <i>O</i> -β-glucopyranoside
2	8.8432	285.0431	C ₁₅ H ₉ O ₆	285,217,175 , 151	Luteolin
3	6.7060	447.0946	C ₂₁ H ₁₉ O ₁₁	285,199,175	Luteolin-7- <i>O</i> -glucoside
4	6.4047	593.1537	C ₂₇ H ₂₉ O ₁₅	447,285	Kaempferol-7- <i>O</i> -neohesperidoside
5	5.7482	609.1475	C ₂₈ H ₃₃ O ₁₅	578,463,301	Hesperidin
6	5.8947	463.0890	C ₂₁ H ₁₉ O ₁₂	301	Quercetin-4'- <i>O</i> -glucoside
7	9.0820	301.0370	C ₁₅ H ₉ O ₇	301,271,151	Quercetin
8	8.2692	609.1293	C ₂₇ H ₂₉ O ₁₆	447,285	Luteolin-3', 7-di- <i>O</i> -glucoside
9	1.9536	353.0896	C ₁₆ H ₁₇ O ₉	191,179	Chlorogenic acid
10	1.1835	191.0567	C ₇ H ₁₁ O ₆	173,127,109,85	D-(-)-Quinic acid
11	9.7857	299.0577	C ₁₆ H ₁₁ O ₆	284,268	3', 5, 7-trihydroxy-4'-methoxyflavone
12	1.2210	153.0185	C ₇ H ₅ O ₄	109	3,4-dihydroxybenzoic acid
13	7.7153	477.1033	C ₂₂ H ₂₁ O ₁₂	315,299,285	Isorhamnetin-3- <i>O</i> -glucoside
14	6.6572	623.1620	C ₂₈ H ₃₁ O ₁₆	477,315	Isorhamnetin-3- <i>O</i> -rutinoside
15	5.4726	431.1931	C ₂₁ H ₁₉ O ₁₀	285	Kaempferol-3- <i>O</i> - α-L -rhamnoside
16	6.1194	431.0995	C ₂₁ H ₂₀ O ₁₀	341,311, 269	Apigenin 8- <i>C</i> -glucoside
17	7.4670	507.1133	C ₂₃ H ₂₃ O ₁₃	477,345,314	Syringetin-3- <i>O</i> -glucoside
18	10.1651	269.0464	C ₁₅ H ₉ O ₅	269,151	Apigenin
19	10.7898	315.0530	C ₁₆ H ₁₁ O ₇	300,199,285	3'-methoxy-4',5,7-trihydroxyflavonol
20	6.2827	461.0753	C ₂₁ H ₁₇ O ₁₂	285	Kaempferol-3- <i>O</i> -glucuronide
21	6.5392	167.0346	C ₈ H ₇ O ₄	167	Homogenetic acid
22	10.0298	271.0725	C ₁₅ H ₁₁ O ₅	271, 175	Naringenin
23	10.0298	507.0399	C ₂₃ H ₂₃ O ₁₃	345	Syringetin-3- <i>O</i> -galactoside
24	5.2471	179.0337	C ₉ H ₇ O ₄	179,135,107	Caffeic acid
25	4.9041	577.1582	C ₂₇ H ₂₉ O ₁₄	431,269	Rhoifolin
26	11.8527	267.0665	C ₁₆ H ₁₁ O ₄	253,237	Formononetin
27	6.5637	591.0120	C ₂₈ H ₃₁ O ₁₄	445,283,268	Acacetin-7- <i>O</i> -rutinoside
28	8.4151	595.0636	C ₂₆ H ₂₇ O ₁₆	463,301	Quercetin-3- <i>O</i> -arabinoglucoside
29	8.8432	433.1046	C ₂₀ H ₁₇ O ₁₁	301	Quercetin-3- <i>D</i> -xyloside
30	7.7851	497.1087	C ₂₂ H ₂₂ ClO ₁₁	463,335,301	Peonidin-3- <i>O</i> -glucoside chloride
31	5.1964	447.0913	C ₂₁ H ₂₀ O ₁₁	285	Cyanidin-3- <i>O</i> -glucoside
32	4.0883	359.0535	C ₁₈ H ₁₅ O ₈	161	Rosmarinic acid
33	1.3099	431.0312	C ₂₁ H ₂₀ O ₁₀	271, 270	Pelargonidin-3- <i>O</i> -glucoside
34	7.7974	491.1168	C ₂₃ H ₂₄ O ₁₂	330,329,314, 299	Malvidin-3- <i>O</i> -galactoside
35	7.1186	289.1456	C ₁₅ H ₁₃ O ₆	271,247,125	Catechin
36	2.8862	283.0232	C ₁₆ H ₁₁ O ₅	283,253	Acacetin
37	6.9123	739.2557	C ₃₃ H ₃₉ O ₁₉	593,431,285	Kaempferol-3- <i>O</i> -robinoside-7- <i>O</i> -rhamnoside
38	6.7305	447.1602	C ₂₁ H ₁₉ O ₁₁	285	Luteolin-6- <i>C</i> -glucoside
39	1.3973	298.9926	C ₁₆ H ₁₂ O ₆	283,270,269	Peonidin
40	1.4101	137.0243	C ₇ H ₅ O ₃	137,93	<i>p</i> - hydroxybenzoic acid
41	4.4711	301.0936	C ₁₆ H ₁₃ O ₆	301,258,143	Hesperetin
42	7.4033	653.1713	C ₂₉ H ₃₄ ClO ₁₇	654,653,491, 329	Malvidin-3,5-di- <i>O</i> -glucoside chloride
43	12.2830	463.1032	C ₂₁ H ₁₉ O ₁₂	317	Myricitrin
44	6.4410	317.0325	C ₁₅ H ₉ O ₈	287,178,151	Myricetin
45	2.9110	477.0414	C ₂₁ H ₁₇ O ₁₃	301	Quercetin-3- <i>O</i> -glucuronide
46	6.2322	579.1379	C ₂₆ H ₂₈ O ₁₅	448,447,286	Cyanidin-3- <i>O</i> -(2"- <i>O</i> -β- xylopyranosyl-β-glucopyranoside)
47	9.7118	433.1039	C ₂₁ H ₂₁ O ₁₀	271	Naringenin-7- <i>O</i> -glucoside

48	1.3099	463.0483	C ₂₁ H ₂₀ O ₁₂	302	Delphinidin-3- <i>O</i> - β -glucopyranoside
49	1.2210	431.1375	C ₂₁ H ₁₉ O ₁₀	269	Apigenin 7- <i>O</i> -glucoside
50	9.6628	445.1456	C ₂₁ H ₁₇ O ₁₁	269	Baicalin-7- <i>O</i> -glucuronide
51	7.0216	624.1066	C ₂₇ H ₂₉ O ₁₇	462,301	Quercetin-3,4'- <i>O</i> -diglucopyranoside
52	7.3153	417.0930	C ₂₀ H ₁₇ O ₁₀	285	Kaempferol-3- <i>O</i> - α -L-arabinoside
53	5.5012	433.0931	C ₂₀ H ₁₇ O ₁₁	301	Quercetin-3-arabinoside
54	7.7533	463.1581	C ₂₁ H ₁₉ O ₁₂	301	Isoquercitrin
55	1.3099	609.0966	C ₂₇ H ₃₀ O ₁₆	448,447,286	Cyanidin-3,5-di- <i>O</i> -glucoside

3.4. Successive Extraction

Successive extraction showed that the percentages of residue of petroleum ether, chloroform, ethyl acetate, 95% ethanol and 70% ethanol extracts were 1.2, 1.4, 1.66, 9.06 and 4.52% respectively. The obtained percentage of total residues was 17.84%. The 95% ethanol extract has the highest percentage among the extracts, while the lowest one was that of petroleum ether extract.

3.5. Cytotoxic Activity

Cytotoxicity of the successive extracts of *L. tubiflorum* (Delile) Kuntze var *tubiflorum* flowers were tested against HEPG2, MCF7, and HCT cell lines. Results showed that successive extracts of the plant flowers exhibited moderate to weak cytotoxic activity against HEPG2, MCF7 and HCT116 compared to Doxorubicin (positive control) which showed *in vitro* cytotoxic effect with IC₅₀ values of 4.57 \pm 0.5, 2.97 \pm 0.9 and 3.73 \pm 0.6 μ g/mL, respectively (Table 2). The 95% ethanolic extract of the flower plant powder exhibited the strongest cytotoxic activity among all the tested successive fractions against HEPG2 and HCT116 cell lines with the same IC₅₀ value of 21 \pm 0.5 and 21 \pm 0.8 μ g/mL, respectively, whereas 70% ethanolic successive extract showed the highest cytotoxic activity against MCF7 cell line among the tested extracts with IC₅₀ value of 26.6 \pm 0.7 μ g/mL.

Table 2. IC₅₀ (Inhibition concentration) of the successive extracts of *L. tubiflorum* (Delile) Kuntze var *tubiflorum* flowers on MCF7, HEPG2 and HCT116

Successive extracts & Doxorubicin (+ve control)	IC ₅₀ (μ g/mL)		
	HEPG2	MCF7	HCT116
Petroleum.ether	37 \pm 0.6	33 \pm 1.0	38.5 \pm 1.1
Chloroform	36 \pm 0.3	34.5 \pm 1.2	39 \pm 1.2
Ethylacetate	27 \pm 0.2	28.9 \pm 0.8	27.5 \pm 1.2
Ethanol 95%	21 \pm 0.5	28.7 \pm 0.7	21 \pm 0.8
Ethanol 70%	31.5 \pm 0.3	26.6 \pm 0.7	34 \pm 1.2
Doxorubicin (positive control)	4.57 \pm 0.5	2.97 \pm 0.9	3.73 \pm 0.6

* The activity was shown as IC₅₀ value, which was the concentration of the tested extract (μ g/mL) that decreased the number of viable cells by 50%. Results are expressed as IC₅₀ \pm SD (n = 3).

4. Discussion

From the above results, it was found that the number of flavonoids were the major chemical constituents present in *L. tubiflorum* (Delile) Kuntze var *tubiflorum* flowers extract. Flavonoids (flavone, flavonols, and flavanones) and/or their conjugates, *O*-glycosides resulted from UPLC-

qTOF-MS, were previously reported in *Limonium* species (Lin and Chou, 2000). In MS analysis, the type of the sugars were observed by the loss of 132 amu (pentose), 146 amu (monodeoxyhexose), 162 amu (hexose), and 176 amu (hexouronic acid) residues. Tandem MS spectra of *L. tubiflorum* (Delile) Kuntze var *tubiflorum* identified quercetin as its aglycone (*m/z* 301.037, C₁₅H₉O₇) in peaks (6-7, 28-29, 45, 51 and 53) and luteolin (*m/z* 285.0431, C₁₅H₉O₆) in peaks (2-3, 8 and 38), (Table 1). For example, hesperidin with *m/z* 609.1475 and molecular formula (C₂₈H₃₃O₁₅) were detected in peak 5. Fragmentation pattern of peak 5 showed losses of 31 amu (-methoxy group), 146 amu (-monodeoxyhexose) and 162 amu (-hexose unit), identified as hesperidin.

Another class of compounds that was detected includes phenolic acids. For instance, chlorogenic acid was recognized from its [M-H]⁻, *m/z* 353.0896 detected at R_t 1.9536 min (peak 9) and showed also fragment ions at 191 amu and 179 amu corresponding to quinic acid and caffeic acid found in the tandem MS spectra of peak 10 and 24, respectively (Table 1).

Anthocyanins and/or their conjugates, *O*-glycosides were also characterized in the negative ion MS spectra including 10 compounds. For example, Petunidin-3-*O*- β -glucopyranoside (peak 1) with (*m/z* 477.1048, C₂₂H₂₂O₁₂) which has fragmentation pattern showed losses of 162 amu (-hexose unit) and 31 amu (-methoxy group). Anthocyanins have been previously recorded in the species *Limonium* (Asen *et al.*, 1973).

UPLC-MS profiling revealed the enrichment of *L. tubiflorum* (Delile) Kuntze var *tubiflorum* flower extract with number of flavonoids especially flavone and flavonol types and their *O*-glycosides in the plant, which is in agreement with Iwashina, 2013. The successive fractions of *L. tubiflorum* (Delile) Kuntze var *tubiflorum* flowers especially the hydro-ethanolic extracts (95% Ethanol and 70% Ethanol) showed a promising cytotoxic activity as a result of their enrichment in phenolic compounds. Our findings were consistent with the results obtained from the previous cytotoxic studies on *L. globuliferum* Kuntze (Eren, 2016).

Data of this study showed that *L. tubiflorum* (Delile) Kuntze var *tubiflorum* collected in Egypt contains appreciable amounts of total phenolic and total flavonoid contents. Also, the current study describes the screening of the metabolic profile of *L. tubiflorum* (Delile) Kuntze var *tubiflorum* via UPLC/qTOF/MS for the first time resulting 55 metabolites dominated by flavonoids of about 38 compounds matches with the high total flavonoid content. Flavonoids are synthesized by plants with *in vitro* cytotoxic activity against various types of cancer cell lines (Oueslati *et al.* 2012, Boulaaba *et al.* 2013 and Boulaaba *et al.* 2019). Flavonoids such as kaempferol, quercetin and their glycosides have been found to possess a protective

effect against cancer by their effect on signal transduction in cell proliferation and angiogenesis (Fateme and Khosro, 2013). Recently, flavonoids enhanced a great interest in the beneficial human health effects such as antitumor, anti-inflammatory, antiviral, anti-diabetic and anti-ageing properties (Cook and Samman, 1996, Ren *et al.* 2003, Zhou *et al.* 2009 and Boulaaba *et al.* 2019). It was declared that these compounds contribute to all the former biological effects via their strong antioxidant and free radical scavenger capabilities (Sharififar *et al.* 2009 and Abdel-Mawgoud *et al.* 2019). Phenolic acids determined in UPLC/qTOF/MS analysis could contribute as well enhance the cytotoxic activity and have the ability to scavenge the free radical that caused cell damage and apoptosis. Various phenolic acids have this activity such as caffeic acid and chlorogenic acid with antiproliferative effect (Ye *et al.* 2010, Yagasaki *et al.* 2000). This effect is attributed to the presence of two OH groups on phenyl group in their structure, giving them the same polyphenols properties.

Furthermore, UPLC/qTOF/MS analysis was able to identify 10 anthocyanin compounds; anthocyanins are a type of flavonoids found naturally in a number of foods and plants possessing antioxidant effects. Anthocyanins were previously characterized for genus *Limonium* (Iwashina, 2013). Numerous studies have confirmed that anthocyanins have anti-proliferative properties (Thomasset *et al.* 2009, Jeong *et al.* 2010 and Szymanowska *et al.* 2018).

5. Conclusion

In summary, this is the first study on the metabolite profile of *L. tubiflorum* (Delile) Kuntze var *tubiflorum* flowers via UPLC-qTOF-MS resulting in tentatively identification of 55 metabolites of phenolic compounds including 38 flavonoids, 7 phenolic acids and 10 anthocyanins. This approach permitted identifying several phenolic compounds in the plant flowers. Also, the results suggest that *L. tubiflorum* (Delile) Kuntze var *tubiflorum* could represent a promising source of natural products. Additionally, the total flavonoid and phenolic content of the plant flowers were determined. *In vitro* cytotoxic activity of the successive plant extracts were investigated against MCF7, HEPG2 and HCT116. The results showed that the 95% ethanolic successive extract among all the tested successive extracts exhibited the strongest cytotoxic activity against HEPG2 and HCT116 cell lines with the same IC_{50} value of 21 ± 0.5 and 21 ± 0.8 $\mu\text{g/mL}$, respectively. The hydro-ethanolic plant flower extracts are enriched in phenolic compounds which are likely to mediate for cytotoxic activity. This research provides useful knowledge for further studies on isolation and characterization of the active compounds as well as the biological screening of these isolated metabolites providing the potential uses of *L. tubiflorum* (Delile) Kuntze var *tubiflorum*.

Acknowledgements

The authors would like to thank Prof. Dr. Sameh Magdeldin, Head of proteomics and metabolomics unit at Children's Cancer Hospital- Egypt (CCHE 57357) for his

kind support and for performing the metabolic analysis of the plant flower via UPLC-qTOF-MS.

References

- Abdel-Mawgoud M, Khedr FG and Mohammed EI. 2019. Phenolic Compounds, Antioxidant and Antibacterial Activities of *Rhus flexicaulis* Baker. *Jordan J Biol Sci*, **12**(1): 17–21.
- Aniya Y, Miyagi C, Nakandakari A, Kamiya S, Imaizumi N and Ichiba T. 2002. Free radical scavenging action of the medicinal herb *Limonium wrightii* from the Okinawa islands, *Phytomedicine*, **9**(3): 239–244.
- Asen S, Norris KH, Stewart RN and Semeniuk P. 1973. Effect of pH, anthocyanin, and flavonoid co-pigments on the color of static flowers. *J Am Soc Hortic Sci*, **98**: 174–176.
- Attard E. 2013. A rapid microtitre plate Folin-Ciocalteu method for the assessment of polyphenols. *Cent Eur J Bio*, **8**(1): 48–53.
- Boulaaba M, Kalai FZ, Dakhlaoui S, Ezzine Y, Selmi S, Bourgou S, Smaoui A, Isoda H and Ksouri R. 2019. Antioxidant, antiproliferative and anti-inflammatory effects of *Glaucium flavum* fractions enriched in phenolic compounds. *Med Chem Res*, **28**(11): 1995–2001.
- Boulaaba M, Mkadmini K, Tsolmon S, Han J, Smaoui A, Kawada K, Ksouri R, Isoda H and Abdelly C. 2013. *In vitro* antiproliferative effect of *Arthrocnemum indicum* extracts on Caco-2 cancer cells through cell cycle control and related phenol LC-TOF-MS identification. *Evid Based Complement Altern Med*, <https://doi.org/10.1155/2013/529375>.
- Boulos L. 2000. Flora of Egypt. Al-Hadara Publishing, Cairo, Egypt, **2**:198–199.
- Christenhusz M. J. M. and Byng, J. W. 2016. The number of known plants species in the world and its annual increase. *Phytotaxa*, **261** (3): 201–217.
- Cook NC and Samman S. 1996. Flavonoids: chemistry, metabolism, cardioprotective effects and dietary sources. *Nutr Biochem*, **7**(2): 66–76.
- Eren y. 2016. Mutagenic and cytotoxic activities of *Limonium globuliferum* methanol extracts. *Cytotechnology*; **68**(5): 2115–2124.
- Fateme, K and Khosro, P. 2013. *In vitro* cytotoxic activity of aqueous root extract of *Althea kurdica* against endothelial human bone marrow cells (line k562) and human lymphocytes. *Bull Env Pharmacol Life Sci*, **2** (6): 23–29.
- Halket JM, Przyborowska A, Stein SE, Mallard WG, Down S and Chalmers RA. 1999. Deconvolution gas chromatography/mass spectrometry of urinary organic acids– potential for pattern recognition and automated identification of metabolic disorders. *Rapid Commun Mass Spectrom*, **13**(4): 279–284.
- Herald TJ, Gadgil P and Tilley M. 2012. High-throughput micro plate assays for screening flavonoid content and DPPH-scavenging activity in sorghum bran and flour. *J Sci Food Agric*, **92**(11): 2326–2331.
- Iwashina T. 2013. Flavonoid Properties of five Families newly incorporated into the order Caryophyllales (Review). *Bull Natl Mus Nat Sci Ser B*, **39**(1): 25–51.
- Jeong JH, Jung H, Lee SR, Lee HJ, Hwang KT and Kim TY. 2010. Anti-oxidant, anti-proliferative and anti-inflammatory activities of the extracts from black raspberry fruits and wine. *Food Chem*, **123**(2): 338–344.
- Kandil FE, Ahmed KM, Hussieny HA and Soliman AM. 2000. A new flavonoid from *Limonium axillare*. *Arch pharm Med Chem*, **333**(8): 275–277.

- Ksouri R, Ksouri W M, Jallali I, Debez A, Magné C, Hiroko I and Abdelly C. 2011. Medicinal halophytes: potent source of health promoting biomolecules with medical, nutraceutical and food applications. *Crit Rev Biotechnol*, **32(4)**: 289–326.
- Lin LC and Chou CJ. 2000. Flavonoids and phenolics from *Limonium sinense*. *Planta Med*, **66(4)**: 382–383.
- Medini F, Fellah H, Ksouri R and Abdelly C. 2014. Total phenolic, flavonoid and tannin contents and antioxidant and antimicrobial activities of organic extracts of shoots of the plant *Limonium delicatulum*. *J Taibah Univ Sci*, **8(3)**: 216–224.
- Murray AP, Rodriguez S, Frontera MA, Tomas MA. and Mulet MC. 2004. Antioxidant metabolites from *Limonium brasiliense* (Boiss.) Kuntze. *Z Naturforsch C*, **59(7–8)**: 477–480.
- Oueslati S, Ksouri R, Falleh H, Pichette A, Abdelly C and Legault J. 2012. Phenolic content, antioxidant, anti-inflammatory and anticancer activities of the edible halophyte *Suaeda fruticosa* Forssk. *Food Chem* **132(2)**: 943–947.
- Ren W, Qiao Z, Wang H, Zhu L and Zhang L. 2003. Flavonoids: promising anticancer agents. *Med Res Rev*, **23(4)**: 519–534.
- Sharififar F, Dehghn G and Mirtajaldini M. 2009. Major flavonoids with antioxidant activity from *Teucrium polium* L. *Food Chem*, **112(4)**: 885–888.
- Skehan P, Storeng R, Scudiero D, Monks A, McMahon J, Vistica D, Warren JT, Bokesch H, Kenney S and Boyd MR. 1990. Newcolometric cytotoxicity assay for anti-cancer drug screening. *J Natl Cancer Inst*, **82(13)**: 1107–1112.
- Szymanowska U, Baraniak B and Bogucka-Kocka A. 2018. antioxidant, anti-inflammatory, and postulated cytotoxic activity of phenolic and anthocyanin-rich fractions from Polana Raspberry (*Rubus idaeus* L.) fruit and juice-*in vitro* study. *Molecules*, **23(7)**: 1812–1829
- Thomasset S, Teller NM, Cai H, Marko D, Berry DP, Steward WP and Gescher AJ. 2009. Do anthocyanins and anthocyanidins, cancer chemopreventive pigments in the diet, merit development as potential drugs? *Cancer Chemother Pharmacol*, **64(1)**: 201–211.
- Yagasaki K, Miura Y, Okauchi R and Furuse T. 2000. Inhibitory effects of chlorogenic acid and its related compounds on the invasion of hepatoma cells in culture. *Cytotechnol* **33(1–3)**: 229–235.
- Ye JC, Hsiao MW, Hsieh CH, Wu WC, Hung YC and Chang WC. 2010. Analysis of caffeic acid extraction from *Ocimum gratissimum* linn. by high performance liquid chromatography and its effects on a cervical cancer cell line. *Taiwan J Obstet Gynecol*, **49(3)**: 266–271.
- Yuh-Chi K, Lie-Chwen L, Wei-Jern T, Cheng-Jen C, Szu-Hao K and Yen-Hui H. 2002. Samarangenin B from *Limonium sinense* suppresses herpes simplex virus type 1 replication in vero cells by regulation of viral macromolecular synthesis, *Antimicrob. Agents Chemother*, **46(9)**: 2854–2864.
- Zhou T, Luo D, Li X and Luo Y. 2009. Hypoglycemic and hypolipidemic effects of flavonoids from *lotus* (*Nelumbo nucifera* Gaertn) leaf in diabetic mice. *J Med Plants Res*, **3(4)**: 290–293.

Expression levels of heat shock proteins through western blot and real-time polymerase chain reaction in maize

Mohamed Abdel-Salam Rashed¹, Mahmoud Hussien Abou-Deif^{2,*}, Kamal Mohamed Khalil² and Fatma El-Sayed Mahmoud²

¹Genetic Dept., Agric. Fac., Ain Shams Univ., Cairo, Egypt; ²Genetic and Cytology Dept., National Research Centre, 12311 Dokki, Giza, Egypt.

Received: March 10, 2020; Revised: September 29, 2020; Accepted: Oct 26, 2020

Abstract

High temperature stress (HTS) is one of the most detrimental abiotic stresses which adversely affect productivity of maize (*Zea mays* L.). Plants respond to HTS by regulating expression of many genes including heat shock proteins (HSPs). We carried out expression analysis of six HSP genes by western blot (WB) and real-time polymerase chain reaction (RT-PCR) in four contrasting Egyptian maize lines, i.e. K1, K7, G342 (heat tolerant) and Rg59 (heat susceptible), subjected to HTS at seedling stage. The six-maize specific HSP genes (*ZmHSP70*, *ZmHSP22*, *ZmHSP17.9*, *ZmHSP17.6*, *ZmHSP16.9* and transcription factor *ZIP60*) exhibited distinctive expression patterns in response to heat stress (HS). Higher upregulation of *ZmHSP70*, *ZmHSP22*, *ZmHSP17.9* and *ZmHSP17.6* were found throughout the stress exposure at 45°C for 2 and 4 hours in the heat tolerant lines as compared to the control (25°C) and susceptible line. *Meanwhile, the susceptible line showed expression of many HSP genes in the control, but these genes were down-regulated by HS. The line K1 showed expression level for ZmHSP70, ZmHSP17.9, ZmHSP17.6 and ZmHSP16.9 genes more than the other lines indicating its highly tolerance against HTS.* Higher upregulation of these six genes in the heat tolerant lines indicated their possible role in protecting plant from adverse effects of HS.

Keywords: Maize, Heat shock proteins, Heat tolerance, Western blot, RT-PCR, Genes.

1. Introduction

Plant productivity is related to the ability of plants to adapt to environmental stress (Sachs and Ho, 1986). Many stress proteins have been proposed to function during stress in the binding of denatured proteins, thus preventing their degradation, and in the refolding of these proteins into their native structure (Schroder *et al.*, 1993; Hendrick and Hartl, 1993). WB is a sensitive immunological method to investigate protein abundance, cellular localization, protein-protein interactions, detection of antigens in crude mixtures of proteins and clinical applications in autoimmune diseases. Specific antibodies are a reliable tool to examine protein expression patterns and to determine the protein localizations within cells (Burnette, 1981; Okegawa *et al.*, 2016; Bass *et al.*, 2017).

Lenne and Douce (1994) reported that when pea (*Pisum sativum*) plants are shifted from 25°C up to 40°C for 3 h, 22-kD protein was produced in mitochondria. HSP22 was used as antigen to prepare antiserum, which the expression of HSP22 was studied using immunodetection methods. Examination of mitochondria matrix extracts by polyacrylamide gel electrophoresis (PAGE) and immune blotting with anti-HSP22 serum revealed HSP complex contains HSP22. Lenne *et al.* (1995) purified HSP22 and developed a polyclonal antibody. Use of antiserum allowed them to show that the HS response is a rapid

process since HSP22 can be detected in total protein extracts as early as 30 min after treatment at 40°C of pea (*Pisum sativum*). Lund *et al.* (1998) identified mitochondrial HSP70 and cpn60 in maize inbred “B73” using two dimensional-PAGE (2D-PAGE) and immune-blot. During HS at 42°C for 4 h, the level of HSP22 increased dramatically. Monoclonal antibodies were developed to maize HSP70, cpn60, and HSP22. Maximal HSP22 expression occurred in etiolated seedling mitochondria after 5 h of a +13°C HS. Li *et al.* (2011) carried out WB to detect the expression of target proteins in a set of 10 rice samples. The results indicated that HSP was the most constantly expressed among all rice proteins tested throughout all developmental stages. They found that the reference proteins and the corresponding antibodies can be used in qualitative and quantitative analysis of rice proteins.

RT-PCR has become one of the most widely used methods of gene quantitation because it has a large dynamic range, can be highly sequence-specific and has little post-amplification processing. In addition, many diagnostic applications have been developed, including microbial quantification, identification of transgenes in genetically modified foods and applications for forensic use (Wong and Medrano, 2005; Berg *et al.*, 2007). The fluorescence-based quantitative RT-PCR (qRT-PCR) is an accurate tool to analyze gene expression, which mRNA normalization requires internal control genes are stably

* Corresponding author e-mail: aboudeif@yahoo.com.

expressed should be used. Reference genes, which serve as endogenous controls to ensure that the results are accurate and reproducible, are vital for data normalization (Lilly *et al.*, 2011; Zhang *et al.*, 2013; Lin *et al.*, 2014).

Li *et al.* (2015) found that, using qRT-PCR, the expression level of *ZmHsf06* was raised by heat stress to different extents in three *Arabidopsis* transgenic lines. Phenotypic observation showed over-expressing of *ZmHsf06* in *Arabidopsis* plants, which enhanced basal and acquired thermo-tolerance under HS conditions. Zhao *et al.* (2017) demonstrated that *ZmHsf04*, analyzed by qRT-PCR, was expressed in multiple tissues of maize. Expression level of *ZmHsf04* was up-regulated significantly by HS at 42°C, especially in pollens with the value of 16 times of the control. Song *et al.* (2016) isolated HSP70 gene from maize designated as *ZmERD2* (Early Responsive to Dehydration 2). Expression of *ZmERD2* was analyzed by qRT-PCR in maize found to be induced by HS and dehydration treatments. The expression was induced at 42°C and reached 40-fold above the control level after one hour of HS. Kumar *et al.* (2019) characterized five HSP genes and their expression analysis in two contrasting maize lines, i.e. LM17 (heat tolerant) and HKI1015WG8 (heat susceptible) subjected to HTS. The five-maize specific HSP genes, viz., *ZmHsp26*, *ZmHsp60*, *ZmHsp70*, *ZmHsp82* and *ZmHsp101* exhibited different expression pattern in response to HS. They found higher upregulation of *ZmHsp70* and *ZmHsp101* throughout the stress exposure in the heat tolerant line as compared to the susceptible line.

The objectives of this study are quantification of expression levels of HSP genes in four Egyptian maize lines by WB and RT-PCR analyses and identification of specific genes playing essential role in HS tolerance for developing stress resistant genotypes.

2. Materials and methods

2.1. Plant materials

Four Egyptian inbred lines of maize (*Zea mays* L.) were used in this study. Two lines K1 and K7 were developed by the plant breeding group, National Research Centre, Giza, Egypt. The other two lines G342 and Rg59 were kindly supplied by the Agriculture Research Center, Giza, Egypt. The four lines were previously studied to identify HSPs under HS at 45°C as protein markers for detecting the thermo-tolerance lines. The results indicated that the three lines K1, K7 and G342 are tolerant and the line Rg59 is susceptible (Mahmoud *et al.*, 2018).

2.2. Western blot analysis

The proteins were separated on one-dimensional gel and transferred to nitrocellulose membranes according to Towbin *et al.* (1979). The membrane was incubated with PBS buffer (1.6 mM PO₄H₂Na.H₂O, 8.4 mM PO₄HNa₂.2H₂O, 150 mM NaCl, pH 7.4.), 0.1% Tween 20 and 3% skimmed milk buffer for one hour at RT on shaker. PBS buffer was used to wash the membrane three times each time for 5 min, then the first antibody (Bib-hsp17.6/ hsp22 with dilution 1:1000 and hsp17.9/ hsp70 with dilution 1:4000) was added in PBS buffer with 0.1% Tween 20 and 3% skimmed milk. The membrane was incubated for 2 h at RT, then washed three times with PBS buffer with 0.1% Tween 20, each time for 5 min. The

second antibody (anti-Rabbit) was added with dilution 1:1000 in PBS buffer with 0.1% Tween 20 and 3% skimmed milk; then incubated for 2 h at RT and washed three times with PBS buffer. The proteins on membrane were detected after maintaining for the needed time, then exposed to autoradiography using LAS 4000 instrument. Immunoreactive bands were visualized with a highly sensitive chemiluminescent substrate for peroxidase detection (GE Healthcare Europe GmbH, Freiburg, Germany). The *Actin* gene was used as reference gene to normalize the expression values.

2.3. Real Time PCR analysis

The expression levels of three HS genes markers (*ZIP60* transcription factor, *hsp22* and *hsp16.9*) were detected by RT-PCR for the four maize lines K1, K7, G342 and Rg59. The primers listed in Table (1) were designed using Primer Express Software (Applied Biosystems, Foster City, CA, USA). Total RNA preparation, first-strand cDNA synthesis and RT-PCR were performed as described by Cui *et al.* (2012). DNaseI-treated total RNA was subjected to reverse transcription using QuantiTect Reverse Transcription kit (Qiagen, Germany), cDNA samples from three independent replicates were analyzed by Fluidigm system (San Francisco, CA, USA). Master mix tubes (Invitrogen, USA) were used in the reactions, each tube containing: dNTPs, MgCl₂, RT-PCR buffer and *Taq* DNA polymerase. The concentration of the primers was 10 µM/µl and cDNA concentration was 15 ng/µl. After the reactions were mixed, vortexed for 30 second then centrifuged at 1600 rpm for one min. The reactions of RT-PCR were applied in Roche Light Cycler 480 instrument using SYBR Green I dye. Three biological replicates were performed. The expression level in leaf tissue from unstressed control plants was selected as calibrator.

Table 1. List of the specific primers for qRT-PCR and their nucleotide sequences.

No.	Gene name	Sequence (primer direction 5'-3')
1	<i>HSP22</i>	F- GAGGGCGAGAAGGAGGATAG R- CTCGACGTTGACTTGAACA
2	<i>HSP16.9</i>	F- GAACGGATAGTAGCGTCCCA R- CAATGCAGGAATACCACCT
3	<i>ZIP60</i>	F- AGGATAGGCCTCTTGGTGCT R- TTCCATGGAGGATGAGTTCC

HSP22: Heat Shock Protein 22, HSP16.9: Heat Shock Protein 16.9, ZIP60: Zipper (ZIP) transcription factor 60, F: Forward, R: Reverse.

3. Results

Resistance of the four maize inbred lines to high temperature correlates with the expression levels of HSP markers was detected through two experiments, WB and RT-PCR.

3.1. WB analysis

A comparative analysis of induction levels of four protein markers (HSP70, HSP22, HSP17.9 and HSP17.6) by WB was carried out using four various antibodies.

3.1.1. Detection of HSP70 in response to HS by BiP antibody

BiP polyclonal antibody was performed in rabbit against C-terminal domain of tobacco HSP70. The reagents of BiP antibody with the extracted proteins from seedling leaves of the inbred lines K1, K7, G342 and Rg59 are shown in Figure (1). The expression bands of reactions were visualized by PAGE analysis. The three lines K1, K7 and G342 showed bands in the control increased in intensity after exposing to HS treatment at 45°C for 2 and 4 h. An intensive band was present in the control of the line Rg59 and decreased with the time of exposing to HS treatment.

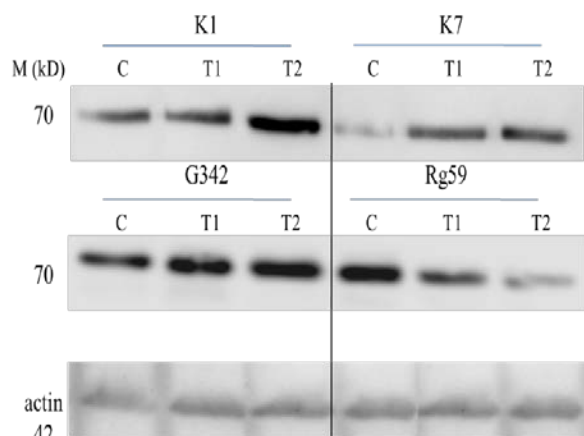


Figure 1. WB of the seedling proteins (10µg/lane) extracted from control and heat-treated plants of indicated inbred lines probed with BiP antibody (dilution 1:1000). C (control) = 25°C, T1 = treatment at 45°C for 2 h and T2 = treatment at 45°C for 4 h. M: molecular weight (kD). Actin antibody is used as a total protein loading control.

3.1.2. Detection of HSP22 in response to HS by HSP22 antibody

HSP22 polyclonal antibody against tobacco mtHSP23 was used to detect HSP22 in maize inbred lines in response to HS (Figure 2). The reaction of HSP22 antibody with the seedling leaves proteins extracted from the lines K1, K7 and G342 did not detect any expression band in the control, while the expression level of up-regulation varied in different lines after exposing to HS treatment at 45°C for 2 and 4 h. The line K1 showed a faint band at 45°C for 2 h and clear band after exposing to 45°C for 4 h, while the contrary was found in the line K7. The expression increased rapidly in the line G342 after 2 and 4 h of heat exposure. In contrast in the line Rg59, the expression level was high in the control but disappeared after treatment at 45°C for 2 h while appeared very faint after exposing to 45°C for 4 h.

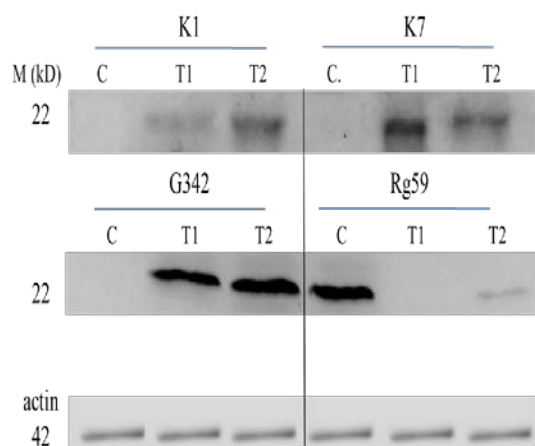


Figure 2. WB of the seedling proteins (25µg/lane) extracted from the control and heat-treated plants of indicated inbred lines probed with HSP22 Antibody (dilution 1:1000). C (control) = 25°C, T1 = treatment at 45°C for 2 h and T2 = treatment at 45°C for 4 h. M: molecular weight (kD). Actin antibody is used as a total protein loading control.

3.1.3. Detection of HSP17.9 in response to HS by HSP17.9 Antibody

HSP17.9 polyclonal antibody against sunflower recombinant proteins made in rabbit was utilized in detection of HSP17.9 in maize inbred lines in response to HS (Figure 3). The reaction of HSP17.9 antibody against inbred line K1 proteins did not manifest any expression band in the control, while an expression band appeared after exposing to HS of 45°C for 2 h and was more visibility after 4 h. The expression level was very faint in the inbred K7 after exposing to HS, while appeared clearly in the line G342 after 4 h of exposure. The expression was very faint in the control of the line Rg59 while disappeared after heat treatment.

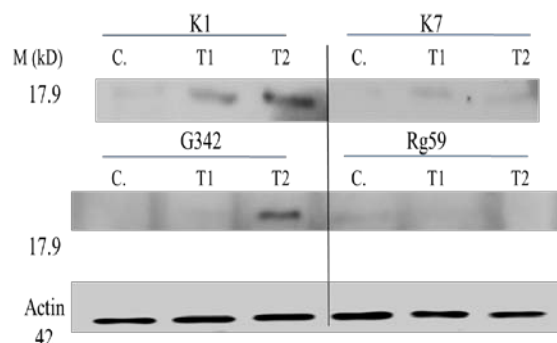


Figure 3. WB of seedling proteins (25µg/lane) extracted from control and heat-treated plants of indicated inbred lines probed with HSP17.9 antibody (dilution 1:4000). C (control) = 25°C, T1 = treatment at 45°C for 2 h and T2 = treatment at 45°C for 4 h. M: molecular weight (kD). Actin antibody is used as a total protein loading control.

3.1.4. Detection of HSP17.6 in response to HS by HSP17.6 antibody

HSP17.6 polyclonal antibody against sunflower recombinant protein made in rabbit was utilized in detection of HSP17.6 in maize lines in response to HS (Figure 4). The reaction of HSP17.6 antibody with the proteins of inbred lines K1 and G342 did not give any expression in the control while intensive expression appeared after exposing to heat treatment at 45°C for 2 h and was more intensity after 4 h. Significant expression

was visualized in the lines K7 and Rg59 which increased gradually after exposing to heat treatment.

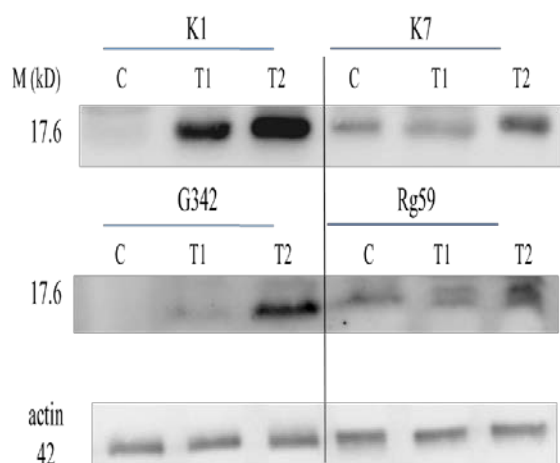


Figure 4. WB of the seedling proteins (25µg/lane) extracted from the control and heat-treated plants of indicated inbred lines probed with HSP17.6 antibody (dilution 1:1000). C (control) = 25°C, T1 = treatment at 45°C for 2 h and T2 = treatment at 45°C for 4 h. M: molecular weight (kD). Actin antibody is used as a total protein loading control.

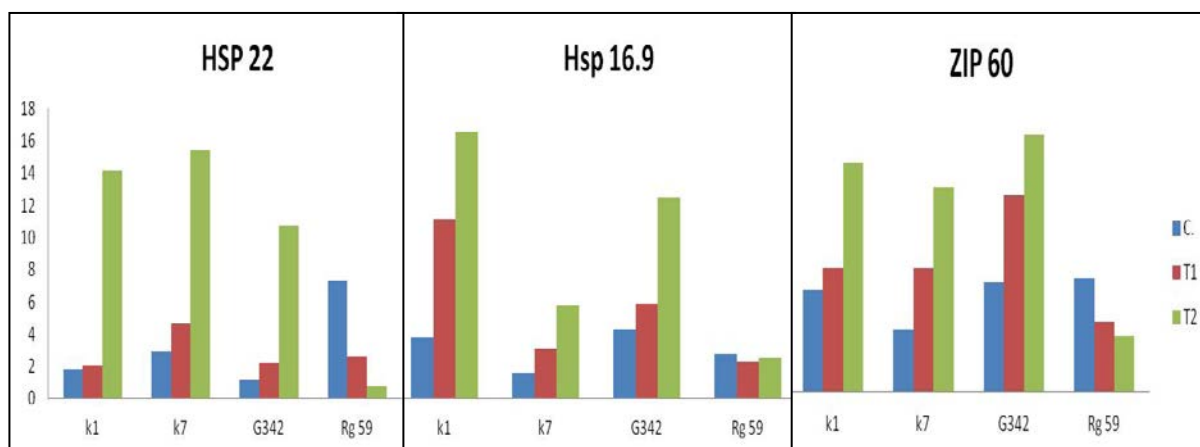


Figure 5. Expression analysis of the three gene markers *ZmHSP22*, *ZmHSP16.9* and *ZIP60* in response to HS treatments in the four maize lines. C: control at 25°C, T1: treatment for 2 h at 45°C and T2: treatment for 4 h at 45°C. The vertical axis represents relative transcript level and the horizontal axis represents the maize lines.

Upregulation of the transcription factor *ZIP60* at 45°C after 4 h in the line K1 was almost twice than the control (25°C) and HS treatment at 45°C after 2 h. *HSP16.9* showed expression level three and four times more than the control after exposing to 45°C for 2 h and 4 h, respectively. Meanwhile, *HSP22* gave gene expression about seven-fold after exposing to 45°C for 4 h more than the control. The transcription factor *ZIP60* expressed in the inbred line K7 two times after exposing to HS at 45°C for 2 h and three times after 4 h as compared to the control. The two genes *HSP16.9* and *HSP22* expressed progressively in the line K7 during time reaching a maximum expression of four and six times respectively after heat exposing to 45°C for 4 h as compared to the control. Regarding the line G342, the transcription factor *ZIP60* expressed in control plants and increased progressively with increasing time of exposing to HS treatment. Both of *HSP16.9* and *HSP22* showed a maximum expression after heat treatment at 45°C for 4 h. In contrast, the expression level of the three genes in the

3.2. RT-PCR analysis

The expression levels of the three heat-induced gene markers *ZmHSP22*, *ZmHSP16.9* and *ZIP60* were estimated by RT-PCR. The quantitation of plant gene expression through RT-PCR method was carried out using the four Egyptian maize lines K1, K7, G342 and Rg59, which cDNA of the three gene markers and SYBR green reagent were used as working model (Figure 5). The primers of each gene that were mentioned in Table (1) were designed according to the sequences from the GenBank, NCBI, USA. All experiments were repeated three replicates to confirm the results.

line Rg59 appeared in the control more than heat treatments (Figure 5).

4. Discussion

The expression levels of the HSP gene markers (*ZmHSP70*, *ZmHSP22*, *ZmHSP17.9* and *ZmHSP17.6*) in the four maize lines K1, K7, G342 and Rg59 were evaluated by WB with four antibodies. The results revealed that: 1) The antibodies against HSPs can recognize the corresponding endogenous proteins of the studied maize lines. 2) HSP expression was absent in the untreated plants but induced in the resistant lines K1, K7 and G342 after exposing to HS treatment. However, the majority of the HSP gene markers expressed only in the untreated plants of the line Rg59 which it is consider a heat sensitive line. 3) There are differences in the induction kinetics of HSP gene markers. For example, induction of *HSP70* was detected after exposing to 45°C for 2 h whereas induction of *HSP17.6* was more evident

after 4 h of HT. Induction of HSP17.6 was more intensity in the line K1 than the other lines after exposing to HT. The gene expression of HSP22 and HSP70 was more intensity in the line G342 than the other lines after exposing to HS treatment, while the same result was shown for HSP70 in the line K7 comparing to the other lines. Higher expression of the four HSP genes that appeared by WB analysis in the heat tolerant lines indicated that they could play a crucial role in conferring heat tolerance. Other researchers revealed similar results such as Verhagen and Kompoliti (2010) who found that WB is a sensitive immunological method for determination of molecular weights of protein antigens and detection of antigens in crude mixtures of proteins. De Vries (2012) reported that linear epitopes can be detected using polyclonal antibodies.

Expression of the three gene markers *ZmHSP22*, *ZmHSP16.9* and *ZIP60* in response to HT by RT-PCR analysis were clearly induced in the three lines K1, K7 and G342 which are considered tolerant lines. The expression levels of the three genes in the line Rg59 after exposing to HT were less than those of the control indicating sensitivity against HT. The results of gene expression using RT-PCR correlated with those of WB analysis in response of the three resistant maize lines to HT, which emphasized that the induced expression of the genes in this study protects the plants from the deleterious effects of high temperature stress. Therefore, identification of specific gene(s) playing essential role in HS tolerance could be useful for developing stress resistant genotypes.

Our results are coincided with those reported by other researchers. The rate of HSP synthesis in plants has been shown to be directly proportional to the temperature applied during the stress (Chen et al., 1990). Our experiments showed that the accumulation of HSPs in leaves tissues was also proportional to temperature by two to seven-fold at 45°C more than at 25°C. Andersen et al. (2004) reported that qRT-PCR provides a useful and rapid means of understanding gene expression in living organisms by measuring the expression of target genes across different samples. Zhao et al. (2017) demonstrated that *ZmHsf04* is expressed in multiple tissues of maize and was up-regulated significantly after exposing to 42°C HS, which the highest value reached 340 times of the control.

Kumar et al. (2019) found five maize specific HSP genes; *ZmHsp26*, *ZmHsp60*, *ZmHsp70*, *ZmHsp82* and *ZmHsp101* exhibited distinctive expression pattern in response to HS, especially *ZmHsp70* showed higher upregulation throughout the stress exposure in a heat tolerant line as compared to a susceptible line. The role of sHSPs in response to environmental stresses has been clearly established by several studies. HSPs have been implicated in functions related to protein assembly or the alteration/maintenance of specific protein conformations (Lindquist and Craig, 1988). *ZmHSP16.9* gene enhances both thermotolerance and oxidative stress resistance through the protection of antioxidative enzymes under heat stress condition (Sun et al., 2012). Overexpression of HSP26 in transgenic *Arabidopsis* enhanced thermotolerance due to increased amount of free proline caused by the elevated proline biosynthetic pathway genes (Xue et al., 2010).

5. Conclusions

The expression analysis of HSP genes was carried out by WB and RT-PCR in the four maize inbred lines K1, K7 and G342 (heat tolerant) and Rg59 (heat susceptible) subjected to high temperature stress at seedling stage. The HSP genes exhibited distinctive expression pattern as response to HS. Higher upregulation of *ZmHSP70*, *ZmHSP22*, *ZmHSP17.9* and *ZmHSP17.6* were found throughout the stress exposure to 45°C for 2 and 4 h in the heat tolerant lines as compared to the control (25°C) and susceptible line. Upregulation of these genes indicated their possible role in protecting plants from the adverse effects of HS. The results indicated that WB and RT-PCR are evident and accurate to detect the gene expression in plants for HSPs induction under abiotic stresses, especially heat stress in maize.

Acknowledgement

The authors thank the Spanish Agency for International Development Cooperation of Spain for funding this work through the research project “11-CAP-2-1151” and for laboratory assistance.

References

- Andersen CL, Jensen JL and Orntoft TF. 2004. Normalization of real-time quantitative reverse transcription-PCR data: a model-based variance estimation approach to identify genes suited for normalization, applied to bladder and colon cancer data sets. *Cancer Res*, **64**: 5245–5250.
- Bass JJ, Wilkinson DJ, Rankin D, Phillips BE, Szewczyk NJ, Smith K and Atherton PJ. 2017. An overview of technical considerations for western blotting applications to physiological research. *Scandinavian J of Med & Sci in Sports*, **27**: 4-25.
- Berg RJ, Vaessen N, Endtz HP, Schulin T, Vorm ER and Kuijper EJ. 2007. Evaluation of real time PCR and conventional diagnostic methods for the detection of *Clostridium* edificial associated diarrhea in a prospective multicenter study. *J Med Microbiol*, **56**: 36–42.
- Bumette WN. 1981. “Western Blotting”: electrophoretic transfer of proteins from sodium dodecyl sulfate-polyacrylamide gels to unmodified nitrocellulose and radiographic detection with antibody and radio-iodinated protein A. *Anal Biochem*, **112**: 195–203.
- Chen O, Lauzon LM, DeRocher AE and Vierling E. 1990. Accumulation, stability, and localization of a major chloroplast heat-shock protein. *J Cell Biol*, **110**: 1873-1883.
- Cui F, Liu L, Zhao Q, Zhang Z, Li Q, Lin B, Wu Y, Tang S and Xie Q. 2012. *Arabidopsis* ubiquitin conjugate UBC32 is an ERAD component that functions in brassinosteroid-mediated salt stress tolerance. *Plant Cell*, **24**: 233–244.
- DeVries E. 2012. Patient-centered screening for primary immunodeficiency, a multi-stage diagnostic protocol designed for non-immunologists. *Clinical & Experimental Immunol*, **167**: 108-119.
- Hendrick JP and Hartl FU. 1993. Molecular chaperone functions of heat-shock proteins. *Annu Rev Biochem*, **62**: 349–384.
- Kumar K, Singh I, Aggarwal C, Tewari I, Kumar A, Yadava P and Rakshit S. 2019. Expression profiling of heat shock protein genes in two contrasting maize inbred lines. *Int J Curr Microbiol App Sci*, **8**: 347-358.

- Lenne C and Douce R. 1994. A low molecular mass heat-shock protein is localized to higher plant mitochondria. *Plant Physiol*, **105**: 1255-1261.
- Lenne C, Block MA, Garin J and Douce R. 1995. Sequence and expression of the mRNA encoding HSP22, the mitochondrial small heat-shock protein in pea leaves. *Biochem J*, **311**: 805-813.
- Li D, Wang L, Liu X, Cui D, Chen T, Zhang H and Zhao L. 2011. Deep sequencing of maize small RNAs reveals a diverse set of micro-RNA in dry and imbibed seeds. *PLoS One*, **8**: e55107.
- Li HC, Zhang HN, Li GL, Liu ZH, Zhang YM, Zhang HM and Guo XL. 2015. Expression of maize heat shock transcription factor gene *ZmHsf06* enhances the thermotolerance and drought-stress tolerance of transgenic *Arabidopsis*. *Functional Plant Biol*, **42**: 1080-1091.
- Lilly ST, Drummond RSM, Pearson MN and MacDiarmid RM. 2011. Identification and validation of reference genes for normalization of transcripts from virus-infected *Arabidopsis thaliana*. *Mol Plant Microbe Interact*, **24**: 294-304.
- Lin Y, Zhang C, Lan H, Gao S, Liu H, Liu J, Cao M, Pan G, Rong T and Zhang S. 2014. Validation of potential reference genes for qPCR in maize across abiotic stresses, hormone treatments, and tissue types. *PLoS One*, **9**: e95445.
- Lindquist S and Craig E. 1988. The heat shock proteins. *Annu Rev Genet*, **22**: 631-677.
- Lund AA, Blum PH, Bhatramakki D and Elthon TE. 1998. Heat-stress response of maize mitochondria. *Plant Physiol*, **116**: 1097-1110.
- Mahmoud FE, Rashed MA, Khalil KM and Abou-Deif MH. 2018. Identification and characterization of heat shock proteins in four Egyptian maize inbred lines (*Zea mays* L.). *Arab Universities J of Agric Sci*, **26**: 1203-1211.
- Okegawa Y, Koshino M, Okushima T and Motohashi K. 2016. Application of preparative disk gel electrophoresis for antigen purification from inclusion bodies. *Protein Expression and Purification*, **118**: 77-82.
- Sachs MM and Ho THD. 1986. Alteration of gene expression during environmental stress in plants. *Annu Rev Plant Physiol*, **37**: 363-376.
- Schröder H, Langer T, Hartl FU and Bukau B. 1993. DnaK, DnaJ and GrpE form a cellular chaperone machinery capable of repairing heat-induced protein damage. *EMBO J*, **12**: 4137-4144.
- Song J, Weng Q, Ma H, Yuan J, Wang L and Liu Y. 2016. Cloning and expression analysis of the *Hsp70* gene *ZmERD2* in *Zea mays*. *Biotechnol & Biotechnological Equipment*, **30**: 219-226.
- Sun L, Liu Y, Kong X, Zhang D, Pan J, Zhou Y et al. 2012. *ZmHSP16.9*, a cytosolic class I small heat shock protein in maize (*Zea mays*), confers heat tolerance in transgenic tobacco. *Plant Cell Rep*, **31**: 1473-1484.
- Towbin H, Staehelin T and Gordon J. 1979. Electrophoretic transfer of proteins from polyacrylamide gels to nitrocellulose sheets: procedure and some applications. *Proc Natl Acad Sci*, **76**: 4350-4354.
- Verhagen L and Kompoliti K. 2010. *Encyclopedia of Movement Disorders*. Academic Press. <https://www.worldcat.org/title/encyclopedia-of-movement-disorders/oclc/614267004>.
- Wong ML and Medrano JF. 2005. Real-time PCR for mRNA quantitation. *BioTechniques*, **39**: 75-85.
- Xue Y, Xiong A, Li X, Zha D and Yao Q. 2010. Over-expression of heat shock protein gene *hsp26* in *Arabidopsis thaliana* enhances heat tolerance. *Biol Plantarum*, **54**: 105-111.
- Zhang X, Rerksiri W, Liu A, Zhou X, Xiong H, Xiang J, Chen X and Xiong X. 2013. Transcriptome profile reveals heat response mechanism at molecular and metabolic levels in rice flag leaf. *Gene*, **530**: 185-192.
- Zhao L, Zhang H, Duan S, Guo X and Li G. 2017. Cloning and characterization of maize (*Zea mays*) *ZmHsf04* gene and its regulating role in thermotolerance. *J of Agric Biotechnol*, **25**: 1411-1422.

Isolation of the Astacin-like metalloprotease coding gene (*astl*) and assessment of its insecticidal activity towards *Spodoptera littoralis* and *Sitophilus oryzae*

Mervat R. Diab^{1,*}, Mahmoud M. Ahmed², Ebtissam H.A. Hussein³ and Ahmed M. A. Mohammed¹

¹Agriculture Genetic Engineering research Institute, Agriculture Research Center, 9 Gamaa St., Giza, Egypt; ²Department of Zoology and Agricultural Nematology, Faculty of Agriculture, Cairo University, Giza, Egypt; ³Department of Genetics, Faculty of Agriculture, Cairo University, Giza, Egypt.

Received: May 25, 2020; Revised: September 26, 2020; Accepted: Oct 26, 2020

Abstract

Astacin-like metalloprotease, possessing a zinc (II) ion in the catalytic center is one of the toxic proteases. It exists in a variety of organisms, including fish, frogs, birds and insects. The present investigation was conducted with the main goal of assessing the efficacy of astacin like metalloprotease toxin for pest control and to determine the probability of using it to produce a new biopesticide that is friendly to the environment. Therefore, the full length of *astl* cDNA was cloned from spider species, *Hasarius adansoni*. Sequencing of the cloned *astl* cDNA has proved that its full length includes 802 bp with 714bp open reading frame encoding 238 amino acids. 486bp of the catalytic domain was cloned and expressed by the yeast expression system *Pichia pastoris*, and its insecticidal activity was determined towards two species of agricultural insects from two different orders, *Spodoptera littoralis* (Lepidoptera:Noctuidae) and *Sitophilus oryzae* (Coleoptera:Curculionidae). Bioassay was performed using three concentrations (100,500 and 1000 µg/ml) for four days for *S. littoralis* and 14 days for *S. oryzae*. At the concentration 1000 µg/ml, the mortality ratio was 69.3%±2.51, 65%±2.6 and 64.0%±3.0 for first instar *S. littoralis*, second instar *S. littoralis* and *S. oryzae* adults respectively. Finally, the present study represents an evidence that the use of zinc metalloproteases derived from different spiders may play an effective role in insect control.

Keywords: Metalloprotease, *Spodoptera littoralis*, *Sitophilus oryzae*

1. Introduction

Spider venoms are a cocktail of several different peptide toxins, most of which are likely to have insecticidal activity towards different insect orders (King et al. 2002, Escoubas et al., 2006 and Windley et al., 2012). Many of the insecticidal peptide toxins have been isolated from spider venoms, and their activity has been examined. Some of spider toxins showed no adverse effects on economically important insects such as Hv1a that is harmless to the pollinating insect honey bee (Nakasu et al. 2014). Zinc metalloproteases (enhancers) expressed by some baculoviruses improve the baculoviral infection into the insect larvae by increasing the permeability of peritrophic matrix (PM) through digestion of the PM proteins (Derksen and Granados 1988; Wang et al. 1994 and Lepore et al., 1996). Therefore, zinc metalloproteases can be exploited in insect control field outside the baculoviruses context (Harrison and Bonning 2010). Astacin-like metalloprotease proteins are secreted as zymogens as low molecular mass proteases that are activated by the cleavage of the prosegment from the catalytic domain (Yiallouris et al. 2002 and Guevara et al. 2010). Stöcker et al. (1988) stated that astacin family consisted of six genes (*bmp1*, *tl1*, *tl2*, *mep1a*, *mep1b* and

astl). Astacin (*astl*) is a multi-domain metalloprotease that is distinguished by the presence of zinc binding motif (HEXXHXXGXXH) and methionine-turn (MXY) (Gomis-Rüth et al. 2012). The *astl* gene is expressed as the hatching enzyme in the oocyte and in the developing embryo (Gomis-Rüth et al. 2012). The hatching enzyme is responsible for degradation of embryonic envelopes in crustaceans, fish, frogs, and birds (Gomis-Rüth et al. 2012). It is also known as ovastacin in mammals (Quesada et al. 2004) and plays a role in egg-sperm interactions (Sachdev et al. 2012).

The agricultural and horticultural pest insects cause 40% loss of the crop yield worldwide, estimated by 17.7 billion dollars annually (Oerke et al. 1994 and Oliveira et al. 2014). *Spodoptera littoralis* and *Sitophilus oryzae* are two of the most dangerous agricultural insect pests that are able to cause a lot of harms to various important crops as cotton, maize, tomatoes and stored grains (Madrid et al. 1990 and Salama et al. 1970). These agriculture pests are controlled by different methods such as chemical insecticides which are extensively used in Egypt (Mansour 2004). Therefore, resistant strains of insect pests have appeared in the field (Sawicki 1986). An alternative control method used in the control strategy is biological agents such as natural enemies, nuclear polyhedrosis virus

* Corresponding author e-mail: mervatdiab10@gmail.com.

(Jones et al. 1994 and Atia et al. 2016), *Bacillus thuringiensis* and its derivatives (Navon et al. 1983 and Moussa et al. 2016) and fumigant toxicity of some plants as *Uvaria afzelli* (Olufemi-Salami et al. 2018). However, *S. littoralis* and *S. oryzae* developed resistance to biological control agents (Salama et al. 1989). New biopesticides are always required to be involved in control strategy. Many spider venoms toxins were exploited as bioinsecticides against various insect pests such as ω -hexatoxin, OAIP-1, brachylin and knottins (Fitches et al. 2012, Hardy et al. 2013, Pyati et al. 2014, Zhong et al. 2014 and Matsubara et al. 2017).

In this article, the astacin like metalloprotease coding gene (*astl*) has been isolated from spider *Hasarius adansoni*, expressed in yeast and the toxicity of the astl protein was demonstrated towards *S. littoralis* and *S. oryzae*.

2. Material and methods

2.1. Spider collection

The spider samples were collected from human houses in Cairo, Egypt. The spider species used in the current study was identified as *Hasarius adansoni* using the DNA barcode technology by amplification of 889 bp of ribosomal RNA (*rRNA*) gene large subunit and 705bp of the 5'-end of mitochondrial cytochrome c oxidase subunit 1 (*COI*) gene. The fragments of *rRNA* and *COI* were amplified using specific primer sets Sp28SN/Sp28SC (Starrett and Hedin, 2007), and SP-LCO 1490FJJ/SP-HCO2198RJJ (Astrin et al., 2016), respectively. The spider species has been confirmed by the complete homology of the two fragments with *H. adansoni* using "BLASTN" NCBI-BLAST alignments tool. The cephalothorax region was dissected in paraffin wax plate and isolated from the rest of the body.

2.2. Total RNA extraction

The total RNA was extracted from the cephalothorax region of the spider by Trizole[®] reagent (Invitrogen, USA, Cat.#15596-026). First strand cDNA was synthesized using SuperScript[™]II reverse transcriptase (Invitrogen Cat.# 18064014) according to the manufacturer's instructions.

2.3. Cloning of astl cDNA

A set of degenerate primers astlFD: CARTTCTCGGAGGTATTGAAGCWGG and astlRD:AATRAAAGGAAGCKAGCAGAA was designed to amplify a part of the nucleotides sequence of the astacin like metalloprotease cDNA using the first strand cDNA as a template. The 5' and 3' ends were amplified using First Choice[®] RLM-RACE kit (Ambion, Austin, TX, USA). According to the kit instructions, two reverse primers, astlR1: CCGTCGAAGATGGAGCCGA and astlR2: CCTTGGGGATGTAGATGGACT, were used to amplify the 5' end. In a similar way, the 3' end was amplified using two forward primers; astlF1: TTCCCCTCCATCAACTGGCTC and astlF2: TTGCCTGTACGCAGCACTGGG TC.

2.4. Sequences and phylogenetic analysis

The alignment of *astl* cDNA sequence was performed using the "BLASTN" and "BLASTX" tools. The ExPASy translate tool (<http://web.expasy.org/translate/>) was

utilized to deduce the amino acid sequences of astl cDNA clones. The phylogenetic tree was carried out by aligning astl amino acid sequence and other spiders and a scorpion sequences using the phylogeny.fr software

(<http://www.phylogeny.fr/index.cgi>). Molecular weight and isoelectric point were predicted by ExPASy Proteomics website (http://web.expasy.org/cgi-bin/compute_pi/pi_tool). The motifs were determined using PROSITE database (<http://prosite.expasy.org>). The glycosylation sites were scanned by NetNGLyc 1.0 software (<http://www.cbs.dtu.dk/services/NetNGLyc/>) and YinOYang program (<http://www.cbs.dtu.dk/services/YinOYang/>).

2.5. Cloning of astl, GNA catalytic regions and astl/GNA fused fragment into the yeast expression vector pPICZaA

The cloning strategy of astl catalytic domain in the expression vector pPICZaA was performed through the digestion by restriction enzymes EcoRI and XbaI then the ligation by T4 DNA ligase. The grown colonies were screened to select the positive clones.

2.6. Transformation of pPICZaA-astl, pPICZaA-GNA and pPICZaA-astl/GNA into yeast "Pichia pastoris", KM71H strain.

pPICZaA-astl (3-5 μ g) was digested using *SacI* followed by purification and transformation into yeast cells, *Pichia pastoris* yeast competent cell strain "KM71H". The transformed cells were incubated at 28°C for 2-3 days on YPDS medium plates containing 100mg/ml Zeocin. Then, the colonies were numbered and transferred to YPD plates containing 100mg/ml Zeocin, and incubated for two more days and allowed to grow.

A number of grown yeast colonies were dissolved in 20mM NaOH then boiled for 45 min at 95°C. After centrifugation, 2 μ l supernatant was used as a template. The putative positive clones were identified using PCR screening.

2.7. Expression of Ha-astl protein

The secreted protein of pPICZaA-Ha-astl was collected through the induction of a single colony of KM71H harboring pPICZaA-Ha-astl by methanol for four days. The expression analysis was conducted on secreted proteins in the supernatant. SDS-PAGE, Western blot analysis and ELISA test were used to analyze the expressed proteins as explained in Salem et al. 2019.

The concentration of protein was determined at protein A280 using Nanodrop 2000/2000C spectrophotometer, (ThermoScientific, USA).

2.8. Insect cultures

The *S. littoralis* colony was reared in the insectory of the Agriculture Genetic Engineering Research Institute (AGERI), Agricultural Research Center (ARC) under standard conditions. The larvae were reared on cleaned castor (*Ricinus communis*) leaves at 25 \pm 2°C and 16 h /8 h light-dark period .

S. oryzae was kindly supplied by the Plant Protection Research Institute (PPRI), ARC. The adults of the same age were reared on wheat seeds in glass jars under standard conditions and then used to assess the insecticidal activity.

2.9. Bioassay

The insecticidal activity of astl was assessed by feeding the *S. littoralis* larvae and the *S. oryzae* adults on three different concentrations (100, 500 and 1000 µg/ml) of the protein. The castor leaves were immersed in solution containing the assayed amount of protein with agitation for half an hour. The leaves were then picked up from the expressed culture supernatant and allowed to air dry. Twenty five and twenty of first and second stadium of *S. littoralis* larvae, respectively, were added to treated castor leaves which were replaced daily with fresh treated leaves for four days. Each treatment was repeated three times. The larval mortality was recorded daily during experiment period. The sensitivity of *S.oryzae* adults to astl was assayed for 14 days period. Ten g of wheat seeds were immersed in protein solution for 30 minutes. The treated wheat seeds were then filtered and allowed to dry. Twenty-five adults were added to each 10 g of treated wheat seeds in glass jar with three replicas for each concentration. The jars were incubated at 27°C for 16h/8h light/dark period. The adult mortalities were recorded on day 14. For all bioassays, both larvae and adults were treated with the control "expressed culture supernatant of native pPICZαA"

2.10. Statistical analysis

the significance of mortality results was calculated by Student's t-test in the Excel program using the calculations (Total, Percentage and STDEV) of the three replicates for each experiment .

3. Results

3.1. Amplification of the full length of Ha-astl cDNA sequence

The first strand cDNA of the *H. adansoni* cephalothorax, was used as a template to amplify Astacin-like metalloprotease coding gene (*astl*). One degenerate

primer set was designed for astacin-like metalloprotease coding gene (*astl*) from the conserved regions of the same gene in the spider *Latrodectus hesperus* and the scorpion *Tityus serrulatus*. A 119 bp fragment was firstly amplified using the degenerate primers. The 5' and 3' ends were amplified using two PCR rounds of RACE based on the sequence of the first amplified fragments; it was deduced that the full length of astacin like metalloprotease of *H. adansoni* (*Ha-astl*) cDNA is 802 nucleotides (accession no. MN453831). The open reading frame consists of 714 nts which encodes 238 amino acids and with catalytic domain between N46 and C238. The calculated molecular weight of encoded protein is 27.33 kDa with an isoelectric point (pI) of 8.29. The analysis of Ha-astl protein reveals the presence of two disulfide bridges between cysteine residues at positions 87-238 and 108-128. In additions, three zinc binding sites at histidine residues were found at positions 136,140 and 146 using the site (<http://prosite.expasy.org>). Also, a putative N-glycosylation site was predicted at aa 149, and O-β-glycosylation sites were predicted at T56, S70 and T94 (Fig 1a).

The deduced amino acid sequence was aligned using the BLASTp tool in the NCBI website. The covered score was 88-99%, and the identity ranged between 74-84% in spiders such as *Trichonephila clavipes*, *Latrodectus hesperus*, *Stegodyp husmimosarum* , *Parasteatodate pidariorum* and scorpion as *Tityus serrulatus* with accession no. PRD25795.1, ADV40108.1, KFM63176.1, XP_015909675.1 and CDJ26716.1, respectively. The alignment results of the deduced amino acids sequence with other published astacin like metalloprotease toxin are shown in Fig (1b). The phylogenetic tree performed by the phylogeny.fr software is shown in Fig (1c). These results demonstrated that the Ha-astl aa sequence is closely related to that of the spider *T. clavipes* and the scorpion *T. serrulatus*.

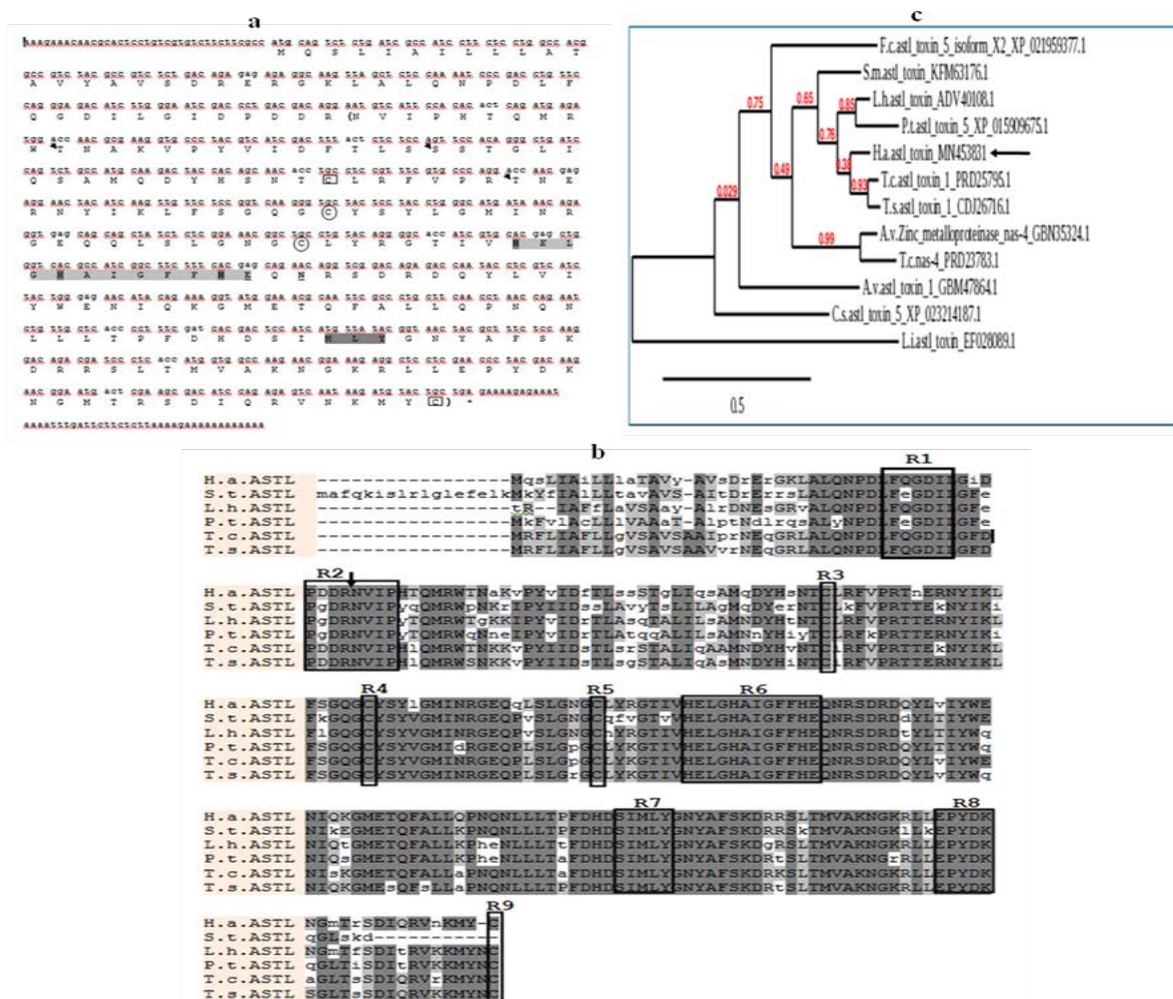


Figure 1. (a) Nucleotides and deduced amino acid sequence of *Hasarius adansoni* Astacin-like metalloprotease. The brackets mark to the active domain that start with asparagine N46 and ended at C238. The zinc motif is grey highlighted containing the three metal sites (Zinc) (H: 136,140 and 146) highlighted by dark grey. The astacin hallmark (E 137) is underlined. The methionine (MXY) turn is highlighted by grey. The first disulphide bridge is between the two squares (C:87 and C: 128). The second disulphide bridge is between the two ovals (C:108 and C: 128). Amino acid that predicted to be N-glycosylated was underlined (N: 149). Predicted O-β-glycosylation sites are noted by arrows (T:56, S70 and T:94). The stop codon is referred by asterisk. (b) amino acid alignment of the astacin like metalloprotease toxin in *Hasarius adansoni* (H.a.) (MN453831) with other spiders *Stegodyphus mimosarum* (S.t.), *Trichonephila clavipes* (T.c.) (PRD25795.1), *Latrodectus hesperus* (L.h.) (ADV40108.1) and *Parasteatoda tepidarium* (P.t.) (XP_015909675.1) and a scorpion *Tityus serrulatus* (T.s.) (CDJ26725.1). The identical aminoacids and the conservative substitution are highlighted in dark and light grey respectively. The rectangles (R) marked the regions containing the conserved aspartic residue "D" within the prosegment (R1), the activation site containing the first amino acid in the mature protein asparagines"N" (R2), the four conserved cysteine residue (R3,R4,R5 and R9), astacin signature sequence containing the hallmark glutamate"E" (R6), the methionine turn (R7) and the segment mainly engaged in shaping of subsite S₁ (R8) respectively. The black arrow referred to the cleavage point between the prosegment and the catalytic segment. (c) Phylogenetic analysis of amino acids of *Hasarius adansoni* (H.a.) Astacin-like metalloprotease (astl) toxin (referred by black arrow) with other correspondings in other spiders *Folsomia candida* (F.c.), *Stegodyphus mimosarum* (S.t.), *Latrodectus hesperus* (L.h.), *Parasteatoda tepidarium* (P.t.), *Trichonephila clavipes* (T.c.), *Araneus ventricosus* (A.v.) and *Loxosceles intermedia* (L.i.) and scorpions *Tityus serrulatus* (T.s.), *Centruroides sculpturatus* (Cs.).

3.2. Expression of pPICZaA-Ha-astl into yeast "Pichia pastoris" "KM71H strain"

Expressing target protein, pPICZaA-Ha-astl bound to His tag, was transformed into the yeast *P. pastoris* "KM71H" competent cells. The cell cultures were induced by methanol to express pPICZaA-- Ha-astl protein. The expressed protein was demonstrated on SDS-PAGE gel.

Expressed Ha-astl showed faint band on the SDS-PAGE at expected molecular mass (Fig. 2a); the extracellular expressed colonies were detected by Western blot analysis (Fig. 2b) in addition to the sandwich ELISA test that detect the expressed proteins targeted His Tag with His-specific antibody with different reading values at OD 450 (Fig 2c).

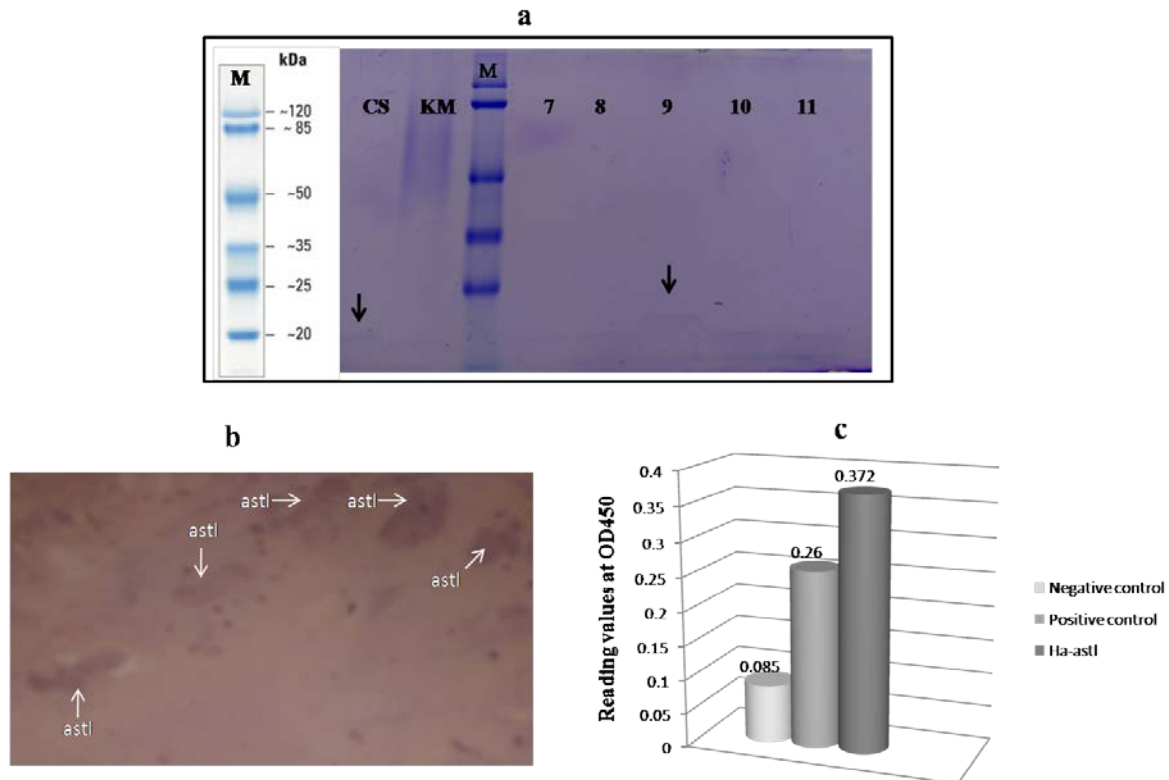


Figure 2. (a) Extracellularly expressing colonies (pPICZ α A-Ha-astl). The black arrow refers to the positive clone that revealed the expected expression. KM: empty KM71H strain and CS: secretion control afforded by invitrogen. M. prestained protein molecular weight marker (Thermoscientific, Cat no. 26612) (b) Western blot analysis for the expressed yeast colonies containing the recombinant vectors pPICZ α A-Ha-astl (c) Sandwich ELISA test showing the average values of negative control, positive control, pPICZ α A-Ha-astl, at OD 450.

3.3. The insecticidal impact of Astacin-like metalloprotease (Ha-astl), protein on *S. littoralis*

The toxic efficacy of Ha-astl was evaluated on the first and second instars of *S. littoralis* larvae *per os* using three different concentrations, i.e. 100, 500, 1000 μ g/ml of the protein. The oral activity was performed on treated castor leaves which were replaced daily for four days. While the control larvae were fed on treated castor leaves with the supernatant of expressed native pPICZ α A for the same period. The mortality was counted daily throughout the experiment period. The larval mortality ratio showed daily increment during the four-day experiment. For the first instar of the *S. littoralis*, the mortality percentages were $42.6\% \pm 2.5$, $46.6\% \pm 3.05$ and $69.3\% \pm 2.51$ for the three concentrations, i.e. 100, 500, 1000 μ g/ml of the protein, respectively. While for the second instar of *S. littoralis* the mortality percentages became $25\% \pm 1.0$, $58.3\% \pm 2.0$ and $65\% \pm 2.6$ for the same three concentrations, respectively. The statistical analysis of the mortality ratio showed significant (b) and highly significant (c) effects of the Ha-astl protein against control larvae at ($p > 0.05$) and ($p > 0.01$) respectively.

Larval mortality of *S. littoralis* and their significance are shown in Fig. (3a) and (3b).

The results of the feeding experiment also demonstrated that the larvae survived in the different treatments showed a significant retardation in their growth (Fig 4a). Some of them retarded to pupate, failed to pupate

or developed to malformed pupae compared to the control (Fig 4b). After a recovery period when larvae were transferred onto untreated castor leaves and allowed to grow for 10 to 15 days, the larvae did not restore normal weight. The difference of consumed castor leaves by control and treated larvae was clearly notable as shown in Fig (4c). The average larval weight of the control and treated larvae was 0.05 and 0.013g after 10 days and 0.08 and 0.0085 g after 15 days, respectively.

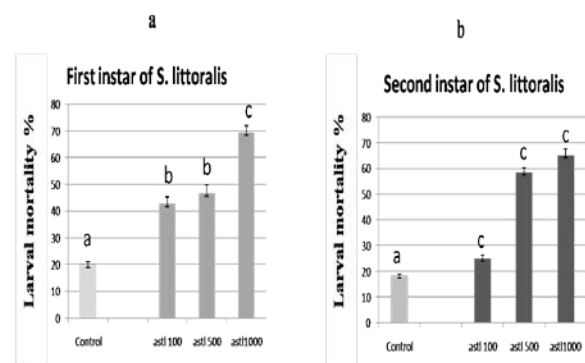


Figure 3. The mortality ratio of the first instar (a) and for the second instar (b) of *Spodoptera littoralis* after 96 hours using three concentrations (100, 500, 1000 μ g/ml) of Ha-astl protein comparing with the control (expressed native pPICZ α A protein). Error bars illustrate \pm SE. Within the same protein concentration different letters indicate significantly (b) at $P < 0.05$. and highly significant (c) at $P > 0.01$.

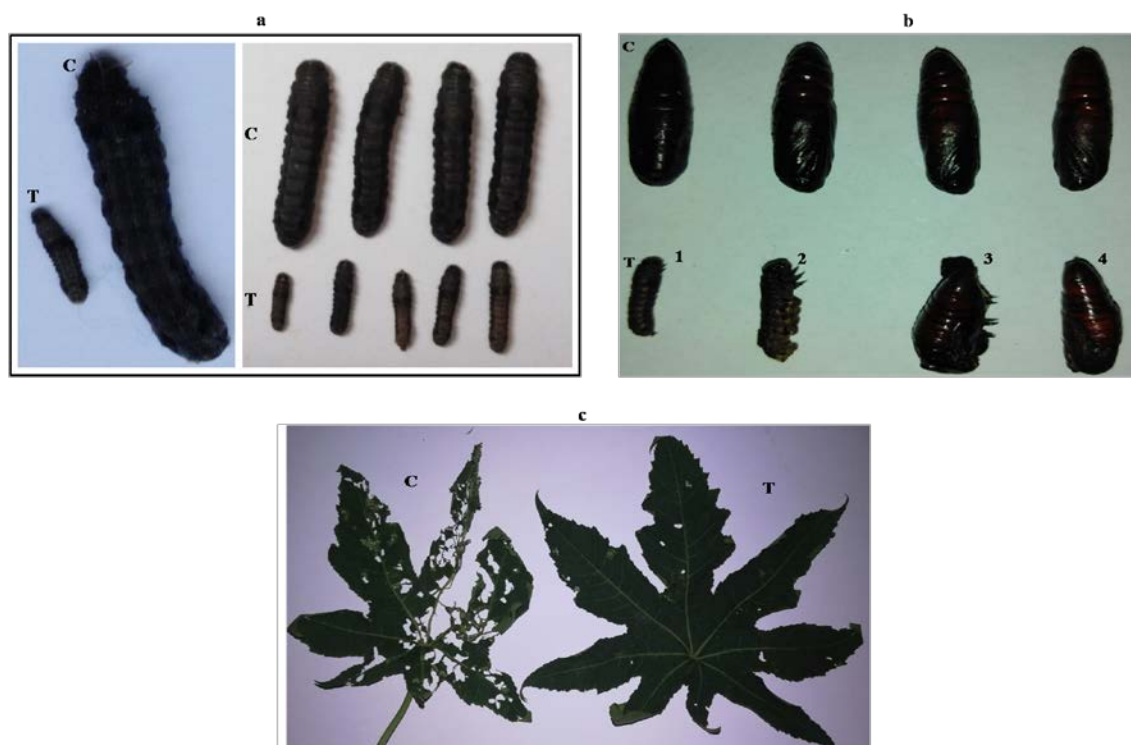


Figure 4. (a) Retardation in growth for the treated larvae using Ha-astl protein (T) against the control (C) in the same age. (b) The development of treated larvae (T) to retarded to pupate (1), failed to pupate (2) or malformed pupae (3 and 4) compared to the control (C). (c) The fed castor leaves by the control (C) and the treated larvae (T).

3.4. The insecticidal activity of Astacin-like metalloprotease (Ha-astl) protein on *S. oryzae*

The toxicity of the astacin-like metalloprotease was evaluated on the adult of *S. oryzae* by *per os* alongside the control (native expressed pPICZαA). Three concentrations were used, i.e.: 100, 500, 1000 µg/ml of the protein with three replicates each and 25 adults per replica. The adult mortality was recorded two weeks post-treatment. The mortality ratio for Ha-astl protein was $46.6\% \pm 0.577$, $48\% \pm 1.7$ and $64\% \pm 3$ for the three concentrations 100, 500, 1000 µg/ml, respectively. The statistical analysis showed that the mortality ratio was highly significant (c) at ($p > 0.01$) for all the concentrations of the Ha-astl protein. (Fig 5).

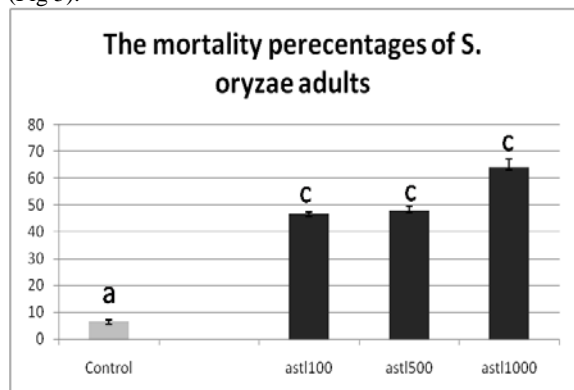


Figure 5. The mortality ratio of the adults of *Sitophilus oryzae* after fourteen days using three concentrations (100, 500, 1000 µg/ml) of Ha-astl protein comparing with the control (expressed native pPICZαA protein). Error bars illustrate \pm SE. Within the same protein concentration different letters indicate highly significant (c) at $P > 0.01$.

4. Discussion

Bioinsecticides are exploited as potential alternatives to pesticides. The sources of biopesticides are natural organisms, or their metabolic products including insecticidal toxins derived from parasitoids and insect predators as spiders and (Hajek 2004, Chandler et al. 2011, Lacey et al. 2015, Silva et al. 2018 and King 2019). This study examined the susceptibility of agricultural insect pests, *S. littoralis* and *S. oryzae*, (belonging to two insect orders lepidoptera and coleoptera towards expressed metalloprotease peptide, astacin, derived from the Adanson's house jumper spider, *H. adansoni*. The Ha-astl sequence was identified in the total RNA content of *H. adansoni* spider venom. The presence of metalloproteases as components of spider venom was previously detected in *Loxosceles* spider species (Feitosa et al. 1998, Young and Pincus 2001, Da Silveira et al. 2002 and 2007, Zanetti 2002 and Barbaro et al. 2005). Moreover, nine possible isoforms of astacin-like metalloproteases were identified from the Peruvian, *L. laeta* venom (Medina-Santos et al., 2019). Presence of metalloproteases in the spider venom provides evidence of its significant biological activity and its conserved feature in the venom of spider species (Da Silveira et al., 2002; Zanetti, 2002 and Barbaro et al., 2005).

The full length of Ha-astl cDNA sequence is a total of 802 nucleotides encoding 238 amino acids peptide. Ha-astl protein shows the same general features of metalloproteases family members (Dumermuth et al. 1991; Bond and Beynon 1995 and Mohrlen et al. 2004). Ha-astl primary structure includes a prosegment region (M1:R45), a catalytic domain (N46:C238) and a conserved methionine- turn MXY (Met192 and Tyr194). The

catalytic domain contains the consensus signature sequence responsible for binding of the catalytic zinc ion, HEXXHXXGXXHE (His136 and Glu147). Approximately 90% of spider-venom toxins possess between one to seven disulfide bridges, however, about 60% of spider toxins have three bridges only (Windley et al. 2012). Two disulfide bridges are potentially present in Ha-astl between Cys108-Cys128 and Cys87-Cys238. The calculated molecular mass and pI of the deduced amino acid of *Hasarius adansoni* (27.3 kDa/8.29) are closely related to other astacin-like metalloproteases in spiders, *Trichonephila clavipes* (27.3 kDa /8.97), *Latrodectus hesperus* (27.1 kDa /8.81) and a scorpion *Tityus serrulatus* (27.3 kDa /8.9).

The biological significance of native astacin-like venom toxin is not clearly known. However, the toxin is assumed to play a role in the predation of the insect prey as well as a defensive role against predators (Da Silveira et al. 2007). The metalloproteases facilitate the diffusion of other venom toxins through prey bodies by increasing the permeability of prey tissues, and then act in complement with other active toxins (Da Silveira et al. 2007).

Astacin may play role, in synergism with other venom toxins, in the deleterious effects of the prey after envenomation (Futrell 1992) as well as in the activation of peptide derived toxins after proteolysis. However, the toxic efficacy of solely astacin-like metalloprotease on insects is questionable. Could these proteases present the venom cocktail be used in insect control? To answer this question, the insecticidal activity of Ha-astl was assayed *per os* on cotton leaf worm and rice weevil. The N-terminal pro-segments of astacin-like metalloproteases inhibit the catalytic zinc domain and its removal is necessary to uncover a deep active-site cleft that contains aspartate residues in the specificity pocket (Gomis-Rüth et al. 2012). Hence, the catalytic region was used for expression as active astl. To maintain functional configuration of the expressed recombinant protein, an expression system performs post translation modifications was required. Thus, *Pichia pastoris* was used to express Ha-astl and secrete the recombinant protein into culture supernatant. The expressed recombinant proteins were exploited for sensitivity assays. A moderate toxic effect (mortality) of Ha-astl was demonstrated in both insect species. 1000 µg/ml of astacin peptide causes 69.3%±2.51 and 65%±2.64 for first and second instars of *Spodoptera* larvae, respectively. On the other hand, 64% ±3 % of *S. oryzae* adults were killed by the same concentration of Ha-astl protein. The similar level of lethality was demonstrated by spider neurotoxins on pest species. The insect-selective neurotoxin µ-agatoxin-Aal from the venom of the Western grass spider, *Agelenopsis aperta*, cause convulsive paralysis in insects and show variable toxicity against different insect orders. It is very potent to dipterans, moderate to orthopterans, while it shows weak activity towards lepidopterans (Adams et al. 1989). The ω-Hexatoxin-Hv1a toxins from the venom of Australian funnel-web spiders have low ED50 values in Orthoptera, Hemiptera, Dictyoptera, Diptera, Coleoptera, Acarina and Lepidoptera (Atkinson et al. 1996, Fletcher et al. 1997 and Bloomquist 2003). However, proper manipulation of these toxins revealed the prospect use of spider toxins in insect pest control. The

transgenic tobacco expressing ω-HXTX-Hv1a shows tolerance levels against *Helicoverpa armigera* and *S. littoralis* larvae (Khan et al. 2006). The topical application of recombinant thioredoxin-ω-HXTX-Hv1a has also been shown to be lethal to these caterpillar species (Khan et al. 2006).

5. Conclusion

The mortality resulting from the feeding of the astl protein in *Spodoptera littoralis* and in *Sitophilus oryzae*, Also, the retardation in growth of the larvae in *Spodoptera littoralis* proved that the astl protein may play an effective role in insect control as oral bioinsecticides. The actual effect of the astl protein will appear when it is used under different field conditions, and this will determine whether it can be used lonely in insect control or maybe introduced as a new biopesticide agent in the integrated pest management programs. Finally, the using of astl protein is considered the starting point for the exploiting zinc metalloproteases derived from different spiders in insect control fields, particularly in the view of the decreasing numbers of bioinsecticides available for use.

Acknowledgments

We would like to thank Dr. Mohamed Atia, Dr. Reda Salem and Dr. Ahmed Ramadan AGERI, for their support and help.

References

- Adams ME, Herold EE and Venema VJ. 1989. Two classes of channel-specific toxins from funnel web spider venom. *J. Comp. Physiol.*, **164**: 333–342
- Astrin JJ, Höfer H, Spelda J, Holstein J, Bayer S, Hendrich L, Huber BA, Kielhorn K, Krammer H, Lemke M, Carlos Monje J, Morinière J, Rulik B, Petersen M, Janssen H and Muster C. 2016. Towards a DNA Barcode Reference Database for Spiders and Harvestmen of Germany. *PLOS ONE*, doi:10.1371/journal.pone.0162624.
- Atia MAM, Osman GH and Elmenofy WH. 2016. Genome-wide In Silico Analysis, Characterization and Identification of Microsatellites in *Spodoptera littoralis* Multiple nucleopolyhedrovirus (SpliMNPV). *SCIENTIFIC REPORTS*, doi: 10.1038/srep33741.
- Atkinson R, Vonarx E and Howden M. 1996. Effects of whole venom and venom fractions from several Australian spiders, including *Atrax* (Hadroneche) species, when injected into insects. *Comp. Biochem. Physiol.*, **114**: 113–117.
- Barbaro K C, Knysak I, Martins R, Hogan C and Winkel K. 2005. Enzymatic characterization, antigenic cross-reactivity and neutralization of dermonecrotic activity of five *Loxosceles* spider venoms of medical importance in the Americas. *Toxicon*, **45**:489–499.
- Bloomquist JR. 2003. Mode of action of atracotoxin at central and peripheral synapses of insects. *Invert. Neurosci.*, **5**: 45–50.
- Bond J S and Beynon R J. 1995. The astacin family of metallo endopeptidases. *Protein Sci.*, **4**:1247–1261.
- Chandler D, Bailey AS, Tatchell GM, Davidson G, Greaves J and Grant WP. 2011. The development, regulation and use of biopesticides for integrated pest management. *Phil. Trans R Soc B.* **366**: 1987–1998.

- Da Silveira RB, Filho JFS, Mangili OC, Veiga SS, Gremski W, Nader HB and Dietrich CP. 2002. Identification of proteases in the extract of venom glands from brown spider. *Toxicon*, **40**: 815–822.
- Da Silveira RB, Wille ACM, Chaim OM, Appel MH, Silva DT, Franco CRC, Toma L, Mangili OC, Gremski W, Dietrich CP, Nader HN and Veiga SS. 2007. Identification, cloning, expression and functional characterization of an astacin-like metalloprotease toxin from *Loxosceles intermedia* (brown spider) venom. *Biochem J*, **406**: 355–363.
- Derksen AC and Granados RR. 1988. Alteration of a lepidopteran peritrophic membrane by baculoviruses and enhancement of viral infectivity. *Virology*, **167**: 242–250.
- Dumermuth E, Sterchi EE, Jiang W, Wolz R, Bond J S, Flannery AV and Beynon RJ. 1991. The astacin family of metalloendopeptidases. *J Biol Chem*, **266**: 21381–21385.
- Escoubas P, Sollod BL, King GF. (2006) Venom landscapes: mining the complexity of spider venoms via a combined cDNA and mass spectrometric approach. *Toxicon* **47**: 650–663.
- Feitosa L, Gremski W, Veiga S S, Elias MCQB, Graner E, Mangili OC and Brentani RR. 1998. Detection and characterization of metalloproteinases with gelatinolytic, fibronectinolytic and fibrinogenolytic activities in brown spider (*Loxosceles intermedia*) venom. *Toxicon*, **36**: 1039–1051.
- Fitches EC, Pyati P, King GF and Gatehouse JA. 2012. Fusion to snowdrop lectin magnifies the oral activity of insecticidal ω -Hexatoxin-Hv1a peptide by enabling its delivery to the central nervous system. *PLoS One*, doi.org/10.1371/journal.pone.0039389.
- Fletcher JI, Smith R, O'Donoghue SI, Nilges M, Connor M, Howden ME, Christie MJ and King GF. 1997. The structure of a novel insecticidal neurotoxin, ω -atracotoxin-HV1, from the venom of an Australian funnel web spider. *Nat. Struct. Biol*, **4**: 559–566.
- Futrell J M. 1992. Loxoscelism. *Am J Med Sci*, **304**: 261–267
- Gomis-Rüth FX, Trillo-Muyo S and Stöcker W. 2012. Functional and structural insights into astacin metallopeptidases. *Biol Chem*, **393**:1027–1041.
- Guevara T, Yiallourou I, Kappelhoff R, Bissdorf S, Stöcker W and Gomis-Rüth FX. 2010. Proenzyme structure and activation of astacin metallopeptidase. *J Biol Chem*, **285**: 13958 – 13965.
- Hajek A. 2004. Natural enemies: an introduction to biological control. Cambridge, UK: Cambridge University Press
- Hardy MC, Daly NL, Mobli M, Morales RAV and King GL. 2013. Isolation of an orally active insecticidal toxin from the venom of an Australian Tarantula. *PLoS One*, doi.org/10.1371/journal.pone.0073136.
- Harrison RL, Bonning BC. 2010. Proteases as Insecticidal Agents. *Toxins*, **2**: 935-953 doi:10.3390/toxins2050935.
- Jones KA, Irving NS, Grzywacz D, Moawad GM, Hussein AH and Fargahly A. 1994. Application rate trials with a nuclear polyhedrosis virus to control *Spodoptera littoralis* (Boisd.) on cotton in Egypt. *Crop Protection*, **13(5)**:337-340.
- Khan SA, Zafar Y, Briddon RW, Malik KA and Mukhtar Z. 2006. Spider venom toxin protects plants from insect attack. *Transgenic Res*, **15**: 349–357.
- King GF, Tedford HW and Maggio F. 2002. Structure and function of insecticidal neurotoxins from Australian funnel-web spiders. *J Toxicol: Toxin Rev*, **21**: 359–389
- King GF. 2019. Tying pest insects in knots: the deployment of spider-venom-derived knottins as bioinsecticides. *Pest Manag Sci* doi.: 10.1002/ps.5452.
- Lacey LA, Grzywacz D, Shapiro-Ilan DI, Frutos R, Brownbridge M and Goettel MS. 2015. Insect pathogens as biological control agents: back to the future. *J Invertebr Pathol*, **132**:1-41
- Lepore LS, Roelvink PR and Granados RR. 1996. Enhancin, the granulosis virus protein that facilitates nucleopolyhedrovirus (NPV) infections, is a metalloprotease. *J Invertebr Pathol* **68**: 131–140.
- Madrid F.J, White NDG and Loschiavo SR. 1990. Insects in stored cereals and their association with farming practices in Southern Manitoba. *Can. Entomol*, **122**: 515-523.
- Mansour SA. 2004. Pesticide exposure--Egyptian scene. *Toxicology*, **20;198(1-3)**:91-115.
- Matsubara FH, Meissner GO, Herzig V, Justa HC, Dias BC, Trevisan-Silva D, Gremski LH, Gremski W, Senff-Ribeiro A, Chaim OM, King GF and Veiga SS. 2017. Insecticidal activity of a recombinant knottin peptide from *Loxosceles intermedia* venom and recognition of these peptides as a conserved family in the genus. *Insect Mol Biol*, **26(1)**:25-34.
- Medina-Santos R, Guerra-Duarte C, Lima SD, Costal- Oliveira F, Aquino PA, Carmo AO, Ferreyra CB, Gonzalez-Kozlova EE, Kalapothakis E and Chávez-Olortegui C. 2019. Diversity of astacin-like metalloproteases identified by transcriptomic analysis in Peruvian *Loxosceles laeta* spider venom and in vitro activity characterization. *Biochimie*, doi: 10.1016/j.biochi.2019.08.017.
- Mohrle F, Bond JS and Stocker W. 2004. Other astacin homologues. In *Handbook of Proteolytic Enzymes*, 2nd ed. Elsevier; London Press
- Moussa S, Kamel E, Ismail IM and Mohammed A. 2016. Inheritance of *Bacillus thuringiensis* Cry1C resistance in Egyptian cotton leafworm, *Spodoptera littoralis* (Lepidoptera: Noctuidae). *Entomological Research*, **46**:61–69.
- Nakasu EYT, Williamson SM, Edwards MG, Fitches EC, Gatehouse JA, Wright GA and Gatehouse AM. 2014. Novel biopesticide based on a spider venom peptide shows no adverse effects on honeybees. *Proc Biol Sci*, doi:10.1098/rspb.2014.0619.
- Navon A, Wysoki M and Keren S. 1983. Potency and effect of *Bacillus thuringiensis* preparations against larvae of *Spodoptera littoralis* and *Boarmia* (Ascotis) selenaria. *Phytoparasitica*, **11(1)**:3-11.
- Oerke E C, Dehne HW, Schoenbeck F and Weber A. 1994. Crop Production and Crop Protection: Estimated Losses in Major Food and Cash Crops. Elsevier Science B: Amsterdam press
- Oliveira CM, Auad AM, Mendes SM and Frizzas MR. 2014. Crop losses and the economic impact of insect pests on Brazilian agriculture. *Crop Protection*, **56**:50–54.
- Olufemi-Salami FK, Akinneye JO and Salami OS 2018. Contact and Fumigant Toxicity of *Uvaria afzelli* (Scott) against *Plodia interpunctella* (Hubner) Infesting Maize Grains in Nigeria. *JJBS*, **12**:49-53
- Pyati P, Fitches E and Gatehouse JA. 2014. Optimising expression of the recombinant fusion protein biopesticide ω -hexatoxin-Hv1a/GNA in *Pichia pastoris*: sequence modifications and a simple method for the generation of multi-copy strains. *J Ind Microbiol Biotechnol*, **41**:1237–1247. doi: 10.1007/s10295-014-1466-8.
- Quesada V, Sánchez LM, Alvarez J and López-Otín C. 2004. Identification and characterization of human and mouse ovastacin: a novel metalloproteinase similar to hatching enzymes from arthropods, birds, amphibians, and fish. *J Biol Chem*, **279**:26627 – 26634.

- Sachdev M, Mandal A, Mulders S, Digilio LC, Panneerdoss S, Suryavathi V, Pires E, Klotz KL, Hermens L, Herrero, MB, Flickinger CJ, Van Duin M and Herr JC. 2012. Oocyte specific oolemmal SAS1B involved in sperm binding through intra-acrosomal SLLP1 during fertilization. *Dev Biol*, **363**: 40 – 51.
- Salama HS, Dimetry NZ and Salem SA. 1970. On the host preference and biology of the cotton leaf worm *Spodoptera littoralis*. *Zeitung für Angewandte Entomologie*, **67**:261-266.
- Salama HS, Foda MS and Sharaby A. 1989. A proposed new biological standard for bioassay of bacterial insecticides vs. *Spodoptera* spp. *Tropical Pest Management* **35(3)**: 326-330.
- Salem, R., El-Kholy, A. A., Omar, O. A., Abu el-naga, M. N., Ibrahim, M. & Osman, G. 2019a. Construction, Expression and Evaluation of Recombinant VP2 Protein for serotype-independent Detection of FMDV Seropositive Animals in Egypt. *Scientific Reports*, **9**:10135, doi.org/10.1038/s41598-019-46596-9
- Sawicki RM. 1986. Resistance to synthetic pyrethroids can be counted successfully. *Agribusiness Worldwide* **8(5)**:20,22-25.
- Silva I M, Martins GF, Melo C R, Santana A S, Faro R R, Blank A F, Alves P B, Picanço M C, Cristaldo PF, Araújo A P A and Bacci L. 2018. Alternative control of *Aedes aegypti* resistant to pyrethroids: lethal and sublethal effects of monoterpene bioinsecticides. *Pest Manag Sci*, doi:10.1002/ps.4801.
- Starrett J and Hedin M. 2007. Multilocus genealogies reveal multiple cryptic species and biogeographical complexity in the California turret spider *Antrodiaetus riversi* (Mygalomorphae, Antrodiaetidae). *Mol Ecol*, **16(3)**:583-604.
- Stöcker W, Wolz RL, Zwilling R, Strydom DJ and Auld D. 1988. Astacus protease, a zinc metalloenzyme. *Biochemistry*, **27**: 5026 – 5032.
- Wang P, Hammer DA and Granados RR. 1994. Interaction of *Trichoplusia ni* granulosis virus- encoded enhancin with the midgut epithelium and peritrophic membrane of four lepidopteran insects. *J Gen Virol*, **75**: 1961–1967.
- Windley MJ, Herzig V, Dziemborowicz SA, Hardy MC, King GF and Nicholson GM. 2012. Spider-Venom Peptides as Bioinsecticides. *Toxins (Basel)*, **4(3)**: 191–227. doi: 10.3390/toxins4030191
- Yiallourous I, Kappelhoff R, Schilling O, Wegmann F, Helms MW, Auge A, Brachtendorf G, Berkhoff EG, Beermann B, Hinz HJ, König S, Peter-Katalinic J and Stöcker W. 2002. Activation mechanism of pro-astacin: role of the pro-peptide, tryptic and autoproteolytic cleavage and importance of precise amino-terminal processing. *J Mol Biol*, **324**:237 – 246.
- Young AR and Pincus SJ. 2001. Comparison of enzymatic activity from three species of necrotising arachnids in Australia: *Loxosceles rufescens*, *Badumna insignis* and *Lampona cylindrata*. *Toxicon*, **39**: 391–400
- Zanetti VC, da Silveira R B, Dreyfuss J L, Haoach J, Mangili OC, Veiga SS and Gremski W. 2002. Morphological and biochemical evidence of blood vessel damage and fibrinogenolysis triggered by brown spider venom. *Blood Coagul Fibrinolysis*, **13**: 135–148.
- Zhong Y, Song B, Mo G, Yuan M, Li H, Wang P, Yuan M and Lu Q. 2014. A novel neurotoxin from venom of the spider, *Brachypelma albopilosum*. *PLoS One*, doi.org/10.1371/journal.pone.0110221.

Embryonic development of the striped spiny eel, *Mastacembelus pancalus* (Hamilton, 1822) in captive condition

Md. Sherazul Islam* and Tandra Rani

Department of Fisheries and Marine Bioscience, Jashore University of Science and Technology, Jessore-7408, Bangladesh

Received: May 8, 2020; Revised: October 8, 2020; Accepted: Oct 26, 2020

Abstract

The striped spiny eel, *Mastacembelus pancalus* is one of the common food fish in Bangladesh, but lacking study on embryonic development of the fish. The present study describes the embryonic progress stages of the fish in the confined state. The embryogenesis is divided into seven major phases: Zygote phase, Cleavage phase, Morula phase, Blastula phase, Gastrula phase, Organogenesis phase and Hatching phase. According to distinct development characteristics, the further sub-stages were also developed whenever possible. Fertilized eggs were sticky, colorless, and demersal with identical perivitelline space. The thickness of the unfertilized eggs ranged from 0.55-0.58 mm, which increased to 0.62-0.71 mm in fertilized eggs. The perivitelline space development happened at 0.35 h after fertilization (AF). The first cleavage groove occurred at the animal pole (two cells) 0.55 h AF. The added cell division such as four cells, eight cells, sixteen cells, thirty-two cells, and multi cells stages was initiated at 1.25, 1.45, 2.15, 2.50, and 4.40 h AF respectively. The morula, blastula, gastrula, yolk plug stage, and organogenesis stages were seen at 8.25, 11.30, 17.15-23.50, 29.20, and 34.15-35.30 h AF respectively. The initial heartbeat was observed at 34.00 h AF. The head and tail ends of the embryo were distinguished at 35.00 h AF. The notochord was also evident at the same hours. The embryo started to hatch at 36.00 h AF which accomplished 39.00 h at 29.11 ± 0.29 °C. The new hatchling was 1.65 ± 0.15 mm in average length. The present findings will serve as baseline information to develop the breeding protocol of the species in the hatchery condition.

Keywords: Embryogenesis, cleavage, organogenesis, hatching

1. Introduction

The Guchibaim (*Mastacembelus pancalus*) is one of the regular food fish found in Asian countries, namely in India, Pakistan, Bangladesh, and Nepal (Talwar and Jhingran, 1991; Froese and Pauly, 2006) and recognized as a striped spiny eel. The species is a common and demandable food fish in Bangladesh and is locally known as 'guchi baim.'

In the past, the fish was available in estuaries and freshwater habitats throughout Bangladesh (Ali, 1967). With the destruction of natural habitat including overexploitation, the fish has diminished abruptly from wildlife (Afroz *et al.*, 2014). Besides drying up of downcast land and using pesticides, the ordinary production lands of this fish are in threat (Rahman *et al.*, 2009). Besides these, the fish is collected only from nature that exaggerates the natural reduction of the fish.

The fish is critically endangered in Bangladesh (FISHWISE, 2013) but has not been shown in the red list of IUCN (Anonymous, 2006). It is needed for the management of natural habitat or to introduce artificial propagation as well as culture. Thus, it is essential to realize the embryonic development stages of the fish to set up a non-natural propagation in a confined condition, it's stocking at mass scale for its expansion and conservation.

Study on biology and breeding has been done on different eel fishes such as on *Mastacembelus pancalus* (Hasan *et al.*, 2016; Karim and Hossain, 1972); *M. armatus* (Serajuddin and Mustafa, 1994); *Macrogathus aculeatus* (Das and Kalita, 2003); *M. pancalus* (Suresh *et al.*, 2006). The development of egg and/or larvae on eel fishes like *M. pancalus* (Rahman *et al.*, 2009; Afroz *et al.*, 2014), *M. aculeatus* (Sahoo *et al.*, 2007; Farid *et al.*, 2008); *Muraenesox cinereus* (Umezawa *et al.*, 1991); *Anguilla rostrata* (Oliveira and Hable, 2010); *Mastacembelus mastacembelus* (Sahinoz *et al.*, 2006) have done, but there are no details of basic work on embryogenesis of *M. pancalus* except Rahman *et al.* (2009). As the embryonic development process differs from species to species, it is important to know the detailed developmental stages of any fish to consider the artificial propagation of the fish in captivity. It is an urgent need to develop a captive breeding protocol of the species due to the declination of natural propagation. It is essential to know the variations of features in embryonic development and to know the development of organs for the management and rearing technology for seed production of any fish species. Thus, detailed embryonic developmental stages with prominent features were carried out in the captive condition of *M. pancalus*.

* Corresponding author e-mail: dms.islam@just.edu.bd.

** **Abbreviations** : AFAfter fertilization; EM Egg membrane ; VM Vitelline membrane ; PS Perivitelline space

2. Materials and Methods

2.1. Study site and preparation of aquarium

The experiment was carried out in the laboratory of the Department of Fisheries and Marine Bioscience, Jashore University of Science and Technology, Jashore, Bangladesh. The experiment was done in rectangular glass aquaria (3 f length × 1.16 f width × 1.25 f depth), each containing thirty liters of water. Water hyacinths were used as a source of plants, and their roots were used as a substrate to lay the eggs of the fishes. The major physicochemical parameters like temperature, pH, and DO were measured at each two hours interval during embryonic development. A pH meter (EZODO, 7200, Taiwan) and a DO meter (LTLutron YK-22DO, Taiwan) were used to measure the water pH, DO and temperature respectively.

2.2. Collection of egg

In the same laboratory, eggs of *M. pancalus* were produced by inducing with PG hormone. Brood fishes were collected from the nearby natural habitat (Baor) and the average body weight was 9 g of each. There were three treatments, and each had two more replications for the inducing of the fish. Three pairs of broods were kept 1:1 (male: female) the ratio in each aquarium for natural propagation after inducing. Fishes were spawned (100%) within sixteen to twenty hours after the administration of the hormone. The sticky eggs of the *M. pancalus* were attached to the aquatic weeds and sometimes on the substrates. Eggs were sampled softly either along with the roots of the water hyacinth or using a father in each sampling.

2.3. Observation of embryonic development

The embryonic development stages were observed, and a snap was taken with a photographable microscope (Carl Zeiss microscopy GmbH, S.N. MKG8639, Germany). The eggs were observed at every 5 to 10 minutes interval till the accomplishment of the morula and then after observed each one-hour intermission until hatching. The diameter of oocytes and eggs was measured at each sampling time using the microscopic camera. The development stages and characteristics were confirmed by following Sahoo *et al.* (2007), Rahman *et al.* (2009), and Honji *et al.* (2012).

3. Results

3.1. Aquarium environment

Water parameters play a major role in the spawning, embryonic development, and hatching of any fish species. In the present study, the physicochemical condition of spawning aquaria such as temperature, dissolved oxygen, and pH ranged from 28.8 to 29.4 °C, 5.25 to 5.75 mg.L⁻¹ and 7.75 to 8.12 respectively.

3.2. Characteristics of the egg

The yellowish eggs were spherical, demersal, and adhesive. They stuck to the roots of water hyacinth in the aquarium. The unfertilized eggs were opaque while the fertilized eggs were transparent with visible egg membrane and yolk (Figure 1A, 1B). The diameter of the fertilized eggs increased 0.62 to 0.71 mm from 0.55 to 0.58 mm of the unfertilized egg.

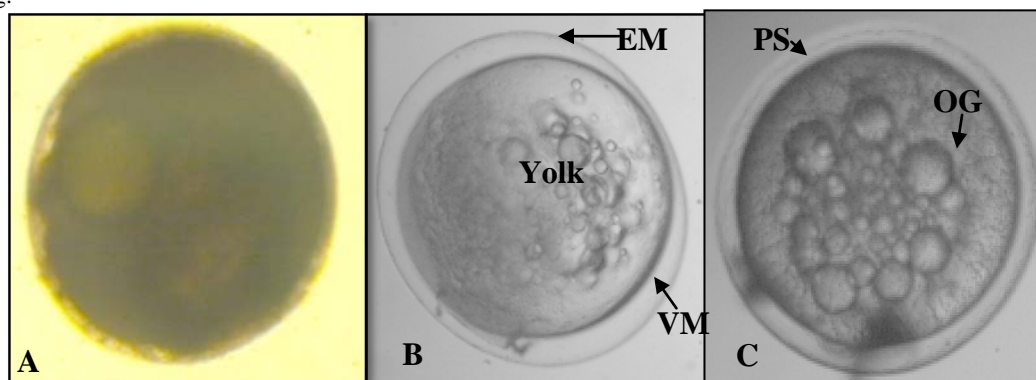


Figure 1. The unfertilized (A) and fertilized (B) egg of *M. pancalus*. The formation of perivitelline space (C) at the early stage of the zygote. EM = Egg membrane; VM = Vitelline membrane; PS = perivitelline space; OG = oil globule.

3.3. Embryonic development

After the fertilization of eggs, the embryonic period started and ended at the time of accomplishment of the general organ systems is common in all fishes. The

fertilized eggs hatched out within 36 to 39 h after fertilization (AF). The events in embryonic progress and their respective time and features of *M. pancalus* are presented in table 1 and figure 1-4.

Table 1. Embryonic developmental stages (major and sub-phases) with the respected time and features of *M. pancalus* in aquarium condition.

Major phase	Sub-phase	Figure	Time (h/min)	Developmental features
Zygote	Fertilized eggs	1	0.00	Eggs adhesive, demersal, spherical, and transparent.
	Perivitelline space formation		0.25- 0.30	Formation of perivitelline space around the yolk
Cleavage	Blastodisc	2	0.35	Formation of blastodisc at the animal pole
	Two cell		0.40-0.50	Aggregated oil globules at the animal pole, the commencement of the first cleavage
	Four cell		1.25	2 nd cleavage, 4-cell
	Eight cell		1.25-1.45	The blastomeres were unequal in size and remain in two rows. 8-cell
	Sixteen cell		2.15	4 th cleavage, 16-cell
	Multi-cell		3.00 -4.40	Quick successive division and transformed into 32, 64, 128 celled stage and so on
Morula			7.15-8.25	Formed a cap at the animal pole, which gradually increased in size.
Blastula		3	11.30-14.45	The marginal blastomeres lost their boundaries and were compressed.
Gastrula	Early gastrula		17.15	Blastoderm started to form a thin layer by invading the yolk and overthrowing over the yolk
	Middle gastrula		22.10	Development of germinal ring in the region of yolk and about ½ of the yolk was possessed by blastoderm.
	Late gastrula		23.50	The embryonic shield was visible and the blastoderm covered ¾ of the yolk.
Organogenesis	Embryonic body		27.15	The embryonic body was visible.
	Yolk plug		29.20	Finished yolk invasion, visible undeveloped head and tail and became differentiated.
	Segmentation	4	34.15- 35.35	Distinguished head and tail, and notify of beating heart. Noticeable notochord in cellular structure.
Hatching			36.00-39.00	The twisting movement became more forceful and the embryo broke the egg pod.

3.3.1. Zygote phase

This phase is characterized by fertilized and perivitelline space formation. The perivitelline space formation occurred at 0.30 h AF in the present study. The perivitelline space (the thin space that separated the egg membrane) was fluid-filled and equal all around the egg membrane (Figure 1C). Oil globules were visible in the yolk in this phase.

3.3.2. Cleavage phase

The single-cell stage became clear with the accumulation of cytoplasm over the animal pole as a protrusion at 0.35 h AF representing the early blastodisc or germinal disc stage (Figure 2A). As the development proceeded, the oil globules were found to aggregate and the cytoplasmic disc became thick and the first cleavage

occurred within 1.00 to 1.25 h AF. The vertical cleavage occurred which divided the blastodisc into two different cells at 0.50 h AF (Fig. 2B). The further cleavage was at a right angle to the first and observed forming four cells within 1.25 h (Figure 2C). Further division of blastomere took place with the advancement of time to reach eight-cell and sixteen cell stages at 1.45 h and 2.15 h AF respectively (Figure 2D, 2E). After quick succession, the sixteen-celled stages resolved into 32, 64, 128 celled stages, and so on. However, due to the rapid occurrence of these cell divisions, it was not possible to observe or count the stages; and hence in the present study, it was considered as a multi-celled stage (Figure 2F). Eggs were measured and noticed the same size (0.62 – 0.71 mm).

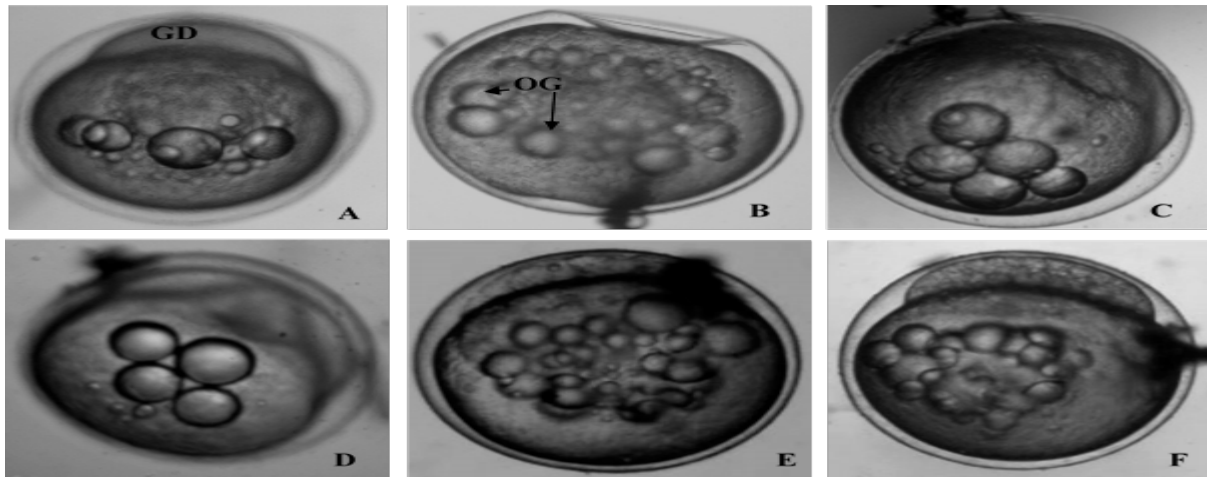


Figure 2. The cleavage phase of *M. pancalus*; Formation of blastodisc (A), 2-cell (B), 4-cell (C), 8-cell (D), 16-cell (E), and Multi-cell stage (F). GD=Germinal disc (blastodisc); OG=Oil globule.

3.3.3. Morula phase

The blastomeres were reduced in size and accumulated around the animal pole during the morula stage. A cap-like creation was seen at the animal pole, which size increased slowly (Figure 3A). The morula phase was recognized at 8.25 h AF.

3.3.4. Blastula phase

The embryo was further divided into numerous cells after the morula and formed a blastoderm by arranging a form of a layer (Figure 3B). The blastodisc was formed by the gradual formation of several layers due to further cell division. At this phase, blastocoels also appeared (a space between yolk and blastoderm). This phase of the embryo is

called 'blastula' which was observed within 11.30 h to 14.45 h AF.

3.3.5. Gastrula phase

The gastrulation phase is subdivided into three stages: like early gastrula, middle gastrula, and late gastrula. The incursion of the yolk started by blastoderm through spreading over the yolk like a thin layer which is denoted as the early gastrula and resulted within 17.15 h AF (Figure 3C). In the middle of gastrulation, noticed a visible germinal ring on every side of the yolk. In this stage, about half of the yolk was engaged by blastoderm (Figure 3D). The embryonic shield was visible at late gastrulation and blastoderm covered $\frac{3}{4}$ th of the yolk (Figure 3E).

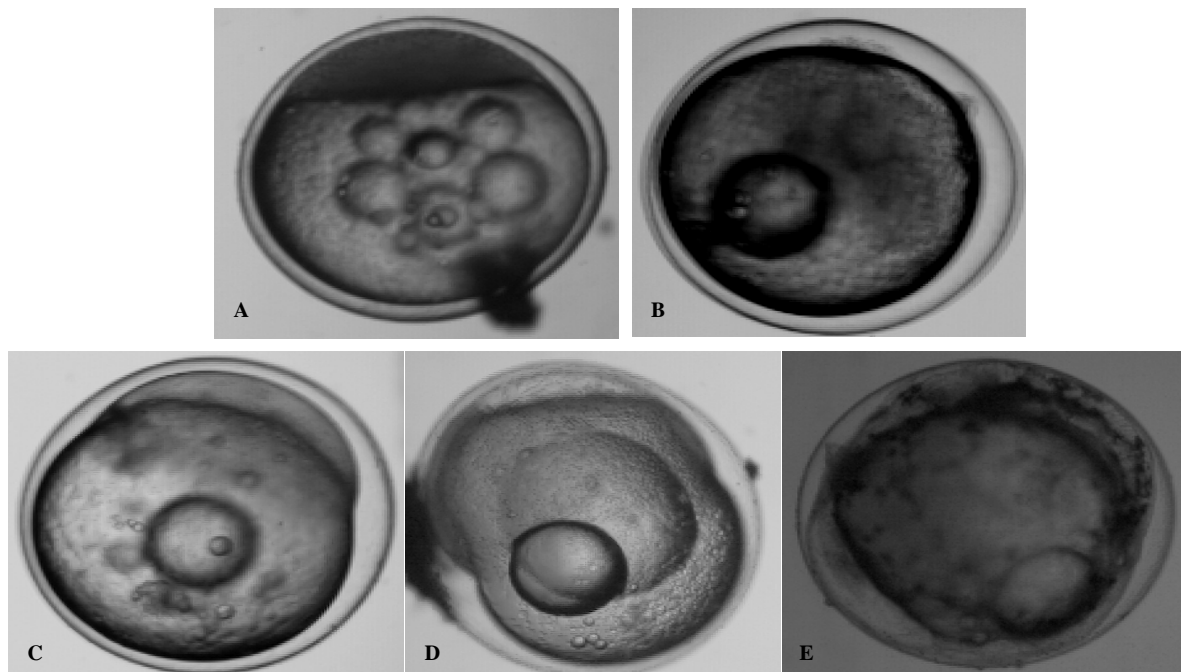


Figure 3. The morula (A), blastula (B) and gastrula phase (C, D, E) of *M. pancalus*; C=Early gastrula, D=Middle gastrula and E=Late gastrula.

3.3.6. Organogenesis phase

The embryonic body formation appeared at 27.15 h AF (Figure 4A). The gradual spreading above the germ layer in the plug stage completed the yolk incursion. The head and tail seemed in this stage within 29.20 h AF (Figure

4B). In addition to this, the embryo was lengthened and bordered the yolk materials and differentiated the tail and head ends (Figure 4C). The first beating heart was visible at about 34.00 h AF. Within the cellular structure, the notochord became noticeable within 34.15 to 35.35 h AF.

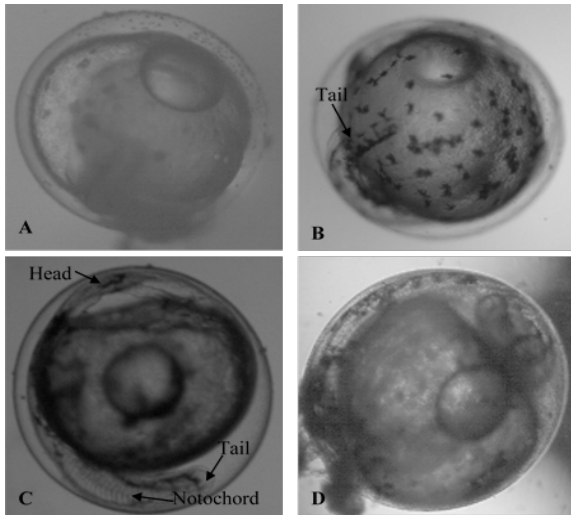


Figure 4. The organogenesis and hatching of *M. pancalus*; Formation of the embryonic body (A), Yolk plug stage (B), segmentation of organ (C), and just before hatching (D).

3.3.7. Hatching phase

In this phase, noticed elongated embryo which progressively separated. The tail became steadily separated from the yolk mass (Fig. 4D). The embryo started an irregular twisting movement. Later, the eggshell started to rupture by the embryos due to the continuous movement. The hatch out of larvae was noticed in 36.00 to 39.00 h after fertilization with its tail portion first and completed within 3.10 h. The size of the newly hatched larvae was 1.65 ± 0.15 mm in length (Fig. 5).

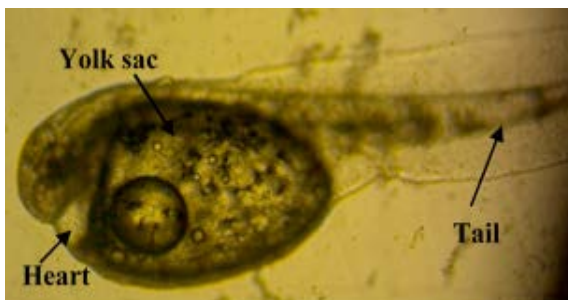


Figure 5. The new hatchling of *M. pancalus* in aquarium condition. Hatching started at 36 h after fertilization.

4. Discussion

4.1. Aquarium environment

The embryonic development of fishes is directly related to the water parameters, particularly water temperature. In the present study, the recorded water parameters were deemed suitable for the species. Water temperature during the time of embryonic development was within 28.8 to 29.4 °C which was close to other studies like 28 to 29 °C (Sahoo *et al.*, 2007) and 27-31 °C (Rahman *et al.*, 2009).

4.2. Characteristics of the egg

The characteristics of the fertilized and unfertilized eggs are more or less similar to other studies. The unfertilized eggs were dense, demersal, sticky and the fertilized eggs were round, clear, and sticky which is supported by Rahman *et al.* (2009). Though the same characteristics of fertilized eggs shown in

Mastacembelidae, different egg color such as 'green color' was observed in the case of *M. aculeatus* (Sahoo *et al.*, 2007). This variation may be due to species variation. The fertilized egg diameter in the present study recorded was 0.62 to 0.71 mm which was smaller than what was reported by Rahman *et al.* (2009). They recorded up to 0.70 to 1.30 mm the size of the fertilized egg in *M. pancalus*. However, further larger (1.20 to 1.40 mm) reported by Sahoo *et al.* (2007) in *M. aculeatus* and 1.50 to 2.02 mm in *M. mastacemblus* reported by Sahinoz *et al.* (2006).

4.3. Embryonic development

The cell division pattern and the further embryonic development stages were more or less similar to other studies of Mastacembelidae. However, differences were noticed in the case of the time of development in different species and even within the same species. The presence of perivitelline space in the present study was also reported in fertilized eggs of New Zealand freshwater eel, *A. dieffenbachia* (Lokman and Young, 2000), and Mesopotamian spiny eel, *M. mastacemblus* (Sahinoz *et al.*, 2006).

The initiation of 1st cleavage, the formation of blastodisc at the animal pole was noticed at 0.35 h AF which was similar to *M. pancalus* (Rahman *et al.*, 2009) and *M. aculeatus* (Sahoo *et al.*, 2007). However, in the case of *M. mastacemblus* it took about 4.00 h (Sahinoz *et al.*, 2006). In the present study, it was noticed that cell division was completed within about 5.00 h AF which was almost the same reported by Rahman *et al.* (2009). However, in the case of *M. aculeatus*, the cell division was completed shortly, and it was by 3.30 h AF (Sahoo *et al.*, 2007). Moreover, within the same species, the induction of morula showed at different times. In the present study, the morula stage appeared within 8.25 h AF whereas Rahman *et al.* (2009) observed this stage at 10.10 h AF. According to Sahoo *et al.* (2007), the same stage in *M. aculeatus* occurred at 4.10 h AF. The blastoderm enclosed nearly 3/4th of the yolk and an embryonic body was formed 27.15 h AF which was noticed 24.30 h AF in the same species (Rahman *et al.*, 2009) and 25.30h AF in *M. aculeatus* (Sahoo *et al.*, 2007) whereas more time (40h) was taken in the case of *M. mastacemblus* (Sahinoz *et al.*, 2006).

The formation of the head and tail of the embryo showed 29.20h AF which was observed in 31.30 h in the same species (Rahman *et al.*, 2009) and even in higher temperatures. However, at a similar temperature, this characteristic was observed at 4.00 h earlier compared to *M. aculeatus* (Sahoo *et al.* (2007) and took more than double duration (77h) in *M. mastacemblus* (Sahinoz *et al.* 2006). The heart pulsation was noticed during about 34.00 h AF in this study alike to Rahman *et al.* (2009) but earlier as compared to Japanese eel, *A. paponica* (Yamamoto *et al.*, 1995). The twisting movement and first hatching were observed at 36.00 h AF. The earlier twisting movement and first hatching were reported by Rahman *et al.* (2009) in the same species and in similar water temperatures. In the case of other eel fishes, different hatching time was reported like 31.45 h in *M. aculeatus* (Sahoo *et al.*, 2007), 38.00-45.00 h in *A. paponica* (Yamamoto *et al.*, 1995) and 85.00 h in *M. mastacemblus* (Sahinoz *et al.*, 2006).

In the present study, it was strong evidence that quick development happens until morula compared to other

studies, but later stages took a longer period particularly in organogenesis and hatching (Figure 6). This may be due to temperature variation as compared to Rahman *et al.* (2009) who recorded more than 30°C after gastrulation whereas in

the present study it was less than 30°C. The other variability like the formation of morula and head and tail due to the different rates of development in different species in addition to temperature.

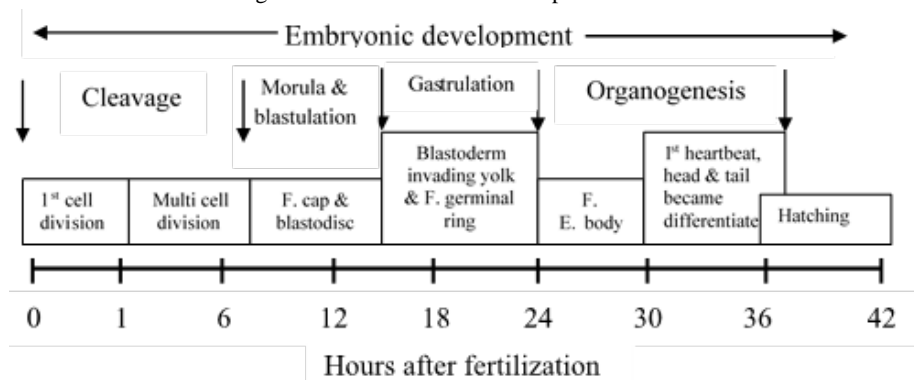


Figure 6. Major events during the embryonic development of *M. pancalus*. C=completion, F=formation, E=Embryonic

5. Conclusion

The study generated detailed information on early developmental commencement with distinguishing characteristics of *M. pancalus*. In conclusion, it is said that the embryonic development of *M. pancalus* commonly imitates that of other eel fishes. However, the period of development varies in some stages. Besides, the development rate of the embryo varied in the variation of water temperature. The development process is noticed faster in the higher the temperature, and vice versa.

Acknowledgement

The present study was financially supported by the Grant for Advanced Research in Education (GARE), Ministry of Education, People's Republic of Bangladesh. We also thank other groups of the project who successfully breed the species in the aquarium by inducing and providing us with the eggs for further study.

References

- Afroz A, Islam MS, Hasan MR, Hasnahena M and Tuly DM. 2014. Larval rearing of spiny eel, *Mastacembelus pancalus* in the captivity with emphasis on their development stages. *Int J Fish Aquat Stud*, **1(6)**: 163-167.
- Ali MH. 1967. Induced breeding of major carps in ponds by pituitary hormone injection. Agricultural Information Service, Dhaka. pp. 23-26.
- Anonymous. IUCN red list of threatened species (2006). International Union for Conservation of Nature. <http://www.redlist.organization> (January 2019).
- Das SK and Kalita N. 2003. Captive breeding of peacock eel, *Macrognathus aculeatus*. *Aquac Asia*, **8**: 17-21.
- Farid SM, Miah MI, Akter MD, Saha D and Rahman MM. 2008. Embryonic and larval development of tarabaim (*Macrognathus aculeatus*). *J Agrofor Env*, **2(2)**: 123-129.
- FISHWISE, <http://www.fishwise.co.za>, Species=*Mastacembelus pancalus* 5 January, 2013.
- Froese R and Pauly D. (eds), 2006. Fishbase, World-wide-Web Electronic publication. <http://www.fishbase.org>

Hasan MR, Islam MS, Afroze A, Bahdur P and Akter S. 2016. Captive breeding of Striped Spiny Eel, *Mastacembelus pancalus* (Hamilton, 1822) considering the various hormonal responses. *Int J Fish Aquat Stud*, **4(3)**: 07-11.

Honji MR, Tolussi CE, Mello PH, Caneppele D and Moreira RG. 2012. Embryonic development and larval stages of *Steindachneridion parahybae*-implications for the conservation and rearing of this endangered Neotropical species. *Neotrop Ichthyol*, **10(2)**: 313-327.

Karim MA and Hossain A. 1972. Studies on the biology of *Mastacembelus pancalus* (Spiny Eel, Hamilton) in artificial pond. Part II. Sexual maturity and Fecundity. *Bangladesh J Agric Bio Sci*, **1(2)**:15-18.

Lokman PM and Young G. 2000. Induced spawning and early ontogeny of New Zealand freshwater eels (*Anguilla dieffenbachii* and *A. australis*). *NZ J Mar Freshwater Res*, **34**: 135-145.

Oliveira K and Hable WE. 2010. Artificial maturation, fertilization, and early development of American eel (*Anguilla rostrata*). *Can J Zool*, **88**:1121-1128.

Rahman MM, Miah MI, Taher MA and Hasan MM. 2009. Embryonic and larval development of guchibaim, *Mastacembelus pancalus* (Hamilton). *J Bangladesh Agril Univ*, **7 (1)**: 193-204.

Sahinoz E, Dogu Z and Aral F. 2006. Development of embryos in *Mastacembelus mastacembelus* (Bank & Solender 1794) (Mesopotamian spiny eel) (Mastacembelidae). *Aquac Res*, **37**: 1611-1616.

Sahoo SK, Giri SS, Shaha A, Chandra S, Sahu AK and Sarangi N. 2007. Embryonic development of the spiny eel, *Mastacembelus aculeatus* (Bloch, 1786). *Indian J Fish*, **54(3)**: 333-337.

Serajuddin M and Mustafa S, 1994. Feeding specialization in adult spiny eel, *Mastacembelus armatus*. *Asian Fish Sci*, **7(1)**:63-65.

Suresh VR, Biswas BK, Vinci GK, Mitra K and Mukherjee A. 2006. Biology and fishery of barred spiny eel, *Macrognathus pancalus* (Hamilton). *Acta Ichthyol Piscat*, **36 (1)**: 31-37.

Talwar PK and Jhingran AG. 1991. Inland Fishes of India and Adjacent Countries. Calcutta: Oxford and IBH Publishing.

Umezawa A, Otake T, Hirokawa J, Tsukamoto K and Okiyama M. 1991. Development of the eggs and larvae of the pike eel, *Muraenesox cinereus*. *Jpn J Ichthyol*, **38(1)**:35-40.

Yamamoto K, Yamauchi K and Kasuga S. 1975. On the development of the Japanese eel, *Anguilla japonica*. *Bull Japan Soc Sci Fish*, **41(1)**: 21-28.

Oxidative Toxic Stress and DNA Damage as a Promising Strategy for Identifying Patients with Nonalcoholic Fatty Liver Disease

Mahshid Abdolmaleki¹, Maryam Mehrpooya², Bahram Sifizarei³, Masoud Saidijam⁴, Ali Reza Soltanian⁵, Maziar Ganji⁶, and Akram Ranjbar^{1,*}

¹ Department of Pharmacology and Toxicology, School of Pharmacy, Medicinal Plants and Natural Products Research Center, ² Department of Clinical pharmacy, School of Pharmacy, ³ Department of Internal Medicine, School of Medicine, ⁴ Department of Molecular Medicine and Genetic, Faculty of Medicine, ⁵ Department of Biostatistics, School of Public Health and Modeling of Noncommunicable Diseases Research Center, Hamadan University of Medical Sciences, Hamadan, 6517838678, ⁶ Department of Medical Genetics, School of Medicine, Shahid Beheshti University of Medical Sciences, Tehran, Iran.

Received: January 13, 2020; Revised: October 27, 2020; Accepted: Oct 31, 2020

Abstract

Non-alcoholic fatty liver disease (NAFLD) is considered as one of the common causes of chronic hepatitis and cirrhosis. The present study was performed to determine paraoxonase 1 (PON 1) and arylesterase (ARE) activities, biomarkers of oxidative toxic stress and DNA damage in patients with NAFLD and their suitability for identifying for NAFLD. In this case-control study, 40 NAFLD patients and 40 normal subjects were studied. Abdominal ultrasonography, serum PON 1 and ARE activities, level of lipid peroxidation (LPO), total thiol groups (TTG), total antioxidant capacity (TAC) and DNA damage biomarker were measured in both NAFLD patients and control group. There was a significant increase in salt stimulated PON 1 activity and LPO level in NAFLD patients compared to the control group ($P < 0.05$). In contrast, TAC decreased in NAFLD patients compared to the control group. No significant difference was observed in biomarkers of DNA damage and ARE activity between the groups ($P > 0.05$). PON 1 activity and LPO level can be considered as biomarkers for NAFLD diagnosis. Along with these biomarkers, total antioxidant capacity can be used for identifying patients with NAFLD.

Keywords: paraoxonase 1, oxidative stress, DNA damage, nonalcoholic fatty liver disease (NAFLD)

1. Introduction

Non-alcoholic fatty liver disease (NAFLD) is characterized by excessive lipid accumulation, inflammation and an imbalanced redox homeostasis. (Damba et al. 2020). NAFLD encompasses a wide spectrum of liver diseases, from simple steatosis to non-alcoholic steatohepatitis (NASH) (Chalasanani et al. 2018). The reported prevalence of NAFLD is 25–30% in Western countries (Ferro et al. 2020). Serum Paraoxonase (PON) and arylesterase (ARE) are esterase enzymes with lipophilic antioxidant characteristics. Serum PON and ARE act as a single enzyme (Ates et al. 2009). Paraoxonase 1 (PON1), a calcium-dependent esterase, is associated with high-density lipoprotein (HDL) cholesterol. It has been established that antioxidant property of PON is conferred by diminishing the storage of the products of lipid peroxidation (LPO) (Aslan et al. 2007). The liver plays an important role in the synthesis of PON 1 which is able to hydrolyse a number of substrates, including phenyl acetate, paraoxon, lipid peroxides, cholesterol esters and hydroperoxides (Shokri et al. 2020). Imbalance between the production of reactive oxygen species (ROS) and inadequate antioxidant defense systems can lead to oxidative toxic stress (OTS) and cell damage

not only directly but also indirectly by changing signaling pathways (Ghadermazi et al. 2018). ROS production results from endogenous factors such as elevation of mitochondrial dysfunction and oxidative enzymes in infections and inflammations and exogenous factors such as air pollution, radiation and drug exposures (Ranjbar et al. 2018). In a previous study, it has been shown that NAFLD was related to an increase in oxidative stress serological parameters (Damba et al. 2020). Since histological changes in liver biopsy for NAFLD diagnosis is invasive, finding non-invasive methods for NAFLD diagnosis is of great importance. The present study was performed to evaluate the presence of oxidative stress, DNA damage and activities of PON 1 and ARE in a sample of patients with NAFLD to find out their valuable potential as future biomarkers for NAFLD diagnosis.

2. Materials and methods

2.1. Chemicals

Reagents and Chemicals used in this study were tetraethoxypropane, 2-thiobarbituric acid (TBA), trichloroacetic acid (TCA), 5,5-Dithiobis-2-nitrobenzoic acid (DTNB), n-butanol, hydrogen peroxide (H₂O₂), Tris base, Propofol, Ketamine, ethylene-di-amine tetra-acetic acid

* Corresponding author e-mail: akranjbar2015@gmail.com.

(EDTA), 2,4,6-tripyridyl-S-triazine (TPTZ) purchased from Sigma-Aldrich (St. Louis, USA). Paraoxonase and DNA damage kits were obtained from Cayman Chemical Co. (Ann Arbor, MI).

2.2. Study subjects

This case-control study was performed in Beheshti teaching hospital, Hamadan city, Iran, in 2016. Forty NAFLD patients who underwent a liver biopsy and 40 normal subjects were studied. All participants signed a formal consent before the commencement of the study. In addition, the protocol of the study was approved by the ethics committee of the Hamadan University of Medical Sciences (No: 940201454).

Histological diagnosis of nonalcoholic Steatohepatitis (NASH) and level of fibrosis were approved by an expert hepatopathologist. Standard (clinical and histological) criteria were used for the diagnosis of NAFLD. Patients were assigned into three distinct groups subjected to liver histology. Group 1, simple steatosis. Group 2, NASH in the absence of advanced fibrosis (NASH is described as steatosis along with portal and/or lobular inflammation and fibrosis stage 0-2). Group 3, NASH in the presence of advanced fibrosis (described as steatosis along with portal and/or lobular inflammation and fibrosis stage 3-4). Patients in the NAFLD group had not the history of alcohol drinking, autoimmune liver diseases, hemochromatosis and viral hepatitis.

Fasting blood samples were taken from the NAFLD patients in the morning of their programmed liver biopsy and control subjects. Samples were withdrawn from a cubital vein and then transferred into blood tubes and immediately stored at +4°C. Separation of cells was performed by centrifugation of samples at 3000 g for 10 min and kept in plastic vials at -80 °C until analysis.

2.3. Biochemical analysis

2.3.1. Paraoxonase 1 (PON1) and Arylesterase (ARE) activities measurement

Basal and salt-stimulated, with presence of NaCl, paraoxonase 1 activities were measured based on previously established findings. Generally, paraoxon (substrate) hydrolysis rate (di-ethyl p-nitro-phenyl-phosphate) was deliberated using an increase in absorbance level at 405 nm wave length at 37 °C. The analysis was carried out originally based upon the formation of p-nitrophenol using the molar absorptivity coefficient of 18050 M⁻¹cm⁻¹ at pH = 8.5. The enzyme activity was expressed as U/L. Molar extinction coefficient of the resultant phenol (1310 M⁻¹cm⁻¹) was used to determine the activity of ARE, and phenyl acetate was utilized as substrate. The reaction was uninterruptedly monitored at 270 nm and 37°C. Under this condition, one unit of ARE activity was considered as the quantity of phenol in mol generated per min and expressed as U/L serum (Hashemi et al. 2011).

2.3.2. Measurement of Total Thiol groups (TTG)

Hu method was utilized to determine total sulfhydryl content in plasma. Briefly, 0.6 ml of the Tris-EDTA buffer (Tris base 0.25 M, EDTA 20 mM, pH = 8.2) was added to an aliquot of 0.2 ml plasma in a test tube. Then, 40 µl of 10 mM DTNB in methanol were added. The volume of the reaction mixture was made up to 4.0 ml by adding 3.16 ml

of methanol. The test tubes were capped and the color was developed for 15–20 min. Then, they centrifuged at 3000 g for 10 min at room temperature. The supernatant was collected, and its absorbance at 412 nm was measured (Hu and Dillard 1994).

2.3.3. Measurement of lipid peroxidation (LPO)

The level of LPO in blood was assessed by TBA reagent, and the LPO is expressed as the extent of aldehyde production, during acid heating reaction. Briefly, 1.5 ml of TCA (20% w/v) was added to 250 µl of each sample and then centrifuged at 3000 g for 10 min. The resultant precipitation was dissolved in sulfuric acid and then 1.5 ml of the mixture was added to 1.5 ml of TBA (0.2% w/v). After incubation in a boiling water bath for one hour, 2 ml of n-butanol was added to the mixture, and then it was centrifuged. After cooling at room temperature, the absorption of the supernatants was measured at 532 nm. Standard solutions of tetraethoxypropane were prepared to obtain calibration curve and to calculate the concentrations of TBA+MDA adducts in samples (Moore and Roberts 1998).

2.3.4. Measurement of Plasma total antioxidant capacity (TAC)

The ability of plasma in reducing Fe³⁺ to Fe²⁺ was used to assess the antioxidant capacity of plasma. The resultant complex of reaction between Fe²⁺ and TPTZ provides a blue color with absorbance at 593 nm (Benzie and Strain 1999).

2.3.5. Measurement of DNA damage

The 8-OHdG content in the extracted DNA solutions was determined using the ELISA method (Highly Sensitive 8-OHdG ELISA kit, Japan). These meticulous assay kits were chosen because they require small amount of sample and provide high sensitivity and specificity, and inter- and intra-assay precision.

2.4. Statistical analysis

Data were analysed using version 16.0 of SPSS version 16 (SPSS, Chicago, IL). Mean and standard error values were ascertained for all the parameters, and the results were stated as Mean ± SEM. Differences between variables of case and control groups were analyzed by student t-test. A P-value less than 0.05 was considered statistically significant.

3. Results

None of the participants (40 NAFLD patients and 40 controls) declined to participate in the study. Three patients were excluded because of the lack of cold chain for their blood samples. Appropriateness of randomization was confirmed by comparison of general characteristics in both groups as shown in Table 1.

Table 1. Demographic characteristics of the studied subjects

Variables	Groups	
	Patients (n=40)	Control (n=40)
Age (years)	42.83±9.84	32.42±10.12
Weight (kg)	81.36±14.63	78.57±9.63
BMI (kg/m ²)	29.31±3.79	24.50±2.13
Height (m)	166.33±11.20	176.17±6.74
Sex (%)	97.5% Male, 2.5% Female	52.8% Male, 47.2% Female

Figures 1 to 7 showed the biomarkers of oxidative stress in both groups. The salt-stimulated PON 1 activity in the NAFLD patients was significantly higher than that of control group ($P = 0.04$, Fig 1). The basal PON1 activity (without NaCl) in the NAFLD patients was higher than the control group; however, the difference was not statistically significant ($P = 0.33$, Fig 2).

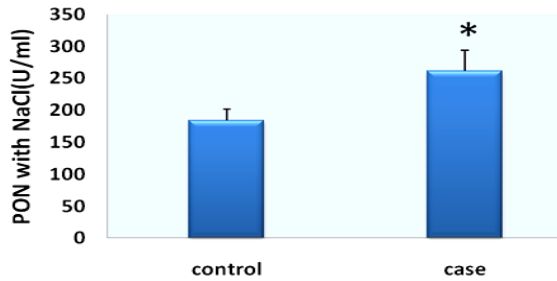


Figure 1. Salt stimulated activity of paraoxonase 1 in serum of patient and control groups. The difference between mean values was assessed by student-t test ($P=0.04$) and is shown by (*).

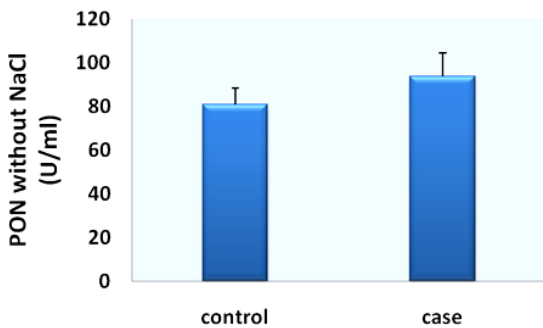


Figure 2. Basal paraoxonase 1 activity in serum of patient and control groups. The difference between mean values was assessed by student-t test ($P=0.33$), and it was not significant

No significant difference of ARE activity was seen between the NAFLD patients and control groups ($P = 0.60$, Fig 3).

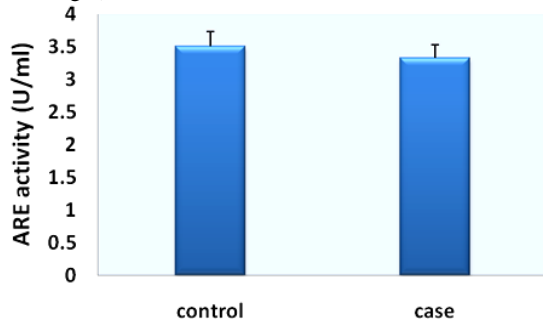


Figure 3. Arylesterase activity in serum of patient and control groups. The difference between mean values was assessed by student-t test ($P=0.60$), and it was not significant.

The LPO level of the NAFLD patients was significantly higher than that of the control group ($P=0.001$, Fig 4). In contrast, the TAC was significantly lower in the NAFLD patients than that of the control group ($P=0.04$, Fig 5). At the same time, total thiol molecules of the NAFLD patients were not significantly lower than that of the control group ($P=0.66$, Fig 6). No significant difference was also observed in the 8-OHdG content of the NAFLD patients and control groups ($P= 0.6$, Fig 7).

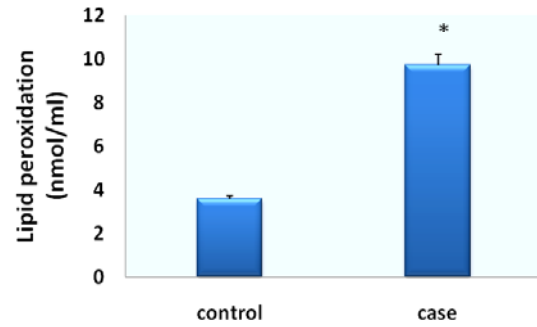


Figure 4. Lipid peroxidation level in serum of patient and control groups. The difference between mean values was assessed by student-t test ($P=0.001$) and is shown by (*).

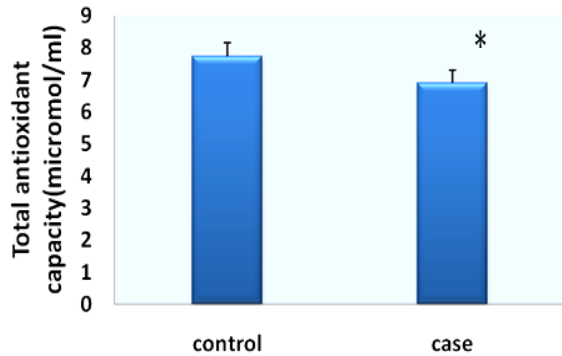


Figure 5. Total antioxidant capacity in serum of patient and control groups. The difference between mean values was assessed by student-t test ($P=0.04$) and is shown by (*).

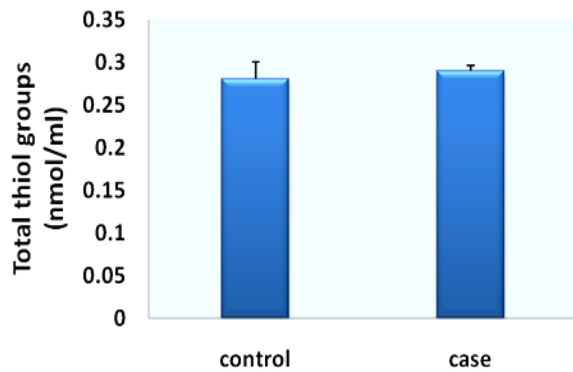


Figure 6. Total thiol groups in serum of patient and control groups. The difference between mean values was assessed by student-t test ($P=0.66$), and it was not significant.

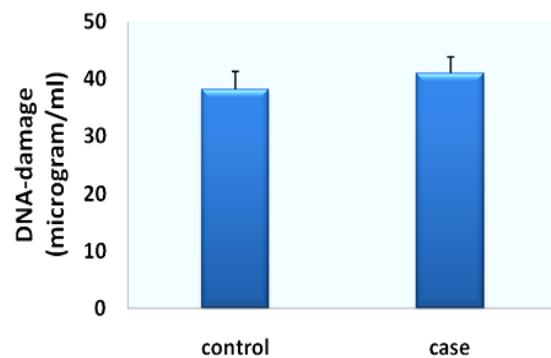


Figure 7: DNA damage level in serum of patient and control groups. The difference between mean values was assessed by student-t test ($P=0.60$), and it was not significant.

4. Discussion

In the present study, we revealed that NAFLD is accompanied by elevations in serum PON 1 activity and oxidative stress biomarkers such as LPO. Previous studies showed that LPO is greatly elevated in Nonalcoholic steatohepatitis (NASH) (Morita et al. 2012). Excess ROS is detoxified by several enzymatic mechanisms. PON 1, a liver-produced peroxidase, is famous for its antioxidant role in the circulation (Ramadan et al. 2012, Zaki et al. 2014). Therefore, our findings provide evidence in support of the theory that PON 1 may act as an antioxidant. This theory was first expressed by Marsillach et al. (2007) when they observed a wide-range of paraoxonases in chronic alcoholics (Marsillach et al. 2007). Previously, Hashemi et al. (2011) studied the effect of PON 1 deficit in a mouse model of NAFLD induced by a high-fat and high-cholesterol diet. They found that PON 1 deficit can induce higher levels of oxidative stress which confirm an antioxidant role for PON 1 in the liver (Hashemi et al. 2011). As mentioned before, liver plays a critical role in PON 1 synthesis. Chronic liver disorders can lead to increased levels of oxidative stress and inflammation (Shokri et al. 2020). PON 1 protects the liver against inflammation, liver disease and fibrosis (Aharoni, Aviram and Fuhrman 2013, Loued et al. 2012). It has already been revealed that increased PON 1 activity could be correlated with the reduction of serum levels of oxidative biomarkers in patients with progressive liver cirrhosis (Desai et al. 2014). Likewise, considering the antioxidant characteristics of PON-1 enzyme in NAFLD patients, the results of the previous studies demonstrated that PON-1 is paradoxically maintained and may even be increased in NAFLD despite its inverse associations with metabolic disorders and low HDL cholesterol (van den Berg et al. 2019). Hepatotoxicity induced by oxidative stress may lead to loss of fundamental biomolecules functions and cell viability due to direct attack of RNS and ROS (Çekmez and Dündar 2013, Awad et al. 2016). Alternatively, indirect activation of nuclear factor κ B (NF- κ B), activator protein-1 (AP-1), and redox-sensitive transcription factors can be induced by ROS, which are initiating the production of cytotoxic, fibrogenic and/or proinflammatory mediators by Kupffer cells and other non-parenchymal cells (Awad et al. 2016, Marí et al. 2015, Wan et al. 2014). Several studies in animal models of NAFLD displayed a higher free radical activity via the following mechanisms: (i) elevation of mitochondrial superoxide radicals and H₂O₂ generation, (ii) induction of microsomal cytochrome P450 isoforms such as CYP2E1 and CYP3A4, characterized by their high pro-oxidant activity, and (iii) LPO responses (Marí et al. 2015, Kumar et al. 2012, Schmilovitz-Weiss et al. 2013, Woolsey et al. 2013). We did not find a significant difference in the level of DNA damage biomarker (8-OHdG) between the NAFLD patients and controls. In addition, no significant difference in the ARE activity was observed between the groups. As a consequence of ROS overproduction and the shortage of endogenous antioxidant molecules, higher oxidative stress is recognized as a well-established cause of liver injury due to extensive oxidative biomolecular damage, and subsequently alterations in PON and ARE activities may lead to progressive fibrosis (Ferro et al. 2020). Furthermore, in previous studies, interference of OTS in NAFLD patients was proved and antioxidants usage for protection against these pathways was suggested,

but in this study patients with NAFLD had the induction of OTS and PON 1 activity which can be used as valuable future biomarkers for NAFLD diagnosis.

5. Conclusions

Patients with NAFLD had the induction of oxidative toxic stress and PON 1 activity which can be used as valuable future biomarkers for NAFLD diagnosis. Further studies are recommended to assess the mechanism of oxidative stress and the beneficial role of antioxidant treatment in patients with NAFLD.

6. Conflict of interest

None.

Acknowledgements

The study is supported by a dissertation grant from Hamadan University of Medical Sciences for student thesis (No:940201454).

References

- Aharoni, S., M. Aviram & B. Fuhrman (2013) Paraoxonase 1 (PON1) reduces macrophage inflammatory responses. *Atherosclerosis*, 228, 353-361.
- Aslan, M., M. Kosecik, M. Horoz, S. Selek, H. Celik & O. Erel (2007) Assessment of paraoxonase and arylesterase activities in patients with iron deficiency anemia. *Atherosclerosis*, 191, 397-402.
- Ates, O., S. Azizi, H. H. Alp, A. Kiziltunc, S. Beydemir, E. Cinici, I. Kocer & O. Baykal (2009) Decreased serum paraoxonase 1 activity and increased serum homocysteine and malondialdehyde levels in age-related macular degeneration. *Tohoku J Exp Med*, 217, 17-22.
- Awad, A. S., E. N. A. Al Haleem, W. M. El-Bakly & M. A. Sherief (2016) Thymoquinone alleviates nonalcoholic fatty liver disease in rats via suppression of oxidative stress, inflammation, apoptosis. *Naunyn Schmiedeberg's Arch Pharmacol*, 389, 381-391.
- Benzie, I. F. & J. Strain (1999) [2] Ferric reducing/antioxidant power assay: Direct measure of total antioxidant activity of biological fluids and modified version for simultaneous measurement of total antioxidant power and ascorbic acid concentration. *Methods Enzymol*, 299, 15-27.
- Çekmez, Ö. P. H. B. F. & H. K. B. N. Dündar (2013) Association between insulin resistance and oxidative stress parameters in obese adolescents with non-alcoholic fatty liver disease. *J Clin Res Pediatr Endocrinol*, 5.
- Chalasanani, N., R. Vuppalananchi, M. Rinella, M. Middleton, M. Siddiqui, A. Barritt IV, O. Kolterman, O. Flores, C. Alonso & M. Iruarizaga-Lejarreta (2018) Randomised clinical trial: a leucine-metformin-sildenafil combination (NS-0200) vs placebo in patients with non-alcoholic fatty liver disease. *Aliment Pharmacol Ther*, 47, 1639-1651.
- Damba, T., A. R. Bourgonje, A. E. Abdulle, A. Pasch, S. Sydor, E. H. van den Berg, R. T. Gansevoort, S. J. Bakker, H. Blokzijl & R. P. Dullaart (2020) Oxidative stress is associated with suspected non-alcoholic fatty liver disease and all-cause mortality in the general population. *Liver Int*, 40, 2148-2159.
- Desai, S., S. S. Baker, W. Liu, D. A. Moya, R. W. Browne, L. Mastrandrea, R. D. Baker & L. Zhu (2014) Paraoxonase 1 and oxidative stress in paediatric non-alcoholic steatohepatitis. *Liver Int*, 34, 110-7.

- Ferro, D., F. Baratta, D. Pastori, N. Cocomello, A. Colantoni, F. Angelico & M. Del Ben (2020) New insights into the pathogenesis of non-alcoholic fatty liver disease: Gut-derived lipopolysaccharides and oxidative stress. *Nutrients*, 12, 2762.
- Ghadermazi, R., F. Khoshjou, S. M. Hossini Zijoud, H. Behrooj, N. Kheiripour, M. Ganji, H. Moridi, M. Mohammadi & A. Ranjbar (2018) Hepatoprotective effect of tempol on oxidative toxic stress in STZ-induced diabetic rats. *Toxin Rev*, 37, 82-86.
- Hashemi, M., D. M. Kordi-Tamandani, N. Sharifi, A. Moazeni-Roodi, M.-A. Kaykhaei, B. Narouie & A. Torkmanzahi (2011) Serum paraoxonase and arylesterase activities in metabolic syndrome in Zahedan, southeast Iran. *Eur J Endocrinol*, 164, 219-222.
- Hu, M. & C. Dillard (1994) Plasma SH and GSH measurement. *Methods Enzymol*, 233, 87.
- Kumar, R., S. Prakash, S. Chhabra, V. Singla, K. Madan, S. D. Gupta, S. K. Panda, S. Khanal & S. K. Acharya (2012) Association of pro-inflammatory cytokines, adipokines & oxidative stress with insulin resistance & non-alcoholic fatty liver disease. *Indian J Med Res*, 136, 229.
- Loued, S., M. Isabelle, H. Berrougui & A. Khalil (2012) The anti-inflammatory effect of paraoxonase 1 against oxidized lipids depends on its association with high density lipoproteins. *Life Sci*, 90, 82-88.
- Marí, M., A. Morales, A. Colell, C. García-Ruiz & J. C. Fernandez-Checa. 2015. Oxidative stress in nonalcoholic fatty liver disease. *Studies on Hepatic Disorders*, 279-308. Springer.
- Marsillach, J., N. Ferré, M. C. Vila, A. Lligoña, B. Mackness, M. Mackness, R. Deulofeu, R. Solá, A. Parés & J. Pedro-Botet (2007) Serum paraoxonase-1 in chronic alcoholics: relationship with liver disease. *Clin Biochem*, 40, 645-650.
- Moore, K. & L. J. Roberts, 2nd (1998) Measurement of lipid peroxidation. *Free Radic Res*, 28, 659-71.
- Morita, M., N. Ishida, K. Uchiyama, K. Yamaguchi, Y. Itoh, M. Shichiri, Y. Yoshida, Y. Hagihara, Y. Naito & T. Yoshikawa (2012) Fatty liver induced by free radicals and lipid peroxidation. *Free Radic Res*, 46, 758-765.
- Ramadan, R., A. Tawdy, R. Abdel Hay, L. Rashed & D. Tawfik (2012) The antioxidant role of paraoxonase 1 and vitamin E in three autoimmune diseases. *Skin Pharmacol Physiol*, 26, 2-7.
- Ranjbar, A., N. Kheiripour, H. Ghasemi, M. A. S. Rabiei, F. Dadras & F. Khoshjou (2018) Antioxidative effects of tempol on mitochondrial dysfunction in diabetic nephropathy. *Iran J Kidney Dis*, 12, 84-90.
- Schmilovitz-Weiss, H., E. Hochhauser, M. Cohen, Y. Chepurko, S. Yitzhaki, E. Grossman, A. Leibowitz, Z. Ackerman & Z. Ben-Ari (2013) Rosiglitazone and bezafibrate modulate gene expression in a rat model of non-alcoholic fatty liver disease-A historical prospective. *Lipids Health Dis*, 12, 41.
- Shokri, Y., A. Variji, M. Nosrati, A. Khonakdar-Tarsi, A. Kianmehr, Z. Kashi, A. Bahar, A. Bagheri & A. Mahrooz (2020) Importance of paraoxonase 1 (PON1) as an antioxidant and antiatherogenic enzyme in the cardiovascular complications of type 2 diabetes: Genotypic and phenotypic evaluation. *Diabetes Res Clin Pract*, 161, 108067.
- van den Berg, E. H., E. G. Gruppen, R. W. James, S. J. Bakker & R. P. Dullaart (2019) Serum paraoxonase 1 activity is paradoxically maintained in nonalcoholic fatty liver disease despite low HDL cholesterol. *J Lipid Res*, 60, 168-175.
- Wan, J., M. Benkdane, F. Teixeira-Clerc, S. Bonnafous, A. Louvet, F. Lafdil, F. Pecker, A. Tran, P. Gual & A. Mallat (2014) M2 Kupffer cells promote M1 Kupffer cell apoptosis: a protective mechanism against alcoholic and nonalcoholic fatty liver disease. *Hepatology*, 59, 130-142.
- Woolsey, S. J., I. Gong, R. Kim, M. Levstik, M. Beaton & R. Tirona (2013) Regulation of Cytochrome P450 3A4 in Non-Alcoholic Fatty Liver Disease by Fibroblast Growth Factor 21. *FASEB J*, 27, 1b537.
- Zaki, M. E., H. El-Bassyouni, S. Kamal, M. El-Gammal & E. Youness (2014) Association of serum paraoxonase enzyme activity and oxidative stress markers with dyslipidemia in obese adolescents. *Indian J Endocrinol Metab*, 18, 340.

The Potential Impact of Different Types of Yogurt Fortified with Inulin and/or Microencapsulated Probiotic Bacteria on Diabetic Rats

Abdel-moniem Naguib¹, Abdel-kader Morsy Abdel- Samad¹, Osama M. Sharaf², Ibrahim M. Hamed³, Shaimaa I. Soltan^{1,3,*} and Mona M. Hussein³

¹Biochemistry Department, Faculty of Agriculture, Cairo University, Egypt; ²Dairy Department, Food Industry and Nutrition Research Division, National Research Centre El-Buhouth St., Dokki, Cairo, Egypt; ³Nutrition and Food Sciences Department, Food Industry and Nutrition Research Division, National Research Centre El-Buhouth St., Dokki, Cairo, Egypt.

Received: March 5, 2020; Revised: October 22, 2020; Accepted: Nov 3, 2020

Abstract

Diabetes is a metabolic disease that is very common in developing countries and responsible for the death of over 1.5 million people each year. This study aimed to investigate the anti-diabetic effect of different types of synbiotic yogurt on experimental rats. Four different types of synbiotic yogurt supplemented with inulin and microencapsulated probiotics (*Lactobacillus acidophilus* CH2, *Lactobacillus plantarum* DSA 20174, *Lactobacillus rhamnosus* NRRL B-442, *Bifidobacterium lactis* LB-12) were used. A fifth type of yogurt supplemented with inulin alone was also prepared. The anti-diabetic effect of different synbiotic yogurt was evaluated in diabetic rats. The results showed that the microencapsulation had improved the survival of probiotic in yogurt samples. The yogurt samples supplemented with inulin and microencapsulated *L. acidophilus* have a mean viability (8.6 ± 0.1 log CFU/g) on the seventh day higher, but not significant, than the viability at zero time (8.1 ± 0.1 log CFU/g). The glucose and total cholesterol levels have significantly decreased (132 mg/dL and 72 ± 5 mg/dL at $P < 0.05$ respectively) in diabetic rats that were fed with yogurt supplemented with inulin and *L. acidophilus* compared to the diabetic control group (glucose 360 mg/dL and total cholesterol 118 ± 4 mg/dL). The administration of yogurt supplemented with inulin and *L. rhamnosus* and yogurt supplemented with inulin and *B. lactis* were the most promising in improving plasma ALT (26 ± 1 U/L) and AST (32 ± 1 U/L) levels respectively, compared to those of diabetic control group (ALT 127 ± 4 U/L and AST 69 ± 0.8 U/L). A significant reduction ($P < 0.05$) was also recorded in the levels of creatinine (0.75 ± 0.09 mg/dL) and urea (30 ± 0.4 mg/dL) in diabetic rats that were fed yogurt supplemented with inulin and *L. plantarum* compared to that of the diabetic control group (creatinine 3.08 ± 0.07 mg/dL and urea 72 ± 2 mg/dL). In general, the results in the current study provided evidence that using the microencapsulation technique can enhance the viability and the performance of the probiotic bacteria. The results also support the application of probiotic bacteria in ameliorating type-2 diabetes and reducing its complications.

Keywords: Probiotics, Synbiotic, Microencapsulation, Yogurt, Diabetic rats.

1. Introduction

Type-2 diabetes mellitus, a metabolic disorder described by hyperglycemia, is being attributed to different physiological, genetic, and environmental factors (Hofe *et al.*, 2014). However, the main cause of type-2 diabetes is a result of the deficiency in insulin secretion or insulin action due to the dysfunction of islet B-cell (Asemi *et al.*, 2013). A series of morphological and functional alterations occur during diabetes mellitus, which can trigger some complications (Ajiboye *et al.*, 2018). Recently, the gut microbiota received considerable attention by nutritionists due to its interesting function in controlling the insulin level (Brunkwall and Orholm-Melander, 2017; Samanta *et al.*, 2018). Probiotic bacteria are living microorganisms present naturally in human and animal gut and have different beneficial effects (Karim and

Hasan, 2019). For instance, they contribute in synthesizing of vitamin and antimicrobial compounds (Karim and Hasan, 2019; Alrabadi *et al.*, 2018), boosting the immune system, reducing cholesterol (AL-Awwad *et al.*, 2014), and use in cancer therapeutic application (Vijayaram and Kannan, 2018). Moreover, the role of gut microbiota in metabolic diseases, including type-2 diabetes, became evident (Gurung *et al.*, 2020; Bera and Ghosh, 2018).

Lactic acid bacteria (LAB), probiotic bacteria which are common in our natural environment, are being commonly used in dairy industries across the world for thousands of years (Evivie *et al.*, 2017). The presence of some *Lactobacillus* strains in human gut flora, in addition to its long history of use in foods and dairy products without significant complications, has led to the conclusion that they are safe for human consumption (Jones *et al.*, 2012; Mahasneh and Abbas, 2010). Nowadays, probiotic bacteria are being widely used in many functional foods

* Corresponding author e-mail: shaimaa.ismail2020@gmail.com.

and also in treating many physiological and metabolic diseases (Jones *et al.*, 2012). Prebiotics are non-digestible oligosaccharides that are enhancing the growth of beneficial commensal organisms (Ooi *et al.*, 2010).

Yogurt is the most popular dairy product that contains probiotic bacteria, and is widely consumed due to its high nutritional benefits (Suliman and El Zubeir, 2014). As such, yogurt is regarded as an ideal form for the successful delivery of probiotic bacteria (Sanders, 2008). There are some factors (e.g. acidity, level of oxygen in products, presence of other lactic acid bacteria, and byproduct produced by other competing bacteria) that might negatively affect the shelf life of probiotic supplemented products. These factors could, individually or collectively, impair the efficacy of probiotic bacteria (Terpou *et al.*, 2019). Recently microencapsulation of probiotic bacteria has been used to enhance the efficiency of functional foods (De Prisco and Mauriello, 2016). The technique of microencapsulation has been proven to enhance the viability of some sensitive microorganisms against the harsh environmental conditions (Huq *et al.*, 2013). This study aimed to manufacture different yogurt samples containing inulin and microencapsulated probiotic bacteria and investigates their anti-diabetic effects on diabetic rats.

2. Materials and Methods

2.1. Preparation of Microorganism

The probiotic bacteria were obtained from different sources. For instance, *Lactobacillus acidophilus* CH2 and *Lactobacillus rhamnosus* NRRL B-442 were purchased from Chr. Hansen's Lab., DENMARK and the Northern Regional Research Laboratory, ILLINOIS, USA, respectively. *Lactobacillus plantarum* DSA 20174 and *Bifidobacterium lactis* LB-12 were purchased from MIRCEN, FACULTY OF AGRICULTURE, AIN SHAMS UNIVERSITY, EGYPT.

All *Lactobacillus* strains, (*L. acidophilus*, *L. plantarum*, and *L. rhamnosus*) were grown on MRS broth (purchased from SRL, INDIA and sterilized for 15 min at 120°C) and incubated at 37°C for 24 hours (De Man *et al.*, 1960), while *Bifidobacterium* strain was grown on modified MRS broth (MRS enriched with L-cysteine hydrochloride 0.05%) to provide anaerobic conditions using the GasPak system (Collins and Hall, 1984; Vinderola and Reinheimer, 1999).

2.2. Microencapsulation of Bacterial Strains

The microencapsulation was prepared using the extrusion technique (Nigam *et al.*, 1988) that was modified by Sharaf *et al.* (2016). The strain biomass was obtained by performing 4000 rpm centrifugation at 4°C for 15 minutes and then rinsed with 0.1% (w/v) sterile peptone (purchased from BACTO, DIFCO Laboratory, USA). The pellets were suspended in 5 ml of 0.1% (w/v) peptone and mixed with the same amount of 2% (w/v) sodium alginate solutions (purchased from JUDEX laboratory, ENGLAND and sterilized at 121°C for 15 minutes). The mixtures were dropped into a sterile CaCl₂ solution through a needle with gently stirring, forming beads to entrap the bacterial cells. The beads (2 mm-diameters) were washed twice in sterile saline to discard free cells and the remains of calcium ions. Finally, beads were washed with 0.1% sterile peptone solution and kept in peptone solution at 4°C. The

entrapped bacteria were released from the capsules using 1g of the microcapsules dissolved in 9 ml of 2% sterile tri-sodium citrate solution and vortexed till complete dissociation (Zhou *et al.*, 1998). The viability of probiotic bacteria inside the microcapsules was estimated using the pour-plate method (Vinderola and Reinheimer, 1999); the results were recorded as colony-forming units for each gram (CFU/g).

2.3. Yogurt Preparation

A control set yogurt was prepared with yogurt starter culture only, without inulin and probiotic cultures. Five batches of set yogurt were prepared and supplemented with inulin and probiotic bacterial cultures except one batch (T5) was prepared and supplemented with inulin only. The yogurt samples were prepared by heating standardized buffalo milk (purchased from the local market) to 85°C for 30 minutes before cooling it to 37°C. Then, the milk was inoculated with a mixture of 3% inulin (purchased from El-SHARQ El-AWSAT company, CAIRO, EGYPT), 2% of the prepared microencapsulated probiotic culture, and 2% of yogurt starter culture, which contained *L. delbruekii bulgaricus* and *Streptococcus thermophilus* (Lee and Lucey, 2010). The probiotic bacteria with the yogurt were incorporated with the yogurt either as microencapsulated cells or free cells. The cultures of probiotic bacteria were added at the same time with the yogurt starter cultures. The inoculated milk was distributed in 100 ml plastic cups and then incubated at 37°C. After that, the yogurt was cooled and stored at 4°C for seven days. The chemical and microbiological analyses were carried out at 'zero' time (after overnight cold storage of samples) and repeated at the third day and seventh day of storage (Kailasapathy, 2006).

2.4. Analysis of Different Synbiotic Yogurt contents

2.4.1. Chemical Analysis

The pH of yogurt samples was determined using a pH meter (AD1000 pH /mV and temperature meter, Adwa Instruments), which was calibrated with reference buffer solutions (pH 4.0 and pH 7.0). All samples of synbiotic yogurt were stirred well before measuring the pH level (Kailasapathy, 2006). The moisture, ash, protein, and fat contents of the samples were determined after 24 hours of product storage at 4°C. For moisture content, a sample of fresh yogurt was accurately weighed and dried in oven at 105°C until reached a constant weight (Bradley, 2010). Ash content was determined by heating the yogurt sample at 550°C in a muffle furnace chamber (Marshall, 2010). The crude protein content was measured using Kjeldahl method (the total nitrogen was multiplied by a factor of 6.25) (Chang, 2010). Fat content was determined following Gerber method (Min and Ellefson, 2010). Total carbohydrate was calculated based on the amount of protein, ash and lipid using the following equation:

$$\text{Total carbohydrate} = 100(\text{dry weight}) - (\text{protein} + \text{lipid} + \text{ash}) \text{ (BeMiller, 2010).}$$

2.4.2. Microbiological Analysis of Different Synbiotic Yogurt

A 10 g of synbiotic yogurt dissolved in 90 ml of 2% sterile citrate buffer. The selective media were used to differentiate the introduced microencapsulated probiotic

cultures from yogurt starter cultures. Both *L. acidophilus* and *L. plantarum* were detected using a selective media of MRS broth—MRS broth supplemented with maltose instead of glucose—and incubated at 37°C for 24 hours. *B. lactis* was grown in MRS broth enriched with L-cysteine hydrochloride 0.05% to allow anaerobic conditions (Collins and Hall, 1984). *L. rhamnosus* was inoculated into MRS supplemented with vancomycin antibiotic, where 0.005 g vancomycin dissolved in 10 ml sterile distilled water, then 0.2 ml of this dissolved antibiotic solution was added to 100 ml MRS broth media at 55°C (Tharmaraj and Shah, 2003).

2.5. Biological Evaluation of Different Synbiotic Yogurt

A total of 42 male rats (Sprague-Dawley), each with an average weight of 110 ± 5 g, were obtained from the animal house of the NATIONAL RESEARCH CENTER, CAIRO, EGYPT. The animal's house ethics committee, NRC, GIZA, EGYPT, approved the safety and ethics. Rats were kept individually in stainless steel wire bottom cages at room temperature (25 ± 2°C) under 12 hours dark and light cycle. Animals were fed with stock diets ad-lib for three weeks until rats weighing 200 ± 10 g. Next, rats have been induced to diabetes disease by injecting them intraperitoneally, while they were fasting, with 5% alloxan solution (135 mg/kg body weight) in saline solution (Federiuk *et al.*, 2004). Blood samples were obtained from the tail vein to test the fasting blood glucose levels. On the seventh day after alloxan injection, rats with a level of blood glucose above 200 mg/dL were included in the study as diabetic rats. The rats were distributed into seven groups (each included six rats) where each group fed with balanced diet supplemented with different synbiotic yogurt as shown in (Table 1).

Table 1. Experimental groups

Groups	Diet
Control normal	Normal rats fed with a balanced diet*
Control diabetes	Diabetes rats fed with a balanced diet
Group (1)	Diabetic rats fed with a balanced diet and synbiotic yogurt have 3% inulin with 2% microencapsulated <i>L. acidophilus</i>
Group (2)	Diabetic rats fed with a balanced diet and synbiotic yogurt have 3% inulin with 2% microencapsulated <i>L. plantarum</i>
Group (3)	Diabetic rats fed with a balanced diet and synbiotic yogurt have 3% inulin with 2% microencapsulated <i>L. rhamnosus</i>
Group (4)	Diabetic rats fed with a balanced diet and synbiotic yogurt have 3% inulin with 2% microencapsulated <i>B. lactis</i>
Group (5)	Diabetic rats fed with a balanced diet and synbiotic yogurt have 3% inulin only

*Balanced diet is a diet that consists of 12% casein, 15% corn oil, 10% sucrose, 3% fiber, 55.5% starch, 3.5% salt mixture, and 1% vitamin mixture has been prepared for rats feeding during the period of the experiment (Reeves *et al.*, 1993).

After five weeks of administration of different synbiotic yogurt, rats were forced to overnight fasting before collecting blood samples to measure the level of fasting blood glucose and HbA1c following Trinder (1969)

and Trivelli *et al* (1971) respectively. The lipid profile of experimental rats was assessed by determining the levels of: (1) total cholesterol (T-CH) according to Allain *et al* (1974), (2) triglycerides (TG) (Fossati and Prencipe, 1982), (3) high-density lipoprotein cholesterol (HDL-CH) (Burstein *et al.*, 1970), and (4) low-density lipoprotein cholesterol (LDL-CH) (Wieland and Seidel, 1983). The liver performance was evaluated by determining the activity of liver enzymes, specifically alanine transaminase (ALT) and aspartate transaminase (AST) (Reitman and Frankel, 1957). To assess changes in kidney functions and performances, the levels of creatinine and urea were evaluated according to Fawcett and Scott (1960) and Bartels *et al.* (1972) respectively.

2.6. Statistical Analysis

Analysis of Variance (ANOVA) with post-hoc Least significant difference (LSD) test was applied to assess the variability between the treatments and the controls (Waller and Duncan, 1969). All statistical analyses were carried out using IBM SPSS Statistics (IBM, 2019).

3. Results and Discussion

3.1. Viability of Probiotic Bacteria inside the Microcapsule

The viable counts of probiotic bacteria within calcium alginate microcapsule are shown in (Table 2). All strains reached 10⁹ CFU/g of their viable counts inside the microcapsule. There was no significant ($P > 0.05$) difference in the viability between the strains. Previous studies suggested a minimum viability threshold of 10⁶ CFU/g to achieve the therapeutic effects from the probiotic bacteria (Dave and Shah, 1997), while a viable count above 10⁷ would maximize the therapeutic effects from the probiotics (Lourens-Hattingh and Viljoen, 2001). These indicate that the viability of the probiotics in our study have high beneficial health properties.

Table 2. Viable counts of probiotic bacteria inside the microcapsule (log CFU/g)

Type	Bacterial count
<i>L. acidophilus</i>	8.64 ± 0.3 ^a
<i>L. plantarum</i>	8.69 ± 0.5 ^a
<i>L. rhamnosus</i>	8.74 ± 0.5 ^a
<i>B. lactis</i>	9.03 ± 0.6 ^a

Each value represents the mean ± SE Means followed by the same letter are not significantly different ($P > 0.05$)

3.2. Analysis of Different Synbiotic Yogurt contents

3.2.1. Chemical Analysis of Different Synbiotic Yogurt

Data displayed in (Table 3) represent the pH values of the yogurt supplemented with microencapsulated probiotic cells, and yogurt supplemented with free probiotic. Our results showed that the pH value of yogurt supplemented with microencapsulated cells at the third and seventh days of storage was less than that of yogurt supplemented with free cells of probiotic bacteria. This decrease in pH value may be contributed positively to microencapsulated cell metabolism.

Table 3. pH of yogurt supplemented with free and microencapsulated probiotic bacteria

Yogurt types	Free probiotic cells			Microencapsulated cells		
	Zero time	Third day	Seventh day	Zero time	Third day	Seventh day
Control*	4.95	4.48	4.42	4.95	4.48	4.42
T1	4.99	4.78	4.53	4.54	4.24	3.95
T2	4.99	4.85	4.43	5.06	4.50	4.14
T3	4.99	4.66	4.52	5.07	4.52	4.24
T4	4.78	4.78	4.46	5.10	4.56	4.33
T5*	5.45	5.10	4.94	5.45	5.10	4.94

*Control yogurt was the same in the case of free cells and microencapsulated cells

Treatment 1 (T1): yogurt supplemented with 3% inulin with 2% microencapsulated *L. acidophilus*. Treatment 2 (T2): yogurt supplemented with 3% inulin with 2% microencapsulated *L. plantarum* Treatment 3 (T3): yogurt supplemented with 3% inulin with 2% microencapsulated *L. rhamnosus* Treatment 4 (T4): yogurt supplemented with 3% inulin with 2% microencapsulated *B. lactis* *Treatment5 (T5): yogurt supplemented with 3% inulin only, was the same in case of free cells and microencapsulated cells

This finding is congruent with that of Afzaal *et al* (2018), who reported a significant decrease in the pH value of the yogurt supplemented with inulin and microencapsulated lactic acid bacterial cells compared with yogurt supplemented with inulin and free cells of lactic acid bacteria. Sultana *et al.* (2000) attributed this decrease in the pH value to the gradual uptake of nutrients and the slow release of metabolites across the shell of microencapsulated alginate beads.

The moisture, protein, and fat of control buffalo yogurt were significantly higher than those of the other treatments (Table 4). However, there was no significant differences ($P=0.086$) between ash content of the control sample and that of the other treatments (Table 4). This finding is incongruence with that obtained by Stijepić *et al.* (2013), who reported high ash content (0.739% w/w) in yogurt supplemented with 3% inulin. This disagreement with our finding because Stijepić *et al.* (2013) have used yogurt

prepared from cow milk, not buffalo. Furthermore, it is known that the ash content depends on the food supplement and also varies between seasons (Rasheed *et al.*, 2016; Barłowska *et al.*, 2011). This is another possible explanation for the disagreement between our finding and finding of Stijepić *et al.* (2013). Our result showed that the carbohydrates content of the control sample was significantly lower than those of other treatments. Previous study showed that carbohydrates can provide an appropriate media for the growth of beneficial bacteria, which, in turn, enhances gastrointestinal health and many physicochemical processes (Chandran *et al.*, 2016). Therefore, the high the carbohydrate contents, the more health benefit. Interestingly, the moisture content value of the control yogurt in our study is in agreement with the moisture content value (86.40%) reported in a previous study (Hassan and Amjad, 2010).

Table 4. Chemical analysis of different synbiotic yogurt (% dry weight)

Treatments	Moisture	Ash/(DM *)	Protein/(DM *)	Fat/(DM *)	Carbohydrate/(DM*)
Control	86 ±0.9 ^a	3.5 ±0.4 ^a	24.7 ±0.1 ^a	41.8 ±0.1 ^a	30 ±1.1 ^b
T1	80.7 ±0.03 ^b	2.9 ±0.1 ^a	21±0.03 ^b	36 ±1.9 ^b	40.1±2.5 ^a
T2	80.7 ±0.05 ^b	3 ±0.1 ^a	20.3 ±0.3 ^b	36.9 ±0.3 ^b	39.8 ±0.1 ^a
T3	80.7 ±0.3 ^b	2.8 ±0.08 ^a	21±0.6 ^b	37 ±0.8 ^b	39.2 ±2.2 ^a
T4	80.7 ±0.6 ^b	3 ±0.1 ^a	20.6 ±0.09 ^b	36.5 ±0.7 ^b	40.9 ±1.3 ^a
T5	80.7 ±0.5 ^b	2.8 ±0.02 ^a	21.1 ±0.9 ^b	35 ±0.4 ^b	41.1±1.1 ^a

Each value represents the mean ± SE.

*DM means dry matter.

Means in the same column followed by the same letter were not significantly different ($P>0.05$). Control yogurt contains no inulin and no microencapsulated probiotic bacteria

Treatment 1 (T1): yogurt supplemented with 3% inulin with 2% microencapsulated *L. acidophilus*. Treatment 2 (T2): yogurt supplemented with 3% inulin with 2% microencapsulated *L. plantarum*. Treatment 3 (T3): yogurt supplemented with 3% inulin with 2% microencapsulated *L. rhamnosus*. Treatment 4 (T4): yogurt supplemented with 3% inulin with 2% microencapsulated *B. lactis*. Treatment 5 (T5): yogurt supplemented with 3% inulin only.

Carbohydrate was calculated not evaluated

Moreover, our result is also incongruence with Rinaldoni *et al.* (2012) who reported low fat content (15g/L) and high protein content (59g/L) in the yogurt sample supplemented with 3% inulin only compared with our results. This incongruence could be because the yogurt samples in Rinaldoni's study were prepared from a different source of milk, soymilk. The content of protein in synbiotic yogurt varies according to the proteolytic activity

of the probiotics, which converts the protein into its functional units, peptides and amino acids (Hassan and Amjad, 2010).

3.2.2. Microbiological Analysis of Different Synbiotic Yogurt during the Storage Period

The differences in viable counts of microencapsulated strains in synbiotic yogurt during storage periods at the refrigerator are shown in (Table 5). All treatments have

shown the appropriate growth of microencapsulated strains. The viable counts of all treatments have increased until the seventh day. The overall means across storage periods for all treatments indicated that the viable counts reached the highest value on the third day of storage (e.g. samples supplemented with inulin and microencapsulated *L. acidophilus*). This increase reflects the protective effect of microencapsulation on the viability of strains. Samples supplemented with inulin and microencapsulated *L. plantarum* have a significant decrease at the seventh day of storage (8.2 ± 0.2 , $P=0.02$) compared to those of the third day of storage.

Table 5. Total viable bacterial counts in synbiotic yogurt during the storage period (log CFU/g)

Treatments	Microencapsulated cells		
	Zero time	Third days	Seventh days
T1	8.1 ± 0.1 ^a	8.7 ± 0.2 ^a	8.6 ± 0.1 ^a
T2	8.2 ± 0.1 ^b	8.4 ± 0.06 ^{ab}	8.2 ± 0.2 ^c
T3	8.1 ± 0.09 ^a	8.8 ± 0.2 ^a	8.3 ± 0.2 ^a
T4	8 ± 0.3 ^a	8.5 ± 0.1 ^a	8.3 ± 0.2 ^a

Each value represents the mean ± SE.

Means in the same row followed by the same letter are not significantly different ($P>0.05$)

Treatment 1 (T1): yogurt supplemented with 3% inulin with 2% microencapsulated *L. acidophilus*. Treatment 2 (T2): yogurt supplemented with 3% inulin with 2% microencapsulated *L. plantarum*. Treatment 3 (T3): yogurt supplemented with 3% inulin with 2% microencapsulated *L. rhamnosus*. Treatment 4 (T4): yogurt supplemented with 3% inulin with 2% microencapsulated *B. lactis*

Our results are in agreement with Brinques and Ayub (2011), who reported high viability for microencapsulated bacteria compared to the viability for free cells. This variation in viability is a result of the effectiveness of microencapsulation in maintaining the stability of the probiotic bacteria under storage at refrigeration temperature (Brinques and Ayub, 2011). Pavunc *et al.* (2011) also found a better growth and high survival rate for *L. helveticus* M92 inside the microcapsule compared to free cells during yogurt fermentation. This growth pattern could be a result of the bidirectional diffusion of nutrients and metabolites through pores of the microcapsule (Pavunc *et al.*, 2011). The reported decrease in the growth of probiotic at the seventh day in the current study was expected because the accumulation of undissociated acids inside the microcapsule, which, in turn, leads to decrease in the growth and the biomass of the probiotics (Klinkenberg *et al.*, 2001).

3.3. Biological Evaluation of Different Synbiotic Yogurt

3.3.1. Anti-diabetic Effect of Different Synbiotic Yogurt

The results of the current study showed that consuming yogurt supplemented with synbiotic could decrease the level of fasting blood glucose and glycosylated hemoglobin of diabetic rats (Table 6). At the end of the experiment, a significant reduction in the level of blood glucose ($P<0.001$) and HbA1c ($P<0.021$) was reported in all groups. However, the rats in group 1 that were fed with a balanced diet supplemented with inulin and microencapsulated *L. acidophilus* showed the highest

significant reduction in the level of blood glucose (132 ± 3 mg/dL, $P=0.001$).

Table 3. Anti-diabetic diet effect on plasma glucose and HbA1c of different experimental rats.

Group	Plasma glucose (mg/dL)	HbA1c %
Control normal	66 ± 1 ^e	<4 ± 0 ^d
Control diabetes	360 ± 2 ^a	8 ± 0.03 ^a
Group (1)	132 ± 3 ^d	4 ± 0.27 ^{cd}
Group (2)	144 ± 3 ^c	4 ± 0.16 ^{cd}
Group (3)	136 ± 5 ^{cd}	6 ± 0.63 ^b
Group (4)	182 ± 4 ^b	5 ± 0.40 ^{bc}
Group (5)	185 ± 5 ^b	5 ± 0.50 ^{bc}

Each value represents the mean ± SE. In each column, the same letters mean no significant difference at $P<0.05$.

It has been suggested that the decrease in the level of blood glucose in diabetic or non-diabetic people is due to the consumption of probiotic bacteria or synbiotic (Nikbakht *et al.*, 2018). Probiotic bacteria play an important role in gut flora modification, which stimulates glucose absorption by producing insulin-tropic polypeptide and glycogen-link peptide (Nikbakht *et al.*, 2018). Another study has also reported that the probiotic strains MTCC 5690 and MTCC 5689 have decreased the blood glucose level (131 mg/dL and 129 mg/dL), respectively, compared to the diabetic group (167 mg/dL) (Balakumar *et al.*, 2018). This decrease attributed to the ability of the probiotic strains to improve the gut integrity, decrease LPS (Lipopolysaccharide), and increase GLP-1 (Glucagon-like peptide-1), which, subsequently, enhances insulin sensitivity (Balakumar *et al.*, 2018).

Probiotic can also indirectly reduce the glucose level by: 1) changing the activities of the autonomic nerve, which, in turn, reduces the secretion of glucagon (Yamano *et al.*, 2006), and 2) enhancing the antioxidant status of diabetic patient, which, in turn, prevents the destruction of β -cells and decreases the oxidative damage (Zhang *et al.*, 2016). Furthermore, probiotic also has the potential to inhibit the absorption of glucose in the intestine, which leads to a reduction in the glucose level (Zhang *et al.*, 2016).

Previous studies could not find significant differences between synbiotic yogurt supplemented with probiotics and conventional yogurt on the glucose levels in patients with diabetes or obesity (Barengolts *et al.*, 2019). These results can be attributed to: 1) using small sample size, 2) sub-therapeutic doses, and 3) short duration for the experiments, which negatively affects the accuracy of the statistical analyses and the final conclusion (Mazloom *et al.*, 2013).

3.3.2. Effect of Different Synbiotic Yogurt on Plasma Lipid Profile

Data in (Table 7) represent the plasma lipid profile for all groups. Diabetic control rats showed a significant increase ($P<0.001$) in the levels of T-CH, TG, HDL-CH, and LDL-CH compared with normal rats. Yogurt supplemented with inulin and microencapsulated *L. acidophilus* was the most promising in improving plasma T-CH, and LDL-CH profile of diabetic rats. Yogurt

supplemented with inulin and microencapsulated *L. plantarum* was the most promising in improving plasma TRG and HDL-CH profile.

Table 4. Effect of different synbiotic yogurt on plasma lipid profile (mg/dL) of the studied group

Groups	T-CH (mg/dL)	TG (mg/dL)	HDL-CH (mg/dL)	*LDL-CH (mg/dL)
Control normal	77 ±2 ^b	86 ±0.2 ^b	35 ±0.7 ^b	24.8 ±2 ^b
Control diabetes	118 ±4 ^a	115 ±4 ^a	35 ±0.7 ^b	60 ±3 ^a
Group (1)	72 ±5 ^b	76 ±4 ^b	47 ±3 ^a	9.8 ±1 ^d
Group (2)	74 ±2 ^b	60 ±2 ^c	48 ±2 ^a	14 ±2 ^{cd}
Group (3)	75 ±2 ^b	64 ±2 ^c	44 ±2 ^a	18.2 ±1 ^c
Group (4)	77 ±3 ^b	82 ±3 ^b	44 ±2 ^a	16.6 ±3 ^c
Group (5)	78 ±4 ^b	86 ±7 ^b	35 ±0.6 ^b	25.8 ±3 ^b

Each value represents the mean ± SE.

Means in the same column, followed by the same letter are not significantly different at $P < 0.05$.

Friedewald Equation for Low Density Lipoprotein (LDL-CH)

*LDL-CH= T-CH – (TG/5) – HDL-CH

Ejtahed *et al.* (2012) found that administrating yogurt enriched with *B. lactis* and *L. acidophilus* has no significant effect on the levels of TG and HDL-CH in diabetic patients. Our result is consistent with the finding of Moroti *et al.* (2012), who showed that administrating of a synbiotic shake supplemented with probiotics (*L. acidophilus* and *B. bifidum*) and prebiotic (oligofructose) led to increase in the level of HDL-CH. This indicates that the use of different prebiotics (inulin or oligofructose) has no influence on the therapeutic activity of probiotic (Azorín-Ortuño *et al.*, 2009). The result of the present study is in accordance with a previous study that found a positive impact for *L. plantarum* LS/07 and *L. plantarum* Biocenol LP96 on lipid profile (Salaj *et al.*, 2013). Probiotic bacteria can positively affect hyperlipidemia through: (1) increasing cholesterol consumption by bacterial growth, (2) binding the cholesterol with the bacterial cell's surface, which inhibiting the cholesterol absorption by the host, (3) probiotic bacteria possessing bile acid hydrolase activity, which, as a consequence, increases cholesterol uptake and metabolism in the liver for synthesizing the bile, and (4) inhibiting the synthesis of hepatic cholesterol and triglyceride due to the presence of short-chain fatty acids such as propionic acid (Salaj *et al.*, 2013; Liang and Shah, 2006; Gill and Guarner, 2004; Noh *et al.*, 1997).

3.3.3. Effect of Different Synbiotic Yogurt on Liver and Kidney Function

The liver and kidney functions of all experimental groups are shown in (Table 8). Compared with the diabetic control group, the administration of synbiotic yogurt has significantly decreased ($P < 0.05$) the liver enzymes (ALT and AST) and kidney enzymes (creatinine and urea) in all diabetic rat groups. The maximum decrease in ALT levels was identified in the group that was fed with yogurt supplemented with *L. rhamnosus* (26 ±1 U/L, $P = 0.001$), while the maximum decrease in AST level was in rat group fed with yogurt supplemented with *B. lactis* (32 ±1

U/L, $P = 0.004$). The maximum decrease in creatinine and urea levels was identified in groups fed on yogurt supplemented with *L. acidophilus* (0.72 ±0.05 mg/dL, $P = 0.012$) and *L. plantarum* (30 ±0.4 mg/dL, $P = 0.005$) respectively.

Table 5. Effect of different synbiotic yogurt on liver and kidney function of diabetic

Groups	ALT (U/L)	AST (U/L)	Creatinine (mg/dL)	Urea (mg/dL)
Control normal	38 ±2 ^c	32 ±0.7 ^d	0.74 ±0.04 ^c	28 ±2 ^e
Control diabetes	127 ±4 ^a	69 ±0.8 ^b	3.08 ±0.07 ^a	72 ±2 ^a
Group (1)	32 ±2 ^{cd}	45 ±2 ^c	0.72 ±0.05 ^c	39 ±2 ^c
Group (2)	35 ±4 ^c	34 ±1 ^d	0.75 ±0.09 ^c	30 ±0.4 ^{de}
Group (3)	26 ±1 ^d	40 ±2 ^c	0.75 ±0.09 ^c	32 ±2 ^{de}
Group (4)	34 ±2 ^c	32 ±1 ^d	0.83 ±0.07 ^{bc}	34 ±2 ^{cd}
Group (5)	47 ±1 ^b	77 ±3 ^a	1 ±0.2 ^b	51 ±3 ^b

ALT (Alanine aminotransferase), AST (Aspartate aminotransferase), Each value represents the mean ± SE.

Means in the same column followed by the same letter are not significantly different at $P < 0.05$.

Lucchesi *et al.* (2015) observed an increase in AST and ALT after two weeks of alloxan induction, whereas ALT remained significantly elevated till 26 weeks because the liver requires longer time to cure the damage resulted from using alloxan. A previous study showed that alloxan increases the oxidative stress and reducing the oxidative defense of hepatic cells (Goel, 1977). Our result is in agreement with Bejar *et al.* (2013), who showed significant protective effects for probiotic bacteria treatment on the kidney and liver functions, which was proofed by a significant decline in serum AST, ALT, urea, and creatinine, 38.20 (U/L), 33.54 (U/L), 0.60 (g/L), and 18.78 (mg/L) respectively. Our result is in line with Kumar *et al.* (2017), who showed that administration of probiotic fermented milk for 60 days has significantly decreased the urea and creatinine in animals fed with probiotics compared to the diabetic control group fed with control diet only.

Diabetes disease is associated with dysfunction and damage of liver and kidney (Ota and Ulrih, 2017). The administration of synbiotic yogurt could reduce damage to the liver and kidney by improving the metabolism of lipid and delaying the hepatic and renal disorder (Sengupta *et al.*, 2019). Probiotics can also improve the liver performance by improving liver histology and decreasing the total fatty acid of the hepatic cells (Bakhshimoghaddam *et al.*, 2018). The mechanism of action of probiotic bacteria on improving kidney function can be summarized as follows: (1) preventing growth of some aerobic bacteria in gut, which, in turn, enhance gut microbial balance and regulate the level of urea (Vaziri *et al.*, 2013), (2) the urease activity of the probiotics can increase the degradation of the urea and, ultimately, reduce its level and enhance kidney functions (Parvez *et al.*, 2006), and (3) probiotics and prebiotics can decrease the inflammatory biomarkers and the oxidative stress, which indirectly affect the performance of kidney (Grimoud *et al.*, 2010).

4. Conclusion

The present work is an attempt to develop a supplementary diet incorporating the health benefits of probiotics and prebiotics. Our findings recommend the use of microcapsulation technique to maximize the benefits from probiotics. The present study suggested that synbiotic yogurt has the potential to regulate the glucose level and the lipid profile (total cholesterol, triglycerides, LDL and HDL) in diabetic rats. Furthermore, the administration of synbiotic yogurt has improved both liver and kidney functions in diabetic rats. The present study demonstrated the anti-diabetic properties of different probiotic strains.

Acknowledgments

I wish to express my sincere gratitude to Dr. Alaa Eldin, Researcher at Ecology Centre, SLU, and Dr. Mohamed El-ssayad, Researcher at National Research Center, Egypt, for their sincere support, valuable advice, and instructive discussion in this study.

References

- Afzaal M, Zahoor T, Sadiq FA, Ahmad F, Khan QF, Yasmeen A, Imran M and Sakandar HA. 2018. Effect of Encapsulation on the Viability of Probiotics in Yoghurt. *Progress in Nutrition*, **20(2-S)**:44–52.
- Ajiboye BO, Ojo OA, Akuboh OS, Okesola MA, Idowu OT, Oyinloye BE and Talabi JY. 2018. The Protective Effect of Polyphenol-Rich Extract of *Syzygium Cumini* Leaves on Cholinesterase and Brain Antioxidant Status in Alloxan-Induced Diabetic Rats. *Jordan J Biol Sci*, **11(2)**:163–169.
- AL-Awwad NJ, Takruri HR and Yamani MI. 2014. Effect of Probiotic Hummus on Blood Lipids of Rats. *Jordan J Biol Sci*, **7(4)**:261–267.
- Allain CC, Poon LS and Chan CSG. 1974. Enzymatic Determination of Total Serum Cholesterol. *Clin Chem*, **20(4)**:470–475.
- Alrabadi NI, Al-Jubury EM, Thalij KM and Hajeej JM. 2018. Lactobacillus Rhamnosus Ability of Aflatoxin Detoxification. *Jordan J Biol Sci*, **11(1)**:87–92.
- Asemi Z, Zare Z, Shakeri H, Sabihi SS and Esmailzadeh A. 2013. Effect of Multispecies Probiotic Supplements on Metabolic Profiles, Hs-CRP, and Oxidative Stress in Patients with Type 2 Diabetes. *Ann Nutr Metab*, **63(1–2)**:1–9.
- Azorín-Ortuño M, Urbán C, Cerón JJ, Teclas F, Allende A, Tomás-Barberán FA and Espín JC. 2009. Effect of Low Inulin Doses with Different Polymerisation Degree on Lipid Metabolism, Mineral Absorption, and Intestinal Microbiota in Rats with Fat-Supplemented Diet. *Food Chem.*, **113(4)**:1058–1065.
- Bakhshimoghaddam F, Shateri K, Sina M, Hashemian M and Alizadeh M. 2018. Daily Consumption of Synbiotic Yogurt Decreases Liver Steatosis in Patients with Nonalcoholic Fatty Liver Disease: A Randomized Controlled Clinical Trial. *J Nutr*, **148(8)**:1276–1284.
- Balakumar M, Prabhu D, Sathishkumar C, Prabu P, Rokana N, Kumar R, Raghavan S, Soundarajan A, Grover S, Batish VK, Mohan V and Balasubramanyam M. 2018. Improvement in Glucose Tolerance and Insulin Sensitivity by Probiotic Strains of Indian Gut Origin in High-Fat Diet-Fed C57BL/6J Mice. *Eur J Nutr*, **57(1)**:279–295.
- Barengolts E, Smith E, Reutrakul S, Tonucci L and Anothaisintawee T. 2019. The Effect of Probiotic Yogurt on Glycemic Control in Type 2 Diabetes or Obesity: A Meta-Analysis of Nine Randomized Controlled Trials. *Nutrients*, **11(3)**:671.
- Barlowska J, Szwajkowska M, Litwińczuk Z and Król J. 2011. Nutritional Value and Technological Suitability of Milk from Various Animal Species Used for Dairy Production. *Compr. Rev. Food Sci. Food Saf.*, **10(6)**:291–302.
- Bartels H, Böhmer M and Heierli C. 1972. Serum Kreatininbestimmung Ohne Enteissein. *Clin Chim Acta*, **37(C)**:193–197.
- Bejar W, Hamden K, Salah R Ben and Chouayekh H. 2013. Lactobacillus Plantarum TN627 Significantly Reduces Complications of Alloxan-Induced Diabetes in Rats. *Anaerobe*, **24**:4–11.
- BeMiller JN. 2010. Carbohydrate Analysis. In: Suzanne Nielsen (Eds.), *Food Analysis*. Springer, Boston, MA, pp. 147–177.
- Bera TK and Ghosh D. 2018. The Corrective Efficacy of the N-Hexane Fraction of the Hydro-Methanol Extract of the *Swietenia Mahagoni* Seeds on Testicular Dysfunctions in Streptozotocin-Induced Diabetic Male Rats. *Jordan J Biol Sci*, **11(2)**:129–139.
- Bradley RL. 2010. Moisture and Total Solids Analysis. In: Suzanne Nielsen (Eds.), *Food Analysis*. Springer, Boston, MA, pp. 85–104.
- Brinques GB and Ayub MAZ. 2011. Effect of Microencapsulation on Survival of Lactobacillus Plantarum in Simulated Gastrointestinal Conditions, Refrigeration, and Yogurt. *J Food Eng*, **103(2)**:123–128.
- Brunkwall L and Orho-Melander M. 2017. The Gut Microbiome as a Target for Prevention and Treatment of Hyperglycaemia in Type 2 Diabetes: From Current Human Evidence to Future Possibilities. *Diabetologia*, **60(6)**:943–951.
- Burstein M, Scholnick HR and Morfin R. 1970. Rapid Method for the Isolation of Lipoproteins from Human Serum by Precipitation with Polyanions. *J Lipid Res*, **11(6)**:583–595.
- Chandran H, Das M and R. K. 2016. Effect of Prebiotics on Synbiotic Fermented Milk. *World J Pharm Pharm Sci.*, **5(2)**:1557–1566.
- Chang SKC. 2010. Protein Analysis. In: Suzanne Nielsen (Eds.), *Food Analysis*. Springer, Boston, MA, pp. 133–146.
- Collins EB and Hall BJ. 1984. Growth of Bifidobacteria in Milk and Preparation of Bifidobacterium Infantis for a Dietary Adjunct. *J Dairy Sci*, **67(7)**:1376–1380.
- Dave RI and Shah NP. 1997. Viability of Yoghurt and Probiotic Bacteria in Yoghurts Made from Commercial Starter Cultures. *Int Dairy J*, **7(1)**:31–41.
- De Man JC, Rogosa M and Sharpe ME. 1960. A Medium for the Cultivation of Lactobacilli. *J Appl Bacteriol*, **23(1)**:130–135.
- De Prisco A and Mauriello G. 2016. Probiotication of Foods: A Focus on Microencapsulation Tool. *Trends Food Sci Technol*, **48**:27–39.
- Ejtahed HS, Mohtadi-Nia J, Homayouni-Rad A, Niafar M, Asghari-Jafarabadi M and Mofid V. 2012. Probiotic Yogurt Improves Antioxidant Status in Type 2 Diabetic Patients. *Nutrition*, **28(5)**:539–543.
- Evivie SE, Huo G-C, Igene JO and Bian X. 2017. Some Current Applications, Limitations and Future Perspectives of Lactic Acid Bacteria as Probiotics. *Food Nutr Res*, **61(1)**:1318034.
- Fawcett JK and Scott JE. 1960. A rapid and precise method for the determination of urea. *J Clin Pathol*, **13(2)**:156–159.

- Federiuk IF, Casey HM, Quinn MJ, Wood MD and Ward KW. 2004. Induction of Type-1 Diabetes Mellitus in Laboratory Rats by Use of Alloxan: Route of Administration, Pitfalls, and Insulin Treatment. *Comp Med*, **54(3)**:252–257.
- Fossati P and Prencipe L. 1982. Serum Triglycerides Determined Colorimetrically with an Enzyme That Produces Hydrogen Peroxide. *Clin Chem*, **28(10)**:2077–2080.
- Gill HS and Guarner F. 2004. Probiotics and Human Health: A Clinical Perspective. *Postgrad Med J*, **80**:516–526.
- Goel KA. 1977. Submassive Necrosis of Liver of Channa Gachua, a Fresh Water Fish during Experimental Alloxan Diabetes. *Anat Anz*, **141(2)**:130–135.
- Grimoud J, Durand H, Souza S de, Monsan P, Ouarné F, Theodorou V and Roques C. 2010. In Vitro Screening of Probiotics and Synbiotics According to Anti-Inflammatory and Anti-Proliferative Effects. *Int J Food Microbiol*, **144(1)**:42–50.
- Gurung M, Li Z, You H, Rodrigues R, Jump DB, Morgun A and Shulzhenko N. 2020. Role of Gut Microbiota in Type 2 Diabetes Pathophysiology. *EBioMedicine*, **51**:102590.
- Hassan A and Amjad I. 2010. Nutritional Evaluation of Yoghurt Prepared by Different Starter Cultures and Their Physicochemical Analysis during Storage. *African J Biotechnol*, **9(20)**:2913–2917.
- Hofe CR, Feng L, Zephyr D, Stromberg AJ, Hennig B and Gaetke LM. 2014. Fruit and Vegetable Intake, as Reflected by Serum Carotenoid Concentrations, Predicts Reduced Probability of Polychlorinated Biphenyl–Associated Risk for Type 2 Diabetes: National Health and Nutrition Examination Survey 2003–2004. *Nutr Res*, **34(4)**:285–293.
- Huq T, Khan A, Khan RA, Riedl B and Lacroix M. 2013. Encapsulation of Probiotic Bacteria in Biopolymeric System. *Crit Rev Food Sci Nutr*, **53(9)**:909–916.
- IBM Corp. 2019. IBM SPSS Statistics for Windows, Version 26.0. Armonk, NY: IBM Corp.
- Jones ML, Martoni CJ, Tamber S, Parent M and Prakash S. 2012. Evaluation of Safety and Tolerance of Microencapsulated Lactobacillus Reuteri NCIMB 30242 in a Yogurt Formulation: A Randomized, Placebo-Controlled, Double-Blind Study. *Food Chem Toxicol*, **50(6)**:2216–2223.
- Kailasapathy K. 2006. Survival of Free and Encapsulated Probiotic Bacteria and Their Effect on the Sensory Properties of Yoghurt. *LWT - Food Science and Technology*, **39(10)**:1221–1227.
- Karim MR and Hasan F. 2019. A Comparative Study of Antibiotics and Probiotics against Pathogens Isolated from Coastal Shrimp Aquaculture System. *Jordan J Biol Sci*, **12(3)**:323–328.
- Klinkenberg G, Lystad KQ, Levine DW and Dyrset N. 2001. Ph-Controlled Cell Release and Biomass Distribution of Alginate-Immobilized Lactococcus Lactis Subsp. Lactis. *J Appl Microbiol*, **91(4)**:705–714.
- Kumar N, Tomar SK, Thakur K and Singh AK. 2017. The Ameliorative Effects of Probiotic Lactobacillus Fermentum Strain RS-2 on Alloxan Induced Diabetic Rats. *J Funct Foods*, **28**:275–284.
- Lee WJ and Lucey JA. 2010. Formation and Physical Properties of Yogurt. *Asian-Australas J Anim Sci*, **23(9)**:1127–1136.
- Liong MT and Shah NP. 2006. Effects of a Lactobacillus Casei Synbiotic on Serum Lipoprotein, Intestinal Microflora, and Organic Acids in Rats. *J Dairy Sci*, **89(5)**:1390–1399.
- Lourens-Hattingh A and Viljoen BC. 2001. Yogurt as Probiotic Carrier Food. *Int Dairy J*, **11**:1–17.
- Lucchesi AN, Cassettari LL and Spadella CT. 2015. Alloxan-Induced Diabetes Causes Morphological and Ultrastructural Changes in Rat Liver That Resemble the Natural History of Chronic Fatty Liver Disease in Humans. *J Diabetes Res*, **2015**:494578.
- Mahasneh AM and Abbas MM. 2010. Probiotics and Traditional Fermented Foods: The Eternal Connection (Mini-Review). *Jordan J Biol Sci*, **3(4)**:133–140.
- Marshall MR. 2010. Ash Analysis. In: Suzanne Nielsen (Eds.), **Food Analysis**. Springer, Boston, MA, pp. 105–115.
- Mazloom Z, Yousefinejad A and Dabbaghmanesh MH. 2013. Effect of Probiotics on Lipid Profile, Glycemic Control, Insulin Action, Oxidative Stress, and Inflammatory Markers in Patients with Type 2 Diabetes: A Clinical Trial. *Iran J Med Sci*, **38(1)**:38–43.
- Min DB and Ellefson WC. 2010. Fat Analysis. In: Suzanne Nielsen (Eds.), **Food Analysis**. Springer, Boston, MA, pp. 117–132.
- Moroti C, Souza Magri L, Rezende Costa M De, Cavallini DCU and Sivieri K. 2012. Effect of the Consumption of a New Symbiotic Shake on Glycemia and Cholesterol Levels in Elderly People with Type 2 Diabetes Mellitus. *Lipids Health Dis*, **11**:1–8.
- Nigam SC, Tsao IF, Sakoda A and Wang HY. 1988. Techniques for Preparing Hydrogel Membrane Capsules. *Biotechnol Tech*, **2(4)**:271–276.
- Nikbakht E, Khalesi S, Singh I, Williams LT, West NP and Colson N. 2018. Effect of Probiotics and Synbiotics on Blood Glucose: A Systematic Review and Meta-Analysis of Controlled Trials. *Eur J Nutr*, **57(1)**:95–106.
- Noh DO, Kim SH and Gilliland SE. 1997. Incorporation of Cholesterol into the Cellular Membrane of Lactobacillus Acidophilus ATCC 43121. *J Dairy Sci*, **80(12)**:3107–3113.
- Ooi LG, Ahmad R, Yuen KH and Liang MT. 2010. Lactobacillus Acidophilus CHO-220 and Inulin Reduced Plasma Total Cholesterol and Low-Density Lipoprotein Cholesterol via Alteration of Lipid Transporters. *J Dairy Sci*, **93(11)**:5048–5058.
- Ota A and Ulrigh NP. 2017. An Overview of Herbal Products and Secondary Metabolites Used for Management of Type Two Diabetes. *Front. Pharmacol.*, **8(July)**:436.
- Parvez S, Malik KA, Ah Kang S and Kim HY. 2006. Probiotics and Their Fermented Food Products Are Beneficial for Health. *J Appl Microbiol*, **100(6)**:1171–1185.
- Pavunc AL, Beganović J, Kos B, Buneta A, Beluhan S and Šušković J. 2011. Influence of Microencapsulation and Transglutaminase on Viability of Probiotic Strain Lactobacillus Helveticus M92 and Consistency of Set Yoghurt. *Int J Dairy Technol*, **64(2)**:254–261.
- Rasheed S, Qazi IM, Ahmed I, Durrani Y and Azmat Z. 2016. Comparative Study of Cottage Cheese Prepared from Various Sources of Milk. *Proc. Pakistan Acad. Sci*, **53(4)**:269–282.
- Reeves PG, Nielsen FH and Fahey GC. 1993. AIN-93 Purified Diets for Laboratory Rodents: Final Report of the American Institute of Nutrition Ad Hoc Writing Committee on the Reformulation of the AIN-76A Rodent Diet. *J Nutr*, **123(11)**:1939–1951.
- Reitman S and Frankel S. 1957. A Colorimetric Method for the Determination of Serum Glutamic Oxalacetic and Glutamic Pyruvic Transaminases. *Am J Clin Pathol*, **28(1)**:56–63.
- Rinaldoni AN, Campderrós ME and Pérez Padilla A. 2012. Physico-Chemical and Sensory Properties of Yogurt from Ultrafiltered Soy Milk Concentrate Added with Inulin. *LWT - Food Science and Technology*, **45(2)**:142–147.

- Salaj R, Štofilová J, Šoltesová A, Hertelyová Z, Hijová E, Bertková I, Strojny L, Kružliak P and Bomba A. 2013. The Effects of Two *Lactobacillus Plantarum* Strains on Rat Lipid Metabolism Receiving a High Fat Diet. *Sci World J*, **2013**:135142.
- Samanta A, Patra A, Mandal A, Roy S, Mandal S, Das K, Sinha B, Kar S and Nandi DK. 2018. Physiological Indications and Gut-Microbial Community in Army Personnel in High- Altitude and Base-Line Environments: A Comparative Study. *Jordan J Biol Sci*, **11(2)**:141–145.
- Sanders ME. 2008. Use of Probiotics and Yogurts in Maintenance of Health. *J Clin Gastroenterol*, **42**:71–74.
- Sengupta S, Koley H, Dutta S and Bhowal J. 2019. Hepatoprotective Effects of Synbiotic Soy Yogurt on Mice Fed a High-Cholesterol Diet. *Nutr*, **63–64(July)**:36–44.
- Shah NJ and Swami OC. 2017. Role of Probiotics in Diabetes: A Review of Their Rationale and Efficacy. *EMJ Diabet*, **5(1)**:104–110.
- Sharaf OM, Ibrahim GA, Mawgoud YA, Dabiza NM and El-sayad MF. 2016. Improvement of Fermentation Processing Conditions for the Production of Lactic Acid by Immobilized *Lactobacillus Delbrueckii* Ssp . *Bulgarius* Lb-12. *Middle East J Appl Sci*, **06(03)**:553–558.
- Stijepić M, Glušac J, Durdević-milošević D and Pešić-Mikulec D. 2013. Physicochemical Characteristics of Soy Probiotic Yoghurt with Inulin Additon during the Refrigerated Storage. *Rom Biotechnol Lett*, **18(2)**:8077–8085.
- Suliman ESK and Zubeir IEM El. 2014. A Survey of the Processing and Chemical Composition of Gariss Produced by Nomadic Camel Women Herders in Algaderif State, Sudan. *Jordan J Biol Sci*, **7(2)**:95–100.
- Sultana K, Godward G, Reynolds N, Arumugaswamy R, Peiris P and Kailasapathy K. 2000. Encapsulation of Probiotic Bacteria with Alginate-Starch and Evaluation of Survival in Simulated Gastrointestinal Conditions and in Yoghurt. *Int J Food Microbiol*, **62(1–2)**:47–55.
- Terpou A, Papadaki A, Lappa IK, Kachrimanidou V, Bosnea LA and Kopsahelis N. 2019. Probiotics in Food Systems: Significance and Emerging Strategies Towards Improved Viability and Delivery of Enhanced Beneficial Value. *Nutrients*, **11(7)**:1591.
- Tharmaraj N and Shah NP. 2003. Selective Enumeration of *Lactobacillus Delbrueckii* Ssp. *Bulgarius*, *Streptococcus Thermophilus*, *Lactobacillus Acidophilus*, Bifidobacteria, *Lactobacillus Casei*, *Lactobacillus Rhamnosus*, and Propionibacteria. *J Dairy Sci*, **86(7)**:2288–2296.
- Trinder P. 1969. Determination of Glucose in Blood Using Glucose Oxidase with an Alternative Oxygen Acceptor. *Ann Clin Biochem*, **6(1)**:24–27.
- Trivelli LA, Ranney HM and Lai HT. 1971. Hemoglobin Components in Patients with Diabetes Mellitus. *N Engl J Med*, **284(7)**:353–357.
- Vaziri ND, Wong J, Pahl M, Piceno YM, Yuan J, Desantis TZ, Ni Z, Nguyen TH and Andersen GL. 2013. Chronic Kidney Disease Alters Intestinal Microbial Flora. *Kidney Int*, **83(2)**:308–315.
- Vijayaram S and Kannan S. 2018. Probiotics: The Marvelous Factor and Health Benefits. *Biomed Biotechnol Res J*, **2(1)**:1-8.
- Vinderola CG and Reinheimer JA. 1999. Culture Media for the Enumeration of Bifidobacterium Bifidum and Lactobacillus Acidophilus in the Presence of Yoghurt Bacteria. *Int Dairy J*, **9(8)**:497–505.
- Waller RA and Duncan DB. 1969. A Bayes Rule for the Symmetric Multiple Comparisons Problem. *J Am Stat Assoc*, **64(328)**:1484–1503.
- Wieland H and Seidel D. 1983. A Simple Specific Method for Precipitation of Low Density Lipoproteins. *J Lipid Res*, **24(7)**:904–909.
- Yamano T, Tanida M, Nijjima A, Maeda K, Okumura N, Fukushima Y and Nagai K. 2006. Effects of the Probiotic Strain *Lactobacillus Johnsonii* Strain La1 on Autonomic Nerves and Blood Glucose in Rats. *Life Sci*, **79(20)**:1963–1967.
- Zhang Q, Wu Y and Fei X. 2016. Effect of Probiotics on Glucose Metabolism in Patients with Type 2 Diabetes Mellitus: A Meta-Analysis of Randomized Controlled Trials. *Medicina*, **52(1)**:28–34.
- Zhou Y, Martins E, Groboillot A, Champagne CP and Neufeld RJ. 1998. Spectrophotometric Quantification of Lactic Bacteria in Alginate and Control of Cell Release with Chitosan Coating. *J Appl Microbiol*, **84(3)**:342–348.

Molecular Characterization and Expression Analysis of *aflR*, *aflS*, and *aflD* in Non-Aflatoxigenic and Aflatoxigenic *Aspergillus flavus* Treated with Gallic Acid.

Ghada M. El-Sayed¹, Rasha G. Salim¹, Soher E-S. Aly² and Nivien A. Abosereh^{3,*}

¹Microbial Genetic Department, National Research Centre, Dokki, Cairo, Egypt; ²Food Toxicology and Contaminants Department, National Research Centre, Dokki, Cairo, Egypt; ³Microbial Genetic Department, National Research Centre, Dokki, Cairo, Egypt.

Received: June 6, 2020; Revised: October 10, 2020; Accepted: Nov 3, 2020

Abstract

In this study, from five *Aspergillus flavus* strains, only three strains have been aflatoxin B producers. Gallic acid as antioxidant was used to assay its potential in aflatoxin diminishing. Gallic acid treated aflatoxin B producing isolates showed a slightly inhibition in aflatoxin production and a remarked diminishing in spore formation and growth as compared with untreated isolates. Three genes, *aflR*, *aflS*, and *aflD* were successfully amplified by a conventional polymerase chain reaction in aflatoxigenic and gallic acid treated *Aspergillus flavus* strains. These genes have been sequenced and deposited in Genbank under the accession numbers LC537158, MW055253, and LC537157, respectively. It has been demonstrated that there was no difference in nucleotide sequences in the amplified fragments of these genes in both aflatoxigenic and gallic acid treated *Aspergillus flavus* isolates, qRT-PCR was employed to test the effect of gallic acid on the transcription of *aflR*, *aflS*, and *aflD* genes and that ensured the negative effect of gallic acid on these genes transcription and therefore production of aflatoxin production

Keywords : *Aspergillus flavus*, conventional PCR, Gallic acid, qRT-PCR

1. Introduction

Production of acute toxic, mutagenic, teratogenic, or estrogenic responses in higher vertebrates was reported via mycotoxin exposure such as Aflatoxins (AF) (Jelineket al., 1989); they are secondary metabolites, poly-ketide that have been produced by *Aspergillus flavus* and *Aspergillus parasiticus*. Aflatoxins are carcinogenic and contaminate food and feed worldwide (Bhatnagaret al., 1987). The complete elucidation of the gene cluster involved in aflatoxin biosynthesis in *A. parasiticus* was achieved by Yu and Ehrlich (2002) and Yu et al. (2004); another study conducted by O'Brian et al. (2007) demonstrated the role of microarray to explain the regulation of aflatoxin biosynthesis genes.

Aflatoxin Genes in *A. flavus* and *A. parasiticus* have highly homologous sequences and the same order within the cluster. Aflatoxin B1 (AFB1) and B2 (AFB2) are known to be produced by *A. flavus* strains, whereas *A. parasiticus* produces aflatoxins B1, B2, G, and G2 (Giorniet al., 2007). Yan et al. (2012) reported the opportunistic and pathogenic infection of *A. flavus* for humans and animals besides its pathogenicity for plants. In the 1960s, aflatoxins, the basic reason for Turkey-X disease, were reported to be mainly produced by *A. flavus* (Nesbitt et al., 1962). While aflatoxins are considered the first fungal secondary metabolites shown to have all genes organized within a DNA cluster,

there have since been significant efforts to realize regulation mechanism involved in aflatoxin biosynthesis.

Several interconnecting networks are involved in the regulation of AF biosynthesis which can be divided into three parts; the most important one comprises the regulation in the AF biosynthetic by *aflR* and *aflS*, positioned adjacent to each other in a 70 kb DNA cluster (Desjardins and Proctor, 2007). These genes are differentially transcribed with independent promoters; with short intergenic regions that share binding sites for regulatory elements or other transcription factors (Ehrlich et al., 2005). Woloshuk et al. (1994) and Yu et al. (1996) reported that a putative 47-kDa protein encoded by the gene of *aflR*, has a similar sequence to a zinc binucleate cluster DNA-binding protein, Todd and Andrianopoulos (1997) classified these proteins and renamed them as Zn (II) 2Cys6 proteins. *aflR* is a remarkable gene in AF biosynthesis for the following discoveries: Yu et al. (1996) take up *aflR* from *A. flavus* to drive ST cluster expression in an *A. nidulans* which lack *aflR* despite clear differences in AF biosynthesis pathway. Another study conducted by Lee et al. (2007) announced the presence of differences in PacC and AreA binding sites, promoter regulatory elements for *aflR* in *A. parasiticus* and *A. flavus* aflatoxin biosynthesis. Carbone et al. (2007) reported the presence of conserved domain of the *aflR* gene in both *A. nidulans* and *A. fumigatus*.

Another gene, *aflS*, has a precise role in AF biosynthesis. A study by Meyers et al. (1998) observed

* Corresponding author e-mail: nivienabdelrahman@yahoo.com.

unchanged mRNA expression levels of genes, *aflC*, *aflD*, *aflM*, and *aflP* in an *aflS* disrupted strain, with all this; AF pathway intermediates could not be converted to aflatoxin. Regarding a relationship between AFLS (a protein encoded by *aflS*) and AFLR (a protein encoded by *aflR*), Chang (2004) showed that activation of AFLR requires AFLS binding in *A. parasiticus*. However, in *A. flavus*, there was no need of AFLS to activate AFLR in AF biosynthesis (Du *et al.*, 2007), while they explained the roles of *aflR* and *aflS* as follows: transcription of early and mid-aflatoxin pathway genes require AFLR, but AFLS enhances this pathway.

Several environmental and cultural conditions such as light, temperature, pH, nitrogen, carbon source, and metals can modulate AF biosynthesis (Calvo *et al.*, 2004; Price, 2005). Over the past decade, research proved the increase in AF production by oxidative stress (Reverberi *et al.*, 2008); antioxidants, for example, Gallic and caffeic acid reduce AF production via expression reduction or inhibition of some AF pathway genes such as *aflD* (*nor-1*) (Mahoney and Molyneux, 2004). Kim *et al.* (2008) announced the down-regulation of the most genes in AF biosynthesis due to caffeic acid treatment using microarray technique. Reverberi *et al.* (2008) also used glucans from *Lentinula edodes* to induce the antioxidant enzymes which subsequently caused to delay in *aflR* transcription as well as AF cluster genes. Several studies conducted different genes assigned in aflatoxin biosynthesis, for example, The *nor-1* (*aflD*), *apa-2*, and *omt-1* (*omtA*) genes by Shapira *et al.* (1996), The *omt-1*, *nor-1*, and *ver-1* genes individually (Färber *et al.*, 1997) and *aflR*, *aflJ*, and *omtB* genes (Rahimi *et al.*, 2008).

The objective of this study was to investigate the *aflR*, *aflS*, and *aflD* genes profile in aflatoxigenic and non-aflatoxigenic isolates of the *A. flavus* using genomic DNA as a template by traditional PCR and assay the potential of gallic acid in aflatoxin suppression through down regulation of *aflR*, *aflS*, and *aflD* using Rti-PCR technique

2. Materials and Methods

2.1. Culture Conditions and Fungal Strains

Five strains of *A. flavus* isolated from contaminated food, used in this study, were friendly provided from the toxicology department, National Research Centre, Egypt. About 10^3 spores *A. flavus* were inoculated into 250 mL Erlenmeyer flasks containing 50 mL Potato dextrose broth (PDB), cultured for three days at 28°C, 200 rpm incubator (thermoscientific, UK) and Potato dextrose agar (PDA Difco) at 28°C for three for further analysis.

2.2. Aflatoxin Analysis Using High Performance Liquid Chromatography (HPLC)

A total of 10^3 *A. flavus* spores were inoculated on PDB medium and cultured at 28°C, 200 rpm incubator (thermoscientific, UK) for three days. Aflatoxin was extracted from 50 mL culture medium for each sample by high performance liquid chromatography according to (Yu *et al.*, 2004 and Salim *et al.*, 2019).

2.3. Investigation the effect of gallic acid on aflatoxin production and colony diameter

A. flavus isolate 5 (the highest aflatoxin producer) was cultured on both PDB for aflatoxin analysis, and PDA

media for measurement of colony diameter, supplemented with a concentration of 1% gallic acid (w/v), for three days at 28°C, but only, 200 rpm shaking conditions in case of PDB (treatment) in parallel with media without gallic acid (control).

2.4. Isolation, Molecular Detection and Sequencing of *aflR*, *aflS* and *aflD* Genes

2.4.1. Extraction of Genomic DNA from *Aspergillus flavus* Isolates

One strain of aflatoxigenic and another of non-aflatoxigenic *A. flavus* strains were separately grown on a 100 mL conical flask (Pyrex, USA) containing 20 mL PDB without 1% (w/v) GA, (control) and with GA (treatment). Incubation was at 28 °C for 3-7 days. About 100 mg mycelium was scraped off and used for genomic DNA extraction as follows: it was ground to a fine powder with liquid nitrogen, fine powder was subsequently put into a 1.5 mL sterile Eppendorf. Plant Genomic DNA Miniprep Kit (QIAamp DNA Mini Kit, QIAGEN, Germany) was used to extract DNA. DNA was used as a template for PCR amplification of *aflR*, *aflS*, and *aflD* for both aflatoxigenic and non-aflatoxigenic isolates.

2.4.2. Primer Design and PCR Optimization

Simultaneously, based on (<http://frodo.wi.mit.edu/primer3/>), all primers used for detection, and sequencing of aflatoxin genes were developed using NCBI reference sequences. These primers are listed in Table 1. The primers were synthesized by HVD life sciences GMBH, Germany. Genomic DNA of *A. flavus*, as a template, was conducted with GeneAmp PCR system (PerkinElmer, Norwalk, Connecticut, USA). According to the method described by Ausubel *et al.* (1990), amplification was carried out in a 50 µl reaction mixture using a PCR master mix kit (Qiagen, Germany). The following program was used: 94°C for 3 min as initial denaturation step, 35 cycles start with 94°C for 30 sec for denaturation, 55°C for 30 sec for annealing and 72°C for 30 sec for extension, finally, an extension step at 72°C for 10 min. The PCR products were separated on 1% agarose gel using TAE buffer 1X (pH = 8.3) and run at 80 V for 45 min, the bands were isolated and purified after agarose gel electrophoresis using a gel extraction kit (Qiagen, Germany). Purified gene fragments were sent to (Clinilab, colors lab, Egypt) for sequencing. The obtained sequences were compared to other known sequences found in Genbank database via the Blast program (<http://www.ncbi.nlm.nih.gov/BLAST/>).

Table 1. The primers used in PCR amplification of *aflR*, *aflS*, and *aflD*

primers	Sequence (5' → 3')	NCBI reference sequence
AFLR_F	GGATGAGGAAGACCAGCCGC	AY650938
AFLR_R	CCTGTCATCTGCTCCTGGCG	
AFLS_F	GGCCGAAGATTCCGCTTGGA	FN398168
AFLS_R	GAGCGAGGGCAACAACCAAGT	
AFLD_F	CTGACGGCGTACGGAGTGTGTC	MH280091
AFLD_R	GAGCACAGATGCCTGCCACA	

Notes: ((AFLR_F and AFLR_R, are forward and reverse primers for *aflR* PCR amplification, AFLS_F and AFLS_R, are forward and reverse primers for *aflS* PCR amplification, and

AFLD_F and AFLD_R, are forward and reverse primers for *aflD* PCR amplification).

The obtained Sequences were translated to amino acids using <https://web.expasy.org/translate/>. Deduced protein sequences of all genes were aligned using CLUSTAL multiple sequence alignment using MUSCLE 3.8 analysis according to Thompson *et al.* (1994).

2.4.3. Isolation of Total RNA

Total RNA was isolated from GA untreated aflatoxigenic *A. flavus* (control) and GA treated one (treatment) by following the manufacturer's instructions of standard TRIzol® Reagent extraction method (cat#15596-026, Invitrogen, Germany). Purity assessment of total RNA was done by the 260/280 nm ratio between 1.8 and 2.1 (<https://www.agilent.com/cs/library/applications>).

Additionally, visualization of 28S and 18S bands was used to assure RNA integrity via formaldehyde-containing agarose gel electrophoresis. For reverse transcription (RT), Aliquots of RNA were used immediately (Mahrous *et al.*, 2020).

2.4.4. Reverse Transcription (RT) Reaction and cDNA Synthesis

According to the manufacturer's instructions of RevertAid™ First Strand cDNA Synthesis Kit (MBI Fermentas, Germany), RNA isolated control and treated samples were reverse transcribed into cDNA in a total volume of 20 µl. The thermocycler (Biometra GmbH, Göttingen, Germany) was used for carrying out the RT reaction at 25°C for 10 min, followed by 1 h at 42 °C, and the reaction was stopped by heating for 5 min at 99 °C. Then, the reaction tubes were flash-cooled in an ice chamber until getting used for DNA amplification via qRT-PCR .

2.4.5. Quantitative Real Time-Polymerase Chain Reaction (qRT-PCR)

StepOne™ Real-Time PCR System from Applied Biosystems (Thermo Fisher Scientific, Waltham, MA USA) was used to determine the control and treated samples of fungal genes transcripts. Sequencing results of different genes were used to design gene specific primers, for qPCR by using the Primer3 program (http://frodo.wi.mit.edu/cgi-bin/primer3/primer3_www.cgi). PCR reactions were set up in 25µL reaction mixtures containing 12.5 µL 1× SYBR® Premix

ExTaq™ (TaKaRa, Biotech. Co. Ltd.), 0.5 µL of 0.2 µM sense primer, 0.5 µL of 0.2 µM antisense primer, 6.5 µL distilled water, and 5 µL of cDNA template.

The reaction program was allocated to 3 steps. Firstly, it started at 95.0°C for 3 min. Secondly, 40 cycles in which each cycle divided to 3 steps: (a) at 95.0°C for 15 sec; (b) at 55.0°C for 30 sec; and (c) at 72.0°C for 30 sec. thirdly, 71 cycles started at 60.0°C and every 10 sec, it increased about 0.5°C until reach to 95.0°C. Each experiment included a distilled water control. GAPDH (housekeeping gene) was used as a control gene for differences in total cDNA input between samples. To check the quality of the used primers, a melting curve analysis was performed at 95.0° at the end of each qRT-PCR. We were careful to make three replicates for each experiment. The relative amount of the genes of interest was calculated according to the method described by Ruijter *et al.* (2009).

2.5. Statistical Analysis

All the wet-lab experiments were conducted in triplicate. The data were subjected to analysis of variance and Duncan's multiple rang test was used to differentiate means at 5% (Duncan, 1955). The error bars in all figures indicate the standard error of the mean.

3. Results

3.1. Identification of Aflatoxin production Using High Performance Liquid Chromatography (HPLC) in *A. flavus*

Direct extraction of aflatoxins from *A. flavus* cultures filtrates via chloroform and subsequent analysis by (HPLC), enables us to identify of AFB1, and AFB2 from three *A. flavus* isolates. The total AF of these strains are reported in (table 2) as follows; isolate 1 (11.17 µg/ml), isolate 2 (26.65 µg/ml), and isolate5 (34.97 µg/ml). The concentrations of aflatoxin (µg/ml) were calculated in three replicates of cultures average for every isolate and expressed as mean ± SEM (Standard Error of the Mean). Simultaneously, these toxins were not detected in isolate 3 and isolate 4. In this research, Isolate 5, as aflatoxigenic and isolate 3 as non-aflatoxigenic samples were taken as examples to elucidate the molecular differences on the level of *aflR*, *aflS*, and *aflD* genes in both of them and investigate the effect of GA on aflatoxin biosynthesis in *A. flavus* strain no.5.

Table 2. Aflatoxins production from *Aspergillus flavus* isolates

Fungal isolates	sample name	Production of mycotoxins	Mycotoxins types	Mycotoxin production ug/ml	Total Mycotoxins production ug/ml
<i>A. flavus</i>	isolate 1	+	AFB1, AFB2	8.63± 2.1	11.17
		+		2.54± 0.56	
	isolate 2	+	AFB1, AFB2	18.22±3.2	26.65
		+		8.43±1.7	
	isolate 3	-	--	ND	ND
	isolate 4	-	--	ND	ND
isolate 5	+	AFB1, AFB2	23.30±3.12	34.97	
	+		11.67± 2.54		

ND: Not Detectable, +: present, -: not present

3.2. Molecular Identification and Sequencing of *aflR*, *aflS* and *aflD* in Aflatoxigenic and non-Aflatoxigenic *A. flavus* isolates

Interestingly, unexpected results were observed, whereas AFLR_F and AFLR_R specific primers succeeded in *aflR* amplification at ~320 bp in both aflatoxigenic and non-aflatoxigenic *A. flavus* isolates figure (1a), the same situation occurred in *aflS*, ~550 bp using AFLS_F and AFLS_R specific primers figure (1b),

and *aflD*, ~420 bp using AFLD_F and AFLD_R specific primers figure (1c) using genomic DNA as a template.

These amplified bands were isolated, purified from agarose gel, and subjected to nucleotide sequencing. The amplified regions of the isolated genes using the previously mentioned primers showed no differences in nucleotides sequences in the case of aflatoxigenic and non-aflatoxigenic isolates. Nucleotide sequences of genes were submitted to (<https://www.ncbi.nlm.nih.gov/>) and took accession numbers LC537158, MW055253, and LC537157 for *aflR*, *aflS* and *aflD*, respectively.

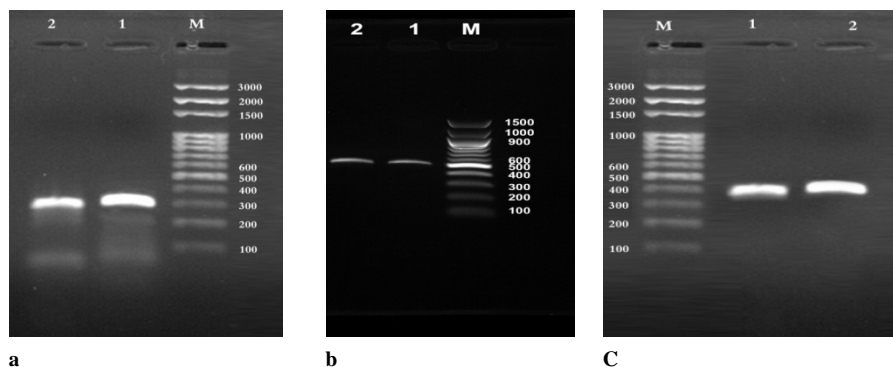


Figure 1. Agarose gel electrophoresis of PCR amplification (a): *aflR*, ~320 bp in aflatoxigenic isolate 5 (lane1) and non-aflatoxigenic isolate 3 (lane 2). (b): *aflS*, ~550 bp in aflatoxigenic isolate 5 (lane 1) and non-aflatoxigenic isolate 3 (lane 2). (c): *aflD*, 420 bp in non-aflatoxigenic isolate 3 (lane 1) and aflatoxigenic isolate 5 (lane 2)

CLUSTAL multiple sequence alignment (<https://www.ebi.ac.uk/Tools/msa/>) was used to align the deduced protein sequences of the isolated genes. Figure (2) showed that deduced protein sequence of *aflR* (our isolated gene) that consists of 86 amino acids, had 98.8%, and 100.0% identity in 86 residues overlap With AFLR deduced amino acids sequence accession numbers, AAM02997 and AAM02991, respectively, while figure (3)

illustrated 94.7% and 96.5% identity between *aflS* (our isolated gene) and that of AFLS accession numbers FN398166 and AF077975, respectively. Identity of 100.0% and 90.6% were detected in 138 residues overlap between *aflD* (in this study) and that of AFLD accession numbers AXG50934 and CAZ61375 as shown in Figure (4)

AAM02997.1	MVVLIVLKVLAWYAAAAGTQCTSTAAGGETNSGSCSNPATVSSGCLTEERVLHLPMMG	360
AFLR	-----MG	2
AAM02991.1	MVVLIVLKVLAWYAAAAGTQCTSTAAGGETNSGSCSNPATVSSGCLTEERVLHLPMMG	360
	*****	**
AAM02997.1	EDCVDEEDQPRVAAQLVLSSELHRVQSLVNLLAKRLQEGGDDAAGIPAHHPASPFSLLGFS	420
AFLR	EDCVDEEDQPRVAAQLVLSSELHRVQSLVNLLAKRLQEGGDDAAGIPAHHPASPFSLLGFS	62
AAM02991.1	EDCVDEEDQPRVAAQLVLSSELHRVQSLVNLLAKRLQEGGDDAAGIPAHHPASPFSLLGFS	420

AAM02997.1	GLEANLRQLRAVSSDIIDYLHRE	444
AFLR	GLEANLRHRLRAVSSDIIDYLHRE	86
AAM02991.1	GLEANLRHRLRAVSSDIIDYLHRE	444

Figure2. Alignment of deduced amino acid sequences of the AFLR accession no. BCD52745, AFLR, Accession no. AAM02991 and AFLR, Accession no. AAM02997

AFLS	-----MSETLAPSASAMGTQTRRFGASEQAEDSA	29
FN398166.1	FLCEPSPGHVAHSVLSKQFVTQPALLDAILFMSETLAPSASAMGTQTRRFGASEQAEDSA	78
AF077975.1	FLCEPSPGHVAHSVLSKQFVTQPALLDAILFMSETLAPSASAMGTQTRRFGASEQAEDSA	180

AFLS	WNMAVGSDSPFAACLQQRKLVKVRQLGDYLSYVSSSIDAGVEDTLTRMNWQNLGMATVVHV	89
FN398166.1	WNMAVGSDSPFAACLQQRKLVKVRQLGAYLSYVSSSIDAGVEDTLTRMNWQNLGMATVVHV	138
AF077975.1	WNMAVGSDSPFAACLQQRKLVKVRQLGAYLSYVSSSIDAGVEDTLTRMNWQNLGMAT---V	237
	*****	*
AFLS	RILSPDRGIQPMT---NLIFM-----	107
FN398166.1	GAQSPSLVVALAPQFSLRFLVQTEAKAESGGHQPCLDNHGISALKLASIPLHLRARITW	198
AF077975.1	GAQSPSLVVALAPQFSLRFLVQTEAKAESGGHQPCLDNHGISALKLASIPLHLRARITW	297
	** . : . * * :	

Figure 3.Alignment of deduced amino acid sequences of the AFLS (under submission), AFLS, Accession no. FN398166 and AFLS, Accession no. AF077975

CAZ61375.1	TVYLVGTGASRGIGRGLIEAFLQRPKSTVVACVRNVATATPALSALTVAEGSRMIIIVQLNC	60
AFLD	-----MIIWHLNC	8
AXG50934.1	-VYLVGTGASRGIGRGLIEAFLQHPKSTAVPCVPNVATATPALSALTYAEGSQMIIWHLNC	59
	*** :***	
CAZ61375.1	DSETDAQAAVQTLREEHGVTHLDVVVANAAMATNFGPASTMPLQHLQAHMMVNMYPVLL	120
AFLD	YSKTDAQASVQTLREEHGVTHLDLEVANAAMATNFGPASTMPLQHLQAHMMVNMHAPVLL	68
AXG50934.1	YSKTDAQASVQTLREEHGVTHLDLEVANAAMATNFGPASTMPLQHLQAHMMVNMHAPVLL	119
	* :***** :***** :***** :***** :***** :***** :***** :***** :*****	
CAZ61375.1	FQATRLMLQQSKQAKFVLI GAPISTITNMHDYARAPLTAYGVSKLAANYMVRKFHFENK	180
AFLD	FHATRLMLQQAKKQAKFVLI GAPIITITNMHDYARAPLTAYGVSKLAANYMVRKFHFENK	128
AXG50934.1	FHATRLMLQQAKKQAKFVLI GAPIITITNMHDYARAPLTAYGVSKLAANYMVRKFHFENK	179
	* :***** :* :***** :***** :***** :***** :***** :***** :*****	
CAZ61375.1	WLTAFIIDP GHVQ TDMGDQ GARLMGRPQAP TTVADSVAGI CARIDE	226
AFLD	WLTAFIIDP G-----	138
AXG50934.1	WLTAFIIDP GHVQ TDMGDQ GARLMGRPQAP TTVADSVAGI CARIDE	225

Figure 4. Alignment of deduced amino acid sequences of the *aflD* gene accession no. BCD52744, AFLD, Accession no. AXG50934 and AFLD, Accession no. CAZ61375.

3.2.1. Effect of GA on Growth of Aflatoxigenic *A. flavus* and Aflatoxin Production

Treatment of *A. flavus* strain no. 5, as the highest aflatoxin producer, with 1% (w/v) GA caused colony diameter reduction, besides the decrease in the formation of spores after three days of cultivation figure (5A) as compared with its growth on PDA medium not containing GA figure (5B). Simultaneously, production of aflatoxin in PDB Medium containing GA with 1% concentration (w/v) was significantly reduced from 34.97 ug/ml to 8.12 ug/ml as follow; AFB1 yield decreased from 23.30 to 6.09 and that of AFB2 reduced from 11.67 to 2.03 (figure 6). We concluded that AF production was directly proportional to colony diameter in *A. flavus*, i.e. GA affected the growth and AF production negatively.

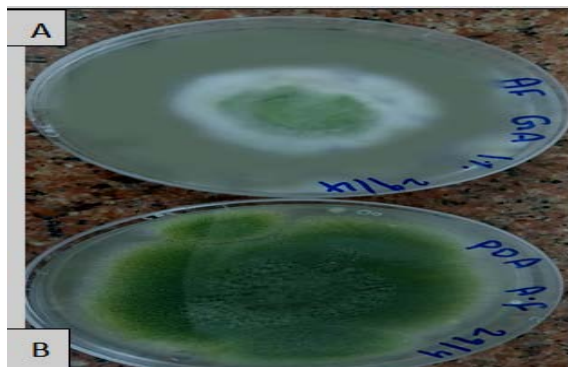


Figure 5. The effect of gallic acid on *A. flavus* growth, A: Growth of *A. flavus* on PDA containing 1% gallic acid (treatment). B: Growth of *A. flavus* on PDA (control) at 28 °C after three days.

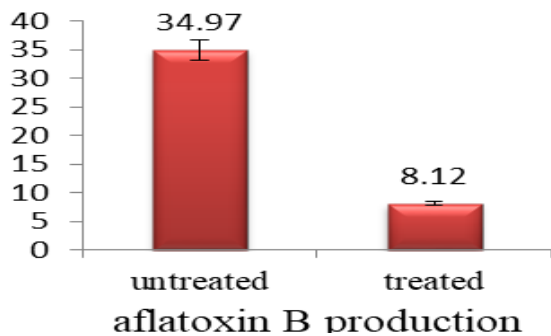
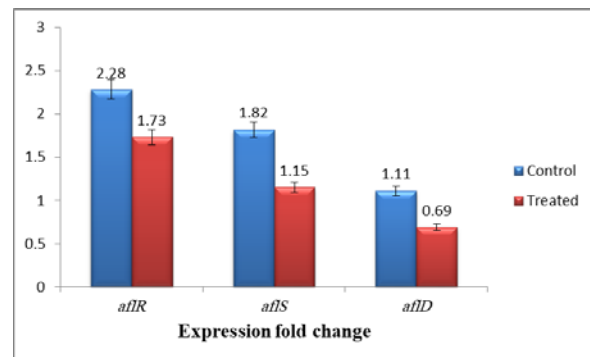


Figure 6. The effect of gallic acid on aflatoxin production from *A. flavus* isolates 5 in PDB containing 1% gallic acid (treated) compared with control at 28 °C after three days .

3.2.2. Analysis the Effect of GA on *aflR*, *aflS* and *aflD* Expression in Aflatoxigenic *A. flavus* using qRT-PCR

The increase in genes expression required for AF biosynthesis mainly depending on *aflR* transcription, supports the hypothesis that for AF-pathway induction, AFLR as transcription regulator is important, therefore, the blocking of undesirable AF production through designing approaches such as utilization of antioxidant substances requires understanding the mechanisms that are being followed by environmental and physiological factors and its effect on *aflR* transcription. From figure (7), expression analysis for transcripts of genes (*aflR*, *aflS* and *aflD*) in 1% gallic acid-treated aflatoxigenic *A. flavus* strain no. 5 indicated that these transcripts expression have to correlate GA treatment. Interestingly, all three assigned genes expressions significantly down regulated due to GA



treatment of concentration of 1% (w/v).

Figure 7. The effect of gallic acid on *aflR*, *aflS* and *aflD* expression in aflatoxigenic *A. flavus* using qRT-PCR

4. Discussion

Many Egyptian researchers directed their efforts for exploring the fungal contamination and their role in aflatoxin production in Egyptian crops. El-Shanshoury *et al*, (2014) investigated *A. flavus* in soybean, peanut seeds, wheat maize, and rice. As mentioned in the result section, the metabolic profile of mycotoxins in the aflatoxigenic *A. flavus* strains was similar to that reported in the study conducted by Rank *et al*, (2012), they announced the production of only B-types in *A. flavus*. Interestingly, the metabolism of mycotoxigenic fungi and its molecular genetics study is a good strategy to deal with mycotoxin contamination in crops (El-Kad and Youssef, 1993). It is

of interest to discover and understand the genetic differences between aflatoxigenic and non-aflatoxigenic strains. This conclusion has been employed to direct these differences to control aflatoxin biosynthesis. In this study, traditional PCR technique was used to investigate the presence of three genes; the first is *aflR*, which is considered as an indicator for aflatoxin production in *A. flavus* and its homolog in *A. parasiticus* (*apaR*) that regulate aflatoxin biosynthesis (Woloshuk *et al.*, 1994). Its role is to control *nor-1* and *ver-1* genes expression (Yu *et al.*, 2004). These genes are sufficient to stimulate transcription of early, mid, and late AF pathway biosynthesis genes. The second is *aflS* that positively regulates biosynthesis of AFB₂ and the third gene is *aflD*, (formally, *nor-1*) as an important structure gene in aflatoxin cluster genes encodes norsolorinic acid reductase to convert norsolorinic acid to averantin (Payne *et al.*, 1993). To connect the presence of *aflR*, *aflS*, and *aflD* genes profiles in aflatoxigenic and non-aflatoxigenic, a single set of PCR primers was used to detect these genes and reliably succeed in amplification of these genes in aflatoxigenic and non-aflatoxigenic *A. flavus* strains. These conflicting results can be explained as follows: specific mutation may occur in *aflR*, and resulted in malfunction gene and subsequently failure in aflatoxin production in non-aflatoxigenic isolates even though in the presence of functional copies of *aflD* and *aflS*. In a similar study conducted by Bok and Keller, (2004), they investigated and explained the block in *omtA* (a structural gene in AF biosynthesis expression in *A. flavus* although presence of AFLR, a protein encoded by *aflR* as follows: the presence of specific mutation in *aflR* resulted in nonfunctional AFLR, therefore, *omtA* expression did not take place. However, Liu and Chu, (1998) explained this phenomenon by the presence of a mutation in DNA binding site in *omtA* gene caused to not producing *omtA* mRNA. Similar nucleotide sequences of detected genes between aflatoxin producing and nonproducing strains told no information about the characterization of these genes. Consequently, this research concluded that successful PCR amplification of aflatoxin genes should not be considered as a proof of aflatoxin synthesis due to undetected mutation external to the amplicon sequence that subsequently caused cryptic and not expressed genes. The study conducted by Patterson (2006), demonstrated that the *aflR* gene may be present in a number of non-aflatoxigenic and functions for conserved regulation of aflatoxin precursors. Twelve strains of *A. flavus* were investigated by Shapira *et al.* (1996), nine of them were non-aflatoxin producers in which some genes involved AF biosynthesis were successfully PCR amplified in varying band patterns; however, only three strains were aflatoxin producers in which the expected amplicon bands were produced. From the previous notifications, the presence of un-expressed genes in non-aflatoxigenic strains may be explained by the occurrence of non-functional gene products due to base-pair substitution mutations.

Our attempts were directed to inhibit the AF production by reducing the oxidative stress using antioxidant such as Gallic acid which proved its efficiency in diminishing of AF production in GA treated *A. flavus* isolate. In order to gain insight into the mechanism by which GA inhibits aflatoxin synthesis, we employed qRT-PCR to assess the expression of *aflS*, *aflR*, and *aflD*. Down regulation of

these genes in GA treated sample as compared with untreated one explain the reason of diminishing of aflatoxin production. Mahoney and Molyneux, (2004) illustrated the role of GA in the inhibition of expression of several genes in AF pathway such as *aflM* (*ver-1*). Another study was conducted by Zhao *et al.*, (2018), they used gallic acid as an antioxidant agent to reduce aflatoxin production. Addition of gallic acid in different doses (0.5%, 0.8%, and 1%) slightly inhibited aflatoxin and growth of *A. flavus*; they showed the inhibition of AF by 0.8% of GA on *farB* gene encodes a factor for transcription of β -oxidation of peroxisomal fatty acid which contributes in AF biosynthesis. Another gene, *creA*, the carbon repression regulator encoding gene and necessary for aflatoxin biosynthesis, was also inhibited by GA treatment. Total inhibition for AF by gallic acid treatment was through the control of polyketide synthase (fatty acid synthase) required for the formation of norsolorinic acid, the first intermediate in the biosynthesis pathway of aflatoxin. It is striking that we noticed incompatibility between our results and the results of Zhao *et al.*, (2018) in terms of the effect of GA on the expression of *aflR* and *aflS*, gallic acid concentration of 0.8% (w/v) inhibited nearly all the genes of aflatoxin except *aflR* and *aflS*.

In our research, taking these results together, we proposed that the down regulation of *aflR* as a master gene in AF regulation may result in down regulation of other genes such as *aflS* and *aflD*; this explanation is agreed with Cotty (2006) who acknowledged that introduction of an additional correct copy of the *aflR* compensates for the disrupted one in *A. flavus* and caused the transcription of AF biosynthesis structural genes and aflatoxin intermediates production. Clevstrom *et al.* (1983) also studied the inhibition of the biosynthesis of AF caused by *aflR* transcription delay as well as other cluster genes of AF by induction anti-oxidant enzymes via β -glucans from *Lentinula edodes*. The previously reported studies, besides our research, proved the potential of gallic acid in biosynthesis inhibition of aflatoxin in *A. flavus* through the expression modulating of *aflR*, *aflS* and *aflD*.

5. Conclusion

Successful PCR amplification of specific genes such as *aflR*, *aflS*, and *aflD* should not be considered evidence of biosynthesis of aflatoxin due to the lack of gene expression as a result of cryptic form and undetected mutation outside to the amplicon sequence and this conclusion explained presence of *aflR*, *aflS*, and *aflD* genes in aflatoxigenic and non-aflatoxigenic *A. flavus* isolates by traditional PCR using genomic DNA as a template. In addition, upon finding that GA as antioxidant, it was used to effectively suppress aflatoxin synthesis. Interestingly, qRT-PCR, a potential tool was employed to investigate the effects of GA on the transcription of aflatoxin genes, *aflR*, *aflS*, and *aflD*, as these genes were down-regulated.

Acknowledgment

The authors thank the National Research Centre at Dokki, Cairo, Egypt for laboratory assistance.

References

- Ausubel FM, Brent R, Kingston RE, Moore DD, Seidman JG, Smith JA and Kevin S. 1990. Current Protocols in Molecular Biology. In: the polymerase chain reaction Mullis KB, Ferre F, Gibbseditors RA (eds.)
- Bhatnagar D, McCormick SP, Lee LS and Hill RA. 1987. Identification of O- methylsterigmatocystin as aflatoxin Bi and Gl precursor in *Aspergillus parasiticus*. *Appl Environ Microbiol.*, **53**:1028-1033.
- Bok JW and Keller NP. 2004. LaeA, a Regulator of Secondary Metabolism in *Aspergillus* spp. *Eukaryot Cell*, **3**: 527-535
- CalvoAM, Bok J, Brooks W and Keller NP. 2004. VeA is required for toxin and sclerotial production in *Aspergillus parasiticus*. *Appl Environ Microbiol.*, **70**: 4733–4739.
- Carbone I, Ramirez-Prado JH, Jakobek JL and Horn BW. 2007. Gene duplication, modularity and adaptation in the evolution of the aflatoxin gene cluster. *BMC EvolBiol*, **7**: 111.
- Chang PK. 2004. Lack of interaction between AfIR and AfII contributes to non-aflatoxicity of *Aspergillus sojae*. *J Biotechnol.*, **107**: 245–253.
- Clevstrom G, Ljunggren H, Tegelstrom S and Tideman K. 1983. Production of aflatoxin by an *Aspergillus flavus* isolate cultured under a limited oxygen supply. *Appl Environ Microbiol.*, **46**: 400–405.
- Cotty PJ, Barug D, Bhatnagar D, van-Egmond HP, van der Kamp JW, van Osenbruggen WA and Visconti A. 2006. Bio competitive exclusion of toxigenic fungi. In the Mycotoxin Factbook, Eds, Wageningen Academic Publishers: Wageningen, The Netherlands: 400p.
- Desjardins AE and Proctor RH. 2007. Molecular biology of *Fusarium* mycotoxins. *Int J Food Microbiol.*, **119**: 47–50.
- Du W, O'brian GR and Payne GA. 2007. Function and regulation of *aflJ* in the accumulation of aflatoxin early pathway intermediate in *Aspergillus flavus*. *Food Addit Contam.*, **24**: 1043–1050.
- Duncan DB. 1955. Multiple ranges and multiple F test. *Biometrics.*, **11**:11–24
- Ehrlich KC, Yu J and Cotty PJ. 2005. Aflatoxin biosynthesis gene clusters and flanking regions. *J Appl Microbiol.*, **99**: 518–527.
- El-Kady IA and Youssef MS. 1993. Survey of mycoflora and mycotoxins in Egyptian soybean seeds. *J Basic Microbiol.*, **33**: 371–378.
- El-Shanshoury AR, El-Sabbagh SM, Emara HA and Saba HE. 2014. Occurrence of moulds, toxicogenic capability of *Aspergillus flavus* and levels of aflatoxins in maize, wheat, rice and peanut from markets in central delta provinces, Egypt. *Int J Curr Microbiol App Sci.*, **3**: 852–865.
- Färber P, Geisen R and Holzapfel W. 1997. Detection of aflatoxigenic fungi in figs by a PCR reaction. *Int J Food Microbiol.*, **36**: 215–220.
- Giorni P, Magan N., Pietri A, Bertuzzi T and Battilani P. 2007. Studies on *Aspergillus* section Flavi isolated from maize in northern Italy. *Int J Food Microbiol.*, **113**: 330–338.
- Jelinek CF, Pohland AE and Wood GE. 1989. Review of mycotoxin in food and feeds-an update. *J Assoc Anal Chem.*, **72**: 223-230.
- Kim JH, Yu J, Mahoney N, Chan KL and Molyneux RJ. 2008. Elucidation of the functional genomics of antioxidant-based inhibition of aflatoxin biosynthesis. *Int J Food Microbiol.*, **122**: 49–60.
- Lee JW, Roze LV and Linz JE. 2007. Evidence that a wortmannin-sensitive signal transduction pathway regulates aflatoxin biosynthesis. *Mycologia.*, **99**: 562–568.
- Liu B and Chu F. 1998. Regulation of *aflR* and its product, AfIRS, associated with aflatoxin biosynthesis. *Appl Environ Microbiol.*, **64**: 3718–3723.
- Mahoney N and Molyneux RJ. 2004. Phytochemical inhibition of aflatoxigenicity in *Aspergillus flavus* by constituents of walnut (*Juglansregia*). *J Agric Food Chem.*, **52**: 1882–1889.
- Mahrous KF, Abd El – Kader HA, Mabrouk DM, Aboelenin MM, Osman NM, Khalil WK and Hassanane MS. 2020. Molecular characterization and expression analysis of hepc1 and hepc2 in three tilapia species collected from Lake Manzala. *Bulletin of the National Research Centre.*, **44**: 1-13.
- Meyers DM, O'brian G, Du WL, Bhatnagar D and Payne GA. 1998. Characterization of *aflJ*, a gene required for conversion of pathway intermediates to aflatoxin. *Appl Environ Microbiol.*, **64**: 3713–3717.
- Nesbitt BF, O'Kelly J, Sargeant K and Sheridan A. 1962. *Aspergillus flavus* and turkey X disease, toxic metabolites of *Aspergillus flavus*. *Nature.*, **195**: 1062–1063.
- O'Brian GR, Georgianna DR, Wilkinson JR, Yu J, Abbas HK, Cleveland D, Bhatnagar TE, Nierman W and Payne GA. 2007. The effect of elevated temperature on gene transcription and aflatoxin biosynthesis. *Mycologia.*, **99**: 232–239.
- Patterson R. 2006. Identification and quantification of mycotoxigenic fungi by PCR. *Process Biochemistry.*, **41**: 1467–1474.
- Payne G, Nystorm G, Bhatnagar D, Cleveland T and Woloshuk C. 1993. Cloning of the *afl-2* gene involved in aflatoxin biosynthesis from *Aspergillus flavus*. *Appl Environ Microbiol.*, **59**: 156–162.
- Price MS. 2005. Classical and modern genetic approaches reveal new gene associations with aflatoxin biosynthesis in *Aspergillus parasiticus* and *A. flavus*. Ph.D. Thesis.
- Rahimi KP, Sharifnabi B and Bahar M. 2008. Detection of aflatoxin in *Aspergillus* species isolated from pistachio in Iran. *J Pathol.*, **156**: 15–20.
- Rank C, Klejnstrup ML, Petersen LM, Kildgaard S, Frisvad JC, Gotfredsen HC and Ostenfeld LT. 2012. Comparative Chemistry of *Aspergillus oryzae* (RIB40) and *A. flavus* (NRRL 3357). *Metabolites.*, **2**: 39–56.
- Reverberi M, Zjalic S, Ricelli A, Punelli F and Camera E. 2008. Modulation of antioxidant defence in *Aspergillus parasiticus* is involved in aflatoxin biosynthesis: a role for ApyapA gene. *Eukaryot Cel.*, **1** **25**: 25.
- Ruijter JM, Ramakers C, Hoogaars WM, Karlen Y, Bakker O, Hoff MJ and Moorman AF. 2009. Amplification efficiency: linking baseline and bias in the analysis of quantitative PCR data. *Nucleic Acids Res.*, **37**:45.
- Salim RG , Aly SE , Abo-Sereh NA , Hathout AS and Sabry BA. 2019. Molecular identification and Inter-Simple Sequence Repeat (ISSR) differentiation of toxigenic *Aspergillus* Strains. *Jordan J Biol Sci.*, **12**:609-616
- Shapira R, Paster N, Eyal O, Menasherov M, Mett A and Salamon R. 1996. Detection of aflatoxigenic molds in grains by PCR. *Appl and Environmen Microbiol.*, **62**: 3270–3273.
- Thompson JD, Higgins DG and Gibson TJ. 1994. CLUSTAL W: improving the sensitivity of progressive multiple sequence alignment through sequence weighting, position-specific gap penalties and weight matrix choice. *Nucleic acids res.*, **22**: 4673–4680.

Todd RB and Andrianopoulos A. 1997. Evolution of a fungal regulatory gene family: the Zn (II)₂Cys₆ binuclear cluster DNA binding motif. *Fungal Genet Biol.*, **21**: 388–405.

Woloshuk CP, Foutz KR, Brewer JF, Bhatnagar D, Cleveland TE and Payne GA. 1994. Molecular characterization of *aflR*, a regulatory locus for aflatoxin biosynthesis. *Appl Environ Microbiol.*, **60**: 2408–24014.

Yan S, Liang Y, Zhang J and Liu CM. 2012. *Aspergillus flavus* grown in peptone as the carbon source exhibits spore density- and peptone concentration-dependent aflatoxin biosynthesis. *BMC Microbiol.*, **12**: 106-112.

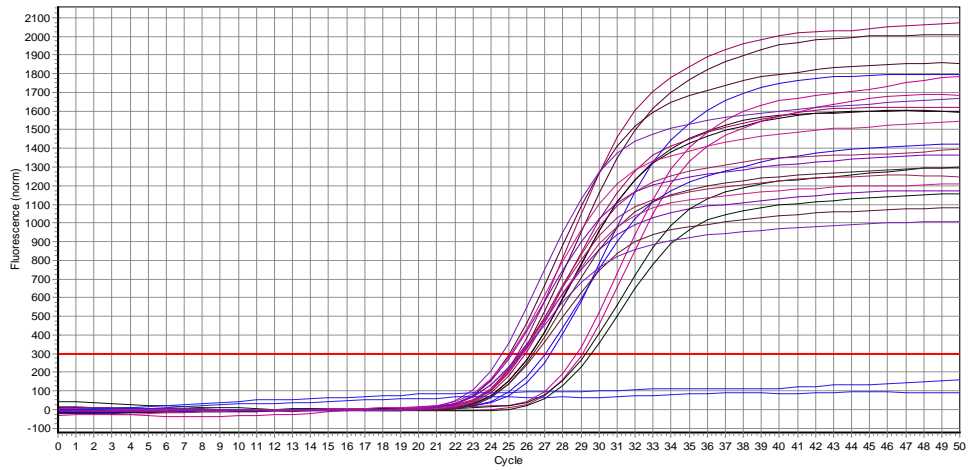
Yu JH, Bhatnagar D and Cleveland TE. 2004. Completed sequence of aflatoxin pathway gene cluster in *Aspergillus parasiticus*. *FEBS Lett.*, **564**: 126–130.

Yu JH and Ehrlich KC. 2002. Aflatoxin biosynthesis. *Rev Iberoam Micol.*, **19**: 191–200.

Yu JH, Butchko RA, Fernandes M, Keller NP, Leonard TJ and Adams TH. 1996. Conservation of structure and function of the aflatoxin regulatory gene *aflR* from *Aspergillus nidulans* and *A. flavus*. *Curr Genet.*, **29**: 549–555.

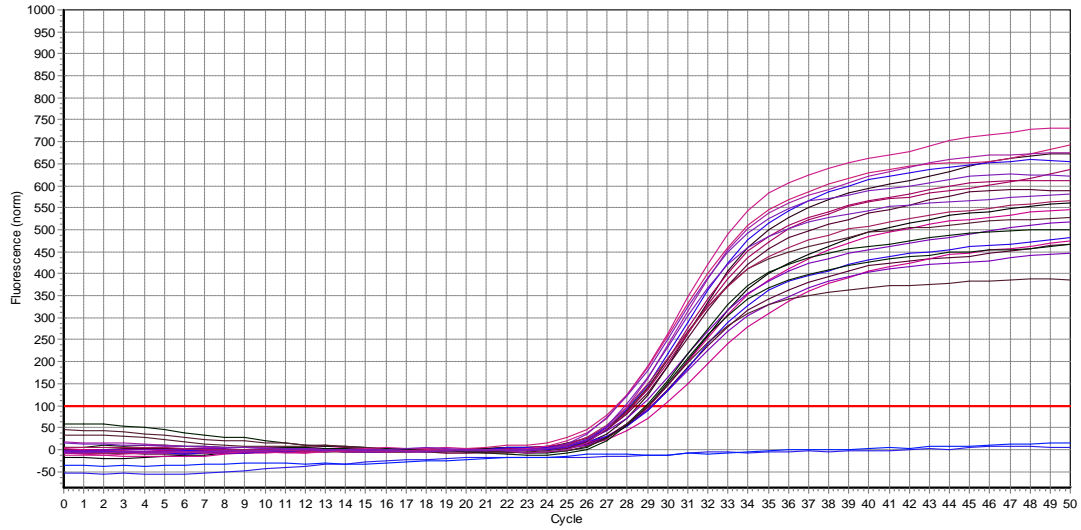
Zhao X, Qing-Qing Z, Jie-Ying L, Nancy P, Keller ID and Zhu MH. 2018. The Antioxidant Gallic Acid Inhibits Aflatoxin Formation in *Aspergillus flavus* by Modulating Transcription Factors FarB and CreA. *Toxin.*, **10**: 2-17.

Appendix

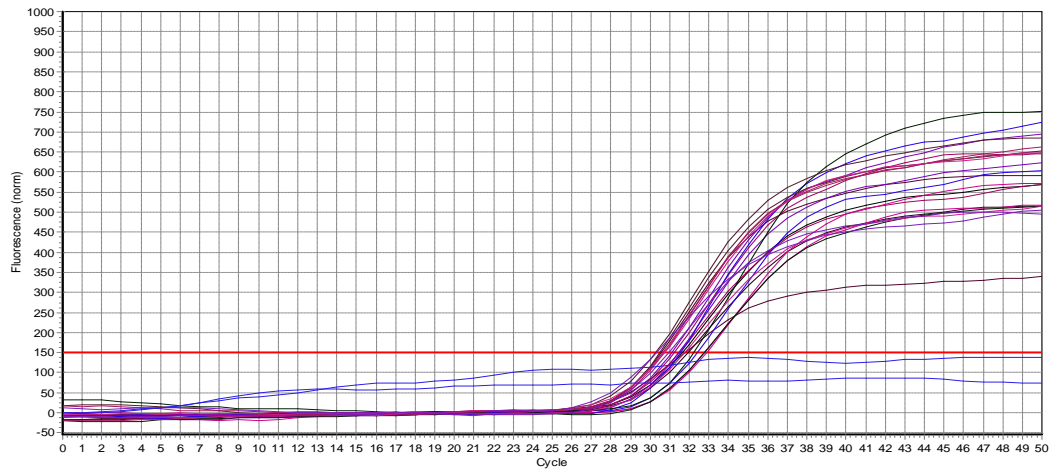


Threshold: 300 (Adjusted manually)
Baseline settings: automatic, Drift correction OFF

The linear and log amplification curves representing the Ct values of *aflR* gene.



Threshold: 100 (Adjusted manually)
Baseline settings: automatic, Drift correction OFF



Threshold: 150 (Adjusted manually)
Baseline settings: automatic, Drift correction OFF

Mycobiota and Fungal Metabolites in Improved Groundnut Varieties in Nigeria

Toba S. Anjorin^{1,*}, Alhassan Usman², Stephen O. Fapohunda³, Adobe Kwanashie⁴, Michael Sulyok⁵ and Rudolf Krska⁵

¹Department of Crop Protection, Faculty of Agriculture, University of Abuja, PMB 117, Abuja, Nigeria; ²Department of Plant Science, Institute of Agriculture Research, Faculty of Agriculture, Ahmadu Bello University, Zaria, Nigeria; ³Department of Microbiology, Babcock University, Ilishan Remo, Ogun State, Nigeria; ⁴Department of Crop Protection, Ahmadu Bello University, Zaria, Nigeria; ⁵Center for Analytical Chemistry, Department of Agrobiotechnology (IFA-Tulln), University of Natural Resources and Life Sciences Vienna (BOKU), Konrad Lorenzstr, 20, A-3430 Tulln, Austria

Received: April 4, 2020; Revised: Sept 18, 2020; Accepted: Nov 10, 2020

Abstract

The study investigated the incidence of mycobiota, *Aspergillus* spp metabolites and aflatoxin biosynthesis precursors in 60 samples of seeds and haulms of improved groundnut genotypes in Nigeria. Culturing of the infected seeds was done using the agar plate method and mycobiota identification was done using conventional cultural and microscopy method. The occurrence of *Aspergillus* toxins, and aflatoxin biosynthesis precursors were evaluated using liquid chromatography-mass spectrometry (LC-MS/MS). Three identified species and four unidentified species of fungi were isolated from the seeds with *Aspergillus niger* (47.19%) and *A. flavus* (17.82%) having higher incidence more than others. The seed samples from ICGX 86024 and ICGX 01276 had the highest and lowest fungal incidence respectively. No aflatoxin B₁, ochratoxin A or fumonisins were detected in the seeds and haulms samples of the improved groundnut despite the incidence of *A. flavus*. Fifteen fungal metabolites were found including eight *Aspergillus* metabolites and seven aflatoxin biosynthesis precursors. From our result, STC which is involved in aflatoxin biosynthesis pathway was below limit of detection and thus aflatoxin formation in the groundnuts might be interrupted. This report is foremost in elucidating the aflatoxins biosynthesis precursors in seeds and haulms of improved groundnut varieties in Northern Nigeria.

Keywords: Aflatoxin precursors, *Aspergillus* metabolites, groundnut, haulm, seeds, incidence, mycobiota.

1. Introduction

Groundnut (*Arachis hypogaea* L.) is a valuable oilseed and food legume crop in the savannah and semi-arid regions of the world. It is a commercial crop for local markets as well as for export in many developed and developing countries (Guchi, 2015a). Major groundnut producing areas in Nigeria are in the Central, Eastern and Western Northern zones (Ntare, 2007; Ifeji *et al.*, 2014; Vabi *et al.*, 2018). The production of quality marketable seeds especially from local varieties and some improved ones are constrained by *Aspergillus* species (Guchi, 2015b). The fungus often causes quantitative losses and produces highly poisonous chemical substances called aflatoxins. Aflatoxins are produced by *Aspergillus* species which are soil-borne fungi that occur Worldwide (Granados-Chinchilla, 2017; Gruber-Dorninger *et al.*, 2017).

In an attempt to improve groundnut v

arieties for resistance against fungal foliar diseases and aflatoxins, breeding techniques and recombinant DNA technology are now employed (Dwivedi 2003; Bhatnagar-Mathur, 2015). The International Crops Research Institute

for the Semi-Arid Tropics (ICRISAT) in West Africa has bred and released groundnut varieties that are high yielding in terms of the pods and fodders and also free of aflatoxins.

Though some improved groundnut cultivars were bred to resist aflatoxigenic fungi and aflatoxins formation by the crop breeders, there are several other minor mycotoxins or metabolites that could be produced in their seeds or in the haulms. There is however paucity of multi-mycotoxin research-based on such roughages within animal feed chain in developing countries like Nigeria. This investigation was therefore carried out to determine the incidence of mycobiota, the profile of *Aspergillus* metabolites and aflatoxin biosynthesis precursors in the seeds and haulms of improved groundnut varieties in Nigeria using multi-mycotoxins LC-MS/MS. The study has risk assessment significance and also gives plausible explanation to how improved groundnut varieties with the presence of *Aspergillus flavus* resist aflatoxin biosynthesis.

2. Materials and Methods

2.1. Experimental field

The experimental groundnut varieties were grown on farmers' participatory lines trial at location T19, Institute of Agricultural Research (IAR) Experimental Field,

* Corresponding author e-mail: toba.anjorin@uniabuja.edu.ng.

Ahmadu Bello University, Samaru Zaria, Kaduna State, Nigeria (Long. 7° 38' and 7° 50'E and Lat. 11° 01' and 11 10'N) with altitude of 686m above sea level under rain-fed conditions in the Northern Guinea Savannah of Nigeria. The mean daily air temperature of the area during the planting season was 24.3°C, while the mean annual rainfall was 1201 mm. The soil texture of the field was sandy loam and with a mean soil pH of 5.5. The unit plot size was 5m x 3m, and they were laid out in a randomized complete block design (RCBD) with each treatment replicated thrice. The plant spacing was 30 cm and 15 cm while plot to plot and replication to replication distance was 0.5 and 1.0 m, respectively. Total area of the farm was 17m x 37m i.e. 629m². The seeds of eight groundnut genotype (Short duration - ICGV-IS 07999, ICGV 94379 and ICGV 86024; Medium duration - ICGV 01276, ICGV-IS-09992, ICGX 24, ICGV-1S-09926 and ICGV 08540) were collected from International Crops Research Institute for the Semi-Arid Tropics (ICRISAT). Also seeds of two local checks – medium-maturing SAMNUT 22 and early-maturing SAMNUT 24 collected from IAR&T were all sown on the flat at the mean depth of 3.5 cm on the 3rd week of July, 2018. Each of the plots was applied with basal dose of 20:40:20 NPK fertilizer at 400 kg ha⁻¹.

2.2. Sample collection

The haulms of each groundnut variety from each plot were separately collected and properly packed in polystyrene bags and then labelled accordingly. Harvested dried unshelled samples were collected in brown envelopes from the farm store in IAR, Samaru, before being transferred to and kept in the Mycotoxin and Pesticidal Residue laboratory of Department of Crop Protection, ABU, Zaria. Prior to commencing laboratory analysis procedures on the samples which was within a month of harvest, they were stored at 4° C to prevent further fungal growth and metabolite production within the samples (Garcia-Cela *et al.*, 2020). Each sample was divided into two portions. The samples from one portion were used for mycological analysis. The second portion was separately packed in zip lock and transported in to University of Natural Resources and Life Sciences Vienna (BOKU), Tulln, Austria for multi-mycotoxins analysis.

Identification of fungal species using Agar plate method. The Potato Dextrose Agar (PDA) was prepared following the method of Giorni *et al.*, 2019. It was then autoclaved, allowed to cool and poured aseptically in the Petri dishes. When the PDA was about to gel, four seeds from each groundnut genotypes were aseptically plated in the Petri dishes. The experimental design was complete randomized design and replicated 4 times. The individual colony of fungi species growing on the agar was examined after seven days of plating. The identification of fungi was carried out based on the colony characters and morphology of the fungus under stereoscopic microscope and by referring to the production of food-borne fungi manual (Joanne *et al.*, 2008).

2.3. Analysis of mycotoxin

2.3.1. Reagents

Liquid chromatographic grade of methanol (CH₃COOH) and acetonitrile were purchased from Merck (Germany) and VWR (Belgium) respectively. The Mass Spectrometry grade ammonium acetate and standards for

fungi metabolite were brought from Sigma-Aldrich (Austria). Decontamination of water was carried out consecutively through reverse osmotic pressure and ultra analytic system was purchased from Veolia water (UK). A total of 34 working solutions were made and kept at -20 °C in the refrigerator (Labcold®, FKvsl 4113, Fishers Scientific, UK) but were brought to 25 °C before use. Fresh final working solution was mixed accordingly for the spiking experiment.

2.4. Groundnut Extraction

Each grain and haulm samples were milled using a cyclone pulverizer which has one millimetre square sieve (Cyclotech, Sweden) before being homogenized. Five grams each were measured into the centrifuge tube (0.05 L polypropylene). Twenty millilitres of the separation solvent (acetic acid/water/acetonitrile 1:20:79, v/v/v) were added before being vortexed using laboratory rotary shaker (Model GFL 3017, Germany). Ratio of the dilution of the sample with the solvent was 1:1 and 5 millilitres of the dilution obtained from the extract was shot into the LC-MS/MS.

2.5. LC-MS/MS Parameters

Analysis of the extracts was achieved with a QTrap 5500 multimycotoxin LC-MS/MS system (Applied Biosystem, California, United State of America) furnished with Turbolon spray ESI source and High Performance Liquid Chromatography (Agilent, Germany). Other liquid chromatography/Mass Spectrometry protocols applied for chromatographic separation, identifying analytes that are positive, quantification of liquid standard identification were as described by Malachova *et al.*, 2015. The method precision was tested through proficiency testing organized by Bureau Interprofessionnel des Etudes Analytique (BIPEA) (Gennevilliers, France) in accordance with ISO 13525:2015. All the 60 results of the groundnut were between -2 < x < 2 which was a satisfactory range.

Maximum and median concentration (µgkg⁻¹) of toxins and metabolites were determined from the data collected for each of the samples analysed. The fungi isolated from the seeds of the improved groundnut varieties were tabulated based on their species. The mean percentage of seeds infected with fungi per treatment were separated with Tukey's test at 5% level of probability.

3. Results

3.1. Mycobiota load in the groundnut seeds

The three *Aspergillus* species detected in the groundnut seed samples were *Aspergillus niger*, *A. flavus* and *A. fumigatus* (Table 1, Figures 1 and 2). Other four genera observed were *Penicillium* spp, *Rhizopus* spp, *Fusarium* spp and *Sclerotium* spp as shown in Table 1. The percentage of SAMNUT 22 (100%), SAMNUT 24 (96.67%), ICGV-1S-09992 (96.67%) and ICGV 94379 (100%) seeds infected with fungi were significantly higher ($p \leq 0.05$) than other varieties. There were total of 303 fungal isolates recovered from all samples, out of which 143 (47.19%) and 54 (17.82%) were *A. niger* and *A. flavus* respectively. The seed samples from ICGX 86024 and ICGX 01276 had the highest and lowest total fungal incidence respectively.

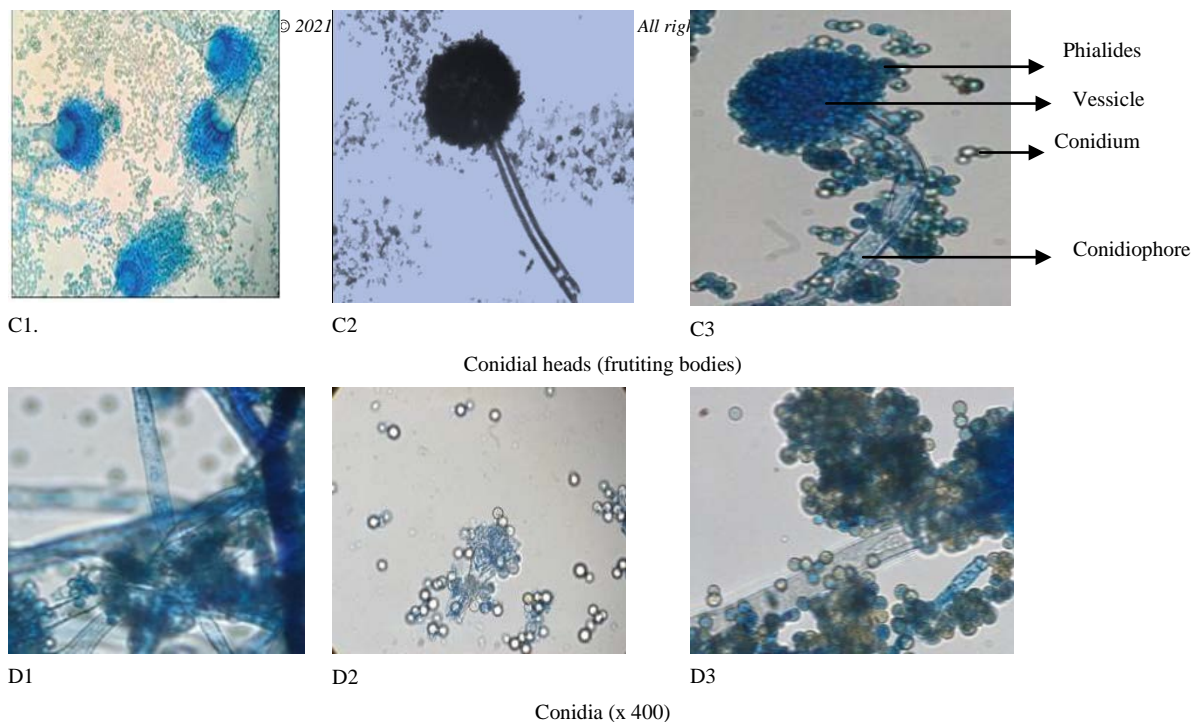


Figure 2. Microscopic features of the three identified *Aspergillus* species. Conidial heads (C1-C3) and conidia - x400 (D1-D3)

Table 2. Microscopic characteristics of the identified *Aspergillus* spp isolates

Fungus	Microscopic features							
<i>Aspergillus</i> species	Size (μm)	Stipes colour	Surface	Vesicle serration	Vessicle size	Metula covering	Shape	Conidia surface
<i>A. flavus</i>	400-800	Pale brown roughened	Quietly spherical	Biserate	30 - 40 μm)	2/3	Glubose ellipsoid	Smooth finely roughened
<i>A. niger</i>	400-3000	Slightly brown	Smooth walled	Biserate, large size	15.45 -20.45 μm	entirely	Glubose	Very rough, irregular
<i>A. fumigatus</i>	200 -400	Grayish near ape	Smooth walled	Uniserate, pyriform	15.45 - 20.45 μm	Upper2/3	Globose, small in columns	Smooth or spinose

3.2. Occurrence of fungal toxins and metabolites in groundnut seeds and haulms

Major mycotoxins such as aflatoxin B₁, ochratoxin A, fumonisin B₁, fumonisin B₂, fumonisin B₃, fumonisin B₄, fumonisin B₆ were below the limit of detection by LC-MS/MS analyser in all the seeds and haulms of the ten groundnut genotypes investigated. The occurrence of 8 emerging *Aspergillus* toxins, sterigmatocystin (STC) and other six biosynthesis precursors were detected in the groundnut and haulm samples. In addition, a bacterial toxin; monactin (0.017 $\mu\text{g kg}^{-1}$) was detected in the haulm of variety ICGV-1509926 (Tables 3 and 4). The only bacterial toxin detected was monactin found in the haulm of variety ICGV-1509926 with a low median concentration of 0.017 $\mu\text{g kg}^{-1}$.

No *Aspergillus* toxin and metabolites were detected in the seeds of ICGV-IS-09992 and ICGV-IS-09926. Also, no toxins and metabolites were detected in the haulms of ICGV-IS-09992. The seeds of ICGV-85024 had the highest co-occurrence of seven out of eight *Aspergillus* emerging toxins and metabolites, while in the haulms, the

highest co-occurrence of six metabolites was found in ICGV-1S-09926. Lower occurrence and concentration of *Aspergillus* toxins and metabolites were detected in the seeds of ICGV-01276, ICGV-SM 08540, SAMNUT 22 and SAMNUT 24 varieties than in their haulms (Table 3).

High median concentration of 3-Nitropropionic acid (2716.3 $\mu\text{g kg}^{-1}$) was detected in the seeds of ICGV-94379. Also, highest median concentration of 3-Nitropropanoic acid (3716 $\mu\text{g kg}^{-1}$) was detected in the haulms of the ICGV-94379 genotype.

Only the seeds of ICGV- IS-09926 had all the seven aflatoxin biosynthesis precursors including STC (Table 4). The median concentration level of STC in the seeds of ICGV-1S-09926 had a maximum concentration of 2.6 $\mu\text{g kg}^{-1}$ with a median of 0.87 $\mu\text{g kg}^{-1}$. The result also revealed that that 7 out of the 10 groundnut varieties' seeds were contaminated with versicolorin A, versicolorin C, and averufin (Table 3), but none of the aflatoxin biosynthesis precursors was detected in the haulms of ICGV- 07999, ICGV-24, ICGV-1S-09926, ICGV-85024.

Table 3. Maximum and median concentration ($\mu\text{g kg}^{-1}$)* of *Aspergillus* metabolites in groundnut seeds and haulms

Groundnut genotype/ <i>Aspergillus</i> metabolite	ICGV-07999		ICGV-24		ICGV-01276		ICGV-1S-09926		ICGV-1S-09992		ICGV-85024		ICGV-94379		ICGV-SM 08540		SAMNUT 22		SAMNUT 24	
	Sd	Hlm	Sd	Hlm	Sd	Hlm	Sd	Hlm	Sd	Hlm	Sd	Hlm	Sd	Hlm	Sd	Hlm	Sd	Hlm	Sd	Hlm
3-Nitropropionic acid	0.4 (0.1)	1.0 (0.6)	0.3 (0.1)	-	-	-	-	-	-	-	0.3 (0.1)	8149 (2716)	8279 (3716)	-	0.4 (0.14)	-	-	-	-	-
gragillin	-	-	-	-	-	-	-	-	5533 (1844)	-	-	-	-	-	-	7279 (2426)	-	-	-	-
Malformin A	-	-	-	-	-	0.04 (0.01)	0.07 (0.02)	-	-	0.01 (0.003)	-	-	5.7 (1.8)	-	-	-	-	-	-	-
Malformin C	-	-	-	-	-	-	0.02 (0.02)	-	-	0.03 (0.01)	-	-	0.4 (0.14)	-	-	-	-	-	-	-
Kojic acid(KJ)	-	-	5.2 (1.7)	7.5 (3.2)	-	-	4.6 (1.5)	-	-	6.7 (2.2)	8149 (2716)	1889 (630)	-	6.6 (2.2)	-	-	-	-	-	6.1 (2)
Methyl funicone	-	-	0.7 (0.2)	0.1 (0.01)	-	0.2 (0.07)	0.8 (0.3)	-	-	0.3 (0.1)	-	-	-	1.16 (0.4)	-	0.04 (0.01)	-	-	0.5 (0.2)	
Emericellamide A	-	-	-	-	1516 (505)	1670 (605)	1156 (385)	-	-	2272 (757)	2.03 (0.7)	4.6 (0.2)	2748 (978)	2948 (998)	2663 (888)	2863 (890)	5642 (1881)	6642 (2881)	-	-
Sydowinin A	-	-	1.21 (0.3)	-	-	-	-	-	-	1.13 (0.4)	-	-	-	-	-	-	-	-	-	-

- = < limits of detection; sd = seed; hlm= haulm

Table 4. Maximum and median concentration ($\mu\text{g kg}^{-1}$) of sterigmatocystin (STC) and other aflatoxin biosynthesis precursors in groundnut seeds and haulms

G/nut genotype	ICGV-07999		ICGV-24		ICGV-01276		ICGV-1S-09926		ICGV-1S-09992		ICGV-85024		ICGV-94379		ICGV-SM 08540		SAMNUT22		SAMNUT24	
	Sd	Hlm	Sd	Hlm	Sd	Hlm	Sd	Hlm	Sd	Hlm	Sd	Hlm	Sd	Hlm	Sd	Hlm	Sd	Hlm	Sd	Hlm
Sterigmatocystin	-	-	-	-	-	-	2.6 (0.87)	-	-	-	-	-	-	-	-	-	-	-	-	-
Nidurufin	6.4 (2.1)	-	21.9 (1.0)	-	2.1 (0.8)	1.13 (0.38)	23.88 (7.96)	-	0.03 (0.1)	14.14 (4.7)	6.8 (2.3)	-	0.04 (0.01)	68.3 (22.8)	-	17.38 (5.75)	-	3.33 (1.1)	-	47.15 (16)
Versicolorin A	9.6 (3.2)	-	37.8 (13)	-	2.3 (0.8)	1.26 (0.4)	30.55 (10.2)	-	0.10 (0.33)	16.0 (5.30)	8.5(2.8)	-	4.4 (1.7)	74.6(25)	-	15.1 (5.02)	-	3.6(1.2)	-	48.3 (16.1)
Versicolorin C	26.1 (8.7)	-	91.8 (30.6)	-	4.8 (1.5)	3.7 (1.23)	84.3 (28.1)	-	0.19 (0.1)	51.99 (13.97)	25.4 (8.5)	-	5.4 (2.1)	213(70.9)	-	56.49 (18.9)	-	10.1 (3.4)	-	160 (53.3)
Averantin	0.4 (0.15)	-	1.6 (0.5)	-	0.9 (0.4)	0.07 (0.02)	1.66 (0.5)	-	-	1.1 (0.4)	0.4 (0.13)	-	-	3.56(1.2)	-	0.7 (0.2)	-	0.19(0.1)	-	2.9(0.9)
Averufin	3.4 (1.14)	-	13.4 (4.5)	-	1.6 (0.9)	0.44 (0.13)	12.61 (4.2)	-	0.08 (0.03)	9.11 (3.4)	3.29 (1.1)	-	0.05 (0.03)	25.4(8.5)	-	7.3 (2.41)	-	1.5 (0.03)	-	25.1 (8.4)
Norsolorinic acid	0.85 (0.3)	-	4.14 (1.4)	-	-	-	4.37 (1.4)	-	-	2.8 (0.95)	1.15 (0.4)	-	-	10.3(3.8)	-	1.7 (0.57)	-	0.5 (0.17)	-	8.1(2.7)

= < limits of detection; sd = seed; hlm= haulm; () = median concentration

4. Discussion

Several *Aspergillus* strains, their metabolites and aflatoxin biosynthesis precursors have been isolated from groundnut seeds and in feeds of ruminants such as cattle feed (Ranjbar *et al.*, 2011) and dairy goat feed from Brazil (da Silva *et al.*, 2015). Ruminant animals are often fed with groundnut haulms as roughages in order to contribute energy and nutrients to their diet (Granados-Chinchilla, 2017). *Aspergillus* species and aflatoxins have been found to be associated with the silages of corn and sorghum (Alonso *et al.*, 2013). Thus studies concerning safety of animals and humans that consume groundnut and/or their haulms should not be neglected.

Some isolated fungi from Jordan Desert leaves and fruits were identified as *Aspergillus*, *Alternaria*, *Rhizopus*, *Penicillium* and *Fusarium* at the genus level by using macroscopic and microscopic examinations depending on colony colour, shape, hyphae, conidia, conidiophores and

arrangement of spores (Alsohaili and Bani-Hasan, 2017) as was carried out in this study. They further molecularly identified the isolated fungi at species level as the extracted fungal DNA was amplified by PCR using specific internal transcribed spacer primer (ITS1/ITS4).

A. niger had the highest incidence (47.20%) of fungal species isolated from the seeds in this study. It is reported that there are up to 145 different secondary metabolites isolated and detected from *A. niger* (Nielson *et al.*, 2009). These include intricate compounds such as naphtho- γ -pyrones, nigragillin, ochratoxin A and fumonisin B₂. *A. flavus* with the second highest incidence (17.8%) is popularly known for being a producer of carcinogenic aflatoxins. About 46 secondary metabolites have been identified in *A. flavus*, and these non-regulated fungal metabolites include 3-NPA, aflatrem, cyclopionic acid aflavorin, aflavozole, aflavine, aspergillilic acid, cladosporin, aspergillilic acid, cladosporin and gliotoxin (Adetunji *et al.*, 2014; Cary *et al.*, 2018). Other toxic regulated compound produced by *A. flavus* is kojic acid

which is implicated as a neurological poison and mitochondrial toxin (Ahuja, 2008).

The incidence of *Sclerotium* spp in the samples was 16.2%. Amber et al. (2012) reported that phenolic acids were detected by HPLC analysis of secondary metabolites in the fungus isolated from chickpea. They observed that this metabolite is responsible for severe collar rot infection in chickpea. The incidence of *Fusarium* spp in the sampled seeds was 9.6%. Nesic et al. (2014) identified 10 species of *Fusarium* and the mycotoxins produced by each of them. *F. culmorum* is known to be a producer of up to 10 mycotoxins which include fusarins, moniliformin, trichothecenes and zearalenone. Other *Fusaria* such as *F. graminearum*, *F. sporotrichioides*, *F. crookwellense* and *F. acuminatum* can produce up to eight mycotoxins each, while *F. equiseti* and *F. proliferatum* can produce six each, *F. verticillioides* - 4, *F. armeniacum* -3 and *F. pseudograminearum* - 2 (Berthiller et al. (2013).

The merits of LC-MS/MS based analytical method used in this study include allowing the sensitive concurrent determination of several fungal metabolites in many matrices (Sulyok et al., 2010; Berthiller et al., 2015; Malachova et al., 2018). LC-MS could tremendously assist in the discovery of recently produced mycotoxins (Varga, 2015), as well as hidden (Berthiller, 2013) or other altered forms (Rychlik, 2014) of mycotoxins in crop produce like groundnut.

Major mycotoxins like aflatoxin and their precursors were below level of detection in almost all the groundnut varieties investigated in this study. This is unlike other several previous studies on the natural occurrence of aflatoxins in groundnut samples from other countries. From the samples of stored peanut kernels collected from four different areas in Sudan, Bakhiet et al. (2011) using TLC techniques, reported AFB₁ concentration ranges of 17.57 - 404 µg kg⁻¹.

Eight *Aspergillus* metabolites in groundnut seeds and haulms were detected in this study. Nigragillin and Malformin C are being produced by *A. niger* (Burdock et al., 2001), Malformin A are produced by *A. ficuum*, *A. awamori* and *A. phoenicis* while Emericellamide A are produced by *A. nidulans* and Sydowinin A by *A. sydowinin* and *A. versicolor*. Kojic acid is known to be produced by *A. flavus* and *A. oryzae*, 3-NPA on the other hand is produced by *A. wentii*, *A. niger* and *A. oryzae*.

STC was not found in nine out of the 10 improved groundnuts varieties understudied. Out of the 10 analysed improved groundnut varieties, STC was only found in the seeds of ICGV-1S-09926 at low median concentration of 0.87 µg kg⁻¹. Sterigmatocystin is normally produced by *A. flavus*, *A. nidulans*, *A. parasiticus* and mainly *A. versicolor* (Versilovskis and De Saeger, 2010). It was reported to often occur where grains and cereal-based food are contaminated with aflatoxigenic fungi (Rank, 2011).

The outcome of this study suggested that the STC (and thus the aflatoxin) pathway is interrupted in the improved groundnut genotypes; thus, such genotypes where not able to produce aflatoxin. Chang et al., (2005) similarly reported that absence of interplay between *afIR* and *afII* contributes to non-aflatoxigenicity of *A. sojae*. They also reported a sequence stopping points in the aflatoxin biosynthesis gene cluster and flanking zones in non-aflatoxigenic *A. flavus* isolates. The non-occurrence of aflatoxins in most of the improved groundnut varieties

indicated that the use of breeding for resistance could be a better intervention needed in the mitigation of mycotoxin contamination in crops. This is, however, in addition to using cultural practice such as pre-and post-harvest managements, and chemical control methods.

STC is one of the precursors of aflatoxin B₁ and G₁ as indicated in a AF biosynthesis pathway as described by Jallow, 2015. Apart from STC being an aflatoxin precursor, it is with toxicity second to AFB₁ (Gao et al., 2015). The aflatoxin pathway really requires the presence of STC which often forms O-methylsterigmatocystin (OMST) with the help of O-methyltransferase. OMST could then be converted to AFB₁ & AFG₁ with the presence of cytochrome P-450 monooxygenase encoded by *ord-1* (Audebert et al., 2014; Bertuzzi et al., 2017; Wartu et al., 2017).

5. Conclusion

In this study identification of the fungal isolates up to species was impossible due to non-involvement of molecular characterization techniques. The producing fungus of some of the fungal metabolites detected could not be identified. Thus, molecular identification of fungi in further studies on this subject is necessary in future studies

The analysis indicated that there was no major mycotoxin detected in all the seeds and haulms of the ten groundnut genotypes despite the presence of *Aspergillus* spp. The improved groundnut varieties might have been bred to resist aflatoxin production, and thus were below detectable level. Planting of such improved varieties with good crop management practices can help reduce aflatoxin and other major mycotoxins contamination in groundnut before storage. In most of the groundnuts analysed, there were incidences of contamination of some minor mycotoxins and metabolites in the seeds more than their haulms.

The non-occurrence of aflatoxins in most of the improved groundnut varieties indicated that the use of breeding for resistance could be a better intervention needed in the mitigation of mycotoxin contamination in crops. This is, however, in addition to using cultural practice such as pre-and post-harvest managements, and chemical control methods. This report is believed to be the first in elucidating the aflatoxins biosynthesis precursors in seeds and haulms of improved groundnut varieties in Northern Nigeria. The result could serve as base information for groundnut breeders to produce a broad spectrum of mycotoxin-resistant groundnut.

Declaration of Interest Statement

There is no conflict of interests.

References

- Adetunji M, Atanda O, Ezekiel CN, Sulyok M, Warth B, Beltrán E, Krska R, Obadina O, Bakare A and Chilaka CA. (2014). Fungal and bacterial metabolites of stored maize (*Zea mays* L.) from five agro-ecological zones of Nigeria. *Mycotoxin Res.* 30(2):89-102.
- Ahuja M, Bishnoi M and Chopra KT. (2008). Protective effect of minocycline, a semi-synthetic second-generation tetracycline against 3-nitropropionic acid (3-NP)-induced neurotoxicity.

- International Nuclear Information System (INIS). *Toxicol.* **244**: (2-3): 111-122.
- Alonso VA, Pereyra CM, Keller LAM, Dalcero AM, Rosa CAR and Chiacchiera SM. (2013). Fungi and mycotoxins in silage: An overview. *J of Appl Microbiol*, **115**(3):637- 643.
- Alsohaili SA and Bani-Hasan BM. (2017). Morphological and Molecular Identification of Fungi Isolated from Different Environmental Sources in the Northern Eastern Desert of Jordan. *Jordan J Biol Sci.*, **11**(3):229-337.
- Amber P, Akram A, Qureshi R and Arid S.. (2012). HPLC analysis for secondary metabolites detection in *Sclerotium rolfsii* isolated from chickpea. *Pak. J. Bot.* **44**: 417-422.
- Audebert M, Theumeur M, Henneb Y, Payros D, Borin C, Tadriss S, Beltz S, Puel O and Oswald I. (2014). Genotoxicity of aflatoxin precursors. Abstracts of Lectures and Posters of the World Mycotoxin Forum 8th Conference, Wien, Austria, 10–12 November 2014, **43**: 102.
- Bakhiet SEA and Musa AAA. (2011). Survey and Determination of Aflatoxin Levels in Stored Peanut in Sudan: *J Biol Sci.*, **4**(1): 13-20.
- Berthiller F, Brera C, Crews C, Iha MH, Krska R, Lattanzio VMT, MacDonald S, Malone R. J, Maragos C, Solfrizzo M, Stroka J and Whitaker TB. (2015). Developments in mycotoxins analysis: an update for 2013–2014. *World Mycotoxin J.*, **8**: 5-35.
- Berthiller F, Crews C, Dall'Asta C, De Saeger S, Haesaert G, Karlovsky P, Oswald IP, Seefelder W, Speijers G and Stroka J. (2013). Masked mycotoxins: a review. *Mol. Nutr. Fd Res.* **57**: 165–186.
- Bertuzzi T, Romani M, Rastelli S, Mulazzi A, and Pietri A. (2017). Sterigmatocystin Occurrence in Paddy and Processed Rice Produced in Italy in the Years 2014–2015 and Distribution in Milled Rice Fractions. *Toxins* **9** (86) : 1-11.
- Bhatnagar-Mathur P, Sunkara S, Bhatnagar-Panwar M, Waliyar F and Sharma KK. (2015). Biotechnological advances for combating *Aspergillus flavus* and aflatoxin contamination in crops. *Plant Sci.* **234**: 119-132.
- Burdock GA, Soni MG and Carabin IG. (2001). Evaluation of health aspects of kojic acid in food. *Regulatory Toxicol and Pharmacol*, **33** (1) : 80–101.
- Cary, JW, Gilbert, MK, Lebar RM, and Calvo AM. (2018). *Aspergillus flavus* Secondary Metabolites: More than Just Aflatoxins. *Food Saf* (Tokyo). **6**(1): 7–32. doi: 10.14252/foodsafetyfscj.2017024.
- Chang PK, Horn BW and Dorner JW. (2005). Sequence breakpoints in the aflatoxin biosynthesis gene cluster and flanking regions in non-aflatoxigenic *Aspergillus flavus* isolates. *Fungal Genet. Biol.* **42**:914–923.
- Changwa R, Abia W, Msagati, T, Nyoni, H, Ndeve, K and Njobeh, P. (2018). Multi-mycotoxin Occurrence in Dairy Cattle Feeds from the Gauteng Province of South Africa: A Pilot Study Using UHPLC-QTOF-MS/MS. *Toxins* **10** (7): 294.
- da Silva JL, Aparecido CC, Hansen D, Pereira TAM, D'arc-Felício J and Gonçalves E. (2015). Identification of toxigenic *Aspergillus* species from diet dairy goat using a polyphasic approach. *Ciência Rural, Santa Maria*, **45**(8):1466-1471.
- Dwivedi SL, Crouch JH, Nigam SN, Ferguson ME and Paterson AH. (2003). Molecular breeding of groundnut for enhanced productivity and food security in the semi-arid tropics: opportunities and challenges. *Adv in Agron*, **80**: 153–22.
- Garcia-Cela E, Kiaitsi E, Sulyok, M, Krska, R, Medina A and I. Petit Damico IP. (2019). Influence of storage environment on maize grain: CO₂ production, dry matter losses and aflatoxins contamination. *Food Addit Contam: Part A*, **36**: 175-185.
- Gao W, Jiang L, Ge L, Chen M, Geng C, Yang G, Li, Q, Ji F, Yan Q, Zou Y. (2015). Sterigmatocystin-induced oxidative DNA damage in human liver-derived cell line through lysosomal damage. *Toxicol.* **29**: 1–7.
- Giorni P, Bertuzzi T and Battilani P. (2019) Impact of Fungi Co-occurrence on Mycotoxin Contamination in Maize During the Growing Season. *Front. Microbiol.* **10**:1265. doi: 10.3389/fmicb.2019.01265.
- Granados-Chinchilla F. (2017). A Focus on Aflatoxin in Feedstuffs: New Developments in Analysis and Detection, Feed Composition Affecting Toxin Contamination, and Interdisciplinary Approaches to Mitigate It. Aflatoxin - Control, Analysis, Detection and Health Risks, Lukman Bola Abdulla'uf, *IntechOpen*. **12**:251-280.
- Gruber-Dorninger C, Novak B, Nagl V, and Berthiller F. (2017). Emerging Mycotoxins: Beyond Traditionally Determined Food Contaminants. *J of Agric and Food Chem.* **65**: 7052–7070.
- Guchi E. (2015a). Implication of aflatoxin contamination in agricultural products. *American J of Food and Nutri.* **3** (1):12-20.
- Guchi E. (2015b). Aflatoxin Contamination in Groundnut (*Arachis hypogaea* L.) Caused by *Aspergillus* Species in Ethiopia." *J Appl & Environ Microbiol.* **3**(1): 11-19.
- Ifeji EI, Makun HA, Mohammed, HL, Adeyemi, RYH, Mailafiya SC, Mohammad KH. and Olurunmowaju YB. (2014). Natural occurrence of aflatoxin and roasted groundnut from Niger State, Nigeria. *Mycotoxicology*, **1**(1): 35–45.
- International Organization for Standardization (2015). ISO guide 13528:2015(en) statistical methods for use in proficiency testing by interlaboratory comparison.
- Jallow EAA. (2015). Determination of aflatoxin-producing fungi strains and levels of aflatoxin B₁ in some selected local grains. MPhil Degree Thesis in Biochemistry. Department of Biochemistry and Biotechnology, Kwame Nkrumah University of Science and Technology (KNUST), Kumasi, Ghana.
- Joanne MW, Linda MS and Christopher JW. (2008). Prescott, Harley & Kleins Microbiology. 7th edition. Mcgraw hill publishers, New York. 1028-1048.
- Malachova A, Sulyok M, Beltrán E, Berthiller F, Krska R. (2015). **Multi-toxin determination in food - The power of "Dilute-and-shoot approaches in LC-MS-MS**. LCGC Europe, **28**(10): 542-555.
- Malachová A, Stránská M, Václavíková M, Elliot CT, Black C, Meleely J, Hajslova J, Ezekiel CN, Schuhmacher R and Kriska R. (2018). Advanced LC–MS-based methods to study the co-occurrence and metabolization of multiple mycotoxins in cereals and cereal-based food. *Anal Bioanal Chem* **410**: 801–825.
- Nesic K, Ivanovic S and Nesic V. (2014) Fusarial Toxins: Secondary Metabolites of *Fusarium* Fungi. In: Whitacre D. (eds) *Rev Environ Contam Toxicol* **228**: 101-120.
- Nielsen KF, Mogensen JM, Johansen, M, Larsen, TO and Frisvad, JC (2009). Review of secondary metabolites and mycotoxins from the *Aspergillus niger* group. *Anal. bioanal Chem.* **395**:1225–1242.
- Ntare BR. (2007). *Arachis hypogaea* L. In: van der Vossen, H.A.M. & Mkamilo, G.S. (Editors). PROTA (Plant Resources of Tropical Africa/Ressources végétales de l'Afrique tropicale), Wageningen, Netherlands. Accessed 2 June 2018.
- Ranjbar S, Nazari R and Noori M. (2011). Isolation and molecular identification of *Aspergillus* species of Cattle. *Vet. Res.* **7**(1):11-17.
- Rank C, Nielsen KF, Larsen TO, Varga J, Samson RA and Frisvad JC. (2011). Distribution of sterigmatocystin in filamentous fungi. *Fungal Biol.* **115**: 406–420.

Rychlik M, Humpf HU, Marko D, Dänicke S, Mally A, Berthiller F, Klaffke H and Lorenz N. (2014). Proposal of a comprehensive definition of modified and other forms of mycotoxins including “masked” mycotoxins. *Mycotoxin Res.* **30**: 197–205.

Sulyok M, Krska R and Schuhmacher R. (2010). Application of an LC-MS/MS based multi-mycotoxin method for the semi-quantitative determination of mycotoxins occurring in different types of food infected by moulds. *Food Chem.* **119**:408–416.

Vabi MB, Ogara I, Anjorin TS; , Oluwabaniwo F; , Alabi O, Ajeigbe HA and Denloye S. (2018). Aflatoxins in Nigerian groundnut: Continuous threat to health,, agriculture and foreign trade. *Policy brief* 35, (April, 2018).

Varga E, Wiesenberger G, Hametner C, Ward TJ, Dong Y, Schöfbeck D, McCormick S, Broz K, Stückler R, Schuhmacher R, Krska R, Kistler HC, Berthiller F and Adam G. (2015). New tricks of an old enemy: isolates of *Fusarium graminearum* produce a type A trichothecene mycotoxin *Environ. Microbiol.*, **17**: 2588 – 2600.

Versilovskis A and De Saeger SA. (2010). Strigmatocystin: occurrence in foodstuffs and analytical methods: An overview. *Mol Nutri and Food Res.* **54**(1) : 136-147.

Wartu JR, Whong, CMZ, Abdullahi IO, and Ameh JB. (2017). Phylogenetics of aflatoxin from in-process wheat and flour from selected major stores within Northern Nigeria. *Sci. World J.* **12**(4): 1-5

Homology modeling of apoprotein Opsin and covalent docking of 11-cis retinal and 11-cis 3, 4-didehydroretinal to obtain structures of Rhodopsin and Porphyropsin from Zebra danio, *Danio rerio* (Hamilton, 1822)

Susmita Dey¹, Gitartha Kaushik², Saurav Mahanta³ and Arijit Chakraborty^{4,*}

¹ Dept. of Zoology, Royal Global University, Guwahati, Assam, India- 781035; ² Faculty of Science, Assam Downtown University, Assam, India – 781026; ³ Bioinformatics Center, National Institute of Electronics and Information Technology, Assam, India-781008; ⁴ Department of Sports & Exercise Science, Somaiya Sports Academy, Somaiya Vidyavihar University, Vidyanagar, Mumbai, Maharashtra 400077, India

Received: April 6, 2020; Revised: Sept 20, 2020; Accepted: Nov 10, 2020

Abstract

Opsin proteins are classically seven transmembrane receptor proteins which detect light. The present investigation describes the stereoscopic structure of the apoprotein Opsin by online structure determining tools using the crystallographic structure of Rhodopsin from *Bos taurus* as the template. The modeled structure was validated and checked through validated data tools for stereochemical quality of a protein structure, ProSa and the square root of the mean square deviation between the templates and the predicted structure was calculated using PyMol. It was found that the chromophores, 11-cis retinal and 11-cis 3, 4-didehydroretinal was covalently docked with apoprotein which gives the structures of Rhodopsin and Porphyropsin respectively. Due to its close homology to the human rhodopsin (accession P08100), zebra fish rhodopsin may serve as an excellent model for study of human diseases in future. This article represents the test of structure/function relationship of apoprotein opsin in this ornamental aquarium fish and provides a foundation for future work exploring cellular and molecular pathways of photoreception in retinal development and disease models.

Keywords: Zebra fish, Opsin, Rhodopsin, Porphyropsin, 11-cis retinal, 11-cis 3,4-didehydroretinal

1. Introduction

Studies have shown the use of visual pigments by representatives of almost all the vertebrates, where visual pigments are Rhodopsin and Porphyropsin. Both rod visual pigments contain the same apoprotein Opsin; however, they are covalently linked to different groups. Rhodopsin binds 11-cis-retinal, whereas Porphyropsin is linked to 11-cis 3, 4-didehydroretinal (La Franco *et al.*, 2018; Ganong 2005). These pigments possess various spectral characteristics like maximum absorbance and absorbency index (Marschall, *et al.*, 2012). The absorption maxima of Rhodopsin are nearly 500 nm, whereas Porphyropsin is in the range of 520 – 535 nm. It has been found that the visual pigments may vary in response to light, temperature, and other environmental stimuli (Korenyak and Govardovskii, 2013).

Studies suggest that certain fish retinas comprise a visual purple pigment rather than the contemporary Rhodopsin of red - color which was confirmed spectrophotometrically (Enright *et al.*, 2015). Similar studies suggested that Porphyropsin a purple rod-pigment, is a characteristic of freshwater fishes, whereas the red rod visual pigment, Rhodopsin is characteristic of terrestrial craniate and most of the Sea fishes. It has also been found that many freshwater fishes have Porphyropsin and/or

admixture of Rhodopsin and Porphyrins (Corush., 2019; Toyama *et al.*, 2008, Ochuko *et al.*, 2014).

The organism *Danio rerio* was selected for the current investigation as its visual system shares high similarities with other vertebrates (Gestri *et al.*, 2012; Golsmith and Harris 2003). Preliminary studies on *D. rerio* suggested that it possesses only Rhodopsin as visual pigment (Morrow and Chang 2015, Cameron 2002; Chinen *et al.*, 2003), whereas in a later study it has been confirmed that they have a paired visual system involving both Rhodopsin and Porphyropsin (Allison *et al.*, 2004).

In the present scenario, computational method such as homology modeling has been used to bridge the gap between sequence information and structures. The current investigation represents 3D models of Rhodopsin and Porphyropsin by homology modeling and docking methods for *D. rerio* which can be used to study the biochemical mechanism underlying the working of both the visual pigments.

2. Materials and Methods

2.1. Protein sequence analysis

Protein sequence analysis including, physicochemical parameters, molecular weight, sum of cationic and anionic residues, theoretical isoelectric point (pI), absorbency index (Porterfield and Zlotnick, 2010), aliphatic index

* Corresponding author e-mail: say.arijit22@gmail.com, arijit@somaiya.edu

(Sahay and Shakya, 2010), Grand Average hydropathy (GRAVY) (Wanyonyi *et al.*, 2011), half-life (Sharma *et al.*, 2014) and instability index (Gamage *et al.*, 2019) was calculated using the ExPasy's ProtParam prediction server (Gasteiger *et al.*, 2003).

2.2. Prediction of the three-dimensional structure

The protein sequence of the apoprotein from the organism *D. rerio* was obtained from the UniProt database (accession number: P35359). The sequence was analyzed using the G protein coupled receptor- Sequence-structure-feature-extractor (GPCR –SSFE) database (Worth *et al.*, 2011). Further, a protein BLAST was also carried out (Altschul *et al.*, 1990). After obtaining the template, homology modeling was carried out using MODELLER 9v8 software. It makes use of a command interpreter for designing stereochemical structures of proteins along with their confounders by summation of spatial restraints (Sali and Blundell 1993). The reliability of the model was analyzed by three (3) ways: (i) PROCHECK (Laskowski *et al.*, 1993), (ii) by calculation of the RMSD (root mean square deviation) between the template and the predicted structure using PyMol (version 1.8, Schrödinger, Inc, USA), and (iii) using ProSa (Wiederstein and Sippl 2007).

2.3. Covalent docking

The receptor and the ligand structures were prepared with Glide and Prime. The Protein Preparation Wizard was used for preparing the receptor, and LigPrep was used for preparing the ligands (Reddy and Vanga 2017). A maximum of 10 poses per ligand are established and are subject to minimization of post-docking. The apoprotein Opsin is covalently bonded to 11-cis-retinal and 11-cis 3, 4-didehydroretinal to form structures of Rhodopsin and Porphyropsin respectively. Covalent docking to the nitrogen of Lysine 296 was performed using the Prime module of Schrodinger. The covalent docking facility allows the selection of the attachment point to the receptor and the possible attachment point on the ligand and then runs a prime loop prediction to find all feasible poses for the ligand.

3. Results and Discussion

In the current study, the sequence of Opsin from *D. rerio* has been reprocessed from the UniProt database. The predicted physicochemical characteristic of Opsin showed that the protein has a molecular weight of 39.7064 kDa. Opsin has 20 (Arg + Lys) amino acid composition of positively charged and 22 (Asp + Glu) residues that are negatively charged. This also correlates with more number of negatively charged residues present in Opsin. The coefficient extinction of Opsin at 280 nm is $69175 \text{ M}^{-1} \text{ cm}^{-1}$ in lieu of the concentration of amino acids Phenylalanine, Trptophan and Tyrosine. It has been well established that for a protein is stable if the measured instability index is smaller than 40 and corresponding value above 40 foresees that the protein may be virtually unstable (Sahay and Shakya, 2010). The instability index of Opsin was found to be 46.09, which indicate that the protein is unstable in vitro. The aliphatic index for the protein sequence was found to be 85.90, which indicated thermo stability (Ashokan *et al.*, 2010). The GRAVY value computed for carotenoid binding protein was 0.457. Molecular orientation using Ramachandran plot showed the modelled

structure ha most of the residues (88.6%) in the fully allowed region, 11.1% in the additionally allowed region, 0.3% in the generously allowed region and nothing in the prohibited region.

3.1. Assessment of the three-dimensional structure

The sequence of the apoprotein from *D. rerio* was analyzed by the GPCR – SSFE database. Current result suggests the structure of Rhodopsin from organism *Bos taurus* (Protein data bank, PDB ID -1U19) as the template for the query sequence. The reasons for the selection of the template are presented in table 1.

Table 1. Reasons for the selection of the template

Helix	Template	Sequence Similarity	Reason for template choice
TMH1	1U19	89.7	Has Pro in same position
TMH2	1U19	100.0	Has Gly-Gly motif in same position
TMH3	1U19	91.4	No insertion or 2nd disulphide bridge and the highest sequence similarity to suggested template
TMH4	1U19	92.0	No second disulphide bridge between TMH3 and ECL2, no insertion and highest sequence similarity to suggested template
TMH5	1U19	96.3	No intra-ECL2 disulphide bridge, no disulphide bridge between ECL1-ECL2, no sequence similarity to the TMH5 extension of sRHO
TMH6	1U19	100.0	No disulphide bridge between TMH6 and ECL3, no sequence similarity to the TMH6 helix extension of sRHO and highest sequence similarity to suggested template
TMH7	1U19	95.8	Has insertion and highest sequence similarity to suggested template
Helix 8	1U19	100.0	Highest sequence similarity to suggested template

Further the sequence of amino acid for the apoprotein was also compared with the known structured sequence using PDB BLAST (Altschul *et al.*, 1990). The result signifies that the co-crystallized structure of Rhodopsin from organism *Bos taurus* (PDB ID-1U19) had the best sequence identity (83%) and had no gaps. After many rounds of loop refinement, an optimum structure was obtained (Fig 1). The arrangement of the phi and psi angles for the amino acid residues was presented in Fig. 2 A (Table 2). The percentage of phi and psi angles in the favorably allowed region was 88.6% and none of the residues was located in the prohibited region. The considered mean square root deviation among the intended model and template structure was found to be 0.213 \AA (Fig. 2 D). The Z-scores of the model and the template were -3.5 and -4.11 validated the quality of the model. Comparative study of the model and the guided structure shows similar profiles, as seen in Fig. 2B, C.

Table 2 . Ramachandran plot statistics for the 3D model of rhodopsin, calculated using PROCHECK

Residues in most favoured regions	88.6%
Residues in additional allowed regions	11.1%
Residues in generously allowed regions	0.3%
Residues in disallowed regions	0.0%

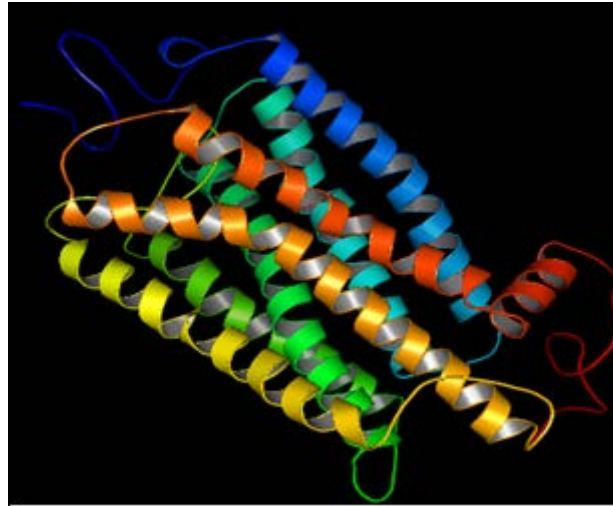


Figure 1. Using *Bos taurus* sequence as the template, the 3D model was built using MODELLER. Extensive loop refinements were carried out as it was found through the Ramachandran plot that residues in the loops were present in the disallowed region. Thus, after many rounds of loop refinement an optimum structure was obtained. In the image, blue represents the template and orange represents the structure of rhodopsin.

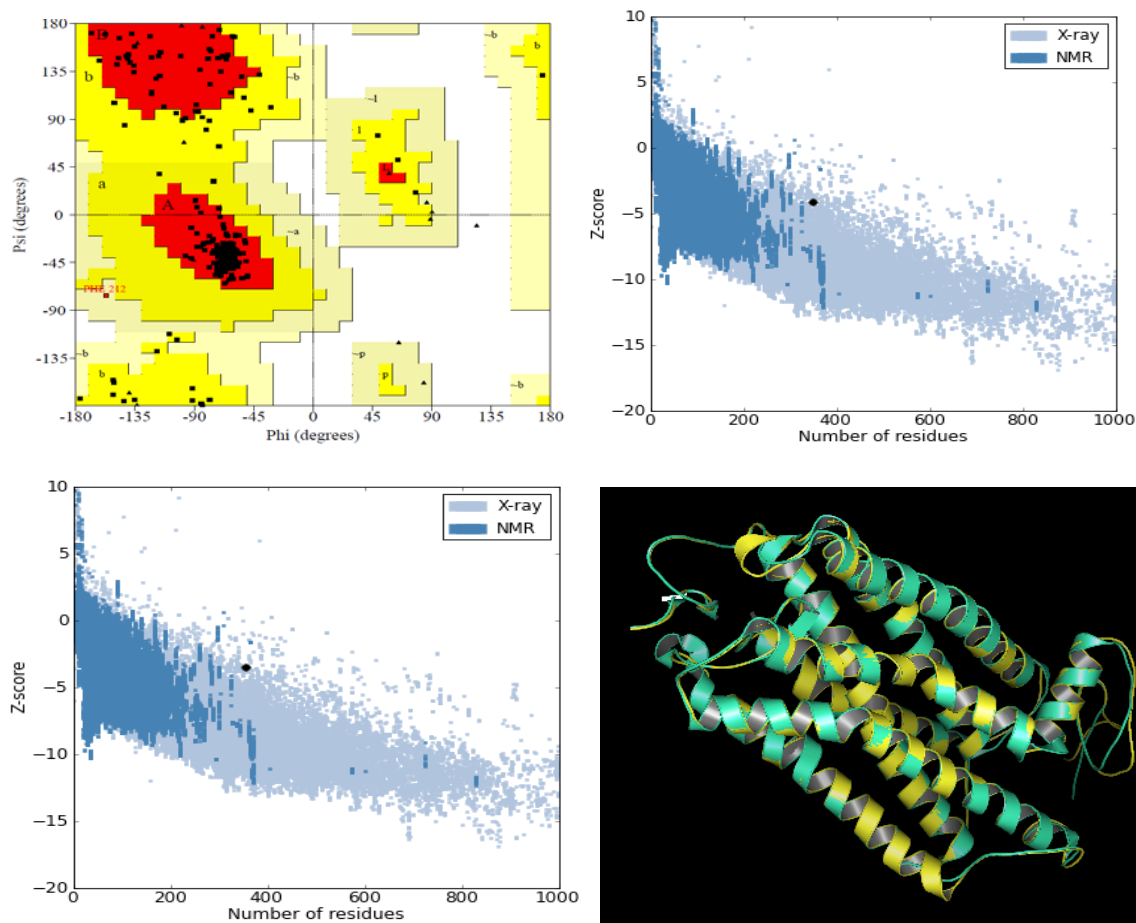


Plate 2. A. Ramachandran plot for the modeled structure of apoprotein from organism *D. rerio*. Red color represents most favored region. Additional allowed, generously allowed and disallowed regions are represented by yellow, light yellow and white colors respectively. B. and C: The plot contains the Z-scores of all experimentally determined protein chains in the current PDB that have been solved by either X-ray diffraction or NMR. The plot is used to check whether the Z-score of the 3D structure is within the range of scores typically found for native proteins of a similar size. The Z-score of -4.11 and -3.5 (fig: 2 B and 2 C respectively) represents the overall quality of the template structure and the target respectively.

3.2. Covalent docking

Covalent docking was performed using the prime Schrodinger. Apoprotein opsin is covalently attached to the chromophore 11 cis retinal to obtain the structure of rhodopsin and in porphyrosin, 11 cis 3,4, di-

dehydroretinol is the chromophore that is attached to the apoprotein. In Rhodopsin and Porphyrosin, the chromophores are covalently attached to opsin through the nitrogen of Lysine 296 (Fig 3 A and Fig 3 B). On comparing the residues that are involved in the binding of

11-cis-retinal and 11-cis 3, 4-didehydroretinal, residues like Glutamic acid 113, Alanine 117, Threonine 118, Glycine 121, Glutamic acid 122, Serine 186, Cysteine 187, Tyrosine 191, Methionine 207, Histidine 211, Phenylalanine 212, Phenylalanine 261, Trptophan 265, Tyrosine 268, Alanine 269, Alanine 292, Lysine 296 were found to be common (Fig. 3 C, D). Out of all these residues, lysine 296 is covalently attached and rests are encompassed in hydrophobic interactions with both the chromophores. The alignment of the template and the covalently docked structures (Rhodopsin and Porphyropsin) were checked and confirmed. It was found

that the chromophores were bound in a similar fashion as that in the template (Fig 3 E, F). The considered RMSD between Rhodopsin and the template was found to be 0.299 Å and the root mean square deviation between Porphyropsin and the model template was 0.302 Å. The backbone atoms were considered for these calculations. These results indicate great similarity of the structure with that of the template and can be used for further analysis. It is also important to mention that zebra fish rhodopsin shares ~80.4% homology to the human rhodopsin (accession P08100). Therefore, it may serve as an excellent model for the study of human diseases.

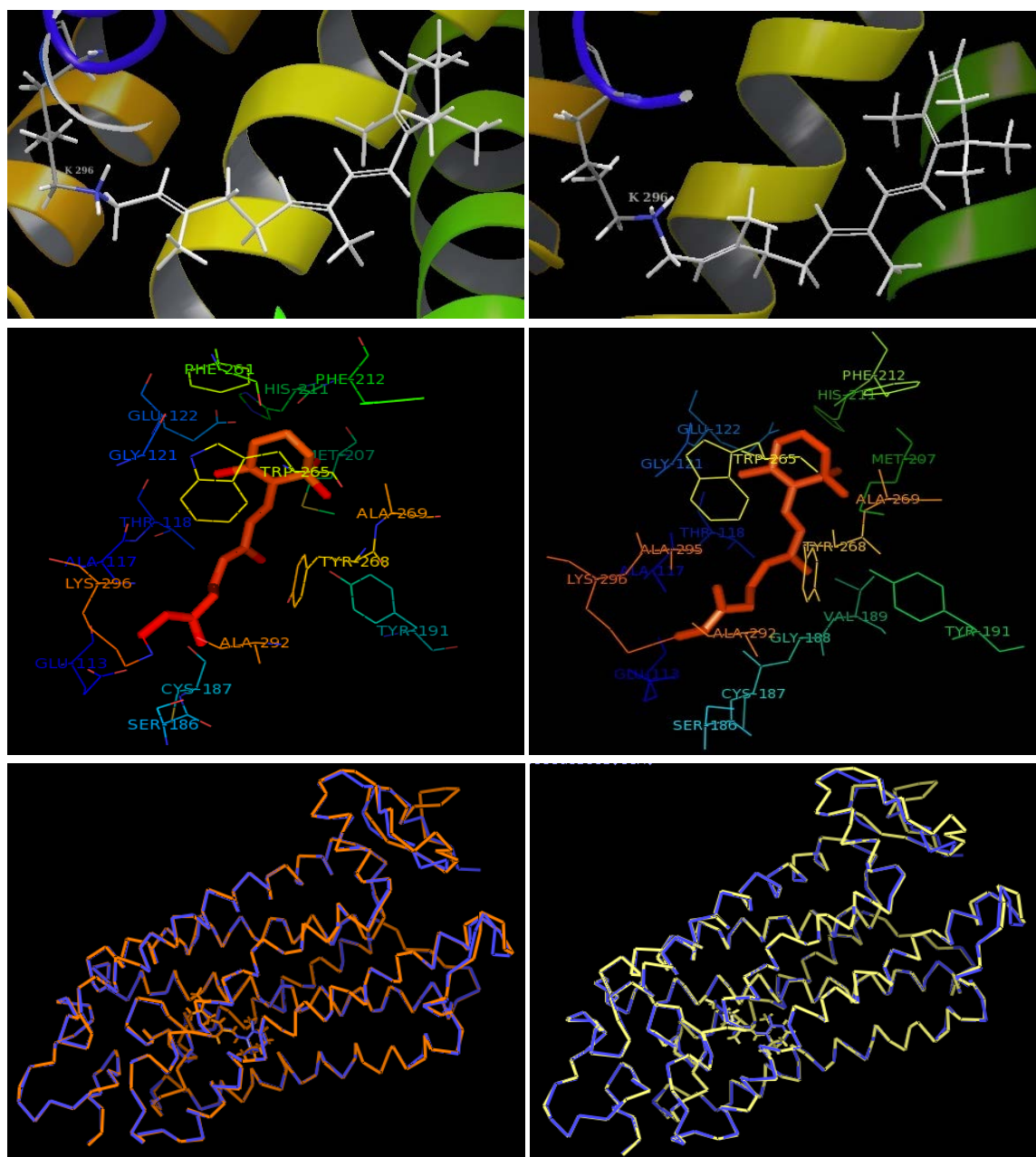


Figure 3. A, B Covalent binding of the chromophore 11-cis-retinal and 11-cis 3, 4-didehydroretinal to apoprotein Opsin through nitrogen of lysine 296 to obtain structures of rhodopsin and porphyropsin respectively. C and D show the amino acids that are involved in the binding of the chromophores, 11-cis-retinal and 11-cis 3, 4-didehydroretinal in rhodopsin and porphyropsin respectively. E The image of superimposed template and rhodopsin generated using PyMol. In the image, blue represents the template and orange represents the structure of rhodopsin. It can be observed that the 11-cis-retinal aligns in a similar fashion as in the template. F The image of superimposed template and porphyropsin generated using PyMol. In the image, blue represents the template and yellow represents the structure of porphyropsin. It can be observed that the 11-cis 3, 4-didehydroretinal aligns in a similar fashion as that of retinal in the template.

- Laskowski RA, MacArthur MW, Moss DS, Thornton JM. 1993. PROCHECK: a program to check the stereochemical quality of protein structures. *J Appl Crystallogr*, **26**: 283-291.
- Marschall, S., Pedersen, C. and Andersen, P.E., 2012. Investigation of the impact of water absorption on retinal OCT imaging in the 1060 nm range. *Biomed Optics Exp*, **3(7)**:1620-1631.
- Morrow JM, Chang BS. 2015. Comparative mutagenesis studies of retinal release in light-activated zebrafish rhodopsin using fluorescence spectroscopy. *Biochemistry*, **54(29)**:4507-18.
- Ochuko, J.E., Ovie, K.S. and Faith, I.I. 2014. Serum enzymes as a result of *Azadirachta indica* extract injection to African catfish *Clarias gariepinus* (Burchell, 1822). *Jordan J Biol Sci*, **147(1573)**:1-5.
- Porterfield JZ, Zlotnick A. 2010. A simple and general method for determining the protein and nucleic acid content of viruses by UV absorbance. *Virology*, **407(2)**:281-288.
- Reddy, P. and Vanga, U.M.R., 2017. Homology Modeling and In silico Docking Studies of DszB Enzyme Protein, Hydroxyphenyl Benzene Sulfinatase Desulfinate of *Streptomyces* sp. VUR PPR 101 *Jordan J Biol Sci*, **10(4)**: 309-316
- Sahay A, Shakya M. 2010. In silico analysis and homology modelling of antioxidant proteins of spinach. *J Proteomics Bioinform*, **3**:148-154.
- Šali A, Blundell TL. 1993. Comparative protein modelling by satisfaction of spatial restraints. *J Mol Biol*, **234**: 779-815.
- Sharma A, Singla D, Rashid M, Raghava GP. 2014. Designing of peptides with desired half-life in intestine-like environment. *BMC Bioinformatics*, **15**:282-287.
- Toyama, M., Hironaka, M., Yamahama, Y., Horiguchi, H., Tsukada, O., Uto, N., Ueno, Y., Tokunaga, F., Seno, K. and Hariyama, T., 2008. Presence of rhodopsin and porphyropsin in the eyes of 164 fishes, representing marine, diadromous, coastal, and freshwater species—a qualitative and comparative study. *Photochem*, **84(4)**: 996-1002.
- Wanyonyi SS, Sharp JA, Khalil E, Lefevre C, Nicholas KR. 2011. Tammar wallaby mammary cathelicidins are differentially expressed during lactation and exhibit antimicrobial and cell proliferative activity. *Comp Biochem Physiol Part A Mol Integr Physiol*. **160(3)**:431-439.
- Wiederstein M, Sippl MJ. 2007. ProSA-web: interactive web service for the recognition of errors in three-dimensional structures of proteins. *Nucleic Acids Res*, **35**: 407-410.
- Worth CL, Kreuchwig A, Kleinau G, Krause G. 2011. GPCR-SSFE: a comprehensive database of G-protein-coupled receptor template predictions and homology models. *BMC Bioinformatics*, **12**:185-198.

A preliminary study of Aminoglycoside Modifying Enzymes (AMEs) of Multiple Antibiotic Resistance of Methicillin-resistant *Staphylococcus aureus* (MRSA) isolated from clinical specimens in Al-Diwaniya/Iraq

Firas Srhan Abd Al- Mayahi*

Biology Department, College of the Science/ University of Al-Qadisiyah, P.O.Box.1895, Diwaniyah / Iraq

Received: June 6, 2020; Revised: Sept 15, 2020; Accepted: Nov 11, 2020

Abstract

Staphylococcus aureus (SA) plays a significant role in numerous serious life-threatening infections that present a major challenge to public health in controlling it, especially those resistant to methicillin (MR) known as (MRSA). These pathogens have resistance to other classes of antimicrobial agents including aminoglycoside molecules which mostly resist it through three types of medically significant enzymes: APH (3')-III, ANT (4')-I and (6')/APH(2"). In this paper, seventy-two MRAS were isolated from different lesions from Al-Diwaniya teaching hospital, and Maternity and Children teaching hospital, during the period from January to July 2018. Disc diffusion method, minimum inhibitory concentration(MIC), and bactericidal (MBC) were carried out to MRAS strains subjected to phenotype and genotype identification as well as to detect AMEs genes. Susceptibility of 29 drugs of MRAS strains was: 100% susceptible to vancomycin and chloramphenicol, but 100% resistant to penicillin, cefoxitin, ceftriaxone, aztreonam, and nitrofurantoin. Thus, a (72.2%) of MRAS were found to be either MDR or XDR including 20 aminoglycoside resistant (AR) strains. Multiple antibiotic resistance (MAR) index of a total of 20(100%)AR strains were recorded high values>0.2 ranged(0.48-0.83) from the maximum MAR index:1. Moreover, MIC and MBC values of vancomycin, for *S. aureus*, ranged from 2 µg/mL to 8 µg/mL. Phenotype resistance of MRSA strains to aminoglycoside molecules was: kanamycin 20(27.8%)tobramycin 18(25%); gentamicin 16(22.2%);amikacin 14(19.4%); and netilmicin 8(11.1%). PCR analysis led to all 100% MRSA caring for the *mecA* gene. Frequency of genes encoding aminoglycosides resistance *aac(6')/aph (2")*;80%, *aph (3')-IIIa*;45%, and *ant (4')-Ia*; 35%. The *aac(6')/aph (2")* and *ant (4')-Ia* genes was the only determinant of resistance in 5 and 1 strains respectively. Correlation between MRSA-AR strains and AMEs genes was 90%. In conclusion, MRSA strains harbouring the *mecA* gene are currently widely distributed in the Al-Diwaniya governorate. Co-production with AMEs may increase the risk of the spreading of multiple drug resistance clinical strains in communities and hospitals.

Keywords: MRSA, MDR, XDR, MAR, *mecA* gene, AME genes.

1. Introduction

Opportunistic *Staphylococcus aureus* (SA) infections are among the significant bacterial infections in the inpatients and outpatients (Goudarzi *et al.*, 2019c; Baines *et al.*, 2019; Xu *et al.*,2019; Kavusi *et al.*, 2019; Elshabrawy *et al.*, 2020) and the most serious worldwide especially which show resistance to methicillin (MR) drug abbreviated called MRSA (Peacock *et al.*, 2015; Gajdacs, 2019; Goudarzi *et al.*,2019e; Hadyeh *et al.*,2019 Navidinina *et al.*, 2019). MRSA has been classified within the high resistance priority tiers (WHO, 2017). Gene is responsible for MRSA named *mecA*(Cikman *et al.*, 2019). This gene is encoded to important protein in the synthesis of MRSA cell wall it is termed an acronym PBP2', while abbreviated SCC*mec* refers to the chromosomal elements transfer of this protein (Gajdacs, 2019). Therefore, MRSA infections cure is considered a major public health concern (Goudarzi *et al.*, 2019d). It causes much mortality of patients because

of multiple drug resistance to antimicrobial categories (Watkins *et al.*, 2019). This will reduce therapeutic options for infections caused by MRAS strains (EIFeky *et al.*, 2019). Aminoglycosides are mostly used in the treatment of infection that caused by staphylococcal bacteria when it combination with glycopeptide and β-lactam drugs (Kavusi *et al.*, 2019), while lincosamide, streptogramin B, and macrolide antibiotics are used as alternatives in treating such infections. (Razeghi *et al.*, 2019). Thus, currently, MRSA strains possess multiple drug resistance (MDR) including the previously mentioned(Khosravi *et al.*, 2017). Development of this resistance is strongly associated with the production of aminoglycoside modifying enzymes (AMEs) which is the majority mechanism to inactivate aminoglycoside molecules(Garneau-Tsodikova and Labby, 2016; Seyed-Marghaki *et al.*, 2019). *Aph (3')-IIIa*, *ant (4')-Ia* and *aac(6')/aph (2")* genes are encoded to the most prevalent types of AMEs which are aminoglycoside-3'-O-phosphoryltransferase III, aminoglycoside-4'-O-

* Corresponding author e-mail: firas.abd@qu.edu.iq.

nucleotidyltransferase I and aminoglycoside-6'-N-acetyltransferase/2''-phosphoryltransferases respectively (Ramirez and Tolmasky, 2010; Namvar *et al.*, 2017). Medically, in staphylococci these enzymes that are known abbreviation [(APH (3')-III, ANT (4')-I and (6'')/APH(2'')] are the most frequent AMEs and, which inactivate aminoglycosides of curative importance including respective kanamycin, tobramycin, and gentamicin (Klingenberg *et al.*, 2004; Szymanek-Majchrzak, *et al.*, 2018a). In different parts of the world including the Middle East, there are several neoteric studies expounding the growing prevalence of AMEs in MRSA strains (Goudarzi *et al.*, 2018; Seyedi-Marghaki *et al.*, 2019; Kavusi *et al.*, 2019; Beigverdi *et al.*, 2019). Nevertheless, in Iraq, the resistance problem of antimicrobial drugs is exacerbated by the overuse and misapply of them. There is no systematic national control of AR, scanty data is available to identify this problem, and there is no database of the genes encoding AMEs among gram-positive bacteria especially MRSA strains. So, the study aimed to assess the occurrence of genes encoding clinically important AMEs such as *aph (3')-IIIa*, *ant (4')-Ia*, and *aac(6'')/aph (2'')*, and to estimate the relationship between MRSA phenotypes of aminoglycosides resistance and the occurrence of genes responsible for this resistance in patients were attending to Al-Diwaniya hospitals.

2. Methodology

2.1. The population of the study, *S. aureus*, and MRSA identification

For the period January to July 2018, 72 MRSA were isolated from different lesions (wound, abscess, throat swab, blood, and urine) from randomly the 72 patients (without data related patients) were attending to Al-Diwaniya teaching hospital, and Maternity and Children teaching hospital which is two main hospitals in Al-Diwaniya province centre of Iraq. Bacterial isolates were identified depending on the traditional morphological (Gram stain/Himedia, India) and bacteriological tests (Haemolysis on blood agar, mannitol salt medium / Oxoid, UK, and coagulase production) in microbiology laboratory belong to the Faculty of Science- University of Al-Qadisiyah. The media were incubated at 37°C for 48 hours according to the method of (Forbes *et al.*, 2007). All *S. aureus* isolates were tested for detecting phenotypic MRSA depending on the cefoxitin disc-diffusion method (Kirby-Bauer) following (CLSI, 2019)

2.2. Antibacterial susceptibility testing

Antibacterial sensitivity patterns of the MRSA strains were performed through Bauer *et al.* (1966) and CLSI (2019), on Mueller-Hinton medium (Oxoid, UK) plates. Bacterial inoculum was modified according to the 0.5

Table 1: Oligonucleotides sequence of primers used to encode genes of AMEs and PBP2'.

Gene target	Forward primer (5' to 3')	Reverse primer (5' to 3')	Amplicon size (bp)	Annealing temperature	Reference
<i>mecA</i>	aaaatc gatg gtaaggttggc	agttctgcagtaccggattgc	533	55°C	Munger and Kelly, (1973)
<i>ac(6'')/aph (2'')</i>	gaa gta cgc aga aga ga	aca tgg caa gct cta gga	508	54°C	Choi <i>et al.</i> (2003)
<i>aph (3')-IIIa</i>	ggctaaaatgagaatcaccgg	ctttaaataatcatacagctcgcg	526	55°C	Vakulenko <i>et al.</i> (2003)
<i>ant (4')-Ia</i>	tggggatgatgtaagc	gcgtttgacacatccac	670	50°C	Riesen and Perreten. (2009).

McFarland tube. Antibacterial discs were selected carried out based on the (CLSI, 2019). All isolates tested for sensitivity of 10 molecules classes were divided into 29 antibacterial agents, which are: penicillin (PEN, 10 units), cefoxitin (FOX, 30 µg), ceftriaxone (CRO, 30 µg), ceftazidime (CAZ, 30 µg), cefotaxime (CTX, 30 µg), amoxicillin/clavulanic acid (AUG, 30 µg), kanamycin (K, 30 µg), netilmicin (NET, 30 µg), amikacin (AK, 30 µg), gentamicin (GM, 10 µg), tobramycin (TOB, 10 µg), aztreonam (ATM, 30 µg), ciprofloxacin (CIP, 5 µg), moxifloxacin (MXF, 5 µg), ofloxacin (OFX, 5 µg), norfloxacin (NOR, 10 µg), tetracycline (T, 30 µg), doxycycline (DXT, 30 µg), trimethoprim (TM, 5 µg), trimethoprim/sulfamethoxazole (SXT, 25 µg), chloramphenicol (C, 30 µg), nitrofurantoin (NI, 300 µg), vancomycin (VA, 30 µg), imipenem (IMP, 10 µg), erythromycin (E, 15 µg), rifampin (RA, 5 µg), teicoplanin (TEC, 30 µg), clindamycin (CD, 2 µg) and oxacillin (OX, 5 µg) (Bioanalyse, Turkey and Mast Diagnostics, UK). Furthermore, the MRSA strains were stratified to MDR and XDR based on (Magiorakos *et al.*, 2012). A laboratory stock culture of genus *S. aureus* ATCC 25923 was used as a quality control organism to confirm the accuracy of the antibacterial disks. Strain giving intermediate sensitivity was calculated as resistant. MICs and MBCs values were detected (Andrews, 2001) and calculation of the multiple antibiotic resistance (MAR) index of 20 MRSA-AR was conducted based on (Krumpal, 1983; Riaz *et al.*, 2011).

2.3. Isolation of deoxyribonucleic acid

DNA isolation was perfect using a specific procedure of (+)ve bacteria (proteinase K) and according to the manufacturer's instructions of Kit (Geneaid, USA).

2.4. PCR analysis

PCR assay was done by components that were accumulated in a PCR tube and mixed under sterile conditions on an ice bag. The reaction was performed using a 25 µl mixture including 12.5 µl Go Tag Green Master mix (Promega, USA), 2.5 µl of 10 µM each primer (Macrogen, Korea), 5 µl of genomic DNA, and 2.5 µl nuclease-free water. The PCR program was done with a (Biometra, Germany). Universal specific primer sequence listed in table 1, the amplification conditions of each primer of *ant (4')-Ia*, *mecA*, *aph (3')-IIIa*, *aac(6'')/aph (2'')* genes describe in the same references in table 1. The amplifications were electrophoresed (Biometra, Germany) through 1.5% agarose gel pretreated with ethidium bromide, utilizing a UV imager (Biometra, Germany). The results were documented. Times of electrophoresis were at 75 volts for 90 minutes. Molecular weight DNA markers were used (Ladder 100 bp Promega, USA).

2.5. Analysis

χ^2 test was used to determine the significant frequencies of resistance results. P-value < 0.01, Prism 5 (Graphpad Software Inc., San Diego, CA, USA).

3. Results

72 MRSA strains were obtained from patients who were suffering from various infections. The main different lesions of this causative agent were: urine 32 (44.5%), wounds 18(25), abases 13 (18.0%), blood cultures 5 (6.9%), and throat swabs 4 (5.6%). Of these 72.2% were found to be either MDR or XDR, thus a (44/72; 61.1%) of MRSA were found to be MDR while the remaining (8/72;11.1%) were XDR. Whole, 100% strains were sensitive to vancomycin(MICs and MBCs values ranged 2 μ g/mL to 8 μ g/mL.) and chloramphenicol. Strains

exhibited significant frequencies of antibacterial agents resistance (P < 0.01)(Figure 1).The highlight indicates cases considered to be resistant to the respective drugs. Penicillin, cefoxitin, ceftriaxone, aztreonam, and nitrofurantoin showed a resistance of 100% from all the isolates. A high rate of resistance (94.5, 88.9, 83.3, 79.2, 77.8, 73.6, and 61.2)% showed that *S. aureus* to ceftazidime, cefotaxime, trimethoprim, erythromycin, oxacillin, tetracycline, and teicoplanin respectively. The resistance of clindamycin and Amoxicillin/clavulanic acid were 37.5% and 30.6%. Also, the most effective of antibacterial agents were imipenem, rifampin, ofloxacin, doxycycline, moxifloxacin, ciprofloxacin, norfloxacin and trimethoprim/sulfamethoxazole with resistance rates 11.1%, 11.1%, 22.2%, 22.2%, 26.4%,27.8%, 27.8% and 33.3% (Figure 1).

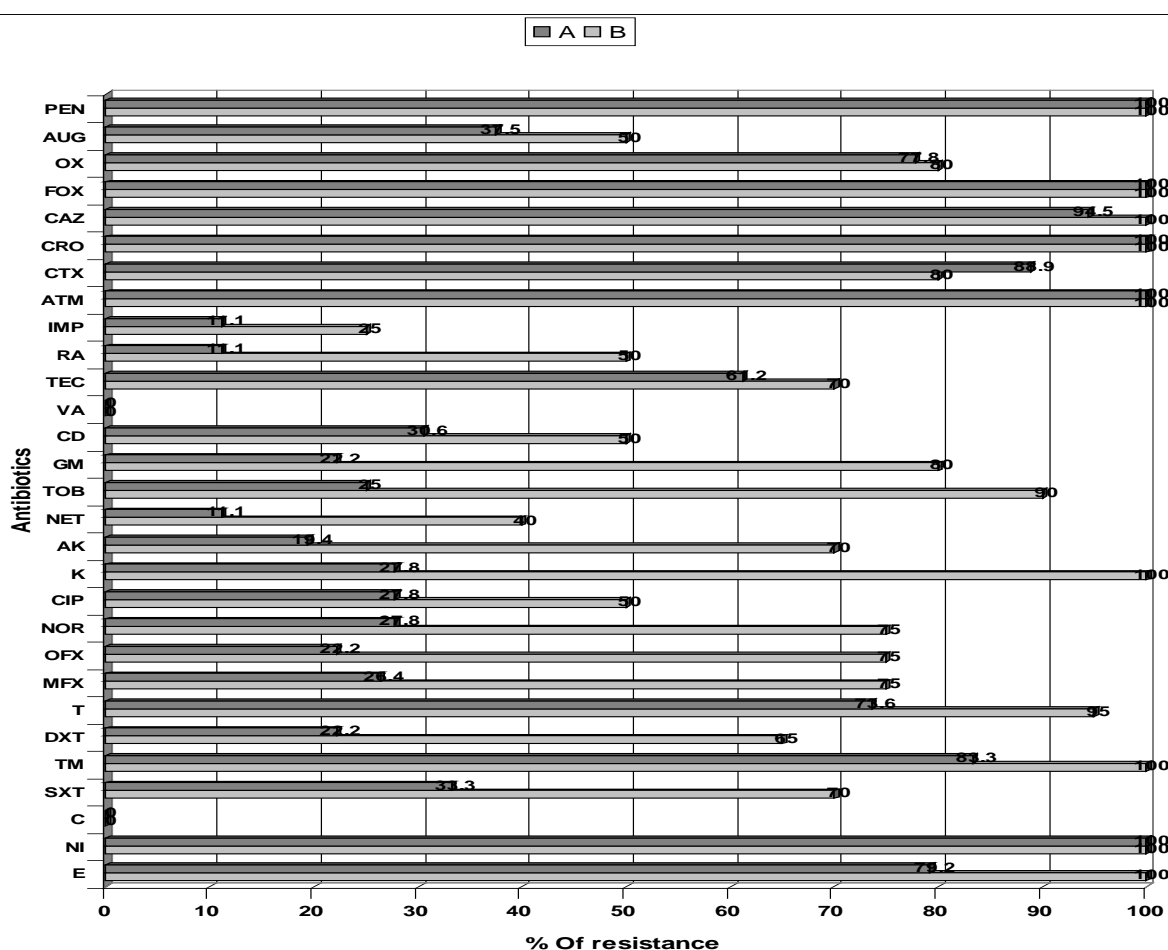


Figure 1. Comparison between the rates of resistance for 72 strains of MRSA(A) and 20 strains of MRSA which show resistance to aminoglycosides(B).

PEN, penicillin; AUG, amoxicillin-clavulanic acid; OX, oxacillin; FOX, cefoxitin; CAZ, ceftazidime; CRO, ceftriaxone; CTX, cefotaxime; ATM, aztreonam; IMP, imipenem; RA, rifampin; TEC teicoplanin; VA, vancomycin; CD, clindamycin; GM, gentamicin; TOB, tobramycin; NET, netilmicin; AK, amikacin; K, kanamycin; CIP, ciprofloxacin; NOR, norfloxacin; OFX, ofloxacin; MFX, moxifloxacin; T, tetracycline; DXT, doxycycline; TM, trimethoprim; SXT, trimethoprim/sulfamethoxazole; C, chloramphenicol; NI, nitrofurantoin; E, erythromycin.

ethoprim/sulfamethoxazole; C, chloramphenicol; NI, nitrofurantoin; E, erythromycin.

The aminoglycosides resistance rate among the tested *S. aureus* strains ranged from 27.8%-11.1%. The present study showed that netilmicin was the most potent aminoglycoside; its overall potency over the isolated *S. aureus* was 11.1%, while amikacin, gentamicin, tobramycin, and kanamycin were 19.4%, 22.2%, 25%, and 27.8% respectively. The full (100%) dissemination of the *mecA* gene in MRSA strains is shown in (Figure2).

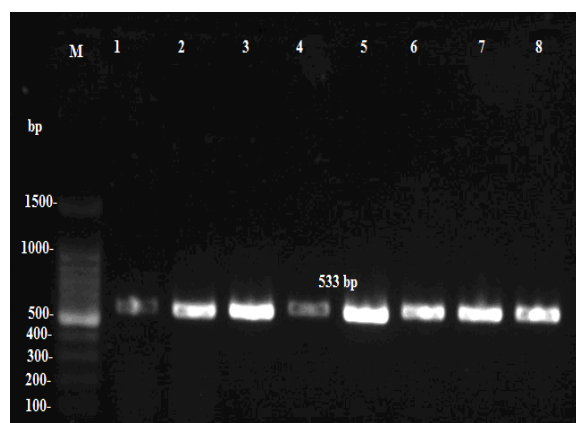


Figure 2. Image of electrophoresis gel of *S. aureus*. Lane M, PCR ladder (100-1500 bp), amplified products of the *mecA* gene (533 bp). Lanes (1-8) positive results.

Out of 20, MRSA was AR eighteen (90%) carrying at minimum 1 of genes encoded AR. The most common of genes encoded AMEs were *aac(6')/aph(2'')*; 80%, *aph(3')-IIIa*; 45%, and *ant(4')-Ia*; 35% (Figure 3,4 and 5 respectively).

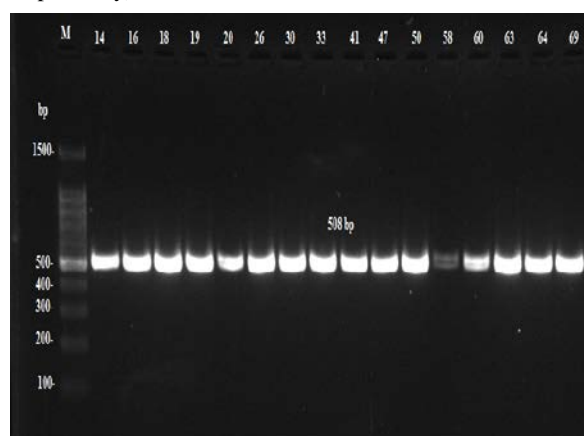


Figure 3. Image of electrophoresis gel of *S. aureus*. Lane M, PCR ladder (100-1500 bp), amplified products of the *ac(6')/aph(2'')* gene (508 bp). Lanes (14,16,18,19,20,26,30,33,41,47,50,58,60,63,64,69) positive results.

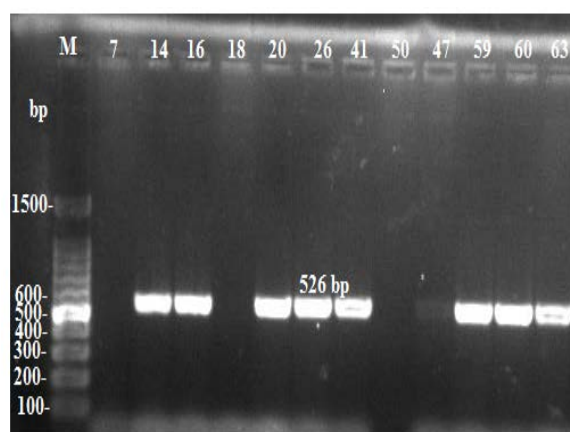


Figure 4. Image of electrophoresis gel of *S. aureus*. Lane M, PCR ladder (100-1500 bp), amplified products of the *aph(3')-IIIa* gene (526bp). Lanes (14,16, 20,26,41,47,59, 60,63) positive results, lanes (7,18,50) negative results.

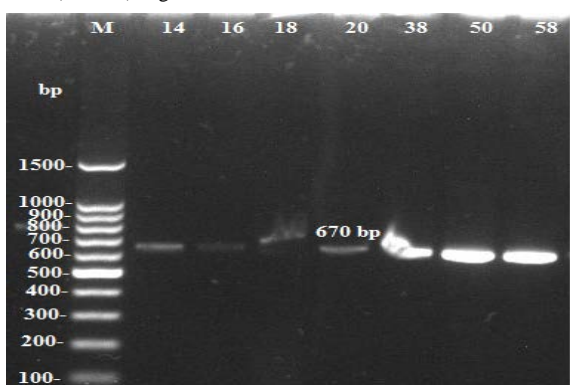


Figure 5. Image of electrophoresis gel of *S. aureus*. Lane M, PCR ladder (100-1500 bp), amplified products of the *ant(4')-Ia* gene (670 bp). Lanes (14, 16,18, 20,26,38,50,58) positive results.

Interestingly, it is observed that all(100%) strains in which positive results of AR genes were resistant to at least three aminoglycoside molecules. The highest resistance of 20 AR isolates compares with 72 MRSA isolates against all drugs, especially aminoglycoside as mentioned in figure 1. 100% of MRSA-AR were either MDR(12/20; 60%) or XDR(8/20; 40%). The dissemination, frequency of co-occurrence genes encoding AMEs, and relationship within phenotypic AR among MRSA harboring *mecA* gene are listed in Table (2).

Table 2: Phenotypic and molecular analysis of aminoglycosides resistance patterns possessed 20 MRSA strains harboring the *mecA* gene.

No.	Phenotypic	No. (%)	Genotypic	No. (%)	Profile type
G1	NET, AK, GM, TOB, K	6(30)	<i>aac(6')/aph(2'')</i>	6(33.3)	3G2,2G3,1G4
G2	AK, GM, TOB, K	6(30)	<i>aph(3')-IIIa</i>	0	-
G3	NET, GM, TOB, K	2(10)	<i>ant(4')-Ia</i>	1(5.6)	G6
G4	GM, TOB, K	2(10)	<i>aac(6')/aph(2'')</i> + <i>aph(3')-IIIa</i>	5(27.8)	3G1,2G2
G5	AK TOB, K,	1(5)	<i>aac(6')/aph(2'')</i> + <i>ant(4')-Ia</i>	2(11.1)	1G2,1G4
G6	TOB, K	1(5)	<i>aph(3')-IIIa</i> + <i>ant(4')-Ia</i>	1(5.6)	G5
G7	K	2(10)	<i>aac(6')/aph(2'')</i> + <i>aph(3')-IIIa</i> + <i>ant(4')-Ia</i>	3(16.7)	3G1
Total		20(100)		18(100)	

The most frequent 11/18(61.1%) of MRSA strains which comprise AMEs genes were as combinations or simultaneously. Correlation between the AR patterns and their presence of plasmid-mediated AR genes among MRSA isolates tested are shown in (Table 2 and 3). The results showed that there is 100% compatibility between

the presence of *aac(6')/aph(2'')* and resistance to gentamicin. It was discovered in all strains resistant to gentamicin (Table 3). Lastly, only 2 strains of MRSA were resistant to kanamycin did not give any result with AMEs genes.

High values >0.2 ranged (0.48-0.83) from the maximum MAR index (1) were documented in all 20 (100%) MRSA-AR strains which summarize in figure 6.

Moreover, the relationship between phenotypic resistance indicators and AR genes among MRSA strains was mentioned in Table(4)

Table 3: Relatedness between phenotypic and the main molecular description of aminoglycosides resistance patterns in a total of 18 MRSA strains harboring AMEs genes.

Genotypic description of AMEs	No. (%)	(%) Of phenotypic expression AMEs				
		NET	AK	GM	TOB	K
<i>aac(6')/aph(2'')</i>	16(80)	50	75	100	100	100
<i>aph(3')-IIIa</i>	9(45)	66.7	100	88.9	100	100
<i>ant(4')-Ia</i>	7(35)	42.8	71.4	71.4	100	100

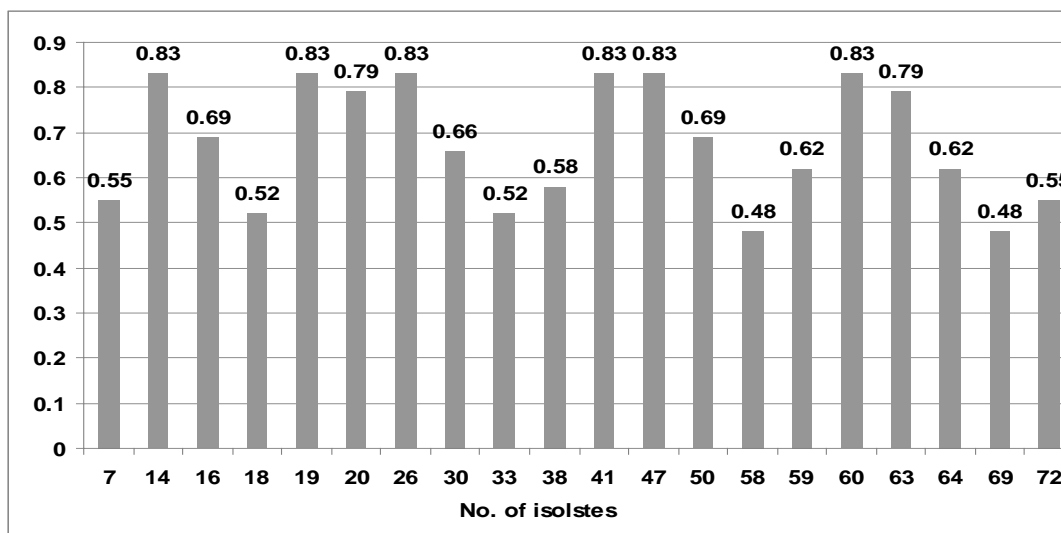


Figure 6. MAR indexes of 20 aminoglycosides resistance MRSA isolates.

Table 4: Dissemination of multiple resistance of drug patterns among MRSA-AR genes.

No. of strain	<i>mecA</i> gene	Phenotypic profile		AMEs genes profile		
		MDR / XDR	MAR index	<i>aac(6')/aph(2'')</i>	<i>aph(3')-IIIa</i>	<i>ant(4')-Ia</i>
S7	+	MDR	0.55	-	-	-
S14	+	XDR	0.83	+	+	+
S16	+	MDR	0.69	+	+	+
S18	+	MDR	0.52	+	-	+
S19	+	XDR	0.83	+	-	-
S20	+	XDR	0.79	+	+	+
S26	+	XDR	0.83	+	+	-
S30	+	MDR	0.66	+	-	-
S33	+	MDR	0.52	+	-	-
S38	+	MDR	0.58	-	-	+
S41	+	XDR	0.83	+	+	-
S47	+	XDR	0.83	+	+	-
S50	+	MDR	0.69	+	-	+
S58	+	MDR	0.48	+	-	-
S59	+	MDR	0.62	-	+	+
S60	+	XDR	0.83	+	+	-
S63	+	XDR	0.79	+	+	-
S64	+	MDR	0.62	+	-	-
S69	+	MDR	0.48	+	-	-
S72	+	MDR	0.55	-	-	-
Total	20			16	9	7

4. Discussion

Antimicrobial stewardship is important to prevent the spread and expansion of MDR strains and to overcome the development of increased resistance to antibiotics in general and aminoglycoside in particular, and continued national surveillance programs are crucial. Aminoglycosides are broad-spectrum bactericidal antibiotics of high potency that have been traditionally used for the treatment of serious and of life-threatening Gram-negative and some Gram-positive infections (Zacharczuk *et al.*, 2011; Becker and Cooper, 2013; Garneau-Tsodikova and Labby, 2016). In different parts of the world including in Iraq, aminoglycosides are used for treating severe infections caused by Gram-Positive bacteria. As a result, multiple resistance determinants to these antimicrobial agents have emerged in various pathogenic microbes including MRSA. This organism is a major public health concern representing about 60% of *S. aureus* isolated from hospitalized patients in countries such as the USA and Brazil in the last years (Dos Reis *et al.*, 2020).

72 MRSA strains were obtained from patients who were suffering from various infections. The main different lesions of this causative agent were: urine 32 (44.5%), wounds 18(25), abscesses 13 (18.0%), blood cultures 5 (6.9%), and throat swabs 4 (5.6%). Of these 72.2% found to be either MDR or XDR, thus a (44/72; 61.1%) of MRSA were found to be MDR while the remaining (8/72;11.1%) were XDR. The full (100%) dissemination of the *mecA* gene in MRSA strains are in (Figure 2 and Table 4). This finding matches with other reports in West Bank-Palestine and Sri Lanka that found all 112 and 94 *S. aureus* (100%) isolated from different lesions as MRSA strains were carrying *mecA* gene (Hadyeh *et al.*, 2019; McTavish *et al.*, 2019) respectively. This agrees with Goudarzi *et al.* (2019b) in Iran as 78.6% (66/84) of MRSA strains were found to be MDR. The vast majority of our results were matched with another report of MRSA strains isolated from the holy shrine in Najaf, Iraq which found that most strains (100%) were resistant to penicillin, ceftriaxone, ceftazidime, (72.7%) to erythromycin, and the most susceptible (100%) to vancomycin, chloramphenicol, (72.3%) to gentamicin and 8/11 (72.7%) of MRSA strains were found to be MDR (Al-Mohana *et al.*, 2012). Based on the above results, it can be said that vancomycin is considered the best choice of treatment MRSA infections in various parts of the world (Szymanek-Majchrzak *et al.*, 2018b) including Iraq, despite some resistance cases that have been observed in this area (Al-Jumaily *et al.*, 2012; ElFeky *et al.*, 2019) and the world (Szymanek-Majchrzak *et al.*, 2018b). Also, these results were close to other results of a study documented in Sulaimani city, Iraq concerning the resistance MRSA of a β -lactams drug (Al-Jumaily *et al.*, 2012). Moreover, resistance of β -lactam, vancomycin, and gentamicin was documented in MRSA strains which were isolated from West Bank-Palestine (Hadyeh *et al.*, 2019). Due to the widespread and indiscriminate use of antibiotics in treatment, a major problem has emerged as the multiple resistance of these drugs from different bacterial species, especially *S. aureus*. This maybe via the biofilms formation which increases from the pathological ability (Gomes *et al.*, 2019). Interestingly, in this

investigation there was a low level of AR among MRSA strains compared with other studies in Iraq and other parts of the world, which may be explained by a decrease in the number of MRSA strains from the various regions of central Iraq or by low-level description of this drug in the treatment infections of this pathogen. For more than half a century, aminoglycoside has been mainly used against gram-negative and some gram-positive bacterial infections (Garneau-Tsodikova and Labby, 2016), and this reinforces the second reason. The first cause may be close to reality and corresponds to an antibiotic sensitivity analysis performed in the Al-Diwaniya governorate (unpublished) which documented that approximately 30.5% (7/23) of MRSA strains were gentamicin resistant (Al-Mayahi, 2018). Thus, ElFeky *et al.* (2019) who found that 63% (63/100) of MRSA strains were resistant to gentamicin. The resistance pattern in the Al-Diwaniya governorate is somewhat harmonious with other investigations in the Najaf governorate centre Iraq, which showed that MRSA strains were 27.7% (15/54) resistant to gentamicin (Al-Mohana *et al.*, 2012). Aminoglycoside molecules still have significant effects alone or in combination with other molecules in treating infections causing staphylococci, despite the emergence of resistance to them in different parts of the world (Kavusi *et al.*, 2019). In a previous study, Goudarzi *et al.* (2019e) found that MRSA strains and AMEs production have been developed rapid resistance to a wide range of drugs including tetracyclines, and this agreed with our study at a rate of resistance (73.6%). High values >0.2 ranged (0.48-0.83) from the maximum MAR index Baines *et al.* (2018) were documented in all 20 (100%) MRSA-AR strains. A MAR index resistance to >0.20 antibiotics indicates that bacteria originate from an environment where antibiotics are freely available, leading to a high potential for misuse and a 'high-risk' source of contamination (Krumpernam, 1983; Riaz *et al.*, 2011). There is scanty information regarding the level of antibiotics resistant to MRSA strains associated with multiple infections in Iraq, thus possibly posing a public health challenge for physicians. Consequently, this study determined the MAR index of these isolates. However, the elevation of MAR index values was observed in our investigation (Figure 5 and Table 4). All MRSA-AG strains had MAR index of >0.20, confirming that there was widespread use of antibiotics and high selective pressure in the Al-Diwaniya population. The MAR indices obtained in the present study is a probable signal that a very major ratio of the MRSA strains was displayed to numerous antimicrobial drugs. The high MAR identified in the present research warns us that any use of antibiotics in treatment should be preceded by an accurate diagnosis of the causative agents, followed by an antimicrobial sensitivity test. Such a thing will not only contribute to the effective use of these drugs but also will control the prevalence of resistant isolates of antibiotics in Iraqi hospitals and communities.

Out of 20, MRSA was AR eighteen (90%) carrying at minimum 1 of genes encoded AR. The most genes encoded AMEs common were namely *aac(6')/aph(2'')*; 80%, *aph(3')-IIIa*; 45%, and *ant(4')-Ia*; 35% (Tables 2 and 4). Many reports from Iran have reported that the *aac(6')/aph(2'')* gene was the most frequent AMEs gene followed by *aph(3')-IIIa* gene and *ant(4')-Ia* gene in MRSA isolates (Fatholahzadeh *et al.*, 2009; Emaneini *et*

al., 2013; Mohammadi *et al.*, 2014; Khosravi *et al.*, 2017; Khoramrooz *et al.*, 2017; Seyedi-Marghaki *et al.*, 2019; Goudarzi *et al.*, 2019d), from Turkey (Ardic *et al.*, 2006), from Australia (Baines *et al.*, 2019), from India (Perumal *et al.*, 2016) and Europe (Vanhoof *et al.*, 1994). However, the prevalence of MRSA strains containing *aac(6')/aph(2'')* gene in Al-Diwaniya (80%), is similar with Goudarzi *et al.* (2019a), Szymanek-Majchrzak, *et al.* (2018a), Baines *et al.* (2019), Kavusi *et al.* (2019), Mohammadi *et al.* (2014) and Mahdiyoun *et al.* (2016) in Iran (80%), Europe (80.5%), Australian clade (79.7%), Iran (78.3%), (77.8%) and (77%) respectively, and is less compared to similar studies in Iran (97.22%) (Khoramrooz *et al.*, 2017) and Asian-Australian clade (93.2%) (Baines *et al.*, 2019). The results showed there is 100% compatibility between the presence of *aac(6')/aph(2'')* and resistance to gentamicin (Table 3). It was discovered in all strains resistant to gentamicin. This concordance matches with previous researches (Choi *et al.*, 2003; Yadegar *et al.*, 2009). The present investigation shows that *aph(3')-IIIa* gene was the second dominant gene (45%), and was in agreement with the reports from, Australia (45.0%) (Baines *et al.*, 2019), Europe (44%) (Mlynarczyk *et al.*, 2010), Iran (46.3%) (Goudarzi *et al.*, 2019e) and (46.7%) (Goudarzi *et al.*, 2019c), while Seyedi-Marghaki *et al.* (2019) and Khoramrooz *et al.* (2017) in Iranian work documented rate of this gene in (19% and 61.1%) of MRSA strains. Dissemination of *ant(4')-I* was detected as 35% (7/20) (Tables 2 and 4). This was similar with other reports from Australia 34.1% (Baines *et al.*, 2019), Iran 38.6% (Goudarzi *et al.*, 2018), and less than the ratio mentioned in a big Japanese report (84.5%) (Ida *et al.*, 2001) and Europe (55.3%) (Szymanek-Majchrzak, *et al.*, 2018b). The presence of the *aac(6')/aph(2'')*, *aph(3')-IIIa* and *ant(4')-Ia* genes was sufficient to express the resistance phenotype (100%) to GM/TOB/K, AK/TOB/K and TOB/K respectively (Table 3). AAC(6')/APH(2'') enzyme grant resistance to aminoglycosides molecules including GM/TOB/K, APH(3')-IIIa grant resistance AK/TOB/K, and ANT(4')-Ia enzyme grant resistance to TOB/K (Vakulenko and Mobashery, 2003). The relatedness between phenotypic and genotypic AR with MRSA were 27.8% and 25%. This relationship was reported in other studies such as (Yadegar *et al.*, 2009; Mohammadi *et al.*, 2014; Khosravi *et al.*, 2017), where the last study recorded a high correlation (72.7%).

5. Conclusion

In conclusion, this is the first paper that provided baseline prevalence data on the presence of AMEs genes in MRSA strains containing the *mecA* gene in Al-Diwaniya governorate in the centre of Iraq which reached alarming tiers; thus, Aminoglycosides should be used carefully by physicians. The execution of a local and global monitoring system to observe antibiotic resistance, particular aminoglycosides, and growing consciousness of AMEs genes among physicians are necessary for guiding empirical therapy-specific measures against a specific pathogen

Acknowledgement

Thank you for the microbiology laboratory staff at the Al-Diwaniya province hospitals for help with collection specimens, and also thank you for the microbiology laboratory in the Department of Biology in the College and University of the researcher for help in providing a place for research.

Funding

None.

Conflict of interest

None.

Authors' contribution sections

Not applicable.

References

- Al-Jumaily EF, Mohamed DA and Khanaka HH. 2012. Molecular epidemiology and Antibiotic susceptibility patterns of clinical strains of methicillin resistant *Staphylococcus aureus* (MRSA) in Sulaimani city-Iraq. *Glo Adv Res J Microbiol*, **1**(6): 81- 89.
- Al-Mayahi MHM .2018. Bacteriological and molecular study of *Staphylococcus aureus* bacteria isolated from women breast abscess in Al Qadisiyah governorate. MSc dissertation, The Al-Qadisiya University, Diwaniya, Iraq.
- Al-Mohana AM, Al-Charrakh AH, Nasir FH and Al-Kudhairi MK. 2012. Community-acquired methicillin-resistant *Staphylococcus aureus* carrying *mecA* and Panton-Valentine leukocidin (PVL) genes isolated from the holy shrine in Najaf, Iraq. *J Bacteriol Res*, **4**(2):15-23.
- Andrews JM. 2001. Determination of minimum inhibitory concentration. *J Antimicrob Chemother*, **48**(S1):5-16.
- Ardic N, Sareyyupoglu B, Ozyurt M, Haznedaroglu T and Ilga U. 2006. Investigation of aminoglycoside modifying enzyme genes in methicillin-resistant staphylococci. *Microbiol Res*, **161**(1):49-54.
- Baines SL, Jensen SO, Firth N, da Silva AG, Seemann T, Carter GP, Williamson DA, Howden BP and Stinear TP. 2019. Remodeling of pSK1 family plasmids and enhanced chlorhexidine tolerance in a dominant hospital lineage of methicillin-resistant *Staphylococcus aureus*. *Antimicrob Agents Chemother*, **63**(5): e02356-18.
- Bauer AW, Kirby WMM, Sherris JC and Turck M. 1966. Antibiotic susceptibility testing by a standardized single disc method. *Am J Clin Pathol*, **45**:493-496.
- Becker B and Cooper MA. 2013. Aminoglycoside antibiotics in the 21st century. *ACS Chem Biol*, **8**:105-115.
- Beigverdi R, Sattari-Maraji A, Jabalameli F and Emaneini M. 2019. Prevalence of Genes Encoding Aminoglycoside-Modifying Enzymes in Clinical Isolates of Gram-Positive Cocci in Iran: A Systematic Review and Meta-analysis. *Microb Drug Resist*, **26**(2): 126-135.
- Choi SM, Kim S-H, Kim H-J, Lee D-G, Choi J-H, Yoo J-H, Kang J-H, Shin W-S and Kang M-W. 2003. Multiplex PCR for the detection of genes encoding aminoglycoside modifying enzymes and methicillin resistance among *Staphylococcus* species. *J of Korean Med Sci*, **18**(5):631-636.

- Cikman A, Aydin M, Gulhan B, Karakeçili F, Kurtoglu MG, Yuksekçaya S, Parlak M, Gultepe BS, Cicek AC, Bilman FB, Ciftci IH, Kara M, Atmaca S and Ozekinci T. 2019. Absence of the *mecC* gene in methicillin-resistant *Staphylococcus aureus* isolated from various clinical samples: The first multi-centered study in Turkey. *J Infect Public Health* **12**: 528-533.
- Clinical and Laboratory Standards Institute. 2010. Performance standards for antimicrobial susceptibility testing; twentieth ed. Informational supplement approved standard M07-A8. Wayne, PA, USA.
- Clinical and Laboratory Standards Institute. 2019. Performance standards for antimicrobial susceptibility testing; twentieth nine ed. Informational Supplement. Approved standard M100. Wayne, PA, USA.
- Dos Reis SV, de Couto NMG, Brust FR, Trentin DS, da Silva JKR, Arruda MSP, Gnoatto SCB and Macedo AJ. 2020. Remarkable capacity of brosimine b to disrupt methicillin-resistant *Staphylococcus aureus* (MRSA) preformed biofilms. *Microb Pathog*, **140**: 103967.
- EIFeky DS, Awad AR, Elshobaky MA and Elawady BA. 2019. Effect of Ceftaroline, Vancomycin, Gentamicin, Macrolides, and Ciprofloxacin against Methicillin-Resistant *Staphylococcus aureus* Isolates: An In Vitro Study. *Surg Infect*, **21**(2):150-157
- Elshabrawy MA, Abouelhag HA, Khairy EA, Marie HSh. and Hakim AS. 2020. Molecular divergence of *Staphylococcus aureus* isolated from Dogs and Cats. *Jordan J Biol Sci*, **13**(2):139-144.
- Emaneni M, Bigverdi R, Kalantar D, Soroush S, Jabalameli F, Khoshnab BN, Asadollahi P and Taherikalani M. 2013. Distribution of genes encoding tetracycline resistance and aminoglycoside modifying enzymes in *Staphylococcus aureus* strains isolated from a burn center. *Ann Burns Fire Disasters*, **26**(2): 76-80.
- Fatholahzadeh B, Emaneni M, Feizabadi MM, Sedaghat H, Aligholi M, Taherikalani M and Jabalameli F. 2009. Characterisation of genes encoding aminoglycoside-modifying enzymes among methicillin-resistant *Staphylococcus aureus* isolated from two hospitals in Tehran, Iran. *Int J Antimicrob Agents*, **33**(3):264-265.
- Forbes BA, Sahn DF and Weissfeld AS. 2007. Bailey and Scott's **Diagnostic Microbiology**, twelfth ed. Mosby Inc, Maryland Heights, Mo, USA.
- Gajdác M. 2019. The continuing threat of methicillin-resistant *Staphylococcus aureus*. *Antibiotics*, **8**(2):52.
- Garneau-Tsodikova S and Labby KJ. 2016. Mechanisms of resistance to aminoglycoside antibiotics: overview and perspectives. *Med Chem Comm*, **7**:11-27.
- Gomes F, Martins N, Ferreira ICFR and Henriques M. 2019. Antibiofilm activity of hydromethanolic plant extracts against *Staphylococcus aureus* isolates from bovine mastitis. *Heliyon*, **5**: e01728
- Goudarzi M, Navidinia M, Beiranvand E and Goudarzi H. 2018. Phenotypic and molecular characterization of methicillin-resistant *Staphylococcus aureus* clones carrying the Pantone-Valentine leukocidin genes disseminating in Iranian hospitals. *Microb Drug Resist*, **24**(10):1543-1551.
- Goudarzi M, Eslami G, Rezaee R, Heidary M, Khoshnood S, and Nia RS. 2019a. Clonal dissemination of *Staphylococcus aureus* isolates causing nosocomial infections, Tehran, Iran. *Iran J Basic Med Sci*, **22**(3), 238-245.
- Goudarzi M, Fazeli M, Eslami G, Pouriran R, Hajikhani B, and Dadashi M. 2019b. Genetic Diversity Analysis of Methicillin-resistant *Staphylococcus aureus* Strains Isolated from Intensive Care Unit in Iran. *Oman Med J*, **34**(2), 118-125.
- Goudarzi M, Kobayashi N, Hashemi A, Fazeli M and Navidinia M. 2019c. Genetic Variability of Methicillin Resistant *Staphylococcus aureus* Strains Isolated from Burns Patients. *Osong Public Health Res Perspect*, **10**(3):170-176.
- Goudarzi M, Mohammadi A, Goudarzi H, Fazeli M and Sabzehali F. 2019d. Genetic Variability and Integron Occurrence in Methicillin Resistant *Staphylococcus aureus* Strains Recovered from Patients with Urinary Tract Infection. *Arch Pediatr Infect Dis*, e86189:1-9.
- Goudarzi M, Razeghi M, Dadashi M, Miri M, Hashemi A, Amirpour A, Nasiri MJ and Fazeli M. 2019e. Distribution of SCC*mec* types, tetracycline and aminoglycoside resistance genes in hospital-associated methicillin-resistant *Staphylococcus aureus* strains. *Gene Reports*, **16**:100454.
- Hadyeh E, Azmi K, Seir RA, Abdellatif I and Abdeen Z. 2019. Molecular Characterization of Methicillin Resistant *Staphylococcus aureus* in West Bank-Palestine. *Front Public Health*, **7**(130): 1-9.
- Ida T, Okamoto R, Shimauchi C, Okubo T, Kuga A and Inoue M. 2001. Identification of aminoglycoside-modifying enzymes by susceptibility testing: epidemiology of methicillin-resistant *Staphylococcus aureus* in Japan. *J Clin Microbiol*, **39**(9): 3115-3121.
- Kavusi M, Nematimansour F and Mahdiyoun M. 2019. The prevalence of antibiotic resistance in methicillin-resistant *Staphylococcus aureus* and the determination of aminoglycoside resistance gene *aac(6')-Ie/aph(2'')* isolated from hospitalized patients in Imam Hossein, Loghman Hakim, and Pars hospitals in Tehran using polymerase chain reaction. *SJIMU*, **27**(1):85-94.
- Khoramrooz SS, Dolatabad SA, Dolatabad FM, Marashifard M, Mirzaei M, Dabiri H, Haddadi A, Rabani SM, Shirazi HRG and Darban-Sarokhali D. 2017. Detection of tetracycline resistance genes, aminoglycoside modifying enzymes, and coagulase gene typing of clinical isolates of *Staphylococcus aureus* in the Southwest of Iran. *Iran J Basic Med Sci*, **20**(8):912-919.
- Khosravi AD, Jenabi A and Montazeri EA. 2017. Distribution of genes encoding resistance to aminoglycoside modifying enzymes in methicillin-resistant *Staphylococcus aureus* (MRSA) strains. *Kaohsiung J Med Sci*, **33**(12): 587-593.
- Klingenberg C, Sundsfjord A, Rønnestad A, Mikalsen J, Gaustad P and Flægstad T. 2004. Phenotypic and genotypic aminoglycoside resistance in blood culture isolates of coagulase-negative staphylococci from a single neonatal intensive care unit, 1989-2000. *J Antimicrob Chemother*, **54**:889e96.
- Krumpnam PH. 1983. Multiple antibiotic resistance indexing *Escherichia coli* to identify risk sources of fecal contamination of foods. *Appl Environ Microbiol*, **46** : 165-170.
- Magiorakos AP, Srinivasan A, Carey RB, Carmeli Y, Falagas ME, Giske CG, Harbarth S, Hindler JF, Kahlmeter G, Olsson-Liljequist B, Paterson DL, Rice LB, Stelling J, Struelens MJ, Vatopoulos A, Weber JT and Monnet DL. 2012. Multidrug-resistant, extensively drug-resistant and pandrug-resistant bacteria : an international expert proposal for interim standard definitions for acquired resistance. *Clin Microbiol Infect*, **18**(3):268-281.
- Mahdiyoun SM, Kazemian H, Ahanjan M, Hourii H and Goudarzi M. 2016. Frequency of aminoglycoside-resistance genes in methicillin-resistant *Staphylococcus aureus* (MRSA) isolates from hospitalized patients. *Jundishapur J Microbiol*, **9**(8): e35052.
- McTavish, SM, Snow SJ, Cook EC, Pichon B, Coleman S, Coombs GW, Pang S, Arias CA, Díaz L, Boldock E, Davies S, Udukala M, Kearns AM, Siribaddana S and de Silva TI. 2019. Genomic and epidemiological evidence of a dominant Pantone-Valentine leukocidin-positive Methicillin Resistant *Staphylococcus aureus* lineage in Sri Lanka and presence among

- isolates from the United Kingdom and Australia. *Front Cell Infect Microbiol*, **9**(123):1-6.
- Młynarczyk A, Szymanek-Majchrzak K and Młynarczyk G .2010. Occurrence of aminoglycoside transferase genes in methicillin-resistant strains of *Staphylococcus aureus*. *Med Dośw Mikrobiol*, **62**(4):289-295.
- Mohammadi S, Sekawi Z, Monjezi A, Maleki M-H, Soroush S, Sadeghifard N, Pakzad I, Azizi-Jalilian F, Emaneini M, Asadollahi K, Pourahmad F, Zarrilli R and Taherikalani M.2014. Emergence of SCCmec type III with variable antimicrobial resistance profiles and spa types among methicillin-resistant *Staphylococcus aureus* isolated from healthcare-and community-acquired infections in the west of Iran. *Int J Infect Dis*, **25**:152-158.
- Munger LL and Kelly BL.1973. Staphylococcal granulomas in a Leghorn hen. *Avian Dis*, **17**:858-860.
- Namvar AE, Havaei SA, Azimi L, Lari AR and Rajabnia R .2017. Molecular characterization of *Staphylococcus epidermidis* isolates collected from an intensive care unit. *Arch Pediatr Infect Dis*, **5**(2):e36176.
- Navidinia M, Amirpour A, Goudarzi M, Pouriran R, and Tabrizi MS. 2019. Diversity of prophages, spa, and SCCmec types in Methicillin-Resistant *Staphylococcus aureus* strains isolated from burn patients: A study in a referral burn hospital in Tehran, Iran. *Mol Genet Microbiol Virol*, **34**:124-130.
- Peacock SJ and Paterson GK.2015.Mechanisms of methicillin resistance in *Staphylococcus aureus*. *Annu Rev Biochem*, **84**(1):577-601.
- Perumal N, Murugesan S and Krishnan P .2016. Distribution of genes encoding aminoglycoside-modifying enzymes among clinical isolates of methicillin-resistant staphylococci. *IJMM*, **34**(3): 350.
- Ramirez MS and Tolmasky ME .2010. Aminoglycoside modifying enzymes. *Drug Resist Updat*, **13**:151-171.
- Razeghi M, Saffarian P and Goudarzi M .2019. Incidence of inducible clindamycin resistance and antibacterial resistance genes variability in clinical *Staphylococcus aureus* strains: A two-year multicenter study in Tehran, Iran. *Gene Reports*, **16**: 100411.
- Riaz S, Faisal M and Hasnain S .2011. Antibiotic susceptibility pattern and multiple antibiotic resistances (MAR) calculation of extended spectrum β -lactamase (ESBL) producing *Escherichia coli* and *Klebsiella* species in Pakistan. *Afr J Biotechnol*, **10** (33):6325-6331.
- Riesen A and Perreten V .2009. Antibiotic resistance and genetic diversity in *Staphylococcus aureus* from slaughter pigs in Switzerland. *Schweiz Arch Tierheilkd*, **151**(9):425-431.
- Seyedi-Marghaki F, Kalantar-Neyestanaki D, Saffari F, Hosseini-Nave H, and Moradi M .2019. Distribution of Aminoglycoside-modifying enzymes and molecular analysis of the coagulase gene in clinical isolates of methicillin-resistant and methicillin-susceptible *Staphylococcus aureus*. *Microb Drug Resist*, **25**(1), 47-53.
- Szymanek-Majchrzak K, Młynarczyk A, Kawecki D, Pacholczyk M, Durlik M, Deborska-Materkowska D, Paczek L and Młynarczyk G .2018a. Resistance to Aminoglycosides of Methicillin-Resistant Strains of *Staphylococcus aureus*, Originating in the Surgical and Transplantation Wards of the Warsaw Clinical Center-A Retrospective Analysis. *Transplant Proc*, **50**(7):2170-2175.
- Szymanek-Majchrzak K, Młynarczyk A and Młynarczyk G .2018b. Characteristics of glycopeptide-resistant *Staphylococcus aureus* strains isolated from inpatients of three teaching hospitals in Warsaw, Poland. *Antimicrob Resist Infect Control*, **7**(105): 1-6.
- Vakulenko SB, Donabedian SM, Voskresenskiy AM, Zervos MJ, Lerner SA and Chow JW.2003. Multiplex PCR for detection of aminoglycoside resistance genes in enterococci. *Antimicrob Agents Chemother*, **47**: 1423-1426.
- Vakulenko SB and Mobashery S .2003. Versatility of aminoglycosides and prospects for their future. *Clin Microbiol Rev*, **16**:430-450.
- Vanhoof R.1994. Detection by polymerase chain reaction of genes encoding AMEs in methicillin-resistant *Staphylococcus aureus* isolates of epidemic phage types. *J Med Microbiol*, **41**:282-290.
- Watkins RR, Holubar M and David MZ .2019. Antimicrobial resistance in methicillin-resistant *Staphylococcus aureus* to newer antimicrobial agents. *Antimicrob Agents Chemother*, **63**(12): e01216-19.
- World Health Organization .2017. Global priority list of antibiotic-resistant bacteria to guide research, discovery, and development of new antibiotics. Geneva, Switzerland.
- Xu F, Chen J, Xiao C, Cong F, Ma L, Moore RJ, Huang R. and Guo P .2019. Development of a Luminex xTAG Assay for the Rapid Detection of Five Aminoglycoside Resistance Genes Both in *Staphylococci* and *Enterococci*. *Microb Drug Resist*, **25**(6): 874-879.
- Yadegar A, Sattari M, Mozafari NA and Goudarzi GR .2009. Prevalence of the genes encoding aminoglycoside-modifying enzymes and methicillin resistance among clinical isolates of *Staphylococcus aureus* in Tehran, Iran. *Microb Drug Resist*, **15**(2):109-113.
- Zacharczuk K, Piekarska K, Szych J, Jagielski M, Hidalgo L, San Millan A, Gutiérrez B, Rastawicki W, González-Zorn B and Gierczynski R .2011. Plasmid-borne 16S rRNA methylase ArmA in aminoglycoside resistant *Klebsiella pneumoniae* in Poland. *J Med Microbiol*, **60** (9) :1306-1311.

Isolation and evaluation of culture media for mycelia growth of an emerging faba bean (*Vicia faba* L.) gall-forming disease causal agent in Ethiopia

Alemayehu Dugassa^{1,*}, Tesfaye Alemu¹, Yitbarek Woldehawariat²

¹Department of Microbial, Cellular and Molecular Biology, Addis Ababa University, P.O. Box 1176, Addis Ababa, Ethiopia. ²Department of Zoological Science, College of Natural and Computational Sciences, Addis Ababa University, P.O. Box.1176, Addis Ababa, Ethiopia

Received: June 12, 2020; Revised: Nov5, 2020; Accepted: Nov 12, 2020

Abstract

The current study aimed to identify suitable preliminary culture media for the isolation of faba bean gall-forming disease causal agent and confirm by pathogenicity test. Five separate media were evaluated for isolation. Infected faba bean stem disc and the mycelial disc of a pure isolate of the test pathogen were used for the in-vitro pathogenicity test on detached leaves. Pots filled with sterilized field soil were arranged in complete random block design and sown with disease susceptible FB-26869 faba bean health seeds for pot pathogenicity test. Pycnidium of the test pathogen appears filled with mature conidia and scattered inside the infected cells. At the initial stage, it was difficult to isolate the disease causal agent on the Potato Dextrose Agar medium. The Coon's medium was found to be suitable for the preliminary isolation of the test pathogen and showed statistically significant mycelial growth (90.00 mm), while Malt Extract Agar and Tryptone Soy Agar favors a large number of conidia production at 14th day of the incubation period. The Chlamydo-spore and conidia of the isolates were similar to *Peyronellaea pinodella* and *Phoma* related species. The optimum mycelial growth of the isolates was recorded at temperature 20 °C and pH value 6.50 on both Coon's and Potato Dextrose Agar medium. No significant differences ($P > 0.05$) were recorded among leaf lesions caused by infected stem and mycelial discs. All the tested isolates exhibited similar virulence levels both in-vitro and in pot experiments. The disease incidence and severity were significantly ($P \leq 0.05$) affected by seasonal variations. The highest percent severity index (91 – 95 %) was recorded from June to September. Synthetic culture media which inhabits other fast-growing fungus favors the mycelial growth of the test pathogen. The molecular characterizations were recommended for further confirmation.

Keywords: culture media, detached leaf, faba bean, gall-forming disease, pathogenicity

1. Introduction

The faba bean (*Vicia faba* L.) locally known as "Bakela" is one of the major pulse crops commonly cultivated in the high lands of Ethiopia. Based on seed size, faba bean is known by the common names including broad bean, horse bean, tic bean, and field bean (Fateme et al., 2019). It is the leading protein source for rural people and is used to make various traditional dishes (Yitayih and Azmeraw, 2017; Etemadi et al., 2019). The new emerging faba bean gall-forming disease is locally called "Kormid" threatening faba bean and causes up to complete crop failure over vast areas within a short time with disastrous economic consequences (Nigir et al., 2016; Bitew and Tigabie, 2016; Bekele et al., 2018). Faba bean gall-forming disease was first reported in July 2010 from high lands of farmers' faba bean fields around Selale and Degem, North Shoa, Oromia National Regional State of Ethiopia (Bekele et al., 2018; Anteneh et al., 2018; Alehegn et al., 2018).

A similar disease that attacks the stem and leaves of broad bean known as broad bean blister disease caused by

Olpidium viciae Kusano was first reported as a new species in Japan and later in China (Yan, 2013). According to Yan (2013), the life history of *Olpidium viciae*, is parasitic on the aquatic plant *Vicia unijuga*. It has numerous but short discharging tubes and binucleate resting sporangia. *Olpidium viciae* Kusano was seldom reported throughout the world apart from Japan and China.

Depending on its field symptoms descriptions and microscopic examination, most of the Ethiopian researchers reported the fungal pathogen *Olpidium viciae* Kusano as the causative agent of faba bean gall-forming disease (Nigir et al., 2016; Bitew and Tigabie, 2016; Getaneh et al., 2018). However, these reports were not confirmed yet by colony morphology, fruiting structures, and molecular characterization. Thus, this could not be the case in Ethiopia.

Physiological and environmental factors were known to influence the growth of fungi. The causal agent of the gall-forming disease requires several specific growth conditions. Growth and sporulation are essential phases during the life of fungi, which are considerably influenced by external growth factors (Mishra and Tripathi, 2015). Among the external growth factors, nutrition was one of

* Corresponding author e-mail: alemayehudugassa2008@gmail.com.

the determinants that were previously proved by several workers in fungal pathogens using different culture media sources (Adhikari *et al.*, 2017; Karaoglu *et al.*, 2018).

One of the most commonly exploited culture media for the growth of many fungal pathogens, Potato Dextrose Agar (PDA), was not suitable for the preliminary isolation of the fungus under study. Searching for suitable culture media for growth, conidia production, and cultural characteristic studies of the pathogen is the first step in pathological research. Synthetic culture media which supported the isolation, radial growth, and sporulation of gall-forming causal agent were not reported yet. As to our knowledge, the current study is the first attempt to find out suitable culture media and obtain the isolates of the gall-forming causal agent.

The lack of suitable culture media that support vegetative growth and sporulation of gall-forming causal agent has hindered *in-vitro* physiological and morphological studies of the test pathogen. Hence, to deal with this problem the present study was undertaken to identify the suitable culture media for mycelia growth and conidia production of the gall-forming causal agent under controlled conditions. This study mainly focused on *in-vitro* cultural practice, isolation of the causal agent, and testing the pathogenicity of the isolates both *in-vitro* and in pot experiments.

2. Materials and Methods

2.1. Sampling techniques

Simple random sampling techniques were used to address the representative of the whole faba bean plant population.

2.2. Sample collection

A total of 100 naturally infected faba bean stem/leaf with typical symptoms (small tumors) were collected from the farmers' field of Angolelana tera (50 samples), and Sululta (50 samples) districts during the 2018 main cropping season. All samples were packed in polyethylene bags and labeled with the name of the zone, district, and date of collection. The samples were transported to Mycology laboratory, College of Natural and Computational Sciences, Addis Ababa University for detection and isolation of causal agents of faba bean gall-forming diseases. It was stored at 4°C until use.

2.3. Sample preparation for detection of the causal pathogen in the plant tissue

Infected parts of the leaves and stems were excised with a sterile scalpel. The samples of infected faba bean stem/leaf were treated with 20 ml of ethyl alcohol (80%) kept in test tubes and then dipped in boiling water until complete evaporation of ethyl alcohol to remove the chlorophyll in the plant tissues. After washing the bleached plant tissues thrice in distilled water, they were immersed in NaClO (4%) for 30 min followed by rinsing thrice with distilled water. The tissues were transferred to NaClO solution and kept at 60 °C for 15 min, followed by washing thrice in distilled water (Caiazza *et al.*, 2006). The tissue was stained with lactophenol cotton blue and examined under a 40 x objective lens of the compound light microscope (MAX BINO BELGIUM).

2.4. Preliminary isolation and purification of the gall-forming causal agent

Initially, the small pieces (1 cm) of infected faba leaves were excised and surface-sterilized by dipping them in 2% sodium hypochlorite for 5 minutes, followed by washing three times with sterile distilled water for 2 minutes. The sterilized fragments of infected faba bean leaves were inoculated on 90 mm Petri dishes containing sterilized Coon's medium (4 g/l maltose, 2 g/l KNO₃, 1.20 g/l MgSO₄.7H₂O, 2.68 g/l KH₂PO₄, and 20 g/l agar) (Adnan *et al.*, 2017) amended with chloramphenicol. A 0.1 ml of the last washes was spread plated on Coon's medium as a control to check the quality of surface sterilization. The inoculated medium was incubated at 23 ± 2 °C for 14 days. The actively growing parts of the isolates were purified on the Coons medium using single hyphal tip techniques suggested by Ahmed and El-Fiki (2017).

2.5. Evaluation of culture media for mycelial growth and conidia production

To find out the medium that best suits for the mycelia growth, conidia production, and other cultural characteristics of gall-forming disease causal agent, five culture media were compared, including Coon's medium (CN), Potato Dextrose Agar (PDA) (Oxoid), Malt Extract Agar (MEA) (Oxoid), Tryptone Soy Agar (TSA) (Oxoid), and Water Agar (WA) in solid states. Pure mycelia Coon's agar plug measuring 4 mm diameter were taken from the actively growing margin of 12 day-old pure culture using a sterile cork borer and placed upside down in the center of each medium in a 90 mm Petri dish. The Petri plates were immediately sealed with parafilm with four replications. All the plates were incubated at 23 ± 2°C for 14 days and all the activities were done under aseptic conditions inside the laminar flow cabinet. Visual observations concerning colony growth were made starting from the fourth day after incubation. The mycelia diameter of the isolates on different media was measured and compared quantitatively, whereas the conidia productions were recorded qualitatively (Smita and Dhutraj, 2017).

2.6. Morphological characterization

2.6.1. Macroscopic morphology

The cultural morphology studies of the isolates were performed on MEA, WA, PDA, Coon's Medium, and TSA following the standardized procedure. The colony diameters (mm) were measured starting from the fourth day after incubation at every two days interval until the mycelium fully covered the Petri dish. Colony morphology, shape, and other cultural characteristics were observed with the naked eye throughout the incubation period and characterized at full plate colony growth on 14 days of incubation. Colony growth was measured in two days intervals. Colony colors and texture were rated 14 days after incubation (Ahmed and El-Fiki, 2017).

2.6.2. Microscopic morphology

Pure fungal isolates were mounted in distilled water with a scalpel blade to study the structure of Pycnidia, chlamydospores, and conidia (Ahmadpour *et al.*, 2017). The microscopic examinations were carried with the 40X objective lens of the compound light microscope (MAX BINO BELGIUM). Macroscopic and microscopic morphological characters were used to compare the fungal

isolates with the assistance of current mycological literature (Johnston *et al.*, 2017).

2.7. Effect of temperature and pH on growth of gall-forming causal agent

2.7.1. Effect of temperature

The ability of faba bean gall-forming diseases causing pathogen to grow at restrictive temperature was assessed by growing the cultures on PDA and Coon's medium and incubating at 20, 23, and 25 °C until full growth of the mycelia in 90 mm plate followed by You *et al.* (2016). For measuring the diameter of mycelia growth rate, the fungal isolate was inoculated in triplicates at the center of the medium. The inoculum was aseptically punched with a cork borer in the form of four mm mycelial discs from the seven days old margin of colonies. The plates were incubated at different temperatures and the diameter of the mycelial growth was measured (in mm) every two days interval up to full growth of mycelia in the plates.

2.7.2. Effect of pH

The pH values 6.50, 7.00, and 7.50 within the range of soil pH of the study sites were used for the study of the effect of pH on the growth rate of faba bean gall-forming disease-causing pathogen as described by You *et al.* (2016). PDA and Coon's medium were prepared in triplicates and its pH was adjusted by adding HCl and NaOH before autoclaving. A four mm disc from the margin of seven days old culture of the gall-forming pure isolate was inoculated on the plates containing PDA and Coon's medium. The inoculated plates were incubated at the temperature mentioned above. Measurements of the diameter of the mycelia growth were recorded as described above.

2.8. Detached leaf in-vitro pathogenicity test

This was done by two experiments. Experiment 1 was conducted to determine the pathogenicity of infected faba bean stems/leaf with typical gall disease symptoms. Experiment 2 was conducted to determine the pathogenicity of faba bean gall-forming diseases causing suspected isolates. In-vitro pathogenicity of both the infected disc of stem/leaf and suspected isolates was done on fresh leaflets of faba bean as stated by Kayim *et al.* (2018).

2.8.1. Preparation of leaflets

Faba bean seeds (FB-26869) were sown in pots at the College of Natural and Computational Sciences, Addis Ababa University greenhouse on December 4, 2018. Leaves were collected from 60 days old seedlings. Leaflets were surface-disinfected by immersion in dilute sodium hypochlorite (2% active chlorine) for 1 min, rinsed three times with sterile distilled water, and placed under an air stream to remove excess water followed by Ermias *et al.* (2013).

2.8.2. Inoculum preparation and inoculation

The infected and healthy portions of faba bean stem were separately cut into four mm discs by corks borers. Both infected and healthy faba bean stem discs were surface sterilized with 2 % Sodium hypochlorite. Similarly, 14 days old culture of agar plugs containing five different faba bean gall-forming diseases causing suspected isolates were removed using a cork borer. A four

mm disc of infected faba bean stems and the agar plugs were inoculated at the center of pre-prepared leaflets separately followed by Kayim *et al.* (2018). The healthy faba bean stems disc and isolates free agar plugs were placed on leaflets as control. All were done in triplicates. Then the inoculated leaflets were placed face-up on the filter paper impregnated with sterile distilled water in the sterilized Petri plates to serve as a moist chamber. All cultures were kept at room temperature (20 ± 3 °C) for five days. The length and width diameters of the leaves lesion formed around each stem disc and agar plugs were measured separately. The lesions of artificially infected leaflets were examined by microscope (MAX BINO BELGIUM) and confirmed as the original inoculated isolates and natural infections.

2.9. Pot experiment pathogenicity test

2.9.1. Experimental design and details

The pot experiment pathogenicity test was conducted three times at the College of Natural and Computational Sciences, Addis Ababa University greenhouse. The first, second, and third experiment was carried out during December 2018 – February 2019, March 2019 – May 2019, and June 2019 – September 2019, respectively. A total of 18 pots (20 cm diameter) were surface sterilized by using 70 % alcohol and arranged in Complete Random Block Design (CRBD) in three blocks (Zakawa *et al.*, 2018). A 2 kg of 2 mm sized sieved autoclaved field soils were added to each pot. The pots were kept for one week and irrigated regularly. The most susceptible faba bean accession (FB-26869) to gall-forming diseases causing pathogen was used for the pathogenicity test.

2.9.2. Inoculum preparation and inoculation of the pathogen

Based upon the in-vitro antigenicity test result, four mm discs of five selected faba bean gall-forming diseases causal agent suspected isolates were removed by using sterilized cork borers. Three discs of each isolate were separately inoculated in a 250 ml flask containing 100 ml Coon's broth and incubated at 23 ± 2 °C for 14 days. Twelve faba bean seeds (FB-26869) were impregnated with 30 ml of conidia suspensions (10^5 spores/ml) of each isolates separately in a 250 ml flask and incubated at 23 ± 2 °C for 48 hr. The level of conidia suspensions was adjusted by using a hemocytometer. Four faba bean seeds impregnated with the suspected isolates were sown in each pot as stated by Khaleedi and Taheri (2016).

Besides, for the mass production of the isolates, 10 ml of each suspension (10^5 spores/ml) of suspected isolates were separately added to 100 g sterilized ground faba bean stems and incubated at 23 ± 2 °C for 21 days (Karaoglu *et al.*, 2018). Fourteen days after the emergence of seedlings, each pot was inoculated with 10 g of the corresponding mass-produced faba bean gall-forming causal agent suspected isolates to increase the inoculum sources. Twelve faba bean seeds impregnated with sterile distilled water served as control. Three replications were maintained. The pathogenicity of each isolate was evaluated through observation and recording the disease incidence and severity per seedlings 30 days after the seedling emergence. The pathogenic isolates were re-isolated from the newly infected faba bean seedling stems and leaves. Then, compared and confirmed with the

original inoculated isolates by microscopic morphological characterization.

2.9.3. Disease data

Terminal disease incidence and present severity index were recorded on plant bases to evaluate the faba bean gall-forming disease causal agent. Percent disease incidence computed over the number of diseased plants from the total number of inspected plants. The disease percent severity index (PSI) was calculated using a 0–9 scale to determine the area of the affected plant part, according to Aghajani *et al.* (2009), with little modifications.

$$PSI = \frac{(a + 3b + 5c + 7d + 9e)}{9(a + b + c + d + e)} \times 100$$

Where, 9 = highest rating value, a = number of plants in class 1, b = number of plants in class 3, c = number of plants in class 5, d = number of plants in class 7, e = number of plants in class 9.

2.10. Statistical data analysis

The data were subjected to SPSS statistical software version 20 and one way ANOVA. The effect of culture

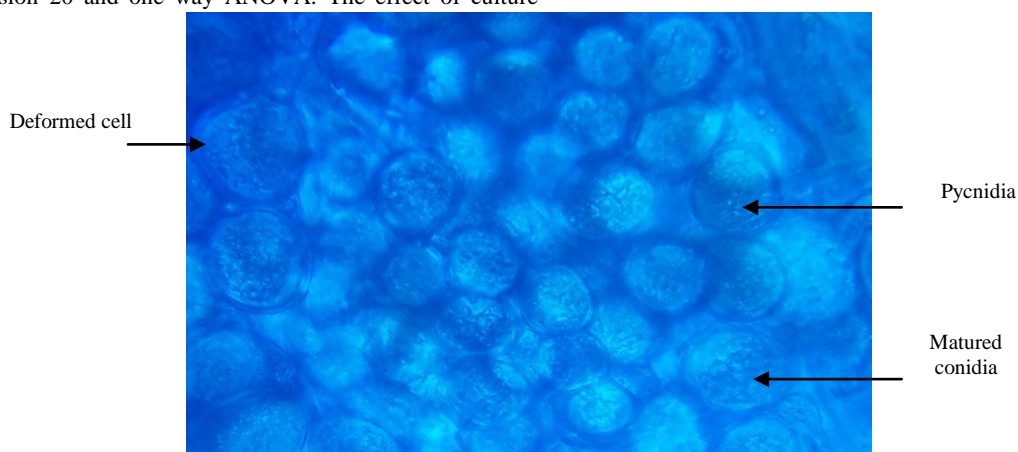


Figure 1. Light microscopy observation of the infected faba bean stem cell stained with lactophenol cotton blue

3.2. Preliminary isolation and purification of the isolates

Different synthetic culture media were tested for isolation of faba bean gall-forming pathogen. It was difficult to isolate the pathogen by using potato dextrose agar from the infected plant parts at the initial stage. However, Coon's medium was very important for the isolation and purification of the pathogen at the preliminary stage. The pure isolates can grow on potato dextrose agar. Thus, potato dextrose agar slant could be used for the storage of the pure isolates at 4 °C for further use.

3.3. Evaluation of culture media for mycelia growth

The mycelial growth rate of the test pathogen was affected by variation in culture media sources. The tested

media on the mycelial growth of faba bean gall-forming disease causal agent was compared using the least significant difference (LSD) at a 5% probability level ($P \leq 0.05$). The slopes were used as measures of mycelia radial growth rates (mm day^{-1}) for each culture medium source treatment (Smita and Dhutraj, 2017).

3. Results

3.1. Detection of faba bean gall-forming disease causal agent inside the infected cells

Light microscopy observations of infected faba bean stem with the gall-forming disease were presented in Figure 1. The infected cells appeared plasmolyzed and disorganized. Pycnidia of the gall-forming causal agent scattered inside the infected faba bean cells. It appears filled with a large number of mature conidia.

culture media supported the growth of the pure isolates of faba bean gall-forming disease causal agent to various degrees and significantly ($P \leq 0.05$) affected mycelia growth of the pathogen at the end of the growth period (Table 1). The mean colony diameter measured with the entire test media ranged from 70.00 (WA) to 90.00 mm (Coon's medium) at 14 days after incubation. Among the tested culture media, Coon's medium (90.00 mm) showed statistically higher mycelial growth followed by PDA (84.00 mm) than others. Coon's medium was found to be more suitable for vegetative growth than the other culture media.

Table 1. *In-vitro* evaluation of different growth culture media on colony growth (mm), growth rate (mm/day) of faba bean gall-forming causal agent incubated at 23 ± 2°C

Medium type	Mean diameter ± SD of colony growth (mm) after different incubation periods (hr)							Radial growth rate (mm/day)	R ² (%)
	48	96	144	192	240	288	336		
MEA	12 ^a ± 2	18 ^a ± 5	24 ^a ± 0	36 ^a ± 2	52 ^a ± 2	70 ^a ± 1	80 ^c ± 1	0.12 ^a	96
WA	12 ^a ± 1	16 ^a ± 4	20 ^a ± 2	36 ^a ± 3	48 ^a ± 2	64 ^a ± 2	70 ^b ± 2	0.89 ^b	99
PDA	16 ^a ± 1	24 ^b ± 3	36 ^b ± 4	50 ^b ± 1	64 ^b ± 5	76 ^b ± 1	84 ^d ± 2	1.08 ^c	96
Coon's	16 ^a ± 3	24 ^b ± 2	40 ^b ± 3	52 ^b ± 2	68 ^b ± 6	84 ^b ± 2	90 ^a ± 3	1.10 ^c	99
TSA	12 ^a ± 4	16 ^a ± 1	28 ^a ± 2	36 ^a ± 1	50 ^a ± 4	68 ^a ± 2	76 ^c ± 2	0.85 ^b	98
Average	13 ^a ± 1	19 ^a ± 2	29 ^a ± 4	41 ^a ± 5	56 ^a ± 4	72 ^a ± 4	80 ^c ± 4	0.81 ^b ± 0.4	97.6 ± 2
CV (%)	16	21	28	22	16	11	10	50	2

Means of mycelial growth followed by a different letter (s) in the same column are significantly ($p \leq 0.05$) different, MEA: Malt Extract Agar, WA: Water Agar, PDA: Potato Dextrose Agar, TSA: Tryptone Soy Agar, R²: Coefficient of determination, SD: Standard deviation

3.4. Macroscopic morphological characteristics

The test pathogen exhibited a wide range of colony characteristics about shape, and color on MEA, WA, PDA, Coon's medium, and TSA on 14th day of incubation period (Figure 2). Mycelia growth patterns included both light and dense radial extending mycelium. Radial mycelia growth was consistently a characteristic feature of the fungus on all media sources. Both the reverse and the front sides of the colony exhibited various colors and shapes on different culture media (Table 2 and Figure 2). Light mycelia, brown-black ring center followed by white ring regular margins were recorded on the reverse side, whereas white regular double rings were recorded on the front side of Coon's medium.

On the other hand, dense mycelia, brown color at center with regular colony margins were recorded on the reverse side of the PDA medium. The black center followed by the white and regular brown rings was recorded on the front side of the PDA medium. Light mycelia were recorded on MEA, Coon's, and TSA medium. Very light and irregular shaped black center mycelia were recorded on WA. The microscopy of a colony grown on different media showed that large numbers of conidia were recorded on MEA and TSA (Table 2 and Figure 2).

Table 2. Cultural characteristics and conidial production of gall-forming disease causal agents on 14 days of incubation at 23 ± 2 °C

Medium	Conidia	Cultural characteristics	
		Reverse side color and shape	Front side color and shape
MEA	+++	white irregular shape at the center greenish-brown irregular shape at the middle white irregular margin	white irregular shape at the center black with a double ring in the middle white irregular margin
WA	-	very light mycelia with irregular black color at the center	very light mycelia with irregular black color at the center
PDA	+	brown at the center and middle with a white regular margin	black center followed by a white and brown ring with a white ring
Coon's	++	a brown black ring at the center followed by a regular white ring	white double-ring followed by white regular ring
TSA	+++	yellowish white with regular margin	white with regular margin

- = no conidia, + = poor, ++ = fair, and +++ = good

MEA: Malt Extract Agar, WA: Water Agar, PDA: Potato Dextrose Agar, TSA: Tryptone Soy Agar

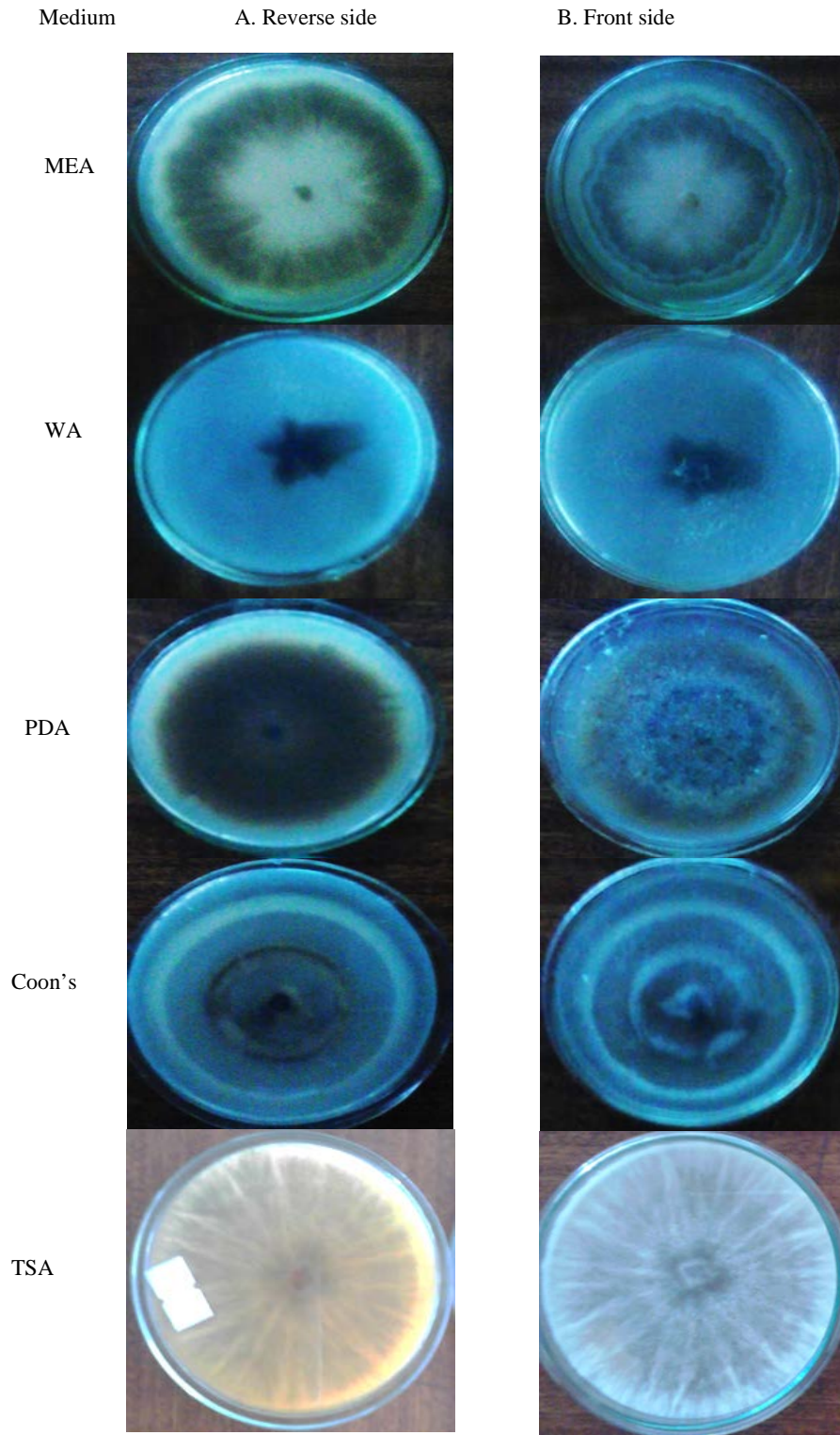


Figure 2. Colony morphology of gall-forming causal diseases agent on different media on 14th day of the incubation period at 23 ± 2 °C. MEA: Malt Extract Agar, WA: Water Agar, PDA: Potato Dextrose Agar, TSA: Tryptone Soy Agar

3.5. Microscopic morphological characteristics

The microscopic structures pycnidia, chlamydospore, and conidia were commonly observed in the 14 days old culture of faba bean gall-forming disease-causing isolates. Mature pycnidium was often observed on the tip of

mycelium (Figure 3 A). Chlamydospore was observed frequently in a chain and separately on mycelia intercalary and terminally (Figure 3 C). Sub cylindrical to the narrow ellipsoid shape of conidia with two nuclei were observed frequently (Figure 3 B) under light microscope.

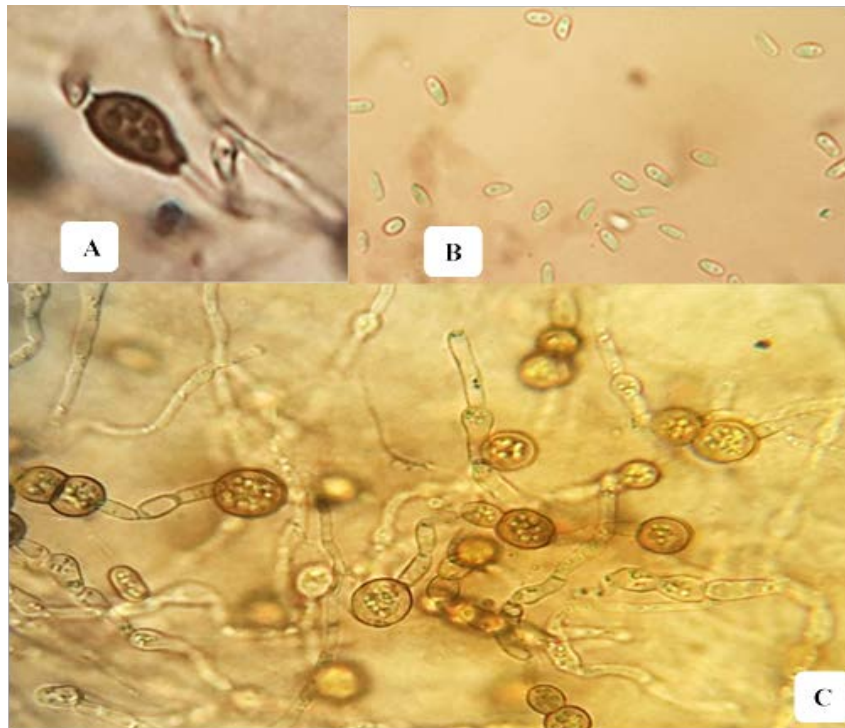
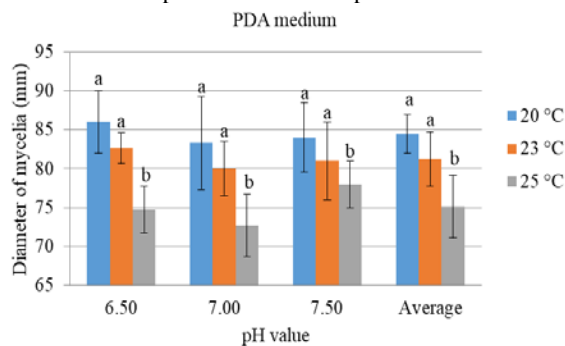


Figure 3. The microscopic structure of gall-forming disease causal agent stained with sterilized distilled water, A: Pycnidia, B: Conidia, C: Chlamydospore

3.6. Effect of temperature and pH on the in-vitro growth of gall-forming causal agent

Incubation temperature significantly ($P \leq 0.05$) affected the mycelia growth of the gall-forming causal agent. As the temperature increased from 20 °C to 25 °C, the mycelia growth of the isolates were significantly decreased. On the other hand, the current evaluated pH values had not significantly influenced the mycelial growth. The maximum mycelial growth (86 mm) was recorded at temperature 20 °C and pH value 6.50, whereas the minimum (72.67 mm) was recorded at temperature 25 °C and pH value 7.00 on PDA medium (Figure 4). At temperature 20 °C and pH value 6.5, 88.67 mm mycelia diameter of the gall-forming isolates was recorded on Coon's medium (Figure 5). Thus, Coon's medium was more suitable for the growth of gall-forming pathogen than the PDA medium. The optimum growth of the isolates was recorded on temperature 20 °C and pH value 6.50 on both



mediums.

Figure 4. The effect of temperature and pH on the mycelia growth of gall-forming pathogen on PDA medium at 14th day of the incubation period there was no significant difference between bar graphs labeled with the same letters, a vertical line on the graphs indicates the standard deviation

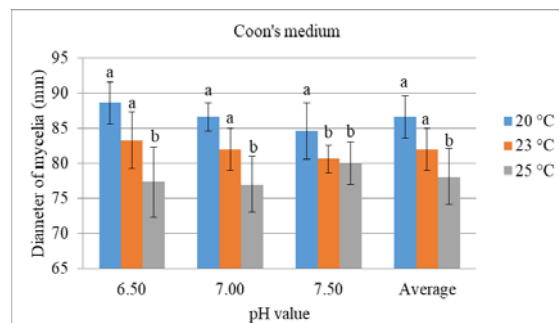


Figure 5. The effect of temperature and pH on the mycelial growth of gall-forming pathogen on Coon's medium at 14th day of the incubation period

there was no significant difference between bar graphs labeled with the same letters, a line on the graphs indicates the standard deviation

3.7. Detached leaves in-vitro pathogenicity test of gall-forming disease causal agent

A significant difference ($P \leq 0.05$) were observed between the average length diameter of the leaf lesion, whereas there was no significant difference ($P > 0.05$) in the average width diameter of the leaf lesion caused by infected stem disc (Experiment 1) and mycelia disc of gall-forming disease-causing isolates (Experiment 2). Among infected stem disc inoculated leaves, the maximum lesion length diameter (28 mm) and width diameter (17.33 mm) were recorded by disc 4. But, the minimum lesion length diameter (6.66 mm) and width diameter (7.33 mm) recorded by infected stem disc 5. On the other hand, the maximum lesion length diameter (29.67 mm) were recorded by the mycelia disc of isolate 6, whereas the maximum lesion width diameter (25 mm) was recorded by the mycelia disc of isolate 4. Leaflets inoculated with health stem disc and mycelia free agar plug did not develop infection symptoms (Table 3 and Figure 6).

Table 3. Average leaf lesions in detached leaf pathogenicity test

Inoculum sources	LD of the leaf lesions (mm) ± SD	WD of the leaf lesions (mm) ± SD	LD/WD leaf lesions
Experiment 1			
Infected stem disc 1	14.00 ^a ± 0.00	13.33 ^d ± 1.15	1.05
Infected stem disc 2	15.33 ^a ± 1.15	15.33 ^d ± 1.15	1.00
Infected stem disc 3	22.00 ^e ± 15.62	12.33 ^d ± 7.37	1.78
Infected stem disc 4	28.00 ^d ± 21.37	17.33 ^d ± 11.54	1.62
Infected stem disc 5	6.66 ^b ± 3.05	7.33 ^e ± 3.05	0.91
Infected stem disc 6	20.67 ^e ± 17.01	10.00 ^e ± 6.00	2.07
Infected stem disc 7	21.67 ^e ± 21.08	12.67 ^d ± 8.08	1.71
Infected stem disc 8	24.67 ^d ± 18.58	13.33 ^d ± 8.32	1.85
Control	0.00 ^f	0.00 ^f	
Average	19.13 ^e ± 6.79	12.71 ^d ± 3.06	1.51 ± 0.44
CV (%)	35.49	24.07	29.13
LSD (P = 0.05)	0.73	0.74	
Experiment 2			
Mycelia disc of isolate 1	6.00 ^b ± 0.00	6.00 ^a ± 0.00	1.00
Mycelia disc of isolate 2	14.00 ^a ± 6.00	13.33 ^d ± 7.02	1.05
Mycelia disc of isolate 3	10.00 ^g ± 6.00	8.00 ^a ± 3.46	1.25
Mycelia disc of isolate 4	16.00 ^a ± 5.29	25.00 ^b ± 13.23	0.64
Mycelia disc of isolate 5	9.33 ^g ± 4.62	9.33 ^c ± 5.03	1.00
Mycelia disc of isolate 6	29.67 ^d ± 22.37	16.00 ^d ± 10.58	1.85
Mycelia disc of isolate 7	8.00 ^b ± 6.93	6.00 ^a ± 3.46	1.33
Mycelia disc of isolate 8	22.67 ^e ± 16.29	12.00 ^d ± 6.93	1.89
Control	0.00 ^f	0.00 ^f	
Average	14.46 ^a ± 8.11	11.96 ^d ± 6.35	1.25 ± 0.43
CV (%)	56.12	53.07	34.65
LSD (P = 0.05)	0.18	0.08	

LD: length diameter of the leaf lesions, WD: width diameter of the leaf lesions, SD: standard deviation

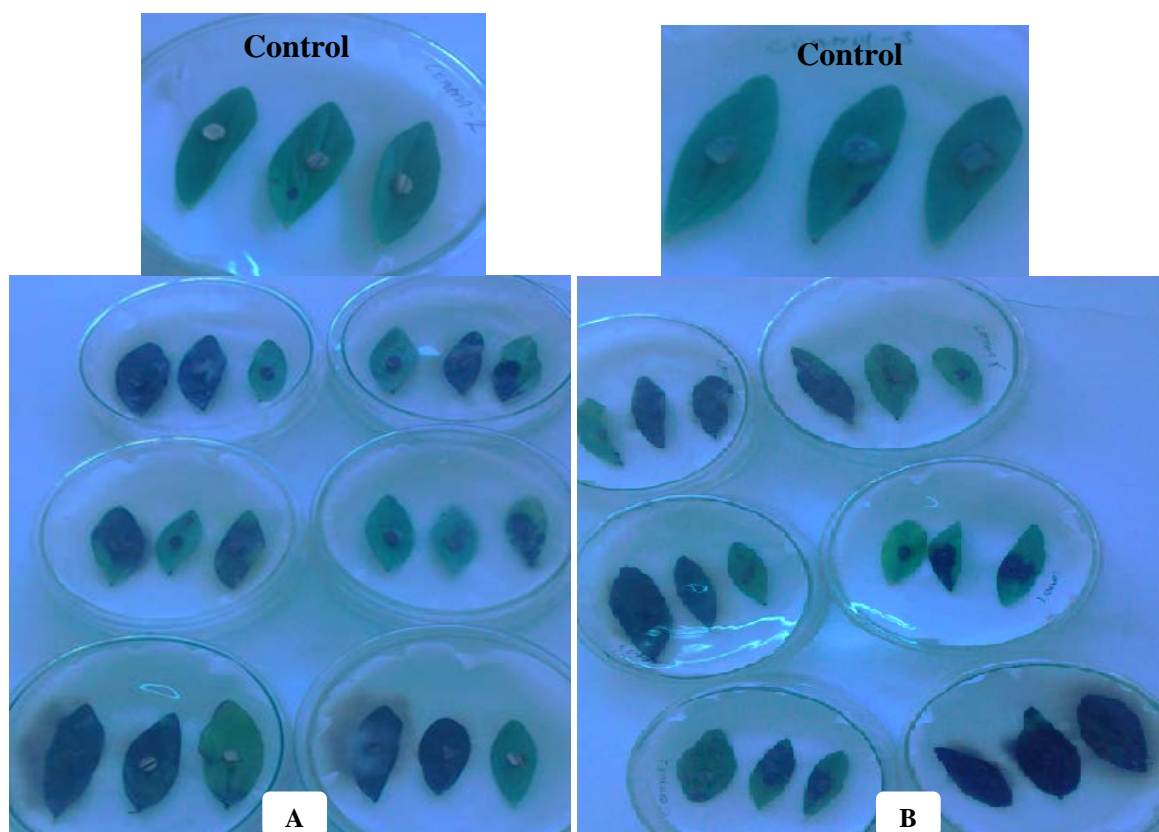


Figure 6. *In-vitro* pathogenicity test on detached leaves, A. Experiment 1: infected faba bean stem disc B. Experiment 2: Mycelia disc of gall-forming disease-causing isolates

3.8. Pot experiment pathogenicity test of gall-forming disease causal agent

It has been noted that gall-forming disease symptoms appeared after thirty days of plant emergence and

continues until flowering. The symptoms appear on leaves and stems. Ten to 25 chlorotic small galls formed on a single leaf. The gall progressively enlarged and became light brown, circular, or elliptical rough spots (Figure 7 C).

At the later stage, it turns to black or brown, the tissues decay, and a few galls break to form necrotic areas (Figure 7 D). Galls often coalesce adjacently to form huge galls, resulting in rolling up (cupping) and finally kill the

infected leaves (Figure 7 E). Faba bean seedlings not inoculated with the pathogens (control) did not develop infection symptoms (Figure 7 B).

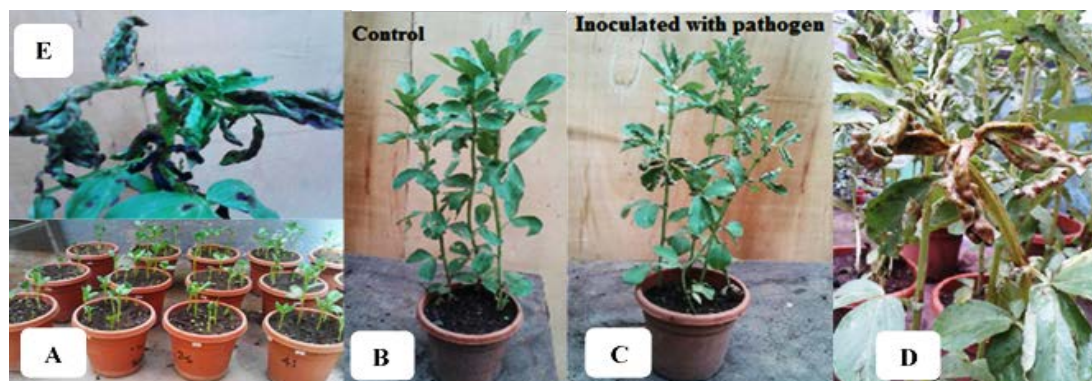


Figure 7. Faba bean gall-forming disease causal agent pathogenicity test in pot experiment during June 2019 – September 2019; A: 14 days faba bean seedlings, B: none inoculated with a pathogen, C: inoculated with pathogen D: faba bean gall-forming disease symptoms, E: faba bean leaves dead by gall-forming disease.

3.9. Percent disease incidence and severity index

During December 2018 – February 2019 (Experiment 1) and March 2019 – May 2019 (Experiment 2) no isolates caused disease incidence on faba bean seedlings (Table 4), whereas, during June 2019 – September 2019 (Experiment 3), both isolates caused faba bean gall-forming disease symptoms on all (100%) faba bean seedlings expect in

control. The highest significant ($P \leq 0.05$) disease incidence and severity were recorded on experiment 3 than experiment 2, and experiment 1. There was no significant difference ($P \geq 0.05$) both in disease incidence (100 %) and PSI (91 – 95 %) among isolates in experiment 3 (Table 4).

Table 4. Disease incidence and severity index of faba bean gall-forming disease-causing isolates in a pot experiment

Control and disease causing isolates	Experiment 1 (December 2018 – February 2019)		Experiment 2 (March 2019 – May 2019)		Experiment 3 (June 2019 – September 2019)	
	Incidence (%)	PSI (%)	Incidence (%)	PSI (%)	Incidence (%)	PSI (%)
Control	0	0	0	0	0	0
Isolate 2 (AAUO2)	0	0	0	0	100	91
Isolate 3 (AAUO3)	0	0	0	0	100	93
Isolate 4 (AAUO4)	0	0	0	0	100	95
Isolate 6 (AAUO6)	0	0	0	0	100	94
Isolate 8 (AAUO8)	0	0	0	0	100	95
Average	0	0	0	0	100	93.60

PSI: a percent severity index

4. Discussion

An emerging faba bean gall-forming disease is one of the most devastating fungal diseases infecting and constraining faba bean cultivation in Ethiopia (Bekele *et al.*, 2018). Recently, the disease is expanding in faba bean growing areas of the country, especially in altitudes above 2400 m above sea level (a. s. l.) (Anteneh *et al.*, 2018). The pathogen-infected and parasitized in the epidermal cells of the faba bean leaf and stem. The host responded quickly to the invasion and then it induces the gall symptom (Figure 1).

In this study, culture media strongly influenced the growth and conidial productions of faba bean gall-forming disease causal agent. Several studies also found similar results concerning the effect of culture media on growth, sporulation, and other cultural characteristics of various types of fungi (Koley and Mahapatra, 2015; Mishra and Tripathi, 2015). Coon's culture medium supported the slow grower faba bean gall-forming causal agent. It was found to be the most suitable for the preliminary isolation and

favors the mycelial growth of the fungus under study. This could be attributed to the low glucose content of the medium and its ability to inhibit other competing fast grower fungus.

Malt extract agar and Tryptone soy agar resulted in good and abundant, whereas the rest tested culture media showed no (Water agar), poor (Potato dextrose agar), and fair (Coon's medium) in conidia production. Good conidia production of the media could be attributed to the low sugar content of the medium. Similarly, another study by Koley and Mahapatra (2015) pointed out that Oat Meal Agar (OMA) supported better sporulation of *A. solani* than PDA due to lower sugar content. In contrast to the current study, Smita and Dhutraj (2017) indicated that PDA and other culture media having good sugar content allowed the best mycelial growth of *A. solani*.

This study found that the colony characteristics of gall-forming disease causal isolates on various culture media were similar to Phoma related species. Phoma related species are associated with disease on many hosts, including legumes (Ahmadpour *et al.*, 2017). Besides, the

diagnosis of microscopic structures showed that the chlamydospore (Figure 3 C) and conidia (Figure 3 B) of the isolates were similar to *Peyronellaea pinodella*. *Peyronellaea pinodella* is associated with a black stem (summer back stem) of clover and peas (Johnston *et al.*, 2017).

At the same time, temperature significantly influenced the mycelia growth rate. Low temperature (20 °C) was preferred by gall-forming disease causal isolates among the tested temperature. However, 6.5 – 7.5 pH values had no significant influence on the mycelia growth of the isolates. In line with our study, Zehra *et al.* (2017) reported that temperature has a great influence on radial growth and sporulation of the fungus. The pH values of the nutrient medium determine mineral availability and influence metabolic rates of the fungus (Poosapati *et al.*, 2014).

The artificially inoculated test pathogen on detached leaflets produced progressive lesions that expanded from the inoculation point through the leaf. The virulence of both infected faba bean stem disc and agar plug of each isolate were consistent (Table 3 and Figure 6). This result coincides with the report of Kayim *et al.* (2018) and Ahmadpour *et al.* (2017) who reported the effect of leaf spot disease on faba bean detached leaves, and the pathogenicity of *Didymella microchlamydozpora* causing stem necrosis of *Morus nigra* in Iran, respectively. Detached leaf tests could be interesting because they can be performed rapidly, and results can be measured in a shorter period (5 – 7 days). Light microscopy observations demonstrated that the test pathogen can penetrate, colonize, and infect the leaf tissues since progressive tissue deterioration and cell plasmolysis were observed five days after pathogen inoculation. These changes in cell structure can be compared with those reported by Ahmadpour *et al.* (2017) and Johnston *et al.* (2017).

In a previous study, Bitew and Tigabie (2016) reported that at the initial stage small chlorotic galls are formed on faba bean leaves, and then progressively enlarge to become light brown, circular, or elliptical rough spots. The small tumor-like galls are formed adjacently to form huge galls, resulting in rolling up and abnormal growth of leaves. The current study also found similar disease symptoms only during June 2019 – September 2019 (experiment 3) in the pot experiment pathogenicity test. This showed that seasonal variation significantly affected the occurrence of disease symptoms on faba bean seedlings. The faba bean gall-forming disease incidence, conidia germination, and virulence of the fungus understudy were favored by the low temperature and high humidity of the cropping season. This result coincides with Yan (2013) findings who reported on blister disease of broad bean in China.

5. Conclusion and Recommendations

Coon's culture medium was suitable for the preliminary isolation and mycelia growth of faba bean gall-forming disease-causing isolates, whereas Malt extract agar and Tryptone soy agar supported good conidia formation. Seasonal variations significantly affected the incidence of faba bean gall-forming disease. Particularly, low temperature and high humidity favor disease incidence and severity. The macroscopic colony morphology and

microscopic morphological structures of the test pathogen were similar to *Peyronellaea pinodella* and Phoma related species. Therefore, the whole genome analysis and molecular characterization should be conducted for further confirmation of the disease causal agent.

Acknowledgment

We would like to express our sincere gratitude to Addis Ababa University for funding this research.

References

- Adhikari M, Dil Raj Y, Sang W, Young H, Seong Ch, Jeong Y, Hong G and Youn S. 2017. Biological Control of Bacterial Fruit Blotch of Watermelon Pathogen (*Acidovorax citrulli*) with Rhizosphere Associated Bacteria. *Plant pathol J.*, **33** (2): 170 – 183.
- Adnan Š, Jelena B and Maria RF. 2017. Endophytic *Fusarium equiseti* stimulates plant growth and reduces root rot disease of pea (*Pisum sativum* L.) caused by *Fusarium avenaceum* and *Peyronellaea pinodella*. *Eur J Plant pathol.*, **148**: 271–282.
- Aghajani A. 2009. Stemphylium leaf blight of broad bean in Iran. *J Plant Pathol.*, **91** (4): 97–112.
- Ahmadpour SA, Farokhinejad R and Mehrabi-Koushki M. 2017. Further characterization and pathogenicity of *Didymella microchlamydozpora* causing stem necrosis of *Morus nigra* in Iran. *Mycosph.*, **8** (7): 835 – 852.
- Ahmed F and El-Fiki A. 2017. Effect of Biological Control of Root Rot Diseases Strawberry Using *Trichoderma* spp. *Middle East J Appl Sci.*, **7**: 482 – 492.
- Alehegn M, Tiru M and Taddess M. 2018. Screening of Faba Bean (*Vicia faba* L.) varieties against faba bean gall diseases (*Olpidium viciae*) in East Gojjam Zone, Ethiopia. *J Biol Agric and Healthcar.*, **8** (1): 50 – 55.
- Anteneh A, Yohannes E, Mesganaw G, Solomon G and Getachew T. 2018. Survey of faba bean (*Vicia faba* L.) diseases in major faba bean growing districts of North Gondar. *Afr J Plant Sci.*, **12** (2): 32 – 36.
- Bekele B, Dawit W, Kassa B and Selvaraj T. 2018. Assessment of Faba Bean Gall Disease Intensity in North Shoa Zone of Central, Ethiopia. *Int J Res Agric Sci.*, **5** (1): ISSN: 2348 – 3997.
- Bitew B and Tigabie A. 2016. Management of Faba Bean Gall Disease (Kormid) in North Shewa Highlands, Ethiopia. *Adv Crop Sci Tech.*, **4**:4. DOI: 10.4172/2329-8863.100022
- Caiazza R, Tarantino P, Porrone G and Lahoz E. 2006. Detection and early diagnosis of *Peronospora tabacina* Adam in tobacco plant with systemic infection. *J Phytopathol.*, **154**: 432 – 435.
- Ermias T, Chemedo G, Samuel S and Mariam W. 2013. *In vivo* Assay for Antagonistic Potential of Fungal Isolates against Faba bean (*Vicia faba* L.) Chocolate Spot (*Botrytis fabae* Sard.). *Jor J Biol Sci.*, **6**: 183 – 189.
- Etmedi F, Hashemi M, Barker A, Zandvakili O and Liu X. 2019. Agronomy, Nutritional Value, and Medicinal Application of Faba Bean (*Vicia faba* L.). *Horticult Plant J.*, **5** (4): 170 – 182.
- Fatemeh E, Masoud H, Allen V, Barker O, Reza Z and Xiaobing L. 2019. Agronomy, Nutritional Value, and Medicinal Application of Faba Bean (*Vicia faba* L.). *HorticultPlant J.*, **5** (4): 170 – 182. <https://doi.org/10.1016/j.hpj.2019.04.004>
- Getaneh G, Hailu E, Sadessa K, Alemu T and Megersa G. 2018. The Causal Pathogen, Inoculum Sources and Alternative Hosts Studies of the Newly Emerged Gall Forming Faba Bean (*Vicia faba* L.) Disease in Ethiopia. *Adv Crop Sci Tech.*, **6**:3. DOI: 10.4172/2329-8863.1000368

- Johnston P R, Park D, Hob W and Alexander J. 2017. Genetic validation of historical plant pathology records – a case study based on the fungal genus *Phoma* from the ICMP culture collection. *Plant Pathol.*, **66**: 1424 – 1431. Doi: 10.1111/ppa.12728
- Karaoglu S. A., Bozdeveci A and Pehlivan N. 2018. Characterization of Local *Trichoderma* spp. as Potential Bio-Control Agents, Screening of in vitro Antagonistic Activities and Fungicide Tolerance. *Hacettepe J Biol & Chem.*, **46** (2): 247 – 261. <https://doi.org/10.15671/HJBC.2018.233>
- Kayım M, Yones AM and Endes A. 2018. Biocontrol of *Alternaria alternata* causing leaf spot disease on faba bean (*Vicia faba* L.) using some *Trichoderma harzianum* isolates under in-vitro condition. *Harran Tarım ve Gıda Bilimleri Derg.*, **22** (2):169 – 178. <https://doi.org/10.29050/harranziraat.329976>
- Khaledi N and Taheri P. 2016. Biocontrol mechanisms of *Trichoderma harzianum* against soybean charcoal rot caused by *Macrophomina phaseolina*. *J Plant Prot Res.*, **56** (1): 22 – 31. <https://doi.org/10.1515/jppr-2016-0004>
- Koley S and Mahapatra S. 2015. Evaluation of culture media for growth characteristics of *Alternaria solani*, causing early blight of tomato. *J Plant Pathol & Microbiol.*, **S1**-005. doi:10.4172/2157-7471.
- Mishra N K and Tripathi B P. 2015. Effect of culture media on growth, colony character and sporulation of three foliar pathogens of guava. *The Bioscan.*, **10** (4):1701 – 1705.
- Nigir B, Baze T and Tilahun M. 2016. Assessment of faba bean gall (*Olpidium viciae* (Kusano) in major faba bean (*Vicia faba* L.) growing areas of Northeastern Amhara, Ethiopia. *J Agric Env Int Dev.*, **110** (1): 87 – 95. <https://doi.org/10.12895/jaeid.20161.402>
- Poosapati S, Ruvulapalli D, Tippirishetty N, Vishawanthaswamy K and Chunduri S. 2014. Selection of high temperature and salinity tolerant *Trichoderma* isolates with antagonistic activity against *Sclerotium rolfsii*. *Springerpl.*, **3**: 641.
- Smita C and Dhutraj N. 2017. Effect of culture media and temperature on growth and sporulation of *Colletotrichum truncatum* of soybean in-vitro. *Int J Appl P Sci Agric.*, **3** (1):25 – 30.
- Yan JM. 2013. Study On Blister Disease Of Broad Bean Caused By *Olpidium Viciae* Kusano. *Doctoral dissertation*, GTID:1223330395984715, China.
- Yitayih G and Azmeraw Y. 2017. Management of Faba Bean Gall Disease through the use of Host Resistance and Fungicide Foliar Spray in Northwestern Ethiopia. *Adv Crop Sci Tech.*, **5** (1): 254.
- You J, Zhang J, Wu M, Yang L, Chen W and Li G. 2016. Multiple criteria-based screening of *Trichoderma* isolates for biological control of *Botrytis cinerea* on tomato. *Biol contr.*, **101**: 31 – 38. <https://dx.doi.org/10.1016/j.biocontrol.2016.06.006>
- Zakawa NN, Channya KF, Magga B and Akesa TM. 2018. Antifungal effect of neem (*Azadirachta indica*) leaf extracts on mango fruit post-harvest rot agents in Yola, Adamawa state. *J Pharmacog & Phytochem.*, **7**: 23-26.
- Zehra A, Dubey K, Meena M and Upadhyay S. 2017. Effect of different environmental conditions on growth and sporulation of some *Trichoderma* species. *J Env Biol.*, **38**: 197 – 203.

The Agar Production, Pigment and Nutrient Content in *Gracilaria* sp. Grown in Two Habitats with Varying Salinity and Nutrient Levels

Ervia Yudiati^{1,2,*}, Annisa Afifah Nugroho¹, Sri Sedjati¹, Zaenal Arifin³, Ali Ridlo¹

¹Department of Marine Science, Faculty of Fisheries and Marine Science, Diponegoro University, Jl. Prof. Soedarto, SH Tembalang, Semarang, 50275; ²Laboratory of Marine Micro/Macroalgae Technology, Department of Marine Science, Faculty of Fisheries and Marine Science, Diponegoro University, Jl. Prof. Soedarto, SH Tembalang, Semarang, Indonesia 50275; ³Brackishwater Aquaculture Development Centre, Jl. Cik Lanang, Jepara, Central Java, Indonesia

Received: March 22, 2020; Revised: Oct 10, 2020; Accepted: Nov 12, 2020

Abstract

Gracilaria sp. is rich in agar, pigment, carbohydrate and mineral contents. This study aims to determine the content of agar, chlorophyll a, carotenoids and nutrient content (protein, carbohydrate, total lipid, ash, water) in *Gracilaria* sp. grown in different habitats with high and low salinity. Samples were brought from high salinity (44±0.33) ppt from the reservoir habitat and low salinity (26.98±0.15 ppt) from biofilter's shrimp waste pond habitat. Salinity and water quality parameters were observed in three different subsites. Agar was extracted by alkali methods. Agar spectra were compared to standard agarose and characterized by FT-IR analysis. Results showed that agar content (25.79 ± 0.28%), chlorophyll a (25.79 ± 0.28 mg/g), carotenoid (5.90 ± 0.07 µmol/g) on low salinity was significantly higher (P<0.05) than high salinity. In high salinity, the agar (6.6±0.34%), chlorophyll a (3.62±0.15, carotenoids (0.71±0.1 µmol/g) contents was lower. The protein level of low salinity (14.4 ± 0.70%) was also significantly higher compared to high salinity (8.15±0.25%), respectively. The total lipid, carbohydrate, water, and ash content were similar. FT-IR analysis spectra show the presence of 3,6-anhydro-L-galactose. These can be useful data concerning optimum salinity in *Gracilaria* sp. culture.

Keywords: Salinity, *Gracilaria* sp., Agar, Pigment, Nutrient content

1. Introduction

Naturally, *Gracilaria* sp. is a euryhaline macroalga (Kumar *et al.*, 2010), has grown all over the coast with high economic value due to its nutrient content (Du *et al.*, 2016; Hernandez, 2017). *Gracilaria/Gracilariopsis* have been mostly cultivated in Asia, especially Indonesia and China. The production is about 98% of global production (FAO, 2016; Kim *et al.*, 2017). Asian people consume seaweed daily (Cikos *et al.*, 2018). Seaweed empirically improves health and able to reduce the chronic disease incidence such as cancer, cardiovascular and heart diseases (Rioux *et al.*, 2017; Xu *et al.*, 2017). *Gracilaria* sp. serves as an excellent source of polysaccharide, i.e. agar (Xu *et al.*, 2017) also rich in pigmented antioxidants such as chlorophyll and carotenoids (Stengel *et al.*, 2015; Asih *et al.*, 2019). Polysaccharides from seaweed are frequently related to pharmacological activities (Hamed *et al.*, 2015) such as anticoagulant, antioxidant (Yudiati *et al.*, 2018a; 2018b), antitumor, and immunomodulatory of shrimp (*Litopenaeus vannamei*) (Yudiati *et al.*, 2016, 2019) as well as Zebrafish (Yudiati *et al.*, 2020)

Common salinity at sea in marine waters is around 35 ppt. Precipitation or freshwater influxes, as in reservoir and mangrove areas, may lead to salinity variation from 10 to 70 (Graham & Wilcox, 2000; Kumar *et al.*, 2010). Some

former researchers have reported the response of estuarine macroalgae to the abiotic factors such as salinity light, pH, temperature, nutrient load (Kumar *et al.*, 2010; Choi *et al.*, 2010) associated to agar yield (Israel *et al.*, 1999) and photosynthetic performance (Phooprong *et al.*, 2007). Later studies have also discussed the possible effects of environmental stresses on seaweed extracts according to its kinetic parameters (Deyab, 2016).

Salinity has been displayed to the reason of osmotic (Kumar *et al.*, 2010) as well as turgor pressure regulation (Pereira *et al.*, 2017). Salinity will improve the upregulation and accumulation of the essential enzymes (Odat, 2018). The seaweed tolerance to high salinity is supported by the internal and external osmotic capacities and on elasticity of the cell wall (Wu *et al.*, 2018). When the cell is located in hypertonic solution, water will flow quickly out of the cell, and turgor pressure will be decreased affecting plasmolysis, which is commonly permanent. If the cell is located in hypotonic solution, water will go into the cell, causing an enlarge of cell volume. Salinity in plants also stimulates the ROS generation which produces cellular oxidative damage when overproduced in large amounts (Luis *et al.*, 2018). These mechanisms play a role in combating the accumulation of reactive oxygen species (ROS) by a diverse set of enzymes such the superoxide dismutase (SOD), which dismutase the O₂-radicals to H₂O₂ (Luis *et*

* Corresponding author e-mail: eyudiati@gmail.com.

al., 2018). *Gracilaria* sp. is abundant in chlorophyll a and carotenoids. The pigment important role is to neutralize the free radicals (Sedjati *et al.*, 2020). In some periods of time, these mechanisms influence the agar, pigment as well as protein and mineral content caused by salinity stress. The objective of this study is to determine the agar, pigment (chlorophyll a and carotenoids) and nutrient content (water, protein, total lipid, ash, carbohydrate) from low (reservoir) and high (biofilter habitats) salinity of *Gracilaria* sp.

2. Materials and Methods

2.1. Water Quality Parameters

Measurements of water quality parameters such as salinity (Atago Refractometer), pH (pH meter RoHS), dissolved oxygen and water temperature (Water Quality Checker "Amstast") nitrate and phosphate content was administered. Assessment on nitrate content (SNI-06-2480-1991) was applied spectrophotometrically (Shimadzu 1900) while the phosphate content was done by Badan Standarisasi Nasional methods (SNI-06-2412-1991).

2.2. Site Location and Sample Preparation

Sample was collected from low salinity/LS (reservoir) and shrimp (*Litopenaeus vannamei*) pond waste (biofilter), which represents high salinity/HS of Center of Brackishwater and Aquaculture Development Center, Jepara, Central Java, Indonesia (Figure 1). Coordinates of sampling sites in HS was S 06°35'12.74" E 110°39'10.32" while in LS was S 06°35'05.64" E 110°38'49.03". The salinity of the reservoir from this study tends to be mild-low salinity. In contrast, biofilter shallow waters illustrate the different condition. The water supply of biofilter came from shrimp (*L. vannamei*) pond waste from uneaten feed and shrimp's fecal. Due to the static and unchanged water supply, biofilter media was relatively high in salinity.

The water and *Gracilaria* sp. sample was taken at three different subsites from two different habitats at 800 cm in depth. Seaweed was taken randomly. Soon as arrived at the laboratory, samples were rinsed with tap water to clean up from debris and salt. This was followed by dried up samples indoor with room temperature. Dried *Gracilaria* sp. was cut off to 0.5 cm and then stored in a clean and dry pack and sealed with aluminium foil



Figure 1. Site location of *Gracilaria* sp. samples (reservoir and shrimp pond biofilter).

2.3. Pigment Extraction

Pigment extraction was administered by single extraction. Ethyl acetate was used (1:10) to extract the dried seaweed for 24 hr maceration at room temperature (Hidayati *et al.*, 2019). Whatman no. 41 was used to sieve the extract. The extract was then concentrated with a rotary evaporator (Bucchi) and stored in a refrigerator and ready to use. Percentage of yield was calculated using the formula:

$$\text{Yield (\%)} = \frac{\text{weight of extract (g)}}{\text{weight of seaweed}} \times 100\%$$

2.4. Determination on Chlorophyll a and Carotenoids Contents

Chlorophyll a and carotenoids (Dere, 1993; Harborne, 1984) content were done spectrophotometrically (Shimadzu 1800). Five g of extract was diluted with acetone p.a. (1:1) The absorbance of samples was recorded at 645 nm, 663 nm dan 470 nm wavelength. The chlorophyll a and carotenoids content was determined based on this formulation

$$\text{Chlorophyll a } \mu\text{g/g sample (Ca)} = 12.21 \times A_{663} - 2.81 \times A_{646}$$

$$\text{Carotenoids } \mu\text{mol/g sample (Cx+c)} =$$

$$\frac{A_{470} + 0.114 \times A_{663} - 0.638 \times A_{646}}{V} \times 1000$$

$$= \frac{112.5 \times 0.1 \times 10}{V}$$

2.5. Agar extraction

Agar extraction methods were basically done by Jayasinghe *et al.*, (2016) with some modifications. Fifty grams of dried seaweed was extracted for 1.5 hr in hot water (85°C) added with 750 mL NaOH 5%. The extract was then rinsed with continuous tap water for discoloration. This was followed by aquadest 750 mL and homogenized. Acetic acid (CH₃COOH) was then added, stirred and boiled at ± 90-95°C for two hrs. The agar was then sieved, dropped with KCl 6 g, homogenized and poured into the container. Finally, 18 hrs later, the gel was performed and yield (%) was counted.

2.6. Nutrient Content

The proximate analysis was referred to as the Association of Official Analytical Chemists (AOAC, 2005) and conducted to 5 g samples.

2.6.1. Water content

Sample was put into the oven (105°C) for three hrs. Dried samples were then placed into dessicator until the weight was constant.

$$\text{Water content (\%)} = \frac{a - b}{c} \times 100\%$$

a = cup + dried sample

b = cup without sample

c = initial samole weight

2.6.2. Protein Analysis

Protein analysis was done by Kjeldahl methods, by located samples into Kjeldahl vial and destructed using 20 mL of hot sulfuric acid. The process was continued until samples were colorless and clear. This was then diluted and distilled with 10 mL of NaOH 10%. The distillate was then put into 25 mL of 3% H₃BO₃ and titered with HCl standard using methyl red as an indicator. The volume of titrants was used to calculate the percentage of total

nitrogen. The protein level was counted by multiplied the total nitrogen and correction factor.

Total nitrogen % = mL HCl x NHCl/sample weight x 14008 x f

Total protein % = total nitrogen x 6.25

denoted : f = correction factor (6.25).

2.6.3. Total Lipid Content

Total lipid analysis was done by soxhlet methods. Dried samples were wrapped with cotton wool. Sample was then placed into soxhlet extractor, using diethyl ether as solvent. Reflux was conducted by the samples until done. Vial was then put into the oven (105°C) and weight. The percentage of total lipid was determined by this formula:

Total lipid (%) = Lipid weight/Sample weight x 100%

2.6.4. Ash Content

Sample was weighed and burned at the top of bunsen until smoke produced and put in the muffle furnace at 500 - 600°C until turned to ash formation. Cup was cooled down and weighed. The ash content was counted using formula:

Ash content (%) = ash weight/sample weight x 100%

2.6.5. Total Carbohydrate

Total carbohydrate was counted simply by this equation:

Total carbohydrate (%) = 100% - (% ash + % water + % protein + % total lipid).

2.6.6. Characterization of Agar

Agar characterization was determined by Fourier Transform Infrared (FT-IR) spectroscopy (Thermo Nicolet 380 FTIR, Germany). Samples were mixed with KBr pellets (10% w/w). Similar to alginate, the pellet was recorded at 4000-500 cm⁻¹ (Yudiati and Isnansetyo, 2017).

3. Statistical Data Analysis

All data surveys were analyzed non parametrically (Mann Whitney test) using SPSS version 20.0 computer software. The laboratory data were analyzed using One Way ANOVA (Analysis of variance) using the same software, with a 95% level of significance.

4. Results

4.1. Water Quality Parameters

Salinity, nitrate and phosphate contents and others water quality parameter LS and HS with three subsites are shown in Table 1. There was a differences in salinity, nitrate and phosphate contents, while other parameters were similar.

Table 1. Water quality parameters of *Gracilaria* sp. grown in low salinity (reservoir) and high salinity (pond waste biofilter)

Parameter	LS	HS
Temperature (°C)	29.74 ± 0.15 ^a	29.70 ± 0.03 ^a
Salinity (ppt)	26.89 ± 3.15 ^a	44.00 ± 0.33 ^b
pH	8.0 ± 0 ^a	8.3 ± 0 ^a
Dissolve Oxygen (ppm)	3.55 ± 0.72 ^a	3.45 ± 0.05 ^a
Nitrate (mg/L)	0.43 ± 0.56 ^b	1.77 ± 1.44 ^a
Phosphate (mg/L)	0.78 ± 0.26 ^b	0.29 ± 0.19 ^a

4.2. Yield of pigment extraction, chlorophyll a and carotenoids content

Yield, chlorophyll a and carotenoids content in reservoir and shrimp pond biofilter is shown in Figure 1. Yield were similar, chlorophyll a and carotenoids of *Gracilaria* sp. sample in reservoir was higher.

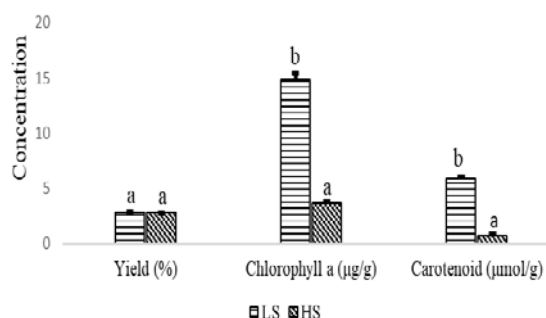


Figure 2. Yield, Chlorophyll and Carotenoids Content of *Gracilaria* sp. grown in high and low salinity. Different superscript indicates a significantly difference (p<0.05).

4.3. Agar Percentage and Characterization

Percentage of agar in *Gracilaria* sp. samples from LS and HS is shown at Table 2. Agar characterization of sample and standard agarose (Merck, USA) is depicted in Figure 3a, b and Table 3. Concentration of agar sample from LS habitat was significantly different compared to HS (p<0.05). On the other hand, pairwise comparison spectra of agar either from low or high salinity were fit to the standard.

Table 2. Percentage agar yield of *Gracilaria* sp. samples from low salinity (reservoir) and high salinity (biofilter)

Habitat	Agar (% w/w)
LS	25.79 ± 0.28
HS	6.60 ± 0.34

turgor pressure, this then leads to restrict division of cells and at last, affected the growth (Lee and Liu, 1999).

Nitrate content at HS in this study was higher than LS (Table 1). This is probably caused by instant efflux nutrient from the shrimp pond. Pond's feed waste and shrimp faecal contribute the nitrate content. Nutrient factor highly fluctuates on photosynthesis especially nitrate and phosphate (Ismail and Osman, 2016). Research by Wu *et al.*, (2018) reported that the nitrate and phosphorus uptake were higher at lower salinities (less than 20 psu) than higher salinity conditions (up to 20 psu). Study from Choi *et al.* (2010) exhibits that nitrate and phosphate uptake of macroalgae were greater in certain levels of salinity (20 and 25 ppt). These reports demonstrate similar suggestion to this study. Moreover, the water supply in LS from this study was more diverse, either from upside regimes from the sea as well as freshwater influxes from the river. Table 1 noted that phosphate content in LS was higher. The role of phosphate pathway is by transferring the high adenosine triphosphate (ATP) energy and other high energy compounds. This occurs in respiration and photosynthetic process (Ismail and Osman, 2016). These researchers' results were similar to our previous data, that photosynthetic pigments (chlorophyll a and carotenoids) of *Gracilaria* sp. in LS was higher when compared to the HS habitat (data is not shown).

5.2. Agar Percentage and Characterization

Data from Table 2 pointed that agar percentage of *Gracilaria* sp. in LS was significantly higher than HS. This is probably due to a relationship between salinity and the agar content. Research by Sasikumar *et al.* (1999) stated that a high salinity of *G. verrucosa* in summer (43.8%) was found to be negatively correlated with agar yield. The best agar production of *Gracilaria tenuistipitata* (24.8 ± 3.0 %DW) in laboratory was found at 25 psu (Bunsom and Prathep., 2012). Rocha *et al.* (2018) stated that, often, yield of agar of *G. tikvahiae* has been clearly connected with salinity and adversely with nitrogen content, similarly reported to *G. gracil* species (Martin *et al.*, 2013). Nitrogen concentration in LS, in fact, is lower than HS (Table 1). Less concentration of nitrogen, synthesis of protein declines in favor of polysaccharide synthesis. However, other factors such as nutrient availability, environmental and geographic factors, seasonal variations can influence the yield, chemistry and biosynthesis of agar (Lahaye and Rochas, 1991). Moreover, Lee *et al.* (2017) also stated that it is not easy to investigate the effects of a single factor on the yield of agar extracted from seaweeds grown in the natural habitat.

Based on spectra of FT-IR analyses, (Figure 2) shows that two *Gracilaria* sp. samples are fit to the standard agarose (Merck) and positively fingerprinted at a specific agar (1500-400 cm^{-1}) with galactose bond (around 1070 cm^{-1}). The vibration signal is slightly different, but overall those are agar characterizations. Agarose has a basic repeating unit of 1,3-linked β -D-galactopyranose and 1,4-linked 3,6-anhydro- α -L-galactopyranose. Based on figure 3 above, there is a 3,6 anhydrogalactose unit at a wave number of 928-933 cm^{-1} (Hii *et al.*, 2015). Observed bands at 930 cm^{-1} indicates O-H bending. The hydroxyl (O-H) unit appears at 3400 cm^{-1} wavenumber. Alkene (CH_3 or CH_2) associated to metoxil appeared at 2900 cm^{-1} .

Aldehyde group (-CHO) markedly appears at 1600 cm^{-1} (Pereira *et al.*, 2009).

Based on Figure 4, it can be seen that protein content in *Gracilaria* sp. samples from LS was significantly higher compared to HS ($p < 0.05$). Protein percentage is related to the nitrate content. In high salinity, nitrate compound has not taken up, easily (Choi *et al.*, 2010). However, in special cases, nutrient uptake can be occasionally imbalanced during unfavorable periods of situations (Trimmer *et al.*, 2000).

Results from Table 1 show that phosphate compound from the LS habitat was higher, and this may force the production of protein in the algal cell. Energy from photosynthesis will be used for amino acid biosynthesis that comes from the surrounding water. ATP is energy synthesized by photosynthesis, and these surely need phosphate. The reduction of protein synthesis triggered the decrease of the protein content and this was then affected the other cell components such as chlorophyll and other pigments (Ismail and Osman, 2016). This phenomenon was performed in *Gracilaria* sp. from HS habitat. Compared to other research, protein content in this study (14.40%) was higher than *G. changii* from Sarawak, Malaysia (12.57%) (Chan and Matanjun, 2016). Even though, this protein content was lower compared to the study on *G. corticata* by Rosemary *et al.* (2019).

Carbohydrate percentages from *Gracilaria* sp. samples grown in LS and HS were similar ($p > 0.05$) (Figure 4). Carbohydrate content in this study was higher than *G. changii* (Chan and Matanjun, 2016) and *G. edulis* (Rosemary *et al.*, 2019). Total lipid, water and ash content of *Gracilaria* sp. in both samples was not significantly different ($p > 0.05$). Generally, total lipid from all macroalgae, including *Gracilaria* sp. in this research, was relatively low at the range of 0.9-40% (Khairy and El Shafay, 2013). Seaweed is rich in minerals. The high ash content indicates high mineral content. In accordance to our finding, the results from Wu *et al.* (2018) reported that nutrient uptake, tissue nutrient contents were affected by salinity and the ideal salinity was around 20 psu. This information could be beneficial to define optimal salinity in *Gracilaria* sp. culture systems to get the maximal agar yield and pigment quality, protein and mineral content. This initiates better economic incomes for agarophyte farming.

6. Conclusion

Agar, chlorophyll a, carotenoids, protein and mineral contents of *Gracilaria* sp. grown from low salinity habitat (reservoir) were higher compared to high salinity habitat (biofilter shrimp ponds). Other compounds such as the total lipid, carbohydrate, water, and ash content from high and low salinity were similar. In this study, it can be concluded that salinity affected *Gracilaria* sp. nutrient content. Similar to the standard agar, FT-IR spectra from different salinity show the existence of 3,6-anhydro-L-galactose. Our findings can be useful for considering the application of *Gracilaria* sp. culture in the future.

References

- AOAC. 2005. Official Methods of Analysis of the Association of Official Analytical Chemists. Benjamin Franklin Station. Washington D.C.
- Asih T, Khayuridlo M, Noor R and Muhfahroyin. 2019. Biodiversity and Potential Use of Macro Algae in Pesisir Barat Lampung. *Biosaintifika*, **11**(1): 100-107.
- Badan Standarisasi Nasional. 1991. SNI 06-2412-1991. Metode Pengambilan Contoh Uji Kualitas Air.
- Badan Standarisasi Nasional. 1991. SNI 06-2480-1991. Cara Uji Nitrat Secara Spektrofotometri.
- Bunsom C and Prathep A. 2012. Effects of salinity, light intensity and sediment on growth, pigments, agar production and reproduction in *Gracilaria tenuistipitata* from Songkhla Lagoon in Thailand. *Phycological Research*, **60**: 169-178
- Chan PT, and Matanjun P. 2016. Chemical Composition and Physicochemical Properties of Tropical Red Sea Weed, *Gracilaria changii*. *Food Chem*, **(16)** : 1-37. Cikos AM, Jokic S, Subaric D and Jerkovic I. 2018. Overview on the application of modern methods for the extraction of bioactive compounds from marine macroalgae. *Mar Drugs*, **16**(10): 348-368.
- Dere S, Gunes T and Sivaci R. 1998. Spectrophotometric determination of chlorophyll-a, b, and total carotenoid content of some algae species using different solvent. *J of Botany*, **22**:13-17.
- Deyab MA. 2016. Inhibition activity of Seaweed extract for mild carbon steel corrosion in saline formation water. *Desalination*, **385**: 60-67.
- Du Q, Guiqi B, Yunxiang M and Zhenghong S. 2016. The complete chloroplast genome of *Gracilariopsis lemaneiformis* (Rhodophyta) gives new insight into the evolution of family Gracilariaceae. *J Phycol*, **52** (3): 441-450
- FAO. 2016. *The State of World Fisheries and Aquaculture 2016 – Contributing to food security and nutrition for all*. Rome.
- Graham LE and Wilcox LW. 2000. Algae. Prentice Hall, New York. (640pp.)
- Hamed I, Özogul F, Özogul Y and Regenstein JM. 2015. Marine bioactive compounds and their health benefits: A review. *Compr Rev Food Sci Food Saf*, **14**: 446-465
- Harborne JB. 1984. **Phytochemical Methods: A Guide to Modern Techniques of Plant Analysis**. second ed. Chapman and Hall, London.
- Hernandez A. 2017. The Effect of Salinity on the Growth of the Red Alga, *Gracilaria ehippisor*. Marine Science Department University of Hawai'i at Hilo.
- Hidayati JR, Yudiati E, Pringgenies D, Arifin Z and Oktavianti DT. 2019. *Sargassum* sp. Extract Macerated In Different Solvents Polarity. *Jurnal Kelautan Tropis*, **22** (1) : 73 – 80.
- Hii SL, Lim JY, Ong WT and Wong CL. 2015. Agar From Malaysian Red Seaweed as Potential Material for Synthesis of Bioplastic Film. *Journal of Engineering Science and Technology Special Issue on SOMCHE*, : 1 – 15.
- Ismail MM and Osman MEH. 2016. Seasonal fluctuation of photosynthetic pigments of most common red seaweeds species collected from Abu Qir, Alexandria, Egypt. *Revista de Biología Marina y Oceanografía*, **51**(3): 515-525.
- Israel A, Martinez-Goss M and Friedlander M. 1999. Effect of salinity and pH on growth and agar yield of *Gracilaria tenuistipitata* var. liui in laboratory and outdoor cultivation. *J Appl Phycol*, **11**: 543-549.
- Jayasinghe P, Pahalawattaarachchi S and Ranaweera KKDS. 2016. Effect of Extraction Methods on the Yield and Physicochemical Properties of Polysaccharides Extracted from Seaweed Available in Sri Lanka. *Poultry, Fisheries and Wildlife Sciences*, **4**(1): 1 - 6.
- Khairy HM and El-Shafay SM. 2013. Seasonal Variations In The Biochemical Composition of Some Common Seaweed Species From The Coast of Abu Qir Bay, Alexandria, Egypt. *Oceanologia*, **55**(2):435-452.
- Kim JK, Yarish C, Hwang EK, Park M and Kim Y. 2017. Seaweed aquaculture: cultivation technologies, challenges and its ecosystem services. *ALGAE*, **32**(1): 1-13.
- Kumar M, Kumari P, Gupta PV, Reddy CRK and Jha B. 2010. Biochemical responses of red alga *Gracilaria corticata* (Gracilariales, Rhodophyta) to salinity induced oxidative stress. *J Exp Mar Bio Ecol*, **391**: 27-34
- Lahaye M. and Rochas C. 1991. Chemical-structure and physicochemical properties of agar. *Hydrobiologia*, **221**: 137-148
- Lee, TM and Liu, CH. 1999. Correlation of decreased calcium contents with proline accumulation in the marine green macroalga *Ulva fasciata* exposed to elevated NaCl contents in seawater. *J Exp Bot*, **50**:1855-1862.
- Lee W-K, Lim Y-Y, Leow AT-C, Namasivayam P, Abdullah JO and Ho C-L. 2017. Factors affecting yield and gelling properties of agar. *J Appl Phycol*, **29**:1527-1540 DOI 10.1007/s10811-016-1009-y
- Luis A, Corpas FJ, López-Huertas E and Palma JM. 2018. **Plant Superoxide Dismutases: Function Under Abiotic Stress Conditions**. *Antioxidants and Antioxidant Enzymes in Higher Plants*. Springer, pp1-26.
- Martin LA, Rodriguez MC, Matulewicz MC, Fissore EN, Gerschenson LN and Leonardi PI. 2013. Seasonal variation in agar composition and properties from *Gracilaria gracilis* (Gracilariales, Rhodophyta) of the Patagonian coast of Argentina. *Phycological Research*, **61**(3): 163-171
- Odat N. 2018. Differential Gene Expression of Durum Wheat (*Triticum turgidum* L. var. durum) in Relation to Genotypic Variation under NaCl Salinity Stress. *Jordan Journal of Biological Science*, **11**(5): 591-595
- Phooprong S, Ogawa H and Hayashizaki K. 2007. Photosynthetic and respiratory responses of *Gracilaria salicornia* (C. Agardh) Dawson (Gracilariales, Rhodophyta) from Thailand and Japan. *J Appl Phycol*, **19**: 795-801.
- Pereira L, Amando AM, Critchley AT, Velde FVD and Ribeiro PJA. 2009. Identification of Selected Seaweed Polysaccharides (Phycocolloids) by Vibrational Spectroscopy (FTIR-ATR and FT-Raman). *Food Hydrocol*, **300**: (1-7).
- Pereira, DT, Simioni C, Filipin EP, Bouvie F, Ramlov F, Maraschin M., Bouzon ZL and Schmidt EC. 2017. Effects of salinity on the physiology of the red macroalga, *Acanthophora spicifera* (Rhodophyta, Ceramiales). *Acta Bot Brasilia*, **31**(4):555-565
- Rioux LE, Beaulieu L and Turgeon SL. 2017. Seaweeds: A traditional ingredients for new gastronomic sensation. *Food Hydrocoll*, **68**: 255-265.
- Rocha CMR, Sousa AMM, Kim JJ, Magalhães JMCS, Yarish C and Gonçalves MP. 2018. Characterization of agar from *Gracilaria tikvahiae* cultivated for nutrient bioextraction in open water farms. *Food Hydrocoll*, doi: <https://doi.org/10.1016/j.foodhyd.2018.10.048>.
- Rosemary T, Arulkumar A, Paramasivam S, Mondragon A and Miranda JM. 2019. Biochemical, Micronutrient and Physicochemical Properties of the Dried Red Seaweeds *Gracilaria edulis* and *Gracilaria corticata*. *Molecules*, **24** (2225) : 1-5.

- Sasikumar C, Rao VNR and Rengasamy R. 1999. The effect of environmental factors on the qualitative and quantitative characteristics of agar from the marine red alga *Gracilaria verrucosa* (Gracilariales, Rhodophyta). *Indian J Mar Sci*, **28**:270–273
- Sedjati S, Pringgienis D and Fajri M. 2020. Determination of the Pigment Content and Antioxidant Activity of the Marine Microalga *Tetraselmis suecica*. *Jordan Journal of Biological Sciences*, **13**(1): 55-58
- Stengel DB and Connan S. 2015. Marine algae: a source of biomass for biotechnological applications, in: D.B. Stengel, S. Connan (Eds.), *Natural Products From Marine Algae - Methods and Protocols*, Humana Press, New York, NY, 2015, pp. 1–37, https://doi.org/10.1007/978-1-4939-2684-8_1.
- Trimmer M, Nedwell DB, Sivyer DB and Malcolm SJ. 2000. Seasonal organic mineralisation and denitrification in intertidal sediments and their relationship to the abundance of *Enteromorpha* sp. and *Ulva* sp. *Mar Ecol Prog Ser*, **203**:67-80.
- Wong SL and Chang J. 2000. Salinity and light effects on growth, photosynthesis, and respiration of *Grateloupia filicina* (Rhodophyta). *Aquaculture*, **182**:387–395
- Wu H, Shin SK, Jang S, Yarish C and Kim JK. 2018. Growth and Nutrient Bioextraction of *Gracilaria chorda*, *G. vermiculophylla*, *Ulva prolifera*, and *U. compressa* Under Hypo- and Hyper-Osmotic Conditions. *ALGAE*, **33**(4): 329-340.
- Xu SY, Xuesong H and Kit-Leong C. 2017. Recent Advances in Marine Algae Polysaccharides: Isolation, Structure, and Activities. A review. *Mar Drugs*, **15** (388) : 1-16
- Xu SY, Huang X and Cheong KL. 2017. Recent Advances in Marine Algae Polysaccharides: Isolation, Structure, and Activities. *Mar Drugs*, **15** (388): 1-16
- Yudiati E and Isnansetyo A. 2017. Characterizing the Three Different Alginate Type of *Sargassum siliquosum*. *ILMU KELAUTAN: Indonesian Journal of Marine Sciences*, **22**(1):7-14
- Yudiati E, Isnansetyo A, Ayuningtyas, Handayani CR, Murwantoko and Triyanto. 2016. Innate immune-stimulating and immune genes up-regulating activities of three types of alginate from *Sargassum siliquosum* in Pacific white shrimp, *Litopenaeus vannamei*. *Fish & Shellfish Immunol*. **54**: 46-53.
- Yudiati E, Santosa GW, Tontowi MR, Sedjati S, Supriyanti E and Khakimah M. 2018a. Optimization of alginate alkaline extraction technology from *Sargassum polycystum* and its antioxidant properties. *IOP Conf. Ser.: Earth Environ. Sci.* **139**. 012052. doi :10.1088/1755-1315/139/1/012052
- Yudiati E, Pringgienis D, Djunaedi A, Arifin Z and Sudaryono A. 2018b. Free radical Scavenging of Low Molecular Weight Sodium Alginate (LMWSA) from *Sargassum polycystum* Produced by Thermal Treatment. *Aquac Ind*, **19** (1): 21-27.
- Yudiati E, Isnansetyo A, Murwantoko, Triyanto and Handayani CR. 2019. Alginate from *Sargassum siliquosum* Simultaneously Stimulates Innate Immunity, Upregulates Immune Genes, and Enhances Resistance of Pacific White Shrimp (*Litopenaeus vannamei*) Against White Spot Syndrome Virus (WSSV). *Marine Biotechnology* **21**(4):503-514. <https://doi.org/10.1007/s10126-019-09898-7>
- Yudiati, E, Rustadi, Ginzel FI, Hidayati JR., Rizfa MS, Azhar N, Djarod MSR, Heriyati E, and Alghazeer R. 2020. Oral Administration of Alginate Oligosaccharide from *Padina* sp. Enhances Tolerance of Oxygen Exposure Stress in Zebrafish (*Danio rerio*). *ILMU KELAUTAN: Indonesian Journal of Marine Sciences* **25**(1):7-14.

Biochemical changes in the liver, kidney and serum of rats exposed to ethanolic leaf extract of *Ziziphus spina-christi*

Sabah M. Khaleel¹, Rana A. Almuhur¹, Taghleab M.F. Al-Deeb^{1,*} and Adnan S. Jaran²

¹ Department of Biological Science, Al-Bayt University, Mafraq, Jordan; ² Department of Medical Laboratory Science, Al-Bayt University, Mafraq, Jordan

Received: June 6, 2020; Revised: Nov 18, 2020; Accepted: Nov 28, 2020

Abstract

Ziziphus spina-christi has been used in traditional herbal medicine for the treatment of fever and inflammatory conditions. However, few studies had assessed its toxicological effects. This study was designed to investigate the effect of ethanolic leaf extract of *Z. spina-christi* on biochemical markers of kidney and liver functions. Fourteen male Wistar albino rats were randomly assigned into two groups. Group I was the control group while group II received oral dose of 400 mg/kg ethanolic leaf extract daily for 14 days. On the 15th day of treatment, rats were sacrificed and some biochemical parameters were evaluated. Then, liver, kidney and heart were taken, weighed and relative organ weight was calculated. Oral dose of leaf extract significantly ($P < 0.05$) increased rats' serum levels of lactate dehydrogenase and total bilirubin while had no significant effect on the other liver enzymes. On the other hand, treatment with the extract significantly increased insulin level, decreased triglyceride level and had no significant effect on the other lipid profile components. Kidney function parameters were not significantly affected by the extract treatment. However, relative liver and heart weight ratios were significantly reduced in ($P < 0.05$) treated rats. The results of this study have shown that oral administration of the ethanolic leaf extract of *Z. spina-christi* did not have deleterious effect on liver, kidney and serum biochemical parameters at the dosage used.

Keywords: *Ziziphus spina-christi*, lipid profile, Kidney function, Liver function, Wistar rats

1. Introduction

Many people from diverse cultures use traditional plants as a source of folkloric medicines. The presence of high concentrations of phytochemical compounds in these plants promotes attention to evaluate their potential health-promoting effects (WHO, 1998, Pieme *et al.*, 2006). Since synthetic drugs are not often affordable or safe, many studies were performed to seek new natural bioactive molecules, which are considered to be safe and without side effects (Kunle *et al.*, 2012; Mostafavinia *et al.*, 2016).

Lack of quality control and scientific evidence for the efficacy and safety of medicinal plants are major concerns that have been raised recently; since many plants were consumed at higher dosages and for long time, they could be toxic and directly impact the physiological function of the body (Nuhu and Aliyu (2008; Herrine, 2018). Therefore, there is a need for more scientific evaluations on their efficiency and potential toxicity.

Ziziphus spina-christi belongs to the family *Rhamnaceae*. It is commonly called sedr. It has been used as a medicine in Arabic herbal traditions, especially in Jordan (Abu-Hamdah *et al.*, 2005; Khaleel *et al.*, 2016). The most common therapeutic properties of the *Ziziphus* are antioxidant, anti-cancer, antibacterial, antiviral and anti-inflammation properties (Khaleel *et al.*, 2019). The

major active components of *Z. spina christi* are flavonoids, tannins and phenolic compounds (Khaleel *et al.*, 2018). Despite the wide spread use of this plant, there are a few specific scientific reports on the evaluation of its toxicological effects. Therefore, this study was designed to assess the kidney and liver function indices in male Wistar albino rats administered ethanolic leaves extract of *Z. spina-christi*. Serum biochemical parameters, body and organ weight changes were also screened.

2. Materials And Methods

2.1. Preparation of crude plant extracts

Ziziphus spina-christi leaves (herbarium collection number 3543) were collected from different locations of Jordan valley in spring. The leaves were air dried, ground into a powder and soaked in 75% ethanol. The plant material was then shaken overnight at (30°C) on a shaker for 48 hrs, then filtered, and dried by rotary evaporator and weighed (Khaleel, 2013).

2.2. Experimental Animals and Dosing

Fourteen male Wistar albino rats weighing between 185 and 245 g were obtained from the Department of Biological Science, Faculty of Science, Yarmouk University, Jordan. The rats were divided into two equal groups. Each group was kept in a plastic cage and housed

* Corresponding author e-mail: taghleab@aabu.edu.jo.

in a well ventilated 12 h light and dark cycle. Commercial standard diet and water was supplied for 14 days. This study was performed according to the protocol of animal experiments and confirmed by the research and ethics committee of the department of biological sciences at Al al Bayt University, Mafraq, Jordan.

For a period of 14 consecutive days, experimental animals orally received *Z. spina-christi* ethanolic leaf extract (400 mg/kg), whereas control group orally received normal saline for the same period (Bannooh *et al.*, 2015).

2.3. Body and organs weights

Animals were individually weighed at the beginning and at the end of the experiment using an electronic weighing balance. Body weight change of rats in each group was calculated and expressed in percentage (%). Liver and kidney were harvested and weighed, from which the relative liver and kidney weights per 100 g body weight of rat was calculated according to the following equation:

$$\text{Relative organ weight} = [\text{organ weight (g)} / \text{body weight (g)}] \times 100$$

2.4. Blood sampling

Animals were sacrificed on the 15th day by cervical dislocation. Blood was collected in a wax embedded tube and serum was separated by centrifugation at 5000 rpm for 10 min and collected in a different tube and kept in freezer till the time of assay.

2.5. Biochemical analysis

Different serum biochemical parameters were determined using commercially available diagnostic kits from Biosystems S.A. Costa Brava, Barcelona (Spain). Serum samples were analyzed for the levels of aspartate aminotransferase (AST), alanine aminotransferase (ALT), alkaline phosphatase (ALP), lipase, and lactate dehydrogenase, and for the levels of glucose, insulin, low-density lipoproteins (LDL), high-density lipoproteins (HDL), total protein, creatinine, cholesterol, triglyceride, total bilirubin, uric acid and urea. All tests were analyzed according to the manufacturer's instructions.

2.6. Statistical analysis

Data were analyzed using two-sample t-test. Values were expressed as means \pm SD of three replicates. A probability value $P < 0.05$ was considered to be statistically significant.

3. Results

3.1. Effects of *Ziziphus* leaf extract on liver function parameters in rats

Following oral administration of 400 mg/kg doses of *Z. spina christi*, serum ALP level was reduced compared to the control group. However, ALP level wasn't significantly different between treated group and the control group. ALT and AST levels were not significantly ($P > 0.05$) increased in treated rats. On the other hand, the treated rats showed a significant ($p < 0.05$) elevation of LDH and total bilirubin levels (Figure 1).

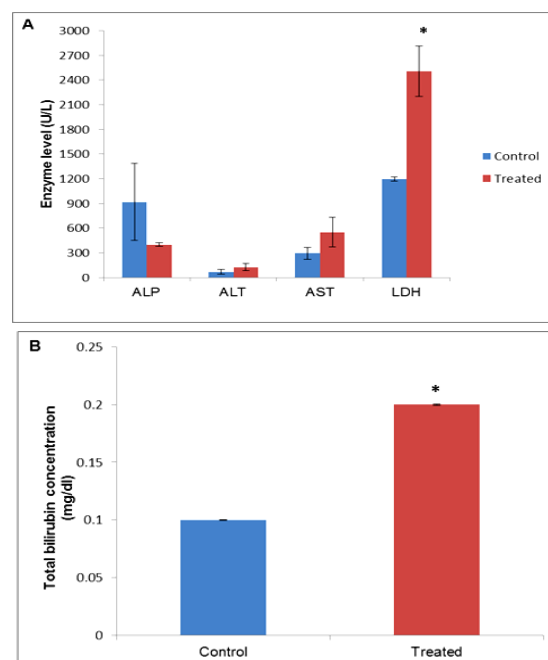


Figure 1. Liver enzymes (A) and total bilirubin (B) levels in control and extract-administered (treated) rats. Values were reported as mean \pm SD (n=3 replicates). Asterisk (*) indicates a statistical significance ($P < 0.05$).

3.2. Effects of *Ziziphus* leaf extract on the kidney function parameters and total protein concentration in rats

The effects of the plant extract on the kidney functions of the rats are revealed in Figure 2. The treated and control rats showed no significant difference ($p < 0.05$) in the levels of urea, uric acid and creatinine (Figure 2A). However, there was a significant elevation in total protein concentration in treated group compared to the control group (Figure 2B).

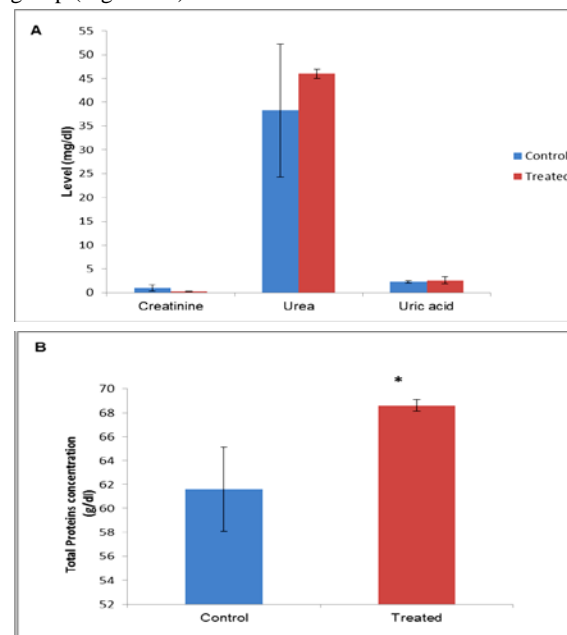


Figure 2. Creatinine, urea, uric acid levels (A) and total protein concentration (B) in control and extract administered (treated) rats. Values were reported as mean \pm SD (n=3). Asterisk (*) indicates a statistical significance ($P < 0.05$).

3.3. Effect of Ziziphus leaf extract on serum glucose and insulin levels in non-fasting rats

Extract-administered rats (treated) showed reduction in glucose level, but this reduction wasn't significantly different from the control. On the other hand, treated rats showed a significant ($P<0.05$) increase in insulin level as compared with control group (Table 1).

Table 1. Serum glucose and insulin levels in control and extract-administered (treated) rats (non-fasting)

	CONTROL	Treated
Glucose (mg/dl)	149.6±8.5	133.0±7.0
Insulin (uIU/mL)	0.7±0.01	0.80±0.02*

Values were reported as mean ± SD (n=3). Asterisk (*) indicates a statistical significance ($P<0.05$).

3.4. Effect of Ziziphus leaf extract on serum lipid profile in rats

As shown in Figure 3, extract-administered rats (treated) showed reduction in the levels of serum triglyceride, cholesterol and LDL, and increase in the levels of serum HDL and lipase, when compared with control group. However, only triglyceride reduction was significantly different ($P<0.05$) between treated rats and the control.

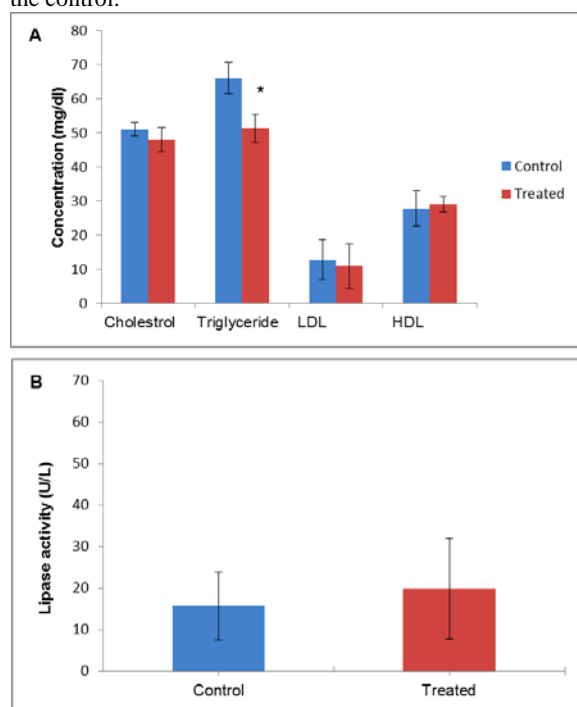


Figure 3. Cholesterol, triglyceride, LDL, HDL (A) and lipase level (B) in control and extract administered (treated) rats. Values were reported as mean ± SD (n=7). Asterisk (*) indicates a statistical significance ($P<0.05$).

3.5. Effects of Ziziphus leaf extract on rat's body weight and relative organ weight.

The mean body weights of rats treated with *Ziziphus* extract did not significantly ($P<0.05$) differ from controls (Table 2). However, the computed relative liver and heart weight ratios were significantly ($P<0.05$) decreased in treated rats (Table 2). This study illustrated that 400 mg/kg dose of *Ziziphus* extracts did not cause mortality in treated rats.

Table 2. Body weight change, and kidney, liver and heart indices in control and extract-administered (treated) rats.

	Control	Treated
% Weight change	2.2±9.8	17.4±13.6
Kidney index	0.82±0.01	0.70±0.071
Liver index	4.1333±0.25	3.1333±0.41*
Heart index	0.4933±0.04	0.3367±0.07*

Values were reported as mean ± SD (n=3 replicates). Asterisk (*) indicates a statistical significance ($P<0.05$).

4. Discussion

Many plants have a variety of properties and various biological components that can be used to treat various diseases. However, some medicinal plants have potential to impair a particular organ or organs' function in many ways (Nuhu and Aliyu, 2008; Herrine, 2018). This study was designed to assess the liver and kidney functions and serum biochemical indices in male Wistar albino rats administered ethanol leaves extract of *Z. spina christi*, a Jordanian medicinal plant.

Liver enzymes such as ALT, AST, LDH and ALP were used to evaluate the hepatic dysfunction. The increased liver enzyme activities significantly reflect liver hepatocytes necrosis and cholestasis, and the high level of transaminases causes inflammation or hepatocellular disorders (Ali *et al.*, 2005, Lavanaya *et al.*, 2011). In the present study, the oral administration of the *Ziziphus* extract to rats resulted a significant increase in LDH level which coincided with insignificant reduction of glucose level in rats' serum (Table 1) suggesting that glucose may have gone through glycolysis to produce pyruvate/lactate. However, there was no significant difference in the glucose level between treated rats and control which might suggest that lactate was converted back to pyruvate then to glucose through gluconeogenesis (Andrew *et al.*, 2005). On the other hand, insignificant change in the serum levels of ALT, AST and ALP levels was found in treated rats compared with the control (Figure 1). It can be observed that the changes in the three enzyme levels are not consistent to indicate liver damage. Although it was insignificant, the reduction in the levels of alkaline phosphatase (ALP), as observed in this present study, could be an indication of a good effects of *Ziziphus* extract on both liver and bone, since the two main sources of ALP are liver and bone. These findings are in agreement with the observations of Nwanjo (2007) and Ibrahim *et al.*, (2016) when they reported insignificant increases in AST and ALT levels in serum to indicate non-hepatotoxic effects of the *Phyllanthus niruri* leaf extract and tuber extracts of *M. psuedopetalosa*, respectively. Moreover, it was reported that ALT, AST and ALP levels insignificantly increased after treating Wistar rats with 500mg/kg oral dose of *Senecio aureus* extract (Osugwe and Margret, 2017). On the contrary, El-Desouky (2014) reported that oral administration of ethanolic *Ziziphus mauritiana* leaf extracts resulted in a significant decrease in level of ALT and AST enzymes in serum of γ -irradiated rats. The same observations were obtained in rats administered *Anthyllis henoniana* ethyl acetate flowers extract (Ben Younes *et al.*, 2018). By contrast, rats treated with ethanolic leaf extract of *Sorghum bicolor* showed extremely significant ($P<0.05$) elevated levels of AST,

ALT and ALP, which indicated intra-hepatic cell damage due to the extract administration (Ogunka-Nnoka *et al.*, 2012). Elevated levels of serum bilirubin, as in certain diseases, is an index of liver damage and the major breakdown product of red blood cells (Baranano *et al.*, 2002; Tano *et al.*, 2013). Osuigwe and Margret (2017) found that 500mg/kg oral dose of *Senecio aureus* extract significantly increased total bilirubin level in Wistar rats suggesting a possible liver damage in the treated rats. In the present study, compared with the control, the serum total bilirubin concentration increased significantly ($P < 0.05$) in extract-administered rats with bilirubin concentration of 0.2 ± 0.0 mg/dL (Figure 2). However, the serum total bilirubin values were still within the normal range (0.1-0.55 mg/dL).

Creatinine, urea and uric acid are major catabolic products of protein metabolism, and an elevation in their serum levels may indicate renal dysfunction (Renugadevi and Prabu, 2010; Mehrdad *et al.*, 2011). Compared with the control (Figure 2), significant differences ($p < 0.05$) were not observed in the levels of creatinine, urea and uric acid in control and extract-administered rats. This indicates that the leaf extract had no negative effect on the kidneys. However, significant difference exists between the treated and control rats in the levels of serum total protein, which implies that the extracts might be able to improve protein synthesis. Determination of serum or plasma protein levels is clinically valuable and reflects major functional changes in kidney and liver functions (Leena *et al.*, 2011). Low total protein levels may suggest liver and/or kidney disorders in which protein is not digested or absorbed properly. High total protein level may be seen in cases of chronic inflammation or liver infections (Ighodaro *et al.*, 2015). These results of kidney functions are in agreement with the findings reported by Ashafa and Olunu (2011) on toxicity of leaf extracts of *Marinda lucida*.

According to the biochemical analysis, *Ziziphus* extract exhibited good improvement in biological evaluation of glucose, insulin and lipid profile. Wistar albino rats given leaf extracts of *Z. spina-christi* showed reduction in the levels of cholesterol, triglycerides, LDL, as well as elevation in the level of serum Insulin and HDL (Table 1, Figure 3). This effect may be due to the inhibition of dietary lipid absorption in the intestine, or low level of lipolysis and/or low activity of cholesterol biosynthesis enzymes which are under the insulin control (Ahmadvanda *et al.*, 2012). A similar result was reported by Al-Qudah *et al.*, (2016) who reported that treatment of diabetic rats with ginger extract produced a significant decrease in serum level of glucose, cholesterol and triglycerides and increase insulin and HDL-C levels when compared with untreated diabetic group. Furthermore, Seufi *et al.*, (2019) found that 150mg/kg oral dose of *Morus nigra* leaf extract significantly decreased serum triglycerides level in chlorpyrifos-exposed male Albino rats.

There was no significant change in the weights seen in all animals treated with ethanolic leaf extract of *Z. spina-christi* at a dose of 400 mg/kg. However, the relative liver and heart weights of the animals treated with the plant extract significantly decreased (Table 2). The decrease in the weight of these organs might be due to the anti-nutritional bioactive components such as tannin probably present in the plant extract. (Alebachew *et al.*, 2014).

Generally, the observed medicinal value of ethanolic extract of *Ziziphus* might be due to the phytochemicals composition of the extract which are flavonoids, tannins and phenol compounds (Khaleel, *et al.*, 2016; 2018b). There is, however, a need for further study so that the molecular mechanism of the observed protective effect and the actual active principles in the extract could be delineated.

5. Conclusions

The current study suggests that oral administration of the ethanolic leaf extract of *Z. spina-christi* is relatively safe and did not have deleterious effect on liver, kidney and on the serum biochemical parameters at the dosage investigated, but may have the tendency to cause reduction in the relative organ weights in rats. Studies for extended period are suggested to determine if the prolonged continuous use of the extract might cause challenge on the functional capacity of the organs. Histological studies are recommended for further assessment.

Acknowledgements

This research was funded by the Deanship of Academic Research at Al al-Bayt University (Project No. 7570/2015).

Conflicts of interest statement

The authors declare that there are no conflicts of interest.

References

- Abu-Hamdah S, Afifi F, Shehadeh M and Khalid S. 2005. Simple quality-control procedures for selected medicinal plants commonly used in Jordan. *Pharm Biol.*, **43**(1): 1–7.
- Ahmadvanda H, Tavafic M and Khalatbary AR. 2012. Hepatoprotective and hypolipidemic effects of *Satureja khuzestanica* essential oil in alloxan-induced type 1 diabetic rats. *Iran J Pharm Sci.*, **11**: 1219-1226.
- Alebachew M, Kinfu Y, Makonnen E, Bekuretsion Y, Urga K and Afework M. 2014. Toxicological evaluation of methanol leaves extract of *Vernonia bipontini* Vatke in blood, liver and kidney tissues of mice. *Afr Health Sci.*, **14**(4).
- Ali AT, Penny CB, Paiker JE, Van Niekerk C, Smit A, Ferris WF, *et al.* 2005. Alkaline phosphatase is involved in the control of adipogenesis in the murine preadipocyte cell line, 3T3-L1. *Clin Chim Acta*, **354**(1-2): 101-9.
- Al-Qudah MA, Haddad MA and EL-Qudah JM. 2016. The effects of aqueous ginger extract on pancreas histology and on blood glucose in normal and alloxan monohydrate-induced diabetic rats. *Biomed Res.*, **27**(2): 350-356.
- Andrew P, Adam LM, and Adam WW. 2005. Lactate-a signal coordinating cell and systemic function. *J Exp Biol.*, **208**:4561-4575.
- Ashafa A and Olunu O. 2011. Toxicological evaluation of ethanolic root extract of *Morinda Lucida* (L) Benth. (Rubiaceae) in male Wistar rats. *J Nat Pharm.*, **2**,108- 114.
- Bannoth CK, Devanna N, Rani S, Krishna OS, Sree MG and Mallikarjun G. 2015 Anti-hyperlipidaemic activity of ethanolic extract of whole plant of *Corallocarpus epigaeus* on wistar rats. *Int J Res Pharm Sci.*, **6**(1):35-43.

- Baranano DE, Rao M, Ferris CK and Snyder SH. 2002. Biliverdin reductase: a major physiologic cytoprotectant. *Proc Natl Acad Sci U S A*, **99** (25): 16093–16098.
- Ben Younes A, Ben Salem M, El Abed H and Jarraya R. 2018. Phytochemical screening and antidiabetic, antihyperlipidemic, and antioxidant properties of *anthyllis henoniana* (coss.) flowers extracts in an alloxan-induced rats model of diabetes. *Evid Based Complement Alternat Med.*, 1-14
- Dkhil MA, Kassab RB, Al-Quraishy S, Abdel-Daim MM, Zrieq R and Abdel Moneim AE. 2018. "Ziziphus spina-christi (L.) leaf extract alleviates myocardial and renal dysfunction associated with sepsis in mice. *Biomed Pharmacother.*, **102**: 64–75.
- El-Desouky WI, Abd El-Aleem IM and Saleh ES. 2014. Effect of ethanolic ziziphus (*ziziphus mauritiana* lam.) leaves extract as radioprotector on some biochemical parameters of γ -irradiated male albino rats. *Int J Adv Res.*, **2**(4): 1046-1057.
- Etim O, Ekpo A, Basse U and Akpan A. 2018. Effect of aqueous and ethanol leaf extracts of *musa paradisiaca* on serum protein, liver and kidney function in albino wistar rats. *IOSR J Biotechnol Biochem.*, **4**(6): 16-19.
- Herrine SK. 2018. Medicinal herbs and the liver. Available online at <https://www.merckmanuals.com/home/liver-and-gallbladder-disorders/drugs-and-the-liver/liver-injury-caused-by-drugs>. (Accessed 1 Nov 2018).
- Ibrahim MA, El Nur E and Gameel A. 2016. Changes in body weight and serum biochemical parameters of Wistar rats orally dosed with *merua psudopetalosa* (gilg and bened.) De wolff tuber extracts. *Eur J Med Res.*, **4** (1): 52-59.
- Ighodaro I, Innih S, Ogedengbe S and Amamina L. 2015. Chronic Toxicity Studies of Aqueous Leaf Extract of *Voacanga africana* in Wistar Rats. *J Appl Sci Environ Manag.*, **19** (4): 639 – 646.
- Khaleel SM and Haddadin MY. 2013. The enhancement of hawthorn leaf extracts on the growth and production of short chain fatty acids of two probiotic bacteria. *Pak J Nutr.*, **12**(2): 144-149.
- Khaleel SM, Jaran SJ and Al-Deeb TM. 2019. Antimicrobial and lipid peroxidation inhibition potential of *ziziphus spina-christi* (sedr), a Jordanian medicinal plant. *J Biol Sci.*, **19**(2): 131-136.
- Khaleel SM, Jaran SJ and Haddadin MY. 2016. Evaluation of total phenolic content and antioxidant activity of three leaf extracts of *Ziziphus spina-christi* (sedr) grown in Jordan. *Br J Med Med Res.*, **14**(6): 1-8.
- Khaleel SM. 2018a. Anti- α -glucosidase, anti- α -amylase and anti-inflammatory effects of leaf extracts of *Ziziphus spina-christi* (sedr) grown in Jordan. *Res J Biol Sci.*, **13**: 1-7.
- Khaleel SM. 2018b. Studying the heavy metals composition and the impact of different common solvents on the extraction efficiency of phytochemical secondary metabolites from the leaves of *Ziziphus spina-christi* grown in Jordan. *Pak J Nutr.*, **17**(8): 392-398.
- Khatab HAH, Al-Amoudi NS and Al-Faleh AA. 2013. Effect of ginger, curcumin and their mixture on blood glucose and lipids in diabetic rats. *Life Sci J.*, **10**(4): 428-442.
- Kunle OF, Egharevba HO and Ahmadu PO. 2012. Standardization of herbal medicines- A review. *Int J Biodivers Conserv.*, **4**(3):101-12.
- Lavanaya S, Ramesh M, Kavitha C and Malarvizhi A. 2011. Haematological, biochemical and ion regulatory response of Indian major Carp, *Carpa catla* during chronic sublethal exposure to inorganic arsenic. *Chemosphere*, **82**(7): 977 – 985.
- Leena K, Veena S, Arti S, Shweta L and Sharma SH. 2011. Protective role of *coriandrum sativum* (coriander) extracts against lead nitrate induced oxidative stress and tissue damage in the liver and kidney in male mice. *Int J Appl Biol Pharm.*, **2**(3):65–83.
- Mehrdad M, Mozghan GP, Sayed AT and Alireza J. 2011. Study of Histopathologic Changes of Zingiber extract on mice kidneys. *International Conference on Food Engineering and Biotechnology – IPCBEE*, **9**: 16 – 20.
- Mostafavinia SE, Khorashadizadeh M and Hoshyar R. 2016. Antiproliferative and proapoptotic effects of crocin combined with hyperthermia on human breast cancer cells. *DNA Cell Biol.*, **35**(7).
- Nuhu AA and Aliyu R. 2008. Effects of *Cassia occidentalis* aqueous leaf extract on biochemical markers of tissue damage in rats. *Trop J Pharm Res.*, **7**(4): 1137–1142.
- Nwanjo H. 2007. Studies on the effect of aqueous extract of *Phyllanthus niruri* leaf on plasma glucose level and some hepatospecific markers in diabetic Wistar rats. *Int J Lab Med.*, **2** (2): 17-21.
- Ogunka-Nnoka CU, Uwakwe AA and Nwachoko NC. 2012. Serum enzyme and histological studies of albino rat treated with ethanol/potash extract of *Sorghum bicolor* leaf sheath. *Indian J Drugs Dis.*, **1** (3): 74-78.
- Osuigwe MJ and Margret N. 2017. Evaluation of the toxicological effects of *Senecio aureus* extract on the liver and hematological parameters in Wistar rats. *Jordan J Biol Sci.*, **10**(1): 29-32
- Pieme C, Penlap V, Nkedoum B, Taziebou C, Tekwu E, Etoa F and Ngongang J. 2006. Evaluation of acute and subacute toxicities of aqueous ethanolic extract of leaves of *Senna alata* (L.) roxb (Cesalipiniaceae). *Afr J Biotechnol.*, **5**: 283-289.
- Renugadevi J and Prabu SM. 2010. Cadmium-induced hepatotoxicity in rats and the protective effect of naringenin. *Exp Toxicol Pathol.*, **62**:171–81.
- Seufi A, Mohammed H, Moussa F, Seif El-Din A, El-Saadani M, Taha T and Hafez E. 2019. Protective Effects of the Aqueous Extract of Black Mulberry Leaves, *Morus nigra*, on Chlorpyrifos Toxicity in Male Albino Rats. *Jordan J Biol Sci.*, **12**(4): 385 – 393.
- Tano KD, Kouadio JH, Yavo W, Djaman AJ and Menan EH. 2013. Toxic effect study of methanol extract of *Terminalia glaucescens* leaves following single or short-term repetitive oral administration in Swiss mice. *Am J Biosci.* **1**(4) : 85–90.
- WHO. 1998. Traditional medicine regulatory situations of herbal medicines. *A worldwide review*, Geneva, 1-5.

Morphological and Phylogenetic Characteristics of *Ditylenchus dipsaci* among Garlic Plants

Miftahul Ajri¹, Siwi Indarti^{1,2,*}, Alan Soffan¹ and Nguyen Ngoc Huu³

¹Department of Crop Protection, Faculty of Agriculture, Universitas Gadjah Mada Jl. Flora No.1 Bulaksumur, Sleman 55281, Yogyakarta Special Region, Indonesia; ²Agrotechnology Innovation Centre (AIC), Universitas Gadjah Mada Jl. Tanjung Tirta, Kalitirto, Berbah, Sleman 55573, Yogyakarta Special Region, Indonesia; ³Department of Plant Biology, Faculty of Agriculture and Forestry, University of Tay Nguyen, 567 Le Duan St. Buon Ma Thuot City, Dak Lak Province, Vietnam, 63100

Received: June 15, 2021; Revised: July 6, 2021; Accepted: Sep 16, 2021

Abstract

Stem and bulb nematode, *Ditylenchus dipsaci* (Kuhn, 1857), is a severe pest on garlic and other vegetables causing yellowing of leaves and rotting of bulbs. The existence of *D. dipsaci* in Indonesia was first reported in Temanggung, Central Java, in 2018. These researches aim to determine the distribution area, identification, and the genetic relationship of *D. dipsaci* which attacked garlic in Central and East Java. The study was conducted by sampling garlic plants attacked by *D. dipsaci* and extraction-isolation by immersion method. Species identification was carried out morphologically, morphometrically, and molecularly using PCR techniques. The results showed that *D. dipsaci* has been spread on garlic plants in Central Java (Magelang, Temanggung, Karanganyar, Tegal, and Brebes) and East Java (Malang and Mojokerto). The varieties that were attacked were Lumbu Kuning, Lumbu Hijau, Sangga Sembalun, and Tawangmangu Baru. The highest population was found in Kaliangkrik, Magelang, with 53.46 nematodes (5 g bulbs)⁻¹. Based on morphological and morphometric identification, the species found was *D. dipsaci*. Based on molecular identification, samples from Jabung Mojokerto and Malang Poncokusumo were amplified at ± 600 bp with the D2A / D3B primers in the 28S rDNA region. *D. dipsaci*, found in East Java, was an indigenous Indonesian species based on phylogenetic studies.

Keywords: *Allium sativum* L., Crop protection, Flagship horticulture, Infected area, Pest control, Stem and bulb nematode

1. Introduction

The import value of garlic (*Allium sativum* L.) in Indonesia reaches 559 728 t yr⁻¹ or 96.6 % of the consumption of garlic in Indonesia (Ministry of Agriculture - Republic of Indonesia, 2018). Planting imported garlic seeds is one of the government's efforts to achieve garlic self-sufficiency. However, imported garlic seeds can be a carrier media for quarantine pests. *Ditylenchus* spp. is one of the quarantine pests that can be spread in Indonesia through imported seeds. *Ditylenchus* species that have attacked garlic plants are *Ditylenchus dipsaci* Kuhn, 1857 (Pethybridge *et al.*, 2016) and *Ditylenchus destructor* Thorne, 1945 (Yu *et al.*, 2012). *D. dipsaci* can cause yield losses in garlic plantations by 15.33 % to 90 % (Abawi and Moktan, 2010; Yavuzaslanoglu *et al.*, 2015).

Ditylenchus spp. or stem and bulb nematodes mainly attack the host plant's root, tubers, and stems. The infective stage of this nematode is the fourth juvenile. Attacked plants show stunted growth, yellowing and twisting leaves. Infested bulbs are necrotic and tend to rot with dark to a black colour, becoming soft (Yavuzaslanoglu *et al.*, 2015).

D. dipsaci is found in various temperate (Wulandari and Indarti, 2020; Wulandari *et al.*, 2021), subtropical to

tropical regions such as Europe and the Mediterranean region, North and South America, North and South Africa, Asia (China, India, Iran, Iraq, Israel, Japan, Taiwan, Turkey, Kazakhstan and South Korea) and Oceania (CABI, 2018). *Ditylenchus* spp. can be spread through infected tubers, seeds, crop residues, attached soil, and other plants or weeds as alternative hosts. Planting infected seeds will increase the attack and losses incurred compared to the previous planting season (Sikora and Fernández, 2005). As with plant-parasitic nematodes, such as root-knot nematodes, infection of *Ditylenchus* spp. exhibits poor growth, a loss in quality and yield of the crop (Youssef and El-Nagdi, 2021)

Ditylenchus spp. has been found in garlic plants in Temanggung Regency, Central Java, and is considered *D. dipsaci* based on symptoms of an attack and morphological characters (Indarti *et al.*, 2018). A survey of the *D. dipsaci* distribution area is needed to prevent the spread of nematodes to other regions in Indonesia. This study aims to determine the distribution area, identification, and genetic relationship of *D. dipsaci* which attacked garlic in Central and East Java, Indonesia.

* Corresponding author e-mail: siwi.indarti@ugm.ac.id.

2. Materials and Methods

2.1. Nematodes sampling and population analysis

Nematode samples were taken by purposive sampling method or by taking symptomatic garlic plants during 2019 at garlic plan in 20 d to 120 d after planting. Sampling locations were Magelang, Temanggung, Karanganyar, Tegal and Brebes Regency (Central Java Province) and Mojokerto and Malang (East Java Province). Nematodes were extracted from bulbs and roots by the water immersion method (Zhang *et al.*, 2013). Bulbs and roots were cut into small pieces then immersed in water for 24 h at 18 °C to 25 °C. The water was filtered with 10 mesh sieve to get a clean suspension nematode. The nematodes of each sample were counted for their population.

2.2. Nematodes identification

Identification of nematodes consisted of morphological, morphometric and molecular identification. Morphological identification was carried out by observing esophagus shape, overlapping the esophageal gland with the intestines, the number of lateral lines, tail shape and spiculum (EPPO, 2017; Karsen and Willemsen, 2010). Morphometric characters were c value (body length/tail length) of female, female body length, stylet length, vulva-anus length and spiculum length (EPPO, 2017). The polymerase chain

reaction (PCR) technique was used for molecular identification. DNA nematodes were extracted using the modified CTAB method (Devi *et al.*, 2013). The primers used were D2A (ACAAGTACCGTGAGGGAAAGTTG) and D3B (TCGGAAGGAACCAGCTACTA) targeting the 28s rDNA region (Douda *et al.*, 2013). PCR was carried out with an initial denaturation stage at 95 °C, 1 min; 30 cycles of denaturation at 95 °C, 15 s, annealing at 57 °C, 15 s and extension at 72 °C, 10 s; final synthesis at 72 °C, 5 min; and the final temperature at 4 °C.

3. Results and Discussion

3.1. Distribution area of *Ditylenchus dipsaci*

The distribution area of *D. dipsaci* was determined based on the population of *D. dipsaci* in the affected garlic plants. In the field observations, garlic plants attacked by *D. dipsaci* showed yellowing leaves, twisting leaves, and rotting bulbs. These symptoms are in accordance with Sikora and Fernández (2005) which stated that the symptoms of *Ditylenchus* attack on garlic are yellowing leaves and rotting tubers. Garlic bulbs attacked by *Ditylenchus* become brighter, turn dark brown, shrink and eventually show cracks and rot due to additional activity from saprophytic soil organisms (Abawi and Moktan, 2010).

Table 1. *Ditylenchus* spp. population on the garlic bulbs in Central and East Java

Location	Varieties	Altitude (m a.s.l.)	Soil temperature (°C)	Population (5 g bulb) ⁻¹
Adipuro, Kaliangkrik, Magelang	Lumbu Kuning	1 420 to 1 748	19.5	52.06
Adipuro, Kaliangkrik, Magelang	Tawangmangu Baru	1 408 to 1 766	21.0	53.46
Tuksari, Temanggung	Lumbu Kuning	1 203	25.4	7.60
Paguyangan, Brebes	Sangga Sembalun	1 013	26.0	27.44
Tuwel, Bojong, Tegal	Tawangmangu Baru	975	25.0	9.99
Tuwel, Bojong, Tegal	Lumbu Putih	975	26.0	0.00
Kalisoro, Tawangmangu, Karanganyar	Tawangmangu Baru	1 183	20.0	0.00
Kalisoro, Tawangmangu, Karanganyar	Lumbu Kuning	1 183	19.0	0.00
Kadipekso, Jenawi, Karanganyar	Sangga Sembalun	1 023	25.0	4.61
Segoro Gunung, Ngargoyoso, Karanganyar	Lumbu Kuning	1 085	24.7	6.5
Segoro Gunung, Ngargoyoso, Karanganyar	Tawangmangu Baru	1 087	25.0	6.8
Sajen, Pacet, Mojokerto	Lumbu Hijau	712	22.3	20.81
Padusan, Pacet, Mojokerto	Lumbu Hijau	867	24.1	11.38
Padusan, Pacet, Mojokerto	Lumbu Kuning	853	23.5	0.00
Taji, Jabung, Malang	Lumbu Hijau	1 173	22.3	10.87
Gubugklakah, Poncokusumo, Malang	Lumbu Kuning	1 100	23.8	46.97
Gubugklakah, Poncokusumo, Malang	Lumbu Hijau	1 100	23.8	44.49

m a.s.l. = meter above sea level

D. dipsaci was detected in the center of garlic crops in Magelang, Temanggung, Karanganyar, Tegal and Brebes (Central Java) and Mojokerto and Malang (East Java) (Table 1). The infested varieties of garlic were Lumbu Kuning, Lumbu Hijau, Tawangmangu Baru, and Sangga Sembalun, and all of them were local varieties. Lumbu Kuning is the most widely cultivated variety due to its relatively short growing age (105 d to 116 d).

The highest population of *D. dipsaci* was found in Kaliangkrik, Magelang, Central Java (53.46 nematodes

(5 g bulb)⁻¹). *D. dipsaci* population that could affect the number and weight of tubers is 14.29 (g of planting medium)⁻¹ or 500 nematodes (g tuber peels)⁻¹ (Mwaura *et al.*, 2015a). *Ditylenchus* populations in all regions are under the damage rate but have caused damage to bulbs and leaves.

Nematode population is influenced by abiotic factors such as temperature, humidity, soil texture, and other soil properties (Mulyadi, 2009). Garlic plants were planted at various heights from 712 m to 1 766 m a.s.l. (Table 1).

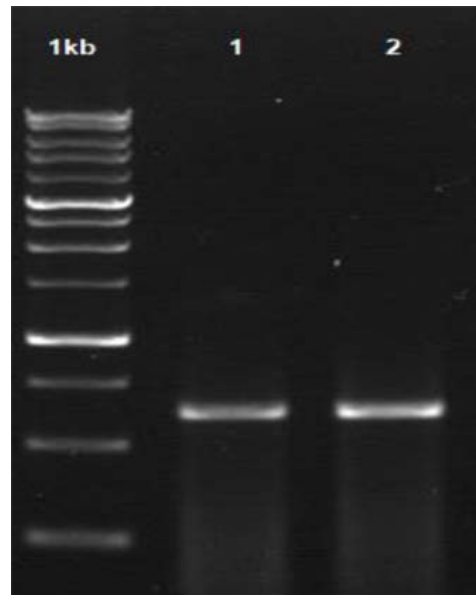


Figure 2. Gel electrophoresis micrograph showing amplicons obtained from PCR reactions; Samples from Jabung Mojokerto (1) and Malang Poncokusumo (2) were amplified at \pm 600 bp with the D2A / D3B primers in the 28s rDNA region

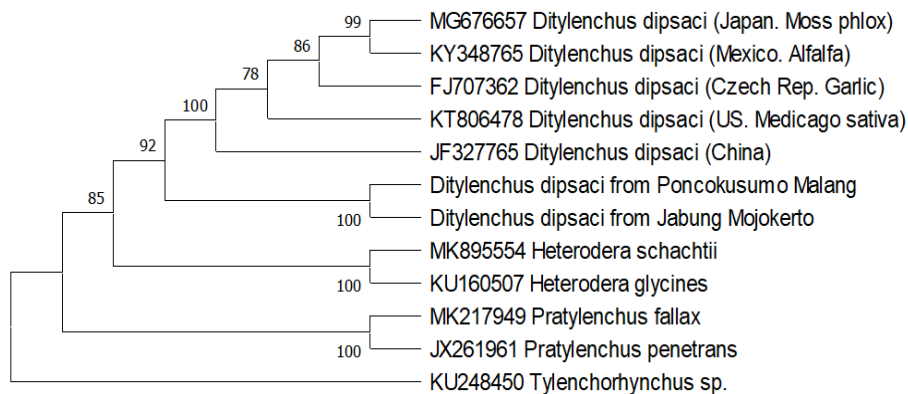


Figure 3. Phylogenetic tree test samples compared to several other nematode species that have been published in the NCBI Database. The method used is the Neighbor-joining (NJ) Kimura 2-parameter model 1.000 bootstraps.

4. Conclusion

D. dipsaci distribution areas in garlic plants in Central and East Java include Magelang, Temanggung, Karanganyar, Tegal, Brebes, Malang, and Mojokerto Regencies. Based on morphological and morphometric identification, the *Ditylenchus* species found was *D. dipsaci* in all affected areas. *D. dipsaci* which attacked garlic in East Java, was an indigenous Indonesian species.

Acknowledgment

The authors would like to thank Universitas Gadjah Mada for the research funded with scheme by RTA (*Rekognisi Tugas Akhir*) with contract No. 2129/UN1/DITLIT/DIT-LIT/LT/2019.

References

Abawi GS and Moktan K. 2010. Bloat Nematode Problem on Garlic: Symptoms, Distribution and Management Guidelines. Cornell University. Geneva.
 CABI, 2018. *Ditylenchus dipsaci* (stem and bulb nematode). Invasive Species Compend. <https://www.cabi.org/isc/datasheet/19287>.

Devi KD, Punyarani K, Singh NS and Devi HS. 2013. An efficient protocol for total DNA extraction from the members of order Zingiberales- suitable for diverse PCR based downstream applications. *Springerplus* **2(669)**: 1–9.

Douda O, Marek M, Zouhar M and Ryšánek P. 2013. Insights into the structure and phylogeny of the 28S rRNA expansion segments D2 and D3 of the plant-infecting nematodes from the genus *Ditylenchus* (Nematoda: Anguinidae). *Phytopathol. Mediterr.* **52(1)**: 84–97.

EPPO. 2017. PM 7/87 (2) *Ditylenchus destructor* and *Ditylenchus dipsaci*. EPPO Bull. **47(3)**: 401–419.

Hajihassani A, Tenuta, M and Gulden RH 2017. Influence of temperature on development and reproduction of *Ditylenchus weischeri* and *D. dipsaci* on yellow pea. *Plant Dis.* **101**: 297–305.

Hazir S, Stock SP, Kaya HK, Koppenhofer AM and Keskin N. 2001. Developmental temperature effects on five geographic isolates of the entomopathogenic nematode *Steinernema feltiae* (Nematoda: Steinernematidae). *J. Invertebrate Pathology* **77(4)**: 243–250.

Indarti S, Wibowo A, Subandiyah S, Ajri M. 2018. First record: A stem and bulb plant parasitic nematode at garlic area centre Temanggung, Central Java, Indonesia with species reference to *Ditylenchus dipsaci*. *Jurnal Perlindungan Tanaman Indonesia.* **22(2)**: 233–237.

- Karssen G. and Willemsen NM. 2010. The spiculum: An additional useful character for the identification of *Ditylenchus dipsaci* and *D. destructor* (Nematoda: Anguinidae). *EPPPO Bull.* **40**: 211–212.
- Mahmoud MAY and Wafaa MA El-Nagdi. 2021. New approach for biocontrolling root-knot nematode, *Meloidogyne incognita* on Cowpea by commercial fresh oyster mushroom (*Pleurotus ostreatus*). *Jordan J Biol Sci*, **14** (1): **173–177**.
- Ministry of Agriculture - Republic of Indonesia. 2018. **Agricultural Statistics 2018**. Center for Agricultural Data and Information Systems, Ministry of Agriculture of the Republic of Indonesia, Jakarta, Indonesia.
- Mulyadi. 2009. **Agricultural Nematology**. Gadjah Mada University Press. Yogyakarta, Indonesia.
- Mwaura P, Niere B and Vidal S. 2015. Effect of initial population densities of *Ditylenchus destructor* and *D. dipsaci* on potato tuber damage and nematode reproduction. *Nematology* **17**(2): 193–202.
- Mwaura P. 2015b. Host-parasite interaction between the potato tuber rot nematode (*Ditylenchus destructor*), stem nematode (*Ditylenchus dipsaci*) and potato. PhD Thesis. Göttingen University.
- Pethybridge SJ, Gorny A, Hoogland T, Jones L, Hay F, Smart C and Abawi G. 2016. Identification and characterization of *Ditylenchus* spp. populations from garlic in New York State, USA. *Trop. Plant Pathol.* **41**: 193–197.
- Sikora RA and Fernández E. 2005. Nematode parasites of vegetables. In: Luc, M., Sikora, RA and Bridge (Eds.), **Plant Parasitic Nematodes in Subtropical and Tropical Agriculture, Ed. 2**. CABI Publishing, Wallingford, UK. pp. 319–392.
- Wulandari AS and Indarti S. 2020. Distribution and abundance of a new pest “root and bulb parasitic nematode” at different elevation levels and soil abiotic factors garlic growing centres in Central Java. In: Tutik DW, Roto R, Rohana A, Laurent C, Kuwat T, Indriana K, Julius M, and Dwi S (Eds.), **Key Engineering Materials**. Vol. 840. Trans Tech Publications Ltd, Switzerland, pp. 124–130.
- Wulandari AS, Indarti S, Massadeh MI and Van Minh N. 2021. The effect of abiotic factors and elevation on the diversity of plant parasitic nematodes in garlic on Central Java, Indonesia. *Sarhad J. Agric.*, **37**(Special issue 1): 75–83.
- Yavuzaslanoglu E, Dikici A, Elekcioğlu İH. 2015. Effect of *Ditylenchus dipsaci* Kühn, 1857 (Tylenchida: Anguinidae) on onion yield in Karaman Province, Turkey. *Turkish J. Agric. For.* **39**: 227–233.
- Yu Q, Zaida MA, Hughes B and Celetti M. 2012. Discovery of potato rot nematode, *Ditylenchus destructor*, infesting garlic in Ontario, Canada. *Plant Dis.* **96**(2): 297–297.
- Zhang SL, Liu GK, Janssen T, Zhang SS, Xiao S, Li ST, Couvreur M and Bert W. 2013. A new stem nematode associated with peanut pod rot in China: morphological and molecular characterization of *Ditylenchus arachis* n. sp. (Nematoda: Anguinidae). *Plant Pathol.* **63**(5): 1193–1206.

Genetic Diversity of Local Cowpea (*Vigna spp.* (L.) Walp.) Accessions Cultivated in Some Regions of Egypt

Ehab M.B. Mahdy^{1,*}, Hossam F.A. El-Shaer², Abd El-Hadi I.H. Sayed² and Abeer El-Halwagi¹

¹ National Gene Bank, Agricultural Research Centre (ARC), Giza, Egypt; ² Botany Department, Faculty of Agriculture, Al-Azhar University, Cairo, Egypt.

Received: August 31, 2020; Revised: January 1, 2021; Accepted: February 4, 2021

Abstract

This work described the ten cowpea accessions using morphological, agronomical, and molecular characterization and select the desirable cowpea accession for improvement. Twenty-four characteristics were quantitative attributes. Data demonstrated by the Principal Component Analysis (PCA) increasing in some components associated with a decrease in eigenvalues, which gave its max at three factors. The PCA was arranged into three main components, which altogether valued at 63.40%. The matrix of PCA data is standardized. The coordinates were calculated for Bi-plot mapping using the Perceptual Mapping (PERMAP). *Radiata* accessions (1 and 2) fell into a group. *Unguiculata* accessions are classified further into two sub-groups. The accessions (4 and 6) dropped into a sub-group, and the rest gathered into another sub-group. The PCR-based marker technique, SSR markers, were also analyzed. These markers gave a total of 64 alleles with 51.32% of polymorphism. A total of 26 alleles were polymorphic. The most informative markers were EH03, EH09, EH06, and EH07. The SSR-phenogram had classified into two main groups at a distance of 0.34. The first one comprises accessions 1 and 2. The second fell further into two sub-groups at a distance of 0.52.

KeyWords: *Vigna*, SSR, SCoT analysis, Principal Component Analysis (PCA), PERMAP Bi-plot mapping.

1. Introduction:

Vigna possesses more than 150 species originating especially in Africa and Asia (Maréchal et al. 1978; Norihiko et al. 2010, 2014). *Vigna* species proliferate in Africa and Asia and grow well below a greater diversity of environmental conditions, including climatic, soil, and cultural features more than most legume crops. They are used as pulses, fodder, and cover crops (Norihiko et al. 2010, 2014; Dachapak et al. 2017; Karuniawan et al. 2006). Having the same uses in Egypt, both species own an excellent protein source, especially the *unguiculata* than *radiata*.

For its improvement, acknowledge the nature and magnitude of genetic divergence are essential for the selection of diverse parents for a breeding program to get an abroad sense of gene recombination for quantitatively inherited traits. Agronomical traits play a significant role in studying and characterizing accessions for a long. Molecular marker analysis with morphological and agronomic evaluation data increase the resolving power of genetic diversity analysis and provide complementary information (Shrivastav et al. 2012).

Recently, more sensitive DNA-based techniques like Inter-Simple Sequence Repeat (ISSR), Cleaved Amplified Polymorphic Sequence (CAPS), Simple Sequence Repeats (SSR), and Start Codon Target (SCoT) markers are most suitable because of easiness in handling, reproducibility, multi-allelic nature, codominant inheritance, relative abundance and genomic wide coverage (Powel et al. 1996). The SSRs are groups of short tandem repeated nucleotides scattered in the genome.

SSR markers are a valuable tool for genetic mapping, genotyping and marker-assisted selection in breeding due to their characterization of codominant loci, high allelic variation and even distribution (Hernandez et al. 2002). This technique is becoming the marker of choice because of its high polymorphism and occurrence throughout the genome. Recently, more efforts are devoted to developing SSR markers in various crops. In cowpea SSR analysis, the earliest research was conducted by Li et al., 2001, and twenty-seven primers have developed. Africa is the diversity centre of wild cowpea, as established by Ogunkanmi et al (2008) using SSR analysis.

Start codon targeted (SCoT) polymorphism has recently emerged as a new and promising marker technique for the genetic diversity assessment in plants (Collard and Mackill 2009) due to longer primer sequences

* Corresponding author e-mail: ehab.mahdy@arc.sci.eg.

** **Abbreviations:** SSR= Simple Sequence Repeats; SCoT= Start Codon Target; PCA= Principal Component Analysis; PERMAP Bi-plot= Perceptual Mapping Bi-plot analysis; Nb= no. of alleles; MB= no. of monomorphic band; PB= no. of polymorphic band; P%= polymorphism; PIC= polymorphic information content; EMR= effective multiplex ratio; MI= marker index; I= Shannon informative index; Ho= observed heterozygosity; He= expected heterozygosity; uHe= unbiased heterozygosity; F= fixation index.

and reproducibility. The SCoT marker is designed based on the conserved region surrounding the translation initiation codon, ATG (Sawant et al. 1999). A single primer is used for SCoT to amplify DNA without prior genomic sequence information. The SCoT could directly be used in marker-assisted breeding programs, unlike random markers (Mulpuri et al. 2013). SCoT markers could evaluate fruitfully genetic diversity, genetic structure, cultivar identification, quantitative trait loci (QTL) mapping, and DNA fingerprinting in various crops such as orange (Jiang et al. 2011), date palm (Al-Qurainy et al. 2015), Pistacia species (Amirbakhtiar and Sorkheh 2015), mango (Leo et al. 2011), and jojoba (Heikrujam et al. 2015).

This investigation assessed the genetic diversity of ten cowpea accessions, representing two *Vigna* species. *Vigna radiata* and *V. unguiculata* subspecies *cv-group: unguiculata* procured by National Gene Bank of Egypt from different local districts. Morphological and agronomical traits as well as molecular markers are used to select desirable accessions for cowpea improvement.

2. Materials and Methods

The viable ten accessions representing two accessions of *V. radiata* and eight of *V. unguiculata* subspecies *cv-group: unguiculata* were procured from local regions (Table 1) by National Gene Bank (NGB), Agricultural Research Centre (ARC), Giza, Egypt. Those selected for this study act as the desirable accessions deposited in NGB, which are more than one hundred accessions of *Vigna*.

2.1. Morphological data:

Experimentations were carried out in the field of National Gene Bank (NGB), Agricultural Research Centre (ARC), Giza, during 2015. The observations follow the standard format descriptor lists for *Vigna* (IBPGR 1983). The data comes from the mean of the twenty-five healthy mature plant materials for each. The morphological terminology follows Stearn (1973). The herbarium voucher-specimens and clean mature seeds were deposited and stored at the herbarium and store-rooms of NGB based on the standard of gene bank (IPGRI, 1994).

Table (1): List of studied accessions of genus *Vigna*.

Code	Taxa	Accession No.	Collected date	Collected area
1	<i>Vigna radiata</i>	19538	2005	Giza
2	Variety: <i>radiata</i>	19537	2004	Giza
3		14176	2008	Dakhla
4		13884	2008	Dakahlyia
5	<i>Vigna unguiculata</i>	101	2010	Luxur
6	Subspecies:	27301	2007	Sohag
7	<i>unguiculata</i> cv-	26983	2007	Qena
8	group: <i>unguiculata</i>	26981	2007	Qena
9		26945	2007	Aswan
10		26738	2006	Menyia

2.2. Genetic variation detected by SSR and SCoT analysis:

Total genomic DNA from 5g of fresh young leaf tissue, collected from five random plants per accession, was extracted following the Zymo Research Kit. Electrophoresis was made on 1% agarose gel electrophoresis at 100 Volt for 30 min. The total genomic DNA was diluted to 10 ng/μl of PCR analysis. Ten SSR primers representing 11 linkage groups designed previously by Kongjaimun et al. (2012) and Wang et al. (2004) and 17-SCoT primers chosen from Collard and Mackill (2009) of *Vigna* species under study evaluated as shown in Table 2. The PCR reactions perform in a 20 μl reaction mixture containing 10 ng template DNA, 200 μM dNTPs, 250 nM of each primer, 1.5 mM MgCl₂, 1x PCR buffer, and 1 unit Taq DNA polymerase. The PCR amplification was performed with an initial denaturation at 94°C for 5 min followed by 35 cycles of 94°C for 1 min, 50 to 60°C (depending on the primer, see Table 2) for 1 min, 72°C for 2 min, and a final extension at 72°C for 5 min before cooling at 4°C (Collard and Mackill, 2009; Kongjaimun et al., 2012).

Each amplicon profile is defined by the presence (1) or absence (0) of bands based on the band positions relative to the ladder sequentially from the smallest to the largest-sized bands. Band profiles are variable when identifying one polymorphic band, at least. Fragments were scored as 1 if present or 0 if absent based on standard marker using Alpha Ease FCTM (version 4.0.1) software. The cluster analysis was computed as the Un-weighted Pair-group Method with Arithmetic averages (UPGMA) method to generate a dendrogram for studying the relationship among accessions based on Nei and Li (1979). Unique alleles defined as those were detected in only one species. A binary matrix was then transformed into genetic similarity (GS) matrices using Jaccard's coefficient (Jaccard, 1908).

Table (2): Sequences of SSR and SCoT markers used for *Vigna* accessions under study.

Code	Marker	Primer sequence	Tm
SSR Primers:			
Eh01	CEDG088	F: TCTTGTCATTTAGCACTTAGCACG R: TTGTTGTTTACTAAGAGCCCGTGT	60
Eh02	CEDG086	F: GAGTTTACAACAGATGGGGCTAA R: AGGTCTTGATTGACTTTCTGGGT	60
Eh03	CEDG073	F: GGTTAGCATCTGAGCTTCTTCGTC R: AACACCCGCCTCTTTCTCC	60
Eh04	CEDG044	F: TCAGCAACCTTGCAATTGCAG R: TTCCCGTCACTCTTCTAGG	57
Eh05	CEDG056	F: TTCCATCTATAGGGGAAGGGAG R: GCTATGATGGAAGAGGGCATGG	60
Eh06	CEDG006	F: AATTGCTCTCGAACCAGCTC R: GGTGTACAAGTGTGTGCAAG	57
Eh07	CEDG014	F: GCTTGCATCACCCATGATTC R: AAGTGATACGGTCTGGTTCC	57
Eh08	CEDG013	F: CGTTCGAGTTTCTTCGATCG R: ACCATCCATCCATTTCGCATC	57
Eh09	CEDG010	F: TGGGCTACCAACTTTTCCTC R: TGAGCGACATCTTCAACACG	57
Eh10	FER	F: TCGCAAAGTTGCCAGTCACT R: TAGAAGGAAGGAGGGCATG	42
SCoT Primers:			
S01	SCoT-02	ACCATGGCTACCACCGGC S10 SCoT-14 ACCATGGCTACCAGCGCG	
S02	SCoT-03	ACGACATGGCGACCCACA S11 SCoT-16 CCATGGCTACCACCGGCA	
S03	SCoT-04	ACCATGGCTACCACCGCA S12 SCoT-24 CCATGGCTACCACCGCAG	
S04	SCoT-05	CAATGGCTACCACTAGCG S13 SCoT-28 CAACAATGGCTACCACCA	
S05	SCoT-06	CAATGGCTACCACTACAG S14 SCoT-34 ACGACATGGCGACCAACG	
S06	SCoT-09	ACAATGGCTACCACTGCC S15 SCoT-35 AACCATGGCTACCACCAC	
S07	SCoT-11	ACAATGGCTACCACTACC S16 SCoT-45 ACCATGGCTACCACCGAG	
S08	SCoT-12	CAACAATGGCTACCACCG S17 SCoT-48 CACCATGGCTACCACCAG	
S09	SCoT-13	ACCATGGCTACCACGGCA	

2.3. Statistical analysis

The averages and standard errors were calculated for all morphological attributes. The Principal Component Analysis (PCA) calculates for morphological attributes was based on Johnson (1998). The data matrix of linkage among accessions and morphological attributes were standardized. The coordinates estimate for Bi-plot mapping is based on the perceptual mapping (PERMAP).

Polymorphism information content (PIC) values were calculated by Anderson et al. (1993) based on the formula: $PIC = 1 - \sum P_i^2$ for co-dominant marker and $PIC = 1 - p^2 - q^2$ for dominant marker; where: P_i is the frequency of the i^{th} alleles, and q is the null allele frequency. The resolving power (Rp) for each primer was calculated as $Rp = \sum I_b$ where: I_b (band informativeness) takes the value: $I_b = 1 - (2 \times (0.5 - p))$ and p is the proportion of the genotype of different *Vigna* accessions containing that band (Prevost and Wilkinson, 1999). The Marker Index (MI) calculates according to Varshney et al. (2007) as per the following formula: $MI = PIC \times EMR$, where EMR (Effective multiplex ratio) = $n\beta$, where: n is the average number of fragments amplified by accession to a specific system marker (multiplex ratio) and, β is the number of polymorphic loci (PB) and the number of non-polymorphic loci (MB); $\beta = PB/(PB + MB)$.

Data sets derived from all averages of attributes were fed into SPSS (version. 14.0) and StatistixL adding in Microsoft Excel (Kovach Computing Service, 2013, version. 1.8) Program, as well as conducted on GenAIEx (Peakall and Smouse, 2006).

3. Results and Discussion

3.1. Diversity revealed by morphological attributes

3.1.1. Morphological characterization:

***Vigna radiata* (L.) R. Wilcz. variety radiata**

An annual herb, erect or sub-erect, up to 50 cm. stems bristly hairy. Leaves trifoliolate, leaflets elongate-ovate, Flowers pale yellow 1.7–2.0 cm long. Pods horizontal, linear-cylindric, 4-10 cm long and 4-6 mm broad, with a dark brown, short, spreading, bristly indument; the 9-12 seeds are greenish to brown, oblong-cylindric to subglobose (Rhomboid), 4.2-4.9 x 3.2-3-8 mm.

Two accessions (1 and 2) were accessed from the National gene bank of Egypt. For more details of morphological attributes, see Table (3 and 4) and plate (1, 2, and 3).

***Vigna unguiculata* (L.) Walp. subspecies unguiculata cv-group unguiculata E. Westphal**

Annual herb, erect or sub-erect, spreading, up to 200 cm tall, glabrous. Stems usually procumbent, often tinged with purple. Leaves are trifoliolate and alternate. The terminal leaflet is often bigger and longer than the two asymmetrical laterals. Leaflets are ovoid-rhombic, entirely or slightly lobed, apex acute, 7.5–15 cm long, 5–11 cm wide. Petiole, stout, grooved, 7–15 cm long. The inflorescence is axillary; peduncles are 2.5–15 cm long. Flowers are white, cream, yellow, and calyx campanulate with triangular teeth; the upper two teeth are connate and longer than the rest. Corona is dull-white, yellow, or violet with standard 2–3 cm in diameter and keel truncate. Pods are curved, straight, 8-20 cm long with 8-14 seeds/pod. Seeds 5–10 mm long, 4-7mm width, globular to reniform,

smooth or wrinkled, brown, green buff or white, as dominant color; full-colored, spotted, marbled, speckled, eyed, or blotched.

A total of the rest, eight accessions were accessed from National Gene Bank. For more details of morphological attributes, see Table (3 and 4) and plate (1, 2, and 3).

Soliman et al. (2008) reported that the plant hairiness, flower color, pod wall thickness, cotyledon color, seed color, eye pattern and color, seed turgidity, and seed crowding are the most significant morphological attributes

to distinguish among subgenera. The type of germination, the thigmotropic movements of hypocotyl and the stem, seedling architecture, and plant longevity were recorded by Ojeda et al. (2013) on four species of *Vigna* Savi. These characteristics permitted us to distinguish the species and construct an identification key that could be useful for agronomic or floricultural purposes. Selvakumar and Kumari (2015) reported that the color of seeds is differed subsequent generations due to the different gene actions, which confirm a further progeny.

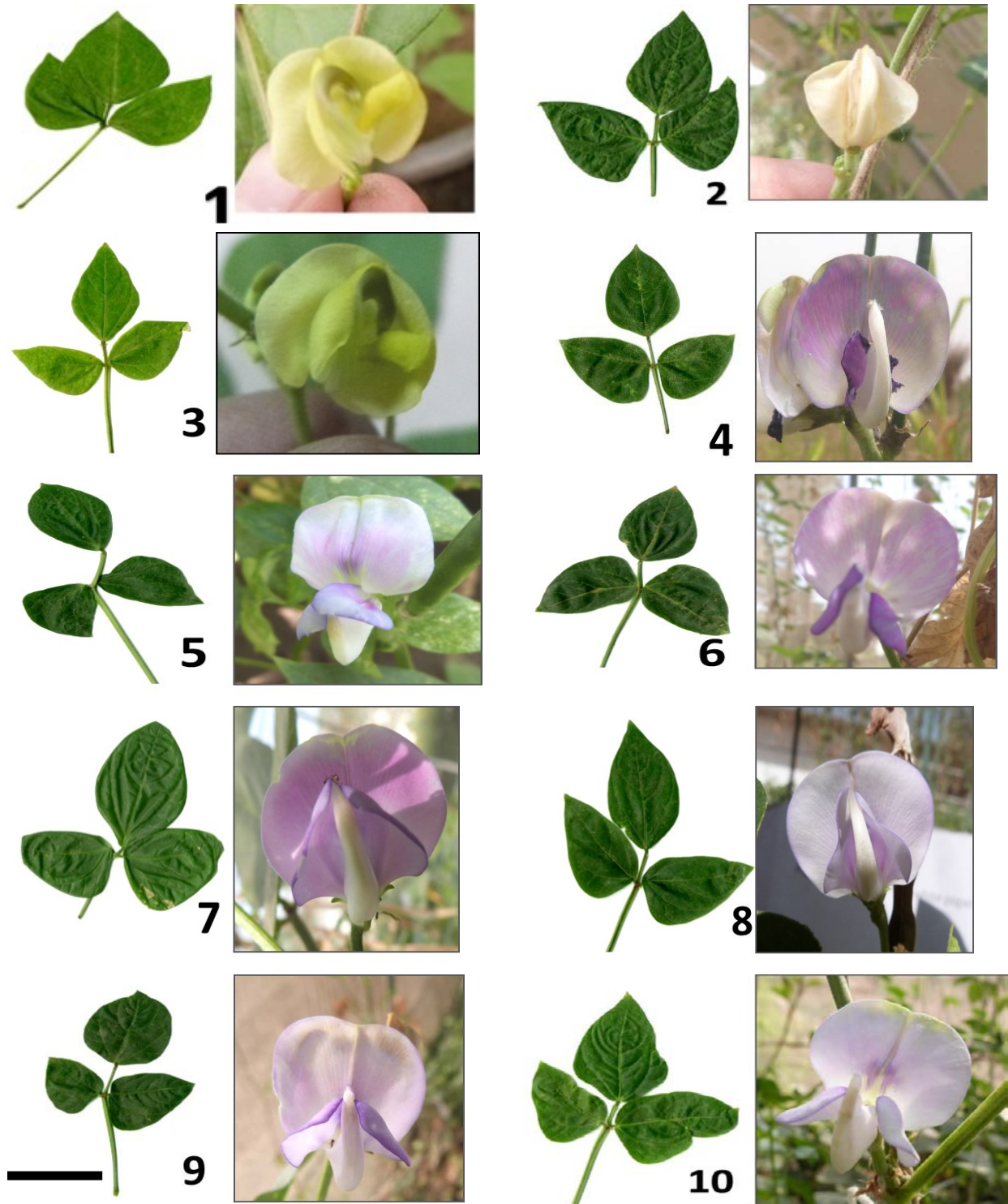


Plate (1): Leaf and flower shapes of the studied accessions of cowpea. For accession name, see table (1). The scale bar equals 15 cm.



Plate (2): Pods of the studied accessions of *Vigna*. For accession name, see table (1). The scale bar equals 1 cm.

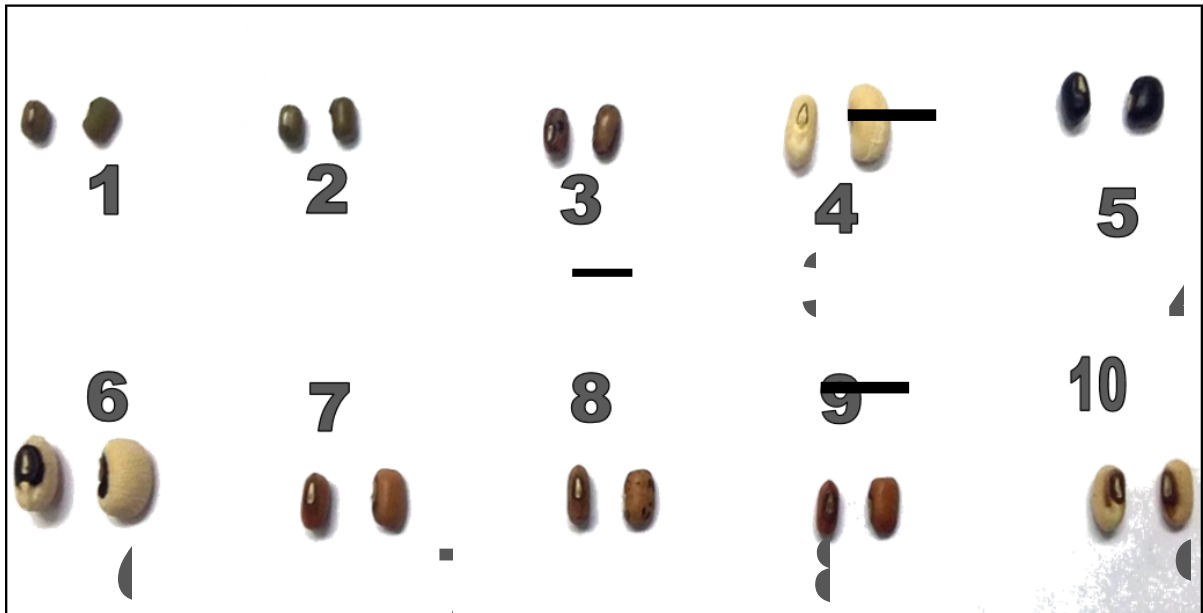


Plate (3): Seeds of the studied accessions of *Vigna*. For accession name, see table (1). The scale bar equals 1 m

Table (4): Morphological characters of the studied accessions of *Vigna*.

Code	Characteristics	1	2	3	4	5	6	7	8	9	10
27	Plant Height (cm)	37.5	39	134	137	62.7	107	115	48	45	204
28	Number of main branches	3.67	3.5	3.33	2.67	3.17	3.17	3	3	2.8	3
29	Terminal leaflet length	11.7	11.7	10.7	10.2	8.06	17.2	12.4	11	14	15.1
30	Terminal leaflet width	5.82	6.31	3.98	5.15	4.99	5.73	4.39	3.6	3.8	4.48
31	Terminal leaflet ratio (length/width)	2	1.85	2.68	1.98	1.62	3.01	2.83	3.1	3.6	3.38
32	Stipule length	6.99	6.34	6.02	3.08	3.39	7.01	4.99	6	4.4	3.52
33	Stipule width	3.9	3.28	2.92	0.92	2.18	3.53	3.3	2.8	2.9	1.99
34	Stipule ratio (length/width)	1.79	1.93	2.06	3.36	1.56	1.99	1.51	2.1	1.5	1.77
35	Days to flowering (week)	8	8	7	8	8	9	8	9	10	10
36	Days to first pods (after flowering)	7.33	10	9.83	9.5	7.17	9.5	9.83	10	6.8	10.2
37	No. of flowers per plant	19.2	18.2	25.8	21.2	14.5	20	22.2	18.8	20.2	23.3
38	Standard length	0.96	1.93	1.95	1.98	2.07	2.04	1.97	2	2.2	1.92
39	Number of pods per plant	17.3	14.2	22.7	16	13.2	18	19.8	18	19	21.2
40	Pods: Flower ratio	0.9	0.78	0.88	0.76	0.91	0.9	0.89	0.9	0.9	0.91
41	Pod Length	9.75	7.8	7.7	18.4	11.1	15.4	10.4	9.15	10.7	10.6
42	No. of seeds / pod	10.2	9.7	10.8	12.2	10.8	11.3	10.7	8.9	11.2	11
43	seed density (seeds no./cm)	1.05	1.24	1.4	0.66	0.98	0.73	1.03	0.97	1.04	1.03
44	Seed length (cm)	0.48	0.48	0.61	0.87	0.5	0.92	0.68	0.66	0.68	0.79
45	Seed width (cm)	0.38	0.37	0.42	0.54	0.41	0.66	0.45	0.44	0.46	0.57
46	Seed thickness (mm)	2.9	3.1	2.5	4	2.3	4.1	3	2.7	2.4	3.5
47	Seeds shape ratio (length/width)	1.26	1.3	1.45	1.61	1.22	1.39	1.51	1.5	1.48	1.39
48	weight of 100 seeds (gm)	4.33	3.93	6.5	14.5	12.1	18.2	5.24	4.8	5.78	12.4

3.1.2. Principal Component Analysis (PCA)

Data presented in Table (5) demonstrated that an increase in the number of components (PC) was associated with a decrease in eigenvalues. This trend reached its maximum at three factors. Accordingly, it is reasonable to assume that the PCA had grouped the estimated variables into three main components, which all accounted for 63.4 % of the total variation of attributes.

The results showed that PC1 correlates well with the attributes of the weight of 100 seeds, Seed thickness, Seed width, seed length, No. of seeds/pod, pod length, pod attachment to the peduncle, plant height, and plant hairiness. Meanwhile, the PC2 correlates well with the attributes of terminal leaflet width and the number of main branches. The PC3 correlates well with eye pattern, terminal leaflet length, terminal leaflet ratio no. of pods/plant, stipule width, and growth habit. Variables that significantly correlated with the first three eigenvectors were the variables with great variability. Data show that PC1 accounted for about 31.65% of the variance among

attributes; PC2 for 18.21%, and PC3 for 13.54%. Therefore, the traits of seed are the weight of 100-seeds, seed thickness, seed width and length, and the number of seeds per pod, following the attribute pod Length, terminal leaflet width, and length, plant height, plant hairiness, eye pattern, pod attachment to peduncle showed to affect the significant grain yield characters.

The factor loading is the coefficient of PCs or the correlation between the component and the variables. This correlation indicates that the variables are associated directly with the maximum of variation thru the data set. A similar result, Yin et al. (2002), reported that the wheat grain yield could be classified into three key components.

The main reason for plant collection is to obtain raw materials that increase useful gene pools for crop improvement. According to Johnson (1998), PCA is a more useful statistical tool for screening multivariate data with significantly high correlations. PCA data assists the breeders to identify limited traits for use in hybridization and selection programs.

Table (5): Loading factor and Eigenvalue of the correlation matrix for the estimated variables of *Vigna* under study using the PCA.

Attributes	PC ₁	PC ₂	PC ₃	PC ₄	PC ₅	PC ₆	PC ₇	PC ₈	PC ₉
Growth habit	0.54	-0.51	-0.35	-0.10	-0.30	-0.30	0.14	-0.27	0.22
Twining tendency	-0.26	-0.52	0.04	0.62	0.32	0.08	-0.35	-0.13	-0.16
Plant pigmentation	-0.64	0.69	0.21	0.06	-0.20	0.09	0.11	-0.06	0.09
Plant hairiness	0.69	-0.57	-0.24	0.04	0.06	-0.30	-0.03	0.17	-0.08
Plant vigor	0.20	-0.49	0.14	-0.20	-0.57	0.01	0.21	0.45	-0.30
Terminal leaflet shape	0.44	-0.12	0.48	-0.57	-0.03	0.38	-0.22	-0.20	0.05
Days to flowering	-0.13	-0.45	-0.32	-0.71	0.06	-0.06	0.33	0.22	0.10
Raceme position	-0.29	0.49	0.51	0.03	-0.64	0.09	-0.04	-0.05	0.05
Flower color	-0.02	0.51	0.02	-0.11	0.54	0.59	0.28	0.11	-0.05
Pod attachment to peduncle	0.73	0.48	-0.26	0.17	0.34	-0.11	0.03	-0.06	-0.02
Seed shape	-0.91	-0.31	-0.10	-0.12	0.17	0.08	0.12	0.05	0.04
Seed color	-0.86	-0.40	-0.17	0.14	0.11	0.02	-0.17	-0.03	-0.07
Testa pattern	-0.23	-0.54	0.00	0.72	0.18	-0.21	-0.07	-0.22	0.06
Testa texture	0.48	0.35	0.31	-0.06	0.59	-0.44	-0.08	0.05	0.07
Eye pattern	0.66	0.16	0.72	0.09	-0.02	-0.10	-0.08	0.01	0.05
Eye color	-0.11	-0.64	0.03	-0.23	0.65	-0.29	-0.05	0.14	0.02
Plant Height	0.71	-0.27	0.15	0.36	-0.45	-0.19	0.07	0.14	-0.03
No. of main branches	-0.71	0.39	0.36	0.19	-0.06	-0.42	0.01	-0.02	-0.02
Terminal leaflet length	0.52	0.13	0.76	-0.14	0.22	0.01	0.15	-0.02	0.18
Terminal leaflet width	-0.10	0.92	0.00	-0.02	-0.12	-0.29	0.05	0.12	0.16
Terminal leaflet ratio	0.41	-0.54	0.60	-0.11	0.24	0.30	0.05	-0.12	0.06
Stipule length	-0.44	0.33	0.53	0.30	0.55	-0.13	0.06	0.00	-0.03
Stipule width	-0.55	0.15	0.60	-0.08	0.44	-0.18	0.26	0.10	0.00
Stipule ratio	0.44	0.35	-0.50	0.56	0.00	0.26	-0.10	-0.17	-0.10
Days to flowering	0.44	-0.12	0.48	-0.57	-0.03	0.38	-0.22	-0.20	0.05
Days to first pods	0.31	-0.02	0.24	0.68	-0.05	0.17	-0.23	0.53	0.11
No. of flowers/plant	0.34	-0.39	0.33	0.64	-0.12	0.06	0.43	-0.08	0.08
Standard length	0.43	-0.48	-0.26	-0.14	0.23	0.08	-0.29	0.23	0.55
Number of pods per plant	0.24	-0.60	0.53	0.40	0.00	0.01	0.33	-0.12	-0.07
Pods: Flower ratio	-0.09	-0.51	0.49	-0.41	0.14	-0.36	-0.05	-0.08	-0.40
Pod Length	0.79	0.37	-0.40	-0.08	0.14	-0.01	0.09	-0.08	-0.17
No. of seeds / pod	0.72	0.04	-0.34	-0.07	-0.15	-0.27	0.44	-0.23	0.14
seed density	-0.69	-0.39	0.27	0.31	-0.22	-0.11	0.08	-0.03	0.36
Seed length	0.96	0.00	0.08	0.11	0.22	0.08	0.03	0.01	-0.04
Seed width	0.94	0.10	0.23	-0.03	0.17	-0.14	-0.08	0.00	-0.03
Seed thickness	0.75	0.59	0.12	0.24	0.01	0.03	0.03	0.17	-0.03
Seeds shape ratio	0.54	-0.32	-0.21	0.35	0.25	0.57	0.24	0.05	-0.03
weight of 100 seeds	0.82	0.21	-0.14	-0.09	0.03	-0.45	-0.21	-0.04	-0.03
Eigenvalue	12.35	7.10	5.28	4.40	3.85	2.49	1.47	1.10	0.96
Variability (%)	31.65	18.21	13.54	11.29	9.88	6.38	3.78	2.81	2.46
Cumulative %	31.65	49.86	63.40	74.69	84.57	90.95	94.73	97.54	100.0

3.1.3. Perceptual Mapping (PERMAP) – Bi-plot analysis:

For getting the linkage among the studied accessions and the most useful morphological attributes, the matrix was standardized, and coordinates were computed for Bi-plot mapping using perceptual mapping (PERMAP) as shown in Figure (1).

PERMAP-Biplot shows that the attributes of plant hairiness, stipule length, flower color, and a number of

main branches are most significant to separate radiata (accessions 1 and 2) in a group. Meanwhile, the rest of the unguiculata accessions are further fell into two groups. The traits of seed thickness, seed crowding, pod length, testa texture, the weight of 100-seeds, and stipule ratio split the accessions (6 and 4) in a group, whereas the rest of the accessions were fell into one group.

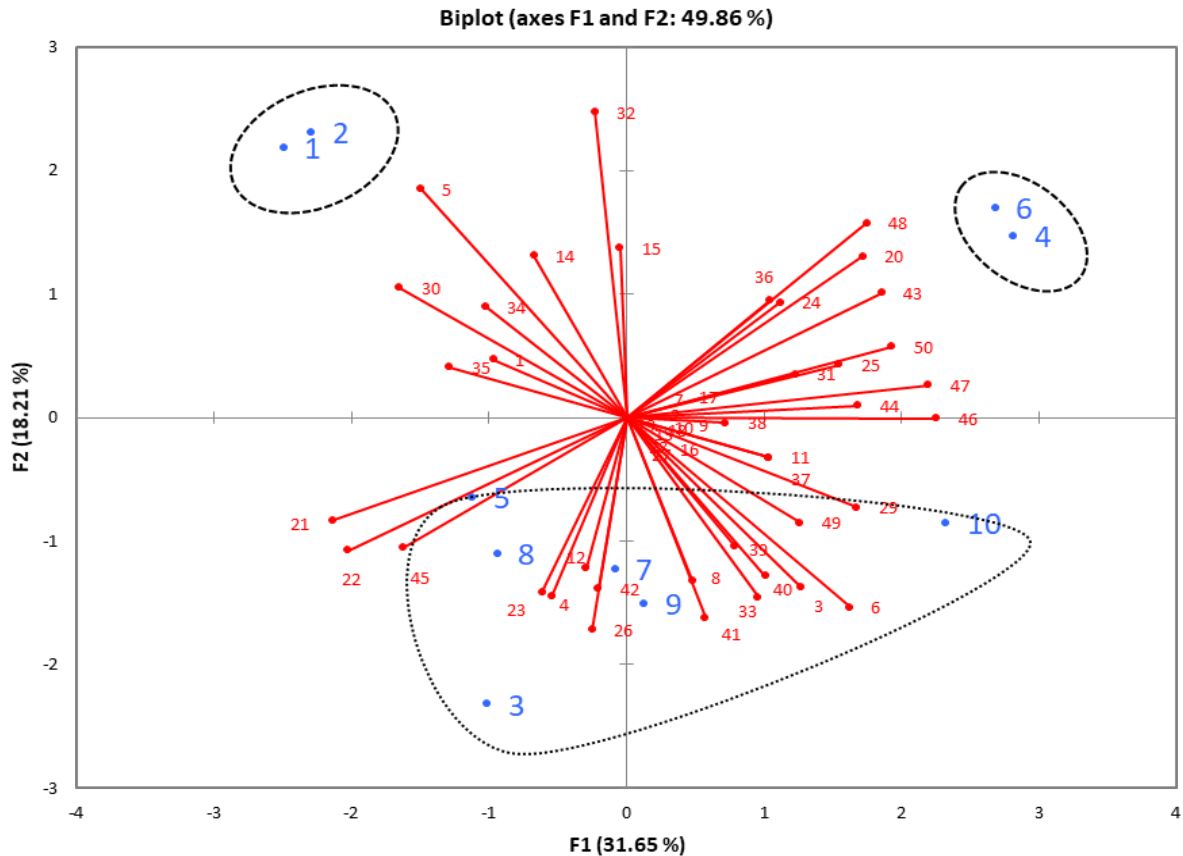


Figure (1): Perceptual mapping (Bi-plot) of the studied accessions of genus *Vigna* (Table 1) for morphological attributes Table (3 and 4).

3.2. Genetic diversity among *Vigna* accessions:

To find more identification among accessions, they were analyzed by the PCR-based marker technique, SSR. The SSR markers employed revealed a total of 64 alleles ranging from 9 to 3 alleles with 51.32% of polymorphism and an average of 6.11 loci by the marker. Table 6 summarizes the data obtained for all the analyzed loci. The polymorphism percentages ranged from 11.11% for EH09 to 75% for EH10.

The slight difference between mean H_o compared to the H_e probably due to one or more reasons. This might reflect small inbreeding and selection against heterozygotes. The markers used might also back to the observed heterozygosity on account of the non-detection of homozygotes because of the null alleles. The H_o values varied from 0.0 to 0.3, with an average value of 0.1. The highest H_o was 0.3 for EH05 and EH06. The Major PIC (H_e) value was 0.86 for EH08 and the minor value (0.62) for EH03; with an average PIC of 0.67. MI values oscillated from 0.85 for EH10 to 13.12 for EH06 primer, with a mean of 5.73. The Shannon's index (I) average was 1.63 for all primers, the lesser value was EH03 (1.03), and the major was 2.10 (EH08). The most informative primers for this data set were EH03, EH09, EH06 and EH07, while the primers EH10, EH02 and EH08 were less informative ones. The effective number of alleles (N_e) is a reciprocal of gene homozygosity (Hartl and Clark 1997). The effective number of alleles (ENA) used to corollary the H_e (when heterozygosity is high, and ENA will be highest). N_e ranged from 2.6 for EH03 to 7.4 for EH08 with an

average of 4.9 per loci. Markers attributes like I, H_e and MI have been used in different studies to evaluate the informative or discriminatory power in the primer combination in genetic diversity studies (Tatikonda et al. 2009).

The slight difference between mean H_o compared to the H_e probably due to one or more reasons. This mirrors small inbreeding, selection against heterozygotes. This marker might naturally back to the H_o by means of the non-detection of homozygotes due to the null alleles. The H_o values varied from 0.0 to 0.3, with an average value of 0.1. The highest H_o was 0.3 for EH05 and EH06, whereas the Major PIC (H_e) value was 0.86 for EH08 and a minor value (0.62) for EH03; with an average PIC of 0.67. MI values oscillated from 0.85 for EH10 to 13.12 for EH06 primer, with a mean of 5.73. The Shannon's index (I) average was 1.63 for all primers, the lesser value was EH03 (1.03), and the major was 2.10 (EH08). The most informative primers for this data set were EH03, EH09, EH06 and EH07, while the primers EH10, EH02 and EH08 were less informative ones. The N_e is a reciprocal of gene homozygosity (Hartl and Clark 1997). The N_e used to corollary the H_e (when heterozygosity is high, ENA will be highest). The N_e ranged from 2.6 for EH03 to 7.4 for EH08 with an average of 4.9 per loci. Markers attributes like I, H_e and MI have been used in different studies to evaluate the informative or discriminatory power in the primer combination in genetic diversity studies (Tatikonda et al. 2009).

Table 6. Details of marker parameters estimated for SSR markers used in *Vigna* accessions under study.

Marker	Size(bp)	Na	PB	P%	N _e	H _o	H _e	EMR	MI	I
Eh01	149-181	4	2	50	2.8	0.0	0.64	4	2.56	1.28
Eh02	130-207	7	2	28.57	5.6	0.0	0.82	4	3.28	1.83
Eh03	464-504	3	3	100	2.6	0.0	0.62	9	5.58	1.03
Eh04	155-197	7	3	42.86	6.3	0.0	0.84	9	7.56	1.89
Eh05	350-679	8	2	25	5.3	0.3	0.81	4	3.24	1.85
Eh06	344-540	7	4	57.14	5.4	0.3	0.82	16	13.12	1.81
Eh07	354-563	6	3	50	4.4	0.1	0.77	9	7.02	1.62
Eh08	247-477	9	3	33.33	7.4	0.2	0.86	9	7.83	2.10
Eh09	122-135	4	3	75	3.3	0.0	0.70	9	6.3	1.28
Eh10	104-189	9	1	11.11	6.4	0.2	0.84	1	0.85	2.04
Average		6.11	2.78	51.32	4.90	0.10	0.76	7.4	5.734	1.63

Na= no. of alleles; PB= no. of polymorphic band; P%= polymorphism; N_e= no. effective alleles; H_o= observed heterozygosity; H_e= expected heterozygosity; EMR= effective multiplex ratio; MI= marker index; I= Shannon informative index.

The SSRs are turning out to be the marker of choice as a result of their high polymorphism and repetitions in the genome. Great efforts are recently powerful to the development of SSR markers applied with various species. In mungbean, polymorphic SSR markers were published by various researchers (Gwag et al. 2006; Somta et al. 2008; Kumar et al. 2002 a and b).

In a study by Somta et al (2008), more than 200 primer pairs while amplifying SSRs were tested for polymorphism among 17 mungbean accessions, however, only 12 (5.7%) primer pairs were polymorphic. Tangphatsornruang et al (2009) assessed 60 polymorphic SSRs. In the mungbean, the number of SSRs reported is not enough for studying genetic diversity with high levels of polymorphism. There is an elementary need to raise the number of SSR polymorphism for genetic mapping and marker-assisted improvement in mungbean. The development of SSRs is a costly and time-consuming endeavor. The SSR development takes in the construction of SSR-enriched libraries, cloning and sequencing, which is costly and labor-intensive (Yu et al. 2009). In this work, the SSR markers showed a high percentage of polymorphism, and it could be useful for DNA and genomic fingerprinting. It may be due to the highly polymorphic, abundant nature of the microsatellites due to slippage in DNA replication (Weber and May 1989).

The details of SCoT primer parameters data are shown in Table (7). The implied seventeen SCoT-primers showed a total of 153 amplified bands (ranged from 4 to 14 bands) with 69.93% of polymorphism. The polymorphism percentages ranged to 33.33% for SCoT-12 to 91.67% for SCoT-02. The variation between the averages of H_o compared to the H_e probably be causing one or more reasons. This difference might reflect the nature of markers used, inbreeding and/or selection against heterozygotes. The H_o values varied from 0.11 to 0.24, with an average value of 0.19. The highest H_o was 0.25 for SCoT-03 following by 0.24 for SCoT-02, SCoT-04 and SCoT-13 primers. While the Major value of a PIC was 0.34 for SCoT-02 and the lowest value was 0.12 for SCoT-12; with PIC average of 0.25. The uH_e oscillated from 0.13 for SCoT-12 to 0.36 for SCoT-02; it was an average mean of 0.27. The Inbreeding Coefficient (Fixation Index, F) ranged from -0.33 to 0.55 for SCoT-13 and SCoT-48 respectively, with the total average being 0.21.

The higher attributes of marker parameter, the MI value was an average of 0.25 and ranged from 0.01 for SCoT-12 to 0.82 for SCoT-02 primer. The average of Shannon Index (I) was 0.39 for all primers, the lesser value was to SCoT-12 (0.18), and the major was 0.51 (SCoT-02).

Table (7). Details of marker parameters estimated for SCoT primers.

Primers	N _b	N _e	PB	P%	PIC	EMR	MI	RP	I	H _o	H _e	uH _e	F
SCoT-02	12	1.56	11	91.67	0.34	2.42	0.82	8.0	0.51	0.24	0.34	0.36	0.29
SCoT-03	6	1.52	5	83.33	0.31	1.04	0.33	3.6	0.48	0.25	0.31	0.33	0.20
SCoT-04	12	1.43	10	83.33	0.27	1.96	0.52	5.4	0.42	0.24	0.27	0.28	0.12
SCoT-34	5	1.36	4	80.00	0.23	0.64	0.15	1.8	0.36	0.20	0.23	0.24	0.13
SCoT-28	7	1.40	5	71.43	0.25	0.81	0.20	3.4	0.39	0.23	0.25	0.26	0.10
SCoT-45	8	1.42	5	62.50	0.25	0.46	0.11	4.0	0.36	0.15	0.25	0.26	0.40
SCoT-48	4	1.58	3	75.00	0.32	0.32	0.10	3.2	0.46	0.14	0.32	0.33	0.55
SCoT-35	10	1.54	8	80.00	0.32	1.49	0.48	5.8	0.49	0.23	0.32	0.34	0.28
SCoT-05	7	1.38	5	71.43	0.24	0.81	0.19	3.0	0.37	0.23	0.24	0.25	0.05
SCoT-06	10	1.49	7	70.00	0.28	0.70	0.20	4.4	0.41	0.14	0.28	0.30	0.49
SCoT-09	14	1.30	8	57.14	0.20	0.84	0.17	4.8	0.31	0.18	0.20	0.21	0.06
SCoT-11	7	1.38	5	71.43	0.23	0.61	0.14	2.6	0.35	0.17	0.23	0.24	0.26
SCoT-12	9	1.22	3	33.33	0.12	0.11	0.01	1.0	0.18	0.11	0.12	0.13	0.08
SCoT-13	10	1.27	6	60.00	0.18	0.88	0.16	3.8	0.30	0.24	0.18	0.19	-0.33
SCoT-14	14	1.44	9	64.29	0.27	1.14	0.30	6.2	0.41	0.20	0.27	0.28	0.26
SCoT-16	10	1.36	7	70.00	0.23	0.96	0.22	3.8	0.36	0.20	0.23	0.24	0.15
SCoT-24	8	1.50	6	75.00	0.28	0.73	0.21	3.8	0.42	0.16	0.28	0.30	0.42
Total	153	24.1	107	69.93	4.3	0.94	4.32	68.6	6.6	3.3	4.3	4.55	3.51
Average	9	1.42	6.3		0.25	0.94	0.25	4.04	0.39	0.19	0.25	0.27	0.21

N_b= no. of alleles; N_e= no. effective alleles; PB= no. of polymorphic band; P%= polymorphism; PIC= polymorphic information content; EMR= effective multiplex ratio; MI= marker index; I= Shannon informative index; H_o= observed heterozygosity; H_e= expected heterozygosity; uH_e= unbiased heterozygosity; F= fixation index

The Resolving Power (RP) was an average of 4.04; oscillated from 1.0 of SCoT-12 primer to 8.0 of SCoT-02 primer. The effective number of alleles (N_e) is a reciprocal of gene homozygosity (Hartl and Clark 1997). The effective number of alleles (ENA) used to corollary the H_e (when heterozygosity is high, ENA will be highest). N_e ranged from 1.22 for SCoT-12 primer to 1.58 for SCoT-48 primer with the mean of 1.42 per primer.

These bands can be considered as potential markers to identify accessions of cowpea or maybe more useful when converted into a simple sequence PCR-based marker that can be used for large-scale screening of accessions. These molecular markers could assess to the acceleration of detection to *Vigna* accessions on the bases of molecular markers at laboratory conditions only with comparison to field screening, which is very difficult and less accurate. In another species, Huq et al (2009) characterized 60 genotypes of *C. olitorius* and *C. capsularis* using SSR marker attained a

high polymorphism value of 92.2%, with a total of 171 different alleles amplified by 27 primer pairs.

3.3. Similarity and genetic distance between accessions

The similarity matrices by Jaccard (1908) coefficient among accessions of cowpea basing on SSR analysis are given in Table 8. The highest values of similarity were recorded between accession 7 and 9 (0.86). On the other hand, between accessions 1 and 6 and accession 1 and 8 (0.29) were recorded the lowest similarity.

The similarity matrices generated by the SCoT marker among accessions showed that the highest similarity value was recorded between accession 5 and 4 and between accession 9 and 6 (0.69). On the other hand, between accessions 2 and 6 the lowest similarity recorded was (0.39), whereas investigation derived from both markers showed the highest similarity was 0.69 between accession 1 and 2, and 0.66 between accession 8 and 9. On the other hand, the lowest value of similarity scored 0.11 among accession 2 and 6.

Table (8): Similarity matrix among ten *Vigna* accessions based on markers used.

Acc.	1	2	3	4	5	6	7	8	9	10
SSR										
1	1.00									
2	0.83	1.00								
3	0.37	0.30	1.00							
4	0.37	0.30	0.79	1.00						
5	0.45	0.38	0.56	0.59	1.00					
6	0.29	0.31	0.58	0.48	0.50	1.00				
7	0.35	0.38	0.68	0.75	0.57	0.59	1.00			
8	0.29	0.31	0.57	0.61	0.55	0.57	0.80	1.00		
9	0.30	0.32	0.68	0.65	0.50	0.52	0.86	0.80	1.00	
10	0.34	0.37	0.48	0.44	0.46	0.65	0.55	0.52	0.55	1.00
SCoT										
1	1.00									
2	0.66	1.00								
3	0.43	0.49	1.00							
4	0.44	0.42	0.63	1.00						
5	0.44	0.41	0.53	0.69	1.00					
6	0.50	0.39	0.44	0.60	0.68	1.00				
7	0.48	0.44	0.50	0.52	0.58	0.58	1.00			
8	0.48	0.45	0.51	0.51	0.48	0.52	0.64	1.00		
9	0.44	0.42	0.50	0.55	0.61	0.69	0.67	0.68	1.00	
10	0.47	0.44	0.51	0.51	0.51	0.50	0.57	0.67	0.67	1.00
Both markers										
1	1.00									
2	0.69	1.00								
3	0.18	0.29	1.00							
4	0.22	0.20	0.56	1.00						
5	0.22	0.19	0.31	0.58	1.00					
6	0.23	0.11	0.16	0.41	0.50	1.00				
7	0.25	0.25	0.30	0.36	0.38	0.38	1.00			
8	0.28	0.28	0.37	0.40	0.31	0.38	0.60	1.00		
9	0.19	0.20	0.32	0.41	0.44	0.54	0.60	0.66	1.00	
10	0.27	0.27	0.32	0.33	0.30	0.35	0.42	0.59	0.57	1.00

Basing on Nei and Li (1979) coefficient, the phenogram generated by UPGMA cluster analysis showed the clustering of ten accessions of *Vigna* (Fig. 2). Investigations derived from the SSR marker (Fig. 2a) are divided into two groups at a distance of 0.338. The first one includes accession 1 and 2. The second group is divided into two sub-groups at a distance of 0.519; the first subgroup includes accession 6 and 10. Whereas, the second subgroup is further divided into sub-sub-groups at a distance of 0.554; one of them consists of accession 5 only, and the other is divided into two sub-sub sub-group at a distance of 0.658. One has accession 4 and 3, whereas the second is divided into sub-sub-sub-sub-group at a

distance of 0.826. The first one includes accession 8 only; the second one consists of accession 7 and 9.

Data generated by SCoT analysis (Fig. 2b) are divided into two groups at a distance of 0.446. The first one includes accession 1 and 2 only. The second group is divided into two sub-groups at a distance of 0.534. The first sub-group was separated into two sub-sub-group at a distance of 0.579; one includes accession 3 only and the other one consists of accessions 4 and 5. Whereas, the second sub-group is further divided into sub-sub-groups at distance of 0.598; one of them consists of accessions 8 and 10 only, and the other is divided into two sub-sub-sub-groups at distance of 0.625. One has accession 7 only, whereas the second one has accessions 6 and 9.

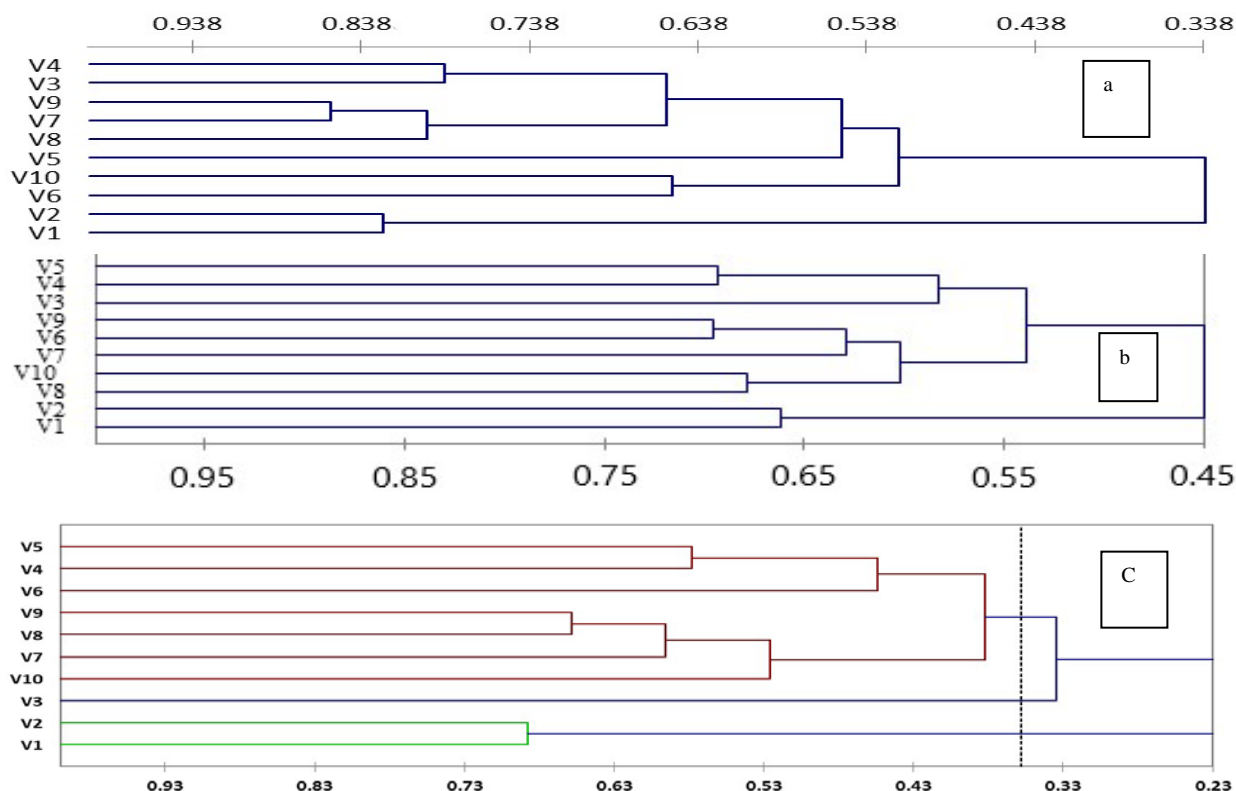


Figure (2): Dendrogram generated by UPGMA-cluster analysis basing on Nei and Li (1979) coefficient.

It is noted from Figure 2c the data based on both markers are separated into two main groups in three classes of objects at a distance of 0.227; the first group includes accession 1 and 2 only, while the second group was divided into two groups at a distance of 0.334; one of them consists of accession 3 whereas the other one is further separated into sub-sub groups at 0.382. Each sub-sub group is further divided into two sub-sub-sub groups. One includes accession 6 only and accessions 4 and 5 at a distance of 0.454. Another one involves accession 10 at a distance of 0.5255 and the rest separated at a distance of 0.578. The distance between the central objects of all classes is presented in Table 9. Data showed the first central-class includes two objects which be accessions 1 and 2; the second class has one object (accession 3 only); whereas the last class consists of seven objects (the rest accessions). The highest distance is recorded between classes 1 and 2 (9.00), while the lowest value was between classes 2 and 3 (8.12); whereas the variance within class recorded 15.00, 26.7 and 0.00 for class 1, 3 and 2, respectively with an average distance ranged from 2.7 to 4.8.

Table 9. Distances between the central objects regenerated by UPGMA cluster analysis.

Class	1	2	3
1	0.00		
2	9.00	0.00	
3	8.89	8.12	0.00
Number of objects	2	1	7
Within-class variance	15.00	0.00	26.67
Average distance to centroid	2.74	0.00	4.77

The choice of molecular markers used in identification when first being selected is very critical to consider. Both markers have great potential in accession identification and can reproduce polymorphisms. The results indicated that the two types of markers were able to effectively identify *Vigna* accessions through DNA assays. Both markers have a high ability to identify specific accession. Therefore, this approach was able to successfully distinguish between the tested germplasm, and we were able to construct unique DNA profiles of each accession for future use. The present study has revealed a broad genetic base in *Vigna* species and suggests the taxonomist review the genotypes using molecular markers. This study would help in the consideration of molecular fingerprinting for germplasm conservation, rectification, purification, and identification of germplasm. This indicates that the *Vigna* species has a broad sense of genetic diversity and allocates in agroclimatic regions.

4. Conclusion

Evaluation of genetic diversity helps in the identification of diverse germplasm that can be utilized by breeding for creating the desired variation. They demand the immediate attention of plant breeders. The available elite accessions are necessarily the products of selection from a few common accessions. For any meaningful plant breeding program, accurate estimates of genetic

diversity and partitioning within and between gene pools are important considerations. The scope for characterizing genetic diversity in cowpea at different levels presents immense opportunities.

Information about the degree and distribution of genetic variation and relationships among breeding materials has a significant effect on crop improvement. In the present study, the used techniques were an efficiency to estimate the genetic variation. Our data indicated that the used markers could effectively identify cowpea accessions because of morphological, agronomical and molecular characterization which give us more insights into the selection of a desirable accession for *Vigna* genetic improvement. In addition, the results revealed a high genetic variation among tested accessions, which can be used in cowpea breeding programs and improvement basing on the overall aims. Our study would help in the reflection of molecular fingerprinting for germplasm conservation, rectification, purification, and identification of germplasm for the genetic diversity of *Vigna* species and its distribution across agroclimatic districts. Thus, that should focus on collecting more landrace collections, as well as obtaining more genetic information for the improvement and development of new cultivars.

Acknowledgments

Authors acknowledge *Dr. Shafiq I. Darweesh*, researcher of Genome mapping, Agricultural Genetic Engineering Research Institute (AGERI), Agricultural Research Center (ARC), for his help and guidance in conducting molecular section, especially CAPS-marker. We wish also to express thanks to the *Taxonomy Dept.*, especially *Prof. Dr. Reda M. Rizk*, director of Taxonomy Dept. National Gene Bank (NGB), Agricultural Research Center (ARC), Egypt, for helping us to identify accessions and completing this study. We acknowledge and appreciate the comments of anonymous reviewers and technical editors of the Journal.

References

Alisa Kongjaimun, Akito Kaga, Norihiko Norihiko, Prakt Somta, Takehiko Shimizu, Yujian Shu, Takehisa Isemura, Duncan A. Vaughan, and Peerasak Srinives
 Al-Qurainy F, Khan S, Nadeem M and Tarroum M. 2015. SCoT marker for the assessment of genetic diversity in Saudi Arabian date palm cultivars. *Pak J. Bot.*, **47(2)**:637-643.
 Amirbakhtiar N and Sorkheh K. 2015. Analysis of diversity and relationships among wild *Pistacia* species using Start Codon Targeted (SCoT) markers. 1st Int and 9th Int. Cong. Islamic Republic of Iran, May 24-26, Shahid Beheshti University, Tehran, Iran p:1-4.
 Anderson JA, Churchill GA, Autrique JE, Tanksley SD and Sorrells ME. 1993. Optimizing parental selection for genetic-linkage maps. *Genome*, **36(1)**:181-186.
 Collard BCY and Mackill DJ. 2009. Start Codon Targeted (SCoT) Polymorphism: a simple, novel DNA marker technique for

generating gene-targeted markers in plants. *Plant Mol. Biol. Rep.*, **27**:86-93.
 Dachapak S, Somta P, Poonchavilaisak S, Yimram T, Srinives P. 2017. Genetic diversity and structure of the zombie pea (*Vigna vexillate* (L.) A. Rich) gene pool based on SSR marker analysis. *Genetica*, **145**:189-200.
 Gwang J, Chung J, Chung H, Lee J, Ma K, Dixit A, Park Y, Cho E, Kim T and Lee S. 2006. Characterization of new microsatellite markers in mung bean, *Vigna radiate* (L.). *Mol. Ecol. Notes*, **6**: 1132-1134.
 Hartl DL and Clark AG (1997) **Principles of Population Genetics**. 3rd ed., Sinauer Associates, Inc., Sunderland, MA, USA.
 Heikrujam M, Kumar J and Agrawal V. 2015 Genetic diversity analysis among male and female Jobba genotypes employing gene targeted molecular markers, start codon targeted (SCoT) polymorphism and CAAT box-derived polymorphism (CBDP) markers. *Meta Gene*, **5**: 90-97.
 Hernandez P, Laurie DA, Martin A and Snape JW. 2002. Utility of barley and wheat simple sequence repeat (SSR) markers for genetic analysis of *Hordeum chilense* and *tritodeum*. *Theor. Appl. Genet.*, **104**:735-739.
 Huq S, Islam MDS, Sajib AA, Ashraf N, Haque S and Khan H. 2009. Genetic diversity and relationships in jute (*Corchorus spp.*) revealed by SSR markers. *Bangladesh J. Bot.*, **38(2)**:153-161.
 IBPGR 1983. INTERNATIONAL BOARD FOR PLANT GENETIC RESOURCES. **Descriptor for cowpea**. IBPGR secretariat, Rome.
 IPGRI 1994. INTERNATIONAL PLANT GENETIC RESOURCES INSTITUTE. **Genebank Standards**. Food and Agriculture Organization of the United Nations, Rome, Rome.
 Jaccard P. 1908 Nouvelles recherches sur la distribution florale. *Bull. Soc. Vaudoise Sci. Nat.*, **44**: 223-270.
 Jiang QQ, Long GY, Li WW and Deng ZN. 2011. Identification of genetic variation in *Citrus sinensis* from Hunan on start codon targeted polymorphism. *Agric. Sci. Technol.*, **12(11)**:1594-1599.
 Johnson DE (1998) Applied multivariate methods for data analysis. Duxbury Press, New York.
 Karuniawan A, Iswandi A, Kale PR, Heinzemann J and Grüneberg WJ. 2006 *Vigna vexillate* (L.) A. Rich. Cultivated as a root crop in Bali and Timor. *Genet. Resour. Crop Evol.*, **53(1)**:213-217.
 Kongjaimun A, Kaga A, Norihiko N, Somta P, Shimizu T, Shu Y, Isemura T, Vaughan DA, and Srinives P. 2012 An SSR-based linkage map of yardlong bean (*Vigna unguiculata* (L.) Walp. subsp. *unguiculata* Sesquipedalis Group) and QTL analysis of pod length. *Genome*, **55**:81-92.
 Kumar SV, Tan SG, Quah SC and Yusoff K. 2002a. Isolation and characterization of seven tetranucleotide microsatellite loci in mungbean, *Vigna radiata*. *Mol Ecol. Notes*, **2**:293-295.
 Kumar SV, Tan SG, Quah SC, Yusoff K. 2002b. Isolation of microsatellite markers in mungbean, *Vigna radiata*. *Mol. Ecol. Notes*, **2**:96-98.
 Leo, C., He XH, Chen H, SJO, Gao MP, Brown JS, Tondo CT and Schnell RJ. 2011. Genetic diversity of mango cultivars estimated using SCoT and ISSR markers. *Biochem. Syst. Ecol.* **39**:676-684.
 Li CD, Fatokun CA, Ubi B, Singh BB and Scoles GJ. 2001. Determining genetic similarities and relationships among cowpea breeding lines and cultivars by microsatellite markers. *Crop Sci*, **41(1)**:189-197.
 Maréchal R, Mascherpa JM, Stainer F. 1978. Etude taxonomique d'un groupe complexe d'espèces des genres *Phaseolus* et *Vigna* (Papilionaceae) sur la base de données morphologiques et polliniques, traitées par l'analyse informatique. *Boissiera* **28**.

- Mulpuri S, Muddanuru T and Francis G. 2013. Start codon targeted (SCoT) polymorphism in toxic and non-toxic accessions of *Jatropha curcas* L. and development of a codominant SCAR marker. *Plant Sci.*, **207**: 117-127.
- Nei M and Li M. 1979. Mathematical model for studying genetic variation in terms of restriction endonucleases. *Proc. Nat. Acad. Sci. USA*, **76**:5269-5273.
- Norihiko T, Kaga A, Isemura T, Vaughan D, Srinives P, Somta P, Thadavong S, Bounphanousay C, Kanyavong K, Inthapanya P, Pandiyan M, Senthil N, Ramamoorthi N, Jaiwal PK, Jing T, Umezawa K, Yokoyama T. 2010. *Vigna* genetic resources. Proceeding of the 14th NIAS international workshop on Genetic Resources, Genetic and Comparative Genomics of Legumes (Glycine and *Vigna*). pp.11–21.
- Norihiko T, Naito K, Kaga A, Sakai H, Isemura T, Ogiso-Tanaka E, Iseki K and Takahashi Y. 2014. Evolution, domestication and neo-domestication of the genus *Vigna*. *Plant Genet. Resour.*, **12**(1):168–171.
- Ogunkanmi LA, Ogundipe OT, Ng NQ and Fatokun CA. 2008. Genetic diversity in wild of cowpea (*Vigna unguiculata*) as revealed by simple sequence repeats (SSR) markers. *J Food, Agric & Environ*, **8**:263–268.
- Ojeda FS, Hoc PS and Garcia MTA. 2013. Morphology of seeds and seedlings of four species of *Vigna Savi* (Leguminosae, Phaseolinae). *Acta Bot. Bras*, **27**(3):483–489.
- Peakall R, Smouse PE (2006). GENALEX 6: genetic analysis in Excel. Population genetic software for teaching and research. *Mol. Ecol. Notes*, **6**:288-295.
- Powell W, Marchary GC and Provan J. 1996. Polymorphism revealed by simple sequence repeats. *Trends in Plant Science*, **1**:215-222.
- Prevost A and Wilkinson MJ. 1999. A new system of comparing PCR primers applied to ISSR fingerprinting of potato cultivars. *Theor. Appl. Genetic*, **98**:107–112.
- Sawant SV, Singh PK, Gupta SK, Madnala R and Tuli R. 1999. Conserved nucleotide sequences in highly expressed genes in plants. *J. Genet.*, **78**:123-131.
- Selvakumar G and Kumari RU. 2015. Phenotypic Expression in Inter Subspecies Crosses of Cowpea (*Vigna unguiculata* (L.) Walp.) and Yard Long Bean (*Vigna unguiculata* (L.) Walp. spp. *sesquipedalis*). *J. Pl. Sci. Res.*, **31**(1):101-108.
- Shrivastav A, Babbar A, Prakash A, Tripathi N and Iquebal MA. 2012. Genetics and molecular diversity analysis of chickpea (*Cicer arietinum* L.) genotypes grown under rice fallow condition. *J. Food Leg.*, **25**(2):147-149.
- Soliman MI, Rizk, RM, El-Eraky NM. 2008. Cytogenetics comparison of cultivated and wild relatives of genus *Vigna* in Egypt. *CATRINA*. **3**(1): 61–70.
- Somta P, Musch W, Kongsamai B, Chanprame S, Nakasathien S, Toojinda T, Sorajjapinun W, Seehalak W, Tragoonrung S and Srinives P. 2008. New microsatellite markers isolated from mungbean (*Vigna radiata* (L.) Wilczek). *Mol. Ecol. Res.*, **8**:1155-1157.
- Stearn WT. 1973. **Botanical Latin**. Newton Abbott: David and Charles.
- Tangphatsornruang S, Somta P, Uthapaisanwong P, Chanprasert J, Sangsrakru D, Seehalak W, Sommanas W, Tragoonrung S and Srinives P. 2009. Characterization of microsatellites and gene contents from genome shotgun sequences of mungbean (*Vigna radiata* (L.) Wilczek). *BMC Plant Biol* **9**:137-147.
- Tatikonda L, Wani SP, Kannan S, Beerelli N, Sreedevi TK, Hoisington DA, Devi P and Varshney RK. 2009. AFLP-Based Molecular Characterization of an Elite Germoplasm Collection of *Jatropha curcas* L. a Biofuel Plant. *Plant Sci.*, **176**:505-513.
- Varshney RK, Chabane K, Hendre PS, Aggarwal RK and Graner A. 2007. Comparative assessment of EST-SSR, EST-SNP and AFLP markers for evaluation of genetic diversity and conservation of genetic resources using wild, cultivated and elite barleys. *Plant Sci.*, **173**:638–649.
- Wang XW, Kaga A, Tomooka N and Vaughan DA. 2004. The development of SSR markers by a new method in plants and their application to gene flow studies in azuki bean [*Vigna angularis* (Willd.) Ohwi & Ohashi. *Theor. Appl. Genet.*, **109**:352-360.
- Weber JL and May JL. 1989. Abundant class of human DNA polymorphism which can be types using the polymerase chain reaction. *Amer. J. Hum. Genet.*, **44**:388–396.
- Yin X, Chasalow SD, Stam PM, Kropff J, Dourleijn CJ, Bos I, Bindraban PS. 2002. Use of component analysis in QTL mapping of complex crop traits: a case study on yield in barley. *Plant Breeding*, **121**(4):314.
- Yu J-W, Dixit A, Ma K-H, Chung J-W and Park Y-J. 2009. A study on relative abundance composition and length variation of microsatellites in eighteen underutilized crop species. *Genet Res Crop Evol*, **56**:237–246.

Isolation and Identification of Dibenzothiophene Desulfurizing Bacteria Occurring in Oil Contaminated Soils of Mechanical Workshops

Praveen Reddy P¹ and UmaMaheswara Rao V^{2,*}

¹Department of Microbiology, Vivekananda Degree and PG College, Karimnagar-505001, Telangana, India; ²Department of Botany and Microbiology, Acharya Nagarjuna University, Nagarjuna Nagar-522 510, Guntur District, Andhra Pradesh, India

Received: September 7, 2020; Revised: December 26, 2020; Accepted: January 7, 2021

Abstract

When fossil fuels are oxidized, a wide range of hazardous gases reach the atmosphere. Among these gases, sulfur oxides which are released because of oxidation of organosulfur compounds occurring in fuels become the sources of environmental pollution and acid rain. Hydrodesulfurization, a traditional practice employed for the removal of sulfur content from petroleum products during refining process is not eco-friendly and effective in removal of sulfur content, especially, recalcitrant organosulfur compounds like dibenzothiophene. Biodesulfurization, which employs microbes for the removal of sulfur from fossil fuels, is an eco-friendly method and a better alternative to hydrodesulfurization. The dibenzothiophene is treated as a model organosulfur compound for biodesulfurization studies. The present paper deals with the isolation of bacteria which exhibit dibenzothiophene biodesulfurization via 4S pathway from oil contaminated soils, detection of intermediates and end product of 4S pathway using Gas chromatography-Mass spectroscopy (GC-MS) in the DBT culture broths of isolates positive for gibb's test, amplification of *dsz* operon genes which regulate 4S pathway in desulfurizing bacteria and identification of DBT desulfurizing bacteria by microscopic examination, biochemical tests and 16S rRNA gene analysis. Two DBT desulfurizing bacteria isolated were found positive for Gibb's test and Dibenzothiophene sulfone (DBTO₂), one of the intermediates and 2-Hydroxy biphenyl, the end product of 4S pathway were detected in DBT containing culture broths of both the desulfurizing bacteria when subjected to GC-MS. In both, the bacteria *dsz* operon genes were detected. The two bacteria were identified as *Streptomyces* sp. VUR PPR 101 and *Streptomyces* sp. VUR PPR 102.

Keywords: Biodesulfurization, Dibenzothiophene, 4S pathway, *dsz* operon, *Streptomyces* sp. VUR PPR 101, *Streptomyces* sp. VUR PPR 102

1. Introduction

The third most abundant element in fossil fuels is sulfur, and numerous organosulfur and sulfur containing inorganic compounds are present in fuels. When fossil fuels are oxidized, sulfur oxides reach the atmosphere (Bordoloi *et al.*, 2016; Sadare *et al.*, 2017) which are potent air pollutants and major source of acid rains (Li *et al.*, 2003). Sulfur dioxide in the environment causes health problems in humans like irritation of eyes, respiratory problems etc. (Wondyfraw, 2014). Even the plants that are exposed to sulfur dioxide exhibit change in their physiology and become susceptible to microbial infections. Prolonged exposure to sulfur dioxide increases rate of transpiration and dark respiration in plants (Khan and Khan, 2011). The conventional hydrodesulfurization (HDS) process used for the removal of sulfur from fossil fuels (petroleum products) which is operated at high temperature and pressure is not so effective in the elimination of sulfur from organosulfur compounds occurring in fossil fuels. Particularly, HDS is not effective in removal of sulfur from recalcitrant organosulfur compounds like Dibenzothiophene (DBT) (Wang *et al.*,

2017; da Silva and Secchi, 2018). To overcome the sulfur dioxide related problems, a new method involving microbes known as Biodesulfurization (BDS) has been developed to remove sulfur content from fossil fuels. The BDS is a very economical and eco-friendly process which does not make use of high temperature and pressure (Wang *et al.*, 2017). For Biodesulfurization studies, DBT which is highly recalcitrant and hazardous is treated as model compound. The DBT is a very persistent compound as compared to most polycyclic aromatic hydrocarbons (PAHs) and other aromatic hydrocarbons. It can remain for 10 years in crude oil polluted sediments, long after most aromatics have disappeared (Li *et al.*, 2005; Mezcua *et al.*, 2008). Microorganisms employ three major pathways for DBT metabolism *viz.*, Kodama, Van Afferden and 4S pathways of which the 4S pathway is regarded as commercially important one (de Araujo *et al.*, 2012). The microbes which metabolize DBT via 4S pathway will not break the ring structure of DBT, and thus calorific value of fuel is unaffected. Specific interest was paid by researchers in isolating bacteria that specifically remove sulfur from organosulfur compounds without breaking the carbon backbone of the original organosulfur compounds. The 4S pathway is such a metabolic pathway exhibited by certain

* Corresponding author e-mail: umrvanga@gmail.com.

microbes during which sulfur element is removed as sulfite from DBT without affecting its ring structure (Labana *et al.*, 2005). The DBT metabolism via other pathways may result in cleavage of DBT ring or sulfur is not removed. Hence, microbes which exhibit 4S pathway for the desulfurization of DBT are eco-friendly and economically important. Various microbes which exhibit 4S pathway include *Rhodococcus erythropolis* XP, *Rhodococcus erythropolis* IGTS8, *Gordonia alkanivorans* RIPI90A etc. (de Araujo *et al.*, 2012; Bordoloi *et al.*, 2016). The 4S pathway is a multienzymatic system with four different activities (Gray *et al.*, 1996). First enzyme of the 4S pathway is monooxygenase (DszC) which catalyzes the DBT oxidation to Dibenzothiophene sulfone (DBTO₂) in two steps. The second is also a monooxygenase (DszA) which converts DBTO₂ to Hydroxyphenyl benzene sulfonate (HPBS), and in the final step DszB (HPBS desulfinase) converts HPBS to 2-hydroxy biphenyl (2-HBP) and sulfite. In this metabolic pathway, FMN-reductase (DszD) has an important role in the activity of the monooxygenases, as it is responsible for the maintenance of reduced flavin levels. The *dszA*, *B* and *C* genes of *dsz* operon synthesize DszA, DszB and DszC enzymatic proteins, respectively (Muraka *et al.*, 2019). The microbial cells have been majorly exploited in pharmaceutical and food industries to produce antibiotics, vitamins, amino acids, alcoholic beverages etc., on large scale. Even various microbial strains are employed in reclamation of polluted sites (bioremediation) and treatment of used engine oils. The biocatalytic desulfurization of fuels is an important and useful emerging process in the present-day context in view of curbing the environmental pollution. The biodesulfurizing microbial strains could pave the way for effective desulfurization process and can be employed in future to generate sulfur free fuels. In the present work, an attempt was made to isolate bacterial strains exhibiting DBT biodesulfurization via 4S pathway using Gibb's assay and by detecting the intermediates and end product of 4S pathway in DBT containing culture broth using Gas chromatography-Mass spectroscopy (GC-MS), identification of *dsz* operon genes responsible for 4S pathway using specific primers and identification of the positive DBT desulfurizing bacteria based on morphological and microscopic examination, biochemical tests and 16S rRNA gene sequencing.

2. Materials and Methods

2.1. Isolation of bacteria growing in DBT supplemented medium

To isolate Dibenzothiophene desulfurizing bacteria, different mechanical workshop sites in Karimnagar town, Telangana, India were selected and designated as A, B, C, D, E and F. Heavy motor vehicles in workshops A and B, light motor vehicles in workshops C and D, and two wheelers in workshops E and F are repaired and serviced. From these sites, oil contaminated soil samples were collected bimonthly for a period of one year. For the isolation of DBT-desulfurizing bacteria, ten grams of each soil sample was suspended in 90 ml of distilled water and 5 ml of the suspension was inoculated into 250 ml flask containing 45 ml of basal salt medium (BSM) supplemented with glucose (5 g/l) as carbon source and 5

mM per liter DBT as sole sulfur source. Cultivation was performed at 30° C in rotary shaker for 5 days. After five sub cultivations, the culture broth medium was spread onto BSM agar medium supplemented with glucose and DBT (Khedkar and Shanker, 2014). All the viable and dominantly growing representative bacterial cultures were isolated from samples of Workshops.

2.2. Gibb's assay

The recovered cultures were grown in BSM broth supplemented with glucose and DBT and tested for the occurrence of 4S pathway within them by detecting 2-HBP, the end product of 4S pathway by the Gibb's assay. The test was used to detect the 2-HBP produced by the bacteria after growing them in the medium containing DBT. Gibb's reagent reacts with aromatic hydroxyl groups such as 2-hydroxy phenyl to form blue colored complex. The pH of bacterial culture broths was adjusted to 8.0 using 10% sodium bicarbonate or sodium carbonate and 100 µl of Gibb's reagent (10 mg of 2,6-dichloroquinone-4-chlorimide prepared in 1 ml of ethanol) was added to 5 ml of each bacterial culture broth and incubated for 30 minutes. Formation of blue color complex indicates the positive result and brown color indicates negative result for Gibb's assay. The cultures positive for Gibb's assay were expected to produce 2-HBP via 4S pathway from DBT (Kayser *et al.*, 1993).

2.3. GC-MS analysis of DBT culture broths of bacteria positive for Gibb's test

The culture broth was centrifuged and the supernatant was acidified with 6N hydrochloric acid to pH 2.0. The acidified supernatant was mixed with equal volume of ethyl acetate, and the extracted samples were subjected to GC-MS analysis. The GC-MS instrument employed was an Agilent 7890A model in which GC was coupled with a Pegasus HT TOFMS. The specifications of GC column include 29.8 m x 0.2 µm and 0.2 m x 320 µm. The initial and final temperatures employed for sample analysis were 60°C and 320°C, respectively. The rate of increase of temperature during sample analysis was 15°C per minute. The temperature maintained during the entire sample run was 280°C. Helium was used as carrier gas with a flow rate of 1.2 ml per minute to run 1 µl of DBT culture broth sample.

2.4. Identification of *dsz* operon genes responsible for 4S pathway

The forward and reverse primers used for the amplification of *dszA* gene were 5'-GCGCGCAAGTTCGATCTGT-3' and 5'-TCCCAGGATGTCCTTGATC-3', respectively. The primers used for the amplification of *dszB* gene were 5'-ATCGAACTCGACGTCCTCAG-3' (forward) and 5'-TCAGGACCACAGCTACAAGG-3' (reverse). For the amplification of *dszC* gene, the forward and reverse primers employed were 5'-CTGTTCGGATACCACCTCAC-3' and 5'-GTGCCTGAAGGTGTTGCA-3', respectively (Duarte *et al.*, 2001; Li *et al.*, 2007).

2.5. Identification of bacterial isolates

2.5.1. Colony characteristics

Colony characteristics of the bacterial isolates positive for DBT desulfurization via 4S pathway were observed on DBT containing basal salt medium. The color, configuration, elevation, margin and size of the colonies were recorded.

2.5.2. Microscopic examination and Biochemical tests

Gram staining and spore staining of the DBT desulfurizing bacteria were performed and the morphological shapes were also noticed. The biochemical tests *viz.*, starch hydrolysis, casein hydrolysis, sucrose test, catalase test, oxidase test, hydrogen sulfide production, lipid activity, indole test, methyl red test, Voges-Proskauer test, citrate utilization test, urea hydrolysis test and nitrate reduction test were performed as per the standard procedures (Kim *et al.*, 2001; Reddy *et al.*, 2011; Bennett *et al.*, 2018).

2.5.3. 16S rRNA sequencing and phylogenetic analysis of the bacterial isolates

The 16s rRNA sequencing and phylogenetic analysis of the bacterial isolates positive for DBT desulfurization were carried out at Bioaxis DNA Research Centre (BDRC), Hyderabad for the identification. The primers used for the amplification of 16S rRNA gene were 5'-GCAATAACAGGTCTGTGATGCCC-3' (forward) and 5'-GCATCACAGACCTGTTATTGC-3' (reverse) (Frank *et al.*, 2008).

2.6. Isolation of chromosomal DNA

The cultures of B39 and B40 were transferred separately into 50 ml BSM broth supplemented with glucose and dibenzothiophene taken in 250 ml flasks and incubated in a shaker at 30° C at 180 rpm for 4 days. After incubation period, the culture broths were subjected to centrifugation at 10,000 rpm for ten minutes. Then 0.1 grams of mycelium of each isolate was crushed with liquid nitrogen in a clean porcelain dish. Then crushed mycelium of each isolate was transferred to a tube consisting of 500 µl TE buffer containing lysozyme enzyme and incubated for half an hour at 37° C. Then, 20 µl SDS (10%) and 20 µl proteinase K were added, and the tube was incubated for thirty minutes at 55° C. After incubation period, the mixture was cooled and centrifuged at 10,000 rpm for five minutes and extracted with phenol-chloroform (1:1) solution. The aqueous phase of the mixture was taken in clean tube and DNA precipitate was obtained by using 90% ethyl alcohol at -20° C. Then DNA pellet was recovered after centrifuging for ten minutes at 10,000 rpm. The pellet was dissolved in TE buffer and 20 µl of RNase enzyme was added and incubated at 37° C for one hour to get RNA free DNA. The DNA is again precipitated by using 90% ethyl alcohol at -20° C. Then, pure DNA pellet was obtained by centrifugation (at 10,000 rpm for 10 minutes) (Kumar *et al.*, 2010), and the purity of DNA was determined by using UV spectrophotometer.

2.7. PCR amplifications

The PCR mixture containing 200 µM dNTPs, 100 ng of genomic DNA, 6 mM magnesium chloride, 10% dimethyl sulfoxide, each primer of 30 pmol and 2.5 units of Taq Pol. in 50µl buffer was prepared. The amplification was performed by initially increasing the temperature of

mixture to 94° C for 1 minute (denaturation), then decreased to 57° C for 60 seconds (annealing) and increased to 72° C for 1 minute (extension of hybridized primers), followed by final extension at 72° C for 5 minutes in thirty-five cycles. Then the PCR reaction mixture was subjected to agarose gel electrophoresis by employing a size marker of 1 kb DNA ladder. The dideoxy chain termination procedure was used for the sequencing of rRNA genes (Kurnijasanti *et al.*, 2017). The 16S rRNA gene sequences of B39 and B40 isolates were submitted to NCBI Genbank. Further, neighbor joining method was employed for the construction of phylogenetic trees of the isolates.

3. Results and Discussion

3.1. Isolation of predominantly growing bacteria on DBT containing medium and screening for bacterial strains positive for Gibb's test

In the present work, a total of 46 predominantly growing bacterial representative types on BSM medium supplemented with DBT were obtained from oil contaminated sites of different mechanical workshops. On screening, all these isolates for the presence of 4S pathway metabolic activity through Gibbs assay, only two bacteria (designated as B39 and B40) isolated from the soil of mechanical workshop B were found positive for 4S pathway. This was confirmed by the development of blue coloration during Gibbs assay indicating the production of 2-HBP which is the end product of 4S pathway (Rahpeyma *et al.*, 2017). The Gibb's assay was used to identify the desulfurization activity of bacteria through 4S pathway by several earlier workers (Sadare *et al.*, 2017; Shahaby and El-din, 2017; Li *et al.*, 2019). The other isolates of our study which were negative for Gibb's assay may be utilizing the other pathways *viz.*, Kodama pathway and Van Afferden pathway for metabolizing DBT as they were also grown abundantly on basal salt medium supplemented with glucose and DBT as sole sulfur source.

3.2. Detection of intermediates and the end product of 4S pathway by GC-MS

The two Gibb's test positive bacterial isolates (B39 and B40) were subjected to GC-MS analysis for the detection of metabolites of 4S pathway. In GC-MS analysis of B39 isolate culture broth, the compounds with retention time of 13.6117 and 9.22667 minutes were identified as DBT sulfone and the 2-HBP, respectively (Figure 1). Similarly, GC-MS of B40 culture broth showed the presence of the same compounds with retention time of 13.61 and 9.23167 minutes that were identified as DBT sulfone and 2-HBP, respectively (Figure 2). Li *et al.* (2003) have detected DBT sulfone and 2-HBP by GC-MS in the DBT culture broth of *Mycobacterium* sp. X7B. Similarly, Rhee *et al.* (1998) during their DBT desulfurizing studies with newly isolated *Gordona* strain CYKS1, observed DBT sulfone and 2-HBP in the GC chromatogram of DBT culture broth. In the mass spectrum of DBT sulfone pertaining to B39 isolate, a molecular [M⁺] ion peak at *m/z* 216 was found corresponding to the molecular mass of DBT sulfone and the major fragmentation ions were seen at *m/z* 139 and 63 (Figure 3). Similarly, in the mass spectrum of 2-HBP of B39, a molecular [M⁺] ion peak at *m/z* 170 was observed corresponding to the molecular mass of 2-HBP and the major fragmentation ions were seen at *m/z* 141,115 and 63

(Figure 4). In the mass spectrum of DBT sulfone of B40 isolate, a molecular $[M^+]$ ion peak at m/z 216 was noticed corresponding to the molecular mass of DBT sulfone and the major fragmentation ions were seen at m/z 187, 136 and 63 (Figure 5). Similarly, in the mass spectrum of 2-HBP of B40, a molecular $[M^+]$ ion peak at m/z 170 was found corresponding to the molecular mass of 2-HBP and the major fragmentation ions were seen at m/z 141, 115, 89 and 63 (Figure 6). This observation is in great concurrence with several earlier reports in this aspect (Mohebbi *et al.*, 2008; Mohammed *et al.*, 2015; Ismail *et al.*, 2016). Even, Akhtar *et al.* (2009) also detected similar molecular ion peaks of DBT sulfone and 2-HBP in the mass spectra of DBT culture broths of *Rhodococcus* species, when subjected to GC-MS.

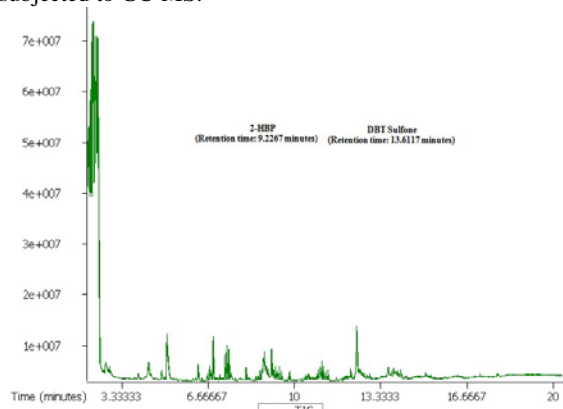


Figure 1. Gas Chromatogram of DBT broth extract of the bacterial isolate B39

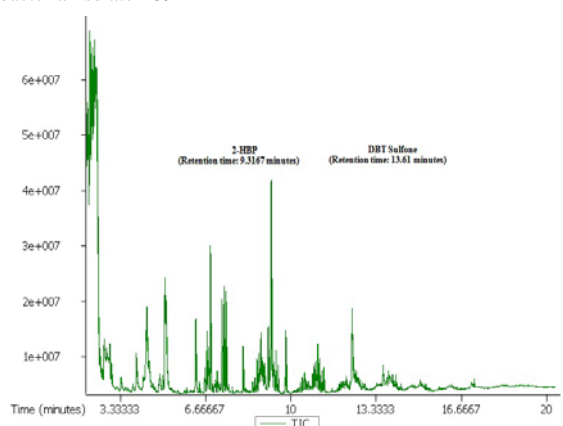


Figure 2. Gas Chromatogram of DBT broth extract of bacterial isolate B40

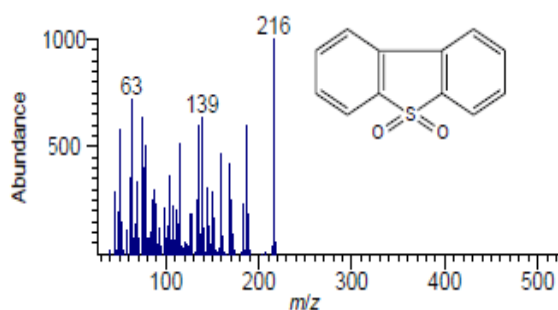


Figure 3. Mass spectrum of DBT sulfone of the bacterial isolate B39

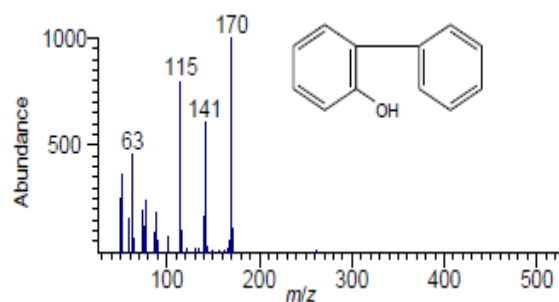


Figure 4. Mass spectrum of 2-HBP of the bacterial isolate B39

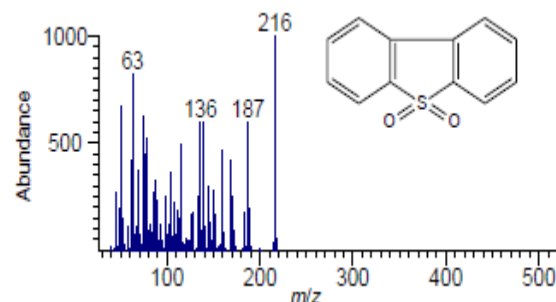


Figure 5. Mass spectrum of DBT sulfone produced by bacterial isolate B40

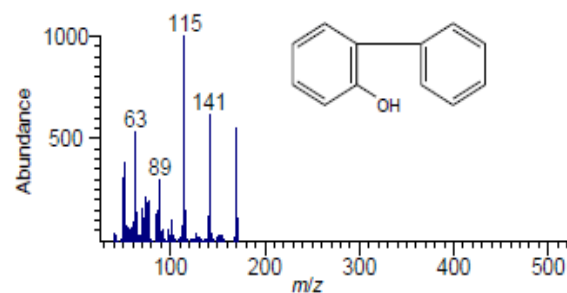


Figure 6. Mass spectrum of 2-HBP produced by bacterial isolate B40

3.3. Amplification of *dsz* operon genes in DBT desulfurizing bacteria

In both the bacterial isolates, *dsz ABC* operon genes were amplified (Figure 7) indicating their presence. Interestingly, the *dsz* operon in both the isolates was located on genomic DNA, which has good concurrence with earlier report of Shavandi *et al.* (2010) who identified the presence of *dsz* operon genes responsible for DBT desulfurization on chromosome in *Gordonia alkanivorans* RIPI90A. However, in *Rhodococcus erythropolis* IGTS8 strain, which is a model strain for biodesulfurization studies, the *dsz* operon was reported to be present on plasmid.

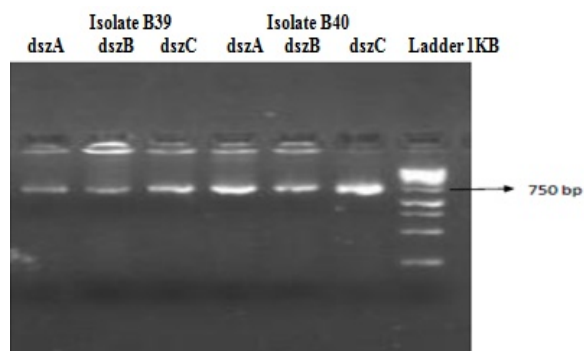


Figure 7. PCR gel picture of amplified *dsz* operon genes of the B39 and B40 bacterial isolates

3.4. Identification of bacteria positive for DBT desulfurization via 4S pathway

Based on colony characteristics (Table 1), morphological (shape), staining (Gram's and Spore) and biochemical studies *viz.*, starch hydrolysis, casein hydrolysis, sucrose test, catalase test, oxidase test, hydrogen sulfide production, lipid activity, indole test, methyl red, Voges-Proskauer test, citrate utilization test, urea hydrolysis and nitrate reduction test (Table 2), the two desulfurizing bacteria are identified as Gram positive, filamentous and tentatively as *Streptomyces* species. Taddei *et al.* (2006) based on the similar morphological and biochemical studies, identified bacteria isolated from Venezuelan soils as *Streptomyces* species.

Table 1. Colony characteristics of the bacterial isolates

Colony character	B39 isolate	B40 isolate
Color	White	Light grey
Configuration	Round	Round
Elevation	Convex	Convex
Margin	Ciliate	Ciliate
Size (Diameter)	4.2 mm	3.5 mm

Table 2. Morphological, Gram staining, Spore shape and Biochemical tests.

Characteristics	Bacterial isolates	
	B39	B40
Microscopic observation		
Morphological shape	Filamentous	Filamentous
Gram staining	Gram positive	Gram positive
Spore shape	Oval to circular	Oval
Biochemical tests		
Starch hydrolysis	Positive	Positive
Casein hydrolysis	Positive	Positive
Sucrose test	Positive	Positive
Catalase test	Positive	Positive
Oxidase test	Positive	Positive
H ₂ S Production test	Positive	Positive
Citrate utilization test	Positive	Positive
Lipid activity	Positive	Positive
Indole test	Negative	Negative
Methyl red test	Positive	Positive
Voges-Proskauer test	Negative	Negative
Urea hydrolysis	Positive	Positive
Nitrate reduction test	Positive	Positive

The 16S rRNA genes of both the bacterial isolates were amplified using the standard primers and sequenced. The

partial length of rRNA gene sequences of bacterial isolates, B39 and B40 were 1,393 and 1,395, respectively. The phylogenetic analysis revealed that B39 and B40 were closely related to *Streptomyces* sp. SPMA113 (Accession No. HQ340163.1) and *Streptomyces* sp. Antag6 (Accession No. JQ417273.1), respectively (Figure 8). The percentage of identity between the *Streptomyces* species was determined using NCBI BLASTn tool. The percentage of identity between B39 and *Streptomyces* sp. SPMA113 was found to be 100%. Similarly, the percentage of identity between B40 and *Streptomyces* sp. Antag6 was also 100%. There was 98.91% of identity between B39 and B40 isolates. The rRNA gene proved to be a universal tool for the phylogenetic analysis and interrelation among the organisms as it is ancient, universally distributed and most conserved region in the genome of the microorganisms. Although there are three different ribosomal RNAs *i.e.*, 5S, 16S and 23S in prokaryotes, only 16S rRNA sequence is used because the nucleotides in 16S rRNA are neither less nor more in length and easy to sequence. The rRNA sequence is used to construct phylogenetic tree by applying distance-matrix method. The evolutionary distance is determined by recording differences in the sequences of two or more organisms by software computer analysis. A statistical correction factor is applied due to the reason that some changes might have taken place in the genome which would lead back to the same sequence. After measuring the evolutionary distance, the phylogenetic tree is constructed. The different evolutionary distances of the two microorganisms are directly proportional to the total length of the branches separating them. Depending on software/computer program and the number of microorganisms, different formats of phylogenetic trees are possibly constructed (Chapus *et al.*, 2005). The gene sequences were submitted to NCBI Genbank designating B39 and B40 isolates as *Streptomyces* sp. VUR PPR101 and *Streptomyces* sp. VUR PPR 102, respectively. The Genbank had accepted and given the accession numbers, KF551242.1 and KF551243.1 to *Streptomyces* sp. VUR PPR 101 and *Streptomyces* sp. VUR PPR 102, respectively.

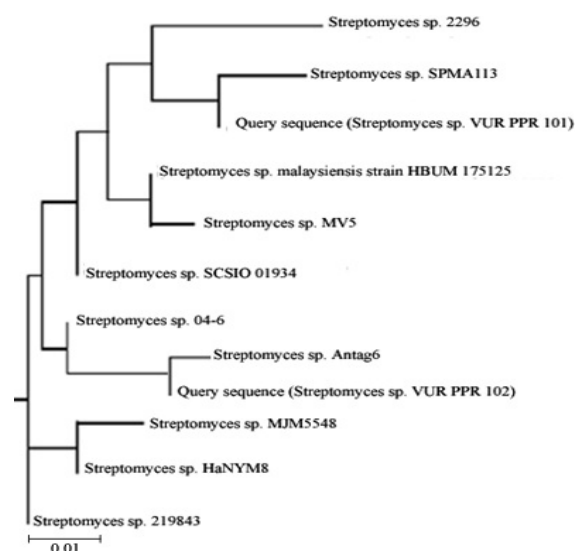


Figure 8. Phylogenetic analysis of *Streptomyces* sp. VUR PPR 101 and *Streptomyces* sp. VUR PPR 102.

The scale bar infers 1% of the estimated nucleotide difference.

The *Streptomyces* species isolated in the present work are aerobic in nature and obviously exhibiting the aerobic DBT desulfurization (4S) pathway. Therefore, they will be commercially and economically important when compared to microbial strains exhibiting anaerobic biodesulfurization pathways. When microbial strains exhibiting oxidative DBT desulfurization pathway are employed during oil refining process, they form water soluble sulfite from DBT which can be easily disposed by employing an aqueous phase. On the other hand, anaerobic desulfurization occurs by a reductive pathway during which sulfur from DBT is removed as hydrogen sulfide which later releases sulfur atom. Though the anaerobic strains can be employed for desulfurization, it is a difficult and costly affair to maintain anaerobic conditions throughout the process, moreover it is time consuming and undesirable products may form from organic constituents of fuels (Sadare *et al.*, 2017). Further, there is a scope to genetically modify these *Streptomyces* species for enhanced DBT biodesulfurization activity. Such genetically improved biodesulfurizing *Streptomyces* strains can be commercially important and potent to employ in desulfurization of fuels during refining process to produce sulfur free fuel products.

4. Conclusion

In the present study, two potential DBT desulfurizing *Streptomyces* species were isolated from oil contaminated soils of mechanical workshops. Both the desulfurizing species are commercially important as they showed the ability to desulfurize the DBT occurring in fuels, the model compound for biocatalytic desulfurization studies by 4S pathway without breaking the ring structure of DBT and not leading to the reduction of calorific value of fuel (mileage). The *dsz* operon genes (*A*, *B* and *C*) responsible for 4S pathway were identified in both the *Streptomyces* species. These two DBT desulfurizing *Streptomyces* species gain ecological and commercial importance in Biodesulfurization of fuels.

Acknowledgments

Both the authors of this manuscript convey thanks to the Department of Botany and Microbiology, Acharya Nagarjuna University, Guntur for the support and facilities provided to carry out the research work.

Conflict of interests

The authors declare that they have no conflict of interests.

References

Akhtar N, Ghauri MA, Anwar MA and Akhtar K. 2009. Analysis of the dibenzothiophene metabolic pathway in a newly isolated *Rhodococcus* spp. *FEMS Microbiol Lett.*, **301**(1): 95-102.

Bennett JA, Kandell GV, Kirk SG and McCormick JR. 2018. Visual and microscopic evaluation of *Streptomyces* developmental mutants. *J. Vis. Exp.*, **139**: e57373.

Bordoloi NK, Bhagowati P, Chaudhuri MK and Mukherjee AK. 2016. Proteomics and metabolomics analyses to elucidate the desulfurization pathway of *Chelatococcus* sp. *PLoS One.*, **11**: e0153547.

Chapus C, Dufraigne C, Edwards S, Giron A, Fertil B and Deschavanne P. 2005. Exploration of phylogenetic data using a global sequence analysis method. *BMC Evol Biol.*, **5**: 63.

da Silva JIS and Secchi AR. 2018. An approach to optimize costs during ultra-low hydrodesulfurization of a blended consisting of different oil streams. *Braz. J. Chem. Eng.*, **35**(4): 1293-1304.

de Araujo HWC, de Freitas SMC, Lins CM, do Nascimento AE, da Silva CAA and Compos-Takaki GM. 2012. Oxidation of dibenzothiophene (DBT) by *Serratia marcescens* UCP 1549 formed biphenyl as final product. *Biotechnology for Biofuels.*, **5**: 33.

Duarte GF, Rosado AS, Seldin L, Araujo W and Van Elsas JD. 2001. Analysis of bacterial community structure in sulfurous-oil-containing soils and detection of species carrying dibenzothiophene desulfurization (*dsz*) genes. *Appl Environ Microbiol.*, **67**(3): 1052-1062.

Frank JA, Claudia IR, Sharma S, Weisbaum JS, Wilson BA and Olsen GJ. 2008. Critical Evaluation of two primers commonly used for amplification of bacterial 16S rRNA genes. *Appl. Environ. Microbiol.*, **74**(8): 2461-2470.

Gray KA, Pogrebinsky OS, Mrachko GT, Xi L, Monticello DJ and Squires CH. 1996. Molecular mechanisms of biocatalytic desulfurization of fossil fuels. *Nat Biotechnol.*, **14**(13): 1705-1709.

Ismail W, El-Sayed WS, Raheem ASA, Mohamed ME and El Nayal AM. 2016. Biocatalytic desulfurization capabilities of a mixed culture during non-destructive utilization of recalcitrant organosulfur compounds. *Front Microbiol.*, **7**: 266.

Kayser KJ, Bielaga-Jones BA, Jackowski K, Odusan O and Kilbane II JJ. 1993. Utilization of organosulphur compounds by axenic and mixed cultures of *Rhodococcus rhodochrous* IGTS8. *J. Gen. Microbiol.*, **139**(12): 3123-3129.

Khan MR and Khan MM. 2011. Plants response to diseases in sulfur dioxide stressed environment. *Plant Pathol. J.*, **10**(1): 1-12.

Khedkar S and Shanker R. 2014. Isolation and classification a soil actinomycete capable of sulphur- specific biotransformation of diebenzothiophene, benzothiophene and thianthrene. *J. Appl. Microbiol.*, **118**(1): 62-74.

Kim EK, Jang WH, Ko JH, Jong SK, Kang JS, Noh MJ and Yoo OJ. 2001. Lipase and its modulator from *Pseudomonas* sp. strain KFCC 10818: Proline-to glutamine substitution at position 112 induces formation of enzymatically active lipase in the absence of the modulator. *J Bacteriol.*, **183**(20): 5937-5941.

Kumar V, Bharti A, Gusain O and Bhist GS. 2010. An improved method for isolation of genomic DNA from filamentous actinomycetes. *Journal of Sci. Engg. & Tech. Mgt.*, **2**(2): 10-13.

Kurnijasanti R, Isnaeni, Poernomo AT and Sudjarwo. 2017. Phylogenetic analysis and anti microbial activity of *Streptomyces* spp. Isolated from compost soil in Surabaya Indonesia on the basis of 16S rRNA gene. *Folia Medica Indonesiana.*, **53**(3): 204-208.

Labana S, Pandey G and Jain RK. 2005. Desulfurization of dibenzothiophene and diesel oils by bacteria. *Lett Appl Microbiol.*, **40**(3): 159-163.

Li FL, Xu P, Ma CQ, Luo LL and Wang XS. 2003. Deep desulfurization of hydrodesulfurization treated diesel oil by a facultative thermophilic bacterium *Mycobacterium* sp. X7B. *FEMS Microbiol Lett.*, **223**(2): 301-307.

Li GQ, Ma T, Li SS, Li H, Liang FL and Liu RL. 2007. Improvement of dibenzothiophene desulfurization activity by

- removing the gene overlap in the *dsz* operon. *Biosci Biotechnol Biochem.*, **71(4)**: 849-854.
- Li L, Liao Y, Luo Y, Zhang G, Liao X, Zhang W, Zheng S, Han S, Lin Y and Liang S. 2019. Improved efficiency of desulfurization of oil sulfur compounds in *Escherichia coli* using a combination of desensitization engineering and DszC overexpression. *ACS Synth. Biol.*, **8(6)**: 1441-1451.
- Li W, Zhang Y, Wang MD and Shi Y. 2005. Biodesulfurization of dibenzothiophene and other organic sulfur compounds by a newly isolated *Microbacterium* strain ZD-M2. *FEMS Microbiol Lett.*, **247(1)**: 45-50.
- Mezcua M, Fernandez-Alba AR, Boltes K, Alonso Del Aquila R, Leton P, Rodriguez A and Garcia-Calvo E. 2008. Determination of PASHs by various analytical techniques based on gas chromatography-mass spectrometry: Application to a biodesulfurization process. *Talanta.*, **75(5)**: 1158-1166.
- Mohammed MES, Yacoub ZHA and Vedakumar JV. 2015. Biocatalytic desulfurization of thiophenic compounds and crude oil by newly isolated bacteria. *Front Microbiol.*, **6**: 112.
- Mohebal G, Ball AS, Kaytash A and Rasekh B. 2008. Dimethyl sulfoxide (DMSO) as the sulfur source for the production of desulfurizing resting cells of *Gordonia alkanivorans* RPI90A. *Microbiology.*, **154(3)**: 878-885.
- Muraka P, Bagga T, Singh P, Rangra S and Srivastava P. 2019. Isolation and identification of TetR family protein that regulates the biodesulfurization operon. *AMB Expr.*, **9**: 71.
- Rahpeyma SS, Mohammadi M and Raheb J. 2017. Biodesulfurization by two bacterial strains in cooperation with Fe₃O₄, ZnO and CuO nanoparticles. *J Microb Biochem Technol.*, **9(2)**: 587-591.
- Reddy NG, Ramakrishna DPN and Raja Gopal SV. 2011. A morphological, physiological and biochemical studies of marine *Streptomyces rocheri* (MTCC 10109) showing antagonistic activity against selective human pathogenic microorganisms. *Asian J. Biol. Sci.*, **4(1)**: 1-14.
- Rhee SK, Chang JH, Chang YK and Chang HN. 1998. Desulfurization of dibenzothiophene and diesel oils by a newly isolated *Gordona* strain, CYKS1. *Appl. Environ. Microbiol.*, **64(6)**: 2327-2331.
- Sadare OO, Obazu F, Rasekh B and Daramola MO. 2017. Biodesulfurization of petroleum distillates - Current status, opportunities and future challenges. *Environments.*, **4(4)**: 85.
- Shahaby AF and El-din KME. 2017. Desulfurization of crude oil and oil products by local isolated bacterial strains. *Int. J. Curr. Microbiol. App. Sci.*, **6(4)**: 2695-2711.
- Shavandi M, Sadeghizadeh M, Khajeh K, Mohebal G and Zomorodipour A. 2010. Genomic structure and promoter analysis of the *dsz* operon for dibenzothiophene biodesulfurization from *Gordonia alkanivorans* RPI90A. *Appl Microbiol Biotechnol.*, **87(4)**: 1455-1461.
- Taddei A, Rodriguez MJ, Marquez-Vilchez E and Castelli C. 2006. Isolation and identification of *Streptomyces* spp. From Venezuelan soils: Morphological and biochemical studies. I. *Microbiol Res.*, **161(3)**: 222-231.
- Wang J, Butler III RR, Wu F, Pomber JF, Kilbane II JJ and Stark BC. 2017. Enhancement of microbial biodesulfurization via genetic engineering and adaptive evolution. *PLoS One.*, **12**: e0168833.
- Wondyfraw M. 2014. Mechanisms and effects of acid rain on environment. *J Earth Sci Clim Change.*, **5(6)**: 204.

Quantitative Probiotic Analysis of Various Kefir Samples

Aylin USKUDAR GUCLU^{1,*}, Esen YESIL², Aylin ALTAY KOCAK¹, Mendane SAKA², Hasan Cenk MIRZA¹, Bedia DINC³, Ahmet BASUSTAUGLU¹

¹Department of Medical Microbiology, Medical Faculty, Baskent University, Ankara, Turkey; ²Department of Nutrition and Dietetics, Health Science Faculty, Baskent University, Ankara, Turkey; ³Department of Medical Microbiology, Ankara City Hospital, Ministry of Health, Ankara, Turkey,

Received: September 28, 2020; Revised: January 15, 2021; Accepted: January 30, 2021

Abstract

This study assessed whether industrial kefir samples have enough probiotic diversity and number, which is important in health benefits, to examine the difference between fruit kefir (FK) and plain kefir (PK) products in terms of probiotic content, and to reveal how much they preserve the probiotic content until the expiry date. The number of total aerobic mesophilic bacteria (TAMB), *Lactobacillus*, *Lactococcus*, *Leuconostoc*, acetic acid bacteria, and yeast was determined using Standard Plate Count Agar, MRS (De Man, Rogosa and Sharpe) agar, M17 agar, MSE (Mayeux, Sandine & Elliker) agar, *Acetobacter* agar and Sabouraud dextrose agar with chloramphenicol. Matrix-assisted laser desorption/ionization-time of flight mass spectrometry (MALDI-TOF-MS) and API 20AUX were used to identify the isolates. TAMB in PK was 4.3×10^5 to 2.9×10^8 ; in FK, 1.8×10^6 to 3.6×10^8 . *Lactobacillus paracasei*, *L. casei*, *Lactococcus lactis*, *Leuconostoc mesenteroides*, *Leuconostoc* spp, *Streptococcus* spp, and *Candida kefir* were isolated in different combinations and number. Acetic acid bacteria were not isolated. There was no difference in FK and PK of the same trademarks. The number of lactic acid bacteria (LAB) in FK and PK at two different times was similar. Total LAB, lactococci, lactobacilli, and yeast populations increased during storage ($p < 0.05$). Although the number of microorganisms of samples decreased at expiration dates, they still had enough microorganism numbers indicated in a codex.

Keywords: Industrial Kefir, Probiotics, Microbial Composition, Fruit Kefir

1. Introduction

Kefir is a fermented-milk beverage produced by the action of lactic acid bacteria, yeasts, and acetic acid bacteria on milk (Ahmed et al., 2013). It originated in the Caucasus Mountains in ancient times and spread from there throughout the world. Kefir is produced by mesophilic bacteria and yeasts as a result of fermenting the lactic acid and alcohol (John and Deeseenthum, 2015). Recently, kefir has strong effects on health as a probiotic food like other fermented milk and dairy products; due to the organic acids, H₂O₂, acetaldehyde, CO₂, and bacteriocins produced as natural metabolites of microorganisms in its components, kefir shows antibacterial activity against many pathogenic microorganisms (Yuksekdag et al., 2004). In addition to its antibacterial and antifungal activities, kefir reduces cholesterol levels in serum and has antitumor, anti-inflammatory, and immunomodulatory effects due to its content of *Lactobacillus* and *Lactococcus* (Otlés and Cagindi, 2003; Vinderola et al. 2005; Prado et al. 2015). It was also reported that acetic acid, polysaccharides, and other chemicals produced by kefir microbial components, effectively wound healing (Hassan et al. 2012). Several studies have shown the positive effect of using probiotic foods, such as kefir, for treating many gastrointestinal disorders, such as diarrhea, irritable bowel syndrome,

colitis, Crohn's disease, traveler's diarrhea, and chronic constipation (Reid et al. 2003; Heyman 2000; Maeda et al., 2004). In pregnant women, kefir consumption prevents the reproduction of *Streptococcus agalactiae* strains that cause sepsis, pneumonia, and meningitis in newborns (John and Deeseenthum, 2015).

There are several methods for producing kefir, in which traditional and industrial processes are widely used. Industrial kefir can be prepared in high volumes by using a starter culture. No matter what method is used, the most important factor affecting kefir characteristics is the number of microorganisms and the ratio of species in the content, where the microbial composition varies depending on the source of kefir grains, the country of origin, and the starter culture used (Guzel-Seydim, 2005). The probiotic content that should be found in most kefir products is expressed in numerical values with no description of its microbial diversity. This study assesses whether kefir products have desired probiotic microorganism diversity and number, examine whether there is a difference between fruit kefir and plain kefir products in terms of probiotic content, and reveal how much they preserve the probiotic content until the expiration date. Thus, the necessity of including individuals in nutrition programs can be demonstrated with scientific data through the outputs and results to be obtained in this study.

* Corresponding author e-mail: uskudaraylin@gmail.com.

2. Materials and Methods

2.1. Data Collection

This study was supported by Baskent University Research Fund (Project No.DA19/12). This study has examined 9 industrial kefir samples and 1 kefir sample fermented using kefir grains. In this study, we examined 4 different fruit kefir (FK) and 5 different plain kefir (PK). For each type, 2 bottles of kefir were bought simultaneously. To prepare the traditional kefir, Pasteurized cow's milk was used to prepare kefir samples with kefir grains from Ankara University Faculty of Agriculture. A ratio of 1:30 weight/volume was used as grain to milk ratio. After adding kefir grains to milk, kefir samples were produced in a closed container at a temperature of 20–25°C and the fermentation time was 24 h. The second measurement of kefir fermented using the traditional method was performed on the 7th day of fermentation.

2.2. Microbiological Analysis

Kefir samples were transferred to sterile tubes, and pH values were measured by pH meter (Inolab, Germany) immediately after they were opened, and then serial dilutions were prepared. Standard plate count agar (SPCA) (Oxoid, UK), MRS (Merck, Germany), M17 (Merck, Germany), MSE (Biokar, France), Acetobacter agar and Sabouraud dextrose (BD Difco) agar with chloramphenicol (Biokar, France) (SDCA) media were used to determine the number of total aerobic mesophilic bacteria, Lactobacillus, Lactococcus, Leuconostoc, acetic acid bacteria, and yeast, respectively. Acetobacter agar was prepared with 3g/L glycose (Merck, Germany), 10g/L yeast extract (Sigma, Germany), 10g/L calcium carbonate (Aromel, Turkey), and 15g/L agar (BD Bacto, USA). All culture procedures were performed in duplicate.

SPCA was incubated for 48 h at 30°C; M17 agar for 18–24 hours at 30°C in 5% CO₂ atmosphere; MSE agar for 4 days at 22°C; MRS agar for 5 days at 30°C in 5% CO₂atmosphere; and SDCA for 5 days at 22°C. Plates with 30–300 colonies were counted at the end of incubation, and the results were recorded in cfu/ml. The same procedures were applied to the expiration date of each kefir sample.

After counting the plates, five randomized colonies from each counted plate were taken to identify isolates. The Matrix-Assisted Laser Desorption/Ionization Time-of-Flight Mass Spectrometry (MALDI-TOF) (VITEK® MS, Biomerieux, France) was used to identify bacteria using direct transfer method according to the direction of the manufacturer. API 20AUX (Biomerieux, France) and conventional methods were used to identify yeast isolates.

2.3. Statistical Analysis

The Shapiro Wilk and Kolmogorov Smirnov tests were used to check whether the data obtained had a normal distribution. The Mann-Whitney U test was used to compare variables without normal distribution. The paired samples t-test was used to compare the numbers of microorganisms measured at two different times. The Wilcoxon test was used to compare non-normally distributed numerical measurements at 2 different times. The data were evaluated using a statistical package

program (SPSS 22.0, IBM SPSS, USA), and $p < 0.05$ was considered statistically significant.

3. Results

Table 1 shows the total number of aerobic mesophilic organisms in kefir samples, including five plain and four fruit kefir and one fermented using kefir grains. The total number of aerobic mesophilic organisms in fruit kefir samples was between 1.8×10^6 and 3.6×10^8 on the packages' opening date (OD); the number of living organisms of the same samples varied between 5.2×10^4 and 1.5×10^7 on the expiration dates (ED). The total number of aerobic mesophilic organisms in plain kefir samples was between 4.3×10^5 and 2.9×10^8 on the OD; and varied between 4.5×10^4 and 1.9×10^7 on the ED (Table 1).

Table 1. Number of aerobic mesophilic bacteria (cfu/mL) and pH value of kefir samples.

	Total number of aerobic mesophilic bacteria			pH values			
	OD	ED	<i>p</i>	OD	ED	<i>p</i>	
FK	1a	3.6×10^8	1.5×10^7	0.000^{p*}	4.5	4.3	0.068^{β}
	2a	3.6×10^8	1.5×10^7	0.066^{β}	4.6	4.4	0.059^{β}
	3a	1.0×10^7	5.2×10^4	0.043^{p*}	4.5	4.3	$0.039^{\beta*}$
	4a	1.8×10^6	6.2×10^4	0.62^{ϵ}	4.4	4.3	0.10^{ϵ}
PK	1b	2.6×10^8	1.3×10^6	0.999°	4.6	4.4	0.090°
	2b	2.9×10^8	9.9×10^5		4.6	4.4	
	3b	6.0×10^7	4.5×10^4		4.6	4.5	
	4b	3.2×10^8	1.9×10^7		4.6	4.5	
	5b	4.3×10^5	2.6×10^5		4.5	4.3	
TK	1c	2.0×10^9	7.8×10^8		4.6	4.7	

FK: fruit kefir, PK: plain kefir, TK: traditional kefir, OD: first opening date of the packages, ED: expiration dates, $p^{\#}$: Difference between OD and ED, p^{β} : Difference between OD and ED of the same samples, p^{ϵ} : Difference between OD of different samples, p° : Difference between ED of different samples, $*p < 0.05$.

The total number of aerobic mesophilic organisms in the kefir sample fermented with kefir grains was 2×10^9 at the 24th hour of the fermentation but did not change after 24 h and decreased to 7.8×10^8 at the end of the seventh day of fermentation. The mean decrease in the total number of aerobic mesophilic organisms was $\log 1.63 \pm 0.43$ in fruit kefir samples and $\log 1.86 \pm 1.14$ in plain kefir samples.

A statistically significant difference was observed between the packages in terms of the average number of living organisms measured at OD and ED ($p < 0.001$), where the average number was significantly lower at ED than at OD. The average number of living organisms was $7.84 \log_{10}$ cfu/mL (6918309) for OD and $6.21 \log_{10}$ cfu/mL (1621810) for ED. The total number of aerobic mesophilic organisms on OD and ED was compared for fruit and plain kefir groups. Accordingly, there was no statistically significant difference between the counts of living organisms measured at two different times for the FK group produced using the industrial method ($p = 0.066$). However, a statistically significant difference was found for the PK group produced using the industrial method ($p = 0.043$). The average number of living organisms in the PK group was lower at ED than at OD. The FK and PK

groups were compared for both ED and OD, and no statistically significant difference was observed between them ($p=0.623$; $p=0.999$) (Table 1).

The pH values of the samples are given in Table 1. There was no statistically significant difference between the pH values measured at two different measuring times ($p=0.068$). Besides, the intragroup comparisons of pH values at OD and ED were examined for each kefir type (plain and fruit). Accordingly, there was no statistically significant difference between OD and ED's pH values for the FK group ($p=0.059$), but a statistically significant difference was found between the values for the PK group ($p=0.039$).

Table 2 shows the number of *Lactobacillus*, *Lactococcus*, *Leuconostoc*, *Streptococcus*, and yeast isolates in kefir samples, and Table 3 shows the microbial diversity of kefir samples included in the study. Accordingly, there was a statistically significant difference between the two counts (OD and ED) in terms of *Lactobacillus* ($p=0.018$), *Lactococcus* ($p=0.005$), *Leuconostoc* ($p=0.012$), and *Streptococcus* ($p=0.021$), where the average value was lower at ED than OD for all

four bacterial groups. An analysis was conducted to determine the difference between the average values at OD and ED, and intragroup comparisons were evaluated for the FK and PK groups. Accordingly, only in the PK group, there was a statistically significant difference between the numbers of *Lactococcus* at OD and ED ($p=0.043$). The logarithmic reduction of *Lactococcus* in plain kefir samples was found as 1.44 ± 0.53 . Four different FK and PK groups' parameters were compared for both counting times, and no statistically significant difference was found between them ($p>0.05$). Table 3 represents the microbial ingredient of each kefir sample indicates the species distribution. Acetic acid bacteria were found in none of the kefir samples included in the study. Only two industrial kefir samples (1 plain and 1 fruit kefir of same brand mark) had yeast, and Table 2 presents the average yeast numbers. Accordingly, there was no statistically significant difference between the yeast counts at OD and ED ($p>0.05$). The yeast isolates were identified as *Candida kefyr*.

Table 2. The number of each bacterial genus of kefir samples (cfu/mL)

	<i>Lactobacillus</i>			<i>Lactococcus</i>			<i>Leuconostoc</i>			<i>Streptococcus</i>			<i>Candida</i>		
	OD	ED	p	OD	ED	p	OD	ED	p	OD	ED	p	OD	ED	p
FK	1a	0		2.0×10^6	4.0×10^5		1.2×10^6	5.5×10^6		2.8×10^8	6.4×10^6				
	2a	2.4×10^4		1.2×10^6	2.8×10^5		1.2×10^6	5.5×10^6		2.8×10^8	6.4×10^6				
	3a	1.7×10^5		6.4×10^5	1.0×10^4		0	0		6.4×10^5	1.0×10^4		1.4×10^5	5.2×10^3	
	4a	2.4×10^4	0.018^{y*}	2.4×10^4	9.0×10^3	0.005^{y*}	2.4×10^4	1.0×10^3	0.012^{y*}	2.1×10^8	2.4×10^8	0.021^{y*}			0.465^{y*}
PK	1b	0	0.109^b	5.4×10^7	2.3×10^6	0.068^b	1.3×10^8	7.8×10^5	0.102^b	5.4×10^7	2.3×10^6	0.141^b			0.655^b
	2b	1.0×10^8	0.068^b	4.0×10^8	5.5×10^6	0.043^b	5.8×10^5	2.6×10^4	0.068^b	4.0×10^8	3.5×10^6	0.080^b			0.180^b
	3b	1.7×10^7	0.539^e	2.7×10^6	4.1×10^4	0.086^e	0	0	0.902^e	1.2×10^5	5.0×10^4	0.999^e	1.2×10^5	5.9×10^5	
	4b	9.0×10^7	0.268^d	1.5×10^7	4.2×10^6	0.176^d	4.1×10^7	6.0×10^6		1.6×10^7	2.2×10^7				
	5b	2.6×10^5		4.2×10^5	1.0×10^4		3.0×10^5	5.0×10^4		3.1×10^9	1.1×10^8				
TK	1c	0		3.1×10^9	2.0×10^3		2.0×10^4	2.0×10^3		0	0				

FK: fruit kefir, PK: plain kefir, TK: traditional kefir, OD: first opening date of the packages, ED: expire dates, p^y : Difference between OD and ED, p^b : Difference between OD and ED of the same samples, $*p<0.05$

Table 3. Microbial diversity of each kefir samples

Samples	<i>Lactobacillus</i>	<i>Lactococcus</i>	<i>Leuconostoc</i>	<i>Streptococcus</i>	<i>Candida</i>
FK	1a	<i>L. lactis</i>	<i>L. mesenteroides</i> , <i>Leuconostoc spp.</i>	<i>Streptococcus spp.</i>	
	2a	<i>L. paracasei</i> , <i>L. casei</i>	<i>L. lactis</i>	<i>L. mesenteroides</i> , <i>Leuconostoc spp.</i>	<i>Streptococcus spp.</i>
	3a	<i>L. paracasei</i>	<i>L. lactis</i>		<i>Streptococcus spp.</i> , <i>C. kefyr</i>
	4a	<i>L. paracasei</i>	<i>L. lactis</i>	<i>Leuconostoc spp.</i>	<i>Streptococcus spp.</i>
PK	1b	<i>L. lactis</i>	<i>L. mesenteroides</i> , <i>Leuconostoc spp.</i>	<i>Streptococcus spp.</i>	
	2b	<i>L. paracasei</i> , <i>L. casei</i>	<i>L. lactis</i>	<i>L. mesenteroides</i> , <i>Leuconostoc spp.</i>	<i>Streptococcus spp.</i>
	3b	<i>L. paracasei</i>	<i>L. lactis</i>		<i>Streptococcus spp.</i> , <i>C. kefyr</i>
	4b	<i>L. paracasei</i>	<i>L. lactis</i>	<i>Leuconostoc spp.</i>	<i>Streptococcus spp.</i>
5b	<i>L. casei</i>	<i>L. lactis</i>	<i>Leuconostoc spp.</i>	<i>Streptococcus spp.</i>	
TK	1c	<i>L. lactis</i>	<i>Leuconostoc spp.</i>		

FK: fruit kefir, PK: plain kefir, TK: traditional kefir

4. Discussion

Kefir is an old and traditional drink with unique taste and properties. In vitro studies and animal experiments have shown that kefir has health benefits due to its probiotic microorganisms (Farnworth, 2005; Walsh et al.,

2016). As kefir is a fermented beverage produced by bacteria and yeasts, its composition is complex due to the high number and diversity of microorganisms and the variety of possible bioactive compounds produced during fermentation. The changes in the process of kefir production from fermentation to consumption are

remarkable. For example, even the size of kefir grains used in production affects the product profile's pH, viscosity, and microbiological properties (Farnworth, 2003). As an alternative to the traditional method using kefir grains and a fermentation period of 20–24 h, industrial kefir with acceptable kefir flavor and longer shelf life, which are produced using starter with lactic acid bacteria and yeast species isolated from kefir grains, are offered to people in their diet. However, it is an issue of concern in selecting and/or recommending fermented products like kefir for consumption, whether industrial kefir products have probiotic values similar to those of traditional kefir. Therefore, this study quantitatively determined the microbial composition of industrial kefir products offered to the market and traditional kefir samples, both at the dates of purchase and expiration date, and to reveal the microbial diversity of these products. This study also compared the fruit and plain kefir products in terms of their probiotic content and pH values.

Kefir contains lactic acid bacteria (*Lactobacilli*, *Lactococci*, *Leuconostocs*, and *Streptococci*), yeast (*Candida* spp., *Kluyveromyces* spp., *Saccharomyces* spp., *Torulopsis* spp., *Zygosaccharomyces* spp.), and rarely acetic acid bacteria (*Acetobacter* spp.) (De Moreno de LeBlanc et al., 2006; Farnworth, 2005; Güzel-Seydim et al., 2011; Motaghi et al., 1997; Witthuhn et al., 2004). Several studies report the benefits of this product with the rich microbial composition (Cevikbas et al., 1994; Vinderola et al., 2006; Maeda et al., 2004; Urdaneta et al., 2007). In particular, lactic acid bacteria's therapeutic effect like reducing cholesterol level, improving immunity, and reducing gastrointestinal symptoms has been emphasized for many years (Tamai et al., 1996; Perdigon et al., 2001; Alm, 1982; Rosa et al., 2017). In the kefir samples examined in this study, *Lactobacillus paracasei*, *Lactobacillus casei*, *Lactococcus lactis*, *Leuconostoc mesenteroides*, *Leuconostoc* spp, *Streptococcus* sp., and *Candida kefir* were isolated from kefir samples included in the study. Acetic acid bacteria were not isolated in any kefir samples. We can conclude from results that the kefir products examined in this study were found to have enough probiotic variety to constitute the kefir flora.

Several studies have highlighted the microorganism diversity of kefir produced using traditional methods (Oner et al., 2010, Guzel-Seydim et al., 2005; Walsh et al., 2016). However, this study determined relatively fewer microorganism varieties in the kefir samples produced using the traditional method. Note that factors such as milk, type of grain, incubation time, or environmental conditions may have affected kefir products' microbial diversity. Nevertheless, industrial kefir with an average shelf life of 20 days had a microbial variety that could provide the expected benefits of kefir in both measurement times.

One study determined that the number of microorganisms remained constant in the first 15 days of kefir's storage time made from cow milk (Oner et al., 2010). Similarly, Leite et al. (2013) observed no change in the number of lactic acid bacteria and yeasts. However, Irigoyen et al. (2005) observed that the number of *Lactobacillus* and *Lactococcus* decreased in the 2nd week in both series prepared by adding 1% and 5% kefir grains, respectively. In this study, the number of *Lactococcus* decreased in the second measurement of plain kefir

samples ($p < 0.05$). Another similar study found a lower number of *Lactococcus* in the second week of the study (Irigoyen et al. 2005). They found that the counts of yeast and acetic acid bacteria remained constant during cold storage, and the count of LAB decreased in the 7–14 days of storage (Irigoyen et al. 2005). Montanuci et al. (2012) reported that the number of yeasts, acetic acid bacteria, and *Leuconostoc* increased or remained unchanged at the end of the storage period, but the total LAB and *Lactococcus* population decreased by 1 to 2 logs or remained unchanged during the storage. In another study, the LAB number of five commercial Norwegian kefir samples decreased in the first 4 weeks of storage, while the number of yeasts increased during the storage period (Grønnevik et al., 2011). This study found a statistically significant difference between the counts of *Lactobacillus*, *Lactococcus*, *Leuconostoc*, and *Streptococcus* at two different times ($p < 0.05$), where the average value in all four parameters was lower at the end of the expiration date than at the beginning of the production date (Table 2). Despite this numerical decrease, all industrial kefir samples complied with the definition of kefir according to Food Codex in both measurements, which suggests that there is no risk/harm in consuming these products until expiry date.

In this study, the yeast was found only in 2 of the 10 samples, including 1 plain and 1 fruit kefir products of the same trademarks. The number of yeasts increased in only a sample with yeast (Table 2). Loretan et al. (2003) determined the number of yeasts in a home-made kefir sample as 8 log₁₀ cfu/mL but found no yeast in it. Contrary to previous studies, the fact that the yeast was not isolated from the kefir samples produced using the traditional method in this study suggests that the stability of microbial content in kefir produced using the traditional method could not be achieved. Note that different microbial contents can be obtained by changing the conditions such as grain, milk, time, and temperature.

One study, conducted in Ireland, has examined the microbial composition of six kefir samples and found a similarity in terms of *Lactobacillus*, *Lactococcus*, *Leuconostoc*, acetic acid bacteria, and yeast numbers (Rea et al. 1996). Similarly, this study compared fruit and plain kefir samples in terms of the number of lactic acid bacteria at two different times and found no statistically significant difference between them. The products sold in the market were compared with their counterparts at two different times and observed to have similar LAB numbers. In this context, there is no risk for individual preferences to come to the fore in selecting fruit or plain kefir samples. However, sugar additives should be considered in selecting kefir in bodyweight management or in the presence of diseases such as diabetes mellitus, where even simple sugar intake should be taken into consideration.

Leite et al. (2013) found that the pH value of Brazilian kefir decreased in the period from fermentation to the expiration date. Another study has emphasized that the pH value continuously decreases in the cold storage period after fermentation (Guzel-Seydim et al., 2005). Similarly, this study determined that the pH values of industrially produced kefir samples decreased in the storage process but found a statistically significant decrease only in plain kefir samples ($p < 0.05$). The pH values of plain and fruit

kefir samples were compared simultaneously and found to be stable, suggesting no statistically significant difference.

This study has some limitations. Only one kefir sample was prepared by the traditional method with one type of kefir grain, and industrial kefir samples included pasteurized milk of only two brands. Therefore, it will be useful for further studies to examine more than one sample by preparing kefirs with the traditional method using pasteurized milk of different brands and grains. Besides, no standardization has been achieved regarding the supply of industrial products in the market, and there was a possibility that the products were not offered for sale in similar conditions (cold chain compatibility, date of arrival, storage conditions, etc.) before purchase, both of which limited this study. However, as a consumer does not have a chance to follow this chain, the existing conditions can be considered suitable.

Microbiological and chemical changes in the process from kefir production to consumption contribute to its unique taste, creating its own unique flavor. The microbiological properties of kefir vary depending on grain to milk ratio, incubation, or storage conditions. This study found that the number of microorganisms in industrial kefir samples decreased at expiration dates. There was a significant decrease in the number of *Lactococcus* only in plain kefir samples sold in the market. No differences were observed between fruit and plain kefir samples in terms of the number of lactic acid bacteria measured at two different times, and all kefir samples examined had probiotic properties. Therefore, there is no difference in preferring plain or fruit kefir to benefit from these bacteria's positive health effects (on gastrointestinal disorders, metabolic diseases, etc.). However, notably the number of microorganisms was relatively lower at the expiration date. Depending on these results, awareness studies on the dates when kefirs are offered to the market should be conducted. Besides, nutritionists should provide detailed information about label reading when they include kefir in nutrition plans. They should also emphasize that individual differences in the selection of flavored or plain kefir do not affect the benefits expected from kefir. Furthermore, there is a need to increase the number of scientific studies on microbiological changes in fermented products and to share the importance of this issue with consumers.

References

Ahmed Z, Wang Y, Ahmad A, Khan, ST, Nisa M, Ahmad H and Afreen A. 2013. Kefir and health: a contemporary perspective. *Crit Rev Food Sci Nutr.*, **53**: 422-434. doi: 10.1080/10408398.2010.540360.

Alm L. 1982. Effect of fermentation on lactose, glucose, and galactose content in milk and suitability of fermented milk products for lactose intolerant individuals. *J Dairy Sci.*, **65**: 46–352. doi: 10.3168/jds.S0022-0302(82)82198-X.

Cevikbas A, Yemni E, Ezzedenn FW, Yardimici T, Cevikbas U and Stohs SJ. 1994. Antitumoural antibacterial and antifungal activities of kefir and kefir grain. *Phytother Res.*, **8**(2): 78-82. doi: 10.1002/ptr.2650080205.

De Moreno de LeBlanc A, Matar C, Farnworth ER and Perdigon G. 2006. Study of cytokines involved in the prevention of a murine experimental breast cancer by kefir. *Cytokine*, **34**: 1-8. doi:10.1016/j.cyto.2006.03.008.

Farnworth ER. 2005. Kefir a complex probiotic. *Food Sci Technol Bull.: Functional Foods*, **2**: 1–17. doi: 10.1616/1476-2137.13938.

Grønnevik H, Falstad M and Narvhus JA. 2011. Microbiological and chemical properties of Norwegian kefir during storage. *Int Dairy J.*, **21**: 601–606. doi: 10.1016/j.idairyj.2011.01.001.

Guzel-Seydim Z, Wyffels JT, Seydim AC and Greene AK. 2005. Turkish kefir and kefir grains: microbial enumeration and electron microscopic observation. *Int. J. Dairy Technol.*, **58**(1): 25-29. doi:10.1111/j.1471-0307.2005.00177.x

Guzel-Seydim ZB, Kok-Tas T, Greene AK and Seydim AC. 2011. Review: Functional properties of kefir. *Crit Rev Food Sci Nutr.*, **51**: 261–268. doi:10.1080/10408390903579029.

Hassan FH, Golnar R, Mohammad RF, Mitra M and Mitra S. 2012. Evaluation of wound healing activities of kefir products. *Burns*, **38**(5): 719-723. doi: 10.1016/j.burns.2011.12.005.

Heyman M. 2000. Effect of lactic acid bacteria on diarrheal diseases. *J Am Coll Nutr.*, **19**: 137-146. doi: 10.1080/07315724.2000.10718084.

Irigoyen A, Arana I, Castiella M, Torre P and Ibanez FC. 2005. Microbiological, physicochemical, and sensory characteristics of kefir during storage. *Food Chem.*, **90**(4): 613-620. doi: 10.1016/j.foodchem.2004.04.021.

John SM and Deeseenthum S. 2015. Properties and benefits of kefir-A review. *Songklanakarinn J Sci Technol.*, **37**(3), 275-282.

Leite AMO, Leite DCA, Del Aguila EM, Alvares TS, Peixoto RS, Miguel MAL, Silva JT and Paschoalin VMF. 2013. Microbiological and chemical characteristics of Brazilian kefir during fermentation and storage processes. *J Dairy Sci.*, **96**(7): 4149-4159.

Loretan T, Mostert JF and Viljeon BC. 2003. Microbial flora associated with South African house hold kefir. *S Afr J Sci.*, **99**: 92–94.

Maeda H, Mizumoto M, Suzuki K and Tsuji K. 2005. Effects of Kefiran-Feeding on Fecal Cholesterol Excretion, Hepatic Injury and Intestinal Histamine Concentration in Rats. *Biosci and Microflora.*, **24**(2): 35-40. doi: 10.12938/bifidus.24.35.

Maeda H, Zhu X, Omura K, Suzuki S and Kitamura S. 2004. Effects of an exopolysaccharide (kefirin) on lipids, blood pressure, blood glucose, and constipation. *Biofactors*, **22**: 197–200. doi: 10.1002/biof.5520220141.

Montanuci FD, Pimentel TC, Garcia S and Prudencio SH. 2012. Effect of starter culture and inulin addition on microbial viability, texture, and chemical characteristics of whole or skim milk kefir. *Cienc tecnol aliment.*, **32**: 850–861. doi: 10.1590/S0101-20612012005000119.

Motaghi M, Mazaheri M, Moazami N, Farkhondeh A, Fooladi MH and Goltapeh E.M. 1997. Short communication: Kefir production in Iran. *World J Microbiol Biotechnol.*, **13**: 579–581. doi:10.1023/A:1018577728412.

Oner Z, Karahan AG and Cakmakci ML. 2010. Effects of different milk types and starter cultures on kefir. *Gida* **35**: 177–182.

Otles S and Cagindi O. 2003. Kefir: A probiotic dairy-composition, nutritional and therapeutic aspects. *Pakistan J Nutr.*, **2**(2): 54-59. doi: 10.1590/S1517-83822013000200001.

Perdigon G, Nader de Macias E, Alvarez S, Medici M, Oliver G and de Ruiz Holgado AP. 1986. Effect of mixture on *Lactobacillus casei* and *Lactobacillus acidophilus* administered orally on the immune system in mice. *J Food Prot.*, **49**: 986–989. doi: 10.4315/0362-028X-49.12.986.

- Prado MR, Blandón LM, Vandenberghe LP, Rodrigues C, Castro GR, Thomaz-Soccol V and Soccol C.R. 2015. Milk kefir: composition, microbial cultures, biological activities, and related products. *Front Microbiol.*, **6**: 1177. doi: 10.3389/fmicb.2015.01177.
- Rea MC, Lennartsson T, Dillon P, Drinan FD, Reville, Heapes M and Cogan TM. 1996. Irish kefir-like grains: their structure, microbial composition and fermentation kinetics. *J Appl Microbiol.*, **81**(1): 83-94.
- Reid G, Jass J, Sebulsky MT and McCormick JK. 2003. Potential uses of probiotics in clinical practice. *Clin Microbiol Rev.*, **16**: 658-72. doi: 10.1128/CMR.16.4.658-672.2003.
- Rosa DD, Dias MM, Grzeszkowiak ŁM, Reis SA, Conceição LL and Maria do Carmo GP. 2017. Milk kefir: nutritional, microbiological and health benefits. *Nutr Res Rev.*, **30**(1), 82-96.
- Tamai Y, Yoshimitsu N, Watanabe Y, Kuwabara Y and Nagai S. 1996. Effects of milk fermented by culturing with various lactic acid bacteria and a yeast on serum cholesterol level in rats. *J Ferment Bioeng.*, **81**(2): 181-182.
- Urdaneta E, Barrenetxe J, Aranguren P, Irigoyen A, Marzo F and Ibanez FC. 2007. Intestinal beneficial effects of kefir-supplemented diet in rats. *Nutr Res.*, **27**(10): 653-658. doi: 10.1016/j.nutres.2007.08.002.
- Vinderola CG, Duarte J, Thangavel D, Perdigón G, Farnworth E and Matar C. 2005. Immunomodulating capacity of kefir. *J Dairy Res.*, **72**(2): 195-202. doi: 10.1017/S0022029905000828.
- Vinderola CG, Perdigon G, Duarte J, Farnworth E and Matar C. 2006. Effects of kefir fractions on innate immunity. *Immunobiology*, **211**:149–156. doi: 10.1016/j.imbio.2005.08.005.
- Walsh AM, Crispie F, Kilcawley K, O’Sullivan O, O’Sullivan MG, Claesson MJ and Cotter PD. 2016. Microbial succession and flavor production in the fermented dairy beverage kefir. *Msystems* **1**(5): e00052-16.
- Witthuhn RC, Schoeman T and Britz TJ. 2004. Isolation and characterization of the microbial population of different South African kefir grains. *Int. J. Dairy Technol.*, **57**: 33–37. doi:10.1111/j.1471-0307.2004.00126.x.
- Yüksekdağ ZN, Beyatli Y and Aslim B. 2004. Determination of some characteristic coccoid forms of lactic acid bacteria isolated from Turkish kefir with natural probiotic. *LWT-Food Sci Technol.*, **37**(6): 663-667. doi: 10.1016/j.lwt.2004.02.004.

Bacterial strain *Pseudomonas avellanae* 6CH2 with anti-Fusarium activity in mitigation of herbicidal stress in wheat plants

Sergey Chetverikov^{*}, Danil Sharipov, Margarita Bakaeva, Daria Chetverikova, Maksim Timergalin and Timur Rameev

Ufa Institute of biology – Subdivision of the Ufa Federal Research Centre of the Russian Academy of Sciences, Ufa, 450054, Russia

Received: September 26, 2020; Revised: December 2, 2020; Accepted: January 15, 2021

Abstract

The aim of this work was to study a new strain of microorganisms resistant to herbicides of different chemical structure and its impact on herbicidal stress in wheat (*Triticum aestivum* L.). Herbicides with synthetic auxins 2,4-D (2-ethylhexyl ether), dicamba (Octapon, Chistalan) and metsulfuron-methyl (Nanomet) had a phytotoxic (stress) effect on wheat plants, decreasing their weight up to 11%, reducing the amount of chlorophylls up to 10% and increasing the proline quantity by 2.5-5.7 times in leaves. The *Pseudomonas avellanae* strain 6CH2 was isolated from chemical factory soil and had a number of useful properties: suppression of phytopathogenic *Fusarium*, herbicide-resistance, synthesis auxins and molecular nitrogen fixation. Its special features did not disappear under the influence of herbicides. Because of these properties, *P. avellanae* strain 6CH2 had an anti-stress effect on wheat plants if they were jointly treated with herbicides and bacteria. Spraying with herbicides increased the concentration of proline in wheat leaves by 1.7-2.8 times, while bacterial addition made it at least the same as in the control group. Inoculation with bacteria *P. avellanae* strain 6CH2 increased the total chlorophyll amount by 1.19-1.26 times against the background of herbicidal stress. Thus, bacteria *P. avellanae* strain 6CH2 can be used as an anti-stress agent when spraying wheat crops with herbicides.

Keywords: *Pseudomonas*, Wheat, Anti-fungal activity, Anti-stress effect, Chlorophyll, Proline.

1. Introduction

When cultivating agricultural crops, traditionally, great attention is paid to combating weed flora. Along with soil tillage and crop rotations, chemical herbicides are the main methods for controlling unwanted vegetation. They are used more often than other plant protection products (Aktar *et al.*, 2009). Such widespread and intensive use provokes the spread of resistant weeds, which in turn prompts agricultural producers to increase the doses of herbicides and combine several active substances in order to improve the efficacy of chemical herbicides (Zargar *et al.*, 2019). The efforts to control perennial and persistent weeds can also inhibit crop plants (Light *et al.*, 2005; Kumar and Singh, 2010) and results in residual effects next year (Su *et al.*, 2018). The current situation will remain until the next generation of products aiming with a different mechanism of action compared to currently produced herbicides.

Therefore, the search for means to reduce herbicidal stress in agricultural crops becomes relevant. The use of specialized strains of microorganisms for this purpose began to be considered only recently and is reflected in a few publications. Bourahla *et al.* (2018) ascertained the ability of the *Pseudomonas putida* strain to improve physiological and biochemical parameters (chlorophyll, carotenoids, malondialdehyde, enzyme activity) and reduce the manifestations of oxidative stress in durum

wheat seedlings against the background of 10^{-4} M norfluazone in hydroponic culture. *Burkholderia cepacia* strain mitigated toxicity, increased the size, dry matter, the ability to form nodules, the content of nutrients in seeds of chickpea plants, reduced the levels of proline and malondialdehyde if the amount of glyphosate in the soil was 4.332 mg/kg (Shahid and Khan, 2018). Strain *Mesorhizobium* in the presence of cladinophope (up to 1.2 mg/kg of soil) increased biomass, nodule and leghemoglobin content, nutrient uptake, seed yield and grain protein in chickpeas (Ahemad and Khan, 2010b). Quizalafop-p-ethyl- and clodinafop-tolerant *Rhizobium* isolate increased biomass, symbiotic properties, nutrients uptake and seed yield of lentil (Ahemad and Khan, 2010a) and pendimethalin resistant cereals growth stimulating *Azotobacter salinestris* (Chennappa *et al.*, 2018) were also described.

The described bacteria, which can increase plant resistance to herbicidal stress, belong to different genera: *Pseudomonas*, *Rhizobium*, *Mesorhizobium*, *Bacillus*, *Azotobacter*. All of them are rhizosphere or endophytic microorganisms that can actively interact with the plant. The authors of the research note that they have such properties as nitrogen-fixing and phosphatemobilizing activity, synthesis of auxins, exopolysaccharides, 1-aminocyclopropane-1-carboxylate deaminase, and siderophores.

It is believed that bacteria associated with plants can enhance the non-specific stress resistance (including

^{*} Corresponding author e-mail: chelab007@yandex.ru.

resistance to herbicides), inducing universal protective reactions in the plants (Tétard-Jones and Edwards, 2015). Therefore, it is possible to obtain a single strain of microorganisms that favorably affects plants against a wide range of different herbicides. The publications we found do not contain data on whether a single bacterium can increase the plant's resistance to herbicides of different structures or to a combination of two herbicides. Therefore, experimental testing of this possibility is actual.

The aim of our work was to study a new strain of microorganisms resistant to herbicides of different chemical structure and its impact on herbicidal stress in wheat.

Wheat was chosen because of its importance in human nutrition and a lot of publications about toxic reactivity of wheat plants to herbicides (Song *et al.*, 2007, Bezuglova *et al.*, 2019).

The presence of other useful qualities (fixing molecular nitrogen, fighting diseases) would increase the practical and commercial value of these bacteria.

2. Materials and methods

2.1. Microorganism

The organism of interest in this research was the bacterial strain 6CH2, isolated of the soil contaminated with petrochemicals from the territory of an industrial enterprise (Republic of Bashkortostan, Russia). The pure culture was characterized according to its cultural, morphological, physiological, and biochemical characteristics using the well-established procedures (Gerhardt *et al.*, 1981; Garrity *et al.*, 2005).

2.2. Molecular identification of bacteria

Isolation of total DNA was carried out according to the method described in (Wilson *et al.*, 1995). Amplification of the 16S rRNA gene fragment was carried out using bacterial primers 27F (5' AGAGTTTGATC (A / C) TGGCTCAG 3') and 1492R (5' ACGG (C / T) TACCTTGTTACGACTT 3') on a My Cycler amplifier (Bio-Rad Laboratories, USA). Isolation and purification of PCR products was carried out from low-melting agarose using the Wizard PCR Preps reagent kit (Promega, United States) according to the manufacturer's recommendations. Sequencing of the obtained PCR fragments of the 16S rRNA gene was performed using the Big Dye Terminator v. 3.1 kit (Applied Biosystems Inc., USA) on an ABI PRIZM 3730 automated sequencer (Applied Biosystems Inc., USA) according to the manufacturer's instructions supplied.

The search for homologous sequences was carried out using the EzBioCloud databases (<http://www.ezbiocloud.net/eztaxon>). A dendrogram of phylogenetic similarity was constructed in the MEGA version 7 program (<http://www.megasoftware.net>) by the Neighbor-Joining method (Saitou and Nei, 1987) using the Kimura model (Kimura, 1980).

2.3. Antagonism against phytopathogens

Antagonistic potential against phytopathogens was determined during joint cultivation of bacteria and filamentous fungi in Petri dishes (Chetverikov and Loginov, 2009) on Czapek Dox agar medium. Test objects were *Bipolaris sorokiniana* (Sacc.) Shoemaker VKM F-

529, *Fusarium culmorum* (W.G. Smith) Sacc. VKM F-844, *F. gibbosum* Appel et Wollenw VKM F-848, *F. graminearum* Schwabe VKM F-1668, *F. solani* (Mart) Sacc. VKM F-142, *F. oxysporum* Schltdl VKM F-137, *F. nivale* (Fr.) Ces. Ex Sacc. VKM F-3106, *F. semitectum* VKM F - 1938, *F. avenaceum* VKM F - 132, *Alternaria alternate* (Fr.) Keissl. VKM F-3047, *Rhizoctonia solani* J.G. Kuehn VKM F-895. Cultures were obtained from the All-Russian Collection of Microorganisms. The fungi were maintained on Czapek Dox agar.

2.4. Measurement of bacterial nitrogenase activity

The acetylene reduction assay was used as an indicator of nitrogenase activity of strain 6CH2, with ethylene used as a label and measured by gas chromatography (Hardy *et al.*, 1973; Korshunova *et al.*, 2013).

2.5. Measurement of bacterial indolyl-3-acetic acid

The capacity of strain 6CH2 to synthesize indolyl-3-acetic acid (IAA) was measured by immunoenzyme assay was carried out as described (Bakaeva *et al.*, 2020).

2.6. Modeling herbicide stress

For modeling herbicide stress in plants, selective herbicides containing auxin-like substances 2,4-D (2-ethylhexyl ether) - Octapon, 2,4-D (2-ethylhexyl ether) and dicamba (sodium salt) - Chistalan (LLC AHK-AGRO, Russia) and metsulfuron-methyl - Nanomet (LLC Pesticides.ru, Russia) were used. They are designed to destroy perennial, annual dicotyledonous weeds that grow among spring barley, spring and winter wheat (State catalog..., 2020).

2.7. Wheat cultivation and treatments

Plants of soft spring wheat (*Triticum aestivum* L.) cultivar Kinelskaya Yubileinaya were grown in Climate Chamber MLR-352H-PE (PHC Europe BV, Netherlands) in one-liter containers filled with a mixture of sand and black soil in a ratio of 1: 9, at a PAR photon flux density of 190 $\mu\text{mol} \cdot \text{m}^{-2} \cdot \text{s}^{-1}$, 14 -hour photoperiod and temperature 26 ° C. Soil humidity was maintained at 60-80% of the total humidity capacity. On the seventh day after germination, when the third shoot start forming, plants were sprayed with a herbicide, a suspension of bacteria *Pseudomonas avellanae* strain 6CH2, or their mixture: per vessel 0.9 μl Octapon, 0.9 μl Chistalan, 13 μg Nanomet, 5×10^7 CFU of the strain 6CH2 (based on the working concentrations of herbicides taking into account the application rates according to the regulations). According to the regulations for herbicides used, the second or third leaf stage is the earliest period when herbicide treatment is acceptable. Control plants were not sprayed.

Growth and weight characteristics of shoots and roots were determined 14 days after spraying. For each variant of the experiment, 30 plants were grown.

On the third day after the treatment of plants, the content of chlorophyll and proline in the leaves was determined. The content of proline and chlorophyll in the leaves, dry weight of roots and shoots, and shoot length were determined using freshly plucked plant parts.

2.8. Chlorophyll measurement

The chlorophyll content was determined spectrophotometrically on spectrophotometer Selecta UV-

2005 (Selecta, Spain) after extraction with 96% alcohol (Vernon, 1960) and was expressed in mg / g dry weight.

2.9. Proline measurement

The proline content was determined using a ninhydrin reagent, as described previously (Bates *et al.*, 1973), using a calibration curve constructed with standard L-proline («Sigma», United States) and expressed in $\mu\text{g} / \text{g}$ dry weight.

2.10. Statistical analyses

Statistical analyses were performed with descriptive statistics (mean) and two-sample unpaired t-test ($p=0.05$) to determine statistically significant differences ($P < 0.05$) between treatments using MS Excel. Data were expressed as averages \pm confidence interval.

3. Results

The cells of the 6CH2 strain are Gram-negative non-spore-forming mobile rods with 1-4 polar flagella, grow slowly on nutrient agar. When they are cultivated on sucrose media, colonies with a diameter of 2-4 mm, round,

shiny, translucent are formed. The optimum growth temperature is 23-25 ° C. The maximum growth temperature is 35 ° C. The metabolism is respiratory. Bacteria liquefied gelatin, did not reduce nitrates, formed levan, did not hydrolyze starch, did not form indole, and curdled milk poorly. They produced acid during fermentation of dextrose, sucrose, glycerin and formed a blue-green fluorescent pigment, when cultured on King B medium (King *et al.*, 1954).

The sequence (1413 bp) of the 16S rRNA gene from the isolated strain corresponding to 21-1433 positions of the *E. coli* nomenclature was determined and subsequently deposited in GenBank as number MT703877. The bacterial species *Pseudomonas avellanae*, *P. syringae*, *P. cannabina*, and *P. mandelii* were closest to the studied sample. The sequence similarity between strains 6CH2 and *P. avellanae* BPC 631 was 99.15%, and with *P. syringae* KCTC 12500, *P. cannabina* CFBP 2341, and *P. mandelii* NBRC 103147 - 98.94%. To clarify the phylogenetic position of the strain, we compared its nucleotide sequence of the 16S rRNA gene and that of nearby *Pseudomonas* species and constructed a dendrogram (Fig. 1).

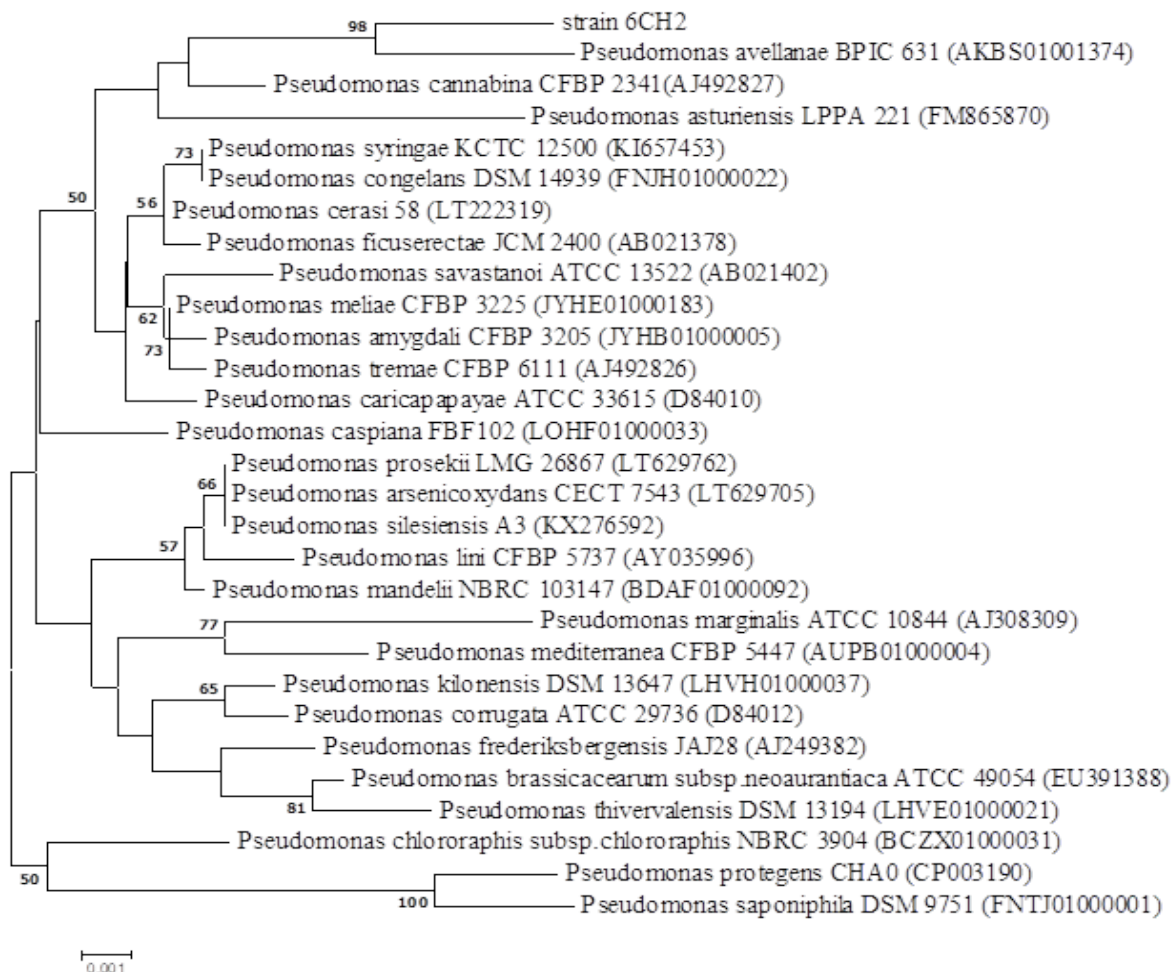


Figure 1. Phylogenetic position of the 6CH2 strain according to the analysis of the nucleotide sequence of the 16S rRNA gene. The scale shows the evolutionary distance corresponding to 1 nucleotide change in every 1000 nucleotides. The numbers show the statistical significance of the branching order determined using the "bootstrap" analysis (the values of the "bootstrap" analysis are shown above 50%). The data obtained was presented in this way to make it possible to identify the studied strain as *Pseudomonas avellanae* 6CH2.

The investigated strain showed antagonism against the spectrum of phytopathogenic *Fusarium* and other phytopathogenic micromycetes (table 1), without exerting much growth suppression of micromycetes from other genera. It was found that the direct interaction of test fungi of the genus *Fusarium* and the strain *P. avellanae* 6CH 2 significantly slowed the formation of mycelium compared to the control without bacteria (the spore germination delay was 24-96 h), and the morphology of the pathogens hyphae was strongly changed.

Table 1. Antagonistic activity of the bacterial strain *Pseudomonas avellanae* 6CH2

Phytopathogenic micromycetes	Diameter of the fungal growth inhibition zone, mm
<i>Fusarium culmorum</i> VKM F - 844	12.0±1.5
<i>F. gibbosum</i> VKM F – 848	16.8±2.0
<i>F. graminearum</i> VKM F – 1668	14.6±1.4
<i>F. nivale</i> VKM F – 3106	10.4±0.5
<i>F. semitectum</i> VKM F – 1938	14.2±1.2
<i>F. solani</i> VKM F – 142	16.2±1.5
<i>F. avenaceum</i> VKM F – 132	20.6±2.2
<i>F. oxysporum</i> VKM F-137	14.4±1.3
<i>Bipolaris sorokiniana</i>	≤5.0
<i>Alternaria alternate</i> VKM F-3047	≤5.0
<i>Rhizoctonia solani</i> VKM F-895	≤5.0

The nitrogen-fixing activity of *P. avellanae* 6CH2 was 19.8 nmol C₂H₄ • h⁻¹ • ml⁻¹. The nitrogenase activity did not decrease under the influence of the studied herbicides in the above-mentioned concentrations.

The herbicide-resistant strain 6CH2 was able to synthesize IAA both when grown in the presence and in the absence of the herbicides. The maximum IAA production was 189 ± 12 ng / ml in the culture liquid without herbicides and did not decrease by more than 10% in their presence.

In our study, treatment of wheat plants with herbicides Nanomet and Chistalan at the stage of emergence of the third leaf resulted in suppression of their growth; shoot (up to 14%) and root weight (up to 18%) (Fig. 2), shoot length (up to 12%) (Fig. 3) were significantly less than in the control group of plants not exposed to the herbicide. The variant with the herbicide Octapone, which slightly stimulated the mass accumulation and shoots growth, stood out from the general paradigm. This synthetic auxin, whose effect on sensitive plants is due to the excessive accumulation of auxins in them and a violation of their distribution between organs (Grossmann, 2007), worked in our case as a weak growth stimulant.

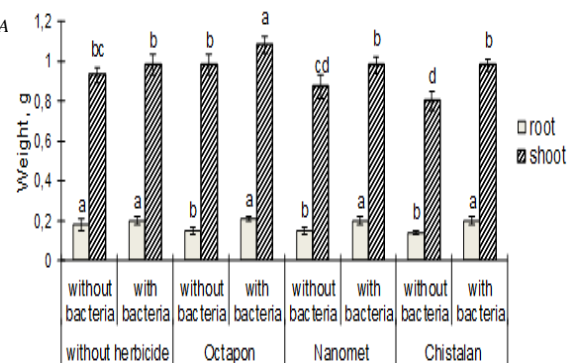


Figure 2. Effect of herbicides and spraying with strain *P. avellanae* 6CH2 on root and shoot weight of wheat measured 14 days after. Mean values ± confidence interval are presented (n=30). Significantly different means of each parameter are marked with different letters (p<0.05)

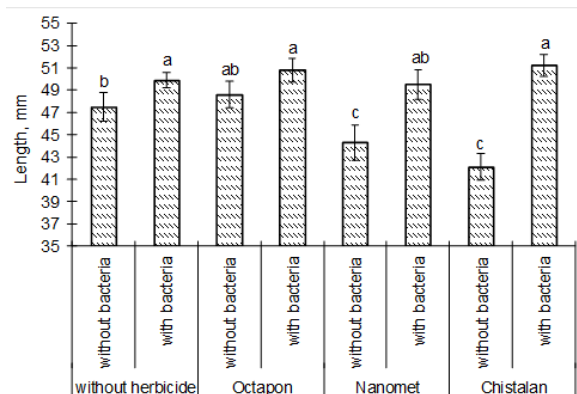


Figure 3. Effect of herbicides and spraying with strain *P. avellanae* 6CH2 on shoot length of wheat measured 17 days after. Mean values ± confidence interval are presented (n=30). Values sharing same letters differ non-significantly (P>0.05)

Another manifestation of the negative effect of all tested herbicides on plants was a decrease in the total content of chlorophylls a and b (up to 10%) (Fig. 4).

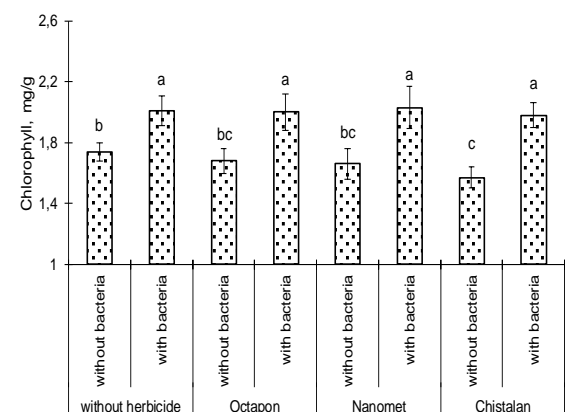


Figure 4. Effect of herbicides and spraying with strain *P. avellanae* 6CH2 on chlorophyll amount in wheat leaves measured 3 days after. Mean values ± confidence interval are presented (n=30). Values sharing same letters differ non-significantly (P>0.05)

Bacterial treatment without herbicides had a positive effect on the length of the shoots and, accordingly, on the chlorophyll amount (an increase of 16%). Taking into account that the chlorophyll content is an important indicator of the state of plants under stress (Ashraf and Harris, 2013), it can be unambiguously asserted that bacterial treatment with the strain 6CH2 was not stressful for the tested plants. The positive effect of bacteria was expressed in mitigation the negative influence of the herbicide on the photosynthetic apparatus. It was reflected in the pigments quantity in plants. In all variants, inoculation with bacteria led to an increase in the total chlorophyll amount against the background of herbicidal stress.

When treating wheat plants with mixtures of bacteria and herbicides, a significant increase in all growth characteristics was observed relative to plants treated with herbicides only. The mass of plant roots reached the control parameters, and the mass and length of shoots exceeded the values in the control group by 8-16%. The increase in the mass of plant can be attributed to the bacterial indolylacetic acid responsible for root system extension and improvement of absorption of mineral elements and water. Bacteria can also increase the nitrogen and phosphorus available to plants, as shown above. The assumption of improved nutrition seems plausible because the increase in plant mass occurred in all variants of the experiment with the bacterium regardless of the herbicide type.

In our experiment, spraying with herbicides increased the concentration of proline in plants (Fig. 5). If the spraying with synthetic auxins increased the concentration of proline by 3 times relative to the control, then in the case of treatment with Nanomet, the increase was more than 500%. The treatment of plants with a mixture of herbicides and bacteria did not initiate the accumulation of proline; its concentration in them practically did not differ from the plants of the control group.

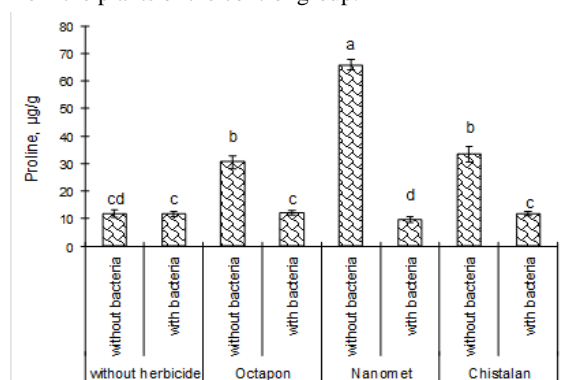


Figure 5. Effect of herbicides and spraying with strain *P. avellanae* 6CH2 on proline amount in wheat leaves measured 3 days after. Mean values \pm confidence interval are presented (n=30). Values sharing same letters differ non-significantly ($P>0.05$)

4. Discussion

The main problem of using herbicides is their negative effect on basic agricultural crops. Herbicide treatment can cause oxidative stress in plants, which is manifested in a slowdown in growth processes and a decrease in productivity in the final (Light *et al.*, 2005). At the same time, herbicidal treatment is the only real way to control weeds on an industrial scale, even taking into account the non-absolute selectivity of herbicides. And reducing the toxic load of herbicides on cultivated plants is a real problem.

Although it is believed that monocotyledonous plants are insensitive to the herbicides based on the synthetic auxin 2,4-D, in the case of their application before the onset of the tillering stage, inhibition of wheat plant growth was noted (Kumar and Singh, 2010). It is also believed that cereals are relatively resistant to the action of sulfonylurea herbicides, but in some cases they do not cope with their toxic effects (Barrett, 1989), not to mention the problems of dicotyledons crops that follow them in the crop rotation.

In our experiment we observed a tendency to slow growth and reduce the amount of chlorophyll in plants treated with certain herbicides. But a more obvious marker of stress was the accumulation of proline in the leaves.

The formation and accumulation of the amino acid proline is a possible physiological reaction of wheat plants to stress caused by toxic substances including herbicides (Sharma and Dietz, 2006). To date, the osmoprotective, antioxidant, signal-regulatory and other functions of this multifunctional amino acid have been established (Szabados and Savoure, 2009; de Carvalho *et al.*, 2013).

Some authors associate the ability of cells to accumulate proline with a selective assessment of drought resistance of plant varieties and species (Chaves and Oliveira, 2004). Taking into account the fact that proline plays an important role in maintaining cellular metabolism and ensures the survival of plants in extreme conditions, we also determined its amount in wheat leaves.

Metsulfuron-methyl most strongly provoked the accumulation of proline in the leaves. We tend to associate this additional increase with the mechanism of action of sulfonylurea class herbicides on plants, the primary target of which is the acetolactate synthase (ALS) enzyme. ALS is the first enzyme on the biosynthetic pathway of branched-chain amino acids (valine, leucine and isoleucine) that functions in fungi, bacteria and higher plants (Brown and Cotterman, 1994). When it is inhibited, an excess of pyruvate and oxaloacetate are formed in plant cells, then they are transformed into α -ketoglutarate (Fig. 6). After that, the metabolic pathway leading to the synthesis of glutamate begins to function as much as possible. It is known that in plants proline can be synthesized in two ways - from glutamate or ornithine. However, it is believed that the synthesis of proline under the influence of stress occurs mainly along the glutamate pathway (Liang *et al.*, 2013). In some plants, more than a hundredfold increase in proline content was noted in response to unfavorable factors.

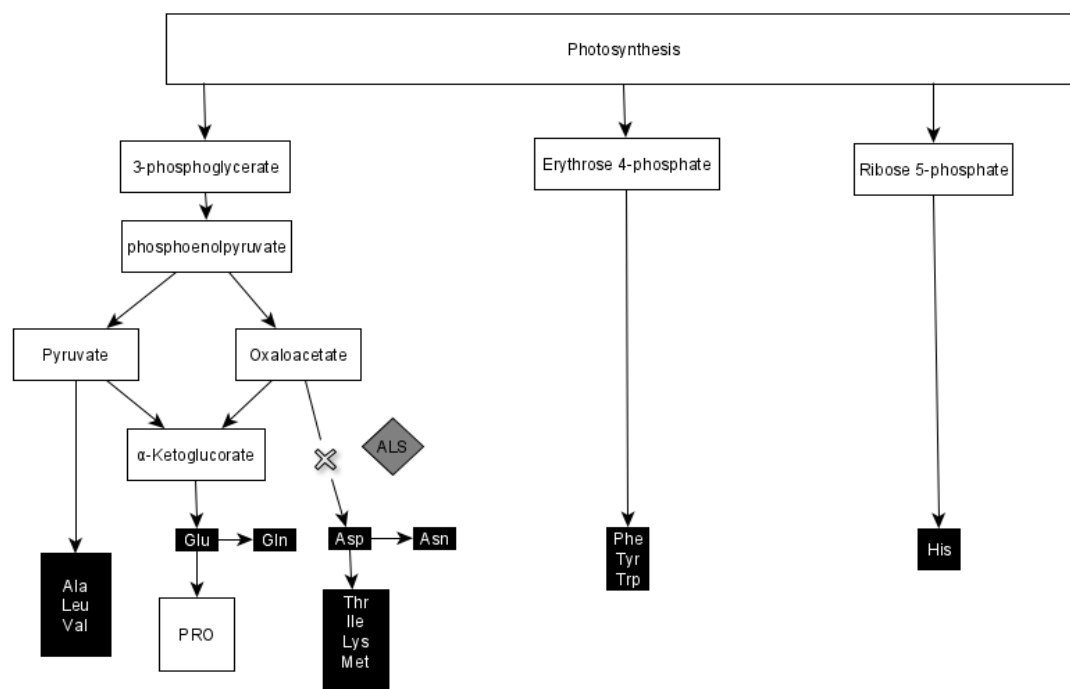


Figure 6. Biosynthesis of amino acids in plants under the influence of herbicides of the sulfonylurea class

We have previously shown that the investigated bacterial strain *P. avellanae* 6CH2 is stable and capable of growing at a high rate in media in the presence of herbicides based on synthetic auxins (Octapone, 10 ml / L; Chistalan, 5 ml / L) and sulfonylureas (Nanomet, 0.05 g / L) (Chetverikov, 2019).

These results show that the studied bacteria exhibited other properties characteristic of PGP - bacteria: antagonism to phytopathogens, synthesis of a nitrogenase complex and phytohormones, including in the presence of herbicides. Inhibition of mycelium growth of *Fusarium* fungi and changes in hyphae morphology are the result of an action of metabolites of the antagonistic bacterial strain. Metabolites of *Bacillus* (Melentyev and Galimzyanova, 1999) and *Azotobacter* (Chetverikov and Loginov, 2009) had a similar impact on *Fusarium*. The nitrogen-fixing activity of *P. avellanae* 6CH2 correlated well with the values characteristic of other known nitrogen fixers (Bakaeva et al., 2020). According to the literature, the amount and activity of nitrogenase in bacteria decreases due to various stresses (Tripathi et al., 2002; Choi and Gal, 1998). Apparently, *P. avellanae* 6CH2 did not experience stress in the presence of herbicides and therefore the activity of nitrogenase did not decrease, while herbicides had almost no effect on nitrogen fixation and inhibition of fungal growth, their presence led to a slight decrease in the indolylacetic acid produced by bacteria. A similar decrease in IAA secretion was observed for the *Burkholderia cepacia* PSBB1 strain resistant to the herbicide glyphosate (Shahid and Khan, 2018).

Auxin synthesis by bacteria may be the main reason for the stimulating effect of PGPB strains on plants. Herbicide-resistant PGPB are likely to secrete auxin sufficiently even when they are applied to herbicide-contaminated soil. High production of auxins, on the contrary, can inhibit plants, as in the case of *Enterobacter* sp. I-3 (Park et al., 2015).

It was shown that PGPBs can change the concentration of auxins not only by their synthesis, but also by their degradation. For example, *P. putida* 1290 can use auxins as a nutrient substrate, thereby eliminating the inhibitory effect of high concentrations of exogenous auxins on the plant (Leveau and Lindow, 2005). Therefore, for achievement of a stimulating effect, the final amount of auxin must correspond to the optimum for the given species under the given environmental conditions.

Thus, will the strain 6CH2, which is tolerant to 2,4-D and sulfonylureas and capable of synthesizing IAA in their presence, mitigate herbicidal stress in plants? Will the amount of phytohormones synthesized by them be sufficient?

The treatment of plants with bacteria 6CH2 in addition to herbicides initiated some positive consequences: stimulation of growth, production of chlorophyll, no need to accumulate a lot of proline. Similar effects from exposure to bacteria were observed under stresses induced by herbicides paraquat (Agafonova et al., 2016), fusilad (Osman et al., 2016), and glyphosate (Shahid and Khan, 2018). In the case of herbicides of the synthetic auxins group, it should be noted that the ability to degrade 2,4-D may be one of the factors providing a favourable effect of PGPR bacteria on plants (Jacobsen, 1997, Han et al., 2015).

In the case of metsulfuron-methyl, an active substance of the herbicide Nanomet, bacteria can mitigate its negative effect on a cultivated plant, taking the impact on itself. First, detoxification can occur by accelerating the biodegradation process. Secondly, the toxicity of the herbicide can be reduced due to its primary binding to the bacterial enzyme ALS, since it has a more convenient conformation.

5. Conclusion

Herbicides with synthetic auxins (Octapone, Chistalan) and sulfonylureas (Nanomet) have a phytotoxic (stress) effect on wheat plants, significantly influencing their growth, reducing the amount of chlorophylls and increasing the proline quantity. The strain *P. avellanae* 6CH2 isolated in this study was capable of suppressing phytopathogenic micromycetes from the genus *Fusarium*, resistant to the herbicides, and also exhibited properties characteristic of PGPB: the synthesis of a nitrogenase complex and phytohormones, including in the presence of herbicides. These properties allowed the *P. avellanae* strain 6CH2 to have an anti-stress effect (to make studied parameters at least the same as in the control group) if wheat plants were jointly treated with herbicides and bacteria.

Acknowledgement

The study was supported by funding for the theme AAAA-A19-119021390081-1 by the Ministry of Science and Higher Education of the Russian Federation

Authors' contributions

SC, DS, MB designed study, performed the statistical analysis, wrote and edited the manuscript. DC, MT, TR, DS carried out the experiments and analyzed the samples.

References

Agafonova NV, Doronina NV and Trotsenko YA. 2016. Enhanced resistance of pea plants to oxidative stress caused by paraquat during colonization by aerobic methylobacteria. *Appl Biochem Microbiol.*, **52**: 199–204.

Ahemad M and Khan MS. 2010a. Growth promotion and protection of lentil (*Lens esculenta*) against herbicide stress by *Rhizobium* species. *Ann Microbiol.*, **60**: 735–745.

Ahemad M and Khan MS. 2010b. Ameliorative effects of *Mesorhizobium* sp. MRC4 on chickpea yield and yield components under different doses of herbicide stress. *Pestic Biochem Physiol.*, **98**: 183–190.

Aktar W, Sengupta D and Chowdhury A. 2009. Impact of pesticides use in agriculture: their benefits and hazards. *Interdiscip Toxicol.*, **2**: 1–12.

Ashraf M and Harris PJC. 2013. Photosynthesis under stressful environments: An overview. *Photosynthetica*, **51**: 163–190.

Bakaeva M, Kuzina E, Vysotskaya L, Kudoyarova G, Arkhipova T, Rafikova G, Chetverikov S, Korshunova T, Chetverikova D and Loginov O. 2020. Capacity of *Pseudomonas* strains to degrade hydrocarbons, produce auxins and maintain plant growth under normal conditions and in the presence of petroleum contaminants. *Plants*, **9**: 379.

Barrett M. 1989. Protection of grass crops from sulfonylurea and imidazolinone toxicity. In: Hatzios KK and Hoagland RE (Eds.), **Crop Safeners for Herbicides, Development, Uses, and Mechanisms of Action**. London: Academic Press, Inc. pp. 195–220.

Bates LS, Waldren RP and Teare IJP. 1973. Rapid determination of free proline for water-stress studies. *Plant Soil*, **39**: 205–207.

Bezuglova OS, Gorovtsov AV, Polienko EA, Zinchenko VE, Grinko AV, Lykhman VA, Dubinina MN and Demidov A. 2019. Effect of humic preparation on winter wheat productivity and

rhizosphere microbial community under herbicide-induced stress. *J Soils Sediments.*, **19**: 2665–2675.

Bourahla M, Djebbar R, Kaci Y and Abrous-Belbachir O. 2018. Alleviation of bleaching herbicide toxicity by PGPR strain isolated from wheat rhizosphere *An Univ Oradea Fascicula Biol*, **XXV**: 74–83.

Brown HM and Cotterman JC. 1994. Recent advances in sulfonylurea herbicides. In: Stetter J. (Eds.), **Herbicides Inhibiting Branched-Chain Amino Acid Biosynthesis. Chemistry of Plant Protection**. Berlin: Springer, Vol 10. pp. 47–81.

de Carvalho K, de Campos MK, Domingues DS, Pereira LF and Vieira LGV. 2013. The accumulation of endogenous proline induces changes in gene expression of several antioxidant enzymes in leaves of transgenic Swingle citrumelo. *Mol Biol Rep*, **40**: 3269–3279.

Chaves MM and Oliveira MM. 2004. Mechanisms underlying plant resilience to water deficits: prospects for water-saving agriculture. *J Exp Bot.*, **55**: 2365–2384.

Chennappa G, Sreenivasa MY and Nagaraja H. 2018. *Azotobacter salinestrus*: a novel pesticide-degrading and prominent biocontrol PGPR bacteria. In: Panpatte D, Jhala Y, Shelat H and Vyas R (Eds.), **Microorganisms for Green Revolution. Microorganisms for Sustainability**. Singapore: Springer, Vol 7. pp. 23–43.

Chetverikov SP. 2019. Selection of anti-stress bacterial agents for the protection of agricultural plants. *Estestvenny'e i tekhnicheskie nauki*, **11**: 81–84.

Chetverikov SP and Loginov ON. 2009. New metabolites of *Azotobacter vinelandii* exhibiting antifungal activity. *Microbiology*, **78**: 428–432.

Choi Y-J and Gal S-W. 1998. Effects of Osmoprotectants on the Growth and Nitrogenase Activity of Rhizobium and Azospirillum under Osmotic Stress. *Appl Biol Chem.*, **41**: 53–59.

Garrity G, Brenner DJ, Krieg NR and Staley JT. 2005. **Bergey's manual of systematic bacteriology**, volume 2: the Proteobacteria, Part B: The Gammaproteobacteria. Springer, New York.

Gerhardt P, Murray RGE, Costilow RN, Nester EW, Wood WA, Krieg NR and Phillips GB. 1981. **Manual of Methods for General Bacteriology**. Amer Soc Microbiol, Washington.

Grossmann K. 2007. Auxin herbicide action: lifting the veil step by step. *Plant Signal Behav.*, **2**: 421–423.

Han L, Zhao D and Li C. 2015. Isolation and 2,4-D-degrading characteristics of *Cupriavidus campinensis* BJ71. *Braz J Microbiol*, **46**: 433–441.

Hardy RWF, Burns RC and Holsten RD. 1973. Application of the acetylene-ethylene assay for measurement of nitrogen fixation. *Soil Biol Biochem.*, **5**: 47–81.

Jacobsen CS. 1997. Plant protection and rhizosphere colonization of barley by seed inoculated herbicide degrading *Burkholderia* (*Pseudomonas*) *cepacia* DBO1 (pRO101) in 2,4-D contaminated soil. *Plant Soil*, **189**: 139–144.

Kimura M. 1980. A simple method for estimating evolutionary rates of base substitutions through comparative studies of nucleotide sequences. *J Mol Evol.*, **16**: 111–120.

King EO, Ward MK and Raney DE. 1954. Two simple media for the demonstration of pyocyanin and fluorescein. *J Lab Clin Med.*, **44**: 301–307.

Korshunova TU, Chetverikov SP, Mukhamatdyarova SR and Loginov ON. 2013. Oxidizing and nitrogenase activity of the bacterium *Ochrobactrum* sp. IB DT-5.3/2. *Izvestiya samarskogo nauchnogo centra rossijskoj akademii nauk*, **3–5**: 1637–1640.

- Kumar S and Singh AK. 2010. A review on herbicide 2, 4-D damage reports in wheat (*Triticum aestivum* L.). *J Chem Pharm Res.*, **2**: 118–124.
- Leveau JH and Lindow SE. 2005. Utilization of the plant hormone indole-3-acetic acid for growth by *Pseudomonas putida* strain 1290. *Appl Environ Microbiol.*, **71**: 2365–2371.
- Liang X, Zhang L, Natarajan SK and Becker DF. 2013. Proline mechanisms of stress survival. *Antioxid Redox Signal*, **19**: 998–1011.
- Light GG, Mahan JR, Roxas VP and Allen RD. 2005. Transgenic cotton (*Gossypium hirsutum* L.) seedlings expressing a tobacco glutathione S-transferase fail to provide improved stress tolerance. *Planta*, **222**: 346–354.
- Melentyev AI and Galimzyanova NF. 1999. Effects of metabolites of antagonistic bacilli on spore germination and development of fungi causing common root rot. *Appl Biochem Microbiol.*, **35**: 353–357.
- Osman MEH, Abo-Shady AM and El-Nagar MMF. 2016. Cyanobacterial *Arthrospira* (*Spirulina platensis*) as safener against harmful effects of fusilade herbicide on faba bean plant. *Re Lincei*, **27**: 455–462.
- Park JM, Radhakrishnan R, Kang SM and Lee IJ. 2015. IAA producing *Enterobacter* sp. I-3 as a potent bio-herbicide candidate for weed control: a special reference with lettuce growth inhibition. *Indian J Microbiol*, **55**: 207–212.
- Saitou N and Nei M. 1987. The neighbor-joining method: a new method for reconstructing phylogenetic trees. *Mol Biol Evol.*, **4**: 406–425.
- Shahid MA and Khan MS. 2018. Glyphosate induced toxicity to chickpea plants and stress alleviation by herbicide tolerant phosphate solubilizing *Burkholderia cepacia* PSBB1 carrying multifarious plant growth promoting activities. *3 Biotech*, **8**(2): 131.
- Sharma SS and Dietz K-J. 2006. The significance of amino acids and amino acid-derived molecules in plant responses and adaptation to heavy metal. *J Exp Bot.*, **57**: 711–726.
- Song NH, Yin XL, Chen GF and Yang H. 2007. Biological responses of wheat (*Triticum aestivum*) plants to the herbicide chlorotoluron in soils. *Chemosphere.*, **68**: 1779–1787.
- MARF. 2020. State catalog of pesticides and agrochemicals allowed for use on the territory of the Russian Federation: part 1. Pesticides. Moscow. <https://mcx.gov.ru>
- Su WC, Sun LL, Ge YH, Wu RH, Hu HL and Lu CT. 2018. The residual effects of bensulfuron-methyl on growth and photosynthesis of soybean and peanut. *Photosynthetica*, **56**: 670–677.
- Szabados L and Saviouré A. 2009. Proline: a multifunctional amino acid. *Trends Plant Sci*, **15**: 89–97.
- Tétard-Jones C and Edwards R. 2016. Potential roles for microbial endophytes in herbicide tolerance in plants. *Pest Manag Sci.*, **72**: 203–209.
- Tripathi A, Nagarajan T, Verma S and Le Rudulier D. 2002. Inhibition of Biosynthesis and Activity of Nitrogenase in *Azospirillum brasilense* Sp7 Under Salinity Stress. *Curr Microbiol.*, **44**: 363–367.
- Vernon LP. 1960. Spectrophotometric determination of chlorophylls and pheophytins in plant extracts. *Anal Chem.*, **32**: 1144–1150.
- Wilson K. 1995. Preparation of genomic DNA from bacteria. In: Ausube FM, Brent LR, Kingston RE, Moore DD, Seidman JG, Smith JA, and Struhl K (Eds.), **Current Protocols in Molecular Biology**, Green Publishing Associates, New York, pp. 241–245.
- Zargar M, Bayat M, Lyashko M and Chauhan B. 2019. Postemergence herbicide applications impact canada thistle control and spring wheat yields. *Agron J*, **111**: 2874–2880.

Evaluation of Quorum-Sensing, Antibiotics Resistance, and Biofilm Formation in Pathogenic Bacteria from the Hospital Environments

Fadhl A. S. Al Gashaa^{1,2,*}, Laith B. Alhuseini³, Shayma M. A. Al Baker¹,
Mohammed F. AL Marjani⁴, Zahraa A. Khadam⁴, Dunya J. Ridha⁵ and Aws H. Al
Rahhal⁵

¹Department of Biology, Al Farabi University College, Baghdad, Iraq; ²Department of Medical Microbiology, College of Science, Ibb University, Yemen; ³Department of Ecology, College of Science, Kufa University, Kufa, Najaf, Iraq; ⁴Department of Biology, College of Science, Mustansiriyah University, Baghdad, Iraq; ⁵Ministry of Higher Education and Scientific Research, Research and Development Department.

Received: October 8, 2020; Revised: December 19, 2020; Accepted: January 7, 2021

Abstract

Background: Multidrug-resistant bacteria (MDR) often contaminate hospital environment and cause serious illnesses. Quorum Sensing (QS) regulates a variety of downstream cellular processes, including antibiotics resistance mechanisms and biofilm formation, and causes harm to the host. This study investigates antibacterial susceptibility and biofilm formation of pathogenic bacteria in hospital environment.

Methods: Hundred bacterial isolates were collected from various environments in the Medical City hospital. The antimicrobial susceptibility technique was evaluated through disk diffusion method. Next, biofilms formation was detected by the microliter plate assay. Finally, PCR was used to analyze the frequency of QS system genes.

Results: Current findings showed that the predominant isolates were *Acinetobacter baumannii* (34%), *Escherichia coli* (30%), *Pseudomonas aeruginosa* (19%), and *Klebsiella pneumonia* (17%). In general, significant resistance was found related to trimethoprim (88%), Augmentin (88%), and cefotaxime (72%). Among all isolates, 62% of sensitivity was related to ciprofloxacin. Biofilm had been formed by 39% of isolates. PCR results showed that the frequency of *lasI* and *rhlI* gene was 70% and 61%, respectively.

Conclusion: Current findings revealed that the hospital environment is a potential reservoir of MDR gram-negative pathogenic bacteria. Thus, we suggest that the health policymakers in Iraq must critically apply the guidelines and recommendations for monitoring the environments in the health sector.

Keywords: Antibiotics Footprint, *Acinetobacter baumannii*, Antibiotics Resistance, Quorum-Sensing, PCR.

1. Introduction

Nosocomial infections, also known as hospital-acquired infections, are serious global health concerns, mainly occurring during hospitalization and causing increased morbidity and mortality (Labi *et al.*, 2019). A hospital environment is undoubtedly a great source of potentially pathogenic bacteria (Bouzada *et al.*, 2010). It can be contaminated with bacterial pathogens, mainly Gram-negative (G-ve) rods such as *Acinetobacter*, *Escherichia coli*, *Pseudomonas spp*, *Klebsiella sp*, *Shigella spp*, *Salmonella spp* and *Proteus spp*, and Gram-positive (G+ve) cocci such as *Staphylococcus aureus*, *Enterococcus* and *Streptococcus*. Environmental surfaces serve as a reservoir for pathogenic bacteria (Otter *et al.*, 2013). The development of nosocomial infection depends on a multifaceted relationship between the rate of contamination of the hospital environment, characteristics of the pathogen, and a susceptible host (Worku *et al.*, 2018). Biofilm bacteria can share nutrients and are

shielded from harmful environmental factors such as desiccation, antibiotics, and the immune system of a host body (Nirwati *et al.*, 2019). In the hospital environment, biofilm-forming bacteria can associate with the ability to survive on surfaces, resist antibiotics, and face host defenses. Therefore, it contributes to cause chronic infections (Ali *et al.*, 2019).

Quorum sensing are used by pathogenic bacteria to regulate gene expression. QS bacteria produce and release signals called autoinducers molecules (Häussler, 2010). Target genes regulate virulence factors, biofilm formation, and broad behaviors including swarming, swimming, twitching motility, and conjugation (Rutherford and Bassler, 2012). The most common QS system in G-ve bacteria involves the production of N-acylated homoserine lactones (AHLs) or autoinducer (Netotea *et al.*, 2009). QS signaling will trigger biofilm formation, resulting in antimicrobial resistance of the pathogens, thereby increasing the therapeutic complexity of bacterial diseases (Jiang *et al.*, 2019). In this regard, the main aim of

* Corresponding author e-mail: fad974@gmail.com.

the current study is to identify the seriousness of a hospital environment as a potential reservoir of multidrug-resistant bacteria capable of infecting patients.

2. Materials and Methods

2.1. Bacterial isolates collection and identification

A total of one hundred bacterial isolates were collected from the surfaces, laundries, health care workers, and medical equipment in Medical City hospital in Baghdad, Iraq. Sterile swabs were used for the collected samples. These isolates were identified by routine biochemical tests and the Vitek 2 system.

2.2. Antibiotic Susceptibility test

The pattern of antibiotic susceptibility was done by the Kirby-Bauer method and interpreted according to the Clinical Laboratory Standard Institute guidelines (CLSI, 2020). Eight antibiotic discs were used in this study, which are Amikacin (AK, 30µg), Augmentin (AMG, 20 µg), Cefotaxime (CTX, 30µg), Cefepime (CPM, 30µg), Ceftriaxone (CTR, 30µg), Ciprofloxacin (CIP, 5µg), Trimethoprim (TMP, 5µg) and Piperacillin (PI, 30µg). These discs are provided from Bioanalyse in Turkey. The duplicated antibiotic was made and quality controlled using *P. aeruginosa* ATCC 27853 (incubated at 37°C for 18-24hr.). Bacterial isolates were resistant to at least three different antimicrobials classes considered as MDR.

2.3. Biofilm formation assay

Microliter Plate Assay was performed for biofilm formation according to the method described by Babapour *et al.* (2016). First, 200 µl of bacterial suspension overnight culture (equivalent to 0.5 McFarland standard) was used to inoculate wells of a flat-bottom 96-well polystyrene microtiter plate (Coastar, USA), containing 180 µl of Brain Heart Infusion broth (Himedia, India) with 2% sucrose. After incubation at 37°C for 24 hours, unattached cells were gently rinsed three times with phosphate buffer saline (pH: 7.2). Then, cells were dried at room temperature for 15 min. Later, adherent bacteria

Table 1: Primers oligonucleotide sequence and molecular size of PCR products

Gene	Oligonucleotide	Product size bp	Reference
<i>lasR</i>	F: 5'-TGCCGATTTTCTGGGAACC-3'	401	(Cotar <i>et al.</i> , 2010)
	R: 5'-CCGCCGAATATTTCCCATATG-3'		
<i>lasI</i>	F: 5'-TCGACGAGATGGAAATCGATG-3'	402	
	R: 5'-GCTCGATGCCGATCTTCAG-3'		
<i>rhlI</i>	F: 5'-CGAATTGCTCTCTGAATCGCT-3'	182	
	R: 5'-GGCTCATGGCGACGATGTA-3'		
<i>rhlR</i>	F: 5'-TCGATTACTACGCCTATGGCG-3'	208	
	R: 5'-TTCCAGAGCATCCGGCTCT-3'		

3. Results

The study aimed to identify the seriousness of hospitals environment as a potential reservoir of multidrug-resistant bacteria and inform policy to monitoring the hospital environment. Thus, the current finding showed that pathogenic bacteria heavily contaminate the surfaces of the hospitals. A hundred of bacterial Gram-negative isolates were identified. Among all isolates, *A. baumannii* were

were fixed with 200 µl of 99% methanol per well. The bacteria attached to the surface were stained with 200 µl of crystal violet (0.1%), rewashed, and extracted with 200 µl ethanol (95%). A total of 200 µl of the mixed solution was analysis using a spectrophotometer at optical density (OD₆₃₀) 630 nm (OPTIMA/Japan). Each assay was performed in triplicate, and the mean OD₆₃₀ value of tested wells was applied to biofilm-forming ability. Uninoculated medium was considered as negative control. Finally, adherence capabilities of the isolates were divided into four categories, and above the mean optical density of the negative control was considered as the cut-off optical density (ODc). Based on the ODs in brain heart infusion broth, the isolates with OD₃₆₀ < ODc₃₆₀ were defined as biofilm non-formers, isolates with (ODc < OD < 2×ODc) were defined as biofilm formers of weak level, isolates with (2×ODc < OD < 4×OD) were defined as moderate level, and isolates with (4×OD < OD) were defined as strong level.

2.4. DNA extraction and gene amplification

DNA was extracted according to the manufacturer's instructions of the DNA extraction kit (WizPrep™ gDNA Mini Kit, South Korea). Polymerase Chain Reaction was performed for amplification of *lasR*, *rhlR*, *lasI* and *rhlI* quorum sensing genes (See Table 1). Each PCR mix (25µl) was composed from 12.5µl of Go Taq® Green master mix, template DNA 5µl, forward & reverse primers (1µl for each), and 5.5µl of deionized nuclease-free water (Promega, USA).

PCR amplification conditions were as follows (all primers): initial denaturation at 95°C/5min followed by 36 cycles of 95°C/30sec, 59°C/1min and 72°C/1min, and a final extension at 72°C/10min (Cotar *et al.*, 2010). The products were analyzed by 1% gel agarose (Promega, USA), containing 0.5 µg/mL of ethidium bromide and visualized under UV light.

34%, *E. coli* were 30%, *P. aeruginosa* were 19%, and *K. pneumoniae* were 17%. The results of the antibiotics susceptibility test showed that most isolates were highly resistant against most antibiotics. The highest resistance was recorded for trimethoprim (88%), Augmentin (88%), and cefotaxime (72%). At the same time, ciprofloxacin (38%) was recorded as the most effective antibiotic against isolates. All isolates showed resistance to the rest of antibiotics ranging between (44%) and (66%), as shown in Figure 1.

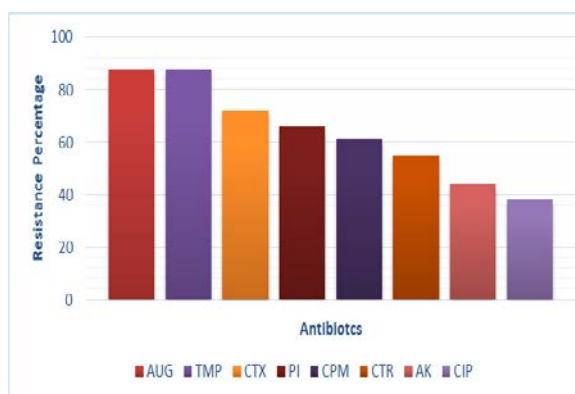


Figure 1: Percentage of Antibiotic susceptibility test of bacterial isolates.

The current obtained results showed that 39% of the environmental isolates were biofilm producers. The results recorded that four isolates with a percentage of 11.76% of *A. baumannii* isolates were strong biofilm producers. At the same time, most isolates were producers with weak biofilm with percentage of 66.66%. In general, *K. pneumoniae* was the high biofilm producers with percentage of 52.94%, followed by *E. coli* (43.33%), *A. baumannii* (35.29%), and *P. aeruginosa* (26.32%) (See Table 2).

Table 2: Adhesion patterns of isolates

Isolates (Number)	Adhesion patterns			Total (%)
	Strong	Moderate	Weak	
<i>A. baumannii</i> (n=34)	4	Non former	8	12 (35.29%)
<i>E. coli</i> (n=30)	Non former	5	8	13 (43.33%)
<i>P. aeruginosa</i> (n=19)	Non former	Non former	5	5 (26.32%)
<i>K. pneumoniae</i> (n=17)	Non former	4	5	9 (52.94%)
Total (%)	4 (10.26%)	9 (23.08%)	26 (66.66%)	39 (39%)

PCR analysis revealed that 70% of isolates carried the *lasI* gene, 61% of isolates carried the *rhII* gene, 57% of isolates had the *lasR* gene, while 4% isolates carried the *rhIR* gene (See Figure 2 and Table 3). *A. baumannii* was the most bacterial isolate harboring quorum sensing genes, *lasI*, *lasR*, and *rhII* genes found in 25 (73.52%) isolates, while 4 (11.76%) of isolates carried *rhIR* gene. The *lasI*, *lasR*, and *rhII* genes were found in all isolates of *P. aeruginosa* (100%) and 13 (76.43%) isolates of *K. pneumoniae*. Finally, 13 (43.33%) *E. coli* isolates contained *lasI* gene, and 4 (13.33%) isolates had *rhII* genes.

Table 3: Number and percentage of QS genes presence in isolates

Genes	<i>lasI</i>	<i>lasR</i>	<i>rhII</i>	<i>rhIR</i>
Isolates				
<i>baumannii</i> (n=34)	25 (73.52%)	25 (73.52%)	25 (73.52%)	4 (11.76%)
<i>P.aeruginosa</i> (n=19)	19 (100%)	19 (100%)	19 (100%)	Negative
<i>K. pneumoniae</i> (n=17)	13 (76.43%)	13 (76.43%)	13 (76.43%)	Negative
<i>E. coli</i> (n=30)	13 (43.33%)	Negative	4 (13.33%)	Negative
Total	70 (70%)	57 (57%)	61 (61%)	4 (4%)

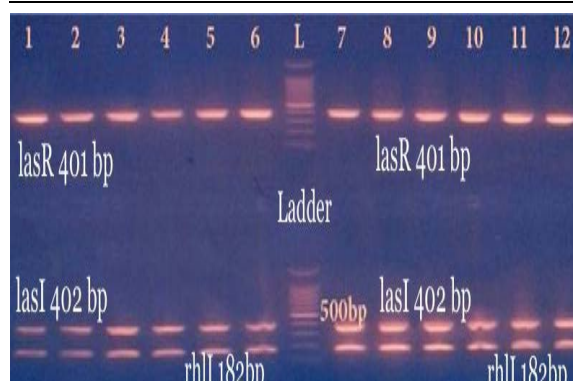


Figure 2: Agarose Gel Electrophoresis (1% agarose, 5-10 V/cm for 50 min) of *lasR*, *lasI*, and *rhII* genes. Lane L 100 bp DNA Ladder, Lanes 1-12 Represent of Isolates Bands.

4. Discussion

Many studies showed that hospitals' environment (surfaces, clothes, air, water, food, waste, and medical devices) harbor bacteria such as *Staphylococcus*, *Enterococcus*, *A. baumannii*, *E. coli*, *P. aeruginosa*, and *K. pneumoniae*. Bacterial isolates in the hospital setting are characterized as MDR, not only for the irrational use of antibiotics but also for the presence of antibiotics residues in fluid effluents (Dougnon *et al.*, 2020). Hospitals' environments are characterized by heavy bacterial density (Ory *et al.*, 2016). Antibiotic resistant bacteria pose a significant threat to public health in the hospitals' environment (Osińska *et al.*, 2017).

Our findings are consistent with several previous studies that showed various components of the hospitals' environment could accommodate many pathogenic bacteria. According to Kim and co-workers, the areas around patients are generally contaminated by bacteria. The bacterial contamination on surfaces was supported by the formation of biofilms and prolonged survival in the environment (Kim *et al.*, 1981, Talon, 1999, Bertrou *et al.*, 2000).

Current findings revealed local isolates carrying one or more QS genes. The Iraqi study conducted by Sallman *et al.* (2018) reported 82.53% isolates carrying *lasI/lasR* and *rhlI/rhlR* genes. Senturk *et al.* (2012) displayed that 77.7%, 88.8%, 66.6%, and 77.7% of isolates were positive for *rhlR*, *rhlI*, *lasR*, and *lasI*, respectively. QS involves generation, release and detection of extracellular signal molecules called auto-inducers (AI). It regulates behaviors requiring cells to synchronize in order to achieve successful results (Paluch *et al.*, 2020). The QS system facilitates the bacterial population to grow and proliferate in an environment with effective intercellular communication (Subhadra *et al.*, 2016). QS-controlled processes include antibiotic resistance, biofilm formation and virulence (Paluch *et al.*, 2020).

Antibiotic-resistant *A. baumannii* has been represented as one of the most problematic hospitals acquired bacteria. *A. baumannii* can colonize in the hospital setting, and constitutes a significant problem in intensive care units (Espinal *et al.*, 2012). *A. baumannii* was isolated from 11% (7/64) of air samples. Hospitals and healthcare settings are regarded as reservoirs of *Pseudomonas spp* isolates, which are a worldwide health concern due to the increasing development of MDR isolate (Alhousseini *et al.*, 2019). Several therapeutic challenges exist with MDR *P. aeruginosa* due to the limit of effective treatment strategies (Aloush *et al.*, 2006). The presence of pathogenic bacteria in the hospitals' environment poses a significant risk to health. *K. pneumonia* is recognized as an urgent threat to human health because of the emergence of MDR isolates associated with hospital outbreaks and hyper-virulent strains associated with severe community-acquired infections (Holt *et al.*, 2015). Recorded hospital settings showed the highest percentage of 23% of extended-spectrum β -lactamase producing *K. pneumonia* (Chaudhry *et al.*, 2019). Biofilm becomes a significant problem in health care (Dewasthale *et al.*, 2018). Bacteria in a biofilm are a protective mechanism to survive in harsh conditions. These bacteria become more resistant to antibiotics; therefore, this biofilm structure represents an important virulence factor (Espinal *et al.*, 2012).

Antibiotics resistance in biofilms is complex and results from contributions of intrinsic, acquired, and adaptive mechanisms. Most notably, biofilm specific features such as the differential expression of multiple gene networks, extracellular matrix, and the metabolic heterogeneity of subpopulations within a biofilm colony are significant contributors to antibiotic resistance (Taylor *et al.*, 2014). *P. aeruginosa* and *K. pneumoniae* exhibited strong biofilm-forming ability on hospital clinical laboratory surfaces. *Klebsiella spp.* was found to persist on dry inanimate surfaces between 2 Hr. to 30 months, while the persistence of *P. aeruginosa* was 6 Hr. to 16 months (Chen *et al.*, 2020).

5. Conclusion

The extracted findings from this study reported the prevalence of gram-negative pathogenic isolates in the hospitals' environment. So, appropriate measures could help reduce pollutants in the hospitals' environment and reduce related serious illnesses. As a result, the current findings recommend the routine screening and disinfection of the hospitals' environment to prevent contamination.

6. Author's contributions

Laith B. Alhousseini, Dunya J. Ridha, Zahraa A. Khadam: Conceptualization, Design of methodology. Mohammed F. Al Marjani: Supervision, Validation. Laith B. Alhousseini, Zahraa A. Khadam: Writing-Reviewing and Editing. Fadhl A. S. Al Gasha, Shayma M. A. Al Baker, Awas H. Al Rahal: Writing and Reviewing the manuscript.

7. Ethical approval

The authors do not see any ethical issues that may arise after the publication of this manuscript.

Acknowledgements

We thank the clinical staff of the Medical City hospital in Baghdad. We are grateful for the useful comments and suggestions from anonymous referees.

Conflict of interest

The authors declare that they have no conflict of interest in the publication.

References

- Alhousseini LB, Maleki A, Kouhsari E, Ghafourian S, Mahmoudi M and Al Marjani MF. 2019. Evaluation of type II toxin-antitoxin systems, antibiotic resistance, and biofilm production in clinical MDR *Pseudomonas aeruginosa* isolates in Iraq. *Gene Reports*, **17**: 100546.
- Ali FS, Authman SH and Al-Marjani MF. 2019. Imipenem Resistance and Biofilm Formation In *Klebsiella pneumoniae* from some Hospitals in Baghdad City. *J Pharm Sci Res.*, **11**: 233–238.
- Aloush V, Navon-Venezia S, Seigman-Igra Y, Cabili S and Carmeli Y. 2006. Multidrug-resistant *Pseudomonas aeruginosa*: risk factors and clinical impact. *Antimicrob Agents Chemother.*, **50**: 43–48.
- Babapour E, Haddadi A, Mirnejad R, Angaji S and Amirmozafari N. 2016. Biofilm formation in clinical isolates of nosocomial *Acinetobacter baumannii* and its relationship with multidrug resistance. *Asian Pac J Trop Biomed.*, **6**: 528–533.
- Bertrou A, Chapuis C and Hajjar J. 2000. Relations entre contamination et environnement hospitalier. *Hygiènes (Lyon)*, **8** (3): 143–146.
- Bouzada ML, Silva VL, Moreira FA, Silva GA and Diniz CG. 2010. Antimicrobial resistance and disinfectants susceptibility of persistent bacteria in a tertiary care hospital. *J Microbiol Antimicrob.*, **2**: 105–112.
- Chaudhry TH, Aslam B, Arshad MI, Nawaz Z and Waseem M. 2019. Occurrence of ESBL-producing *Klebsiella pneumoniae* in hospital settings and waste. *Pak J Pharm Sci.*, **32**(2):773-778.
- Clinical and Laboratory Standards Institute. 2020. Performance standards for antimicrobial susceptibility testing, 30th ed CLSI supplement M100 *CLSI.*, Wayne, PA.
- Cotar AI, Chifiriuc MC, Dinu S, Pelinescu D, Banu O and Lazăr V. 2010. Quantitative real-time PCR study of the influence of probiotic culture soluble fraction on the expression of *pseudomonas aeruginosa* quorum sensing genes. *J Arc Microbiol Immunol.*, **69**(4):213-223.
- Dewasthale S, Mani I and Vasdev K. 2018. Microbial biofilm: current challenges in health care industry. *J Appl Biotechnol Bioeng.*, **5**: 156–160.

- Dougnon VT, Koudokpon H, Chabi Y, Fabiyi K, Legba B, Dougnon j and Baba-Moussa L. 2020. Infection Risks and Antimicrobial Resistance in Tertiary Hospitals in Benin: Study Cases of Sakété-Ifangni and Menontin Hospitals. *Int J Infect.*, **7(1)**:e99649.
- Espinal P, Marti S and Vila J. 2012. Effect of biofilm formation on the survival of *Acinetobacter baumannii* on dry surfaces. *J Hosp Infect.*, **80(1)**: 56–60.
- Häussler S. 2010. Multicellular signalling and growth of *Pseudomonas aeruginosa*. *Int J Med Microbiol.*, **300(8)**: 544-548.
- Holt KE, Wertheim H, Zadoks RN, Baker S and *et al.* 2015. Genomic analysis of diversity, population structure, virulence, and antimicrobial resistance in *Klebsiella pneumoniae*, an urgent threat to public health. *Proc Natl Acad Sci.*, **112**: E3574–E3581.
- Jiang Q, Chen J, Yang C, Yin Y and Yao K. 2019. Quorum sensing: a prospective therapeutic target for bacterial diseases. *Biomed Res Int.*, **7**:1-15.
- Kim KH, Fekety R, Batts DH, Brown D, Cudmore M, Silva J and Waters D. 1981. Isolation of *Clostridium difficile* from the environment and contacts of patients with antibiotic-associated colitis. *J Infect Dis.*, **143(1)**: 42–50.
- Labi, AK, Obeng-Nkrumah N, Owusu E, Bjerrum S and *et al.* 2019. Multi-centre point-prevalence survey of hospital-acquired infections in Ghana. *J Hosp Infect.*, **101(1)**: 60–68.
- Chen Lh, Li Y, Qi Y and *et al.* 2020. Evaluation of a pulsed xenon ultraviolet light device for reduction of pathogens with biofilm-forming ability and impact on environmental bioburden in clinical laboratories. *Photodiagnosis Photodyn Ther.*, **29**: 101544.
- Netotea S, Bertani I, Steindler L, Kerényi A, Venturi V and Pongor S. 2009. A simple model for the early events of quorum sensing in *Pseudomonas aeruginosa*: modeling bacterial swarming as the movement of an "activation zone". *Biol Direct.*, **4(1)**: 1–16.
- Nirwati H, Sinanjung K, Fahrnunisa F and *et al.* 2019. Biofilm formation and antibiotic resistance of *Klebsiella pneumoniae* isolated from clinical samples in a tertiary care hospital, Klaten, Indonesia. *BMC proceedings.*, **13(11)**: 1–8.
- Ory j, Bricheux G, Togola A, Bonnet JL, Donnadiou-Bernard F, Nakusi L, Forestier Ch and Traore O. 2016. Ciprofloxacin residue and antibiotic-resistant biofilm bacteria in hospital effluent. *Environ Pollut.*, **214**: 635–645.
- Osińska A, Korzeniewska E, Harnisz M and Niestępski S. 2017. The prevalence and characterization of antibiotic-resistant and virulent *Escherichia coli* strains in the municipal wastewater system and their environmental fate. *Sci Total Environ.*, **577**: 367–375.
- Otter JA, Yezli S, Salkeld JA and French GL. 2013. Evidence that contaminated surfaces contribute to the transmission of hospital pathogens and an overview of strategies to address contaminated surfaces in hospital settings. *Am J Infect Control.*, **41(5)**: S6–S11.
- Paluch E, Rewak-Soroczyńska J, Jędrusik I, Mazurkiewicz E and Jermakow K. 2020. Prevention of biofilm formation by quorum quenching. *Appl Microbiol Biotechnol.*, **104**: 1871–1881.
- Rutherford ST and Bassler BL. (2012). Bacterial quorum sensing: its role in virulence and possibilities for its control. *Cold Spr Harbor perspectives med.*, **2(11)**: a012427.
- Sallman R, Hussein S and Ali M. 2018. ERIC- PCR Typing, RAPD-PCR Fingerprinting and Quorum Sensing Gene Analysis of *Pseudomonas aeruginosa* Isolated from Different Clinical Sources. *Al-Mustansiriyah J Sci.*, **29(2)**: 50-62.
- Senturk S, Ulusoy S, Boşgelmez-Tinaz G and Yagci A. 2012. Quorum sensing and virulence of *Pseudomonas aeruginosa* during urinary tract infections. *J Infec Develop Count.*, **6(06)**: 501-507.
- Subhadra B, Oh MH and Choi CH. 2016. Quorum sensing in *Acinetobacter*: with special emphasis on antibiotic resistance, biofilm formation and quorum quenching. *AIMS Microbiol.*, **2(1)**: 27-41.
- Talon D. 1999. The role of the hospital environment in the epidemiology of multi-resistant bacteria. *J Hosp Infect.*, **43(1)**: 13-17.
- Taylor PK, Yeung AT and Hancock RE. 2014. Antibiotic resistance in *Pseudomonas aeruginosa* biofilms: towards the development of novel anti-biofilm therapies. *J. Biotechnol.*, **191**: 121–130.
- Worku T, Derseh D and Kumalo A. 2018. Bacterial profile and antimicrobial susceptibility pattern of the isolates from stethoscope, thermometer, and inanimate surfaces of Mizan-Tepi University Teaching Hospital, Southwest Ethiopia. *Int J Microbiol.*, **2018**: ID 9824251, 7 pages.

Antioxidant and Apoptotic Effect of *Muscari muscarimi*, an Endemic Geophyte Species from Turkey

Cennet Ozay^{1,*}, Ege Riza Karagur², Ramazan Mammadov³ and Hakan Akca²

¹Izmir Katip Celebi University, Faculty of Pharmacy, Department of Basic Pharmaceutical Sciences, Izmir 35620, Turkey; ²Pamukkale University, Faculty of Medicine, Department of Medical Genetics, Denizli 20070, Turkey; ³Muğla Sıtkı Koçman University, Faculty of Science, Department of Molecular Biology and Genetics, Muğla 48121, Turkey

Received: October 16, 2020; Revised: January 19, 2021; Accepted: January 28, 2021

Abstract

Muscari muscarimi Medik., which is an endangered and endemic geophyte species of Turkey, was studied for antioxidant, cytotoxic and apoptotic potentials. The antioxidant effect of the extracts (ethanol and methanol) provided from the flower and bulbs of *M. muscarimi* was tested through the antioxidant potency by phosphomolybdenum assay, the reducing power assay, metal chelating ability, nitric oxide scavenging and ABTS radical cation scavenging capability methods. Also, total flavonoid and saponin content of the extracts was specified. Cytotoxic activity of the extracts was assessed and screened against human MCF-7, HeLa and H1299 cancer cells. Terminal transferase dUTP nick end-labeling (TUNEL) assay was applied to cancer cells for the determination of the late apoptotic changes. Antioxidant potencies in bulb extracts were observed to be lower than the flower extracts. However, the cytotoxicity and TUNEL assay revealed that the bulb extracts exhibited more marked anticancer activity against H1299 cell line than the other cell lines. Based on the in vitro data, *M. muscarimi* warrants further studies to isolate novel compounds for chemotherapeutic use.

Keywords: Antioxidant activity, Apoptosis, Cancer cell lines, *Muscari muscarimi*, Turkey

1. Introduction

The use of plants as medicines has a history as old as mankind. Traditional medicinal plants have been used to cure several diseases for thousands of years in different parts of the World (Adebayo & Krettli, 2011). Turkey is one of the most prominent floristic regions on the earth due to its geologic, topographic and climatic features. Floristic studies have shown that Turkey houses about 12000 plant taxa on its soils and more than 3000 taxa among them are endemic (Hoekstra *et al.*, 2005). Geophytes are a considerable component of this generous biodiversity and include a lot of significant endangered and endemic species such as *Muscari muscarimi* Medik. The genus *Muscari* Mill. was formerly classified in the family Liliaceae but recently has been reclassified in the family Asparagaceae (Mulholland *et al.*, 2013). The total number of *Muscari* species recorded in Turkish flora is approximately 39, and 24 of them (61.5%) are endemic (Eker, 2019). *M. muscarimi* is a perennial bulbous plant known as 'misk sümbülü', growing in south-west Turkey. This endemic species is most fragrant species in the genus *Muscari* and has high ornamental potential. It bears fascinating dirty bluish-gray flowers that bloom between March and May each year. The indigenous populations of *M. muscarimi*, is critically affected by enhanced environmental impurity and urbanization (Ozel *et al.*, 2015). It has been used in the folk medicine in Turkey. In addition to this, it has also been used as ornamental plants

in gardens, dye and as food for animals and humans (Oztas *et al.*, 2018). Some species of *Muscari* have been utilized in conventional medicine as hypoglycemic, diuretic, antirheumatic, antiverruca, antiallergic and expectorant (Kayıran & Özkan, 2017, Loizzo *et al.*, 2010). Different investigations have also been notified to the antioxidant, antimicrobial and anticancer effects of *Muscari* (Mammadov *et al.*, 2012, Mammadov *et al.*, 2016, Eroğlu Özkan *et al.*, 2018).

Antioxidants preserve the cell constituents towards oxidative loss caused by free radicals. Phenolic compounds, alkaloids, terpenoids and other secondary metabolites present in plants are superb in antioxidative effects. Researchers have found out that many of these antioxidant components have anticancer, antiinflammatory, antimutagenic, antimicrobial and antiviral potentials (Shahidi & Ambigaipalan, 2015). *Muscari* Mill. contains different phytochemicals with biological activities including homoisoflavonoids, glycosides and water-soluble polysaccharides (Urbancikova *et al.*, 2002, Adinolfi *et al.*, 1985). Lanosterol and tetranorlanosterol glycosides from *Muscari paradoxum* (bulbs) were assessed for their cytotoxic effect on HSC-2 cancer cells. Even though the tetranorlanostane glycosides did not display any cytotoxicity on HSC-2 cells, the lanostane glycosides exhibited high cytotoxic activity (Ori *et al.*, 2003). It was reported that homoisoflavonoid compounds isolated from *M. neglectum* had antiinflammatory, estrogenic, antiestrogenic, anticancer and angioprotective bioactivities (Lim, 2014).

* Corresponding author e-mail: cennet.ozay@ikcu.edu.tr.

Cancer is a fatal universal illness of these times and a crucial obstacle in the ever-increasing lifetime of affected inhabitants (Bray *et al.*, 2018). Despite a general choice for cancer therapy, chemotherapy is restricted by drug resistance and noxious adverse effects (Hanahan & Weinberg, 2011). Natural products can inhibit cancer and restrain tumor growth via cell fate pathways containing apoptosis (Fulda, 2010). Cancer cells are invulnerable to apoptosis owing to the activation of anti-apoptotic proteins or suppression of pro-apoptotic proteins (Pandey *et al.*, 2016). In recent times, a lot of plant extracts or their isolated compounds have been evaluated for apoptotic effect, and several mechanisms of actions have been proposed for their toxicity against cancer cells. Hence, in this study, *M. muscarimi*, which is an endemic and endangered species, was assessed for cytotoxicity and possible apoptotic ability taking into consideration that there has been no paper about such activities previously. The antioxidant activity of *M. muscarimi* was investigated through mainly five methods, and its total flavonoid and saponin content was also determined.

2. Materials and Methods

2.1. Plant material and extraction

Approximately, 250 g of *M. muscarimi* were picked up in May 2013 from Antalya (900 m), located in the southern part of Turkey and identified by (Voucher No: RM1001) Dr. Ramazan Mammadov, Muğla Sıtkı Koçman University, Turkey. The plant was divided into two parts as bulb and flowers and dried in shade at room temperature. The pulverised plant parts were separately subjected to solvent extraction in a shaker water bath with methanol and ethanol at 48-50°C for 6h. The extraction was repeated twice at the same condition. Then solvents were removed with a rotary evaporator (IKA RV, Germany), samples were lyophilised (Labconco FreeZone, USA). The crude samples were kept at -20°C until needed (Ozay & Mammadov, 2017).

2.2. Total flavonoid and saponin contents

The total amounts of flavonoid and saponin substances of the plant extracts were detected by using the aluminum chloride (Moreno *et al.*, 2000) and vanillin-sulphuric acid (Hiai *et al.*, 1976) colorimetric methods, respectively. These substances were expressed as quercetin (mg QEs/g) and quillaja (mg QAEs/g) equivalents, respectively.

2.3. Antioxidant activity assays

2.3.1. Total antioxidant capacity (TAC)

The phosphomolybdenum method was used to evaluate the TAC of the extracts. To keep it short, different extract solutions were mixed with the reagent solution and incubated at 95°C for 90 min. The absorbance values were determined at a wavelength of 695 nm (Prieto *et al.*, 1999). TAC is denoted as ascorbic acid (mg AEs/g) equivalents.

2.3.2. Ferric reducing antioxidant power (FRAP) assay

FRAP assay was applied as defined by Zengin *et al.*, (2015). with small modifications. Extracts solutions were added to FRAP reagent which was mixed in advance. After measuring the absorbances at 593 nm, FRAP potential is denoted as Trolox (mg TEs/g extract) equivalents.

2.3.3. Metal chelating activity

Extracts solutions at different concentrations were added to FeCl₂. The reaction that started directly after adding ferrozine was read at 562 nm after being left for 10 min left at 25°C. Metal chelating effect is denoted as EDTA (mg EDTAEs/g extract) equivalents (Zengin *et al.*, 2015).

2.3.4. ABTS radical scavenging activity

The scavenging activity towards ABTS (2,2 azino-bis (3-ethylbenzothiazoloine-6-sulfonic acid)) radical was analyzed as described by Re *et al.*, (1999) with slight modifications. Freshly prepared and diluted ABTS solution was joined in the extracts of *M. muscarimi* (20-1000 µg/mL), and the absorbances were read after 30 min at 734 nm. The outcomes were indicated as IC₅₀.

2.3.5. Nitric oxide (NO) scavenging activity

NO was produced from sodium nitroprusside (SNP) which read as defined by Balakrishnan *et al.*, (2009) in the Griess reaction. SNP (5mM) in PBS was incubated with several concentrations (20-1000 µg/ml) of the extracts, and the tubes were kept waiting for 3 hours at 25°C. The absorbance value was determined at 546 nm wavelength. Ascorbic acid was employed as an antioxidant standard. The results were indicated as IC₅₀.

2.4. Cytotoxicity assay

HeLa (cervix adenocarcinoma), MCF-7 (breast adenocarcinoma) and H1299 (non-small cell lung adenocarcinoma) human cancer cell lines were employed in this research. The cells were cultured in RPMI 1640 medium in a CO₂ incubator. 24 hours incubation after seeding into 96-well plates (2×10³ cells/well), the medium was removed from the well leaving the adherent cells and cells were applied with extract for 72 hours in the range of 25-1000 µg/mL. After time was up, cell viability was determined by using CytotoxGlo kit (Promega, USA), in accordance with the manufacturer's instructions. The percentage of cell viability was calculated relative to control cells. A plot of cell viability (%) against concentration was created, and the concentration of the plant extract that decreased cell viability by 50% (IC₅₀) was calculated.

2.5. TUNEL assay

The apoptotic effects of *M. muscarimi* bulb extracts in HeLa, MCF-7 and H1299 cells were evaluated using the TUNEL assay. The cells were treated with IC₅₀ values of each extract for 24 h at 37°C. To determine cell death, the *In Situ* Cell Death Detection Kit (Millipore, USA) was used in accordance with the manufacturer's instructions. The TUNEL-stained apoptotic cells were visualized by use of a microscope and then counted. The data were expressed as a percentage of the area of TUNEL-positive cells in 10 random fields.

2.6. Statistical analysis

Statistical analysis was performed using the software SPSS version 22.0 program. Statistical significance was determined using the one-way ANOVA. Multiple group comparisons were analyzed with Tukey's multiple comparison test. Data were expressed as mean ± standard error of three separate experiments. *p* value of < 0.05 was considered statistically significant.

3. Results

3.1. Antioxidant activity

Antioxidant activity of the bulb and flowers of *M. muscarimi* was assayed by using FRAP, ABTS, NO, phosphomolybdenum and metal chelating assays. Also, total amounts of flavonoid and saponin substances of the extracts were calculated by using the aluminum chloride and vanillin-sulphuric acid assays, respectively. The outcomes of all these assays are presented in Tables 1 and 2. According to the data that were obtained, the highest total flavonoid content was found for the methanolic flower extract as 27.22 mg QEs/g, while the highest total saponin content was detected for the methanolic bulb extract as 140.41 mg QAEs/g ($p < 0.05$) (Table 1). Flower methanolic extract had the highest ABTS (IC_{50} value=52.16 μ g/ml) and NO (IC_{50} value=64.35 μ g/ml) radical scavenging activities ($p < 0.05$) followed by the flower ethanolic extract (Table 2). Likewise, the highest results of the FRAP, phosphomolybdenum and metal chelating assays for *M. muscarimi* were determined in the flower methanolic extract as 77.53 mg TEs/g, 62.05 mg AEs/g and 24.10 mg EDTAEs/g extract, respectively.

Table 1. Total antioxidant capacity, total flavonoid and saponin contents of *M. muscarimi* extracts (mean \pm SE).

Extracts	TFC	TSC	TAC
BE	19.35 \pm 0.45 ^b	134.01 \pm 4.12 ^a	44.33 \pm 2.27 ^b
BM	15.33 \pm 0.63 ^b	140.41 \pm 4.35 ^a	47.24 \pm 2.41 ^b
FE	23.12 \pm 0.71 ^a	110.63 \pm 3.06 ^c	58.32 \pm 2.65 ^a
FM	27.22 \pm 0.75 ^a	128.17 \pm 3.52 ^b	62.05 \pm 2.73 ^a

TFC (Total flavonoid content): quercetin equivalents (mg QEs/g). TSC (Total saponin content): quillaja equivalents (mg QEs/g). TAC (Total antioxidant capacity): ascorbic acid equivalents (mg AEs/g). BM/FM: Bulb/Flower Methanol, BE/FE: Bulb/Flower Ethanol. Different letters in the same column indicate a significant difference ($p < 0.05$)

Table 2. Antioxidant activities of *M. muscarimi* extracts (mean \pm SE).

Extracts	ABTS (IC_{50} μ g/mL)	NO (IC_{50} μ g/mL)	FRAP assay (mg TEs/g)	Metal chelating activity (mg EDTAEs/g)
BE	63.29 \pm 1.24 ^b	76.14 \pm 1.55 ^b	58.24 \pm 0.30 ^c	12.16 \pm 0.04 ^b
BM	68.70 \pm 1.38 ^a	81.42 \pm 1.67 ^a	62.48 \pm 0.33 ^c	14.03 \pm 0.07 ^b
FE	55.01 \pm 0.17 ^c	72.21 \pm 1.01 ^b	71.02 \pm 1.54 ^b	17.85 \pm 0.15 ^b
FM	52.16 \pm 0.12 ^c	64.35 \pm 0.56 ^c	77.53 \pm 1.63 ^a	24.10 \pm 0.26 ^a
Ascorbic acid	08.11 \pm 0.03 ^d	19.02 \pm 0.05 ^d	nt	nt

BM/FM: Bulb/Flower Methanol; BE/FE: Bulb/Flower Ethanol, TEs: Trolox equivalents, EDTAEs: EDTA equivalents, nt: no tested. Different letters in the same column indicate a significant difference ($p < 0.05$)

3.2. Cytotoxic activity and TUNEL assay

To evaluate the cytotoxic activity of the *M. muscarimi* bulb extracts at several concentrations (25-1000 μ g/mL) towards MCF-7, HeLa and H1299 cancer cell lines for 72 h, CytotoxGlo assay was carried out. A decrease in viability in cancer cells was observed in a concentration-dependent manner ($p < 0.05$) (Fig. 1 and 2). The IC_{50}

values (μ g/mL) of ethanolic and methanolic bulb extracts in different cancer cell lines were tabulated (Table 3). Methanolic bulb extracts were found to have lower IC_{50} values in all cancer cells than ethanolic extracts. The IC_{50} values for the methanolic extract were 90.43, 140.13 and 58.20 μ g/mL on MCF-7, HeLa and H1299 cells, respectively. The apoptosis-inducing potential of *M. muscarimi* bulb extract was evaluated in the cancer cell lines using the TUNEL assay after treatment with the extracts at their IC_{50} doses for 24 h. A remarkable rise in apoptotic cells was noticed in the H1299 cells treated with methanolic bulb (45.0 \pm 2.38%) and ethanolic bulb (41.4 \pm 2.35%) extracts, compared with the control ($p < 0.05$) (Fig. 3). Apoptotic cells in H1299 cells were shown in Fig. 4.

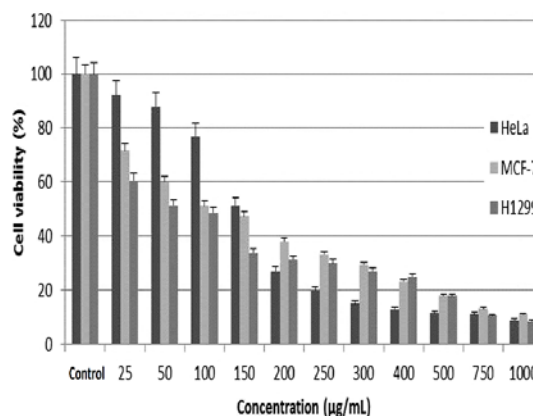


Figure 1. Cytotoxic activity of *M. muscarimi* ethanolic bulb extracts against different cancer cell lines. Data are presented as mean \pm SE.

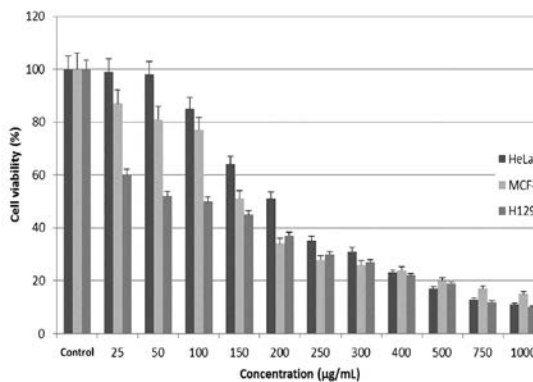


Figure 2. Cytotoxic activity of *M. muscarimi* methanolic bulb extracts against different cancer cell lines. Data are presented as mean \pm SE.

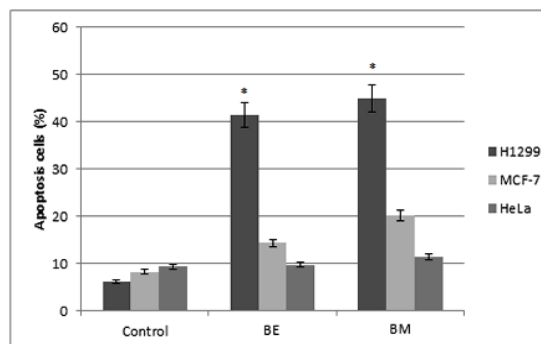


Figure 3. Apoptotic effects of *M. muscarimi* bulb extracts in different cancer cell lines. Data are presented as mean \pm SE.

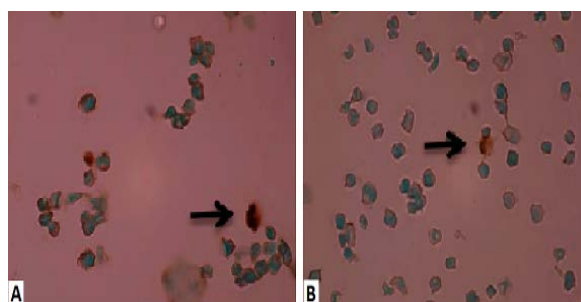


Figure 4. Apoptotic cells in H1299 cells treated by *M. muscarimi* bulb extracts (A: methanol, B: ethanol) using TUNEL assay. The arrows show the apoptotic cells.

Table 3. IC₅₀ (µg/mL) values of *M. muscarimi* in different cancer cell lines

Extracts	HeLa	MCF-7	H1299
BE	205.01±1.46	135.08±1.28	62.05±1.24
BM	140.13±1.30	90.43±1.26	58.20±1.20

BE: Bulb Ethanol, BM: Bulb Methanol. Data are presented as mean±SE.

4. Discussion

The plants extensively include substances that high antioxidant activity owing to the being of phenolic complexes particularly flavonoids (Tungmunnithum *et al.*, 2018). Antioxidants were called as bioactive substances that prevent the generation of free radicals or neutralize free radicals in living organisms. To prevent oxidative degradation of food, some antioxidants called synthetic (BHT, BHA, etc.) are extensively used in the food industry, but these synthetic antioxidants are suspected of being responsible for tumorigenesis (Lourenço *et al.*, 2019). Therefore, the improvement and usage of more powerful antioxidants from natural resource are needed.

In studies evaluating the antioxidant activity of *M. muscarimi*, two free radicals (NO and ABTS) were used, and the studies determined the rate at which these radicals are scavenged by the extracts. Transition metals act as a catalyst for lipid peroxidation. Therefore, chelating these metals is considered as an important antioxidant mechanism (Zengin & Aktumsek, 2014). In this study using the phosphomolybdenum assay, FRAP assay and metal chelating activity, it was found that the flower extracts demonstrated higher antioxidant potency than the bulb extracts. We have previously published data representing the antioxidant activity of *M. muscarimi* using two assays namely, β-carotene/linoleic acid assay and DPPH assay and similarly, the flower extracts were detected to have higher antioxidant activity than the bulb extracts. Also, the highest total phenolic content was determined in the methanolic flower extract (38.13 mg GAEs/g) (Mammadov *et al.*, 2016). In the current research, the highest total flavonoid content was determined in the methanolic flower extract as 27.22 mg QEs/g. Therefore, the higher antioxidant activity of methanolic flower extract may be depending on its total phenolic and flavonoid contents.

To assess the cytotoxic activity of the extracts of *M. muscarimi* on the growth of HeLa, MCF-7 and H1299 cell lines, the bulb extracts were examined. The low cytotoxicity of the flower extracts has directed us to this

choice (data not shown). Also, in our previous report, the brine shrimp lethality test results of the *M. muscarimi* extracts showed that the flower extracts were less cytotoxic than the bulb extracts (Mammadov *et al.*, 2016).

Many phytochemicals are biologically active, and they may interact to protect against cancer. Flavonoids are quite strong antioxidants, which scavenge free radicals, prevent the progression of cancer and protect towards oxidative stress related diseases (Abotaleb *et al.*, 2019, Vrancheva *et al.*, 2020). Flavonoids demonstrate powerful anticancer potencies against different cancer cells, mediated through coordinating of primary signaling pathways involved in the migration and invasion of cancer cells and metastatic spread, plus increase apoptosis (Ravishankar *et al.*, 2013). It was reported that the chemical components of the genus *Muscari* are homo-isoflavanones, flavonoids, glycosides, alkaloids and terpenoids (Urbancikova *et al.*, 2002; Lim, 2014). It has been shown that *M. racemosum* homoisoflavanoids have antimutagenic features and may be important for the prevention from cancer (Miadokova *et al.*, 2002). In the current study, we found that the bulb extracts had higher saponin content than the flower extracts. Cytotoxicity of the bulb extracts containing a high amount of saponin was higher than the flower extracts. Studies in recent years have stated that saponins indicate remarkable anticancer activity, like anti-proliferation via mechanisms that contain induction of apoptosis (Man *et al.*, 2010). Not surprisingly, the percentages of TUNEL-positive cells were escalated in all human cancer cell lines, especially in the H1299 cells, treated with the extracts comparison to their untreated controls, referring that the strong cytotoxic effects of the bulb extracts towards cancer cells are mediated by induction of apoptosis. Lanosterol glycosides, named scillasaponins E–G, were isolated from *M. paradoxum* bulb extract, and these isolated compounds exhibited cytotoxic activity against HSC-2 human oral squamous cell carcinoma cells with IC₅₀ values ranging from 6.3 to 59 mg/mL when etoposide (positive control) had an IC₅₀ value of 24 mg/mL (Ori *et al.*, 2003). It can be concluded that the high amounts of saponins in the bulbs of *M. muscarimi* may result in cytotoxic activity.

5. Conclusion

In conclusion, this study is the first research that describes the potential antiproliferative and apoptotic efficacy on the cancer cells of *M. muscarimi*, which is an endemic and endangered geophyte species for Turkey. Further phytochemical and biological studies are needed to state the active constituents of *M. muscarimi*.

Acknowledgments

We would like to thank Busra Donmez and Sirin Ozturk who were members of the Secondary Metabolites Lab., (Pamukkale University) for assistance with the studies and would also like to extend particular thanks to Onur Tokgun and Aydin Demiray for their valuable support during the experiments in the Medical Biology Lab., Pamukkale University, Turkey.

References

- Abotaleb M, Samuel SM, Varghese E, Varghese S, Kubatka P, Liskova A and Büsselberg D. 2019. Flavonoids in Cancer and Apoptosis. *Cancers (Basel)*, **11**: 28.
- Adebayo JO and Krettli AU. 2011. Potential antimalarials from Nigerian plants: a review. *J Ethnopharmacol*, **133**: 289-302.
- Adinolfi M, Barone G, Belardini M, Lanzetta R, Laonigro G and Parrilli M. 1985. Homoisoflavanones from *Muscari comosum* bulbs. *Phytochemistry*, **24**: 2423-2426.
- Balakrishnan N, Panda AB, Raj NR, Shrivastava A and Prathani RB. 2009. The evaluation of nitric oxide scavenging activity of *Acalypha indica* Linn Root. *Asian J Res Chem*, **2**: 148-150.
- Bray F, Ferlay J, Soerjomataram I, Siegel RL, Torre LA and Jemal A. 2018. Global cancer statistics 2018: GLOBOCAN estimates of incidence and mortality worldwide for 36 cancers in 185 countries. *CA Cancer J. Clin.*, **68**: 394-424.
- Eker I. 2019. *Muscari fatmacereniae* (Asparagaceae, Scilloideae), a new species from southern Anatolia, *Phytotaxa*, **397**: 99-106.
- Eroğlu Özkan E, Demirci Kayıran S, Taşkın T and Abudayyak M. 2018. In vitro antioxidant and cytotoxic activity of *Muscari neglectum* growing in Turkey. *Marmara Pharm J*, **22**: 74-79.
- Fulda S. 2010. Modulation of apoptosis by natural products for cancer therapy. *Planta Med*, **76**: 1075-1079.
- Hanahan D and Weinberg RA. 2011. Hallmarks of cancer: the next generation. *Cell*, **144**: 646-674.
- Hiai S, Oura H and Nakajima T. 1976. Color reaction of some sapogenins and saponins with vanillin and sulfuric acid. *Planta Med*, **29**: 116-122.
- Hoekstra JM, Boucher TM, Ricketts TH and Roberts C. 2005. Confronting a biome crisis: global disparities of habitat loss and protection. *Ecol. Lett*, **8**: 23-29.
- Kayıran SD and Özkan EE. 2017. The ethnobotanical uses of Hyacinthaceae species growing in Turkey and a review of pharmacological activities. *Indian J Tradit Know*, **16**: (2017) 243-250.
- Lim TK. 2014. *Muscari neglectum*. Edible Medicinal And Non-Medicinal Plants. Springer Netherlands 122.
- Loizzo MR, Tundis R and Menichini F. 2010. Chelating, antioxidant and hypoglycaemic potential of *Muscari comosum* (L.) Mill. bulb extracts. *Int J Food Sci Nutr*, **61**: 780-791.
- Lourenço SC, Moldão-Martins M and Alves VD. 2019. Antioxidants of Natural Plant Origins: From Sources to Food Industry Applications. *Molecules*, **24**: 4132.
- Mammadov R, Ili P and Dusen O. 2012. Phenolic contents and antioxidant properties of *Muscari parviflorum* Desf. *J. Chem. Soc. Pak*, **34**: 651-655.
- Mammadov R, Ozay C, Dusen O, Aydin C, Yaka H and Dusen S. 2016. Evaluation of antioxidant, antimicrobial and cytotoxic activities of *Muscari muscarimi* Medik. bulb and flower extracts from Turkey. *Fresenius Environ Bull*, **25**: 1680-1685.
- Man S, Gao W, Zhang Y, Huang L and Liu C. 2010. Chemical study and medical application of saponins as anti-cancer agents. *Fitoterapia*, **81**: 703-714.
- Miadokova E, Masterova I, Vlckova V, Duhova V and Toth J. 2002. Antimutagenic potential of homoisoflavanoids from *Muscari racemosum*. *J Ethnopharmacol*, **81**: 381-386.
- Mulholland DA, Schwikkard SL and Crouch NR. 2013. The chemistry and biological activity of the Hyacinthaceae. *Nat Prod Rep*, **30**: 1165-1210.
- Moreno MI, Isla MI, Sampietro AR and Vattuone MA. 2000. Comparison of the free radical-scavenging activity of propolis from several regions of Argentina. *J Ethnopharmacol*, **71**: 109-114.
- Ori K, Koroda M, Mimaki Y, Sakagami H and Sashida Y. 2003. Lanosterol and tetranorlanosterol glycosides from the bulbs of *Muscari paradoxum*. *Phytochemistry*, **64**: 1351-1359.
- Ozay C and Mammadov R. 2017. Screening of some biological activities of *Alyssum fulvescens* var. *fulvescens* known as Ege madwort. *Acta Biol Hung*, **68**: 310-320.
- Ozel CA, Khawar KM and Unal F. 2015. Factors affecting efficient in vitro micropropagation of *Muscari muscarimi* Medikus using twin bulb scale. *Saudi J Biol Sci*, **22**: 132-138.
- Oztas H, Oztas F, Aladag MO and Alas A. 2018. An Endemic Plant of Ermenek Region (Turkey), *Muscari muscarimi*: Economic Importance, and Is There a Useful Way Out Cultivation in Its Natural Habitats? *JFSE*, **8**: 189-190.
- Pandey MK, Prasad S, Tyagi AK, Deb L, Huang J, Karelia DN, Amin SG and Aggarwal BB. 2016. Targeting cell survival proteins for cancer cell death. *Pharmaceuticals*, **9**: 11.
- Prieto P, Pineda M and Aguilar M. 1999. Spectrophotometric quantitation of antioxidant capacity through the formation of a phosphormolybdenum complex: specific application to the determination of vitamin E. *Anal Biochem*, **269**: 337-341.
- Ravishankar D, Rajora AK, Greco F and Osborn HMI. 2013. Flavonoids as prospective compounds for anti-cancer therapy. *Int. J. Biochem. Cell Biol*, **45**: 2821-2831.
- Re R, Pellegrini N, Proteggente A, Pannala A, Yang M and Rice-Evans C. 1999. Antioxidant activity applying an improved ABTS radical cation decolorization assay. *Free Radic Biol Med*, **26**: 1231-1237.
- Shahidi and Ambigaipalan P. 2015. Phenolics and polyphenolics in foods, beverages and spices: antioxidant activity and health effects—a review. *J. Funct. Foods*, **18**: 820-897.
- Tungmunnithum D, Thongboonyou A, Pholboon A and Yangsabai A. 2018. Flavonoids and Other Phenolic Compounds from Medicinal Plants for Pharmaceutical and Medical Aspects: An Overview. *Medicines*, **5**: 93.
- Urbancikova M, Masterova I and Toth J. 2002. Estrogenic/antiestrogenic activity of homoisoflavanoids from bulbs of *Muscari racemosum* (L.) Miller. *Fitoterapia*, **73**: 724-726.
- Vrancheva R, Popova A, Mihaylova D and Krastanov A. 2020. Phytochemical Analysis, In Vitro Antioxidant Activity and Germination Capability of Selected Grains and Seeds. *Jordan J Biol Sci*, **13**: 337-342.
- Zengin G and Aktumsek A. 2014. Investigation of Antioxidant Potentials of Solvent Extracts from Different Anatomical Parts of *Asphodeline anatolica* E. Tuzlaci: an Endemic Plant to Turkey. *Afr J Tradit Complement Altern Med*, **11**: 481-488.
- Zengin G, Nithiyantham S, Locatelli M, Ceylan R, Uysal S, Aktumsek A, Selvi PK and Maskovic P. 2015. Screening of in vitro antioxidant and enzyme inhibitory activities of different extracts from two uninvestigated wild plants: *Centranthus longiflorus* subsp. *longiflorus* and *Cerinthe minor* subsp. *auriculata*. *Eur J Integr Med*, **8**: 286-292.

Fauna of the Ladybird Beetles (Coleoptera: Coccinellidae) and their Associated Host Plants from Southern Syria

Nazir Khalil¹, Abdoulrahman Mourad², Mahmoud Karoum³, Mohammad Abu Baker⁴ and Zuhair Amr^{5,*}

¹Al-Furat University, Sciences Faculty, Al-Raqa, Syria; ²Damascus University, Sciences Faculty, Biology Animal Department, Damascus, Syria; ³Aleppo University, Sciences Faculty, Biology Animal Department, Aleppo, Syria; ⁴Department of Biology, The University of Jordan, Amman, Jordan; ⁵Department of Biology, Jordan University of Sciences and Technology, Irbid, Jordan.

Received: November 4, 2020; Revised: December 27, 2020; Accepted: January 28, 2021

Abstract

The coccinellids of southern Syria were studied based on 7418 specimens collected during 2001 to 2005. Fifty-one species and subspecies belonging to 21 genera of 11 tribes and two subfamilies (Microweiseinae and Coccinellinae) were recorded. Fifteen species are recorded for the first time in Syria. Host plants species for each coccinellid species were recorded.

Keywords: Coccinellids, Coccinellidae, Coleoptera, systematics, Syria, host plant.

1. Introduction

Ladybird beetles (Coccinellidae) constitute one of the largest families of coleopterous insects, including over 6000 species (Hodek *et al.*, 2015). The overwhelming majority of lady beetles are predators, feeding of aphids, psyllids, whiteflies, mealybugs, scales, thrips, spider mites, leaf beetle larvae and other small arthropods (Kuznetsov, 1997).

The species of family Coccinellidae in the Middle East, with 61 species in Iraq (Ali *et al.*, 1990), 142 species in Iran (Biranvand *et al.*, 2016; Mesbah *et al.*, 2016), 16 species in Jordan (Alawi, 1989), 71 species in Palestine (Halperin *et al.*, 1995; Najajrah *et al.*, 2019), 35 species in Saudi Arabia (Fürsch, 1979; Raimundo and van Harten, 2000), 84 species in Turkey (Yurtsever 2001), 22 species in the United Arab Emirates (Raimundo *et al.*, 2008) and 73 species in Yemen (Raimundo and van Harten, 2000). Prior to this study, only 11 species had been recorded from southern Syria without sufficient data on their distribution or ecology (Winkler, 1927; El-Hariri, 1968 and 1971; Kabakibi, 1993; Almatni *et al.*, 1999; Bascheer and Abo Alshamat 2004; Almatni and Khalil, 2008).

The aim of the present work is to study the biodiversity and distribution of the coccinellid beetles in southern Syria, with notes on their host plants.

2. Materials and methods

Sampling was conducted in southern Syria covering five Governorates (Damascus, Damascus Rural, Al-Quneitra, Dar`a and As`Sweida) located at different altitudes (280-2400m asl. (Figure 1, Table 1). A total of 7418 adult ladybirds was collected from agricultural and non-agricultural areas during three years (August 2001-July 2003), and other specimens were collected during 2004 and 2005.

Ladybird beetles were collected from branches and foliage of trees or herbaceous plants. Also, trees were shaken and insects were collected in a cloth tray with an insect net or by an aspirator. Each specimen was labeled with data about host plants, locality, and date. Specimens were preserved in 70% ethanol, and other specimens were dry mounted and preserved in collection boxes. Whole specimens were photographed by Canon camera, while genital structure were extracted (Tegmen and penis, for the males and the spermatheca for the females), boiled in 10% KOH, washed in water, different concentrations of alcohol 70%, 95% and 100%, and xylene, then mounted on slides and drawn using camera lucida. Specimens are deposited at the Department of Animal Biology, Damascus University.

* Corresponding author e-mail: amrz@just.edu.jo.

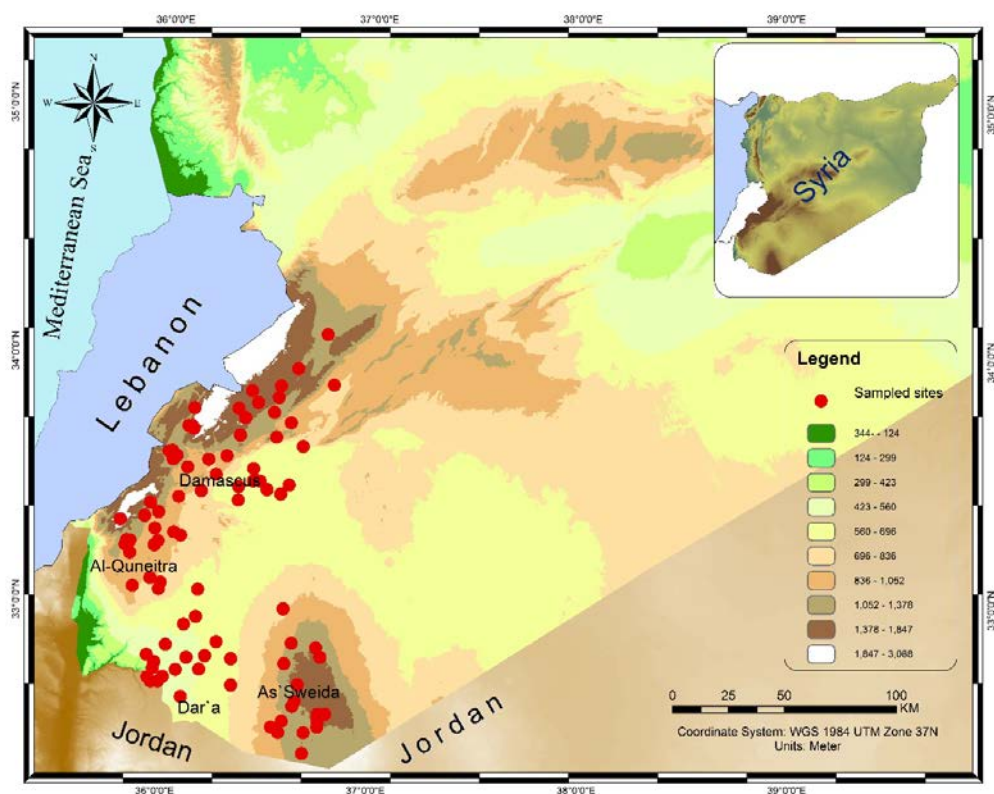


Figure 1: Collecting localities with their coordinates.

Species identification was carried out using different taxonomic keys and taxonomic references (Dauguet, 1949; Chapin, 1965; Fürsch, 1967a; 1979, 1989; Iablokoff-Khnzorian, 1971, 1982; Hodek, 1973; Gourreau, 1974; Chazeau *et al.*, 1974; Leeper 1975; Uygun 1981, Uygun and Fürsch, 1981; Canepari, 1983; Canepari *et al.*, 1985; Klausnitzer and Klausnitzer, 1986; Raimundo and Alves, 1986; Majerus and Kearns, 1989; Duverger, 1991; Kuznetsov, 1997; Raimundo and van Harten, 2000; Le Monnier and Livory, 2003). Identification of most species was confirmed by Prof. Dr. Helmut Fürsch (Passau University, Germany).

Table 1: Collecting localities with their coordinates.

localities	Latitude	Longitude	Localities	Latitude	Longitude
Airport Street	33° 28' 36"	36° 21' 48"	Kulaiaa	33° 17' 12"	36° 03' 30"
Ahmadia	33° 28'	36° 30'	Maalula	33° 50' 21"	36° 32' 57"
Ajami	32° 42'	35° 57'	Ma`adamiyeh Al-sham	33° 27' 21"	36° 11' 06"
Addimass	33° 33'	36° 07'	Maissalon	33° 35' 44"	36° 03' 49"
Al-Dumayr	33° 38' 37"	36° 40' 11"	Masehara	33° 06'	35° 57'
Al-Harra	33° 03' 24"	35° 59' 33"	Mashkok	32° 24' 23"	36° 41' 37"
Al-Hameh	33° 35'	36° 13'	Mugr Almeer	33° 18'	35° 58'
Al-Kafr	32° 36' 56"	36° 39' 16"	Mzireeb	32° 42' 13"	36° 01' 21"
Alqraya	32° 32' 06"	36° 35' 39"	Nahaj	32° 41'	36° 00'
Al-Qutayfeh	33° 44' 17"	36° 36' 35"	Nahta	32° 46' 56"	36° 20' 46"
Annashabyeh	33° 30'	36° 28'	Namer	32° 47' 28"	36° 13' 18"
Ashiphonieh	33° 33'	36° 26'	Nasseria	33° 52' 99"	36° 48' 49"
Attall	33° 35' 55"	36° 18' 15"	Ophania	33° 12'	35° 51'
Attawani	33° 46' 43"	36° 30' 99"	Orman	32° 30' 49"	36° 45' 49"
Assaida Zainab	33° 25' 19"	36° 21' 51"	Orman Mountain	32° 31' 54"	36° 45' 54"
Assal Alwared	33° 51' 48"	36° 25' 10"	Qanawat	32° 46'	36° 36'

To assess the occurrence and preference of coccinellid species on plant hosts, we measured species richness (total number of species recorded), species incidence (the number of plant host at which a species occurred). The number of coccinellid species was plotted against the number of plant hosts to distinguish specialist (coccinellids occurring on less than 10 plant hosts) vs. generalist species (those occurring on over 30 plant hosts). To assess the preferred plant hosts (plants on which more than 15 coccinellid occurred) the number of plant hosts was plotted against the total number of coccinellids.

Table 1. cont

Autaiba	33° 29' 12"	36° 36' 22"	Qatana	33° 25' 50"	36° 04' 38"
Azzabadani	33° 42' 26"	36° 08' 36"	Rankus	33° 45' 16"	36° 23' 23"
Baka	32° 29' 22"	36° 34' 42"	Rankus Mountain	33° 47' 30"	36° 21' 25"
Barad	32° 30' 38"	36° 32' 36"	Sabsaba	33° 05'	36° 00'
Beqaasem	33° 24' 14"	35° 56' 37"	Sad alaa'in	32° 35' 43"	36° 38' 34"
Beer Ajam	33° 04'	35° 52'	Sahm al-joulan	32° 47' 24"	35° 56' 35"
Beet jen- Mazraa	33° 15'	35° 51'	Salkhad	32° 29' 24"	36° 41' 59"
Bludan	33° 43'	36° 07'	Sanameen	33° 03' 32"	36° 10' 48"
Bludan Mountain	33° 43'	36° 08'	Serghaya	33° 47' 21"	36° 08' 37"
Damascus (Qasioun)	33° 31' 23"	36° 15' 15"	Sarkha	33° 53' 10"	36° 33' 31"
Dar`a	32° 36' 90"	36° 06' 40"	Sasaa	33° 15'	35° 59'
Deir Al-ashairr	33° 34' 49"	36° 02' 44"	Saura	32° 59' 16"	36° 35' 27"
Deir Atyeh	34° 05' 48"	36° 46' 42"	Sehaileia	32° 55'	36° 07'
Dorin	33° 14'	35° 58'	Shahba	32° 51'	36° 38'
Durbol	33° 21'	35° 55'	Sheikh Saad	32° 50'	36° 02'
Ein alarab	32° 41'	36° 40'	Sheikh Miskin	32° 47'	36° 08'
Erneh	33° 20'	35° 48'	Seydnaya	33° 41'	36° 22'
Fakiia	32° 56' 55"	36° 10' 24"	Southern Al-Qutayfeh	33° 40' 44"	36° 32' 27"
Ghoujygoujyat Mont.	32° 32' 57"	36° 45' 51"	Taamri Mountain	32° 33' 54"	36° 45' 52"
Hadar	33° 15'	35° 50'	Tafas	32° 44'	36° 05'
Haran Al-awameed	33° 27'	36° 34'	Taima	32° 50'	36° 45'
Houch arab	33° 49'	36° 27'	Tal Shihab	32° 41'	35° 58'
Izraa	32° 50' 56"	36° 15' 89"	Tal-loz	32° 34'	36° 48'
Jeelin	32° 45' 45"	35° 58' 46"	Tarba	32° 47' 44"	36° 46' 19"
Jeesrin	33° 30'	36° 26'	Trounja	33° 14' 40"	35° 50' 48"
Jubata Al-Khashab	33° 13' 56"	35° 49' 36"	Wadi Al-Qaren	33° 36' 44"	36° 01' 31"
Kafir- Hawar	33° 22'	35° 59'	Wadi Jeelin	32° 44' 13"	35° 58' 27"
Kanaker	33° 16' 28"	36° 05' 28"	Wadi Shihab	32° 41'	35° 58'
Karak	32° 40' 31"	36° 20' 57"	Yabrud	33° 57' 24"	36° 38' 23"
Kharabo	33° 30' 08"	36° 27' 19"	Zarzar	33° 36' 54"	36° 02' 30"
Kherbeet Gazaleh	32° 44' 13"	36° 11' 41"	Zeizon	32° 42'	35° 57'

3. Results

Fifty-one species and subspecies belonging to 21 genera representing 11 tribes within two subfamilies were recorded from southern Syria. Fifteen species are new records to Syria (Table 2). Higher taxonomic classification and scientific names were followed according to those in Kovár (2007), Ślipiński (2007), Seago *et al.* (2011) and Robertson *et al.* (2015).

Table 2. List of coccinellid species in Southern Syria.

Species	No. of sites	Total No. collected specimens
Subfamily Microweiseinae		
Tribe Microweiseini		
<i>Pharoscymnus ovoideus</i> Sicard, 1929	38	272
<i>Pharoscymnus setulosus</i> (Chevrolat, 1861)*	1	1
Subfamily Coccinellinae		
Tribe Coccidulini		
<i>Cryptolaemus montrouzieri</i> Mulsant, 1853	3	6
<i>Lindorus lophantae</i> (Blaisdell, 1892)*	4	80

Tribe Diomini		
<i>Diomus rubidus</i> (Motschulsky, 1837)	1	1
Tribe Hyperaspidini		
<i>Hyperaspis (Hyperaspis) femorata</i> (Motschulsky, 1837)*	1	2
<i>Hyperaspis (Hyperaspis) histeroides</i> (Faldermann, 1837)*	8	12
<i>Hyperaspis (Hyperaspis) syriaca</i> Weise, 1885	1	16
Tribe Scymnini		
<i>Clitostethus arcuatus</i> (Rossi, 1794)	3	40
<i>Nephus (Bipunctatus) bipunctatus</i> (Kugelann, 1794)*	32	97
<i>Nephus (Bipunctatus) includens</i> (Kirsch, 1870)	2	2
<i>Nephus (Nephus) ludyi</i> (Weise, 1879)*	11	115
<i>Nephus (Nephus) merkli</i> Fürsch, 1994*	8	115
<i>Nephus (Nephus) quadrimaculatus</i> Herbst, 1783	29	265
<i>Nephus (Sidis) caucasicus</i> Weise, 1929*	1	1
<i>Nephus (Sidis) hiecki</i> Fürsch, 1965*	2	2
<i>Nephus (Sidis) kreissli</i> Fürsch & Uygun, 1980*	4	27
<i>Scymnus (Mimopullus) pharaonis</i> Motschulsky, 1851	39	317
<i>Scymnus (Mimopullus) flagellisiphonatus</i> Fürsch, 1969	17	26
<i>Scymnus (Mimopullus) flavicollis</i> Redtenbacher, 1844	26	416

<i>Scymnus (Mimopullus) marinus</i> Mulsant, 1850	11	109
<i>Scymnus (Parapullus) abietis</i> (Paykull, 1798)*	2	2+
<i>Scymnus (Pullus) apetzii</i> Mulsant, 1846*	34	403
<i>Scymnus (Pullus) auritus</i> Thunberg, 1795*	4	5
<i>Scymnus (Pullus) fraxini</i> Mulsant, 1850*	2	62
<i>Scymnus (Pullus) subvillosus</i> (Goeze, 1777)	30	316
<i>Scymnus (Pullus) syriacus</i> (Marseul, 1868)	28	250
<i>Scymnus (Scymnus) bivulnerus</i> Capra & Fürsch, 1967	16	52
<i>Scymnus (Scymnus) frontalis</i> (Fabricius, 1787)	2	60
<i>Scymnus (Scymnus) interruptus</i> (Goeze, 1777)	13	111
<i>Scymnus (Scymnus) nubilus</i> Mulsant, 1850	31	279
Tribe Stethorini		
<i>Stethorus (Stethorus) gilvifrons</i> (Mulsant, 1850)	48	1368
Tribe Chilocorini		
<i>Chilocorus bipustulatus</i> (Linnaeus, 1758)	7	42
<i>Exochomus octosignatus</i> (Gebler, 1830)*	1	1
<i>Exochomus quadripustulatus</i> (Linnaeus, 1758)	4	54
<i>Exochomus undulatus</i> (Weise, 1878)	2	2
<i>Parexochomus nigromaculatus</i> (Goeze, 1777)	10	24
<i>Parexochomus pubescens</i> (Küster, 1848)	4	6
Tribe Platynaspini		
<i>Platynaspis luteorubra</i> (Goeze, 1777) *	8	14
Tribe Noviini		
<i>Novius cardinalis</i> (Mulsant, 1850)	4	16
Tribe Tychthaspidini		
<i>Anisosticta novemdecimpunctata</i> (Linnaeus, 1758)*	1	1
Tribe Coccinellini		
<i>Adalia (Adalia) bipunctata</i> (Linnaeus, 1758)	6	61
<i>Adalia (Adalia) decempunctata</i> (Linnaeus, 1758)	13	37
<i>Coccinella (Coccinella) septempunctata</i> Linnaeus, 1758	39	330
<i>Coccinella (Spilota) undecimpunctata aegyptica</i> Reiche, 1861	40	152
<i>Harmonia quadripunctata</i> (Pontoppidan, 1763)	10	59
<i>Hippodamia (Adonia) variegata</i> (Goeze, 1777)	56	1042
<i>Oenopia conglobata</i> (Linnaeus, 1758)	41	618
<i>Oenopia oncina</i> (Olivier, 1808)*	5	6
<i>Propylea quatuordecimpunctata</i> (Linnaeus, 1758)	8	121
<i>Psyllobora (Thea) vigintiduopunctata</i> (Linnaeus, 1758)	1	2
Total	94	7418

* new record for Syria

Family Coccinellidae Latreille, 1807

Subfamily Microweiseinae Leng, 1920

Tribe Microweiseini Leng, 1920

Pharoscyrnus ovoideus Sicard, 1929 (Figs. 2A and 3A)

Material examined (272): Damascus Rural: Attall, (1), 26.9.2001; (1), 8.5.2002; (1), 26.6.2002; (2), 5.9.2002. Wadi Al-Qaren, (4), 19.8.2001; (1), 19.9.2001; (7), 5.9.2002. Yabrud, (2), 25.10.2001; (1), 8.8.2002; (3), 11.9.2002. Sasaa, (5), 13.8.2001; (4), 3.10.2001; (1), 20.3.2002; (5), 2.5.2002; (4), 31.7.2002; (3), 12.9.2002.

Kulaiaa, (1), 7.8.2002. Beqaasem, (2), 21.9.2001; (6), 11.7.2002; (1), 29.8.2002. Muqr Almeer, (1), 26.8.2003. Addimass, (4), 5.9.2002; (9), 17.9.2002; (6), 30.4.2003. Al Hameh, (1), 14.6.2003. Sarkha, (1), 26.9.2001; (4), 11.9.2002; (1), 21.5.2003. Seydnaya, 11: (9), 2.8.2001; (2), 21.5.2003. Al-Qutayfeh, (8), 8.8.2002. Annashabyeh, (4), 28.8.2001; (2), 21.11.2001; (5), 24.7.2002; (2), 27.7.2002. Kharabo, (3), 22.8.2001; (1), 26.9.2001; (1), 25.10.2001; (1), 23.5.2002; (1), 11.7.2002; (2), 25.5.2003; (4), 2.7.2003. Ma`adamiyeh Al-sham, (1), 7.10.2001; (2), 6.12.2001; (1), 6.3.2002; (1), 12.4.2002; (16), 30.8.2002; (3), 9.9.2002; (15), 4.10.2002; (1), 1.11.2002; (1), 4.12.2002; (1), 16.1.2003; (1), 13.3.2003; (1), 6.7.2003; (2), 11.7.2003; (2), 23.7.2003; (1), 27.7.2003; (5), 9.8.2003; (3), 13.8.2003. **Damascus:** Qasioun, (3), 13.5.2003. **Al-Quneitra:** Beer Ajam, (1), 20.3.2002; (2), 12.9.2002; (1), 2.10.2002; (1), 19.3.2003. Jubata Al-Khashab, (1), 10.4.2002; (4), 16.5.2002; (2), 11.7.2002; (3), 29.8.2002; (2), 26.8.2003. Hadar, (6), 31.7.2002. Trounja, (1), 29.8.2002. Ophania, (1), 10.9.2001. **As`Sweida:** Al-Kafir, (1), 11.5.2003. Ein alarab 12: (2), 7.8.2001; (2), 29.8.2001; (1), 21.8.2002; (6), 23.10.2002; (1), 2.6.2003. Orman mountain, (1), 27.9.2001. Orman, (1), 21.8.2002. Qanawat, (1), 20.9.2001; (2), 11.4.2002. Taima, (12), 11.9.2001. Mashkok, (1), 20.9.2001. Alqrayya (2), 20.9.2001. **Dar`a:** Jeelin 4: (2), 30.8.2001; (1), 24.10.2001; (1), 3.7.2002. Wadi Jeelin, (1), 25.4.2002; (1), 22.8.2002. Zeizon, (3), 2.10.2002; (1), 13.11.2002; (2), 23.4.2003. Ajami (1), 18.7.2002. Kherbeet Gazaleh, (1), 7.2.2002. Nahaj, (1), 24.10.2001. Sehaileia, (2), 26.9.2001. Fakiia, (1), 28.3.2002. Al-Harra, (4), 4.9.2001; (4), 2.10.2002; (1), 13.11.2002.

Remarks: It was recorded from Egypt, Jordan, Palestine and Syria (Alfieri, 1976; Halperin *et al.*, 1995; Kovár, 2007).

Host species: *Amygdalus* sp., *Cedrus libani*, *Citrus* sp., *Crataegus* sp., *Cupressus* sp., *Ficus carica*, *Juglans regia*, *Medicago sativa*, *Morus alba*, *Quercus calliprinos*, *Olea europaea*, *Phaseolus vulgaris*, *Pinus* sp., *Pistacia vera*, *Punica granatum*, *Prunus armeniaca*, *Prunus persica*, *Pyrus communis*, *Schinus molle*, *Solanum melongena*, *Zea mays*, and thistle plants.

Pharoscyrnus setulosus (Chevrolat, 1861) (Figs. 2B and 3B)

Material examined (1): Damascus Rural: Southern Al-Qutayfeh, (1), 15.8.2001.

Remarks: Known from Spain, North Africa, the Middle East, and Yemen (Raimundo and van Harten, 2000, Kovár, 2007). This species is recorded for the first time in Syria.

Host species: *Pinus* sp.

Subfamily Coccinellinae Latreille, 1807

Tribe Coccidulini Mulsant, 1846

Cryptolaemus montrouzieri Mulsant, 1853 (Figs. 2C and 3C).

Material examined (6): Dar`a: Wadi Jeelin (1), 24.10.2001; (1), 28.3.2002. Zeizon, (1), 24.10.2001; (1), 25.4.2002. Wadi Shihab, (2), 13.5.2003.

Remarks: This species have a wide range of distribution worldwide (Uygun, 1981). It feeds on scale insects. It was introduced to Syria in 1995 for controlling some pest on citrus trees such *Planococcus citri* in the

Syrian Coast. Abboud *et al.* (2020) reported that this species predates on *Protopulvinaria pyriformis*.

Host species: *Inula viscosa* and *Rubus idaeus*.

***Lindorus lophanthae* (Blaisdell, 1892) (Figs. 2D and 3D)**

Material examined (80): Damascus Rural: Sasaa, (1), 13.8.2001. **Dar`a:** Wadi Jeelin, 5: (2), 9.5.2002; (2), 29.5.2002; (1), 3.7.2002. Serghaya, (1), 3.10.2002. **As`Sweida:** Ein alarab, (5), 27.9.2001; (18), 18.10.2001; (13), 29.11.2001; (1), 3.4.2002; (2), 17.7.2002; (1), 1.8.2002; (20), 21.8.2002; (11), 10.9.2002; (2), 23.10.2002.

Remarks: This species have a wide range of distribution almost worldwide (Raimundo and van Harten 2000), with records from Turkey, Jordan and Palestine (Uygun, 1981; Allawi, 1989; Halperin *et al.*, 1995). This species represents a new record to Syria.

Host species: *Citrus* sp., *Cupressus* sp. and *Nerium oleander*.

Tribe Diomini R. D. Gordon, 1999

***Diomus rubidus* (Motschulsky, 1837) (Figs. 2E and 3E)**

Material examined (1): Damascus Rural: Attall, (1), 27.12.2001.

Remarks: Fürsch (1979) recognized three subspecies for this form. Listed by El Hariri (1971) as *Scymnus rubidus* in Syria. Jalilvand *et al.* (2014) found that this species predates on *Planococcus vovae* in Iran.

Host species: *Rubus idaeus*.

Tribe Hyperaspidini Mulsant, 1846

***Hyperaspis (Hyperaspis) femorata* (Motschulsky, 1837) (Figs. 2F and 3F)**

Material examined (2): As`Sweida: Taamri Mountain, (2), 21.6.2002.

Remarks: This species is distributed in the Caucasus, Armenia, Ukraina (Iablokoff-Khznorian, 1971) and Bulgaria (Canepari *et al.*, 1985). This species is recorded for the first time in Syria. Aslan and Uygun (2005) reported this species from Turkey to feed on aphids.

Host species: *Achillea* sp.

***Hyperaspis (Hyperaspis) histeroides* (Faldermann, 1837) (Figs. 2G and 3G)**

Material examined (12): Damascus Rural: Rankus, (1), 11.9.2002. **As`Sweida:** Qanawat, (1), 19.6.2002. Ghoujygujyat Mountain, (1), 1.8.2002; (1), 29.4.2003, Orman Mountain, (2), 4.7.2002; (1), 4.8.2003. Taamri Mountain, (2), 28.6.2003; (1), 4.7.2003. **Al-Quneitra:** Beer Ajam, (1), 27.6.2002. Masehara, (1), 13.8.2001.

Remarks: This species is distributed in the Caucasus, Kazakhstan and Armenia (Iablokoff-Khznorian, 1971). Reported previously from As-Sweida preying on the almond curl leaf aphid, *Brachycaudus amygdalinus* (Almatni and Khalil, 2008).

Host species: *Achillea* sp., *Amygdalus* sp., *Cucurbita pepo*, *Ficus carica*, and *Quercus calliprinos*.

***Hyperaspis (Hyperaspis) syriaca* Weise, 1885 (Figs. 2H and 3H)**

Material examined (16): Dar`a: Wadi Jeelin, (4), 9.5.2002; (1), 29.5.2002; (2), 3.7.2002; (9), 22.8.2002.

Remarks: This species is known from Palestine, Syria and Lebanon (Iablokoff-Khznorian, 1971).

Host species: *Vitex agnus-castus*.

Tribe Scymnini Mulsant, 1846

***Clitostethus arcuatus* (Rossi, 1794) (Figs. 2I and 3I).**

Material examined (40): Damascus Rural: Attall, (1), 25.10.2001; (20), 20.11.2002. Ma`adamiyeh Al-sham, (4), 6.3.2002; (1), 4.10.2002; (3), 1.11.2002; (1), 4.12.2002; (1), 5.2.2003; (4), 6.3.2003; (2), 9.4.2003; (1), 23.6.2003; (1), 11.7.2003. **Damascus:** Damascus, (1), 20.10.2002.

Remarks: This species is known from Europe, the Caucasus and Turkey (Uygun 1981). Reported from the Coastal regions of Syria on whiteflies (Al Jundi and Ahmad, 1999) and Palestine (Halperin *et al.*, 1995).

Host species: *Citrus* sp., *Morus alba*, *Phaseolus vulgaris* and *Punica granatum*.

***Nephus (Bipunctatus) bipunctatus* (Kugelann, 1794) (Figs. 2J and 3J)**

Material examined (97): Damascus Rural: Attall, (2), 26.9.2001; (2), 25.10.2001; (3), 5.9.2002. Wadi Al-Qaren, (1), 5.9.2002; (1), 10.7.2002. Yabrud, (1), 11.9.2002. Sasaa, (6), 3.10.2001; (2), 12.9.2002; (3), 26.8.2003. Kulaiaa, (1), 7.8.2002. Hadar, (1), 12.9.2002; (1), 26.8.2003. Beet-jen Mazraa Mazraa, (1), 3.10.2001; (1), 26.8.2003. Erneh, (1), 11.7.2002. Beqaasem, (1), 29.8.2002, Rankus Mountain, (4), 11.9.2002, Sarkha, (2), 26.9.2001; (3), 11.9.2002. Al-Qutayfeh, (4), 8.8.2002. Qatana, (1), 14.8.2003. Kharabo, (2), 2.4.2003; (2), 6.8.2003. Serghaya, (1), 5.9.2002. Ma`adamiyeh Al-sham, (2), 30.8.2002; (3), 9.9.2002; (2), 4.10.2002; (2), 11.7.2003; (2), 13.8.2003. **As`Sweida:** Al-Kafr, (1), 18.10.2001; (1), 23.10.2002. Ein alarab, (1), 17.7.2002. Orman, (1), 27.9.2001. Orman Mountain, (1), 9.4.2003. Taamri Mountain, (1), 8.8.2003. Qanawat, (1), 11.9.2001; (1), 20.9.2001; (2), 13.3.2002; (1), 21.8.2002. Shahba, (1), 13.3.2002. Salkhad, (1), 22.11.2001. Taima, (2), 11.9.2001. Alqrayya, (2), 10.9.2001, **Dar`a:** Wadi Jeelin, (1), 7.2.2002; (1), 22.8.2002. Zeizon, (1), 22.8.2002; (1), 13.11.2002. Sheikh Miskin, (2), 22.7.2003. Sahn al-joulan, (10), 4.9.2001. **Al-Quneitra:** Beer Ajam, (2), 12.9.2002; (2), 2.10.2002; (1), 19.3.2003. Trounja, (1), 29.8.2002.

Remarks: This is a Palaearctic species with a wide range of distribution in Central Asia, North Africa reaching Japan (Gourreau, 1974; Kuznetsov, 1997). Reported previously from As-Sweida preying on the almond curl leaf aphid, *Brachycaudus amygdalinus* (Almatni and Khalil, 2008).

Host species: *Amygdalus* sp., *Prunus armeniaca*, *Cedrus libani*, *Citrus* sp., *Ficus carica*, *Hibiscus esculentus*, *Malus communis*, *Morus alba*, *Phaseolus vulgaris*, *Pinus* sp., *Populus* sp., *Prunus* sp., *Prunus avium*, *Prunus vulgaris*, *Punica granatum*, *Pyrus communis*, *Quercus calliprinos*, *Urtica* sp., *Vitex agnus-castus*, *Vitis vinifera*, and thistle plants.

***Nephus (Bipunctatus) includens* (Kirsch, 1870) (Figs. 2K and 3K)**

Material examined (2): Dar`a: Wadi Jeelin, (1), 7.2.2002. Sahn al-joulan, (1), 4.9.2001.

Remarks: This species is distributed in some the Mediterranean area and Saudi Arabia (Uygun, 1981). Listed in Syria by El Hariri (1968) and recorded from the Coastal area on *Planococcus citri* (Aslan, 2001). It has been recorded as a predator of the mealybug *Nipaeococcus viridis* on different hosts in Iran (Fallahzadeh *et al.*, 2013).

Other species of this genus in Iran were found to prey on *Planococcus vovae* (Jalilvand *et al.*, 2014).

***Nephus (Nephus) ludyi* (Weise, 1879) (Figs. 2L and 3L)**

Material examined (115): Damascus Rural: Erneh, (1), 29.8.2002. Beqaasem, (1), 29.8.2002. Wadi Al-Qaren, (9), 17.11.2001; (3), 19.9.2001; (2), 5.9.2002; (3), 14.3.2002. **Al-Quneitra:** Jubata Al-Khashab, (3), 8.11.2001; (1), 20.12.2001; (3), 20.3.2002; (4), 28.2.2002; (2), 10.4.2002; (2), 25.4.2002. Beer Ajam, (6), 20.3.2002. **As`Sweida:** Al-Kafr, (11), 20.9.2001; (10), 18.10.2001; (31), 29.11.2001; (1), 21.3.2002; (3), 24.4.2002; (1), 17.7.2002; (1), 1.8.2002; (1), 29.11.2002; (1), 12.12.2002. Ein alarab, (1), 17.7.2002; (1), 1.8.2002; (1), 21.8.2002. Ghoujygujyat Mountain, (1), 22.10.2002; (2), 4.8.2003. Orman Mountain, (3), 4.8.2003. Taamri Mountain, (1), 5.8.2003. Qanawat, (2), 20.9.2001; (1), 13.3.2002; (1), 3.4.2002; (1), 11.4.2002.

Remarks: This species is known from southern France and the Mediterranean region (Gourreau, 1974). Recorded from Jordan (Allawi, 1989). This species is recorded for the first time in Syria.

Host species: *Amygdalus* sp., *Prunus armeniaca*, *Juglans regia*, *Malus communis*, *Prunus avium*, *Prunus vulgaris*, *Pyrus communis* and *Quercus calliprinos*.

***Nephus (Nephus) merkli* Fürsch, 1994 (Figs. 2M and 3M)**

Material examined (115): Damascus Rural: Seydnaya, (3), 21.5.2003. Qatana, (2), 14.8.2003. Attall, (7), 26.9.2001; (4), 25.10.2001; (1), 21.11.2001; (1), 10.7.2002. Kharabo, (46), 22.8.2001; (4), 26.9.2001; (10), 25.10.2001; (3), 21.11.2001; (2), 27.3.2002; (2), 11.7.2002; (1), 24.7.2002; (9), 8.8.2002; (2), 11.9.2002; (2), 25.9.2002; (4), 9.10.2002. Ma`adamiyeh Al-sham, (1), 4.10.2002; (1), 1.11.2002; (1), 23.6.2003; (1), 6.7.2003; (2), 23.7.2003; (1), 9.8.2003; (1), 13.8.2003. **Dar`a:** Wadi Jeelin, (1), 3.7.2002; (1), 18.7.2002. Zeizon, (1), 23.4.2003. **Al-Quneitra:** Masehara, (1), 13.8.2001.

Remarks: Described originally from Palestine (Fürsch, 1994), and very similar to *Nephus quadrimaculatus pictus*. This species is recorded for the first time in Syria.

Host species: *Citrus* sp., *Cupressus* sp., *Ficus carica*, *Juglans regia*, *Ligustrum* sp., *Morus alba*, *Nerium oleander*, *Olea europaea*, *Prunus avium*, *Punica granatum*, *Solanum melongena*, *Urtica* sp. and *Zea mays*.

***Nephus (Nephus) quadrimaculatus* Herbst, 1783 (Figs. 2N and 3N)**

Material examined (265): Damascus Rural: Beet-jen Mazraa, (3), 10.4.2002. Durbol, (1), 29.8.2002. Beqaasem, (3), 21.9.2001; (4), 20.9.8.2002. Wadi Al-Qaren, 12: (2), 17.11.2001; (8), 19.8.2001; (2), 19.9.2001. Sasaa, (1), 13.8.2001; (2), 2.5.2002; (1), 12.9.2002. Kulaiaa, (5), 7.8.2002. Addimass, (1), 30.4.2003. Qatana, (1), 14.8.2003. Attall, (13), 3.9.2001; (12), 26.9.2001; (10),

25.10.2001; (2), 21.11.2001; (1), 27.12.2001; (1), 14.3.2002; (1), 26.6.2002; (11), 10.7.2002; (25), 5.9.2002; (1), 24.8.2003. Kharabo, (1), 25.10.2001; (1), 21.11.2001; (1), 27.3.2002; (1), 25.9.2002; (11), 2.7.2003. Ma`adamiyeh Al-sham, (1), 6.12.2001; (1), 6.3.2002; (1), 30.8.2002; (1), 4.10.2002; (1), 1.11.2002; (1), 11.7.2003; (3), 23.7.2003; (5), 27.7.2003; (1), 9.8.2003. **Al-Quneitra:** Masehara, (1), 13.8.2001. Jubata Al-Khashab, (1), 20.3.2002; (4), 28.2.2002; (5), 16.4.2003; (1), 26.8.2003. Hadar, (5), 10.9.2001. Ophania, (1), 10.9.2001. Beer Ajam, (8), 20.3.2002; (5), 12.9.2002; (3), 2.10.2002; (2), 19.3.2003. **As`Sweida:** Al-Kafr, (2), 18.10.2001; (1), 9.5.2002; (1), 17.7.2002. Ein alarab, (1), 6.6.2002; (1), 23.10.2002. Orman Mountain, (12), 27.9.2001; (1), 21.8.2002. Orman (1), 4.7.2002. Taamri Mountain, (1), 5.8.2003. Qanawat, (1), 12.8.2001; (3), 20.9.2001; (1), 13.3.2002. Shahba, (4), 23.3.2002. Salkhad, (7), 22.11.2001. Baka, (1), 20.9.2001. Taima, (4), 11.9.2001. Alqrayya, (12), 20.9.2001. **Dar`a:** Wadi Jeelin, (3), 21.9.2001; (2), 24.10.2001; (4), 22.11.2001; (2), 7.2.2002; (2), 29.5.2002; (5), 3.7.2002; (2), 18.7.2002; (9), 22.8.2002. Zeizon, (1), 20.12.2001; (1), 25.4.2002; (3), 2.10.2002.

Remarks: This is a Palaearctic species (Gourreau, 1974). Listed by El Hariri (1971) as *Scymnus quadrimaculatus pictus* in Syria. Reported from Palestine, the Golan Heights, Mount Hermon and Lebanon (Canepari and Tedeschi, 1977; Halperin *et al.*, 1995). It feeds on scale insects (Klausnitzer and Klausnitzer, 1986).

Host species: *Amygdalus* sp., *Citrus* sp., *Cupressus* sp., *Ficus carica*, *Juglans regia*, *Morus alba*, *Nerium oleander*, *Olea europaea*, *Prunus vulgaris*, *Pinus* sp., *Pistacia vera*, *Phaseolus vulgaris*, *Populus* sp., *Prunus armeniaca*, *Prunus avium*, *Punica granatum*, *Pyrus communis*, *Quercus calliprinos*, *Rubus idaeus*, *Schinus molle*, and thistle plants.

***Nephus (Sidis) caucasicus* Weise, 1929 (Figs. 2O and 3O)**

Material examined (1): Damascus Rural: Attall, (1), 27.12.2001.

Remarks: This species is recorded for the first time in Syria. Previously recorded from Turkey and the Caucasus (Fürsch, 1965).

Host species: *Urtica* sp.

***Nephus (Sidis) hiekei* Fürsch, 1965 (Figs. 2P and 3P)**

Material examined (2): Damascus Rural: Jeessrin, (1), 29.12.2002. **Dar`a:** Zeizon, (1), 20.12.2001.

Remarks: This species is recorded for the first time in Syria. This species is widely distributed throughout southern Europe and the Middle East (Raimundo and van Harten, 2000), with records from Lebanon and Palestine on *Pseudococcus citri* (Fürsch, 1967b).

Host species: *Urtica* sp.

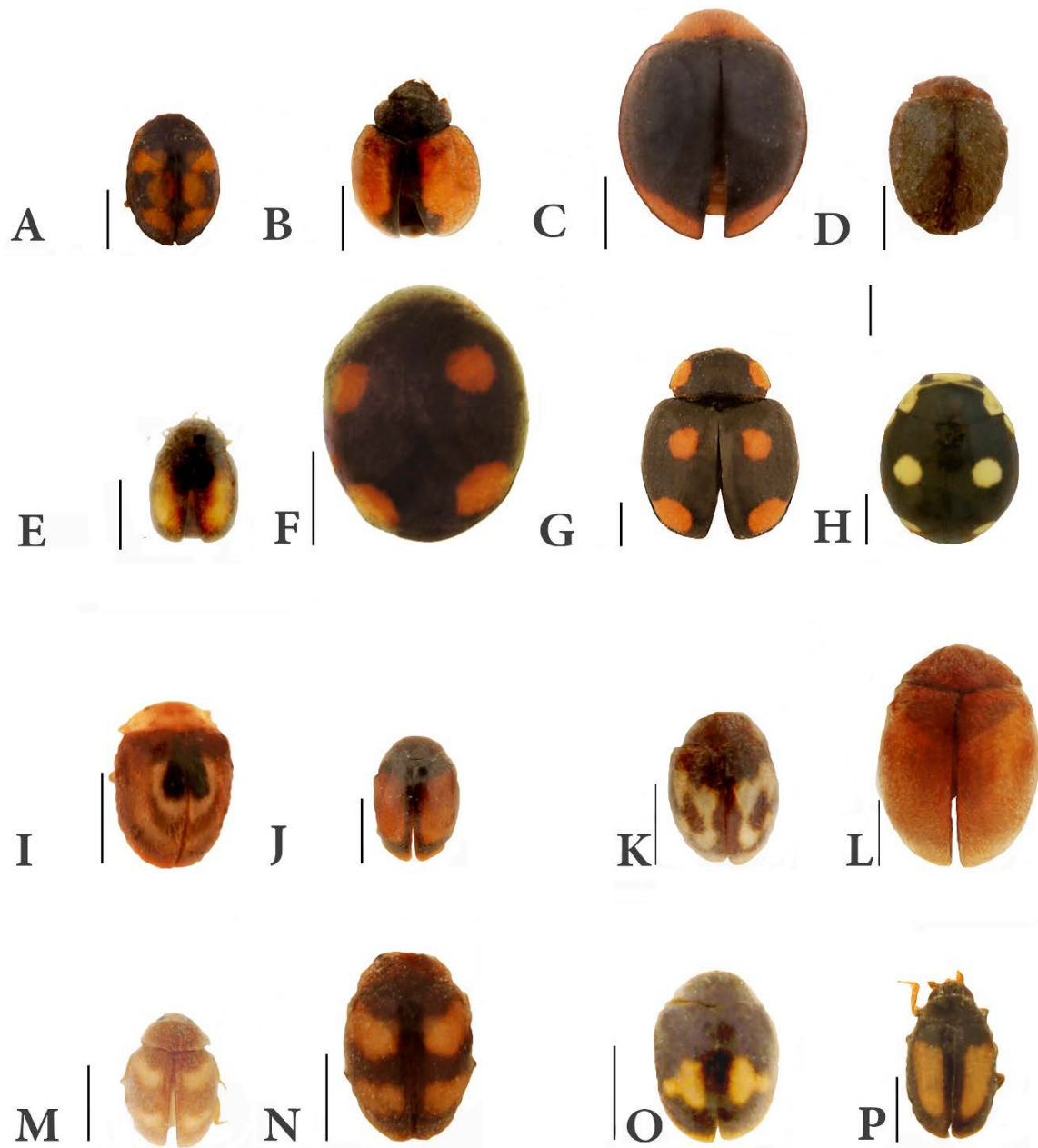


Figure 2: A. *Pharoascymnus ovoideus*. B. *Pharoascymnus setulosus*. C. *Cryptolaemus montrouzieri*. D. *Lindorus lophantae*. E. *Diomus rubidus*. F. *Hyperaspis (Hyperaspis) femorata*. G. *Hyperaspis (Hyperaspis) histeroideus*. H. *Hyperaspis (Hyperaspis) syriaca*. I. *Clitostethus arcuatus*. J. *Nephus (Bipunctatus) bipunctatus*. K. *Nephus (Bipunctatus) includens*. L. *Nephus (Nephus) ludyi*. M. *Nephus (Nephus) merkli*. N. *Nephus (Nephus) quadrimaculatus*. O. *Nephus (Sidis) caucasicus*. P. *Nephus (Sidis) hiekei*. Scale bar=1 mm.

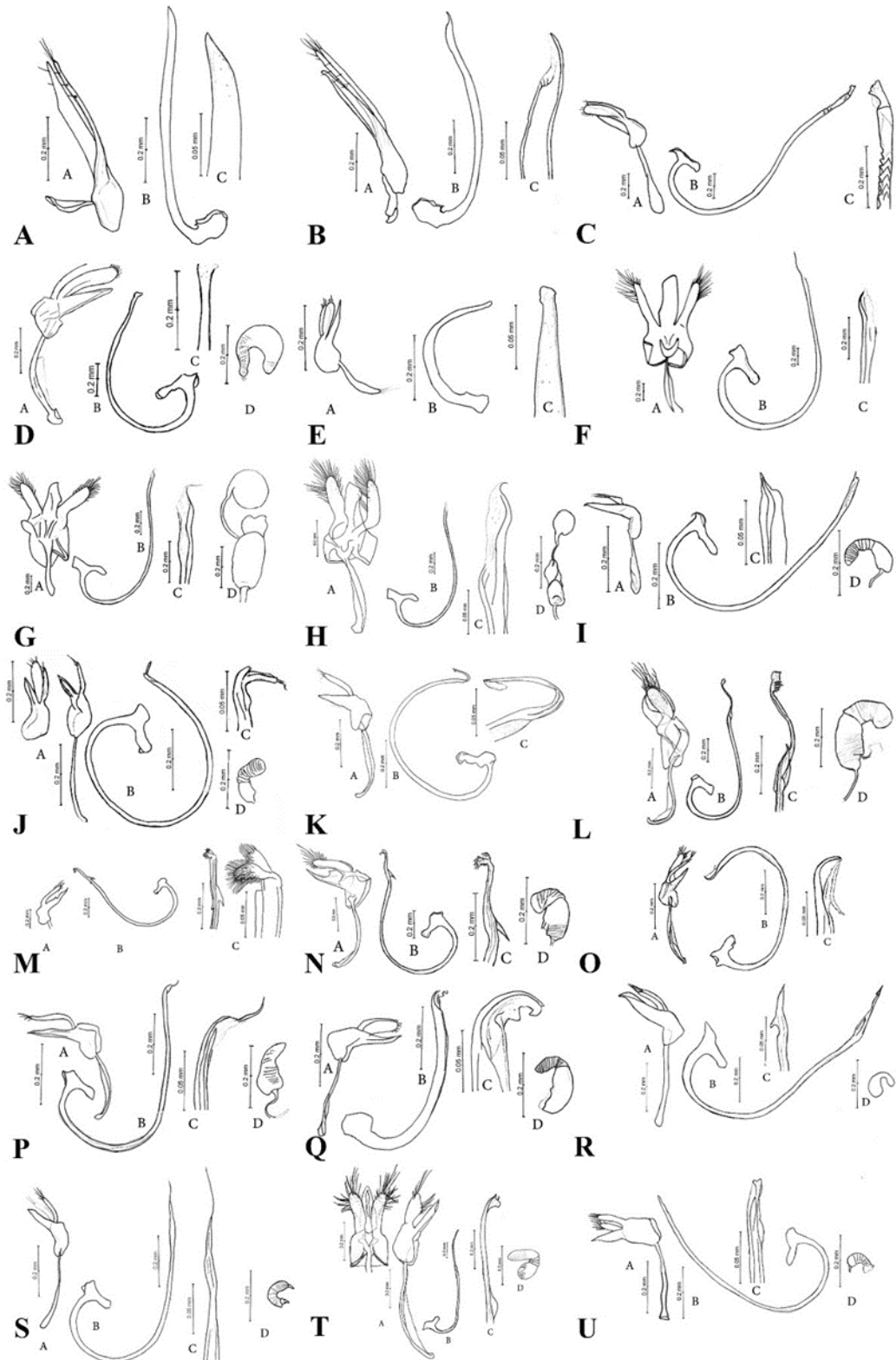


Figure 3: A. *Pharoscymnus ovoideus*. B. *Pharoscymnus setulosus*. C. *Cryptolaemus montrouzieri*. D. *Lindorus lophantae*. E. *Diomus rubidus*. F. *Hyperaspis (Hyperaspis) femorata*. G. *Hyperaspis (Hyperaspis) histeroides*. H. *Hyperaspis (Hyperaspis) syriaca*. I. *Clitostethus arcuatus*. J. *Nephus (Nephus) bipunctatus*. K. *Nephus (Nephus) includens*. L. *Nephus (Nephus) ludyi*. M. *Nephus (Nephus) merkli*. N. *Nephus (Nephus) quadrimaculatus*. O. *Nephus (Nephus) caucasicus*. P. *Nephus (Nephus) hiekei*. Q. *Nephus (Nephus) kreissli*. R. *Scymnus (Mimopullus) pharaonis*. S. *Scymnus (Mimopullus) flagellisiphonatus*. T. *Scymnus (Mimopullus) flavicollis*. U. *Scymnus (Mimopullus) marinus*. Key to darwings: A= Tegmen, B= Penis, C= Penis apex, D= Spermatheca.

***Nephus (Sidis) kreissli* Fürsch and Uygun, 1980 (Figs. 4A and 3Q)**

Material examined (27): Damascus Rural: Attall, (2), 26.9.2001; (1), 25.10.2001; (1), 21.11.2001; (4), 14.3.2002; (9), 8.5.2002; (2), 26.6.2002; (1), 5.9.2002. Ma`adamiyeh Al-sham, (1), 23.6.2003. **Dar`a:** Wadi Jeelin, (1), 22.11.2001; (1), 18.7.2002; (1), 22.8.2002. Zeizon, (1), 22.8.2002; (2), 23.4.2003.

Remarks: This species is recorded for the first time in Syria. This species was known from Turkey (Fürsch and Uygun, 1980).

Host species: *Citrus* sp., *Ficus carica*, *Inula viscosa*, *Malus communis*, *Morus alba*, *Nerium oleander*, *Punica granatum*, *Populus* sp., *Rubus idaeus*, *Urtica* sp. and *Vitex agnus-castus*.

***Scymnus (Mimopullus) pharaonis* Motschulsky, 1851 (Figs. 4B and 3R)**

Material examined (317): Damascus Rural: Wadi Al-Qaren, (6), 19.9.2001; (1), 5.9.2002; (8), 10.7.2002; (1), 15.6.2002; (1), 17.11.2002. Yabrud, (1), 8.8.2002. Kharabo, (1), 26.9.2001; (2), 25.10.2001. Ma`adamiyeh Al-sham, (3), 6.12.2001; (4), 28.6.2002; (11), 30.8.2002; (8), 9.9.2002; (10), 4.10.2002; (2), 1.11.2002; (1), 23.6.2003; (10), 11.7.2003; (2), 23.7.2003; (1), 13.8.2003. Sasaa, (1), 3.10.2002; (3), 12.9.2002. Kulaiaa, (17), 7.8.2002. Dorin, (1), 10.7.2002. Beet-jen Mazraa, (5), 3.10.2001; (1), 8.11.2001; (1), 7.8.2002. Erneh, (7), 21.9.2001. Beqaasem, (2), 21.9.2001; (1), 11.7.2002; (3), 29.8.2002. Muqr Almeer, (1), 26.8.2003. Kafr- Hawar, (1), 7.8.2002. Deir Al-ashairr, (1), 17.9.2002. Addimass, (1), 17.9.2002. Al-Qutayfeh, (3), 8.8.2002. Qatana, (2), 14.8.2003. Assaida Zainab, (1), 13.3.2002. Ashiphonieh, (1), 25.9.2002. Attall, (1), 26.9.2001; (2), 26.6.2002; (3), 10.7.2002; (1), 20.11.2002. **As`Sweida:** Al-Kafr, (3), 20.9.2001; (2), 29.11.2001. Ein alarab, (1), 7.8.2001; (2), 17.7.2002; (1), 1.8.2002. Orman, (1), 27.9.2001; (3), 4.7.2002, (3), 17.7.2002; (1), 6.6.2003. Ghoujygujyat Mountain, (1), 4.7.2002; (4), 1.8.2002; (2), 21.8.2002; (1), 10.9.2002; (4), 23.10.2002; (3), 4.8.2003. Taamri Mountain, (1), 17.7.2002; (2), 4.7.2003; (1), 14.7.2003; (4), 25.7.2003; (7), 5.8.2003; (4), 8.8.2003. Orman Mountain, (4), 4.8.2003. Qanawat, (2), 11.9.2001; (12), 20.9.2001; (1), 19.6.2002; (3), 1.8.2002; (3), 21.8.2002. Shahba, (1), 19.6.2002. Alqrayya, (14), 20.9.2001. **Dar`a:** Jeelin, (9), 3.7.2002, Wadi Jeelin, (4), 18.7.2002; (1), 22.8.2002. Zeizon, (1), 29.5.2002; (1), 22.8.2002; (2), 2.10.2002; (2), 13.11.2002; (1), 19.3.2003. Mzireeb, (1), 9.5.2002. Nahaj, (9), 4.10.2001; (5), 24.10.2001. Tafas, (1), 4.9.2001. Sahm al-joulan, (12), 4.9.2001. Namer, (3), 20.6.2002. **Al-Quneitra:** Beer Ajam, (2), 20.3.2002; (1), 27.6.2002; (9), 12.9.2002; (10), 2.10.2002. Jubata Al-Khashab, (1), 10.9.2001; (1), 20.3.2002; (1), 10.4.2002. Hadar, (2), 31.7.2002; (9), 12.9.2002; (1), 26.8.2003.

Remarks: Its distribution range extends from Central Asia to North Africa to Europe (Gourreau, 1974; Uygun, 1981). *Scymnus (Mimopullus) araraticus* Iablokoff-Khnzorian, 1969 is now considered a synonym for *S. pharaonis* (Kovář 2007). It was recorded by Almatni and Khalil (2008).

Host species: *Aloysia citrodora*, *Amygdalus* sp., *Prunus armeniaca*, *Cedrus libani*, *Citrus* sp., *Cupressus* sp., *Faba vulgaris*, *Ficus carica*, *Hibiscus esculentus*,

Juglans regia, *Lonicera japonica*, *Malus communis*, *Medicago sativa*, *Morus alba*, *Olea europaea*, *Pinus* sp., *Phaseolus vulgaris*, *Pistacia vera*, *Platanus orientalis*, *Populus* sp., *Prunus avium*, *Prunus mahaleb*, *Prunus persica*, *Punica granatum*, *Pyrus communis*, *Quercus calliprinos*, *Triticum* sp. and thistle plants.

***Scymnus (Mimopullus) flagellisiphonatus* Fürsch, 1969 (Figs. 4C and 3S)**

Material examined (26): Al-Quneitra: Beer Ajam, (2), 20.3.2002. Jubata Al-Khashab, (1), 25.4.2002; (1), 16.5.2002. Trounja, (1), 10.4.2002. Masehara, (1), 2.5.2002. **Damascus Rural:** Attall, (1), 26.9.2001. Beet-jen Mazraa, (1), 10.4.2002. Kharabo, (1), 23.5.2002. Serghaya, (1), 30.5.2002, Ma`adamiyeh Al-sham, (1), 12.4.2002; (1), 13.8.2003. **As`Sweida:** Al-Kafr, (1), 9.5.2002, Orman, (1), 4.7.2002. Ghoujygujyat Mountain, (1), 4.7.2002. Qanawat, (5), 11.4.2002. **Dar`a:** Jeelin, (1), 10.8.2001; (1), 3.7.2002. Wadi Jeelin, (1), 28.3.2002. Zeizon, (1), 10.4.2002, Sabsaba, (2), 10.4.2002.

Remarks: Known from the Mediterranean Region (Uygun, 1981) and recorded from Wadi Al Qaren in Syria by Kabakibi (1993). It feeds on aphids (Canepari, 1991).

Host species: *Amygdalus* sp., *Juglans regia*, *Medicago sativa*, *Pinus* sp., *Pistacia vera*, *Prunus avium*, *Punica granatum* and *Quercus calliprinos*.

***Scymnus (Mimopullus) flavicollis* Redtenbacher, 1844 (Figs. 4D and 3T)**

Material examined (416): Damascus Rural: Kharabo, (3), 22.8.2001; (1), 26.9.2001; (1), 25.10.2001; (1), 15.5.2002; (23), 23.5.2002; (6), 5.6.2002; (8), 11.7.2002; (2), 24.7.2002; (5), 11.9.2002; (3), 25.9.2002; (6), 9.10.2002; (13), 25.5.2003; (10), 2.7.2003; (2), 6.8.2003. Serghaya, (6), 7.11.2001; (4), 10.7.2002; (14), 24.7.2002; (18), 14.8.2002; (20), 5.9.2002; (21), 17.9.2002; (12), 3.10.2002; (3), 7.11.2002; (1), 10.4.2003; (1), 22.5.2003; (7), 26.6.2003; (12), 29.7.2003. Ma`adamiyeh Al-sham, (1), 23.5.2002; (10), 28.6.2002; (7), 30.8.2002; (2), 9.9.2002; (4), 4.10.2002; (2), 1.11.2002; (3), 19.5.2003; (13), 23.6.2003; (19), 11.7.2003; (8), 23.7.2003; (1), 9.8.2003; (3), 13.8.2003. Yabrud, (2), 25.10.2001. Sasaa, (1), 31.7.2002; (1), 12.9.2002. Dorin, (2), 10.7.2002. Beet-jen Mazraa, (2), 7.8.2002; (6), 29.8.2002. Zarzar, (3), 19.9.2001. Al Hameh, (9), 14.6.2003. Azzabadani, (2), 27.6.2002. Sarkha, (1), 26.6.2002. Qatana, (3), 5.7.2002. Airport Street, (1), 28.8.2001. Haran Al-awameed, (3), 24.7.2002. Assaida Zainab, (6), 11.9.2001; (2), 18.10.2001. Ashiphonieh, (2), 25.9.2002. Attall, (5), 26.9.2001; (1), 25.10.2001; (8), 26.6.2002; (26), 10.7.2002; (1), 5.9.2002. **As`Sweida:** Ein alarab, (3), 28.6.2002; (3), 1.8.2002; (1), 23.10.2002; (5), 4.8.2003. Orman, (1), 27.9.2001; (18), 4.7.2002; (1), 11.7.2002; (5), 17.7.2002; (2), 12.6.2003. Orman Mountain, (1), 4.7.2002. **Dar`a:** Wadi Jeelin, (1), 22.11.2001; (1), 22.8.2002. Jeelin, (2), 3.7.2002. Namer, (3), 20.6.2002. **Al-Quneitra:** Beer Ajam, (3), 12.9.2002; (1), 2.10.2002. Hadar, (1), 10.9.2002. Trounja, (1), 28.2.2002.

Remarks: Recorded from Iran, Palestine and the Golan Heights (Ahmadi and Yazdani 1993; Halperin *et al.*, 1995). Listed for Syria by El Hariri (1968 and 1971).

Host species: *Althaea officinalis*, *Amygdalus* sp., *Prunus armeniaca*, *Capsicum annum*, *Cedrus libani*,

Citrus sp., *Cucumis melo*, *Cucurbita pepo*, *Cydonia vulgaris*, *Dacus carota*, *Elaeagnus angustifolia*, *Euphorbia* sp., *Ficus carica*, *Foeniculum vulgare*, *Glycyrrhiza glabra*, *Hypericum trinquetifolium*, *Inula viscosa*, *Juglans regia*, *Malus communis*, *Medicago sativa*, *Morus alba*, *Nerium oleander*, *Oncium* sp., *Phaseolus vulgaris*, *Populus* sp., *Prunus avium*, *Prunus mahaleb*, *Punica granatum*, *Pyrus communis*, *Quercus calliprinos*, *Rosa* sp., *Rubus idaeus*, *Solanum melongena*, *Schinus molle*, *Triticum* sp., *Urtica* sp., *Zea mays*, and thistle plants.

***Scymnus (Mimopullus) marinus* Mulsant, 1850 (Figs. 4E and 3U)**

Material examined (109): Damascus Rural: Ma`adamiyeh Al-sham, (2), 6.12.2001; (3), 28.6.2002; (5), 30.8.2002; (4), 9.9.2002; (8), 4.10.2002; (13), 1.11.2002; (5), 4.12.2002; (1), 5.2.2003; (6), 11.7.2003; (2), 23.7.2003; (2), 13.8.2003. Assaida Zainab, (1), 13.3.2002. **As`Sweida:** Taamri Mountain, (4), 6.6.2003; (6), 20.6.2003; (5), 4.7.2003; (1), 14.7.2003; (4), 25.7.2003; (9), 5.8.2003; (6), 8.8.2003. Orman, (3), 6.6.2003. Ghoujygujyat Mountain, (2), 12.6.2003. Shahba, (1), 19.6.2002; (3), 11.12.2002. Barad, (1), 18.10.2001. Baka, (1), 20.9.2001. Taima, (7), 11.9.2001. Tal-loz, (3), 12.8.2001. **Dar`a:** Wadi Jeelin, (1), 22.11.2001.

Remarks: This species is recorded for the first time in Syria. It is distributed in Europe and North Africa (Gourreau, 1974) and was recorded from Palestine (Halperin *et al.*, 1995). *Scymnus mediterraneus* Iablokoff-Khnzorian, 1972 is considered as a synonym (Kovář, 2007).

Host species: *Aloisia citrodora*, *Amygdalus* sp., *Biota orientalis*, *Citrus* sp., *Cupressus* sp., *Faba vulgaris*, *Juglans regia*, *Olea europaea*, *Pinus* sp., *Pistacia vera*, *Phaseolus vulgaris*, *Prunus armeniaca*, *P. avium* and *Punica granatum*.

***Scymnus (Parapullus) abietis* (Paykull, 1798) (Figs. 4F and 5A)**

Material examined (2): Damascus Rural: Wadi Al-Qaren, (1), 19.8.2001. **As`Sweida:** Orman, (1), 17.7.2002.

Remarks: This species is recorded for the first time in Syria. Distribution of this species extends from Europe, North Africa to Mongolia and the Russian Far East (Gourreau, 1974, Kuznetsov, 1997; Kovář, 2007).

Host species: *Pinus* sp. and *Quercus calliprinos*.

***Scymnus (Pullus) apetzii* Mulsant, 1846 (Figs. 4G and 5B)**

Material examined (403): Damascus Rural: Kharabo, (1), 22.8.2001; (1), 26.9.2001; (1), 25.10.2001; (11), 23.5.2002; (1), 5.6.2002; (2), 11.7.2002; (5), 24.7.2002; (1), 11.9.2002; (7), 25.9.2002; (4), 9.10.2002; (9), 25.5.2003; (8), 2.7.2003; (3), 6.8.2003. Serghaya, (2), 7.11.2001; (2), 30.5.2002; (1), 27.6.2002; (4), 10.7.2002; (6), 24.7.2002; (22), 14.8.2002; (17), 15.9.2002; (32), 17.9.2002; (18), 3.10.2002; (1), 7.11.2002; (1), 10.4.2003; (1), 22.5.2003; (6), 26.6.2003; (13), 29.7.2003. Ma`adamiyeh Al-sham, (12), 28.6.2002; (3), 30.8.2002; (1), 9.9.2002; (1), 4.10.2002; (1), 19.5.2003; (7), 23.6.2003; (11), 11.7.2003; (3), 23.7.2003; (1), 9.8.2003. Wadi Al-Qaren, (2), 10.7.2002. Sasaa, (1), 2.5.2002; (1), 12.6.2002; (2), 31.7.2002. Kulaiaa, (1), 7.8.2002. Dorin, (1), 24.8.2003. Beet-jen Mazraa, (2), 7.8.2002; (6), 29.8.2002. Erneh, (2), 11.7.2002. Beqaasem, (1),

21.9.2001; (1), 11.7.2002. Muqr Almeer, (1), 26.8.2003. Zarzar, (2), 19.9.2001. Deir Al-ashairr, (1), 17.10.2001. Al-Hameh, (7), 16.4.2003. Azzabadani, (5), 27.6.2002; (1), 14.6.2003. Al-Qutayfeh, (3), 8.8.2002. Qatana, (2), 14.8.2003. Ashiphonieh, (1), 25.9.2002. Attall, (3), 26.9.2001; (2), 25.10.2001; (3), 8.5.2002; (3), 26.6.2002; (20), 10.7.2002; (2), 5.9.2002; (7), 14.8.2003. **As`Sweida:** Ein alarab, (1), 27.9.2001; (7), 28.6.2002; (2), 4.7.2002; (15), 1.8.2002; (4), 23.10.2002; (3), 22.7.2003; (8), 4.8.2003. Orman Mountain, (1), 1.8.2001; (7), 1.8.2002. Orman, (1), 27.9.2001; (1), 24.6.2002; (21), 4.7.2002; (1), 17.7.2002; (1), 10.7.2002; (1), 12.6.2003. Taamri Mountain, (1), 1.8.2002, Ghoujygujyat Mountain, (5), 23.10.2002. Qanawat, (1), 18.10.2001; (1), 13.3.2002; (1), 1.8.2002. Alqrayya, (1), 20.9.2001. **Dar`a:** Jeelin, (2), 3.7.2002. Wadi Jeelin, (2), 3.7.2002. Zeizon, (1), 29.5.2002; (1), 22.8.2002. Sheikh Miskin, (2), 30.8.2001; (1), 27.5.2003. Nahaj, (3), 4.10.2001. Namer, (1), 26.6.2002. **Al-Quneitra:** Beer Ajam, (2), 12.9.2002. Jubata Al-Khashab, (1), 26.8.2003.

Remarks: This species has a wide range of distribution in Central Europe, the Mediterranean Region, including North Africa and Middle Asia (Gourreau, 1974). It recorded by Almatni and Khalil (2008).

Host species: *Althaea officinalis*, *Amygdalus* sp., *Prunus armeniaca*, *Capsicum annum*, *Cedrus libani*, *Citrus* sp., *Cucumis melo*, *Cucurbita pepo*, *Cydonia vulgaris*, *Dacus carota*, *Elaeagnus angustifolia*, *Euphorbia* sp., *Ficus carica*, *Foeniculum vulgare*, *Glycyrrhiza glabra*, *Hypericum trinquetifolium*, *Inula viscosa*, *Juglans regia*, *Malus communis*, *Medicago sativa*, *Morus alba*, *Nerium oleander*, *Oncium* sp., *Phaseolus vulgaris*, *Populus* sp., *Prunus avium*, *Prunus mahaleb*, *Punica granatum*, *Pyrus communis*, *Quercus calliprinos*, *Rosa* sp., *Rubus idaeus*, *Solanum melongena*, *Schinus molle*, *Triticum* sp., *Urtica* sp., *Zea mays*, and thistle plants.

***Scymnus (Pullus) auritus* Thunberg, 1795 (Figs. 4H and 5C)**

Material examined (5): Al-Quneitra: Jubata Al-Khashab, (1), 16.5.2002. **Damascus Rural:** Wadi Al-Qaren, (2), 5.9.2002. Sasaa, (1), 12.9.2002. Erneh, (1), 11.7.2002.

Remarks: This species is recorded for the first time in Syria. It is distributed in the largest part of temperate Eurasia (Gourreau, 1974; Kovář, 2007). Uygun (1981) reported this species from Turkey It feeds on aphids.

Host species: *Amygdalus* sp., *Malus communis* and *Quercus calliprinos*.

***Scymnus (Pullus) fraxini* Mulsant, 1850 (Figs. 4I and 5D)**

Material examined (62): Al-Quneitra: Beer Ajam, (25), 12.9.2002; (17), 2.10.2002. Jubata Al-Khashab, (4), 10.9.2001; (1), 8.11.2001; (8), 25.4.2002; (5), 16.5.2002; (1), 31.7.2002; (1), 29.8.2002.

Remarks: This species is recorded for the first time in Syria. Reported in the Balkans and other parts of Europe (Gourreau, 1974).

Host species: *Quercus calliprinos*.

***Scymnus (Pullus) subvillosus* (Goeze, 1777) (Figs. 4J and 5E)**

Material examined (316): Damascus Rural: Wadi Al-Qaren, (1), 19.9.2002; (2), 5.9.2002. Nasseria, (1),

5.6.2002. Beet-jen Mazraa, (1), 10.4.2002; (1), 7.8.2002. Erneh, (2), 11.7.2002. Beqaasem, (1), 21.9.2001. Deir Al-ashairr, (4), 17.10.2001; (1), 28.11.2002. Addimass, (1), 30.4.2003. Rankus Mountain (1), 21.5.2003. Attall, (1), 10.7.2002. Kharabo, (4), 22.8.2001; (2), 25.10.2001; (1), 21.11.2001; (2), 23.5.2002; (1), 11.7.2002; (3), 8.8.2002; (1), 9.10.2002; (1), 27.11.2002; (3), 13.5.2003; (3), 25.5.2003; (2), 2.7.2003. Serghaya, (1), 5.9.2002. Ma`adamiyeh Al-sham, (4), 23.5.2002; (1), 4.12.2002; (1), 9.4.2003. **Al-Quneitra:** Beer Ajam, (6), 20.3.2002; (1), 27.6.2002; (1), 12.9.2002; (2), 19.3.2003. Jubata Al-Khashab, (1), 20.3.2002; (1), 10.4.2002; (2), 25.4.2002; (2), 16.5.2002; (1), 16.4.2003. Trounja, (1), 10.4.2002. **As`Sweida:** Al-Kafr, (11), 18.10.2001; (20), 29.11.2001; (11), 24.4.2002; (6), 9.5.2002; (3), 6.6.2002; (1), 17.7.2002; (4), 23.10.2002; (3), 11.5.2003; (1), 12.6.2003. Ein alarab, (4), 9.5.2002; (2), 28.6.2002; (1), 4.7.2002; (4), 17.7.2002; (4), 1.8.2002; (1), 10.9.2002; (2), 12.6.2002. Orman Mountain, (3), 11.4.2002; (1), 9.4.2003. Orman, (4), 21.6.2002; (3), 24.6.2002; (12), 4.7.2002; (6), 17.7.2002; (8), 6.6.2003; (3), 4.8.2003. Taamri Mountain, (1), 21.6.2002; (1), 17.7.2002; (1), 1.8.2002; (2), 21.8.2002; (3), 6.6.2003; (1), 20.6.2003; (1), 28.6.2003; (6), 4.7.2003; (12), 14.7.2003; (6), 25.7.2003; (1), 5.8.2003; (2), 8.8.2003. Ghoujygujyat Mountain, (2), 4.7.2002; (9), 23.10.2002; (4), 4.8.2003. Qanawat, (7),

11.9.2001; (3), 20.9.2001; (4), 18.10.2001; (10), 13.3.2002; (4), 3.4.2002; (14), 11.4.2002; (2), 9.5.2002; (1), 6.6.2002; (2), 19.6.2002; (1), 1.8.2002. Shahba, (5), 13.3.2002; (1), 11.4.2002; (1), 11.12.2002. Salkhad, (1), 22.11.2001. **Dar`a:** Jeelin, (1), 18.7.2002. Zeizon, (1), 21.3.2002; (1), 29.5.2002. Sheikh Miskin, (2), 20.6.2002; (4), 27.5.2003; (10), 22.7.2003. Nahaj, (1), 4.10.2001; (2), 24.10.2001. Fakiia, (1), 28.3.2002. Sahn al-joulan (2), 4.9.2001.

Remarks: Recorded from the Mediterranean Region, Central Europe to North Africa and eastwards to western Asia (Uygun, 1981; Fürsch, 1989; Raimundo and van Harten, 2000). Recorded from Mount Hermon and the Golan Heights (Halperin *et al.*, 1995) and from Wadi Al Qaren (Kabakibi, 1993).

Host species: *Amygdalus* sp., *Cedrus libani*, *Citrus* sp., *Cucumis melo*, *Cupressus* sp., *Euphorbia* sp., *Eucalyptus camaldulensis*, *Ficus carica*, *Galium* sp., *Hypericum trinquetifolium*, *Juglans regia*, *Ligustrum* sp., *Malus communis*, *Medicago sativa*, *Morus alba*, *Nerium oleander*, *Pinus* sp., *Prunus armeniaca*, *Prunus spinosa*, *P. mahaleb*, *Prunus persica*, *Punica granatum*, *Pyrus communis*, *Quercus calliprinos*, *Robinia pseudoacacia*, *Rubus idaeus*, *Spartium junceum*, *Zea mays*, and thistle plants.

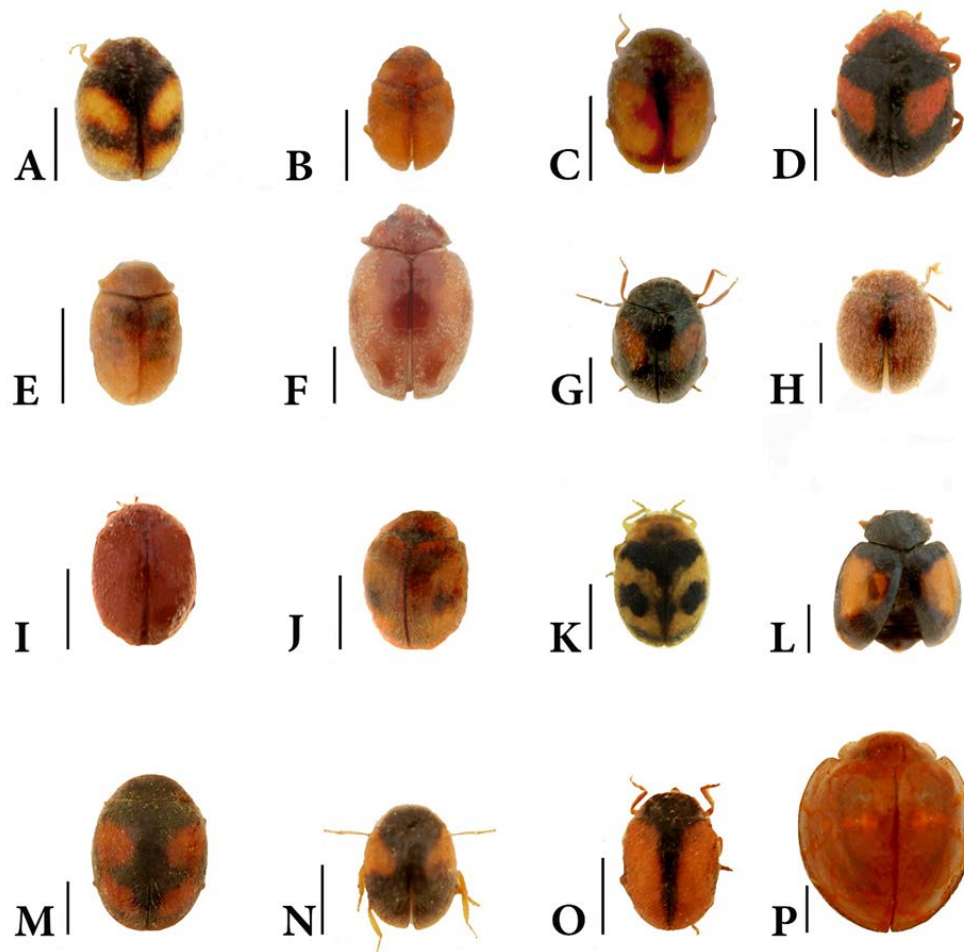


Figure 4: A. *Nephus (Sidis) kreissli*. B. *Scymnus (Mimopullus) pharaonis*. C. *Scymnus (Mimopullus) flagellisiphonatus*. D. *Scymnus (Mimopullus) flavicollis*. E. *Scymnus (Mimopullus) marinus*. F. *Scymnus (Parapullus) abietis*. G. *Scymnus (Pullus) apetzii*. H. *Scymnus (Pullus) auritus*. I. *Scymnus (Pullus) fraxini*. J. *Scymnus (Pullus) subvillosus*. K. *Scymnus (Pullus) syriacus*. L. *Scymnus (Scymnus) bivulnerus*. M. *Scymnus (Scymnus) frontalis*. N. *Scymnus (Scymnus) interruptus*. O. *Scymnus (Scymnus) nubilis*. P. *Chilocorus bipustulatus*. Scale bar= 1 mm.

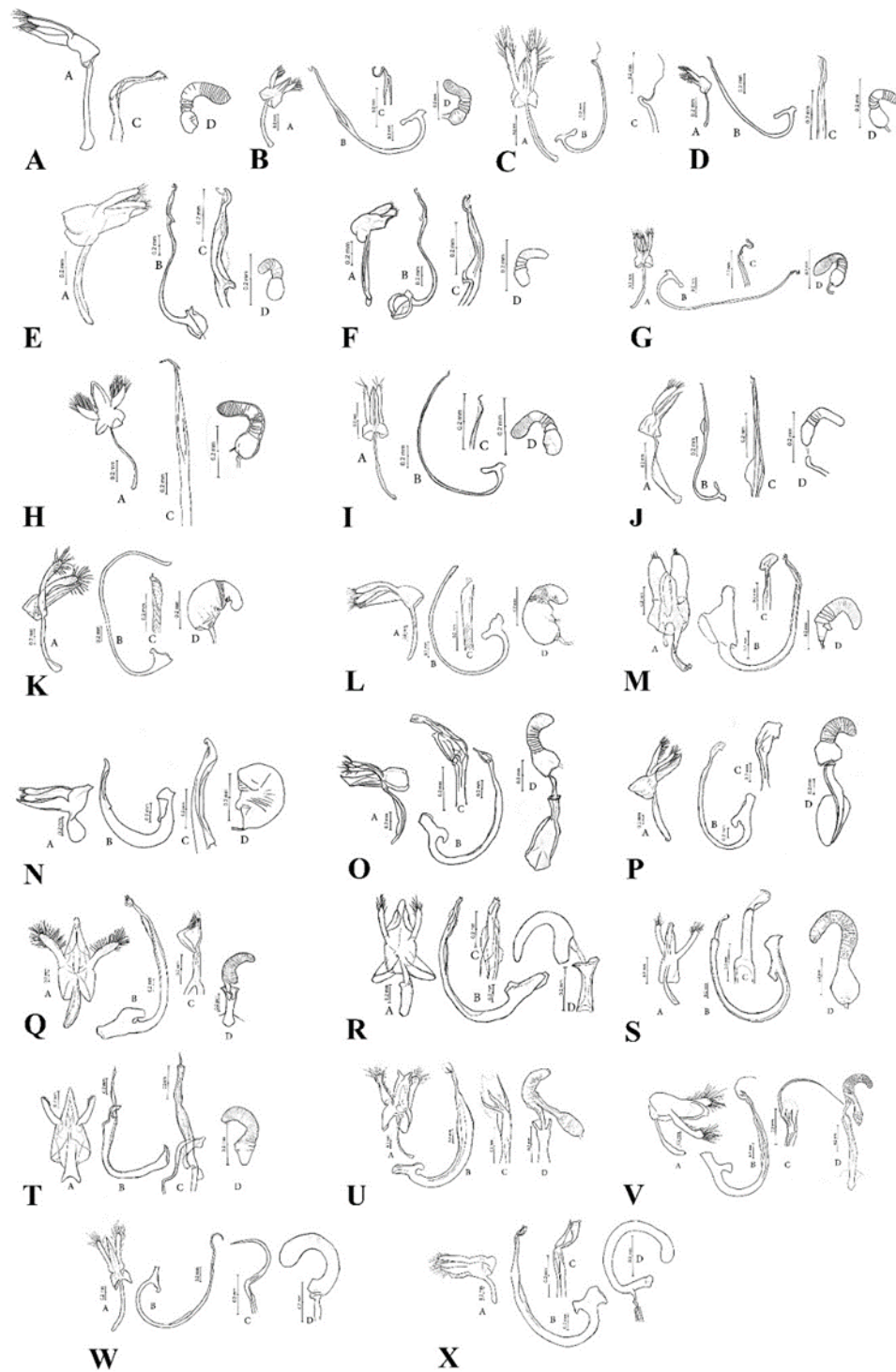


Figure 5: A. *Scymnus (Parapullus) abietis*. B. *Scymnus (Pullus) apetzi*. C. *Scymnus (Pullus) auritus*. D. *Scymnus (Pullus) fraxini*. E. *Scymnus (Pullus) subvillosus*. F. *Scymnus (Pullus) syriacus*. G. *Scymnus (Scymnus) bivulnerus*. H. *Scymnus (Scymnus) frontalis*. I. *Scymnus (Scymnus) interruptus*. J. *Scymnus (Scymnus) nubilus*. K. *Exochomus octosignatus*. L. *Exochomus quadripustulatus*. M. *Platynaspis luteorubra*. N. *Novius cardinalis*. O. *Adalia (Adalia) bipunctata*. P. *Adalia (Adalia) decempunctata*. Q. *Coccinella (Coccinella) septempunctata*. R. *Coccinella undecimpunctata*. S. *Harmonia quadripunctata*. T. *Hippodamia (Adonia) variegata*. U. *Oenopia conglobata*. V. *Oenopia oncina*. W. *Propylea quatuordecimpunctata*. X. *Psyllobora (Thea) vigintiduopunctata*. Key to darwings: A= Tegmen, B= Penis, C= Penis apex, D= Spermatheca.

***Scymnus (Pullus) syriacus* (Marseul, 1868) (Figs. 4K and 5F)**

Material examined (250): Damascus: Damascus, (1), 13.5.2003. **Damascus Rural:** Wadi Al-Qaren, (1), 20.3.2002. Yabrud, (3), 8.8.2002; (1), 11.9.2002. Sasaa, (1), 12.9.2002. Beet-jen Mazraa, (1), 3.10.2001; (1),

8.11.2001; (5), 7.8.2002; (4), 29.8.2002. Erneh, (1), 21.9.2001. Muqr Almeer, (3), 26.8.2003. Addimass, (2), 5.9.2002. Al Hameh, (1), 14.6.2003. Azzabadani, (2), 27.6.2002. Al-Qutayfeh, (9), 15.8.2001; (5), 8.8.2002. Qatana, (3), 14.8.2003. Autaiba, (1), 8.8.2002. Attall, (15), 26.9.2001; (7), 25.10.2001; (7), 26.6.2002; (18),

10.7.2002; (2), 5.9.2002; (4), 24.8.2003. Kharabo, (1), 22.8.2001; (1), 25.10.2001; (1), 23.5.2002; (1), 11.9.2002; (1), 25.9.2002. Ma`adamiyeh Al-sham, (2), 6.12.2001; (3), 6.3.2002; (1), 12.4.2002; (3), 23.5.2002; (4), 9.9.2002; (2), 4.10.2002; (1), 1.11.2002; (2), 4.12.2002; (1), 5.2.2003; (2), 9.4.2003; (7), 23.6.2003; (27), 11.7.2003; (12), 23.7.2003; (4), 27.7.2003; (10), 13.8.2003. **Al-Quneitra:** Beer Ajam, (1), 2.10.2002. Masehara, (2), 13.8.2001. **Dar`a:** Wadi Jeelin, (1), 24.10.2001; (2), 22.11.2001; (1), 7.2.2002; (2), 9.5.2002; (2), 22.8.2002. Zeizon, (1), 8.8.2001; (4), 10.4.2002; (1), 25.4.2002; (1), 9.5.2002; (1), 29.5.2002; (1), 18.7.2002; (2), 18.12.2002; (3), 19.3.2003; (3), 23.4.2003. Sheikh Miskin, (1), 27.5.2003. Sheikh Saad, (1), 13.11.2002. Nahaj, (10), 4.10.2001; (3), 24.10.2001. Sahm al-joulan, (1), 4.9.2001. Namer, (2), 20.6.2002. **As`Sweida:** Al-Kafr, (1), 29.11.2001; (2), 1.8.2002; (1), 29.11.2002. Ein alarab, (1), 29.11.2001; (1), 9.5.2002; (1), 1.8.2002; (1), 10.9.2002; (1), 23.10.2002. Shahba, (4), 23.3.2002; (5), 11.4.2002; (1), 19.6.2002; (1), 11.12.2002.

Remarks: This species is distributed in the Middle East with reports from Syria, Egypt, Iraq, Turkey and Palestine (Uygun, 1981; Halperin *et al.*, 1995). Listed for Syria by El Hariri (1971). Recorded from northern Syria by Ka`ada (2002). In Iran, it has been recorded as a predator of two mealybugs (*Planococcus ficus* and *Phenacoccus solenopsis*) on different hosts (Fallahzadeh *et al.*, 2013).

Host species: *Aloysia citrodora*, *Cedrus libani*, *Citrus* sp., *Elaeagnus angustifolia*, *Ficus carica*, *Hibiscus esculentus*, *Inula viscosa*, *Juglans regia*, *Morus alba*, *Nerium oleander*, *Olea europaea*, *Pinus* sp., *Populus* sp., *Punica granatum*, *Prunus armeniaca*, *Prunus avium*, *Prunus mahaleb*, *Pyrus communis*, *Quercus calliprinos*, *Rubus idaeus*, *Solanum melongena*, *Tamarix orticulatus*, *Vitis vinifera* and *Zea mays*.

Scymnus (Scymnus) bivulnerus Capra and Fürsch, 1967 (Figs. 4L and 5G)

Material examined (52): Damascus Rural: Wadi Al-Qaren, (1), 5.9.2002; (1), 10.7.2002. Yabrud, (1), 25.10.2001. Ma`adamiyeh Al-sham, (1), 28.6.2002; (1), 30.8.2002; (1), 19.5.2003; (4), 23.6.2003; (5), 11.7.2003; (4), 23.7.2003. Nasseria, (1), 5.6.2002. Sasaa, (2), 3.10.2002; (1), 2.5.2002; (6), 26.8.2003. Beet-jen Mazraa, (2), 26.8.2003. Erneh, (1), 11.7.2002; (1), 29.8.2002. Deir Al-ashairr, (5), 17.10.2001. Azzabadani, (2), 17.10.2001. Attawani, (2), 26.6.2002. **As`Sweida:** Ein alarab, (2), 17.7.2002. Orman, (1), 22.9.2002; (2), 4.7.2002. Orman Mountain, (1), 21.8.2002; (1), 4.8.2003. Ghoujygujyat Mountain, (2), 29.4.2003. Qanawat, (1), 6.6.2002.

Remarks: Known from Central and Southern Europe (Gourreau, 1974). Recorded from Palestine (Halperin *et al.*, 1995). Listed by El Hariri (1968) for Syria.

Host species: *Amygdalus* sp., *Citrus* sp., *Cucurbita pepo*, *Daucus carota*, *Eriobotrya japonica*, *Euphorbia* sp., *Faba vulgaris*, *Petrocelinum crispum*, *Populus* sp., *Punica granatum*, *Rubus idaeus*, *Zea mays* and thistle plants.

Scymnus (Scymnus) frontalis (Fabricius, 1787) (Fig. 4M and 5H)

Material examined (60): Damascus Rural: Kharabo, (4), 22.8.2001; (2), 26.9.2001; (1), 27.11.2001; (2), 23.5.2002; (1), 5.6.2002; (5), 11.7.2002; (1), 24.7.2002;

(26), 11.9.2002; (5), 25.9.2002; (1), 9.10.2002; (1), 25.5.2003; (4), 2.7.2003. Serghaya, (1), 10.7.2002; (1), 24.7.2002; (2), 14.8.2002; (2), 3.10.2002; (1), 7.11.2002.

Remarks: This species is known from Central Asia, West Europe, the Middle East and North Africa (Kuznetsov, 1997). It was listed by El Hariri (1971) in Syria.

Host species: *Galium* sp., *Malus communis*, *Medicago sativa*, *Morus alba*, *Triticum* sp., *Urtica* sp., *Zea mays*, and thistle plants.

Scymnus (Scymnus) interruptus (Goeze, 1777) (Figs. 4N and 5I)

Material examined (111): Damascus Rural: Yabrud, (1), 25.10.2001; (2), 26.6.2002. Deir Al-ashairr, (3), 11.6.2002. Al-Hameh, (2), 14.6.2003. Azzabadani, (3), 27.6.2002. Sarkha, (1), 26.6.2002; (1), 11.9.2002. Al-Qutayfeh, (4), 8.8.2002. Qatana, (4), 5.7.2002. Assaida Zainab, (3), 18.10.2001. Ashiphonieh, (1), 25.9.2002. Attall, (5), 26.9.2001; (1), 25.10.2001; (2), 8.5.2002; (11), 26.6.2002; (24), 10.7.2002. Kharabo, (5), 23.5.2002; (1), 11.7.2002; (2), 25.9.2002; (3), 9.10.2002; (3), 2.4.2003; (6), 25.5.2003; (10), 2.7.2003; (1), 6.8.2003. Serghaya, (1), 10.4.2003. Ma`adamiyeh Al-sham, (1), 28.6.2002; (1), 4.7.2002; (3), 23.6.2003; (5), 11.7.2003; (1), 13.8.2003.

Remarks: Known from Central Europe, North Africa and the Middle East (Canepari, 1991). Recorded from northern Syria by Ka`ada (2002).

Host species: *Amygdalus* sp., *Citrus* sp., *Cucurbita pepo*, *Elaeagnus angustifolia*, *Ficus carica*, *Galium* sp., *Juglans regia*, *Malus communis*, *Medicago sativa*, *Morus alba*, *Phaseolus vulgaris*, *Populus* sp., *Punica granatum*, *Rosa* sp., *Rubus idaeus*, *Solanum melongena*, *Triticum* sp., *Urtica* sp., *Zea mays*, and thistle plants.

Scymnus (Scymnus) nubilus Mulsant, 1850 (Figs. 4O and 5J)

Material examined (279): Damascus Rural: Sasaa, (3), 3.10.2002; (1), 7.8.2002; (1), 26.8.2003. Kulaiaa, (2), 7.8.2002. Dorin, (3), 10.7.2002. Zarzar, (1), 14.6.2003. Deir Al-ashairr, (1), 11.6.2002. Qatana, (3), 5.7.2002. Autaiba, (5), 24.7.2002. Assaida Zainab, (8), 18.10.2001; (1), 3.4.2002. Ashiphonieh, (2), 25.9.2002. Attall, (1), 26.9.2001; (6), 26.6.2002; (4), 10.7.2002. Kharabo, (1), 22.8.2001; (2), 25.10.2001; (2), 27.12.2001; (1), 4.5.2002; (2), 15.5.2002; (7), 23.5.2002; (2), 5.6.2002; (15), 11.7.2002; (5), 24.7.2002; (2), 8.8.2002; (3), 11.9.2002; (10), 25.9.2002; (20), 9.10.2002; (1), 29.12.2002; (2), 25.5.2003; (4), 2.7.2003; (1), 6.8.2003. Ma`adamiyeh Al-sham, (1), 23.5.2002; (2), 28.6.2002; (2), 9.9.2002; (1), 1.11.2002; (1), 4.12.2002; (2), 19.5.2003; (30), 23.6.2003; (25), 11.7.2003; (15), 23.7.2003; (5), 13.8.2003. **Al-Quneitra:** Jubata Al-Khashab, (1), 16.5.2002. **As`Sweida:** Ein alarab, (3), 7.8.2001. Ghoujygujyat Mountain, (1), 4.7.2002. Qanawat, (1), 21.8.2002. Saura, (3), 11.6.2002. **Dar`a:** Jeelin, (1), 10.8.2001; (1), 18.7.2002. Wadi Jeelin, (1), 29.5.2002; (3), 3.7.2002; (14), 22.8.2002. Zeizon, (1), 9.5.2002; (3), 29.5.2002; (3), 16.6.2003. Izraa, (1), 27.9.2001. Sheikh Miskin, (4), 20.6.2002; (10), 22.7.2003. Sheikh Saad, (2), 12.5.2003. Karak, (1), 22.8.2002. Nahta, (6), 22.8.2002. Nahaj, (1), 24.10.2001. Sehaileia, (1), 20.6.2002. Tafas, (2), 25.7.2002. Sahm al-joulan, (3), 4.9.2001. Wadi Shihab, (2), 13.5.2003. Namer, (4), 20.6.2002.

Remarks: This species have a wide range of distribution in the Mediterranean Region (Raimundo and van Harten, 2000). Listed by El Hariri (1971) and the Golan Heights (Halperin *et al.*, 1995) in Syria. It feeds on aphids and scale insects. In Iran, it has been recorded as a predator of two mealybugs (*Nipaeococcus viridis* and *Maconellicoccus hirsutus*) on different hosts (Fallahzadeh *et al.*, 2013).

Host species: *Citrus* sp., *Cucumis sativus*, *Cucurbita pepo*, *Cupressus* sp., *Cydonia vulgaris*, *Euphorbia* sp., *Ficus carica*, *Foeniculum vulgare*, *Hibiscus esculentus*, *Juglans regia*, *Medicago sativa*, *Morus alba*, *Nerium oleander*, *Olea europaea*, *Pinus* sp., *Populus* sp., *Prunus armeniaca*, *Prunus vulgaris*, *Punica granatum*, *Quercus calliprinos*, *Solanum melongena*, *Triticum* sp., *Tamarix articulatus*, *Urtica* sp., *Vitis vinifera*, *Vitex agnus-castus*, *Zea mays* and thistle plants.

Tribe Stethorini

Stethorus (*Stethorus*) *gilvifrons* (Mulsant, 1850)

Material examined (1368): **Al-Quneitra:** Beer Ajam, (5), 12.9.2002; (3), 2.10.2002. Jubata Al-Khashab, (2), 10.9.2001; (1), 31.7.2002; (1), 29.8.2002. Hadar, (4), 31.7.2002; (3), 12.9.2002. Masehara, (2), 13.8.2001. **Damascus Rural:** Attall, (1), 26.9.2001; (7), 25.10.2001; (4), 21.11.2001; (1), 27.12.2001; (3), 14.3.2002; (4), 4.4.2002; (1), 8.5.2002; (1), 10.7.2002; (6), 5.9.2002; (7), 20.11.2002; (2), 24.8.2003. Wadi Al-Qaren, (1), 17.11.2001; (3), 5.9.2002. Yabrud, (7), 8.8.2002; (5), 11.9.2002. Sasaa, (4), 13.8.2001; (3), 3.10.2001; (5), 20.3.2002; (7), 2.5.2002; (2), 16.5.2002; (2), 12.6.2002; (1), 7.8.2002; (7), 12.9.2002. Beet-jen Mazraa, (5), 3.10.2001; (1), 7.8.2002; (3), 29.8.2002. Erneh, (7), 21.9.2001; (8), 29.8.2002. Beqaasem, (5), 21.9.2001; (2), 11.7.2002; (1), 29.7.2002. Muqr Almeer, (1), 26.8.2003. Zarzar, (2), 19.9.2001. Deir Al-ashairr, (9), 17.9.2002. Azzabadani, (2), 17.10.2001. Kharabo, (5), 26.9.2001; (8), 25.10.2001; (3), 21.11.2001; (2), 27.12.2001; (6), 23.5.2002; (5), 11.9.2002; (15), 25.9.2002; (18), 9.10.2002; (9), 27.11.2002; (2), 29.12.2002; (3), 9.2.2003; (12), 2.4.2003; (1), 2.7.2003; (2), 6.8.2003. Serghaya, (50), 19.9.2001; (42), 17.10.2001; (9), 7.11.2001; (2), 18.4.2002; (1), 4.5.2002; (1), 10.7.2002; (22), 24.7.2002; (63), 14.8.2002; (39), 5.9.2002; (24), 17.9.2002; (18), 3.10.2002; (16), 7.11.2002; (1), 26.6.2003; (14), 29.7.2003. Ma'adamiyeh Al-sham, (3), 23.5.2002; (46), 30.8.2002; (8), 9.9.2002; (36), 4.10.2002; (30), 1.11.2002; (39), 4.12.2002; (13), 16.1.2003; (8), 5.2.2003; (1), 13.3.2003; (1), 9.4.2003; (1), 23.6.2003. Houch arab (1), 3.9.2001. Assal Alwarded, (14), 26.9.2001. Rankus Mountain, (1), 11.9.2002. Sarkha, (8), 26.9.2001; (31), 11.9.2002. Maalula (4), 2.8.2001. Seydnaya, (1), 2.8.2001. Qatana, (2), 14.8.2003. Ahmadiya, (1), 25.9.2001. Assaida Zainab, (1), 11.9.2001. Jeerlin, (3), 29.12.2002; (5), 9.2.2003. Ashiphonieh, (51), 25.9.2002. Annashabyeh, (2), 21.11.2001; (1), 24.7.2002. **Damascus:** Qasioun, (3), 13.5.2003. **As`Sweida:** Al-Kafr, (8), 20.9.2001. Ein alarab, (28), 7.8.2001; (30), 29.8.2001; (29), 27.9.2001; (6), 18.10.2001; (1), 1.8.2002; (17), 21.8.2002; (48), 10.9.2002; (20), 23.10.2002. Orman Mountain, (18), 1.8.2001; (23), 12.8.2001; (20), 29.8.2001; (15), 27.8.2001; (1), 11.4.2002; (1), 1.8.2002; (49), 10.9.2002; (1), 4.8.2003. Orman, (20), 29.8.2001; (6), 4.7.2002; (6),

17.7.2002. Taamri Mountain, (2), 17.7.2002; (1), 21.8.2002(2), 5.8.2003; (1), 8.8.2003. Ghoujygujyat Mountain, (16), 1.8.2002; (33), 21.8.2002; (10), 10.9.2002; (10), 23.10.2002; (7), 22.10.2003. Qanawat, (1), 12.8.2001; (3), 11.9.2001; (1), 20.9.2001. Taima, (4), 11.9.2001. Tal-loz, (2), 12.8.2001. Mashkok, (1), 20.9.2001. **Dar`a:** Wadi Jeelin, (5), 21.9.2001; (3), 22.11.2001; (4), 7.2.2002; (3), 25.4.2002. Jeelin, (3), 24.10.2001; (5), 3.7.2002. Zeizon, (4), 8.8.2001; (1), 22.8.2002. Mzireeb, (1), 6.8.2001. Sheikh Saad, (2), 13.11.2002. Nahaj, (18), 4.10.2001; (16), 24.10.2001. Sahm al-joulan, (3), 4.9.2001.

Remarks: Distributed in the East Mediterranean Region, covering India, Pakistan, Afghanistan, the Caucasus, Turkey, Iran and Saudi Arabia (Gourreau, 1974; Uygun, 1981; Raimundo and van Harten, 2000).

Host species: *Aloysia citrodora*, *Amygdalus* sp., *Capsicum annum*, *Citrus* sp., *Cucurbita pepo*, *Cupressus* sp., *Eriobotrya japonica*, *Eucalyptus camaldulensis*, *Ficus carica*, *Glycyrrhiza glabra*, *Helianthus annuus*, *Hibiscus esculentus*, *Inula viscosa*, *Juglans regia*, *Ligustrum* sp., *Lonicera* sp., *Malus communis*, *Medicago sativa*, *Morus alba*, *Olea europaea*, *Parietaria judaica*, *Phaseolus vulgaris*, *Pinus* sp., *Populus* sp., *Prunus armeniaca*, *Pyrus communis*, *Pistacia vera*, *Prunus avium*, *Prunus mahaleb*, *Prunus vulgaris*, *Punica granatum*, *Quercus calliprinos*, *Rosa* sp., *Rubus idaeus*, *Schinus molle*, *Solanum melongena*, *Urtica* sp., *Vitis vinifera*, and *Zea mays*.

Tribe Chilacorini Mulsant, 1846

Chilocorus bipustulatus (Linnaeus, 1758) (Fig. 4P)

Material examined (42): **Al-Quneitra:** Jubata Al-Khashab (1), 29.8.2002. **Damascus Rural:** Ma'adamiyeh Al-Sham, (9) 9.9.2002; (15) 13.8.2003; (4) 24.8.2003; (3) 15.8.2004. Addimass, (1), 17.9.2002; (1), 3.4.2003. Airport Street (1), 28.8.2001. Attall (1), 15.8.2002. **As`Sweida:** Ein alarab, (1), 1.8.2002; (2), 10.9.2002; (1), 23.10.2002. **Dar`a:** Wadi Jeelin, (1), 7.2.2002; (1), 29.5.2002.

Remarks: This species has a wide range of distribution covering India, Pakistan, China, Mongolia, Russia and Western Europe (Poorani, 2004), with records from northern Syria and the coastal regions (Lababidi and Zepter, 1995; Al Jundi and Ahmad, 1999) and Damascus (Bascheer and Abo Alshamat, 2004). It feeds on scale insects and aphids. Lababidi and Zebitz (1995) reported it feeding on the pistachio psyllid *Agonoscena targionii* Lich. in northern Syria.

Host species: *Biota orientalis*, *Citrus* sp., *Cupressus* sp., *Olea europaea*, *Pinus* sp., *Populus* sp., *Pyrus communis*, and *Quercus calliprinos*.

Exochomus octosignatus (Gebler, 1830) (Figs. 5K and 6A)

Material examined (1): **Damascus Rural:** Bludan Mountain, (1), 14.6.2003.

Remarks: This species is recorded for the first time in Syria. It was listed under the genus *Brumus*. Distribution of this species extends from Siberia to the Eastern Mediterranean (Duverger, 1991). Uygun (1981) recorded this species to feed on scale insects in Turkey.

Host species: Species of family Asteraceae.

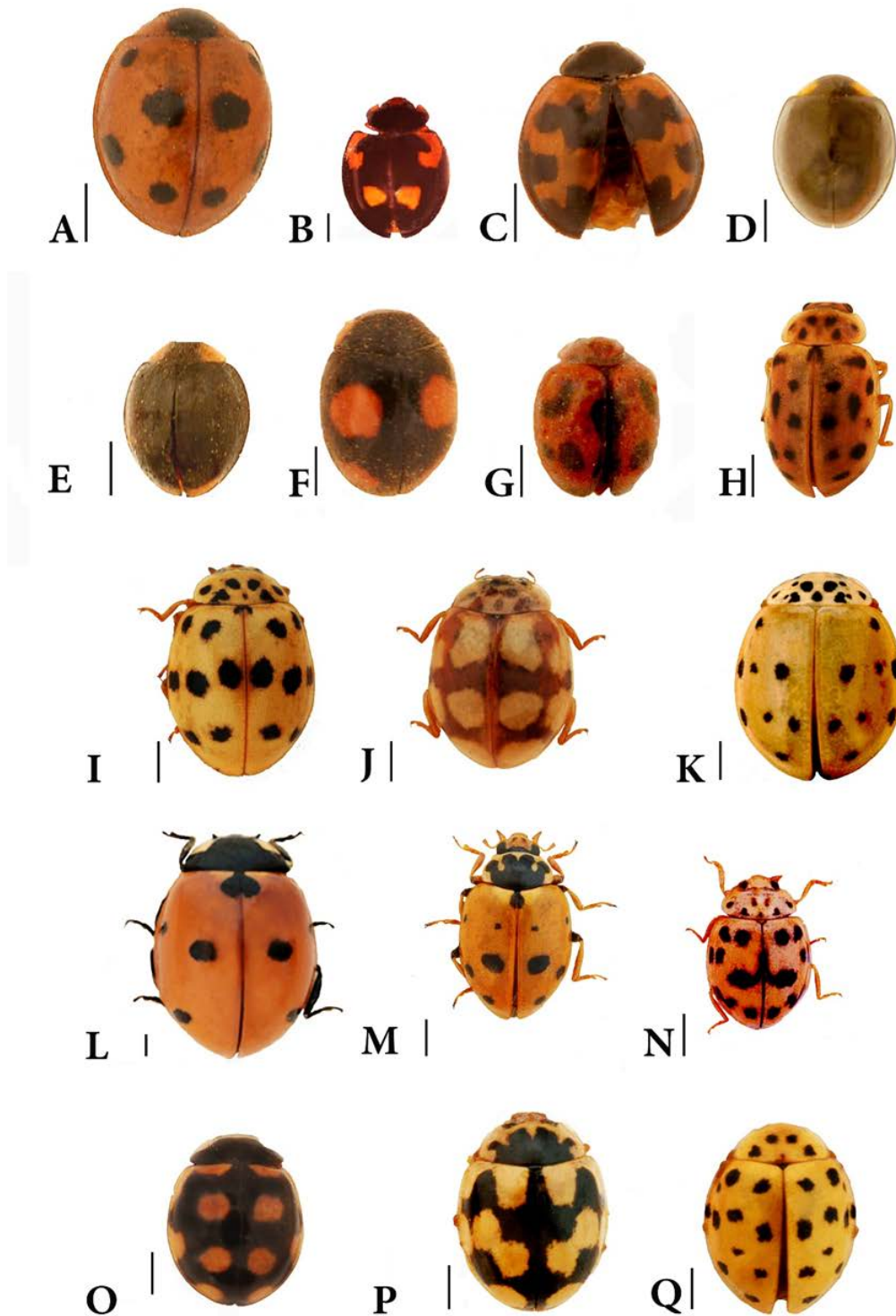


Figure 6: A. *Exochomus octosignatus*. B. *Exochomus quadripustulatus*. C. *Exochomus undulatus*. D. *Parexochomus nigromaculatus*. E. *Parexochomus pubescens*. F. *Platynaspis luteorubra*. G. *Novius cardinalis*. H. *Anisosticta novemdecimpunctata*. I. *Adalia* (*Adalia*) *bipunctata*. J. *Adalia* (*Adalia*) *decempunctata*. K. *Harmonia quadripunctata*. L. *Coccinella* (*Coccinella*) *septempunctata*. M. *Hippodamia* (*Adonia*) *variegata*. N. *Oenopia conglobata*. O. *Oenopia oncina*. P. *Propylea quatuordecimpunctata*. Q. *Psyllobora* (*Thea*) *vigintiduopunctata*. Scale bar = 1 mm.

***Exochomus quadripustulatus* (Linnaeus, 1758) (Figs. 5L and 6B)**

Material examined (54): Damascus Rural: Wadi Al-Qaren, (4), 19.8.2001; (1), 17.11.2001; (1), 14.3.2002; (2), 19.2.2003. **Al-Quneitra:** Beer Ajam, (2), 20.3.2002; (3), 19.3.2003. Jubata Al-Khashab, (2), 28.2.2002; (3), 25.4.2002; (14), 16.5.2002; (10), 16.4.2003; (1),

26.8.2003; (4), 2.5.2005. **As`Sweida:** Al-Kafr, (4), 23.10.2002; (1), 12.12.2002; (2), 11.5.2003.

Remarks: This species is distributed from India, Mangolia, Middle East to Russian Far East and Western Europe (Kuznetsov, 1997; Poorani, 2004; Kovář, 2007). In Syria, it was listed by El Hariri (1968) and recorded from Wadi Al Qaren by Kabakibi (1993), from As`Sweida by

Almatni *et al.* (1999) and from Damascus by Bascheer and Abo Alshamat (2004).

Host species: *Amygdalus* sp. and *Quercus calliprinos*.

***Exochomus undulatus* Weise, 1878 (Fig. 6C)**

Material examined (2): Damascus Rural: Rankus, (1), 6.7.2004. Wadi Al-Qaren, (1), 14.3.2002.

Remarks: This species is known from the southern states of the former Soviet Union, Turkey, Iran, Palestine and Egypt (Alfieri, 1976; Uygun, 1981, Moodi, 1994; Halperin *et al.*, 1995). In Syria, it was listed by El Hariri (1968). Uygun (1981) recorded it feeding on scale insects and aphids in Turkey. Jalilvand *et al.* (2014) found that this species predates on *Planococcus vovae* in Iran.

Host species: *Amygdalus* sp. and *Quercus calliprinos*.

***Parexochomus nigromaculatus* (Goeze, 1777) (Fig. 6D)**

Material examined (24): Damascus Rural: Wadi Al-Qaren, (1), 19.9.2001; (2), 5.9.2002. Jeerin, (1), 29.12.2001. **Al-Quneitra:** Masehara, (1), 13.8.2001. **As`Sweida:** Al-Kafr (1), 18.10.2001. Taamri Mountain, (1), 21.6.2002. Orman Mountain, (1), 21.8.2002; (1), 8.8.2003. Qanawat, (2), 12.8.2001. **Dar`a:** Izraa (4), 27.9.2001. Sheikh Miskin, (8), 30.8.2001. Sanameen, (1), 6.8.2001.

Remarks: This species has a wide range of distribution in South and Central Europe, Africa and Asia (Raimundo and van Harten 2000). This species was recorded previously from Syria by El Hariri (1971) and from the Golan Heights (Halperin *et al.*, 1995). Jalilvand *et al.* (2014) found that this species predates on *Phenacoccus* sp. in Iran.

Host species: *Achillea* sp., *Cucumis melo*, *Cucurbita pepo*, *Daucus carota*, *Nerium oleander*, *Quercus calliprinos* and *Urtica* sp.

***Parexochomus pubescens* (Küster, 1848) (Fig. 6E)**

Material examined (6): Damascus Rural: Jeerin, (3), 9.2.2003. Attall, (1), 24.8.2003. Kharabo, (1), 23.5.2002. **Dar`a:** Wadi Shihab, (1), 13.5.2003.

Remarks: This is widely distributed species with a range extending from India, Middle East, reaching westwards to Spain, with records from Egypt, Palestine, Syria, Saudi Arabia and Yemen (Raimundo and van Harten, 2000; Poorani, 2004).

Host species: *Tamarix articulata*, *Triticum* sp. and *Urtica* sp.

Tribe Platynaspini Mulsant, 1846

***Platynaspis luteorubra* (Goeze, 1777) (Figs. 5M and 6F)**

Material examined (14): Damascus Rural: Kharabo, (1), 22.8.2001; (1), 11.7.2002; (1), 24.7.2002; (1), 6.8.2003. Qatana, (1), 5.7.2002. Attall, (1), 10.7.2002. **As`Sweida:** Ein alarab (1), 22.7.2003. Orman Mountain (1), 27.9.2001. Ghoujygujyat Mountain, (1), 4.7.2002; (2), 29.4.2003. Shahba, (1), 13.3.2002. **Dar`a:** Zeizon, (2), 8.8.2001.

Remarks: Halperin *et al.* (1995) reported *Platynaspis luteorubra* as a rare species in the Golan Heights and Palestine. This is a Palaearctic species with a range extending from North Africa, Europe, and the Middle East reaching the Caucasus (Uygun, 1981).

Host species: *Malus communis*, *Medicago sativa*, *Morus alba*, *Pinus* sp., *Punica granatum*, *Rosa* sp., and *Zea mays*.

Tribe Noviini Mulsant, 1850

***Novius cardinalis* (Mulsant, 1850) (Figs. 5N and 6G)**

Material examined (16): Damascus Rural: Attall, (1), 25.10.2001; (1), 27.12.2001. Ma`adamiyeh Al-sham, (1), 15.2.2002; (1), 23.5.2002; (1), 16.1.2003; (1), 5.2.2003; (1), 13.3.2003; (1), 9.4.2003; (1), 23.6.2003; (1), 11.7.2003; (1), 13.8.2003. **Dar`a:** Wadi Jeelin, (1), 7.2.2002; (2), 25.4.2002. Zeizon, (1), 25.4.2002; (1), 27.5.2002.

Remarks: This species has a world-wide distribution (Uygun, 1981). Listed previously from Syria (El Hariri, 1968). Recorded by Al Jundi and Ahmad (1999) from the coastal regions.

Host species: *Citrus* sp., *Faba vulgaris*, *Punica granatum*, and *Rubus idaeus*.

Tribe Tythaspidini Crotch, 1874

***Anisosticta novemdecimpunctata* (Linnaeus, 1758) (Fig. 6H)**

Material examined (1): Dar`a: Nahta, (1), 22.8.2002.

Remarks: This species is widely distributed in Europe, Central Asia and the Middle East (Uygun, 1981; Kuznetsov, 1997; Kovář, 2007). This species is recorded for the first time in Syria.

Host species: *Zea mays*.

Tribe Coccinellini Latreille, 1807

***Adalia (Adalia) bipunctata* (Linnaeus, 1758) (Figs. 5O and 6I)**

Material examined (61): Damascus Rural: Kafr-Hawar, (1), 7.8.2002. Al-Hameh, (2), 14.6.2003. Jeerin, (30), 29.12.2002; (3), 9.2.2003. Attall, (3), 26.6.2002. Kharabo, (2), 22.8.2001; (1), 25.10.2001; (1), 23.5.2002; (1), 11.7.2002; (1), 24.7.2002; (1), 8.8.2002; (3), 11.9.2002; (1), 25.9.2002; (3), 9.10.2002; (2), 2.4.2003; (2), 25.5.2003; (1), 2.7.2003; (1), 6.8.2003. Ma`adamiyeh Al-Sham, (1), 23.5.2002. **As`Sweida:** Orman Mountain, (1), no date.

Remarks: This species has a world-wide distribution (Harde, 1999; Poorani, 2004). In Syria, it was listed by El Hariri (1968). Recorded from Damascus by Bascheer and Abo Alshamat (2004) and from As`Sweida by Almatni *et al.* (1999).

Host species: *Ficus carica*, *Juglans regia*, *Malus communis*, *Medicago sativa*, *Morus alba*, *Populus* sp., *Punica granatum*, *Rubus idaeus*, *Salix* sp., *Solanum melongena*, *Triticum* sp., *Urtica* sp., and *Zea mays*.

***Adalia (Adalia) decempunctata* (Linnaeus, 1758) (Figs. 5P and 6J)**

Material examined (37): Al-Quneitra: Beer Ajam, (2), 27.6.2002; (1), 2.10.2002. **Damascus Rural:** Wadi Al-Qaren, (4), 10.7.2002. Sarkha, (5), 26.6.2002; (1), 11.9.2002. Beqaasem, (1), 11.7.2002. Kafr Hawar, (1), 7.8.2002. **As`Sweida:** Al-Kafr, (1), 17.7.2002; (2), 23.10.2002. Orman, (1), 24.6.2002; (3), 11.7.2002; (1), 17.7.2002. Taamri Mountain, (1), 4.7.2003. Ghoujygujyat Mountain, (1), 4.7.2003. Qanawat, (2), 6.6.2002. Sad alain, (9), 17.7.2002. **Dar`a:** Zeizon, (1), 9.5.2002.

Remarks: It is distributed throughout the Palaearctic region, North Africa reaching Japan (Harde, 1999; Uygun,

1981). Previous records from Syria include the coastal region (Al Jundi and Ahamd, 1999), Mount Hermon (Halperin *et al.*, 1995), North Syria (Aswad, 1998) and listed by El Hariri (1968).

Host species: *Amygdalus* sp., *Inula viscosa*, *Juglans regia*, *Quercus calliprinos*, *Robinia pseudoacacia*, *Salix* sp., *Pinus* sp., *Populus* sp., and *Prunus vulgaris*.

***Coccinella (Coccinella) septempunctata* Linnaeus, 1758 (Figs. 5Q and 6L)**

Material examined (330): Al-Quneitra: Beer Ajam, (1), 27.6.2002. Jubata Al-Khashab, (12), 12.6.2002; (8), 11.7.2002; (3), 31.7.2002, (2), 26.8.2003. **Damascus:** Qasioun, (6), 13.5.2003. **Damascus Rural:** Kharabo, (1), 22.8.2001; (1), 21.11.2001; (1), 6.2.2002; (2), 18.4.2002; (8), 15.5.2002; (9), 23.5.2002; (1), 5.6.2002; (1), 24.7.2002; (1), 11.9.2002; (1), 2.4.2003; (1), 21.4.2003; (2), 13.5.2003; (3), 25.5.2003; (1), 6.8.2003; (6) 13.5.2005. Yabrud, (1), 25.10.2001; (1), 4.4.2002; (4), 8.5.2002. Sasaa, (1), 2.5.2002; (10), 16.5.2002. Beet-jen Mazraa, (6), 8.11.2001; (5), 16.5.2002. Qatana, (1), 5.7.2002; (1), 28.2.2002. Deir Al-ashairr, (2), 11.6.2002. Bludan, (2), 14.6.2003. Rankaus, (1), 10.6.2003. Maalula, (1), 8.5.2002. Attawani, (1), 20.11.2002. Autaiba, (6), 6.2.2002; (1), 9.2.2003. Deir Atyeh, (4), 21.5.2003. Annashabyeh, (1), 28.8.2001. Attall, (3), 3.9.2001; (6), 25.10.2001; (3), 27.12.2001; (2), 14.3.2002; (1), 4.4.2002; (2), 20.11.2002; (6), 19.2.2003; (1), 7.5.2003. Serghaya, (4), 19.9.2001; (10), 7.11.2001; (2), 6.12.2001; (7), 4.5.2002; (8), 30.5.2002; (12), 11.6.2002; (2), 27.6.2002; (1), 17.9.2002; (4), 3.10.2002; (4), 7.11.2002; (2), 22.5.2003. Ma'adamiyeh Al-sham, (1), 24.11.2001; (2), 19.4.2002; (2), 24.4.2002; (1), 1.5.2002; (1), 23.5.2002; (1), 19.7.2002; (1), 1.11.2002; (1), 4.12.2002; (3), 19.5.2003; (1), 23.6.2003; (1), 23.7.2003. **As'Sweida:** Al-Kafr, (3), 12.6.2003. Ein alarab, (2), 9.5.2002; (16), 6.6.2002; (1), 19.6.2002; (1), 23.10.2002; (5), 2.6.2003. Orman Mountain, (3), 11.4.2002; (1), 6.6.2002; (2), 12.6.2003. Taamri Mountain, (2), 17.4.2002; (1), 17.7.2002. Ghoujygoujyat Mountain, (2), 4.7.2002; (1), 12.6.2003. Qanawat, (1), 29.11.2001; (1), 13.3.2002 (1), 11.4.2002; (1), 9.5.2002; (1), 6.6.2002. Shahba, (2), 29.11.2001; (4), 13.3.2002; (1), 11.4.2002; (3), 11.5.2003. Tarba, (1), 11.9.2001. Saura, (1), 13.3.2002. **Dar'a:** Wadi Jeelin, (1), 9.5.2002. Zeizon, (6), 22.11.2001; (4), 7.2.2002; (1), 10.4.2002; (1), 25.4.2002; (1), 29.5.2002; (1), 18.12.2002; (1), 16.6.2003. Mzireeb, (1), 20.12.2001; (1), 25.4.2002; (4), 9.5.2002; (3), 16.5.2002; (1), 18.12.2002. Sheikh Saad, (8), 12.5.2003. Ajami, (3), 13.11.2002. Sehaileia, (1), 20.6.2002. Tafas (1), 22.11.2001; (4), 25.7.2002. Dar'a, (3), 6.5.2003. Wadi Shihab, (2), 13.5.2003. Namer, (10), 15.4.2002.

Remarks: This species has a world-wide distribution (Zhou *et al.*, 1995). In Syria, it was listed by El Hariri (1968) and collected from Wadi Al Qaren by Kabakibi (1993), from As'Sweida by Almatni *et al.* (1999) and from Damascus by Bascheer and Abo Alshamat (2004). It feeds on aphids. Lababidi and Zebitz (1995) reported it feeding on the pistachio psyllid *Agonoscena targionii* Lich. in northern Syria.

Host species: *Acer* sp., *Achillea* sp., *Amygdalus* sp., *Anthemis* sp., *Beta vulgaris*, *Cardus pycnocephalus*, *Centaurea* sp., *Chenopodium* sp., *Citrus* sp. *Cucumis sativus*, *Cucurbita pepo*, *Cupressus* sp., *Diplotaxis ercoides*,

Elaeagnus angustifolia, *Faba vulgaris*, *Foeniculum vulgare*, *Hibiscus esculentus*, *Hordeum* sp., *Inula viscosa*, *Juglans regia*, *Malus communis*, *Medicago sativa*, *Morus alba*, *Nerium oleander*, *Onobrychus* sp., *Ononis spinosa*, *Onopordum syriacum*, *Quercus calliprinos*, *Petroselinum crispum*, *Pinus* sp., *Punica granatum*, *Prunus avium*, *Prunus armeniaca*, *Prunus vulgaris*, *Pyrus communis*, *Rosa* sp., *Rubus idaeus*, *Tamarix orticulatus*, *Triticum* sp., *Urtica* sp., *Vicia sativa*, *Vitis vinifera*, and *Zea mays*.

***Coccinella (Spilota) undecimpunctata aegyptica* Reiche, 1861 (Figs. 5R)**

Material examined (152): Damascus: Damascus, (1), 16.6.2002; (1), 13.5.2003. **Damascus Rural:** Kharabo, (2), 22.8.2001; (2), 25.10.2001; (2), 15.5.2002; (4), 23.5.2002; (2), 5.6.2002; (2), 11.7.2002; (1), 13.5.2003; (1), 25.5.2003. Serghaya, (1), 27.6.2002. Ma'adamiyeh Al-Sham, (8), 24.4.2002; (5), 23.5.2002; (4), 19.5.2003; (1), 11.7.2003. Yabrud, (5), 8.5.2002. Nasseria, (2), 5.6.2002. Kanaker, (3), 4.9.2001. Zarzar, (1), 14.6.2003. Deir Al-ashairr, (1), 17.10.2001. Bludan, (2), 14.6.2003. Assal Alwared, (1), 26.9.2001. Rankus Mountain, (1), 21.5.2003. Rankaus, (6), 10.6.2003. Al-Dumayr, (15), 15.8.2001. Qatana, (1), 5.7.2002. Seydnaya, (5), 21.5.2003. Ahmadiya, (10), 23.5.2002. Autaiba, (8), 10.7.2001; (1), 28.8.2001; (6), 2.8.2004. Assaida Zainab, (2), 11.9.2001. Deir Atyeh, (1), 21.5.2003. Annashabyeh, (14), 28.8.2001. Attall, (1), 3.9.2001; (1), 7.5.2003. **As'Sweida:** Al-Kafr, (1), 12.6.2003. Ein alarab, (1), 2.6.2003. Orman Mountain, (1), 23.6.2002; (1), 16.5.2003. Ghoujygoujyat Mountain, (1), 4.7.2002. Taamri Mountain, (1), 6.6.2003; (1), 25.7.2003. Orman, (1), 6.6.2003. Qanawat, (2), 29.11.2001. Sad alaaain, (1), 12.5.2003. **Dar'a:** Jeelin, (2), 10.8.2001. Zeizon, (1), 24.10.2001. Sheikh Miskin, (1), 27.5.2003. Mzireeb, (2), 6.8.2001; (1), 20.12.2001. Sheikh Saad, (1), 12.5.2003. Shagara, (1), 9.7.2002. Tafas, (3), 25.7.2002. Daraa, (3), 6.5.2003. Shihab, (1), 25.7.2002. Namer, (1), 15.4.2002.

Remarks: Known from Europe, Asia and Africa (Rainundo and van Hartenl 2000). In Syria, recorded by Al Jundi and Ahmad (1999) as a predator for aphids on citrus tree in the coastal regions and recorded from As'Sweida by Almatni *et al.* (1999). It was listed by El Hariri (1968) from Syria.

Host species: *Amygdalus* sp., *Beta vulgaris*, *Carthamus tinctorius*, *Cerasus avium*, *Citrus* sp., *Crataegus* sp., *Cucumis sativus*, *Cupressus* sp., *Eriobotrya japonica*, *Euphorbia* sp., *Faba vulgaris*, *Foeniculum vulgare*, *Gossypium* sp., *Hordeum* sp., *Juglans regia*, *Malus communis*, *Morus alba*, *Medicago sativa*, *Nerium oleander*, *Pinus* sp., *Pisum sativum*, *Prunus armeniaca*, *Punica granatum*, *Pyrus communis*, *Solanum melongena*, *Triticum* sp., *Vicia sativa* and *Zea mays*.

Harmonia quadripunctata (Pontoppidan, 1763) (Figs. 5S and 6K)

Material examined (59): Damascus Rural: Zarzar, (1), 30.4.2003; (1), 14.6.2003. Maissalon, (4), 30.4.2003. Addimass, (1), 15.5.2002; (2), 30.4.2003. Kafr Hawar, (1), 7.8.2002. **Al-Quneitra:** Trounja 7: (1), 28.2.2002; (5), 29.8.2002; (1), 16.4.2003; (1), 12.6.2002. **As'Sweida:** Al-Kafr, (1), 23.10.2002, Ein alarab, (7), 4.7.2002; (3), 17.7.2002; (9), 1.8.2002; (8), 21.8.2002; (2), 10.9.2002; (3), 23.10.2002; (3), 2.6.2003. Ghoujygoujyat Mountain,

(2), 1.8.2002; (1), 23.10.2002. Taamri Mountain, (1), 25.7.2003. Orman Mountain, (1), 4.8.2003.

Remarks: Known from Europe throughout Central Asia and the Middle East (Allawi, 1989; Canepari, 1991; Halperin *et al.*, 1995; Harde, 1999). It was recorded by Al Jundi and Ahmad (1999) as a predator for aphids on citrus tree in the coastal regions.

Host species: *Amygdalus* sp., *Cedrus libani*, *Cupressus* sp., *Galium* sp., *Pinus* sp., *Prunus avium*, *Prunus vulgaris*, *Quercus calliprinos* and *Rosa damascena*.

***Hippodamia (Adonia) variegata* (Goeze, 1777) (Figs. 5T and 6M)**

Material examined (1042): Damascus Rural: Attall, (25), 3.9.2001; (4), 26.9.2001; (2), 27.12.2001; (4), 4.4.2002; (2), 8.5.2002; (1), 26.6.2002; (11), 10.7.2002; (3), 20.11.2002; (7), 7.5.2002. Kharabo, (1), 22.8.2001; (1), 26.9.2001; (6), 25.10.2001; (3), 21.11.2001; (1), 6.2.2002; (5), 4.5.2002; (11), 15.5.2002; (102), 23.5.2002; (6), 5.6.2002; (11), 11.7.2002; (6), 24.7.2002; (1), 8.8.2002; (24), 11.9.2002; (5), 25.9.2002; (3), 9.10.2002; (3), 25.5.2003; (6), 2.7.2003; (8), 6.8.2003; (2), 13.5.2005. Serghaya, (7), 19.9.2001; (19), 17.10.2001; (25), 7.11.2001; (2), 6.12.2001; (1), 18.4.2002; (2), 30.5.2002; (17), 11.6.2002; (16), 27.6.2002; (14), 10.7.2002; (11), 24.7.2002; (15), 14.8.2002; (2), 5.9.2002; (6), 17.9.2002; (8), 3.10.2002; (15), 7.11.2002; (2), 9.1.2003; (1), 10.4.2003; (2), 26.6.2003; (3), 29.7.2003. Ma'adamiyeh Al-sham, (1), 6.12.2001; (1), 20.1.2002; (12), 19.4.2002; (2), 1.5.2002; (15), 23.5.2002; (6), 28.6.2002; (2), 19.7.2002; (1), 9.9.2002; (2), 16.1.2003; (4), 5.2.2003; (3), 13.3.2003; (8), 19.5.2003; (4), 23.6.2003; (7), 11.7.2003; (2), 23.7.2003; (1), 13.8.2003. Yabrud 14: (4), 2.8.2001; (1), 26.9.2001; (8), 25.10.2001; (1), 11.9.2002. Kanaker, (1), 4.9.2001. Sasaa, (13), 3.10.2001; (1), 12.6.2002. Kulaiaa, (4), 7.8.2002. Dorin, (12), 10.7.2002; (5), 24.8.2003. Beet-jen Mazraa 4: (1), 1.8.2001; (3), 8.11.2001. Erneh (4), 11.7.2002; Zarzar, (7), 19.9.2001; (1), 14.6.2003. Deir Al-ashairr, (12), 17.10.2001; (8), 28.11.2001; (17), 11.6.2002. Al-Hameh, (5), 14.6.2003. Azzabadani, (3), 17.10.2001; (1), 28.11.2001; (6), 27.6.2002. Bludan, (4), 14.6.2003. Houch arab, (2), 3.9.2001. Rankaus, (6), 21.5.2003; (10), 10.6.2003. Attawani, (1), 20.11.2002. Al-Dumayr, (1), 15.8.2001. Qatana, (19), 5.7.2002. Ahmadiya, (3), 25.9.2002. Airport Street, (2), 21.11.2001. Autaiba, (1), 6.2.2002; (1), 24.7.2002. Haran Al-awameed, (1), 24.7.2002. Assaida Zainab, (9), 11.9.2001; (1), 3.4.2002. Deir Atyeh, (1), 21.5.2003. Jeerain, (21), 29.12.2002; (1), 9.2.2003. Ashiphonieh, (6), 25.9.2002. Annashabyeh, (10), 28.8.2001. **Damascus:** Damascus, (9), 13.5.2003. **As'Sweida:** Al-Kafr, (1), 1.8.2002; (1), 12.6.2003. Ein alarab, (1), 21.11.2001; (2), 29.11.2001; (1), 19.6.2002; (5), 17.7.2002; (8), 1.8.2002; (1), 23.10.2002; (2), 2.6.2003. Orman Mountain, (1), 21.11.2001; (4), 4.7.2002; (14), 27.9.2002; (1), 1.8.2002; (2), 21.8.2002; (1), 12.6.2003. Taamri Mountain, (2), 17.4.2002; (3), 6.6.2003; (1), 13.6.2003; (1), 28.6.2003; (1), 4.7.2003; (2), 25.7.2003. Orman, (15), 21.6.2002; (6), 4.7.2002; (1), 17.7.2002; (4), 22.6.2002; (1), 11.7.2002; (4), 25.5.2003; (1), 6.6.2003. Ghoujygujyat Mountain, (3), 10.9.2002; (1), 21.8.2002; (4), 23.10.2002; (2), 29.4.2003; (1), 12.6.2003. Sad alain, (6), 17.7.2002. Qanawat, (9), 12.8.2001; (3), 29.8.2001; (1), 11.9.2001; (8), 18.10.2001;

(10), 15.5.2002; (1), 19.6.2002; (5), 1.8.2002; (8), 21.8.2002; (5), 4.8.2005; **Dar'a:** Shahba, (1), 16.5.2001; (1), 13.3.2002; (1), 11.12.2002; (1), 11.5.2003. Jeelin, (15), 10.8.2001; (3), 30.8.2001; (6), 18.7.2002. Wadi Jeelin, (2), 21.9.2001; (1), 22.11.2002; (1), 25.4.2002; (4), 9.5.2002; (1), 2.10.2002. Zeizon, (9), 8.8.2001; (3), 24.10.2001; (18), 22.11.2001; (3), 20.12.2001; (5), 10.4.2002; (1), 9.5.2002; (2), 29.5.2002; (1), 16.6.2003. Izraa, (6), 27.9.2001. Sheikh Miskin, (6), 30.8.2001; (1), 20.6.2002; (2), 27.5.2003; (4), 22.7.2003. Mzireeb, (4), 6.8.2001; (7), 20.12.2001; (2), 25.4.2002; (4), 9.5.2002; (3), 16.5.2002; (1), 25.7.2002. Sheikh Saad, (1), 12.5.2003. Ajami, (2), 13.11.2002. Nahta, 2: (1), 6.8.2002; (1), 22.8.2002. Sehaileia, (1), 20.6.2002. Tafas 23: (2), 4.9.2001; (13), 22.11.2001; (8), 25.7.2002. Dar'a, (6), 6.5.2003. Shihab, (1), 25.7.2002. Wadi Shihab, (1), 13.5.2003. Namer, (1), 20.6.2002.

Remarks: This species has a wide range of distribution extending from the Russian Far East across Asia southward to India and the Middle East to Europe and North Africa and occurs also in South Africa (Kuznetsov, 1997; Raimundo and van Harten, 2000). Listed from Syria by El Hariri (1968). Recorded by Al Jundi and Ahmad (1999) from the coastal regions. Its principal food is aphids. Özden *et al.* (2006) reported this species from Cyprus feeding on aphids and mites. Lababidi and Zebitz (1995) reported it feeding on the pistachio psyllid *Agonoscena targionii* Lich. in northern Syria.

Host species: *Acer* sp., *Agropyron repens*, *Amygdalus* sp., *Anabasis* sp., *Beta vulgaris*, *Carthamus tinctorius*, *Cedrus libani*, *Citrus* sp., *Crataegus* sp., *Cucurbita pepo*, *Cucumis melo*, *Cupressus* sp., *Diplotaxis ercoides*, *Elaeagnus angustifolia*, *Eriobotrya japonica*, *Euphorbia* sp., *Faba vulgaris*, *Ferula hermonis*, *Ficus carica*, *Galium* sp., *Glycyrrhiza glabra*, *Helianthus innuus*, *Hibiscus esculentus*, *Hordeum* sp., *Hypericum trinquetifolium*, *Inula viscosa*, *Juglans regia*, *Malus communis*, *Malva* sp., *Medicago sativa*, *Nerium oleander*, *Ocimum* sp., *Petrocelinum crispum*, *Papaver syriacum*, *Pinus* sp., *Pistacia vera*, *Populus* sp., *Punica granatum*, *Prunus mahaleb*, *Prunus vulgaris*, *Pyrus communis*, *Quercus calliprinos*, *Rosa* sp., *Rubus idaeus*, *Sinapis alba*, *Solanum melongena*, *Spartium junceum*, *Triticum* sp., *Urtica* sp., and *Zea mays*.

***Oenopia conglobata* (Linnaeus, 1758) (Figs. 5U and 6N)**

Material examined (618): Damascus Rural: Attall, (3), 3.9.2001; (3), 25.10.2001; (1), 14.3.2002; (1), 8.5.2002; (3), 26.6.2002; (3), 10.7.2002; (2), 7.5.2003. Kharabo, (14), 22.8.2001; (1), 26.9.2001; (5), 25.10.2001; (1), 21.11.2001; (4), 23.5.2002; (1), 5.6.2002; (1), 11.7.2002; (3), 24.7.2002; (9), 8.8.2002; (3), 11.9.2002; (1), 25.9.2002; (4), 9.10.2002; (1), 29.12.2002; (1), 2.4.2003; (5), 13.5.2003; (7), 25.5.2003; (9), 6.8.2003; (1), 9.5.2002. Serghaya, (2), 19.9.2001; (5), 17.10.2001; (3), 7.11.2001; (1), 18.4.2002; (4), 4.5.2002; (5), 15.5.2002; (3), 30.5.2002; (1), 11.6.2002; (14), 5.9.2002; (23), 17.9.2002; (22), 3.10.2002; (17), 7.11.2002; (17), 10.4.2003; (6), 22.5.2003; (3), 29.7.2003. Ma'adamiyeh Al-sham, (1), 23.5.2002; (4), 28.6.2002; (7), 19.7.2002; (5), 30.8.2002; (15), 9.9.2002; (1), 4.12.2002; (1), 9.4.2003; (1), 19.5.2003; (7), 23.6.2003; (6), 6.7.2003; (25), 11.7.2003; (7), 23.7.2003; (6), 13.8.2003. Wadi Al-Qaren, (6), 10.7.2002; (2), 14.3.2002; (1), 19.2.2003.

Yabrud, (7), 2.8.2001; (1), 26.9.2001; (1), 4.4.2002; (1), 26.6.2002; (8), 8.8.2002; (6), 11.9.2002. Kulaiaa, (2), 7.8.2002, Beet-jen Mazraa, (14), 7.8.2002; (11), 29.8.2002. Erneh, (5), 11.7.2002. Beqaasem, (1), 21.9.2001; (4), 11.7.2002; (1), 29.7.2002, Muqr Almeer, (2), 16.4.2003. Kafr- Hawar, (1), 7.8.2002. Zarzar, (1), 19.9.2001; (1), 28.11.2001; (4), 30.4.2003; (1), 14.6.2003. Deir Al-ashairr, (9), 17.10.2001; (3), 28.11.2001; (4), 11.6.2002; (4), 17.9.2002. Addimass, (1), 10.7.2002; (10), 5.9.2002; (3), 17.9.2002; (2), 30.4.2003. Al-Hameh, (2), 14.6.2003. Azzabadani, (14), 27.6.2002; (1), 14.6.2003. Rankaus, (6), 10.6.2003. Sarkha, (25), 26.6.2002; (6), 11.9.2002; (6), 21.5.2003. Seydnaya, (7), 2.8.2001; (4), 26.6.2002. Qatana, (1), 14.8.2003. Deir Atyeh, (4), 21.5.2003. Jeerlin, (2), 29.12.2002. Ashiphonieh, (1), 25.9.2002. Annashabyeh, (1), 28.8.2001. **Damascus:** Qasioun, (14), 13.5.2003. **Al-Quneitra:** Jubata Al-Khashab, (2), 20.3.2002; (1), 28.2.2002; (2), 16.5.2002; (2), 26.8.2003; (3), 22.5.2004. Hadar, (2), 10.9.2001; (2), 31.7.2002; (1), 12.9.2002. Beer Ajam, (2), 12.9.2002; (1), 2.10.2002. **As`Sweida:** Al-Kafr, (1), 18.10.2001; (1), 29.11.2001; (2), 9.5.2002; (5), 6.6.2002; (1), 1.8.2002; (10), 23.10.2002; (5), 11.5.2003; (2), 12.6.2003. Shahba, (1), 13.3.2002; (1), 11.12.2002. Ein alarab, (1), 28.6.2002; (2), 4.7.2002; (2), 17.7.2002; (1), 10.9.2002. Orman Mountain, (3), 11.4.2002. Orman, (1), 30.5.2002; (3), 21.6.2002; (1), 4.7.2002; (1), 11.7.2002; (2), 17.7.2002. Ghoujygujyat Mountain, (1), 10.9.2002, (1), 4.8.2003. Taamri Mountain, (2), 25.7.2003; (1), 8.8.2003. Qanawat, (1), 11.9.2001; (1), 13.3.2002; (4), 11.4.2002; (1), 9.5.2002; (1), 17.7.2002; (2), 1.8.2002. **Dar`a:** Shihab, (1), 25.7.2002. Wadi Shihab, (1), 13.5.2003. Zeizon, (1), 21.3.2002; (1), 28.3.2002; (4), 10.4.2002; (2), 25.4.2002; (10), 9.5.2002; (4), 29.5.2002. Nahaj, (6), 4.10.2001.

Remarks: This species has a wide range across Europe, North Africa to the Far East and North America (Kuznetsov, 1997). In Syria, it was recorded from the Golan Heights, Mount Hermon, Wadi Al Qaren, As`Sweida and northern Syria (Kabakibi, 1993; Halperin *et al.*, 1995; Almatni *et al.*, 1999; Ka`ada, 2002). Jalilvand *et al.* (2014) found that this species predates on *Planococcus ficus* in Iran.

Host species: *Acer* sp., *Aloysia citrodora*, *Amygdalus* sp., *Biota orientalis*, *Cedrus libani*, *Citrus* sp., *Cupressus* sp., *Cydonia vulgaris*, *Elaeagnus angustifolia*, *Eriobotrya japonica*, *Eucalyptus camaldulensis*, *Faba vulgaris*, *Ficus carica*, *Glycyrrhiza glabra*, *Hibiscus esculentus*, *Inula viscosa*, *Juglans regia*, *Ligustrum* sp., *Medicago sativa*, *Morus alba*, *Nerium oleander*, *Olea europaea*, *Prunus armeniaca*, *Prunus vulgaris*, *Pinus* sp., *Pistacia vera*, *Populus* sp., *Prunus avium*, *Prunus mahaleb*, *Punica granatum*, *Pyrus communis*, *Quercus calliprinos*, *Robinia pseudoacacia*, *Rosa* sp., *Rubus idaeus*, *Salix* sp., *Solanum melongena*, *Ulmus campestris*, *Urtica* sp., *Vitis vinifera* and *Zea mays*,

***Oenopia oncina* (Olivier, 1808) (Figs. 5V and 6O)**

Material examined (6): Damascus Rural: Deir Al-ashairr, (1), 17.10.2001; (1), 11.6.2002. Bludan, (1), 14.6.2003. Rankus Mountain, (1), 21.5.2003, Rankaus, (1), 10.6.2003. **Dar`a:** Wadi Shihab, (1), 13.5.2003.

Remarks: This species is distributed in the Eastern Mediterranean extending to Central Asia (Iablokoff-

Khznorian, 1982). This species represents a new record to Syria.

Host species: *Amygdalus* sp., *Medicago sativa*, *Onobrychus* sp. and *Punica granatum*.

***Propylea quatuordecimpunctata* (Linnaeus, 1758) (Figs. 5W and 6P)**

Material examined (121): Damascus Rural: Qatana, (1), 5.7.2002. Ahmadiya, (1), 25.9.2002. Assaida Zainab, (2), 11.9.2001; (3), 13.3.2002. Jeerlin, (3), 9.2.2003. Ashiphonieh, (1), 25.9.2002, Attall, (7), 3.9.2001; (2), 4.4.2002; (1), 8.5.2002; (1), 26.6.2002; (18), 10.7.2002; (6), 15.7.2005. Kharabo, (1), 22.8.2001; (1), 26.9.2001; (2), 25.10.2001; (1), 15.5.2002; (9), 23.5.2002; (7), 11.7.2002; (3), 24.7.2002; (1), 8.8.2002; (8), 25.9.2002; (13), 9.10.2002; (3), 2.4.2003; (10), 25.5.2003; (3), 2.7.2003; (3), 6.8.2003. Ma`adamiyeh Al-sham, (3), 28.6.2002; (3), 19.7.2002; (1), 19.5.2003; (1), 23.6.2003; (1), 11.7.2003; (1), 23.7.2003.

Remarks: This is a Trans-Palaeartic species with wide range of distribution through Europe, across Asia reaching Korea and Japan (Iablokoff-Khznorian, 1982). Regionally, it was recorded from Lebanon and Palestine (Talhook, 1961; Halperin *et al.*, 1995). Recorded by Al Jundi and Ahmad (1999) from the coastal regions, and from Damascus by Bascheer and Abo Alshamat (2004).

Host species: *Cucumis sativus*, *Cucurbita pepo*, *Cydonia vulgaris*, *Faba vulgaris*, *Foeniculum vulgare*, *Hordium vulgare*, *Juglans regia*, *Medicago sativa*, *Morus alba*, *Populus* sp., *Punica granatum*, *Solanum melongena*, *Triticum* sp., *Urtica* sp., and *Zea mays*.

***Psyllobora (Thea) vigintiduopunctata* (Linnaeus, 1758) (Figs. 5X and 6Q)**

Material examined (2): Damascus Rural: Attall, (2), 3.9.2001.

Remarks: This is a Palaeartic species with a wide distribution in Europe (Harde, 1999). Aslan and Uygun (2005) reported this species from Turkey on aphids. This species was listed by El Hariri (1968) from Syria. Recorded from northern Syria and the coastal regions by Ka`ada (2002) and Younes *et al.* (2015).

Host species: *Vitis vinifera*.

Association of coccinellids with their host plants

The coccinellids in southern Syria are associated with 90 plant species, number of plants per species of coccinellid ranged between considered 1 and 45 (12.72 ± 13.04 , Average \pm STDEV). 29 coccinellid species were found on fewer than 10 plants, thus specialists; whereas seven species were found on more than 30 plant species and were considered generalists (Figure 7). Generalist species include (from highest to lowest number of plant hosts): *Coccinella septempunctata*, *Oenopia conglobata*, *Coccinella undecimpunctata*, *Stethorus gilvifrons*, *Scymnus apetzi*, *Hippodamia variegata*, and *Scymnus flavicollis*.

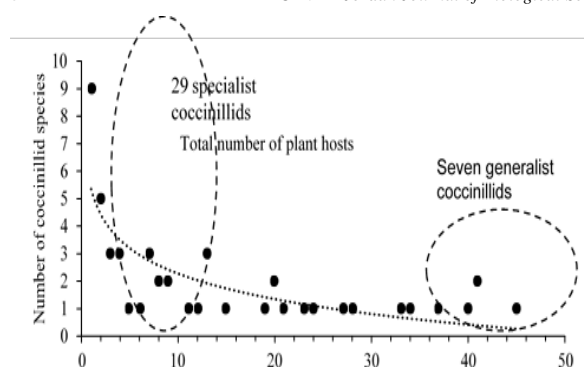


Figure 7. Occurrence of coccinellid species on plant hosts.

On the other hand, the number of coccinellid species per plant host ranged between 1 and 26 different species 7.07 ± 6.87 (Average \pm STDEV). With 54 plant species (60% of all plants) had ≤ 5 different coccinillids, whereas, 18 plants (20% of all plants) had 15-26 different coccinillids (Figure 8). These preferred plants include (from highest to lowest number of coccinillids): *Punica granatum*, *Quercus calliprinos*, *Amygdalus* sp., *Citrus* sp., *Juglans regia*, *Morus alba*, *Zea mays*, *Pinus* sp., *Urtica* sp., *Medicago sativa*, *Ficus carica*, *Populus* spp., *Rubus idaeus*, *Malus communis*, *Pyrus communis*, *Cupressus* sp., *Prunus avium*, and *Prunus armeniaca*. Additionally, at least 75 species of these plant hosts have agricultural value including *Punica granatum*, *Amygdalus* sp., *Malus communis*, *Pyrus communis*, *Morus alba*, and *Citrus* sp.

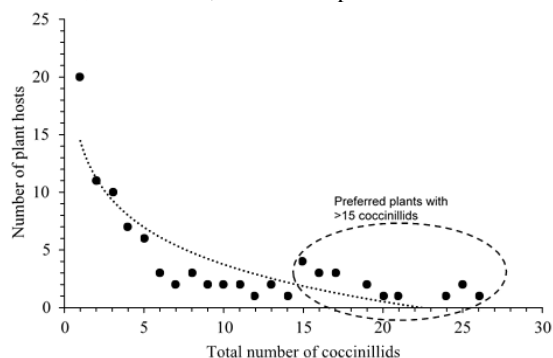


Figure 8. Diversity of coccinellid species on plant hosts.

4. Discussion

In this study, a total of 51 species were recorded. Fifteen are new records for Syria (Table 2). This high number of new records is not surprising, due to the paucity of systematic studies on the coccinellid fauna of Syria. Within the Middle East, Turkey enjoys the highest number of coccinellids reaching up to 84 species (Yurtsever, 2001), followed by Palestine with 71 species (Halperin *et al.*, 1995; Najajrah *et al.*, 2019). The number of coccinellids species of Syria is higher than those recorded from Jordan, Saudi Arabia, and the United Arab Emirates with species 16, 35, and 22 respectively (Fürsch, 1979; Allawi, 1989; aimundo and van Harten, 2000).

Stethorus gilvifrons and *Hippodamia variegata* were the most abundant species, and constituted 18.5% and 14% of the collected specimens respectively. The former species was very efficient predator, essentially feeding on mites. Aslan and Uygün (2005) reported this species from Turkey on aphids. Also, it feeds on all stages of the whitefly *Bemisia tabaci* (Al-Duhawi *et al.*, 2006).

Based on species incidences among sites, three groups of species may be distinguished: there are 19 rare or "satellite" species which were recorded from less than 10 localities with low abundance; 5 modal species found at an intermediate number of sites over larger areas, and 13 ubiquitous "core" species recorded from more than 40 sites with 152-1368 specimens per species (Table 3). Five species (*A. novemdecimpunctata*, *D. rubidus*, *E. octosignatus*, *N. caucasicus* and *P. setulosus*) are considered as very rare species, since only one specimen of each was collected. *Hippodamia variegata*, *Stethorus gilvifrons*, *Oenopia conglobata*, *Coccinella undecimpunctata aegyptica*, *Coccinella septempunctata* and *Scymnus pharaonis* respectively, are widely distributed in the study area.

More coccinellid species were collected in agricultural areas (47 species) than in non-agricultural areas (28 species). Only four species (*E. undulatus*, *E. octosignatus*, *E. quadripustulatus* and *S. fraxini*) were found in non-agricultural areas and were not found in agricultural areas.

Over ninety plant species were identified as hosts for these beetles; some plants have economic value, as fruit trees, crops, woods or ornamentals. The coccinellids on apple, citrus, almond, cherry and other fruit trees were identified. Since Syria is an agricultural country with a wide range of crops, the high diversity of coccinellids in Syria suggests the importance of these insects as biological control agents against harmful agricultural pests.

Acknowledgements

The authors are much indebted to Prof. Dr. Helmut Fürsch (Passau University, Germany) for his help to confirm the identification most species. We wish to thank Dr. Nashat Hamidan for his help in the preparation of figures.

Disclosure statement

No potential conflict of interest was reported by the authors.

References

- Ahmadi AA and Yazdani A. 1993. The coccinellid fauna of Fars Province, part II: tribe Scymnini of subfamily Scymninae. *JESI*, **12/13**: 1-22.
- Al Jundi A and Ahmad M. 1999. [Contribution to the natural enemies for the most important citrus pests in the Coastal region of Syria]. *Tishreen University for Research Studies, Agricultural Sciences Ser*, **21**: 29-40. [In Arabic].
- Al-Duhawi SS, Ali AA and Sameer SH. 2006. The predation efficacy of the predators *Stethorus gilvifrons* (Muls) and *Scolothrips sexmaculatus* (Perg.) on Tobacco Whitefly *Bemisia tabaci* (Gen) which attack cotton plants. *Arab J Plant Prot*, **24**: 112-117.
- Alfieri A. 1976. The Coleoptera of Egypt. *Memoires de la Societe entomologique d'Egypte*, **5**: 1-361.
- Ali HA, Abdul-Rassoul MS and Swail MA. 1990. Systematic list of Coccinellidae recorded for Iraq. *Bull Iraq Nat Hist Mus*, **8**: 45-51.
- Allawi TF. 1989. A list of predaceous coccinellids collected in Jordan. *Dirasat*, **16**: 23-26.

- Almatni W and Khalil N. 2008. A primary survey of aphid species on almond and peach, and natural enemies of *Brachycaudus amygdalinus* in As-Sweida, Southern Syria. In: Ecofruit-13th International Conference on Cultivation Technique and Phytopathological Problems in Organic Fruit-Growing: Proceedings to the Conference from 18th February to 20th February 2008 at Weinsberg/Germany (pp. 109-115).
- Almatni W, Mahmalji M and Al Rouz H. 1999. Recording and preliminary study of some natural enemies of the woolly apple aphid *Eriosoma lanigerum* (Hausmann) (Homoptera: Aphididae) in Syria. Toulouse, France, 39-44.
- Aslan L. 2001. [Biological study of insect *Planococcus citri* (Risso) that strikes the citrus in the Syrian Coast]. *Basel Al Asad Journal of Agricultural Sciences*, **13**: 9-31. [In Arabic].
- Aslan MM and Uygun N. 2005. The aphidophagus Coccinellid (Coleoptera: Coccinellidae) species in Kahramanmaraş, Turkey. *Turk J Zool.*, **29**: 1-8.
- Aswad N. 1998. [Biological Diversity of the Vascular Flora and the Arthropod Fauna in the Fornlok Forest that Represents Wet Forest Ecosystem and Prepared for Declarations as a Nature Reserve]. M. Sc. Theseis, Aleppo University. 252 pp. [In Arabic].
- Bascheer A and Abo Alshamat M. 2004. A preliminary survey of predators and parasitoid insects in Abo-Jarash regoin, Damascus. *Bassel al-Assad Journal for Engineering Sciences- Agricultural, food, Chemical and Biotechnology*. **19**: 65- 85. [In Arabic].
- Biranvand A, Nedvød O, Tomaszewska W, Canepari C, Shakarami J, Fekrat L and Khormizi MZ. 2016. An annotated checklist of Microweiseinae and Sticholotidini of Iran (Coleoptera, Coccinellidae). *ZooKeys*, **587**: 37–48.
- Canepari C and Tedeschi M. 1977. Le sottospecie del *Nephus quadrimaculatus* (Herbst) (Coleoptera: Coccinellidae). *Mem Soc Entomol Ital.*, **55**: 101- 105.
- Canepari C. 1983. Le specie italiane del gruppo *Scymnus frontalis* Fab. con descrizione di due nuove specie (Coleoptera: Coccinellidae). *G Ital Entomol.*, **1**: 179- 204.
- Canepari C. 1991. Coleotteri Coccinellidi della provincia di Ferrara (Coleoptera: Coccinellidae). *Quaderni della Stazione di Ecologia Museo Civico di Storia Naturale di Ferrara*, **4**: 43- 52.
- Canepari C, Fürsch H. and Kreissl E. 1985. Die *Hyperaspis*-Arten von Mittel, West-und Sudeuropa. Systematik und verbreitung (Coleoptera: Coccinellidae). *G Ital Entomol*, **2**: 223-252.
- Chapin EA. 1965. The genera of the Chilocorini (Coleoptera: Coccinellidae). *Bull Mus Comp Zool*, **133**: 227-271.
- Chazeau J, Etienne J and Fürsch H. 1974. Les Coccinellidae de l'île de la Réunion (Insecta, Coleoptera). *Bull Mus Natl Hist Nat 3 Ser.*, n. 210, *Zoologie*, **140**: 265- 297.
- Dauguet P. 1949. **Les Coccinellini de France – L'entomologiste**. Paris, 46pp.
- Duverger C. 1991. Chilocorinae (Coleoptera: Coccinellidae) de France métropolitaine et de Corse. *Bull Soc Linn Bordeaux*, **19**: 75- 95.
- El-Hariri G. 1968. **A List of Recorded Syrian Insects and Acari. Part 1**. Faculty of Agriculture, University of Aleppo, Aleppo, 160 pp.
- El-Hariri G. 1971. **A List of Recorded Insect Fauna of Syria. Part 2**. Faculty of Agriculture, University of Aleppo, Aleppo, 306 pp.
- Fallahzadeh M, Abdmaleki R and Saghaei N. 2013. Contribution to the knowledge of the ladybird beetles (Coleoptera, Coccinellidae), predators of mealybugs (Hemiptera, Pseudococcidae) in Hormozgan Province, Southern Iran. *Linz Biol Beitr*, **45**: 673-679.
- Fürsch 1967a. Familie 62. Coccinellidae (Marienkäfer). In: **Die Käfer Mittel-Europas**. Freude H, Harde K and Lohse G. (Eds.). Band 7. pp. 227-278. Krefeld.
- Fürsch 1967b. *Scymnus (Sidis) hiecki* Fürsch, als feind von *Pseudococcus citri* Risso. *Entomophaga*, **12**: 309- 310.
- Fürsch H and Uygun N. 1980. Neue Scymnini aus der Türkei. *NachrBl Bayer Ent*, **29**: 109-118.
- Fürsch H. 1965. Die palaearktischen Arten der *Scymnus-bipunctatus* Gruppe und die europäischen Vertreter der Untergattung *Sidis*. *Mitt Munch Entomol Ges*, **55**: 178-213.
- Fürsch H. 1979. Insects of Saudi Arabia. Coleoptera: Fam. Coccinellidae. *Fauna of Saudi Arabia*, **1**: 235-248.
- Fürsch H. 1989. The Arabian species of the *Scymnus (Pullus) guimeti*-group (Coleoptera, Coccinellidae). *Fauna of Saudi Arabia*, **10**: 113-123.
- Fürsch H. 1994. Neue Coccinelliden-Art aus Israel (Coleoptera). *Ann Hist-Nat Mus Natl Hung*, **86**: 43- 44.
- Gourreau JM. 1974. **Contribution a l Etude de la fauna de France: Systematique de la Tribu des Scymnini (Coccinellidea)**. Annales de Zoologie, Ecologie Animale. INRA, Institut National De La Recherche Agronomique. Paris. 223 pp.
- Halperin J, Merkl O and Kehat M. 1995. An annotated list of the coccinellidae (coleoptera) of Israel and adjacent areas. *Phytoparasitica*, **23**: 127-137.
- Harde KW. 1999. **A Field Guide in Colour to Beetles**. Blitz editions. Prague. 333 pp.
- Hodek I and Honek A. 1996: **Ecology of Coccinellidae**. Kluwer Academic Publishers. The Netherlands. 464 pp.
- Hodek I. 1973. **Biology of Coccinellidae**. Dr. W. Junk N.V., Pub., The Hage, 260 pp.
- Honek A. 2015. Distribution and habitats, **In: Ecology and Behaviour of the Ladybird Beetles (Coccinellidae)**. Hodek I., van Emden, H.F. and Honek, A. (Eds.). Blackwell Publishing Ltd, pp. 110–140.
- Iablokoff-Khnzorian SM. 1971. Synopsis des *Hyperaspis* Paléartiques (Col.: Coccinellidae). *Ann Soc Entomol Fr (N. S.)*, **7**: 163- 200.
- Iablokoff-Khnzorian SM. 1982. **Les Coccinelles, Coélopteres-Coccinellidae, Tribu Coccinellini des regions Paléartique et Orientale**. Société nouvelles des éditions boubée 11, place Saint-Michel. Paris, 568 pp.
- Jalilvand Kh, Shirazi M, Fallahzadeh M, Vahedi HA, Samih MA and Moeini Naghadeh N. 2014. Survey of natural enemies of mealybug species (Hemiptera, Pseudococcidae) in Kermanshah province, Western Iran to inform biological control research. *J Entomol Res Soc*, **16**: 1-10.
- Ka'ada F. 2002. [Effect of Different Insecticides in Cotton and Their Natural Enemies of Predacious Insects and Parasites in Cotton Fields in Northern Syria]. Ph. D. thesis, Aleppo University. 196 pp. [In Arabic].
- Kabakibi MM. 1993. [Animal biodiversity in a Mediterranean forest ecosystem-Wadi Al Qaren Nature Reserve (West of Damascus)]. 33rd Scientific Week. [In Arabic].
- Klausnitzer B and Klausnitzer H. 1986. **Marienkäfer (Coccinellidae) 3 Überarb.** Aufl. Wittenberg: A. Ziemsen Verlag, 104 pp.
- Kovář I. 2007. Family Coccinellidae Latreille 1807. Pp. 568–631. **In: Catalogue of Palaearctic Coleoptera**. Löbl I. and Smetana A. (eds.). Vol. 4. Elateroidea, Derodontoidea, Bostrichoidea, Lymexyloidea, Cleroidea, Cucujoidea. Apollo Books, Stenstrup, 935 pp.

- Kuznetsov VN. 1997. **Lady Beetles of the Russian Far East**. Memoir No. 1, Center for Systematic Entomology, The Sandhill Crane Press Inc., Gainesville, 248 pp.
- Lababidi MS and Zebitz CP. 1995. Preliminary study on the pistachio psyllid (*Agonoscaena targionii* Lich.) (Psyllidae: Homoptera) and its associated natural enemies in some regions of Syria. *Arab J Plant Prot*, **13**: 62- 68. [In Arabic].
- Le Monnier Y and Livory A. 2003. **Une enquête Manche-Nature: Atlas des Coccinelles de la Manche**. Les Dossiers de Manche-Nature N° 5, 206 p.
- Leeper JR. 1975. **A Review of the Hawaiian Coccinellidae**. Technical Report No. 53, Hawaii national park library, Honolulu, Hawaii, 54 pp.
- Majerus MEN and Kearns P. 1989. **Ladybirds**. No. 10 Naturalists` Handbooks Series. Richmond Publishing Co. Ltd. Slough, England, 103pp.
- Mesbah RA, Nozari J, Allahyari H and Khormizi MZ. 2016. Checklist and distribution of lady beetles (Coleoptera: Coccinellidae) in Iran. *Iran J Anim Biosyst*, **12**: 1-35.
- Moodi S. 1994. **The Coccinellids (Col.: Coccinellidae) Fauna of South East Khorasan, Iran**. M.Sc. Thesis, Shahid Chamran University, Ahvaz, Iran, 158p. [In Persian].
- Najajrah MH, Swaileh KM and Qumsiyeh MB. 2019. Systematic list, geographic distribution and ecological significance of lady beetles (Coleoptera: Coccinellidae) from the West Bank (Central Palestine). *Zootaxa*, **4664**: 1–46.
- Özden Ö, Uygun N and Kersting U. 2006. Ladybird beetles (Coccinellidae: Coleoptera) from northern Cyprus, including six new records. *Zool Middle East*, **39**: 97- 100.
- Poorani J. 2004. An annotated checklist of the Coccinellidae of the Indian region. World Wide Web electronic publication. www.angelfire.com/bug2/j.checklist.pdf. [accessed on 15.3.2010].
- Raimundo AAC, Alves MLG. 1986. **Revisão dos Coccinélidos de Portugal**. Universidade de Évora, Évora, Évora, 103 pp.
- Raimundo AAC and van Harten A. 2000. An annotated checklist of the Coccinellidae (Insecta: Coleoptera) of Yemen. *Fauna of Arabia*, **18**: 211-243.
- Raimundo AC, Fürsch H and van Harten A. 2008. Order Coleoptera, family Coccinellidae. In: **Arthropod Fauna of the United Arab Emirates**. Van Harten A. (Ed.). Dar Al Ummah printing. Adu Dhabi, United Arab Emirates, **1**: 217-239.
- Seago AE, Giorgi JA, Li J and Ślipiński A. 2011. Phylogeny, classification and evolution of ladybird beetles (Coleoptera: Coccinellidae) based on simultaneous analysis of molecular and morphological data. *Mol Phylogenet Evol*, **60**: 137–151.
- Ślipiński A. 2007. **Australian Ladybird Beetles (Coleoptera: Coccinellidae) their Biology and Classification**. Australian Biological Resources Study, Canberra, 286 pp.
- Talhook AS. 1961. Records of entomophagous insects from Lebanon. *Entomophaga*, **6**: 207-209.
- Uygun N and Fürsch H. 1981. Die Hyperaspis-Arten der Türkei (Coleoptera, Coccinellidea). *NachrBl Bayer Ent*, **30**: 12- 16.
- Uygun N. 1981. **Türkiye Coccinellidea (Coleoptera) faunası üzerinde taksonomik arařtırmalar**. Dilek Matbaası, Adana, 111 pp. [In Turkish].
- Winkler A. 1927. **Catalogus Coleopterorum Regionis Palaearcticae**. A. Winkler, Wien, 1698 pp.
- Younes GH, Ahmad M and Ali N. 2015. Morphological, biological and ecological studies of the mycophagous ladybird *Psyllobora vigintiduopunctata* L. (Coleoptera: Coccinellidae) on powdery mildew fungi in the coastal region of Syria. *JJAS*, **11**: 483-494.
- Yurtsever S. 2001. A Preliminary study on the Ladybirds (Coleoptera: Coccinellidae) of Edirne in North-Western Turkey. *Turk J Zool*, **25**: 71-75.
- Zhou X, Honek A, Powell W and Carter N. 1995. Variations in body length, weight, fat content and survival in *Coccinella septempunctata* at different hibernation sites. *Entomol Exp Appl*, **75**: 99-107.

Larvicidal Potentials of Three Indigenous Plants Against Malaria Vector, *Anopheles Gambiae* L.

Sulaimon Adebisi Aina^{1,*}, Ismail Babatunde Onajobi², Ajoke Saidat Sanusi³ and Oluwatobi Shakirat Kolejo⁴

¹Department of Zoology & Environmental Biology, Olabisi Onabanjo University, Ago-Iwoye, Ogun State, Nigeria; ²Department of Microbiology, Olabisi Onabanjo University, Ago-Iwoye, Ogun State, Nigeria; ³Department of Plant Science, Olabisi Onabanjo University, Ago-Iwoye, Ogun State, Nigeria; ⁴Forestry Research Institute of Nigeria State, Jericho, Ibadan, Oyo State, Nigeria

Received: July 18, 2020; Revised: November 21, 2020; Accepted: January 12, 2021

Abstract

Malaria is one of the highest causes of mortality in the populations of African, South Asia, and Latin America as it contributes a large part of the continued impoverishment of these populations. The efficacy of both the ethanolic and aqueous extracts of the fruits of *Calotropis gigantea*, R. Br. (Asclepiadaceae), *Aframomum melegueta* K. Schum (Zingiberaceae), and seeds of *Blighia sapida* (Sapindaceae) were tested on the third instar larvae of *Anopheles gambiae* (L). 200 g of the blended form of each plant material was suspended in 500 mls of water and filtered after 1 day. The filtrates were then dried to get the stock from which serial concentrations (20, 10, 1, 0.1 mg/ml) were reconstituted. The result after a 24 hrs bioassay time shows that the *A. melegueta* (59.4 %) ethanolic extract with LC₅₀ values of 0.3 mg/ml acted most followed by its aqueous form (38.89 %) with LC₅₀ 2.57 mg/ml, ethanolic extract of *C. gigantea* (27.78 %) with LC₅₀ 5.57 mg/ml, the ethanolic form of *B. sapida* (27.5 %) 6.25 mg/ml while the aqueous forms of *C. gigantea* and *B. sapida* were 6.37 at 25 % and 6.5mg/ml at 26.6% respectively. For all the plants used, *A. melegueta* was the most potent plant and there was significant difference (p<0.05) between the ethanolic extract and the aqueous form. The use of insecticides of plant origins may serve as a suitable alternative to chemical insecticides in the future with their characteristic relative safety, degradability, and abundance in many areas of the world.

Keywords: *Calotropis gigantea*, *Aframomum melegueta*, *Blighia sapida*, *Anopheles gambiae*, Ethanolic extract, Aqueous extract.

1. Introduction

There are approximately 3,500 species of mosquitoes grouped into 41 genera. Out of these only *Anopheles* is still the transmitter of human malaria (NCID, 2004). And within the genus *Anopheles* comprising more than 400 described species approximately, 70 species are active vectors of malaria affecting humans (Pimenta *et al.*, 2015). The life cycle starts when the female *Anopheles* mosquito takes a blood meal from a *Plasmodium* infected vertebrate host and ingests gametocytic forms of the parasite that are present in the blood (Pimenta *et al.*, 2015). The mosquito *Anopheles gambiae* is the principal vector of malaria in Africa. According to the WHO statistics, this parasitic disease infects from 300 to 500 million persons per year in the world and kills more than a million and a half each year, mainly African children (Marimo *et al.*, 2016). Together with AIDS, malaria is one of the causes of mortality in the populations of African, South Asia, and Latin America and it contributes a large part of the causes of poverty among these populations (Aina *et al.*, 2009a). ; it contributes a large part of the continued impoverishment of these populations (Aina *et al.*, 2009a).

Calotropis gigantea is a large shrub growing to 4 m tall. Its flowers occur in waxy clusters of either white or lavender. The stem is oval with light green leaves, and milky in appearance (Li *et al.*, 2015). The latex of *C. gigantea* contains cardiac glycosides, fatty acids, and calcium oxalate. The milky juice of *Calotropis* sp. was used against arthritis, cancer, and as an antidote for snakebite (Upadhyay, 2014)

A. melegueta is a perennial herbaceous plant found in swampy areas along the West African coast. Its trumpet-shaped, purple flowers develop into pods 5-7 cm long, containing numerous small, reddish-brown seeds. The presence of aromatic ketones, such as (6)-paradol (systematic name: 1-(4-hydroxy-3-methoxyphenyl)-decan-3-one) caused the pungent, peppery taste of the seeds. The dominating flavor components are the essential oils which closely relate to cardamom and occur in traces (Austin, 2004). In West African folk medicine, "grains of paradise" are valued for their warming and digestive properties, and among the Efik in Nigeria they have been used for divination and ordeals (Simmons, 1956) to determine guilt (Nwaehujor, 2014). *A. melegueta* was brought to the Caribbean and

* Corresponding author e-mail: : aina.sulaimon@oouagoiwoye.edu.ng.

Latin America, where it is used in religious (voodoo) rites (Moret, 2013)

Blighia sapida (Fig. 3) is also known as ackee in English and locally as Okpu (Igbo), Isin (Yoruba), Ukpe (Edo) and Gwanja kusa (Hausais a fruit of the Sapindaceae soapberry family. It is native to tropical West Africa (Kristen, 2003; Simons and Leakey, 2004). The English common name is derived from the West African Akan *akye fufo* (Simons, and Leakey, 2004). It is used for its "soap" properties as a laundering agent or fish poison in West Africa and the Caribbean Islands. The ripe arils, leaves or bark were used to treat minor ailments in traditional African medicine (Sinmisola *et al.*, 2019).



Figure 1. *Calotropis gigantea* fruit (Source, Whistler, 2000)



Figure 2. *Aframomum melegueta* fruit (Source, Osuntokun, 2020)



Figure 3. *Blighia sapida* fruit showing seeds (black)(Source, Kristen, 2003)

At present biocontrol and biopesticide agents are only operational against mosquito larvae and pupae (Thomas, 2018). Plant materials have been used in different forms to

control mosquitoes; for example, ancient peoples used smoke from burning cattle or goat dung to drive out mosquitoes from their caves or huts before sleeping (Kihampa, 2011). Later on, certain herbs and barks of some trees were added to the smoldering fire to enhance the repellent action of smoke. A large number of plant extracts have been reported to have mosquitocidal or repellent activity against mosquito vectors but very few plant products have shown practical utility for mosquito control (Mohan and Ramaswamy, 2007).

Botanical insecticides are made from chemical extracts from plants. Examples are Pyrethrum which is an insecticide derived from the dried flower of *Chrysanthemum cinerariaefolium* grown in Kenya, Australia, and Tanzania. Pyrethrins are chemicals extracted from the pyrethrum flower, Rotenone is extracted from the roots of several tropical legumes such as the cube plant grown in Peru, originally used in India as a fish poison but moderately toxic to human (Sola *et al.*, 2014).

Therefore, the objective of this study is to investigate the effects aqueous and ethanolic extracts of the fruits of *Calotropis gigantea*, R. Br. (Asclepiadaceae), *Aframomum melegueta* K. Schum (Zingiberaceae), and seeds of *Blighia sapida* (Sapindaceae) on third instar larvae (Aina *et al.*, 2009a) of *Anopheles gambiae* (L) to discover more plant products that can be used to control the prevalence of malaria in developing nations.

2. Materials and Methods

2.1. Experimental Site

The research was conducted at the insectaries of the Department of Zoology and Environmental Biology, Olabisi Onabanjo University, Ago-Iwoye, Ogun State, Nigerian located on Lat.6.942374, Long 3.921517.

2.2. Collection of Plant Materials

The matured fruits of *A. melegueta* were bought in from Awolowo Market in Sagamu, while the matured fruits of *C. gigantea* and the seeds of *B. sapida* were collected at Sagamu and Ago-Iwoye respectively, both in the Ogun State, Southwestern Nigeria. The materials were also dried in the Gallemhamp oven (Aina *et al.*, 2009b; Ariyo *et al.*, 2011) and identification of the plants was done at the Herbarium of the Department of Plant Science, OOU, Ago-Iwoye.

2.3. Culture of Mosquito

The 3rd instar *Anopheles gambiae* mosquito larvae used for this study was collected from a culture maintained in the insectary of the Department of Zoology and Environmental Biology, OOU, Ago-Iwoye, Nigerian. The third stage of larvae development is identified morphologically (according to Gillies and Coetzee, 1987) using dissecting microscope to examine characters like: length between 3 and 5 mm, well developed palmate hairs, widened sclerotized head collar and long lateral setae (tufty at thoracic region).

2.4. Aqueous Extraction Preparation

The plant materials were blended using the Moulinex blender (LM243027). 200 grams of each grounded botanical was then soaked separately in 500 mls distilled

water for 1 hour to dissolve the active components for 24 hrs. The suspension was then filtered using the Whatman's No.1 filter paper. The filtrate was freeze-dried to remove the water solvent in each case using the Edwards Modulyo Freeze-drying machine. From the freeze-dried (Stock), serial dilutions were made to obtain different concentrations of 20, 10, 1, 0.1 mg/ml (Ijarotimi *et al.*, 2013).

2.5. Ethanolic Extraction Preparation

Two hundred grams (200 g) of each blended material was mixed with 500 mls of 70% ethanol in separate jars and allowed to stay for 24 hrs. They were then filtered into separate conical flasks using the Whatman's No.1 filter paper and the filtrates were put into the Gallenham Vacuum oven to evaporate the extraction solvent (Aina *et al.*, 2009a). Serial dilutions were made from the stock to obtain different concentrations of 20, 10, 1, 0.1 mg/ml mg/ml (Ijarotimi *et al.*, 2013).

2.6. Bioassay of Extracts

Ten active third instar larvae of the *Anopheles gambiae* were transferred into (100 ml) containers containing 2 ml of distilled water and 50 ml from each graded concentrations of each extract was added. In the controls, the larvae were put in 50 ml of distilled water and 2% ethanol respectively. Three replicates were set-up for each concentration including the control. The set up was allowed to stay undisturbed for 24 hours, after which the larvae were put inside distilled water to observe any recovery. A time of 5 minutes was given to observe such recovery in each treatment. Larvae were counted as dead when they were not coming to the surface for respiration and were probe insensitive. The percentage mortality was reported from the average of three replicates.

$$\text{Percentage mortality} = \frac{\text{Number of dead larvae}}{\text{Number of larvae introduced}} \times 100$$

2.7. Statistical Analysis

Data recorded from the bioassay tests were analyzed using probit analysis based on the Statistical Analysis System (SAS) version 16. Comparison among seeds, fruits, between seeds and fruits, and all the plants were also sorted-out using the Analysis of Variance (ANOVA) and Turkey's multiple comparison test for post hoc comparison which were carried out using SPSS for windows version 21.

Table 2. Comparison between the ethanolic and aqueous extract for each plant

	Levene's Test for Equality of Variances		t-test for Equality of Means		Sig. (2-tailed)	Mean Difference	Std. Error Difference
	F	Sig.	t	df			
<i>C. gigantea</i>	.089	.767	.298	70	.767	.2778	.93232
			.298	69.963	.767	.2778	.93232
<i>B.sapida</i>	.103	.749	-.089	70	.929	-.0833	.93637
			-.089	69.872	.929	-.0833	.93637
<i>A. melegueta</i>	.595	.443	-2.023	70	.470	-2.0556	1.01631
			-2.023	69.796	.470	-2.0556	1.01631

3. Results

For the percentage mortality, Table 1 shows that of *A. melegueta* (59.44%) fruits extracted with ethanol give the highest mortality followed by its aqueous form (38.89%), ethanolic extract of the fruits of *C. gigantea* (27.78%), ethanolic extract of *B. sapida* (27.5%) seeds, the aqueous extract of *B. sapida* (26.67%) while the least mortality was recorded for *C. gigantea* (25%). The LC₅₀ values indicated that the ethanolic extract of *A. melegueta* (0.30 mg/ml) was the most active followed in descending order by its aqueous form 2.57mg/ml, ethanolic extract of fruits of *C. gigantea*, ethanolic extract of seeds of *B. sapida* (6.25mg/ml), and aqueous extract of *C. gigantea* (6.37mg/ml) while the aqueous form of *B. sapida* (6.5mg/ml) was least in performance.

Table 1. Percentage Mortality of *A. gambiae* larvae tested with ethanolic extract and water of the plants

Extraction medium	Plant species	Part used	Total mortality (360) and % mortality	LC ₅₀ (mg/ml)
Ethanol	<i>B. sapida</i>	Seed	99 (27.50%)	6.25
	<i>C. gigantea</i>	Fruit	100 (27.78%)	5.57
	<i>A. melegueta</i>	Fruit	214 (59.44%)	0.30
	Control	NA	0 (0.00%)	0.00
Water	<i>B. sapida</i>	Seed	96 (26.67%)	6.50
	<i>C. gigantea</i>	Fruit	90 (25.00%)	6.37
	<i>A. melegueta</i>	Fruit	140 (38.89%)	2.57
	Control	NA	0 (0.00%)	0.00

Note NA – Not applicable

Table 2 shows the comparisons between the ethanolic and aqueous extracts of each plant; there were no significant differences between the ethanolic and aqueous extract for each of the plants; *C. gigantea* (P = 0.767), *B. sapida* (P = 0.749) and *A. melegueta* (0.443). While in Tables 3 there was no significant difference in the toxicity of the ethanolic extracts of all the plants (P = 0.377), but in contrast there was significant difference among the aqueous extracts of the plants (P = 0.001) and between the ethanolic and aqueous groups (P = 0.028). The post hoc test shows that only *A. melegueta* had a significant difference (0.00) with the two other plants, which shows that it is most potent using Fisher's LSD (Table 4).

Table 3. Comparison within each extraction medium and between the ethanolic and aqueous groups.

		Sum of Squares	df	Mean Square	F	Sig.
Ethanolic extract	Between Groups	32.889	2	16.444	.986	.377
	Within Groups	1751.778	105	16.684		
	Total	1784.667	107			
Aqueous extract	Between Groups	265.574	2	132.787	7.969	.001
	Within Groups	1749.639	105	16.663		
	Total	2015.213	107			
Ethanolic versus Aqueous media	Between Groups	20.782	1	20.782	1.170	.028
	Within Groups	3799.880	214	17.756		
	Total	3820.662	215			

Table 4. Post Hoc Tests for Multiple Comparisons

	Comparison	Mean Difference	Std. Error	Sig.
Duncan	C - A	-2.8704	0.6298	0
	C - B	-3.7002	0.6298	0.953
	A - B	2.8333	0.6298	0

* The mean difference is significant at the .05 level. C – *Calotropis gigantea*; A – *Aframomum melegueta*; B – *Bligia sapida*

4. Discussion

Challenges posed by high cost and development of resistance in many vector mosquito species to many of the patented synthetic insecticides have revived interest in exploring the pest control potentials of botanicals (Karunamoorthi *et al.*, 2008; Karunamoorthi, 2012). Also, the tendency toward the use of “soft” pesticides was encouraged by the economic and environmental concerns about chemicals (Awad and Shimaila, 2003; Sharma *et al.*, 2016).

The assessment of botanicals for the three plant extracts shows that the ethanolic and aqueous extracts of *A. melegueta* were the most effective for the control of *A. gambiae* larvae; this could be due to the similarity shared between the two extracted components of the plants based on the solvent type used while the aqueous extract of *C. gigantea* was the least to pose mortality. This is in line with the report of (Oke *et al.*, 2001) in which the hexanolic extract of *P. guineense* kills both 77% and 95% of the *Aedes aegypti* larvae in 1hour and 24 hours respectively. Fafioye *et al.* (2004) reported that the ethanolic extracts of *Parkia biglobosa* and *R. vinifera* were more potent against the juveniles of *Clarias gariepinus* than the aqueous forms. This is due to the polarity, volatility, and its (ethanol) power to dissolve more of the active constituents. Also, the extract of *Cannabis sativa* (Moraceae) tested on *Anopheles stephensi* within 24 and 48hours gave LC₅₀ of 15.58 and 8.04ppm respectively (Maurya *et al.*, 2007; Aina *et al.*, 2009a).

This result falls in line with the study of Ileke *et al.* (2017) who reported that the leaf and seed of *A. melegueta* were screened for their potential larvicidal and pupicidal properties against *Anopheles* species in the laboratory. After a 24 hrs bioassay time, larval and pupal mortalities increased with increase in concentration irrespective of the type of plant part used for the extraction while the seed extract showed more insecticidal effect on both larvae and

pupae of *Anopheles* species. The powder of *A. melegueta* posed high mortality in adult *Sitophilus zeamais* within 24hours (LC₅₀ of 0.398g/5g maize) (Ribeiro *et al.*, 2017). The mosquitocidal effect of acetone extract of *Cymbopogon citratus* (DC). Stapf., *Momordica charantia* L., *Zingiber officinale* (Rof), *Xylopia aethiopica* (Dunl). A. Rich., *Ocimum gratissimum* L. and *A. melegueta* (Ros) K. Schum tested against the cowpea aphid, *Aphis craccivora* Koch was investigated. Extracts from *Z. officinale* and *A. melegueta* had the greatest effect in causing mortality of *A. craccivora* and also hindered its reproduction (Karunamoorthi and Ilango, 2010).

Govidarajam and Sivakumar, 2014 reported the efficacy of *Eeythrina indica* (Lam.) on *Anopheles stephensi*, *Aedes aegypti*, and *Culex quinquefasciatus* larvae using hexane, benzene, chloroform, ethyl acetate and methanol as solvents for extraction. After 24 hrs of the bioassay, all the extracts showed high larvicidal effects.

The oil extract of *Citrus hystrix* (Kaffir lime) oil exhibits highest repellency activity (95.33%) against German cockroach (*Blattella germanica*) over the oils of *Cymbopogon winteruanus* (Citronella) and *Eucalyptus globulus* (Eucalyptus) in which both had 85.00% mortality (Chooluck *et al.*, 2019, while by comparison the hexane and ethanol extracts of *Achyranthus aspera* had highest Larvicidal potentials with LC₅₀ value of 82.555 ppm and 68.133 ppm over those of *Cassia occidentalis*, *Catharanthus roseus*, *Lantana camara* and *Xanthium strumarium*.

5. Conclusion

Although the statistical analysis revealed that the ethanolic extraction is better in performance, this does not mean that we cannot also use the aqueous form for such control. There is still a need to investigate the use of other volatile solvents to discover the unknown properties of these plants. Invariably, botanical insecticides may serve as suitable alternative to synthetic insecticides in the future as they are safer, easily degradable, and are readily found in many areas of the world (Sreedhanya *et al.*, 2017).

Competing interests

The author(s) declare that they have no competing interests.

Authors' contributions

SAA, ASS and OSK conducted the experiments and drafted the manuscript. IBO participated in the writing of the final versions of the manuscript and provided other logistical issues towards the publication of the article. SAA also oversaw the acquisition of laboratory requirements and provision of literature.

Acknowledgments

The authors appreciate Prof. O.O. Fafioye, Head, Department of Zoology and Environmental Biology, Olabisi Onabanjo University, Ago-Iwoye for allowing the use of the insectaries in the Animal House. Also, we thank Alhaja Hamdallat Funke Aina who assisted in purchasing the fruits of *A. melegueta* from markets and locating the plants for procurement.

References

- Aina SA, Banjo AD, Lawal OA, and Jonathan K. 2009b. Efficacy of some Plant Extracts on *Anopheles gambiae* Mosquito larvae. *Acad. J. Entomol.*, **2(1)**: 31-35.
- Aina SA, Banjo AD, Lawal OA, Okoh HI, Aina OO and Dedek GA. 2009a. The toxicity of extracts of *Tetrapleura tetraptera* (Aridan), *Delonix regia* (Flame of the Forest) and *Raphia vinifera* (Raffia Palm) on the larvae of *Anopheles gambiae*. *Acad J Entomol.*, **2(2)**: 67-70.
- Ariyo OA, Shonubi OO, Oyesiku OO and Akande AO. 2011. Antimicrobial activity of the indigenous liverwort, *Riccia nigerica* Jones, from Southwestern Nigeria. *Evansia*, **28(2)**: 43-48.
- Austin D. 2004. "Florida ethnobotany". CRC Press, p. 170. ISBN 0-8493-2332-0.
- Awad OM and Shimaila A. 2003. Operational use of neem oil as an alternative anopheline larvicide. Part A: Laboratory and field efficacy. *East Mediterr Health J.*, **9(4)**: 637-45.
- Chooluck K, Teeranachaidekul V, Jintapattanakit A, Lomarat P and Phechkrajang C. (2019). Repellency effects of essential oils of *Cymbopogon winterianus*, *Eucalyptus globulus*, *Citrus hystrix* and their major constituents against adult German cockroach (*Blattella germanica*) Linnaeus (Blattaria: Blattellidae). *Jordan J Biol Sci.*, **12(4)**: 519-521.
- Fafioye OO, Adebisi AA and Fayode SO. 2004. Toxicity of *Parkia biglobosa* and *Raphia vinifera* extracts on *Clariis gariepini* juveniles. *Afric J Biotech.*, **3(10)**: 627-630.
- Gillies MT and Coetzee M. 1987. A supplement to the Anophelinae Africa South of the Sahara (Afrotropical region), Johannesburg, South Africa. *S Afr Inst Med Res.*, 55:1-143.
- Govindarajan M and Sivakumar R. 2014. Larvicidal, ovicidal, and adulticidal efficacy of *Erythrina indica* (Lam.) (Family: Fabaceae) against *Anopheles stephensi*, *Aedes aegypti*, and *Culex quinquefasciatus* (Diptera: Culicidae). *Parasitol Research.*, **113**: 777-791.
- Ijarotimi OS, Adeoti OA and Ariyo O. 2013. Comparative study on nutrient composition, phytochemical, and functional characteristics of raw, germinated, and fermented *Moringa oleifera* seed flour. *Food Sci & Nutrition.*, **1(6)**: 452-463. <https://doi.org/10.1002/fsn3.70>.
- Ileke KD, Adesina JM and Okunola OG. 2017. Larvicidal and pupicidal potential of *Aframomum melegueta* K. Schum extract against mosquito, *Anopheles species*. *J Entomol Res Soc.*, **19(1)**: 121-127.
- Karunamoorthi K and Ilango K. 2010. Larvicidal activity of *Cymbopogon citratus* (DC) Stapf. and *Croton macrostachyus* Del. against *Anopheles arabiensis* Patton, a potent malaria vector. *Euro Rev Med & Pharmacol Sciences.*, **14(1)**: 57-62 PMID: 20184090.
- Karunamoorthi K, Ramanujam S and Rathinasamy R. 2008. Evaluation of leaf extracts of *Vitex negundo* L. (Family: Verbenaceae) against larvae of *Culex tritaeniorhynchus* and repellent activity on adult vector mosquitoes. *Parasitol Res.*, 103: 545. <https://doi.org/10.1007/s00436-008-1005-5>
- Karunamoorthi K. 2012. Medicinal and aromatic plants: a major Source of green pesticides/ risk reduced pesticides. *Med Aromat Plants.*, **1**: 8 doi: 10.4172/2167-0412.1000e137.
- Kihampa C. 2011. Tanzanian botanical derivatives in the control of malaria vectors: opportunities and challenges. *J Appl Sci Environ Mgt.*, **15**: 155-160.
- Kristen L. 2003. **Tropical Flowering Plants: A Guide to Identification and Cultivation**. Timber Press. ISBN 0-88192-585-3.
- Li B, Gilbert MG and Stevens WD. 2015. "Calotropis gigantea (Linnaeus) W. T. Aiton, Hortus Kew. ed. 2. 2: 78. 1811", *Flora of China online*, retrieved 19 July 2015.
- Marimo P, Hayeshi R and Mukanganyama S. 2016. Inactivation of *Anopheles gambiae* glutathione transferase $\epsilon 2$ by epiphylloucoumarin. *Biochem Res Int.*, **2016**: 2516092. doi: 10.1155/2016/2516092. PMID: 26925266. PMID: 26925266.
- Maurya P, Mohan L, Sharma P, Batabyal L and Srivastara CN. 2007. Larvicidal efficacy of *Aloe barbadensis* and *Cannabis sativa* against the malaria vector *Anopheles stephensi* (Diptera: Culicidae). *Entomol Research J.*, **37(3)**: 153-156.
- Mohan DR and Ramaswamy M. 2007. Evaluation of larvicidal activity of the leaf extract of a weed plant, *Ageratina adenophora*, against two important species of mosquitoes, *Aedes aegypti* and *Culex quinquefasciatus*. *Afric J Biotech.*, **6(5)**: 631-638. Available online at <http://www.academicjournals.org/AJB>.
- Moret ES. 2013. **Trans-Atlantic Diaspora Ethnobotany: Legacies of West African and Iberian Mediterranean Migration in Central Cuba**. In: Voeks R., Rashford J. (eds) African Ethnobotany in the Americas. Springer, New York, NY. https://doi.org/10.1007/978-1-4614-0836-9_9. ISBN 978-1-4614-0835-2.
- National Centre for Infectious Diseases (NCID). 2004. **Mosquitoes**. Division of parasitic diseases, Atlanta, 6pp. <https://www.ncid.sg> (July 17, 2020).
- Nwaehujor CO, Eban LK, Ode JO, Ejiofor CE and Igile GO. 2014. Hepatotoxicity of Methanol Seed Extract of *Aframomum melegueta* [Roscoe] K. Schum. (Grains of paradise) in Sprague-Dawley Rats. *Am J Biomed Research.*, **2(4)**: 61-66. doi: 10.12691/ajbr-2-4-1.
- Oke OA, Anyale OO, Amusan AAS, and Okorie TG. 2001. Toxicity of Hexanolic extract of *Piper guineense* Schum & Thunn (Piperaceae) seed oil to larvae of *Aedes aegypti* (L). *European J Sci Research.*, **18(1)**: 6-11.
- Osuntokun OT. 2020. *Aframomum melegueta* (grains of paradise). *Ann Microbiol & Infectious Dis.*, **3(1)**: 1-6. ISSN 2637-5346.
- Pimenta PFP, Orfano AS, Bahia AC, Duarte APM, Ríos-Velásquez CM, Melo FF, Pessoa FAC, Oliveira GA, Campos KMM, Villegas LM, Rodrigues NB, Nacif-Pimenta R, Simões RC, Monteiro WM, Amino R, Traub-Cseko YM, Lima JBP, Barbosa MG, Lacerda MV, Tadei WP and Secundino NFC. 2015. An overview of malaria transmission from the perspective of Amazon *Anopheles* vectors. *Mem Inst Oswaldo Cruz.*, **110(1)**: 23-47. doi: 10.1590/0074-02760140266. PMID: 26371216.

- Ribeiro AV, Luz CEA, Bastos CS, Krieger YST, Da Silva NH and Da Silva WB. 2017. Toxicity of botanical and synthetic formulations to the maize weevil, *Sitophilus zeamais* (Coleoptera: Curculionidae). *Revist Colombiana de Entomol.*, **43(2)**: 167-172. DOI: 10.25100/socolen.v43i2.5938.
- Sharma A, Kumar S and Tripathi P. (2016). Evaluation of the larvicidal efficacy of five indigenous weeds against an Indian strain of dengue vector, *Aedes aegypti* L. (Diptera: Culicidae). *J Parasitol Res.*, ID 2857089. <http://dx.doi.org/10.1155/2016/2857089>.
- Simons AJ and Leakey RRB. 2004. Tree domestication in tropical agroforestry. *Agroforestry Sys.*, **61-62**: 167-181.
- Sinmisola A, Oluwasesan BM and Chukwuemeka AP. 2019. "*Blighia sapida* K.D. Koenig: A review on its phytochemistry, pharmacological and nutritional properties". *J Ethnopharm.*, **235**: 446-459. doi: 10.1016/j.jep.2019.01.017.
- Sola P, Mvumi BM, Ogendo JO, Mponda O, Kamanula JF, Nyirenda SP, Belmain SR and Stevenson PC. 2014. Botanical pesticide production, trade and regulatory mechanisms in sub-Saharan Africa: making a case for plant-based pesticidal products. *Food Sec.*, **6(3)**: 369-384. DOI: 10.1007/s12571-014-0343-7.
- Sreedhanya S, Athira A and Pushpalatha E. 2017. Larvicidal and repellent efficacy of some of the weed plant extracts against *Culex quinquefasciatus* Say. *J Adv Lab Research Biol.*, **8(1)**: 6-11. ISSN: 0976-7614.
- Thomas MB. 2018. Biological control of human disease vectors: a perspective on challenges and opportunities. *BioControl*, **63**: 61-69. <https://doi.org/10.1007/s10526-017-9815-y>.
- Upadhyay RK. 2014. Ethnomedicinal, pharmaceutical and pesticidal uses of *Calotropis procera* (Aiton) (Family: Asclepiadaceae). *Int J Green Pharm.*, **8**: 135-46.
- Whistler WA. 2000. **Tropical Ornamentals; A Guide**. Timber Press Inc. Oregon. ISBN 0-88192-448-2.

Examination of Microplastic Particles in Reef Fish Food in Ternate Island Waters, Indonesia

Mimien Henie Irawati Al Muhdhar^{1*}, I Wayan Sumberartha¹, Zainudin Hassan², Muhammad Shalahuddin Rahmansyah³, M. Nasir Tamalene⁴

¹ Faculty of Mathematics and Natural Science, Universitas Negeri Malang, Box 65139 Kota Malang Jawa Timur-Indonesia; ² Faculty Sains Sosial dan Kemanusiaan University Teknologi Malaysia, Box 81310 Skudai Johor Bahru-Malaysia; ³ Sekolah Tinggi Teknik Industri Turen Malang, Box 65175 Turen Kabupaten Malang- Indonesia; ⁴ Biology Universitas Khairun Jl. Bandara Babullah Kampus 1 Akehuda Box 97728. Ternate, Indonesia.

Received: July 20, 2020; Revised: November 27, 2020; Accepted: January 12, 2021

Abstract

Microplastics are pollutants, such as debris from human activities that contaminate several marine biotas and the environment. This research examined the occurrence of microplastic particles in the fish digestive tract in Ternate Island waters, Indonesia. The visual method carried out in the laboratory using a stereo microscope with a magnification of up to 40x was used to identify microplastics in the intestines and stomachs of fish. After observation, the pollutants were systematically counted in the range of 0.3-5 mm based on color, size, number, and shape. They were also classified into: 1) fragments, 2) films, 3) lines/fibers, 4) foams, and 5) pellets categories. Furthermore, six types of fishes including *Epinephelus fuscoguttatus*, *Epinephelus coioides*, *Epinephelus suillus*, *Siganus canaliculatus*, *Synanceia*, and *Scarus psittacus* were collected from four sites, Kasturian, Kampung Makasar, Mangga dua, and Kalumata between August and September 2019. The results showed 183, represented by 83.18%, of the 220 reef fish individuals studied have ingested plastics. Moreover, a total of 594 plastic particles were found in the digestive tract of which 47.81% were fragments, 38.22% films, 2.69% foams, 2.36% fibers, 7.41% line, and 1.52% of 1.8 to 5 mm sized pellets. The color distribution in all locations include 46.80% transparent, 32.15% black, 5.56% pink, 6.06% yellow, 5.22% blue, and 4.21% red. The findings of this study provide the first evidence of microplastic contamination in reef fishes of the Ternate Island waters littoral zone – Indonesia.

Keywords: Microplastic Particles, Reef Fish Food, Ternate Island Waters, Indonesia

1. Introduction

The increase in global plastic production has led to the pollution of oceans with 4.8 to 12.7 million metric tons (MMT) of plastic wastes, and Indonesia was ranked second among the countries with the highest contribution with 0.48-1.29 MMT (Jambeck *et al.*, 2015). Microplastics are generally defined as plastics with a diameter less than 5 mm formed through the decomposition of micro-plastics or abrasive materials used in cosmetics and detonation media (Barnes *et al.*, 2009). They have the potential to cause damage and contaminate the marine ecosystem due to the continuous increase in the global production of plastic wastes (Barnes *et al.*, 2009); (Jundong Wang *et al.*, 2016). Microplastics also cause physical and toxicological damage to the marine organism (Law & Thompson, 2014) and threat to marine biota due to their small size which makes them biologically available for organisms in all food networks (Betts, 2008; Wick *et al.*, 2013; Bergmann *et al.*, 2015).

Marine fauna in the ocean such as marine invertebrates (Murray & Cowie, 2011), fishes (Boerger *et al.*, 2010; Romeo *et al.*, 2015; Davison & Asch, 2011), Zooplankton (Cole *et al.*, 2013), Crustaceans (Goldstein & Goodwin, 2013) sea birds (Ryan *et al.*, 2009), and mammals (Eriksson & Burton, 2003) ingest microplastics

in the water, and this has negative effects on their health. The consumption of these particles reduces the eco-physiological function of the organisms thereby causing physical injuries and physiological stress (Rochman *et al.*, 2013). In addition, microplastics are prone to contamination by toxic organic pollutants in water (Bakir *et al.*, 2014; Rowland *et al.*, 2016), which after being ingested enter the food chain to cause bio-magnification (Farrell & Nelson, 2013; Setälä *et al.*, 2016).

The contamination of waters areas by microplastics has been reported in Cilacap Gulf with 2.5 mg m³ concentration (Syakti *et al.*, 2017), Jakarta Gulf (Manalu *et al.*, 2017), and small islands in Bintan Regency, Kepulauan Riau Province (Syakti *et al.*, 2018). The particles currently existing in the Java sea are assumed to have originated from the South China Sea and the Pacific Ocean (Handyman *et al.*, 2019). Meanwhile, the microplastics found in the Spermonde Islands of Makassar Gulf were contaminating seagrass beds (Tahir *et al.*, 2019) and Muara Jagir of Surabaya City (Firdaus *et al.*, 2020). The fishes from *Trichiurus* sp. and *Johnius* sp. were also reported to have ingested microplastics in Pangandaran Gulf (Ismail *et al.*, 2019) while other pollutions associated with this material have also been discovered in the Karimunjawa national park waters (Lie *et al.*, 2018).

Even though the presence of microplastics in the ocean is a serious threat to marine organism, residents of Ternate

Island of North Maluku Province-Indonesia have a habit of dumping plastic wastes into the sea. Previous research showed the Ternate Island sea is dominated by seven plastic types and these are 1) bottles, 2) bags, 3) glasses, 4) packages, 5) spoons, 6) toys, and 7) straps without any focus on microplastic pollution. This present research was, therefore, conducted to fill this gap by examining the presence of microplastic particles in the reef fish digestive tract in the littoral zone of Ternate Island waters, i.e Katurian, Kampung Makassar, Mangga Dua, and Kalumata.

2. Method

2.1. Study Area

The research was conducted at Ternate Island, Maluku Utara Province shown in Figure. 1 which was selected due to the fact that 80% of its area is made of the ocean and the residents' activities are predominantly centered on the waters.

2.2. Tools

The tools used include gloves, straps, scissors, ropes, plastic containers, a small shovel, beakers, tweezers, nails, glass objects, Petri dishes, fishing nets, stereo microscopes, and pencils Jabeen *et al.* (2017).

2.3. Microplastics Separation Procedures

The saturated salt solution used to separate microplastics and non-microplastics through the floatation technique was prepared at 1.2-1.5 g/mL concentration. The process involved the addition of approximately 850 mL NaCl into a sample bottle and left for 10-15 minutes after which the solution was filtered using a Wattman filter paper. This was followed by the placement of the filter paper in a covered petri dish to observe microplastic particles using a microscope. The procedure was in line with the method used by Li *et al.* (2016); Jabeen *et al.* (2017).

2.4. Microplastic Visual Identification

A visual method was used to identify microplastics in fish intestines and stomach. This involved the observation of the particles visually at the laboratory using a stereo microscope with magnification up to 40x after which they were calculated systematically in a range of 0.3-5 mm based on color, size, number, and shape and further classified based on five categories which are 1) fragment, 2) film, 3) line/fiber, 4) foam and 5) pellet (Hidalgo-Ruz *et al.*, 2012; Free *et al.*, 2014).

2.5. Data Analysis

Microplastic amounts are presented as the mean values. Microsoft Excel software was used to calculate the percentage value of microplastic density data according to type and fish.

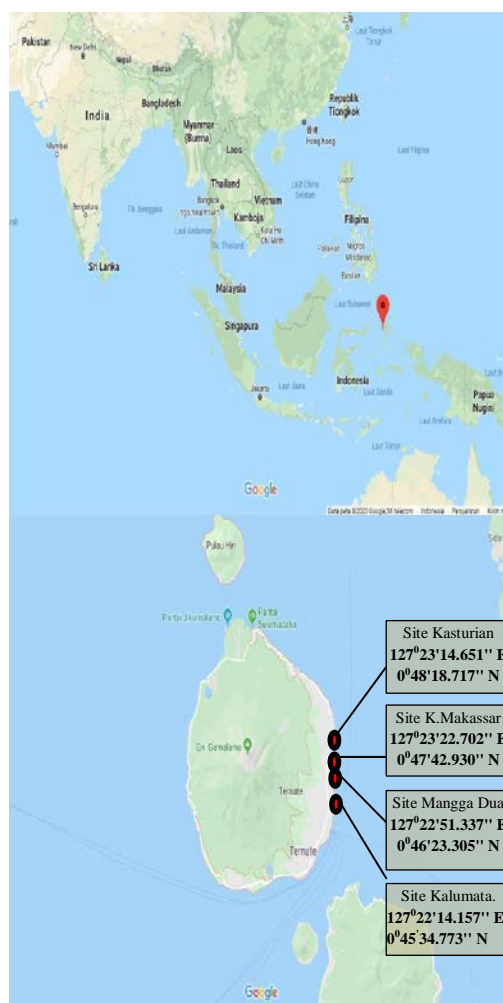


Figure 2. Sample Location (Source: <https://www.google.com/maps/>; Access March 2020)

3. Results and Discussion

3.1. Microplastic abundance in reef fishes

The results showed 183 individuals, represented by 83.18%, of the 220 reef fishes examined had ingested plastics as shown in Table 1. The six types of fish studied include *Epinephelus Fuscoguttatus*, *E. coioides*, *E. suillus*, *Siganus canaliculatus*, *Synanceia*, and *Scarus Psittacus*. Moreover, a total of 594 plastic particles were found in the digestive tract out of which 47.81% were fragment, 38.22% film, 2.69% foam, 2.36% fiber, 7.41% was line, and 1.52% pellet ranged between 1.8 and 5 mm as presented in Figure. 3.

Table 1. The Number of Reef Fishes that have Ingested the Microplastic Waste in Ternate Island Waters

Fish Species	Number of Samples	Number of Fish that Ingested Microplastics	Number of Microplastics based on Shape						Total
			Fragment	Film	Foam	Fiber	Line	Pellet	
<i>Epinephelus fuscoguttatus</i>	29	23	37	32	3	5	12	0	89
<i>Epinephelus coioides</i>	36	31	64	24	0	5	2	0	95
<i>Epinephelus suillus</i>	65	56	60	14	3	2	17	2	98
<i>Siganus canaliculatus</i>	47	35	43	67	2	2	1	1	116
<i>Synanceia</i>	27	27	62	78	4	0	12	4	160
<i>Scarus Psittacus</i>	16	11	18	12	4	0	0	2	36
	220	183	284	227	16	14	44	9	594

Based on the types of fish, *Synanceia* was found to have ingested 26.94% and *S.canaliculatus* 19.53%. Moreover, 89 plastic particles were discovered in the digestive tract of *E. fuscoguttatus*, 95 in *E. coioides*, 98 in *E. suillus*, 116 in *S. canaliculatus*, 160 in *Synanceia*, and 36 in *S.Psittacus* as shown in Table 1 and Figure. 2.

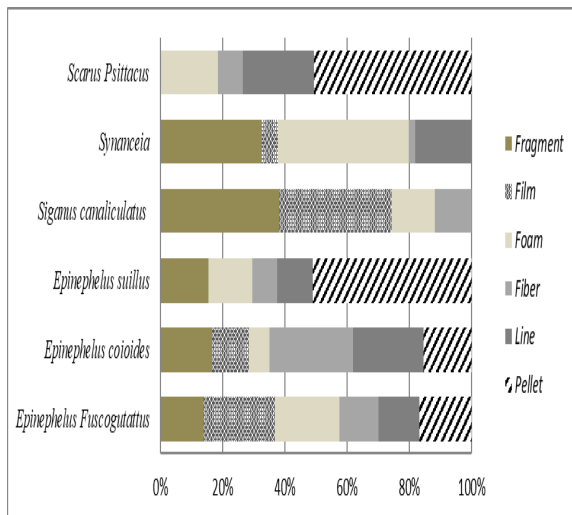


Figure 2. Percentage of microplastic particles ingested by fish

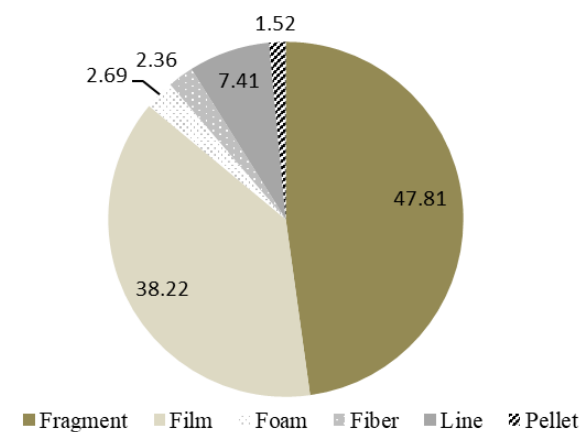


Figure 3. Total Percentage of Microplastic Type ingested by fish

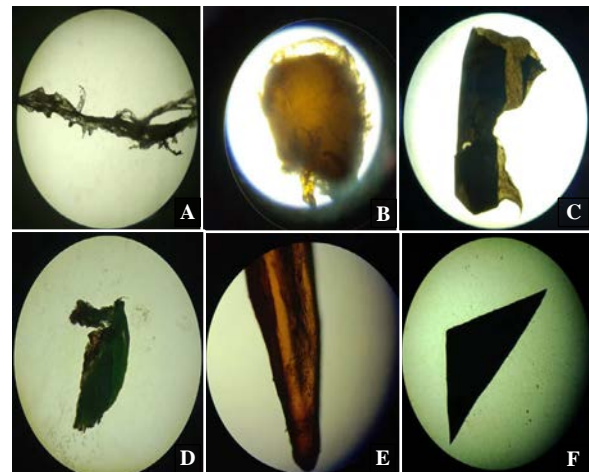


Figure 4. The Stereo shape of microplastic; (A) Pellet (B) foam, (C) film, (D) Fiber, (E) line, (F) fragment

The colors of microplastic particles ingested by *E. fuscoguttatus* fish were found to be transparent with 53.93% followed by black with 26.97%, pink with 13.48%, yellow with 3.37%, and blue and red with 1.12%. Meanwhile, *E. coioides* ingested 33.68% transparent, 28.42% black, 13.68% blue, 15.79% red, 6.32% yellow, and 2.11% pink. *E. suillus* had 57.14% transparent, 34.69% black, 2.04% pink, 1.02% blue, 3.06% yellow, and 2.04% red. Moreover, *S. canaliculatus* ingested 58.62% transparent, 36.21% black, 1.72% pink, 2.59% blue, 0.86% yellow, and no red color was recorded. In *Synanceia*, 41.88% transparent, 25.63% black, 8.13% pink, 7.50% blue, 14.38% yellow, and 2.50% red were recorded. Finally, *S. Psittacus* was recorded to have 19.44% transparent, 63.89% black, 5.56% pink, 2.78% blue, and 8.33% red without any yellow particle as shown in Figure. 3. The total color distribution of microplastics ingested by the reef fishes in all sites includes 46.80% transparent, 32.15% black, 5.56% pink, 6.06% yellow, 5.22% blue, and 4.21% red as shown in Figure. 4.

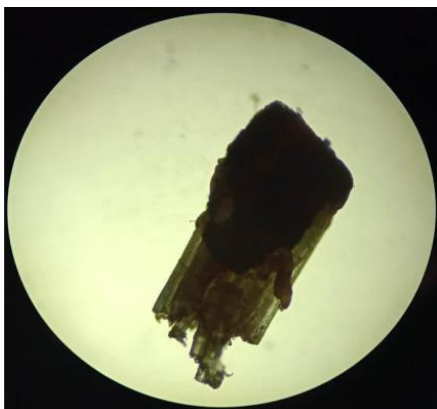


Figure 5. Color distribution of microplastics ingested by five types of fish

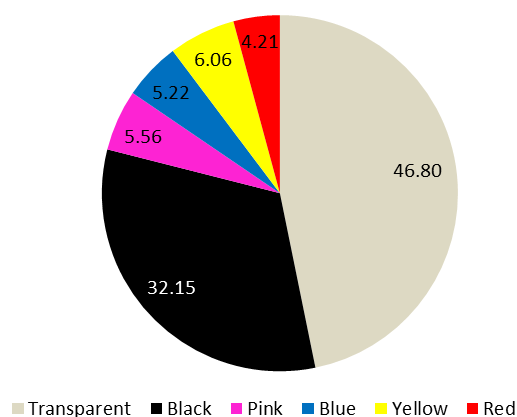


Figure 6. Color distribution of microplastics ingested by fish in all locations

4. Discussions

The result showed the microplastic particles found in the digestive organelle and stomach of reef fishes in the Ternate Island waters littoral zone were likely from several plastics dumped into the ocean by humans and later consumed by the fishes, which later caused a disturbance in their food network. This is in line with the report that the presence of microplastics in sediments and seawater is caused by human activities such as waste disposal (Ng & Obbard, 2006). It has also been discovered that microplastics are not only in the coastal areas but also in the deepest reach of the ocean, East Atlantic Sea, Asia Sea, and the North Pole (Van Cauwenberghe *et al.*, 2013; Lusher *et al.*, 2014; Ivleva *et al.*, 2017; Wagner & Lambert, 2018; Jun Wang *et al.*, 2019; Jamieson *et al.*, 2019;)

Microplastics are found by fishes at 200-478 m depth and ingested by zooplankton in shallow waters (Zhu *et al.*, 2019; Botterell *et al.*, 2019). It has also been reported that they sink and accumulate in sediments causing a risk in the ecological system for benthic communities (Vianello *et al.*, 2013; Jun Wang *et al.*, 2019). Moreover, chronic exposure to microplastics is seldom deadly but has a bad impact on animals (Galloway *et al.*, 2017) due to their ability to cause oxidative and pathological stresses, decrease in body immunity function, cancer, and a change in the chromosome which further leads to infertility and obesity (Sharma & Chatterjee, 2017; Guzzetti *et al.*, 2018).

The microplastic colors found in the fish digestive organs were transparent, black, pink, yellow, and red. The most dominant colors were transparent and black while *Epinephelus fuscogutattus* and *Synanceia* fishes mostly had pink and yellow and *Epinephelus coioides* were observed to have ingested mainly blue and red. The data also showed the particles were carried by water and presumed to be embedded in muddy, sandy, and rocky substrates. However, fishes were unable to differentiate between food and microplastic particles in the littoral zone. Moreover, the predominant microplastic shape was the filament type due to its elongated structure and movement in the water. Previous studies showed the proportion of fish with microplastics in their digestive tract has increased over the last 60 years (Nadal *et al.*, 2016; Pace, 2018). Moreover, transparent and colored particles have been reported to be dominant in fish intestines (Stolte *et al.*, 2015; Hastuti *et al.*, 2019) while blue fibers were found in the fish larva (Steer *et al.*, 2017).

5. Conclusion

The results showed microplastic particles were found in the digestive tracts of *E. fuscogutattus*, *E. coioides*, *E. suillus*, *S. canaliculatus*, *Synanceia*, and *S. Psittacus* collected in four locations in Ternate Island waters – Indonesia littoral zone. The particles ingested were discovered to be fragment, film, foam, fiber, line, and pellet while the colors were transparent, black, pink, yellow, blue, and red. Therefore, further research is recommended to examine and evaluate the microplastic pollution level in deeper sea biota. The sample size should also be increased by including other fish types in future studies. For practical application, the local government needs to manage its coastal environment through a community-based approach to reduce the plastic-type pollution in the Ternate Island waters, Indonesia.

Acknowledgments

This research was funded by PNBP Universitas Negeri Malang (UM)

References

- Bakir, A., Rowland, S. J., & Thompson, R. C. (2014). Enhanced desorption of persistent organic pollutants from microplastics under simulated physiological conditions. *Environ Pol*, **185**, 16–23.
- Barnes, D. K. A., Galgani, F., Thompson, R. C., & Barlaz, M. (2009). Accumulation and fragmentation of plastic debris in global environments. *Philosophical Transactions of the Royal Society B: Biol Sci*, **364** (1526), 1985–1998.
- Bergmann, M., Gutow, L., & Klages, M. (2015). Marine anthropogenic litter. *In Marine Anthropogenic Litter*.
- Betts, K. (2008). Why small plastic particles may pose a big problem in the oceans. *Enviro Sci and Tec*, **42** (24), 8996.
- Boerger, C. M., Lattin, G. L., Moore, S. L., & Moore, C. J. (2010). Plastic ingestion by planktivorous fishes in the North Pacific Central Gyre. *Marine Poll Bulletin*, **60** (12), 2275–2278.
- Botterell, Z. L. R., Beaumont, N., Dorrington, T., Steinke, M., Thompson, R. C., & Lindeque, P. K. (2019). Bioavailability and effects of microplastics on marine zooplankton: A review. *Enviro Poll*, **245**, 98–110.

- Cole, M., Lindeque, P., Fileman, E., Halsband, C., Goodhead, R., Moger, J., & Galloway, T. S. (2013). Microplastic ingestion by zooplankton. *Enviro Sci and Tec*, **47** (12), 6646–6655.
- Davison, P., & Asch, R. G. (2011). Plastic ingestion by mesopelagic fishes in the North Pacific Subtropical Gyre. *Marine Eco Progress Series*, **432** (January), 173–180.
- Derraik, J. G. B. (2002). The pollution of the marine environment by plastic debris: A review. *Marine Poll Bulletin*, **44** (9), 842–852.
- Eriksson, C., & Burton, H. (2003). Origins and Biological Accumulation of Small Plastic Particles in Fur Seals from Macquarie Island. *Ambio*, **32** (6), 380–384.
- Farrell, P., & Nelson, K. (2013). Trophic level transfer of microplastic: *Mytilus edulis* (L.) to *Carcinus maenas* (L.). *Enviro Poll J*, **177**, 1–3.
- Firdaus, M., Trihadiningrum, Y., & Lestari, P. (2020). Microplastic pollution in the sediment of Jagir Estuary, Surabaya City, Indonesia. *Marine Poll Bulletin*, **150** (November), 110790.
- Free, C. M., Jensen, O. P., Mason, S. A., Eriksen, M., Williamson, N. J., & Boldgiv, B. (2014). High-levels of microplastic pollution in a large, remote, mountain lake. *Marine Poll Bulletin* **85** (1), 156–163.
- Galloway, T. S., Cole, M., & Lewis, C. (2017). Interactions of microplastic debris throughout the marine ecosystem. *Nature Eco and Evo*, **1** (5), 1–8.
- Goldstein, M. C., & Goodwin, D. S. (2013). Gooseneck barnacles (*Lepas* spp.) ingest microplastic debris in the north Pacific subtropical gyre. *PeerJ*, **2013** **1**, 1–17.
- Guzzetti, E., Sureda, A., Tejada, S., & Faggio, C. (2018). Microplastic in marine organism: Environmental and toxicological effects. *Enviro Toxic and Pharma*, **64**, 164–171.
- Handyman, D. I. W., Purba, N. P., Pranowo, W. S., Harahap, S. A., Dante, I. F., & Yuliadi, L. P. S. (2019). Microplastics patch based on hydrodynamic modeling in the north Indramayu, Java sea. *Polish J Enviro Studies*, **28** (1), 135–142.
- Hastuti, A. R., Lumbanbatu, D. T. F., & Wardiatno, Y. (2019). The presence of microplastics in the digestive tract of commercial fishes off pantai Indah Kapuk coast, Jakarta, Indonesia. *Biodiversitas*, **20** (5), 1233–1242.
- Hidalgo-Ruz, V., Gutow, L., Thompson, R. C., & Thiel, M. (2012). Microplastics in the marine environment: A review of the methods used for identification and quantification. *Enviro Sci and Tec*, **46** (6), 3060–3075.
- Ismail, M. R., Lewaru, M. W., & Prihadi, D. J. (2019). Microplastics Ingestion by Fish in The Pangandaran Bay, Indonesia. *World News of Natural Sci*, **23** (8), 173–181.
- Ivleva, N. P., Wiesheu, A. C., & Niessner, R. (2017). Microplastic in Aquatic Ecosystems. *Angewandte Chemie International Edition*, **56** (7), 1720–1739.
- Jabeen, K., Su, L., Li, J., Yang, D., Tong, C., Mu, J., & Shi, H. (2017). Microplastics and mesoplastics in fish from coastal and fresh waters of China. *Enviro Poll Sci*, **221**, 141–149.
- Jambeck, J. R., Ji, Q., Zhang, Y.-G., Liu, D., Grossnickle, D. M., & Luo, Z.-X. (2015). Plastic waste inputs from land into the ocean. *Sci J*, **347** (6223), 764–768.
- Jamieson, A. J., Brooks, L. S. R., Reid, W. D. K., Piertney, S. B., Narayanaswamy, B. E., & Linley, T. D. (2019). Microplastics and synthetic particles ingested by deep-sea amphipods in six of the deepest marine ecosystems on Earth. *R S Open Sci* **6** (2).
- Law, K., & Thompson, R. C. (2014). Microplastics in the seas - Concern is rising about widespread contamination of the marine environment by microplastics. In *Sci*. (Vol. **345**, Issue 6193, pp. 144–145).
- Li, J., Qu, X., Su, L., Zhang, W., Yang, D., Kolandhasamy, P., Li, D., & Shi, H. (2016). Microplastics in mussels along the coastal waters of China. *Enviro Poll*, **214**, 177–184.
- Lie, S., Suyoko, A., Effendi, A. R., Ahmada, B., Hadid, N. I., Rahmasari, N., & Reza, A. (2018). **Measurement of microplastic density in the Karimunjawa National Park, Central Java , Indonesia**. **2** (2), 54–58.
- Lusher, A. L., Burke, A., O'Connor, I., & Officer, R. (2014). Microplastic pollution in the Northeast Atlantic Ocean: Validated and opportunistic sampling. *Marine Poll Bulletin*, **88** (1–2), 325–333.
- Manalu, A. A., Hariyadi, S., & Wardiatno, Y. (2017). Microplastics abundance in coastal sediments of Jakarta Bay, Indonesia. *AACL Bioflux*, **10** (5), 1164–1173.
- Murray, F., & Cowie, P. R. (2011). Plastic contamination in the decapod crustacean *Nephrops norvegicus* (Linnaeus, 1758). *Marine Poll Bulletin*, **62** (6), 1207–1217.
- Nadal, M. A., Alomar, C., & Deudero, S. (2016). High levels of microplastic ingestion by the semipelagic fish bogue *Boops boops* (L.) around the Balearic Islands. *Enviro Poll*, **214**, 517–523.
- Ng, K. L., & Obbard, J. P. (2006). Prevalence of microplastics in Singapore's coastal marine environment. *Marine Poll Bulletin*, **52** (7), 761–767.
- Pace, E. Di. (2018). Proceedings of the International Conference on Microplastic Pollution in the Mediterranean Sea. *International Conference on Microplastic Pollution in the Mediterranean Sea*, **22** (5), 238.
- Rochman, C. M., Hoh, E., Kurobe, T., & Teh, S. J. (2013). Ingested plastic transfers hazardous chemicals to fish and induces hepatic stress. *Scientific Reports*, **3**, 1–7.
- Romeo, T., Pietro, B., Pedà, C., Consoli, P., Andaloro, F., & Fossi, M. C. (2015). First evidence of presence of plastic debris in stomach of large pelagic fish in the Mediterranean Sea. *Marine Poll Bulletin*, **95** (1), 358–361.
<https://doi.org/10.1016/j.marpolbul.2015.04.048>
- Rowland, S. J., Galloway, T. S., & Galloway, T. S. (2016). Potential for Plastics to Transport Hydrophobic Contaminants. *ACS Publications*, **41**; 7759–7764.
- Ryan, P. G., Moore, C. J., Van Franeker, J. A., & Moloney, C. L. (2009). Monitoring the abundance of plastic debris in the marine environment. *Philosophical Transactions of the Royal Society B: Biol Sci*, **364** (1526), 1999–2012.
- Setälä, O., Norkko, J., & Lehtiniemi, M. (2016). Feeding type affects microplastic ingestion in a coastal invertebrate community. *Marine Poll Bulletin*, **102** (1), 95–101.
- Sharma, S., & Chatterjee, S. (2017). Microplastic pollution, a threat to marine ecosystem and human health: a short review. *Enviro Sci and Pollution Research*, **24** (27), 21530–21547.
- Steer, M., Cole, M., Thompson, R. C., & Lindeque, P. K. (2017). Microplastic ingestion in fish larvae in the western English Channel. *Enviro Poll*, **226**, 250–259.
- tolte, A., Forster, S., Gerdt, G., & Schubert, H. (2015). Microplastic concentrations in beach sediments along the German Baltic coast. *Marine Poll Bulletin*, **99** (1–2), 216–229.
- Syakti, A. D., Bouhroum, R., Hidayati, N. V., Koenawan, C. J., Boulkamh, A., Sulisty, I., Lebarillier, S., Akhlus, S., Doumenq, P., & Wong-Wah-Chung, P. (2017). Beach macro-litter monitoring and floating microplastic in a coastal area of Indonesia. *Marine Poll Bulletin*, **122** (1–2), 217–225.
- Syakti, A. D., Hidayati, N. V., Jaya, Y. V., Siregar, S. H., Yude, R., Suhendy, Asia, L., Wong-Wah-Chung, P., & Doumenq, P. (2018). Simultaneous grading of microplastic size sampling in the

Small Islands of Bintan water, Indonesia. *Marine Poll Bulletin*, **137** (November), 593–600.

Tahir, A., Samawi, M. F., Sari, K., Hidayat, R., Nimzet, R., Wicaksono, E. A., Asrul, L., & Werorilangi, S. (2019). Studies on microplastic contamination in seagrass beds at Spermonde Archipelago of Makassar Strait, Indonesia. *Physics J: Conference Series*, **1341** (2).

Van Cauwenberghe, L., Vanreusel, A., Mees, J., & Janssen, C. R. (2013). Microplastic pollution in deep-sea sediments. *Enviro=Poll*, **182**, 495–499.

Vianello, A., Boldrin, A., Guerriero, P., Moschino, V., Rella, R., Sturaro, A., & Da Ros, L. (2013). Microplastic particles in sediments of Lagoon of Venice, Italy: First observations on occurrence, spatial patterns and identification. *Estuarine, C and Shelf Sci*, **130**, 54–61.

Wagner, M., & Lambert, S. (2018). **Freshwater Microplastics - The Handbook of Environmental Chemistry** **58** (p. 302).

Wang, Jun, Wang, M., Ru, S., & Liu, X. (2019). High levels of microplastic pollution in the sediments and benthic organisms of the South Yellow Sea, China. *Sci of the Total Envir*, **651**, 1661–1669.

Wang, Jundong, Tan, Z., Peng, J., Qiu, Q., & Li, M. (2016). The behaviors of microplastics in the marine environment. *Marine Enviro Research*, **113**, 7–17.

Wick, A. F., Daniels, W. L., Orndorff, Z. W., & Alley, M. M. (2013). Organic matter accumulation post-mineral sands mining. *Soil Use and Management*, **29** (3), 354–364.

Zhu, L., Wang, H., Chen, B., Sun, X., Qu, K., & Xia, B. (2019). Microplastic ingestion in deep-sea fish from the South China Sea. *Sci of the Total Envir*, **677**, 493–501.

Genetic improvement of *Pseudomonas aeruginosa* and *Bacillus cereus* for controlling root knot nematode and two weeds under laboratory conditions.

Shereen AH. Mohamed^{1,*}, Hoda H. Ameen², Usama S. Elkelany², Mona A. El-Wakeel³, Mostafa MA. Hamman² and Gaziea M. Soliman²

¹Microbial Genetics Department, National Research Centre, ²Plant Pathology Department National Research Centre, ³Botany Department, National Research Centre, Bohouth St, Dokki, P.O.Box12622, Giza, Egypt

Received: August 10, 2020; Revised: November 28, 2020; Accepted: January 2, 2021

Abstract

Plant parasitic nematodes and weeds are among the many biotic stresses that crops production suffers from during their growing season. Their management relies mainly on chemical pesticides. To decrease the extent of environment degradation and hazards to human health and livestock due to the prolonged use of these chemicals, biological control using soil microorganisms is considered as a new ecofriendly and efficient control method. The main objective of this work was to improve the inhibition of two local bacterial strains, *Pseudomonas aeruginosa* and *Bacillus cereus*, against root knot nematode and weed seeds germination. To achieve this goal, protoplast fusion experiments were performed to gather all their properties in bacterial fusants and increase production of such toxic compounds. The results showed that *P. aeruginosa* was Rifampicin (Rif) resistance, but *B. cereus* was sensitive. In contrast to this *B. cereus* was Neomycin (Nm) resistance but *P. aeruginosa* was sensitive. A total of 40 fusants derived from the protoplast fusion experiments were selected by antibiotic resistance markers. SDS-PAGE analysis of the proteins confirmed that six recombinants acquired and expressed many specific protein bands from their parental strains. Three fusants, No. F7, F20 and F35, were selected and evaluated for their nematocidal potential in comparison with their parent against root knot nematode *Meloidogyne incognita* J₂ and *Echinochloa crus-galli* and *Portulaca oleracea* seeds germination during *in vitro* experiments. Data showed that the fusants exhibited more antagonistic effects than their parents. After 72hrs of exposure, the three fusants caused-80.6, 96.5 and 97.7% mortality as compared to control, while the % mortality after the same duration by *P. aeruginosa*, *B. cereus* singly and combined resulted in 52.2, 65.9 and 48.8%, respectively as compared to control. Furthermore, the three fusants completely inhibited the germination of *P. oleracea* seeds and resulted in small radicals *in E. crus-galli* seeds as compared to control. These fusants show great potential to be selected as possible potential biopesticide.

Keywords: Protoplast fusion, SDS-PAGE, *Pseudomonas aeruginosa*, *Bacillus cereus*, Biocontrol, *Meloidogyne incognita*, *Echinochloa crus-galli*, *Portulaca oleracea*.

1. Introduction

Plant parasitic nematodes are one of the most damaging and widespread pathogens that cause global losses to crop production with an estimated loss of \$ 157 billion per year (Singh *et al.*, 2015). Root-knot nematodes, *Meloidogyne* spp. especially *M. incognita*, has been found as the major limiting factor in vegetables production in tropical and subtropical regions. When the infective stage (J₂) penetrates the roots and migrates directly to the vascular cylinder, it causes severe root galling, reduces nutrient and water utilisation efficiency, and affects photosynthetic products (Almaghrabi *et al.*, 2013).

Throughout the world, weeds significantly contribute to reduce crop production, even more than all other pests combined (Adeux *et al.*, 2019). They affect crop yield and quality by competing on space, nutrients, water, light and interfere with the distribution of fertilizers. Weed

infestation resulted in yield losses of up to 45 % in wheat (Hussain *et al.*, 2017). Moreover, weeds act as reservoir for plant pathogens like nematodes, thus facilitating the reinfesting of crops in the next seasons (Byron *et al.*, 2019).

Chemical pesticides have been used against plant parasitic nematodes and weeds with encouraging results since long, but many of these chemicals are proven to be carcinogens, infiltrate into ground water, build up residues in food plants and hazardous to the beneficial soil fauna and flora (Jabran *et al.*, 2015). For more sustainable crop production, scientists are endorsing alternatives pesticides reduced toxicities. Using of non-pathogenic microbes with potential control activity against nematodes and herbicide resistant weeds has emerged as promising solution (Sayed *et al.*, 2014). One of the most promising microorganisms without negative effects on the users, consumers or the environment are Plant-Growth Promoting Rhizobacteria (PGPR) (Lee and Kim 2016). They affect nematodes and

* Corresponding author e-mail: shereen_asba@yahoo.com.

weeds directly through the production of toxic compounds, siderophores, hydrogen cyanide, antibiotic, competition for space and indirectly through promoting plant growth and induction of systemic resistance (Lakshmi *et al.*, 2015; Siddiqui *et al.*, 2003).

Researchers have reported that mixtures of PGPR strains give better protection than one strain. But in certain cases, the establishment of more than one microorganism has no synergistic effect due to their different nutritional and environmental requirements. Furthermore, the combinations considered to exhibit improved efficacy under one set of conditions or one host may not produce equally favorable results under other set of conditions (Schisler *et al.*, 1997). These open the door for utilizing some biotechnological approaches like protoplast fusion to gathering more than one mechanism of controlling in one individual and increasing the production of such toxic substances or enzymes (Abdel Salam *et al.*, 2018; Soliman *et al.*, 2018; Soliman *et al.*, 2020).

The objectives of this study are to improve the antagonistic potential of such isolated bacteria using the protoplast fusion technique and to analyze the fusants products through SDS -PAGE technique. Under *in vitro* conditions, the antagonistic potential of fusants against root knot nematodes *M. incognita* J2 and *E. crus-galli* and *P. oleracea* weed seeds was evaluated in comparison to the parental types.

2. Materials and Methods

2.1. Bacterial strains and growth conditions

Two bacterial strains isolated from the Egyptian soil had nematocidal activity against plant parasitic nematodes. The bacterial isolates were identified based on 16S rDNA sequence analysis in the GenBank database nucleotides, as *Bacillus cereus* GEs (Accession No. LC215052) and *Pseudomonas aeruginosa* (under accession number LC215048) (Soliman *et al.*, 2019). The aforementioned bacterial isolates were used as parent strains in the protoplast fusion experiment and bioassay tests. Bacterial strains were grown in Luria-Bertani (LB) medium (Davis *et al.*, 1980) at 30 °C for 24 h with shaking at 120 r/min.

2.2. Nematode inoculum preparation

Cultrure of root-knot nematode *M. incognita* was established from single egg-mass of an adult female, previously identified by the morphological characteristics of the female perineal patterns (Taylor and Sasser, 1978) and reared on tomato plants (*Lycopersicon esculentum* Mill) cv. Alisa in the greenhouse of the Plant Pathology Department, National Research Centre. Nematode eggs were extracted from the infected tomato roots using NaOCl solution as described by (Hussey and Barker, 1973). To perform *in vitro* tested, eggs were allowed to hatch for 48 h at 30±2°C in an incubator to obtain the 2nd stage larvae (J₂) to perform the *in vitro* test.

2.3. Antimicrobial susceptibility

Eleven antibiotics were used with final concentrations as follows: rifampicin (Rif), 100 µg/mL; ampicillin (Amp), 100 µg/mL; amikacin (Amk), 30 µg/mL; streptomycin (Sm), 200 µg/mL; kanamycin (Km), 40 µg/mL; tetracycline (Tc), 15 µg/mL; chloramphenicol (Cm), 35 µg/mL; gentamicin (Gm), 15 µg/mL; polymyxin (Pmx), 50

µg/mL; neomycin (Nm), 40 µg/mL; and erythromycin (Erm), 20 µg/mL. The Kirby-Bauer disc diffusion method for antimicrobial susceptibility test was followed (NCCLS, 1999).

2.4. Growth conditions and protoplast formation

Cultivation of *Bacillus cereus* and *Pseudomonas aeruginosa* was carried out in 250 ml flasks containing 70 ml of LB medium. Flasks were incubated for 24 hr. at 30°C with shaking at 120 rpm. Cells were harvested at the mid-point of the log phase by centrifugation at 5000 rpm for 10 min and washed once with 1% N-laurylsarcosine. This was followed by washing three times with osmotic stabilizer buffer. The bacterial cells were then pelleted by centrifugation. Lysozyme was dissolved in osmotic stabilizer buffer to a final concentration of 15 mg/ml, sterilized by 0.2µm millipore filter. Lysozyme was then, added to the cell pellets at final concentration of 1/10th the volume and mixed thoroughly to make the suspension. The resulting mixture was incubated at 37°C for 4h. The viable protoplast were counted by spreading appropriate dilution onto LB medium solidified by adding 2% agar, where all inviable protoplasts were lysed and only the intact protoplast will grow after incubation according to (Soliman *et al.*, 2020; Mohamed *et al.*, 2016).

2.4.1. The microscopic examination of the protoplasts

Aliquots (1.0 ml each) of the parental protoplasts were mixed in 25% PloyEthylene Glycol (PEG) 6000 and 100 mM CaCl₂ and incubated for 2 h at 30°C. Aliquots of 100 µl from the mixture were prepared at 10 min intervals and diluted 10 times in protoplasting buffer. A total of six fusants were obtained after 2h of fusion time on selective medium containing antibiotics Neomycin (Nm) and Rifampicin (Rif).

2.4.2. Regeneration of protoplast

The protoplasts in the reaction mixture were collected by centrifugation at 3000 rpm for 10 min. The precipitate was washed with Tris-HCl buffer with an osmotic stabilizer and the resulting precipitate was re-suspended in the same buffer. Protoplast suspension was diluted and overlaid on the LB medium solidified by adding 2% agar. (Mohamed *et al.*, 2016).

2.5. SDS-PAGE protein analysis

The parental and fusant strains were grown in suspensions following the method of (El-Kawokgy *et al.*, 2015). SDS-PAGE 12.5 %, was done according to the method of (Laemmli, 1970) to compare the products secreted by the parental strains and those secreted by fusant strains. After size fractionation, the proteins were visualized by staining with Coomassie Blue R-250 dye. The gels were scanned using Gel Doc 2000 system, and molecular masses were determined using Total Lab version 1.10 software based on protein marker purchased from Biomatik Corporation (Wilmington, Delaware, USA).

2.6. Bioassay Tests

2.6.1. Efficiency of the nematocidal effect of three fusants in comparison with their parents *P. aeruginosa* and *B. cereus* against *M. incognita* J₂

To evaluate the nematocidal activity, Petri dishes 6cm in diameter were supplied separately with 4 ml cell

suspension of *P. aeruginosa* and *B. cereus* singly and combined and three fusants (No. F7, F20 and F35), then added one ml water containing 100 ± 5 freshly hatched *M. incognita* juveniles. Three concentrations were used and standard (S), S/2 and S/4 concentrations were prepared using distilled water. Each ml from standard containing (2×10^6 cfu/ ml) Five ml distilled water containing 100 ± 5 freshly hatched *M. incognita* juveniles served as control. All preparations and the control were replicated in five times. All dishes were kept in incubator at 35°C and loosely covered to permit aeration and lessen evaporation. Number of survived and dead individuals was counted for three days. After the exposure periods, the nematodes in each treatment were transferred to distilled water and left for 24 hrs to see whether immobile nematodes resumed activity or not. The J₂ mortality (%) were assessed as compared to the control according to Mortality% = $[(C1 - C2/C1) \times 100]$, where C1 is the number of live nematodes larvae in control treatment and C2 is the number of live nematodes larvae in other treatments.

2.6.2. Examine the inhibitory effects of *P. aeruginosa* and *B. cereus* as parental strains and their fusants on germination and growth of *P. oleracea* and *E. crus-galli* weed seeds during in vitro analysis

Seeds of targeted weeds were surface sterilized by immersing in 95% ethanol for a few seconds (3–4 s). After surface sterilization with 5% ethanol, seeds of targeted weeds were washed with sterilized distilled water several times to remove sterility. Filter paper was soaked with 3 ml of bacterial suspension (containing approximately 2×10^6 cfu/ ml) from *P. aeruginosa* and *B. cereus* as parental strains and the fusants No. F7, F20 and F35, were placed separately on Petri dish. Ten sterilized seeds from each weed species were placed separately in Petri dishes then incubated at 25°C. For control, ten seeds from the two weed species were placed separately on filter paper soaked with 3 ml of sterile water. Each treatment was replicated three times. Ten days later, germination of shoots and root lengths were observed.

3. Results

3.1. Bacterial strains and antibiotic susceptibility

Isolation of antibiotic genetic markers from *P. aeruginosa* and *B. cereus* was necessary for their manipulation. Data in Table 1 showed that *P. aeruginosa* was Rifampicin resistant and Neomycin sensitive in the contrary, *B. cereus* was Neomycin resistant and Rifampicin sensitive. Thus, Rifampicin and Neomycin were used as genetic markers for fusion products from the two strains.

Table 1. Antibiotics susceptibility of *P. aeruginosa* and *B. cereus*.

Bacterial strains	Antibiotic resistance	
	Nm	Rif
<i>Pa</i> (Rif ^r)	---	+++
<i>Bc</i> (Nm ^r)	+++	---

Pa = *P. aeruginosa*, Bc = *B. cereus* +++: = Very good growth

---: = no growth Rif = Rifampicin Nm = Neomycin

3.2. The microscopic examination of the protoplasts

The protoplast formation between the two selected strains, *P. aeruginosa* and *B. cereus* were tested periodically by microscopic examination. A total of six fusants were obtained after 2h of fusion time on selective medium containing the two antibiotics Nm and Rif as shown in (Figure 1).

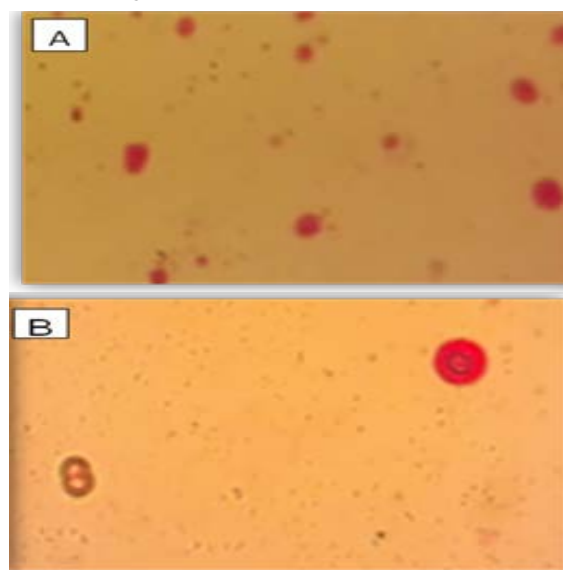


Figure 1. The microscopic examination of the protoplasts of the two parental strains *P. aeruginosa* and *B. cereus* (A) Protoplast formation (B) Protoplast fusion

3.3. Fusants isolation

Neomycin (Nm) and Rifampicin (Rif) were added in LB medium as selective genetic marker, and only the fusants having combined the two selected isolates will grow in this media. Forty single colonies were randomly selected and retested for their ability to grow on the selective media. The fusants' growth was detected as follow: Six fusion products exhibited strong growth (F4, F5, F7, F15, F20 and F35), while forty fusion products showed weak growth and no growth in twenty single colonies refer to no fusion products.

3.4. Expression of the parental strains protein bands in their fusants

The SDS-PAGE protein patterns of the two parental strains *B. cereus* and *P. aeruginosa* and fusants are presented in (Figure 2). SDS-PAGE analysis of the total proteins of the two parental strains revealed a total of 11 and 12 protein bands, respectively. The molecular weights of parental strains ranged from 7 to 179 kDa. While the fusants showed a variable number of protein bands ranging from 11 in four fusants to 7 in one fusant (Table 2).

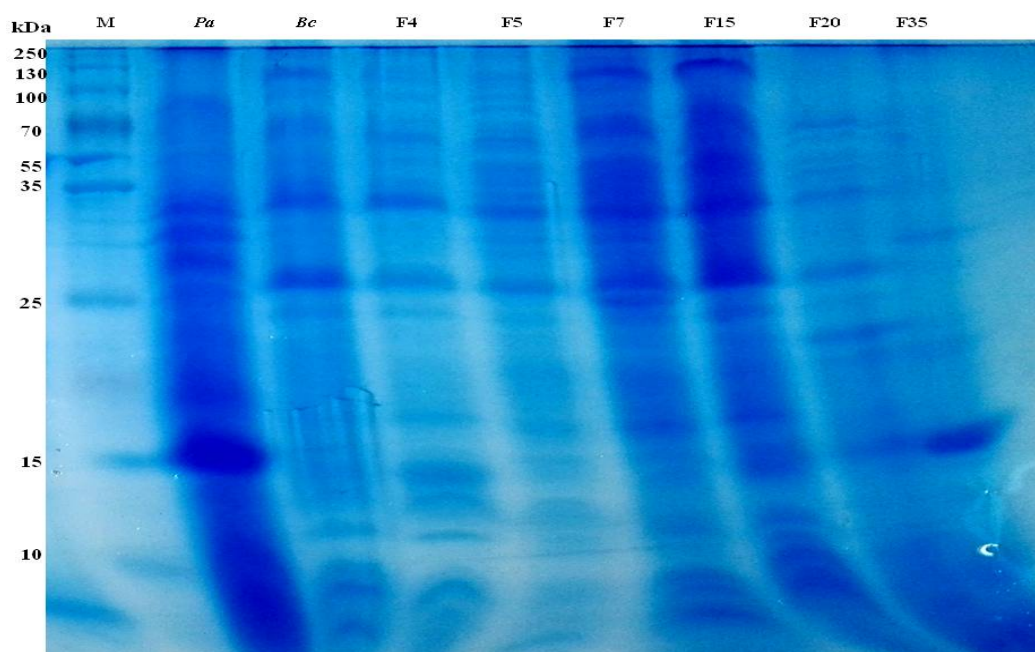


Figure 2. SDS-PAGE protein profiles of the two parental strains; *P. aeruginosa* and *B. cereus* and their fusant (F). M is the protein marker (Biomatik Corp, (Wilmington, USA) with nine molecular weight bands (kDa).

Table 2. SDS-PAGE analysis of total proteins of the two parental strains *P. aeruginosa* and *B. cereus* and six of their fusants.

Band No.	MW KDa	Parental strains		<i>Pa</i> :: <i>Bc</i> fusants					
		<i>Pa</i>	<i>Bc</i>	F4	F5	F7	F15	F20	F35
1	179	+		+	+	+	+	+	+
2	160	+		+	+		+	+	+
3	141		•	•	•	•	•	•	•
4	126	+		+	+	+	+	+	+
5	116	+			+	+	+	+	+
6	109		•	•	•	•	•	•	•
7	100		•	•	•	•	•	•	•
8	92	+			+	+	+	+	+
9	83	+		+	+	+	+	+	+
10	76	+				+	+	+	+
11	67		•	•	•	•	•	•	•
12	57		•	•	•	•	•	•	•
13	48		•	•		•	•	•	•
14	39	+		+	+	+	+	+	+
15	32	+			+	+	+	+	+
16	28		•	•	•	•	•	•	•
17	24		•	•	•	•	•	•	•
18	19		•	•	•	•	•	•	•
19	15		•	•	•	•	•	•	•
20	13		•	•	•	•	•	•	•
21	11	+		+		+	+	+	+
22	8		•	•	•	•	•	•	•
23	7	+		+	+	+	+	+	+
Total no. of protein bands		11	12	18	18	22	23	23	23
Numbers of <i>Pa</i> bands expressed in fusants				7	9	10	11	11	11
<i>Pa</i> bands (%)				38.8	50	45.5	47.8	47.8	47.8
Numbers of <i>Bc</i> bands expressed in fusants				11	9	12	12	12	12
<i>Bc</i> bands(%)				61.2	50	54.5	52.2	52.2	52.2

(+) Refers to presence of protein band of *Pa* . (•) Refers to presence of protein band of *Bc*

The highest number of *P. aeruginosa* bands (11 bands) was displayed in 3 fusants, while the lowest number (7 bands) was shown by F4. The total *P. aeruginosa* expressed bands in the rest of the fusants were classified in ascending order as follows: 9 bands in F5, 10 bands in F7, 11 bands in F15, F20 and F35 fusants. On the other hand, variable number of protein bands of *B. cereus* was shown

in the fusants. The highest number of *B. cereus* (12 bands) was displayed in 4 fusants, while the lowest number (9 bands) was revealed by F5 fusant. The 6 fusants were characterized based on the absence and presence of the 11 *P. aeruginosa* protein bands. A total of 11 *P. aeruginosa* protein bands with different molecular weights were expressed in all the 6 fusants. The presence of the

remaining 11 bands was distributed in descending order as follows: five bands with molecular weights of 179, 126, 83, 39 and 7kDa, and five bands with molecular weights 160, 116, 92, 32 and 11kDa, and one band with molecular weight 76kDa existed in four fusants, respectively.

The 6 fusants were characterized based on the absence or presence of the expression of the 12 *B. cereus* protein bands. A total of 8 protein bands with different molecular weights were found in all fusants. The presence of the remaining 8 bands was distributed in descending order among the 6 fusants as follows: each of the eight bands with molecular weights of 141, 109, 100, 67, 28, 15, 13 and 8kDa was displayed in 6 fusants, while 4 bands with molecular weights of 57, 48, 24 and 19kDa were detected in 5 fusants.

Table 3. The nematocidal potential of *P. aeruginosa* and *B. cereus* and their fusants on mortality of *M. incognita* juveniles under laboratory conditions.

Bacterial strains	Percentage mortality at different exposure periods								
	S			S/2			S/4		
	24hrs	48hrs	72hrs	24hrs	48hrs	72hrs	24hrs	48hrs	72hrs
<i>Pa</i>	7c	28.4d	52.2d	2e	25.2c	35.2e	0 c	10.5c	14.7e
<i>Bc</i>	10c	46.3c	65.9c	5d	10.5d	43.1d	1c	5.2cd	20.4d
<i>Pa+Bc</i>	8c	44.2c	48.8d	2e	5.2e	28.4f	0c	4.2d	17.1de
F 7	29b	48.4c	80.6b	18c	36.8b	62.5c	10b	25.2b	48.8c
F 20	40a	70.5a	96.5a	27a	56.8a	79.5b	20a	31.5a	71.5b
F 35	30b	55.7b	97.7a	22b	37.8b	90.9a	10b	25.2b	86.3a
Control	---	---	---	----	----	----	----	----	----

Pa=*Pseudomonas aeruginosa* *Bc*=*Bacillus cereus* F= fusant S= Standard concentration Averages followed by same letter(s) are not significantly ($P \leq 0.05$) different according to Duncan's Multiple Range Test

3.5.2. Evaluation of the inhibitory effects of *P. aeruginosa* and *B. cereus* and three fusants on germination of *P. oleracea* and *E. crus-galli* weed seeds under laboratory conditions

All bacterial suspensions completely inhibited seeds germination of *P. oleracea* as compared to control. *P. oleracea* seeds were swollen in size but did not germinate in a response to all bacterial suspensions (parents and fusants). However, no radicle growth was observed in plates, while *E. crus-galli* seeds were less influenced than *P. oleracea* seeds. The seeds germinated with small radicle as compared to control. It is worthy to mention that both parents and fusants retard *E. crus-galli* germination. Moreover, fusants suspensions inhibited the weed germination more than parents suspension.

4. Discussion

Protoplast fusion of two parental *Pa* and *Bc* strains was expressed in the 6 selected fusants. SDS-PAGE proteins indicated that some parental protein bands expressed in all fusant strains this study agree with (Khan *et al.*, 1998), who studied the whole cell protein profiles of 42 strains of *P. aeruginosa*, isolated from clinical samples, using the SDS-PAGE method and reported the presence of protein bands, ranging from 340kDa to 14.3kDa. On the basis of Dice Index of similarity, the strains could be grouped into 20 types. Protoplast fusion has been glorified as the method adequate for a new type and good reproducibility.

3.5. Bioassay tests

3.5.1. The nematocidal potential of *P. aeruginosa* and *B. cereus* parental strains and their fusants against *M. incognita* J₂ under laboratory conditions

As illustrated in (Table 3), the bacterial strains under investigation had a lethal effect on *M. incognita* J₂ as detected by the percentage mortality when compared to control. The reduction in the movement was irreversible, and the mortality of the juveniles was confirmed when they were transferred to distilled water for 24 hrs. Nematode mortality was positively correlated with suspension concentration and times of exposure. Fusants were more effective than their parent singly or combined. The fusant F35 had shown a strong nematocidal activity against *M. incognita* J₂. The recorded percentages mortality as compared to control were 97.7%, 90.9% and 86.3% for S, S/2 and S/4 concentration respectively, after 72hrs of exposure (Table 3).

The present study demonstrated that biocontrol of *M. incognita* J₂ could be effectively achieved using *P. aeruginosa*, *B. cereus* strains and their fusants. These rhizobacteria appear to suppress root knot nematode via different mechanisms. Oka *et al.*, (1993) reported that ammonia was excreted during protein degradation by *B. cereus* improving its nematocidal activity. Xioa *et al.*, (2018) mentioned that the extracellular metabolites like protease, chitinase, and siderophore in *B. cereus* cell free supernatant significantly increase the mortality of *M. incognita* J₂ and decrease egg hatching. Chen *et al.*, (2015) mentioned that *P. aeruginosa* can kill nematodes via the production of hydrolytic enzymes, like protease and diffusible toxins like cyanogen, phenazines, and pyocyanin which degrade nematode cuticle and inhibit metabolic pathways. In addition, *P. aeruginosa* has the ability to produce hydrogen cyanide which is responsible for killing nematode (Patil, 2014).

Moreover, the present study indicated that rhizobacterial strains remarkably reduced the germination of *P. oleracea* and *E. crus-galli* seeds. These are in accordance with the previous studies of (Sardar *et al.*, 2020) who reported that bacteria inhabiting plant rhizospheres could be applied as a biocontrol agent to control weeds associated with rice plants. Also, (Carvalho *et al.*, 2007) found that *B. cereus* produced at least two phytotoxins which acted a vital role in the production of sodium vanillate and 2-aminobenzoic acid which inhibit lettuce seedling. (Patil, 2014) confirmed the ability of *P.*

aeruginosa to produce the toxic secondary metabolite hydrogen cyanide inhibiting the enzymes involved in plant respiration, carbohydrate metabolism, CO₂ and nitrate assimilation. Lakshmi *et al.*, (2015) mentioned that seed bacterization with *P. aeruginosa* caused reduction in shoot and root length of *P. oleracea* and *A. spinosus* weed seedlings.

Our results illustrate that fusant products were more efficient in killing *M. incognita* J₂ and inhibiting germination of seeds weed than their parents. Fusants produced more toxins, antibiotics, and lytic enzymes than the parents, according to (Zaied *et al.*, 2009), who discovered that fusion between *Serratia* spp. and *Pseudomonas* spp. produced more chitinases and bacteriocin than the parents, resulting in high mortality levels in nematodes when compared to the parental strains.. Elkylany, (2017) mentioned that fusants from *Anoxybacillus flavithermus* and *B. pumilus* were more effective in killing *M. javanica* J₂ than their parent, and Abdel Salam *et al.*, (2018) discovered that a higher level of chitinase production in the fusants between *B. amyloliquefaciens* subsp. *plantarum* SA5 and *Lysinibacillus sphaericus* Amira than the parents resulted in higher nematode mortality..

5. Conclusion

We are focusing here on genomics and genetic engineering techniques as helpful tools for developing more powerful biocontrol agents. The efficacy of nematode and weed seeds suppression by tested materials depends on the toxic compound released from these organisms. The obtained fusants from the two local bacterial *P. aeruginosa* and *B. cereus* showed high efficacy against *M. incognita* J₂ and *E. crus-galli* and *P. oleracea* seeds germination because they produced more toxins, antibiotic, lytic enzymes than the parent strains. These new strains show great potential to be formulated as an effective biopesticide.

Acknowledgements

This work was funded by a grant code number 11090408 of In-House project from the National Research Centre, Giza, Egypt.

References

Abdel-Salam MS, Ameen HH, Soliman GM, Elkylany US and Asar MA. 2018. Improving the nematocidal potential of *Bacillus amyloliquefaciens* and *Lysinibacillus sphaericus* against the root-knot nematode *Meloidogyne incognita* using protoplast fusion technique. *Egypt J of Biol Pest Co.*, **28**: 211-216.

Adeu G, Vieren E, Carlesi S, Bärberi P, Munier-Jolain N, Cordeau S. 2019. Mitigating crop yield losses through weed diversity. *Nat sustain.*, **2**: 1018–1026.

Almaghrabi OA, Massoud SI and AbdImoneim TS. 2013. Influence of inoculation with plant growth promoting rhizobacteria (PGPR) on tomato plant growth and nematode reproduction under greenhouse conditions. *Saudi J of Biol Sci.*, **20**: 57-61.

Byron M, Treadwell D and Dittmar P. 2019. Weeds as reservoirs of plant pathogens affecting economically important crops. *IFAS Extension Univ of Florida*, **HS1335**:1-7.

Carvalho DC, Oliveira DF, Correa RS. 2007. Rhizobacteria able to produce phytotoxic metabolites. *Braz. Microbiol.*, **38**: 759-765.

Chen L, Jiang H, Cheng Q, Chen J, Wu G, Kumar A, Sun M and Liu Z. 2015. Enhanced nematocidal potential of the chitinase *pachi* from *Pseudomonas aeruginosa* in association with *Cry21Aa*. *Scientific Rep.*, **5**:14395 [https://doi: 10.1038/srep14395](https://doi.org/10.1038/srep14395).

Davis RW, Botstein D and Rotho JR. 1980. Transfection of DNA. in *Bacterial Genetics: A Manual for Genetic Engineering Advanced Bacterial Genetic*. CSHL *New York*, **67**:134-137.

El-Kawokgy TM, Hussein HA, Aly NA and Mohamed SAH. 2015. Highly toxic and broad-spectrum insecticidal local *Bacillus* strains engineered using protoplast fusion. *Can. Journal of Microbiol.*, **61**: 38–47.

Elkelany US. 2017. Controlling of root-knot nematodes in eggplant using genetically improved bacteria. PhD Thesis, *Fac Agric, Ain Shams Univ.*, **197**pp.

Hussain S, Khaliq BAA, Matloob A, Areeb A, Ashraf U, Hafeez A, Imran M. 2017. Crop growth yield losses in wheat due to little seed Canary grass infestation differ with weed densities and changes in environment, *Planta Daninha*, **35** (e017162328): 1-15.

Hussey RS and Barker KR. 1973. A comparison of methods of collecting inocula of *Meloidogyne* spp. including a new technique. *Plant Dis Rep.*, **57**: 1025-1028.

Jabran K, Mahajan G, Sardana V, Chauhan BS. 2015. Allelopathy for weed control in agricultural systems. *Crop Prot.*, **72**: 57–65. Doi: <https://doi.org/10.1016/j.cropro.2015.03.004>

Khan FG, Ashok R, Khan IA, Kalia A. 1998. Study of *Pseudomonas aeruginosa* causing ventilator associated pneumonia. *Ind J Med Res.*, **107**: 68- 74.

Laemmli UK. 1970. Cleavage of structural proteins during assembly of the head of bacteriophage T4. *Nat.*, **227**:680-685.

Lakshmi VS, Kumari S, Singh A and Prabha C. 2015. Isolation and characterization of deleterious *Pseudomonas aeruginosa* KC1 from rhizospheric soils and its interaction with weed seedlings. *J of King Saud Univ Sci.*, **27**(2): 113–119.

Lee Yand Kim K. 2016. Antagonistic potential of *Bacillus pumilus* L1 against root-knot nematode, *Meloidogyne arenaria*. *J Phytopathol.*, **164**:29–39.

Mohamed SAH, Ibrahim SA, Soliman KHA, Abd-El-Aal SKH, Moawad SS, and Attallah AG. 2016. Genetic improvement of some microorganisms that naturally colonize of tomato plants to increase the effect of bio-control on *Tuta absoluta*. *Res J Pharm Biol Chem Sci.*, **7**: 1502- 1518.

National Committee for Clinical Laboratory Standards (NCCLS). 1999. Performance standards for antimicrobial susceptibility testing; ninth informational supplement, Document M100- S9. *Wayne Pennsylvania* 9, 1.

Oka Y, Chet I, Spiegel Y. 1993. Control of the rootknot nematode *Meloidogyne javanica* by *Bacillus cereus*. *Biocontrol Sci Technol.*, **3**:115–126.

Patil VS. 2014. Isolation, characterization and identification of rhizospheric bacteria with the potential for biological control of *sida acuta*. *J of Environ Res and Develop.*, **8**(3): 411-417.

Sardar MF, Siddique S, Abbas T, Aziz MZ, Naveed M, Khan S. 2020. Biological weeds control in rice (oryza sativa) using beneficial plant growth promoting rhizobacteria. *Int J Agric Biol.*, **23**(3):522-528.

Sayed MHE, Aziz ZKA and Abouzaid AM. 2014. Efficacy of extracellular metabolite produced by *Streptomyces levis* strain LX-65 as a potential herbicidal agent. *J Am Sci.*, **10**: 169-80.

Schisler DA, Slininger PJ, Bothast RJ. 1997. Effects of antagonist cell concentration and two-strain mixtures on biological control of *Fusarium* dry rot of potatoes. *J Phytopathol.*, **87**: 177-183.

- Siddiqui IA, Shaukat SS, Khan GH and Ali NI. 2003. Suppression of *Meloidogyne javanica* by *Pseudomonas aeruginosa* IE-6S+ in tomato: the influence of NaCl, oxygen and iron levels. *Soil Biol Biochem.* **35**:1625–1634. <https://doi.org/10.1016/j.soilbio.2003.08.007>.
- Singh S, Singh B, and Singh A P. 2015. Nematodes: a threat to sustainability of agriculture. *Procedia Environ Sci.*, **29**: 215–216. doi: 10.1016/j.proenv.2015.
- Soliman GM, Ameen HH, Abdel-Aziz SHM and El-sayed GM. 2019. In vitro evaluation of some isolated bacteria against the plant parasite nematode *Meloidogyne incognita*. *Bull Natl Res Cent.*, **43**:171. <https://doi.org/10.1186/s42269-019-0200-0>.
- Soliman GM, Ameen HH, Abd-El-Khair H, El-Nagdi WMA and E-Isayed GM. 2018. Isolation, identification, and improving nematotoxicity of rhizobacterial strains against *Meloidogyne incognita*. *Egypt Pharmaceut J.*, **17**:27–31.
- Soliman GM, Mohamed SAH, Haggag LF and El-Hady ES. 2020. Efficiency of biological control of root-knot nematodes in infected grapevines seedling by genetic improved bacteria. *Plant arch.*, **20(1)**: 951-961.
- Taylor AL and Sasser JN. 1978. Biology, identification and control of root-knot nematodes (*Meloidogyne* species) Raleigh, NC, North Carolina State Univ. Graph.
- Xiao L, Wan JW, Yao JH, Feng H and Wei LH. 2018. Effects of *Bacillus cereus* strain Jdm1 on *Meloidogyne incognita* and the bacterial community in tomato rhizosphere soil. *Biotech.*, **8**: 319-327. <https://doi.org/10.1007/s13205-018-1348-2>.
- Zaied KA, Kawther S, Kash S, Ibrahim A and Tawfik TM. 2009. Improving Nematocidal activity of bacteria via protoplast Fusion. *Australian J of Basic and Appl Sci.*, **3(2)**: 1412- 1427.

Smoking increases the premature associated senescence phenotype of circulating Endothelial Progenitor Cells

Kumboyono Kumboyono^{1,*}, Wiwit Nurwidyaningtyas², Indah Nur Chomsy², Fibe Yulinda Cesa³ and Titin Andri Wihastuti⁴

¹ School of Nursing, Faculty of Medicine, University of Brawijaya, Malang, Indonesia; ² Doctoral Program of Medical Science, Faculty of Medicine, University of Brawijaya, Malang, Indonesia; ³ Master Program of Biomedical Science, Faculty of Medicine, University of Brawijaya, Malang; ⁴ Department of Basic Nursing Science, Faculty of Medicine, University of Brawijaya, Malang

Received: August 17, 2020; Revised: November 26, 2020; Accepted: December 21, 2020

Abstract

Smoking is a risk factor for cardiovascular disease. Notably, it is associated with endothelial progenitor cells (EPCs) dysfunction. It also influences the shift of the EPCs mobilisation from bone marrow. We hypothesized that smoking could induce a premature associated senescence phenotype on the circulating population of EPCs, which may contribute to the default of recovery endothelial injury. Peripheral Blood Mononuclear Cell (PBMC) samples were collected from 30 smokers at least for five years and 31 healthy subjects (non-smoker) as control. CD117⁺ and CD133⁺ cells were confirmed as the population of endothelial progenitor cells. Those marked cells with SA- β galactosidase were quantified as senescence phenotype. Then, FACS assessed the targeted cells. The average concentration of CD133⁺/CD117⁺ was 0.05% (\pm 0.03) for smoker subjects and 0.03% (\pm 0.02) for non-smoker ($p < 0.05$). Almost all of the EPCs population (98.33 \pm 3.53%) in the smoker group expressed SA- β gal positive cells ($p < 0.001$). Thus, this study suggests that smoking is associated with a significant elevated premature senescence of EPCs, which may contribute to diminished bioavailability of mature EPCs of the smoker, reducing the potency of vascular maintenance and repair.

Keywords: premature senescence, endothelial progenitor cells, smoking, vascular repair

1. Introduction

Endothelial progenitor cells (EPCs) effluxed from bone marrow (BM) in response to various molecular signalling pathways. The EPCs population is around 0.0001 in the blood circulation (Tagawa *et al.*, 2015; Zhao *et al.*, 2016). EPCs are required for the repair of the endothelium when endothelial injury or dysfunction. Regenerative potential to repair endothelial injury is carried out only by mature EPCs. Mobilization of population endothelial progenitor cells from BM is the initial stage of maturation or differentiation of various cell types, including EPCs (Hur *et al.*, 2004; Zhang *et al.*, 2014; Tagawa *et al.*, 2015; Zhao *et al.*, 2016). Hematopoietic progenitor cells are characterized by CD117 and CD133 surface markers (Hur *et al.*, 2004; Gargett *et al.*, 2009). Changes in the number of hematopoietic progenitor cells in the blood circulation affect the availability of mature EPCs. Various factors that modulate endothelial dysfunction also induce dysfunction of EPCs and induce the reduction in circulating EPCs (Hur *et al.*, 2004; Zhang *et al.*, 2014; Tagawa *et al.*, 2015; Zhao *et al.*, 2016).

The senescence of the human cell is considered an essential hallmark of the ageing process (Honn *et al.*, 2017). Ageing is a complex phenomenon associated with increasing age or the accumulation of long-term oxidative stress exposure. Cells characterised as senescence are

recognised viable, but they cannot perform a functional role due to cell cycle arrest for a certain period; meanwhile, the disrupted factor exposure remains constant. Senescence markers were identified as intracellular specific changes, such as increased senescence-associated β -galactosidase activity (SA- β -Gal). The SA- β -ga is a marker widely used to identify senescence in cells and tissues (Young *et al.*, 2009; Kurz *et al.*, 2000; Lee *et al.*, 2006).

Smoking is an established risk factor for cardiovascular disease (CVD) (Kaplan *et al.*, 2017). Tobacco smoke contains more than 4720 compounds, including well-known harmful chemicals such as polycyclic aromatic hydrocarbons, free radicals, and oxidative gases (Yao *et al.*, 2008; Rafacho *et al.*, 2011). Smoking might become a habit due to the addictive property of nicotine (Kumboyono *et al.*, 2020). Nicotine induces the mesenchymal (MSC) biological function because of its underlying cause of various diseases. But, researchers have argued this phenomenon due to the limited study (Huertas *et al.*, 2010; Kumboyono *et al.*, 2020). Several studies claim that smoking significantly inhibits the regenerative potential of MSC and has been implicated in the early degeneration of mesenchymal tissue (Greenberg *et al.*, 2017). This study investigates the effect of smoking exposure on EPC's biological changes in vivo, further exploring the consequence of smoking-mediated premature senescence in the EPCs population.

* Corresponding author. e-mail: publikasikoe@gmail.com.

2. Methods

2.1. Research design

The study was a cross-sectional study with a simple random sampling technique—informed consent was given to collect peripheral blood from each participant. Participants were divided into two groups; current smokers are participants who smoked >10 cigarettes/day for five years ago (n=30), and participants who had never smoked were considered in the control group (n=31). The participant's inclusion criteria included; having no history of diabetes mellitus, hypertension, and coronary arterial disease, ideal weight, maintaining physical exercise with medium intensity three times a week. Laboratory analysts were blinded to smoking status during data collection and analysis.

2.2. Collection and Isolation of PBMC

Peripheral blood (5 mL/subject) was drawn by a heparinized venous puncture method at the forearm. PBMC isolated by density gradient centrifugation (catalogue#07801/07811, Lymphoperp™, Germany) with a density of 1.077 g/mL as previously reported (Shi *et al.*, 1998; Masuda *et al.*, 2014; Beyth *et al.*, 2015). Mononuclear cells were collected, and the remaining erythrocytes lysed. CD133⁺ and CD117⁺ marked cells were purified by FACS auto-separator, using fluorescence anti-human CD133 APC-conjugated antibody monoclonal mouse IgG2A clone #170411 [FAB no.cat 11331A] and PE anti-human CD117/c-kit [Biolegend; no.cat. 323408].

2.3. Flow cytometry

Freshly isolated PBMC subjected to flow cytometry to detect surface antigen of EPC. The collected cell were resuspended with incubation buffer (0.5 g bovine serum albumin in 100 ml 1X PBS, stored at 4°C). Aliquot made in 1 x 10⁶ cells/100 µl/tube. Suspended were cells incubated in 10 µl CD133 and 5 µl CD117 by 100 µl staining volume at room temperature for 20 minutes. The stained cells were washed with PBS/1% BSA three times, resuspended in 0.5 ml PBS/1% BSA/propidium iodide (PI; Sigma). Flow cytometric profiles were obtained using FACS BD flow cytometer and Cell Quest software (Becton Dickinson Immunocytometry Systems, Mountain View, CA).

2.1. SA-β galactosidase assay

Senescence-associated beta-galactosidase (SA-β gal) activity was detected using Cell Event™ Senescence Green Flow Cytometry Assay Kit (Invitrogen; C10841) following the manufacturer's protocol (Thermo Fisher Scientific Inc.).

2.2. FCM analysis

The scatter diagram of each PBMC population in an individual is gated into a cell-sized population of lymphocytes, monocytes, and the other larger cells. The percentage (%) of the marker positivity (+) obtained from the EPCs population on each gate compared to the total cells in 3 gates.

2.3. Ethical Clearance

This experimental design has been fulfilled and approved by the Ethics Committee of Faculty of Medicine,

Brawijaya University, Malang, Indonesia, by registered number: 1206-KEP-UB/2019.

2.4. Statistical Analysis

The percentage of targeted cells in each group was analysed using SPSS v.23 in value ± standard deviation. Student t-test was used to compare the means between groups. A p-value ≤ 0.05 is statistically significant and indicates strong evidence against the null hypothesis.

3. Result

3.1. Smoking induced the enrichment of circulating CD117⁺ cells

Cell population that was positively selected from PBMC consists of 0.33% – 3.25% CD117⁺ cells and 0.15%-0.31% CD113⁺ cells (Figure 1), indicating the efficacy of the isolation method. The smoking group showed the enrichment of CD117⁺ cells compared to non-smoker (10 fold in CD117⁺ cells; Table 1). The average concentration of CD117⁺ cells in the current smoker group (3.24% ± 1.6) was significantly higher than in the non-smokers' group (0.33% ± 0.07) (*p*<0.001).

3.2. The decrease of CD113⁺ cells in the current smoker group compared to the non-smoker group

The proportion of CD113⁺ cells of the current smoke group was 50% lower than the non-smoker group. Population of CD113⁺ cells in non-smokers (0.31% ± 0.3) was significantly higher than in smokers (0.15% ± 0.01) (*p*<0.05) (Table 1).

3.3. Smoking increased the hematopoietic progenitor cell population compared to the non-smoker group

Based on fluorescent cell sorting, large hematopoietic progenitor cells were proportionally found in PBMC of the current smoker group (0.05% ± 0.03) than the non-smoker group (0.03% ± 0.02) (*p*<0.05) (Table 1).

3.4. The SA-β-galactosidase-expressed Hematopoietic Progenitor Cells elevation in the smoker group

In this study, the EPCs biological phenotype was evaluated by SA-β-galactosidase expression as a premature senescence hallmark. The senescence cells increased significantly in the current smoker group (98.33% ± 3.53). On the other hand, negative marked SA-β galactosidase cell in non-smoker group was significantly higher (55.51% ± 34.96) than in the current smoker group (*p*<0.001) (Table 1). Thus, it indicates that the premature senescence of EPCs increased due to the stress effect of smoking.

Table 1. Diversity of circulating progenitor cell populations in the smokers and non-smoker groups

Marker (% gate)	Circulating Progenitor Cell		t-test
	Smokers [n=30]	Non-smokers [n=31]	
CD133 ⁺	0.15 ± 0.01	0.31 ± 0.3	0.011*
CD117 ⁺	3.24 ± 1.63	0.32 ± 0.07	0.000**
CD133 ⁺ /CD117 ⁺	0.05 ± 0.03	0.03 ± 0.02	0.036*
CD133 ⁺ /CD117 ⁺ /SA-β gal. ⁺	98.33±3.52	55.51 ± 5.10	0.000**
CD133 ⁺ /CD117 ⁺ SA-β gal. ⁻	1.67±3.53	45.40 ± 3.35	0.000**

Data shown are the mean ± SD; Significant value *p*< 0.05*, *p*<0.001**

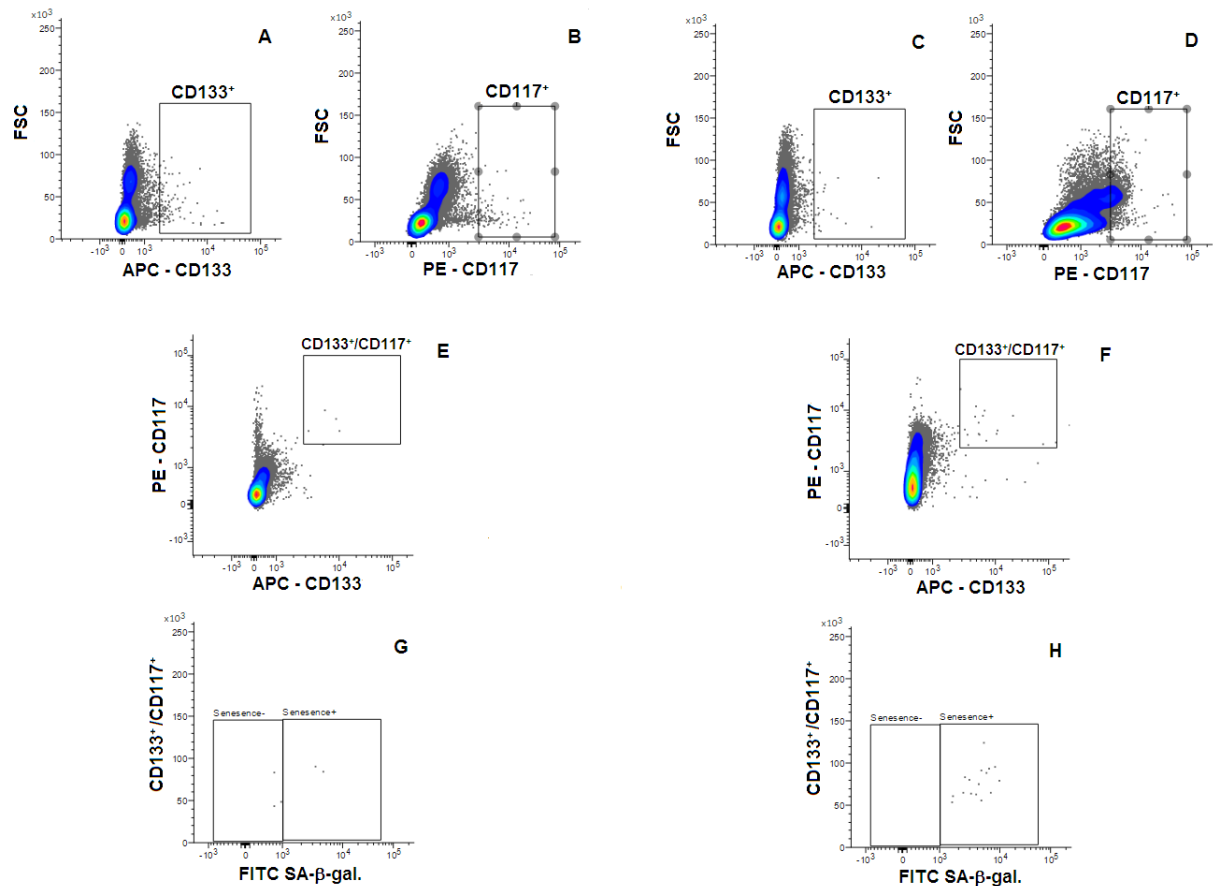


Figure 1. Cytometric analysis of cells that were positively CD133, CD117, and SA-β-galactosidase of each group. The investigated cell surface markers were hematopoietic progenitor cells (PE-CD117⁺, APC-CD133⁺). (A) CD133⁺ in non-smoker group; (B) CD117⁺ in non-smoker group; (C) CD133⁺ in the smoker group; (D) CD117⁺ in the smoker group; (E) CD133⁺/CD117⁺ cells on non-smoker group; (F) CD133⁺/CD117⁺ cells on smoker group were higher than a non-smoker group; (G) senescence scatter plot gate which confirmed with SA-β-gal in non-smoker group; (H) senescence scatter plot visualization in the smoker group—representative analysis for one out of 61 PBMC samples.

4. Discussion

Reparative activity by EPCs has been declared in much research as a good advantage in both clinical approach and laboratory-based research. Still, it hasn't answered the remaining questions regarding the comprehensive framework of EPCs and their maturation in blood circulation. Based on their origin, bone marrow-derived EPCs biology is considered the source of EPCs and their differentiation through the vascular system. In this study, we used and compared different smoking habits that might exhibit different visualizing of biology EPCs.

The present study aimed to investigate EPCs viability through the premature senescence phenotype, confirmed by CD133⁺/CD117⁺. Our finding showed that the premature senescence of EPCs and increased SA-β-galactosidase-expressed hematopoietic progenitor cells population in the smoker group. These results suggest that the elevation of EPCs mobilization from bone marrow modulated by smoking to compensate responses due to the increase of the senescence cells.

Nicotine is the primary addictive component of tobacco. It is a highly toxic compound that exerts its effects on almost every organ and system in the body. Nicotine exposure *in vitro* induced cell death (about 50%) in the MRC-5 cell line (Vajravelu *et al.*, 2015). It also

demonstrated that smoking also induces premature senescence in EPCs due to the effect of nicotine exposure. So, our result is in line with studies that investigate the cytotoxicity of tobacco compounds.

Analysis of aged stem cells in various tissues leads to common effectors and signalling pathways that contribute to stem cell dysfunction in response to toxic metabolites. Reactive oxygen species (ROS) that generated from electron 'leak' during mitochondrial oxidative phosphorylation plays fundamental roles in perturbed stem cell function leading to ageing (Takubo *et al.*, 2013; Harris *et al.*, 2013; Yu *et al.*, 2013; Oh *et al.*, 2014; Vlasceanu *et al.*, 2018). In this study, the induction of actin filament reorganisation after a long time of nicotine exposure can be attributed to elevated cell senescence. Acrolein and other gas-phase oxidants in cigarette smoke remain stable in blood and thus are capable of acting directly on the vascular cells through impairs nitric oxide (NO)-mediated cell function (Bluhm *et al.*, 1971; Barnova *et al.*, 2005; Chung *et al.*, 2005; Witschi *et al.*, 2005; Mossman *et al.*, 2006; Pervaiz *et al.*, 2009; Lennartsson and Ronnstrand, 2012).

Smoking can trigger the ROS production enriched in both the gaseous and particulate components of smoking (Bluhm *et al.*, 1971; Barnova *et al.*, 2005; Kaplan *et al.*, 2017). Alteration in ROS production due to cigarette smoking has a drastic effect on the host immunity through

increasing the production of pro-inflammatory cytokines such as interleukin-8 (IL-8) and tumour necrosis factor- α (TNF- α) (Chung *et al.*, 2005; Witschi *et al.*, 2005). The data demonstrate the elevated circulation of circulating CD117⁺ cells in the smoker group, confirming the statement that expansion in CD117⁺ cells considered to the process of lineage diminished ability to self-renew, occurs in synergy with other cytokines and risk-factor (Mossman *et al.*, 2006)

Surface protein CD117 plays a vital role in regulating survival, maintenance, self-renewal, and endothelial stem cell re-endothelization (Mossman *et al.*, 2006). In addition, our study reports that oxidative stress-mediated by smoking-induced imbalance redox signalling for cellular senescence (Höhn *et al.*, 2017). Also, our results showed that environmental stimuli could regulate stem cell function (Lennartsson and Ronnstrand, 2012; Ren *et al.*, 2017). High premature senescence EPCs in the smoker group of this study impacted the availability of mature EPCs in circulation. The maturation of EPCs in blood circulation is the result of the differentiation of bone marrow-derived EPCs marked by current-EPCs that gradually disappeared and were replaced by endothelial cell markers. This EPCs senescence might be considered EPCs dysfunction, which is the cause of repair endothelial dysfunction failure due to oxidative stress (Tousoulis *et al.*, 2008; Cruciani *et al.*, 2020).

The oxidative stress from smoking influences the cardiovascular system in two ways; by directly delivering free radicals to the vascular system and consuming antioxidants that would generally be available to protect against endogenous free radicals occurring from the respiratory process. DNA damage in mitochondria induced from oxidative stress in smoking might influence the checkpoint phase and result in the cell cycle arrest (Ambrose and Barua, 2004; Lennartsson and Ronnstrand, 2012; Ren *et al.*, 2017). The latest report showed that EPCs stem cells exhibit a series of these age-related changes that could trigger cell dysfunction/death and, in turn, a progressive decline in regeneration capacity (Koyuncu *et al.*, 2015)

5. Conclusion

This research finding showed that smoking increases of EPCs premature senescence. This knowledge is essential for improving senescent cells' identification and characterization *in vivo* and developing rational strategies to modulate the senescence program for therapeutic in high-risk CVD populations.

Conflict OF Interest

The authors declare no conflict of interest.

Acknowledgements

The study was supported by a research grant from the Ministry of Education and Culture, The Republic of Indonesia, through Brawijaya University.

Authors Contributions

KK, TAW, and WN designed this study and prepared the manuscript.

TAW, WN, INC, and KK collected and analysed the clinical data.

FYC and INC significantly revised the manuscript.

TAW and KK are responsible and accountable for the accuracy or integrity of the work.

References

- Ambrose JA, and Barua RS. 2004. The pathophysiology of cigarette smoking and cardiovascular disease: an update. *J Am Coll Cardiol.* **43(10)**: 1731-1737.
- Barnoya J, and Glantz SA. 2005. Cardiovascular effect of secondhand smoke nearly as large as smoking. *Circulation.* **111**: 2684-2698.
- Beyth S, Mosheiff R, Safran O, Daskal A, and Liebergall M. 2015. Cigarette smoking is associated with a lower concentration of CD105⁺ Bone marrow progenitor cells. *Bone Marrow Res.* **2015**: 914935.
- Bluhm A, Weinstein J, and Sousa J. 1971. Free Radicals in Tobacco Smoke. *Nature.* **229**: 500.
- Chung KF. 2005. Inflammatory mediators in chronic obstructive pulmonary disease. *Curr Drug Targets.* **4(6)**: 619-625.
- Cruciani S, Garroni G, Ginesu GC, Fadda A, Ventura C, and Maioli M. 2020. Unravelling Cellular Mechanisms of Stem Cell Senescence: An Aid from Natural Bioactive Molecules. *Biology (Basel).* **9(3)**: 57. Published 2020 Mar 20.
- Gargett CE, Schwab KE, Zillwood RM, Nguyen HP, and Wu D. 2009. Isolation and culture of epithelial progenitors and mesenchymal stem cells from human endometrium. *Biol Reprod.* **80(6)**: 1136-1145.
- Greenberg JM, Carballosa CM, and Cheung HS. 2017. Concise Review: The Deleterious Effects of Cigarette Smoking and Nicotine Usage and Mesenchymal Stem Cell Function and Implications for Cell-Based Therapies. *Stem Cells Transl Med.* **6(9)**: 1815-1821.
- Harris JM, Esain V, Frechette GM, Harris LJ, Cox AG, Cortes M, Garnaas MK, Carroll KJ, Cutting CC, Khan T, Elks PM, Renshaw SA, Dickinson BC, Chang CJ, Murphy MP, Paw BH, Vander Heiden MG, Goessling W, and North TE. 2013. Glucose metabolism impacts the spatiotemporal onset and magnitude of HSC induction *in vivo*. *Blood.* **121(13)**: 2483-2493.
- Höhn A, Weber D, Jung T, Ott C, Hugo M, Kochlik B, Kehm R, König J, Grune T, and Castro JP. 2017. Happily (n)ever after: Aging in the context of oxidative stress, proteostasis loss and cellular senescence. *Redox Biol.* **11**: 482-501.
- Huertas A, Testa U, Riccioni R, Petrucci E, Riti V, Savi D, Serra P, Bonsignore MR, and Palange P. 2010. Bone marrow-derived progenitors are greatly reduced in patients with severe COPD and low-BML. *Respir Physiol Neurobiol.* **170**: 23-31.
- Hur J, Yoon CH, Kim HS, Choi J, Kang H, Hwang KK, Oh B, Lee M, and Park YB. 2004. Characterization of Two Types of Endothelial Progenitor Cells and Their Different Contributions to Neovascularogenesis. *Arterioscler Thromb Vasc Biol.* **24**: 288-293.
- Kaplan A, Abidi E, Ghali R, Booz GW, Kobeissy F, and Zouein FA. 2017. Functional, Cellular, and Molecular Remodeling of the Heart under Influence of Oxidative Cigarette Tobacco Smoke. *Oxid Med Cell Longev.* **2017**: 3759186.
- Koyuncu S, Irmak D, Saez I, and Vilchez D. 2015. Defining the General Principles of Stem Cell Aging: Lessons from Organismal Models. *Curr Stem Cell Rep.* **1**: 162-9.
- Kumboyono K, Hamid AYS, Sahar J, and Bardosono S. 2020. Community response to the initiation of smoking in Indonesian early adolescents: a qualitative study. *Int J Adolesc Youth.* **25(1)**: 210-220.

- Kurz DJ, Decary S, Hong Y, and Erusalimsky JD. 2000. Senescence-associated (beta)-galactosidase reflects an increase in lysosomal mass during replicative ageing of human endothelial cells. *J Cell Sci.* **113** (Pt 20): 3613-3622.
- Lee BY, Han JA, Im JS, Morrone A, Johung K, Goodwin EC, Kleijer WJ, DiMaio D, and Hwang ES. 2006. Senescence-associated beta-galactosidase is lysosomal beta-galactosidase. *Aging Cell.* **5**(2): 187-195.
- Lennartsson J, and Ronnstrand L. 2012. Stem Cell Factor Receptor/c-Kit: From Basic Science to Clinical Implications. *Physiol Rev.* **92**: 1619-1649.
- Masuda H, Tanaka R, Fujimura S, Ishikawa M, Akimaru H, Shizuno T, Sato A, Okada Y, Iida Y, Itoh J, Itoh Y, Kamiguchi H, Kawamoto A, and Asahara T. 2014. Vasculogenic conditioning of peripheral blood mononuclear cells promotes endothelial progenitor cell expansion and phenotype transition of anti-inflammatory macrophage and T lymphocyte to cells with regenerative potential. *J Am Heart Assoc.* **3**(3): e000743.
- Mossman BT, Lounsbury KM, and Reddy SP. 2006. Oxidants and signaling by mitogen-activated protein kinases in lung epithelium. *Am J Respir Cell Mol Biol.* **34**(6): 666-669.
- Oh J, Lee YD, and Wagers AJ. 2014. Stem cell aging: mechanisms, regulators and therapeutic opportunities. *Nat Med.* **20**(8): 870-880.
- Pervaiz S, Taneja R, and Ghaffari S. 2009. Oxidative stress regulation of stem and progenitor cells. *Antioxid Redox Signal.* **11**: 2777-2789.
- Rafacho BP, Azevedo PS, Polegato BF, Fernandes AAH, Bertoline MA, Fernandes DC, Chiuso-Minicucci F, Roscani MG, dos Santos PP, Matsubara LS, Matsubara BB, Laurindo FRM, Paiva SAR, Zornoff LAM, and Minicucci MF. 2011. Tobacco smoke induces ventricular remodeling associated with an increase in NADPH oxidase activity. *Cell Physiol Biochem.* **27**(3-4): 305-312.
- Ren R, Ocampo A, Liu GH, and Izpisua Belmonte JC. 2017. Regulation of Stem Cell Aging by Metabolism and Epigenetics. *Cell Metab.* **26**(3): 460-474.
- Shi Q, Rafii S, Wu MH, Wijelath ES, Yu C, Ishida A, Fujita Y, Kothari S, Mohle R, Sauvage LR, Moore MA, Storb RF, and Hammond WP. 1998. Evidence for circulating bone marrow-derived endothelial cells. *Blood.* **92**: 362-367.
- Tagawa S, Nakanishi C, Masayuki M, Yoshimuta T, Shimojima YS, Yokawa M, Kawashiri J, Yamagishi M, and Hayashi K. 2015. Determination of Early and Late Endothelial Progenitor Cells in Peripheral Circulation and Their Clinical Association with Coronary Artery Disease. *Int J Vasc Med.* 674213.
- Takubo K, Nagamatsu G, Kobayashi CI, Nakamura-Ishizu A, Kobayashi H, Ikeda E, Goda N, Rahimi Y, Johnson RS, Soga T, Hirao A, Suematsu M, and Suda T. 2013. Regulation of glycolysis by Pdk functions as a metabolic checkpoint for cell cycle quiescence in hematopoietic stem cells. *Cell Stem Cell.* **12**(1): 49-61.
- Tousoulis D, Andreou I, Antoniadis C, Tentolouris C, and Stefanadis C. 2008. Role of inflammation and oxidative stress in endothelial progenitor cell function and mobilization: Therapeutic implications for cardiovascular diseases. *Atherosclerosis.* **201**(2): 236-47.
- Vajravelu BN, Hong KU, Al-Maqtari T, Cao P, Keith MCL, Wysoczynski M, Zhao J, Moore JB 4th, and Bolli R. 2015. C-Kit Promotes Growth and Migration of Human Cardiac Progenitor Cells via the PI3K-AKT and MEK-ERK Pathways. *PLoS ONE.* **10**(10):
- Vlasceanu AM, Baconi DL, Galateanu B, Miriana S, and Cristian B. 2018. Comparative cytotoxicity study of nicotine and cotinine on MRC-5 cell line. *Mind Med Sci.* **5**(1): 117-122.
- Witschi H. 2005. Carcinogenic activity of cigarette smoke gas phase and its modulation by beta-carotene and N-acetylcysteine. *Toxicol. Sci.* **84**:1:81-7.
- Yao H, Edirisinghe I, Yang SR, Rajendrasozhan S, Kode A, Caito S, Adenuga D, and Rahman I. 2008. Genetic ablation of NADPH oxidase enhances susceptibility to cigarette smoke-induced lung inflammation and emphysema in mice. *Am J Pathol.* **172**(5): 1222-1237.
- Young AR, Narita M, Ferreira M, Kirschner K, Sadaie M, Darot JF, Tavaré S, Arakawa S, Shimizu S, Watt FM, and Narita M. 2009. Autophagy mediates the mitotic senescence transition. *Genes Dev.* **23**(7): 798-803.
- Yu WM, Liu X, Shen J, Jovanovic O, Pohl EE, Gerson SL, Finkel T, Broxmeyer HE, and Qu CK. 2013. Metabolic regulation by the mitochondrial phosphatase PTPMT1 is required for hematopoietic stem cell differentiation. *Cell Stem Cell.* **12**(1): 62-74.
- Zhang M, Rehman J, and Malik AB. 2014. Endothelial progenitor cell and vascular repair. *Curr Opin Hematol.* **21**(3): 224-228.
- Zhao J, Mitrofan CG, Appleby SL, Morrell NW, and Lever AML. 2016. Disrupted Endothelial Cell Layer and Exposed Extracellular Matrix Proteins Promote Capture of Late Outgrowth Endothelial Progenitor Cells. *Stem Cells Int.* Volume, **2016**: 1406304.

Light Microscopic Changes in The Epididymis of Different Age Groups of The African Greater Cane Rat (*Thryonomys swinderianus*, Temminck 1827)

Omirinde Jamiu Oyewole^{1,*}, Olukole Samuel Gbadebo² and Oke Bankole Olusiji²

¹Department of Veterinary Anatomy, Faculty of Veterinary Medicine, University of Jos, Jos, Plateau State, Nigeria; ²Department of Veterinary Anatomy, Faculty of Veterinary Medicine, University of Ibadan, Ibadan, Oyo State, Nigeria.

Received: August 30, 2020; Revised: February 2, 2021; Accepted: February 13, 2021

Abstract

The mammalian epididymis is an important tubular epithelial structure with key functions in spermatozoa maturation and storage. There is a dearth of information on age-related changes in the light microscopic details of the epididymis in cane rat. This study evaluated light microscopic changes in the epididymis of different age groups of the African greater cane rats (AGCR) using histological, histochemical, and histomorphometric techniques. Twenty (20) African greater cane rats were used for this study. The rats were randomly assigned into 4 groups of 5 rats each as i. prepubertal (≤ 4 months), ii. pubertal ($>4 \leq 12$ months), iii. adult ($>12 \leq 30$ months) and iv. aged (>30 months). Sequel to intra-cardiac perfusion with fixative (10% buffered formalin), routine histology, and histomorphometry using GIMP2 Software was carried out on the processed epididymal tissues. Also, the glycogen and connective tissue content of the epididymis of each group was demonstrated using Periodic-Acid Schiff and Masson Trichrome stains, respectively. The epididymis was lined by simple cuboidal epithelium in prepubertal compared to the pseudostratified columnar cells observed in others. Both Periodic-Acid Schiff and Masson Trichrome intensities were significantly higher in pubertal and adult rats relative to others. Histomorphometric parameters displayed a progressive age-related increase across the groups of cane rats. These sets of data could probably be associated with reproductive quiescence in the prepubertal and remarkable vigor more particularly in the adult cane rats investigated. Consequent upon this, adult cane rats are recommended for optimal breeding.

Keywords: Age, light microscopy, epididymis, cane rat

1. Introduction

The mammalian epididymis is an important epithelial tube with prime functions of spermatozoa maturation and storage (Cornwall, 2009). Morphologically, epididymis was originally thought to be divided into three distinct regions (segments): the caput which is situated at the testicular cranial pole, the corpus found by the side of the testes and the cauda segment occupying the caudal pole of the testis (Hermo, 1995). The epididymis was later discovered to contain an additional segment, the initial segment, especially in the rat (Hermo et al., 1991; 1998).

The epididymal histoarchitecture has been observed to be divided into segments and zones by connective tissue stroma and typified by epithelial compositions with different cell types (principal, basal, apical, clear, and halo cells) of diverse functions (Robaire et al., 2006). In terms of cell population on the epididymal epithelium, the principal and basal cells constitute the major cells while the remaining cells on the epididymal epithelium are regarded as accessory cells (Agnes and Akbarsha, 2001). Studies on different mammalian species have identified several other slight histo-architectural differences such as additional zones and segments along the ductus

epididymal length (Jones et al., 1979; Oke, 1989; Adebayo and Olurode, 2010).

The ductal diameter, epithelial height, parenchymal cell types and their distribution differ in the various segments of the mammalian epididymis (Akbarsha et al., 2015). The epididymal epithelial thickness has been established to vary along the tubule being thickest at the proximal caput and thinnest at the caudal region (Arrotéa et al., 2012). In most mammals, the proximal to the distal segment of the epididymis usually has a progressive increase in luminal diameter and periductal muscle coat thickness (Lasserre et al., 2001). Also, spermatozoa concentrations are usually scanty in the initial segment but are largely concentrated in the lumen of the cauda epididymal region (Yanagimachi et al., 1985; Cornwall, 2009). The epididymal external ductal diameter, epithelial height, periductal muscular wall width, and stereocilia height have been reported to vary in different age-category of hamster rats (Calvo et al., 1999).

African greater cane rat (AGCR) is a wild herbivorous rodent currently undergoing massive domestication to augment the acute shortage of animal protein in sub-Saharan Africa (Fayenuwo et al., 2003; Olude et al., 2014; Monadjem et al., 2015). Earlier investigations on the epididymal morphology of the cane rat paid attention to the adult-only (Olukole et al., 2009; Adebayo and Olurode,

* Corresponding author e-mail: oimirindejamiu@yahoo.com.

2010; Adebayo et al., 2016). There is a dearth of reports on the light microscopic changes in the epididymis of different age groups of the African greater cane rat (*Thryonomis swinderianus*, Temminck 1827). Therefore, this study was designed to evaluate light microscopic changes in the epididymis of different age-category of cane rat using histological, histochemical and histomorphometric approaches.

2. Materials and Methods

2.1. Animals

Twenty (20) healthy male African greater cane rats used for this study were procured from a commercial farm (Pavemgo cane rat, Lagos State, Nigeria) with a record of birth. The rats were stabilized for one week in the Experimental Animal Unit of the Faculty of Veterinary Medicine. They were fed daily on dry corn feed and water provided *ad libitum*. The protocol for this experiment was approved by the University of Ibadan Animal Care and Use Research Ethics Committee (UI-ACUREC) and issued an ethical clearance (UI-ACUREC/18/0120).

2.2. Experimental Design

Modified age-classification earlier reported by Soro et al. (2014) was adopted. The AGCR were randomly sorted into four groups of five (n=5) rats per group as highlighted below:

(A). Prepubertal (Pre); ≤ 4 months, (B). Pubertal (Pub); $>4 \leq 12$ months, (C). Adult; $>12 \leq 30$ months and (D). Aged (AG); >30 months). At the end of stabilization on day 8, the rats were sedated with combined sedatives; xylazine and ketamine (20:80 mg/kg body weight respectively) injected intramuscularly. Thereafter, primary perfusion fluid (0.9% sodium chloride (Aventra, Fidson, Nigeria) plus 25,000 IU of heparin (2IU\ML) (Heparinum; Polfa) and fixative proper (10% buffered formalin) were intracardially perfused.

2.3. Tissue processing for histology, histochemistry and histomorphometry

For histology, epididymal tissues were processed using the protocol of Adebayo and Olurode (2010). The stained tissues were then examined under a light microscope (Olympus BX3-CBH, USA) for variation in histo-architecture concerning age. Photomicrographs of the slides of the epididymides of different age groups of AGCR were evaluated for histomorphometric variations in epididymal (ductal diameter, ductal height, luminal diameter, stereocilia height and peritubular muscle coat thickness) parameters using GIMP2 Software. Following routine histology, the glycogen and connective tissue content of the epididymis of each group were demonstrated using Periodic-Acid Schiff (PAS) and Masson Trichrome (MT) stains, respectively. Also, the images of PAS and MT stained slides were quantified using ImageJ software.

2.4. Statistical analysis

Data obtained from histomorphometry and image J quantification of PAS and Masson trichrome staining intensities were statistically analyzed using GraphPad Prism Version 4.00 for Windows, GraphPad Software (San Diego, CA, USA). The results were expressed as group

mean \pm standard error of the mean (SEM), with a level of significance at $p < 0.05$. The differences across the four groups of AGCR were compared using a one-way analysis of variance (ANOVA), and Tukey was used for multiple comparisons post hoc.

3. Results

3.1. Histological changes in the epididymis of different age groups of the African greater cane rat

The epididymis of the AGRC comprised six distinct zones: Zones I, II and III (initial segment), Zone IV (caput), Zone V (corpus) and Zone VI (cauda) (Fig 1 A-C). The first (initial) segment unlike others is further partitioned by connective tissue septae into three (3) histologically distinct sub-segments or regions or zones, namely: proximal (zone I), middle (zone II) and caudal (zone III) initial segments (Fig. 1 A and B). The shape of the lumen of all the epididymal segments in the pre-pubertal rat was round (Fig. 2). However, in the pubertal and aged AGCR, the proximal to the distal sub-segments of the initial epididymal segment had stellate-shaped lumen (Figs. 2-4), while their caput, corpus and cauda segments bear characteristic round luminal shape (Figs. 5-7). Concerning age-related differences in the nature of the epithelial lining of the epididymal segments, pre-pubertal epididymal duct was lined by predominantly simple cuboidal to columnar cells (Figs. 2-7), while the epithelial lining of the epididymal duct in pubertal and adult rats were the typical pseudostratified ciliated columnar epithelium (Figs. 2-7).

3.2. Age-related changes in the content of glycogen and collagen fibres in the epididymis of the African greater cane rat

Positive Masson's Trichrome stained areas within the segments of the epididymal duct of all AGCR groups were observed as bluish collagen substances in the ductal interstices and in the peritubular muscle coats (Figs. 2-7). Concerning PAS staining of the epididymis, positive areas appeared as magenta colour in the epididymal interstitium, lamina propria, peritubular muscle coat, perinuclear region of epididymal epithelial cells, ductal stereocilia and luminal content especially in the caput, corpus and caudal segments (Figs. 2-7). On the intensity of MT and PAS (Figs. 2-7) expressions in the segments of epididymal duct, significant age-related increase ($p < 0.05$) in values were consistently observed for both stains. Strong PAS and MT intensities were displayed in most of the segments of pubertal and adult epididymis compared to other AGCR groups.

3.3. Histomorphometric parameters of the epididymis of different age-groups of the African greater cane rat

3.3.1. Ductal diameter (DD)

The DD was the smallest in all the segments of the epididymis in the prepubertal AGCR relative to others. The various segments of the epididymal duct showed a significant increase in DD from prepubertal to aged AGCR. The comparison along the rest of the epididymal duct of each AGCR group showed a significant ($p < 0.05$) craniocaudal increase in the DD with the highest in the caudal segments (Table 1).

3.3.2. Ductal luminal diameter (DLD)

The ductal luminal diameter was significantly low ($p < 0.05$) in the prepubertal relative to other AGCR groups. Also, the DLD of the entire epididymal segment was significantly higher ($p < 0.05$) in the aged AGCR compared to others. The DLD of the epididymal duct in all age groups showed a significant increase ($p < 0.05$) with advancing age. On the difference along the epididymal duct within each group, a significant craniocaudal increase ($p < 0.05$) in luminal diameter was observed (Table 1).

3.3.3. Ductal epithelial height (DEH)

The ductal epithelial height of the prepubertal AGCR was significantly low ($p < 0.05$) when compared to other groups. The DEH in nearly all the epididymal segments (initial, middle and distal segments) were not significantly different ($p > 0.05$) from pubertal to aged groups, though a markedly reduced DEH was noticed in the caudal segment of the aged AGCR. In the comparison along the epididymal duct, a progressive significant craniocaudal decrease in DEH was seen in this study (Table 1).

3.3.4. Ductal stereocilia height (DSH)

The ductal stereocilia height of the prepubertal epididymis was significantly low ($p < 0.05$) relative to other groups. The DSH values from the pubertal to aged AGCR were not significantly different ($p > 0.05$), though an insignificant decrease in DSH was exclusively found in the epididymal segments of aged AGCR. Concerning variation along the segments of the epididymal duct of each AGCR group, a craniocaudal decrease in the trend of DSH values was noted. Also, the initial segments of each group bear significantly higher ($p < 0.05$) stereocilia (Table 1).

3.3.5. Periductal muscle coat thickness (PMCT)

The periductal muscle coat thickness was significantly higher ($p < 0.05$) in the adult AGCR compared to other groups. The PMCT appeared to increase significantly ($p < 0.05$) with age. A fairly progressive increase in PMCT was noticed with consistently significant ($p < 0.05$) values obtained in the caudal epididymal segment of all AGCR groups (Table 1).

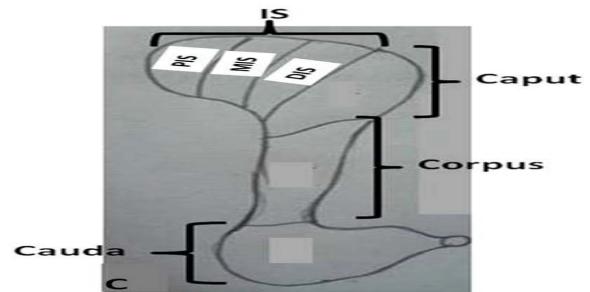
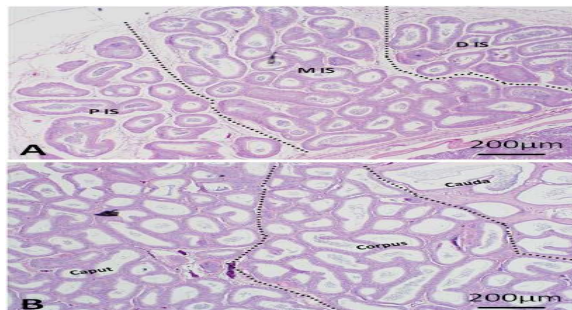


Figure 1 A-C. Photomicrographs and schematic diagram of the epididymal segments of the African greater cane rat. Note the four main segments of the epididymis; Initial segment (IS), caput, corpus and cauda. The initial segment (IS) is partitioned by connective tissue septae (dashed lines) into the proximal initial segment (P-IS), middle initial segment (M-IS) and distal initial segment (D-IS). Scale bar: 200 μ m.

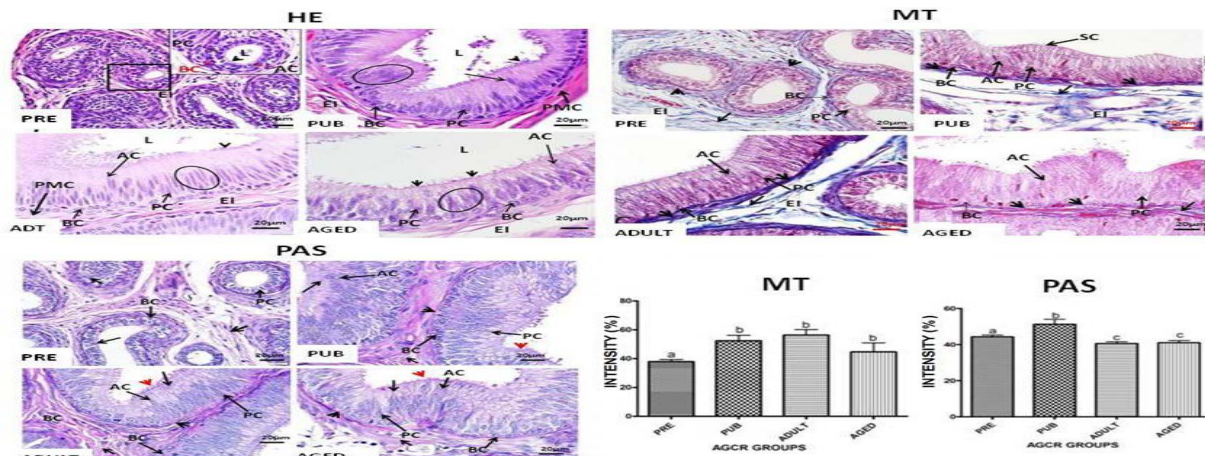


Figure 2. Photomicrographs of the proximal initial segment of the epididymis in different AGCR groups. In HE sections, the conspicuously reduced but almost absent stereocilia height (arrowhead), a round ductal lumen (L) lined by simple columnar epithelial cells and more cellular epididymal interstitium (EI) in prepubertal (Pre) AGCR. While in others, note the display of stellate-shaped ductal lumen prominently lined by pseudostratified columnar epithelium (oval) with prominent stereocilia (arrowhead) as well as component cell types; basal cells (BC), Principal cells (PC) and apical (AC). For the Masson trichrome (MT) sections, Note the blue staining collagen fibres (arrow) in the epididymal ductal interstices (EI) together with pink-staining smooth muscles (arrowheads) surrounding the epididymal ducts. Concerning the PAS section, note the PAS-positive areas in the interstitium (short arrow), lamina propria (arrowhead), ductal stereocilia (red arrowhead), and supranuclear region (long arrow) of the epididymal epithelium. Scale bar: 20 μ m. Bars with different superscripts (a, b, c) are significantly different.

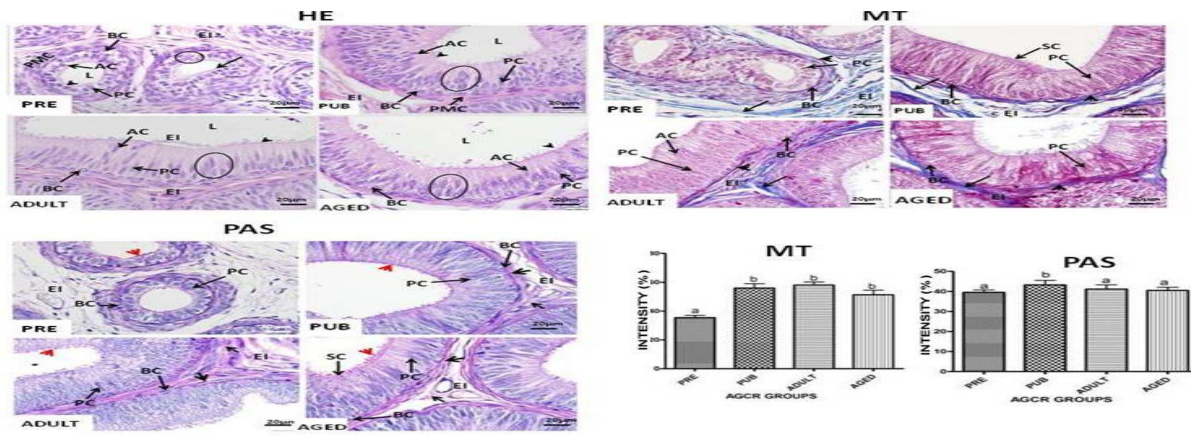


Figure 3. Photomicrographs of the middle initial segment of the epididymis in different AGCR groups. In the HE sections, note the markedly reduced stereocilia height (arrowhead), the round ductal lumen (L) lined by simple columnar epithelium and more cellular epididymal interstitium (EI) in pre-pubertal rat compared to the stellate-like lumen, duct lined by pseudostratified columnar epithelium (oval) with prominent stereocilia (arrowhead) as well as the presence of basal cells (BC), Principal cells (PC) and a moderate increase in apical cells (AC) seen in other AGCR. Also, observe in Masson trichrome (MT) sections the blue staining collagen fibers (arrow) in the epididymal ductal interstices (EI) together with pink-staining smooth muscles (arrowheads) surrounding the epididymal ducts. Note the PAS-positive areas in the interstitium (short arrow), lamina propria (arrowhead) and supranuclear region (long arrow) of the epididymal epithelium in the PAS sections. Scale bar: 20µm. Bars with different superscripts (a, b) are significantly different.

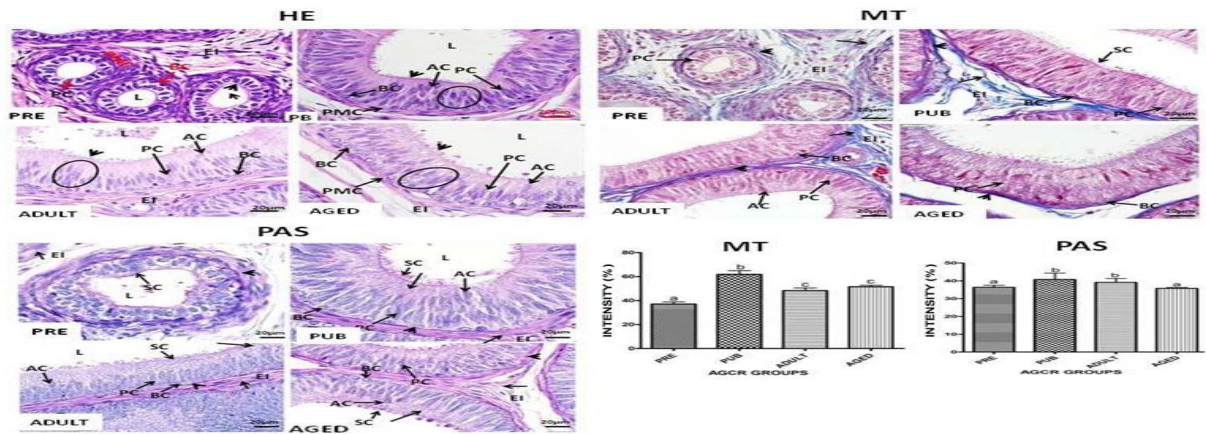


Figure 4. Photomicrographs of the distal initial segment of the epididymis in different AGCR groups. Note in the HE sections the reduced stereocilia height (arrowhead), the round ductal lumen (L) lined by simple columnar epithelium and more cellular interstitium in the prepubertal rat compared to the stellate-like luminal shape, ducts lined by pseudostratified columnar epithelium (oval) with prominent stereocilia (arrowhead) as well as the presence of basal cells (BC), Principal cells (PC) and markedly increase in apical cells (AC) in other groups. Note also the blue staining collagen fibres (arrow) in the epididymal ductal interstices (EI) together with pink-staining smooth muscles (arrowheads) surrounding the epididymal ducts in all the MT sections. Observe the PAS-positive areas in the interstitium (short arrow), lamina propria (arrowhead), and supranuclear region (long arrow) of the epididymal epithelium of all AGCR. Scale bar: 20µm. Bars with different superscripts (a, b, c) are significantly different.

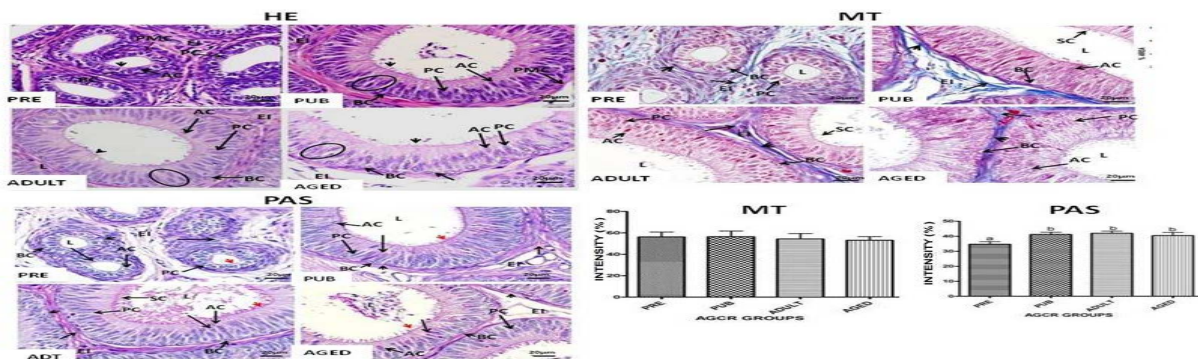


Figure 5. Photomicrographs of the caput segment of the epididymis in different AGCR groups. Observe in prepubertal (Pre) the display of markedly reduced stereocilia height (arrowhead), roundish ductal luminal (L) shape lined by simple cuboidal to columnar epithelial lining relative to the stellate like luminal shape, ducts lined by pseudostratified columnar epithelium (oval) with prominent stereocilia (arrowhead) as well as the presence of basal cells (BC), principal cells (PC) and more apical cells (AC) in other groups. Take note of the bluish staining collagen fibers (arrow) in the epididymal ductal interstices (EI) together with pink-staining smooth muscles (arrowheads) surrounding the epididymal ducts in the MT sections of all groups. Note the PAS-positive areas in the interstitium (short arrow), lamina propria (arrowhead), ductal stereocilia (red arrowhead), epithelial perinuclear region (long arrow) and luminal spermatozoa especially from pubertal to aged AGCR. Scale bar: 20µm. Bars with different superscripts (a, b) are significantly different.

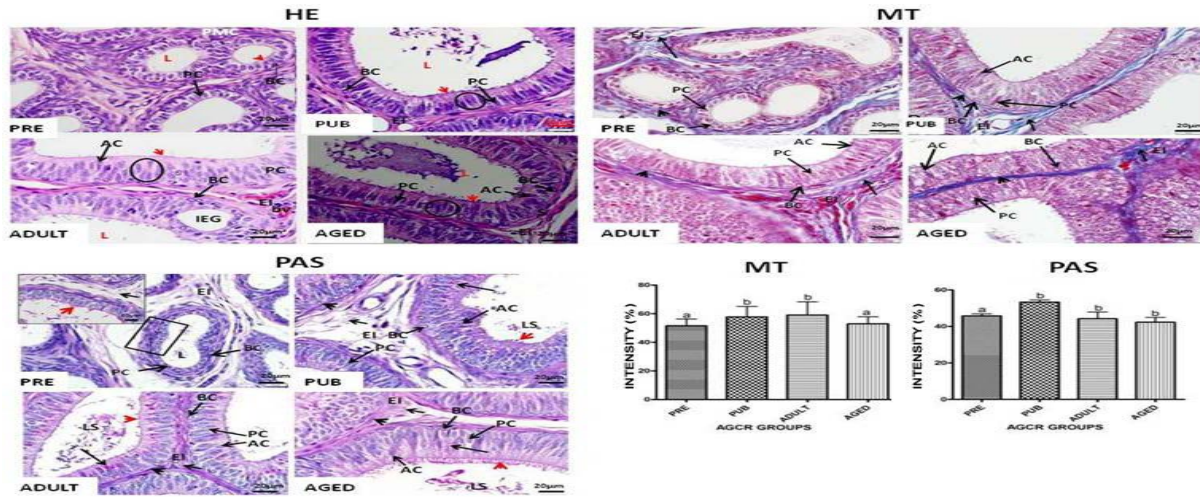


Figure 6. Photomicrographs of the corpus segment of the epididymis in different AGCR groups. In the HE sections, note the reduced stereocilia height (arrowhead) and roundish ductal luminal (L) shape lined by simple cuboidal to columnar epithelial cells in the prepubertal rat compared to the numerous intraepithelial glands (IEG), large roughly around ductal lumen shape containing spermatozoa, ducts lined by pseudostratified columnar epithelium (oval) with prominent stereocilia (arrowhead) as well as the presence of basal cells (BC), Principal cells (PC) and reduced apical cells (AC) seen in others. Also, note in MT stained sections the bluish staining collagen fibers (arrow) in the epididymal ductal interstices (EI) together with pink-staining smooth muscles (arrowheads) surrounding the epididymal ducts. Bv- blood vessel. Scale bar: 20µm. Bars with different superscripts (a, b) are significantly different.

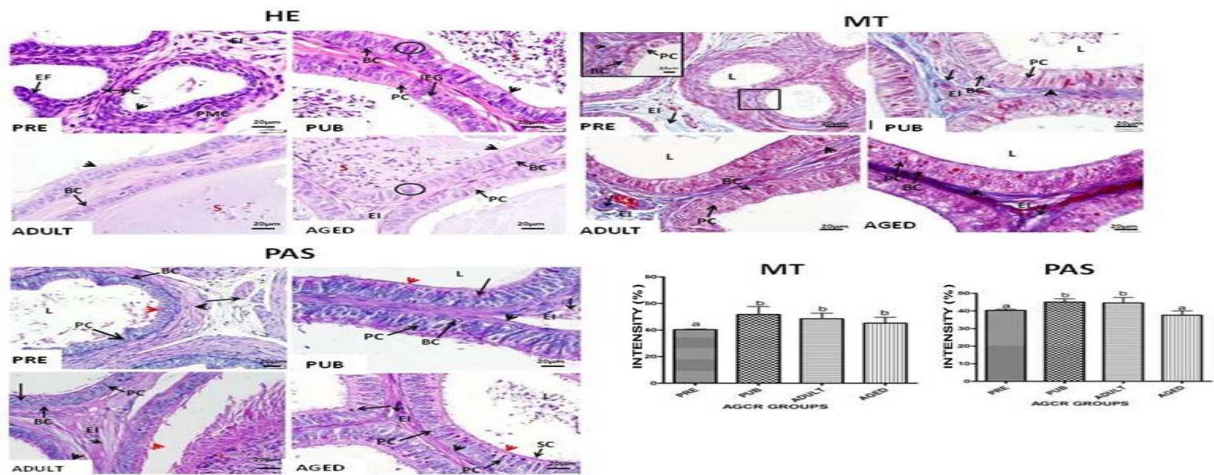


Figure 7. Photomicrographs of the cauda segment of the epididymis in different age groups of AGCR. Note in the HE sections the display of reduced stereocilia height (arrowhead), almost roundish ductal luminal (L) shape and copious epithelial fold (EF) in pre-pubertal rats when compared to the numerous intraepithelial glands (IEG), large roughly around ductal lumen shape containing spermatozoa (S), ductal lining bears a markedly reduced pseudostratified columnar epithelium (oval) with prominent stereocilia (arrowhead) as well as the dominating population of basal cells (BC) and Principal cells (PC) present in other groups. Also, note in MT sections the bluish staining collagen fibres (arrow) in the epididymal ductal interstices (EI) together with pink-staining smooth muscles (arrowheads) surrounding the epididymal ducts in inset A and other groups. Observe in the PAS sections positive areas to PAS staining in the interstitium (short arrow), lamina propria (arrowhead), epithelial supranuclear region (long arrow) and lumina (L) spermatozoa especially from pubertal to aged. Scale bar: 20µm. Bars with different superscripts (a, b) are significantly different.

Table 1. Age-related changes in epididymal parameters of African greater cane rat

Parameter	AGCR Group	Pro. Ini. Seg	Middle Ini. Seg	Distal Ini. Seg	Caput	Corpus	Cauda
Ductal Diameter (µm)	Prepub.	166.90 ± 8.89 ^a	151.20 ± 6.98 ^a	168.40 ± 15.51 ^a	106.50 ± 5.47 ^{a##}	167.60 ± 11.91 ^a	239.20 ± 13.18 ^{a#}
	Pub.	329.50 ± 16.42 ^{b##}	250.50 ± 6.65 ^b	257.50 ± 8.58 ^b	282.10 ± 11.06 ^b	252.30 ± 7.60 ^b	430.10 ± 21.86 ^{b#}
	Adult	309.00 ± 18.50 ^{b##}	274.80 ± 7.64 ^b	289.70 ± 16.86 ^b	270.50 ± 13.70 ^b	272.20 ± 16.28 ^b	440.80 ± 25.86 ^{b#}
	Age	329.00 ± 8.78 ^b	295.80 ± 9.87 ^b	305.70 ± 12.13 ^b	370.80 ± 10.49 ^b	308.80 ± 12.30 ^c	685.60 ± 34.26 ^{c#}
Luminal Diameter (µm)	Prepub.	75.27 ± 6.73 ^{a###}	60.14 ± 3.99 ^a	53.32 ± 3.08 ^a	49.95 ± 4.39 ^a	112.30 ± 8.80 ^{a###}	149.40 ± 12.84 ^{a#}
	Pub.	133.50 ± 10.57 ^{b###}	118.60 ± 5.38 ^b	110.40 ± 6.35 ^b	171.80 ± 9.36 ^{b##}	158.90 ± 9.44 ^{b##}	379.90 ± 30.18 ^{b#}
	Adult	187.80 ± 12.77 ^{c##}	117.40 ± 7.15 ^b	107.50 ± 8.25 ^b	161.90 ± 10.64 ^{b##}	183.20 ± 7.56 ^{c###}	396.00 ± 23.47 ^{b#}
	Age	213.70 ± 9.53 ^c	190.60 ± 13.89 ^c	190.20 ± 8.82 ^c	219.90 ± 16.20 ^c	208.80 ± 10.52 ^d	576.30 ± 36.66 ^{d#}

Epithelial Height (μm)	Prepub.	41.74 \pm 1.90 ^{a#}	47.32 \pm 2.21 ^{a#}	47.80 \pm 0.95 ^{a#}	33.33 \pm 1.65 ^{a##}	39.23 \pm 2.42 ^{a###}	26.56 \pm 3.39 ^{a####}
	Pub.	65.43 \pm 2.41 ^{b##}	76.54 \pm 2.35 ^{b#}	73.41 \pm 4.11 ^{b#}	61.58 \pm 2.37 ^{b###}	55.95 \pm 2.53 ^{b####}	50.03 \pm 1.66 ^{b####}
	Adult	85.75 \pm 3.39 ^{c#}	86.43 \pm 4.37 ^{b#}	77.86 \pm 2.55 ^{b#}	66.61 \pm 3.09 ^{b##}	51.10 \pm 1.64 ^{b###}	55.01 \pm 3.07 ^{b###}
	Age	90.77 \pm 4.06 ^{c#}	64.50 \pm 1.75 ^{c##}	72.47 \pm 5.01 ^{b##}	70.24 \pm 2.93 ^{b##}	50.61 \pm 2.52 ^{b###}	23.50 \pm 1.16 ^{a####}
Stereocilia Height (μm)	Prepub.	3.96 \pm 0.24 ^{a#}	2.76 \pm 0.09 ^a	2.59 \pm 0.12 ^a	2.44 \pm 0.10 ^a	2.53 \pm 0.23 ^a	2.11 \pm 0.13 ^a
	Pub.	8.51 \pm 0.45 ^{b###}	10.51 \pm 0.47 ^{b###}	8.71 \pm 0.24 ^{b###}	7.62 \pm 0.30 ^{b###}	7.94 \pm 0.31 ^{b###}	5.59 \pm 0.48 ^{b###}
	Adult	8.73 \pm 0.49 ^{b###}	7.74 \pm 0.19 ^{b###}	7.62 \pm 0.24 ^{b###}	6.47 \pm 0.14 ^{b###}	7.24 \pm 0.14 ^{b###}	5.03 \pm 0.13 ^{b###}
	Aged	6.95 \pm 0.25 ^{b###}	7.45 \pm 0.38 ^{b###}	6.99 \pm 0.36 ^{b###}	6.21 \pm 0.29 ^{b###}	5.79 \pm 0.34 ^{b###}	4.72 \pm 0.24 ^{b###}
Perimuscular Coat Thickness (μm)	Prepub.	13.25 \pm 0.90 ^{a#####}	16.17 \pm 1.21 ^{a#####}	10.54 \pm 0.65 ^{a#####}	23.3 \pm 2.40 ^{a#####}	21.12 \pm 1.40 ^{a#####}	46.01 \pm 4.30 ^{a#####}
	Pub.	14.74 \pm 0.80 ^a	17.93 \pm 1.01 ^a	13.20 \pm 0.75 ^a	11.36 \pm 0.91 ^a	16.87 \pm 1.60 ^a	51.30 \pm 5.70 ^a
	Adult	20.00 \pm 0.90 ^a	21.03 \pm 1.90 ^a	17.10 \pm 1.40 ^a	14.28 \pm 1.30 ^a	15.90 \pm 1.40 ^a	60.99 \pm 8.20 ^a
	Aged	17.22 \pm 1.70 ^a	12.40 \pm 0.91 ^a	16.10 \pm 1.90 ^a	8.97 \pm 0.44 ^a	14.17 \pm 0.88 ^a	51.20 \pm 3.70 ^a

Prepub – Prepubertal, Pub – Pubertal, Pro. Ini. Seg – Proximal Initial Segment

- Values with the different alphabet superscripts (a,b,c,d) within the column (comparison within an epididymal segment) are significantly different

- Values with the different number of harsh tag (#) in the same row (comparison along each epididymal segment i.e Pro. Ini. Seg to Cauda) are significantly different.

4. Discussion

The epididymal segments and zones of the AGCR in this study are in agreement with documentations on the epididymis of adult cane rats (Adebayo and Olurode, 2010) as well as the boar (Wrobeland Fallenbacher, 1974). These observations, however, contrasted the documentations of 3 segments in dog and camel (Chandler et al., 1981; Ruhl, 2001), 4 segments in rat and cat (Hamilton, 1975; Sánchez et al., 1998), 5 segments in the hamster, mouse, African giant rat and buck (Flickinger et al., 1978; Takano, 1980; Goyal and Williams, 1991; Oke, 1982). It is, therefore, suggested that the segments and zones of the epididymis of animals vary based on species.

The simple cuboidal to the columnar epididymal epithelial lining of the pre-pubertal unlike the classical pseudostratified stereociliated columnar epithelium observed in other groups conforms with earlier reports on the epididymal epithelial lining in immature and mature mammals (Oke, 1982; Adebayo and Olurode, 2010; Elzoghby et al., 2014). The functional relevance of this variation in epididymal epithelial lining could be correlated with the ongoing active secretory and absorptive activities on the epithelium of the pubertal to aged cane rats as opposed to the quiescent nature of the prepubertal rats.

Also, the observed progressive age-related increase in epididymal histomorphometric parameters in the different age groups of cane rat, as well as craniocaudal alterations (increase or decrease) to some of the parameters along the epididymal duct in this study, agree with the reports of Adebayo and Olurode (2010) in adult cane rat as well as Kishore et al. (2012) in the goat. The variations noticed in the histomorphometric parameters between the segments and within cane rat groups might be to accommodate the varied physiological activities of the different segment of the epididymis across age groups. For instance, the increase in stereocilia height of the initial segment functionally has been attributed to an additional resorptive ability of the epithelium in this segment (Alkafafy, 2005) or aiding the movement of spermatozoa along the duct.

The increased periductal muscle coat thickness towards the caudal segment in each group of cane rat is in accord with the pattern previously reported for the epididymal segments in most mammals (Delhon and von Lawzewitsch, 1994; Sánchez et al., 1998; Calvo et al., 1999; Ruhl, 2001). The functional implication of periductal smooth muscular coat presence along the epididymal segments has been suggested to be essential in the movement of the sperm toward the terminal segment (Goyal, 1985; Zayyed et al., 2012). The pronounced thickness of the PMC in the cauda epididymis could be linked to ejaculation. Also, the presence of an age-dependent increase in the thickness of the epididymal coat of the different groups of the cane rat more particularly in the cauda segment of the pubertal group could be suggestive of morphological compensation needed for the initiation of ejaculatory activity of the rats in this group.

The observation of round ductal luminal shape in all the epididymal segments of prepubertal rats, as well as the display of variable luminal shape (stellate to roundish) in other rat groups, agree with the numerous reports of round luminal shape in the lower segments of the epididymal duct of most mammals (Sánchez et al., 1998; Alkafafy, 2005; Shagufta et al., 2012). The roundish shape of epididymal ducts has been attributed to the regular nature of the epithelium in lower segments especially the cauda segment where the epithelium is uniformly low and luminal diameter is at maximum thereby favouring adaptation for sperm storage and maturation (Delhon and von Lawzewitsch, 1994; Zayyed et al., 2012). However, the irregularly long nature of the epithelium in the initial segments has been suggested to contribute to the stellate shape of their lumen (Sánchez et al., 1998; Alkafafy, 2005). Based on the above morpho-functional assumptions regarding the ductal luminal shape, it is understandable to attribute the fairly uniform epididymal epithelium height in prepubertal rats to their roundish ductal luminal shape.

The presence of positive PAS staining in the epididymal interstitium, lamina propria region, the perinuclear region of the epithelium, ductal stereocilia and lumen of different age groups of cane rat is consistent with glycogen-rich parts of the epididymis previously reported

in most mammals (Goswami et al., 1990; Oke et al., 1988; Kishore et al., 2012; Kumari, 2013). The significantly higher PAS staining intensity observed in all the epididymal segments of pubertal cane rat relative to others implies the active functional status of this age group. The demonstration of intense PAS staining in pubertal rats is consistent with the reports of Kishore et al. (2012) and Kumari (2013) on similar age-related studies in the epididymis of goats.

The demonstration of MT-positive epididymal duct interstices and the smooth muscles surrounding the epididymal ducts is consistent with the reported sites of collagen fibres in the epididymis (Shagufta et al., 2012). Owing to the resilience of collagen fibres (Bacha and Bacha, 2000), it suffices to assume that its presence in the epididymal interstices and periductal muscle coat correlates with its functional roles of maintaining the ductal architecture. The demonstration of exceptionally high MT intensity in nearly all the epididymal segments of the pubertal rat can be linked to the reproductive activeness of this age group.

In conclusion, this study has demonstrated that epididymal light microscopic details in cane rats were remarkably influenced by age increment as evidenced in the changes in the epididymal epithelium from simple cuboidal in prepubertal to pseudostratified columnar in other cane rat groups, significantly higher glycogen and connective tissue components in the pubertal and adult rats and progressive age-related increase in the histomorphometric parameters. These sets of data could probably be associated with reproductive quiescence in the prepubertal and remarkable vigor more particularly in the adult cane rat investigated. Even though previous authors have described light microscopic changes in the epididymis of the adult AGCR, this work is possibly the first report of the age-related changes in histology, histochemistry and histomorphometric changes in the epididymis of cane rat.

Acknowledgment

The authors are appreciative of the technical assistance rendered by Mrs. R. Phaswane of the Pathology Laboratory Unit, University of Pretoria, South Africa.

References

Adebayo AO and Olurode SA. 2010. The morphology and morphometry of the epididymis in the greater cane rat (*Thryonomys swinderianus Temmincks*). *Folia Morphol.*, **69** (4): 246 – 252.

Adebayo AO, Akinloye AK, Ihunwo AO, Taiwo VO and Oke BO. 2016. Zonal changes in the ultrastructure of the epididymal principal cell of the greater cane rat (*Thryonomys swinderianus*). *Alex. J Vet Sci.*, **48** (1): 99 – 106.

Agnes VF and Akbarsha MA. 2001. Pale vacuolated epithelial cells in the epididymis of aflatoxin-treated mice. *Reprod (formerly J Reprod Fertil)*, **122**: 629 – 41.

Akbarsha MA, Faisal K, Radha A. 2015. The epididymis: Structure and function. In: Singh SK editor. **Mammalian Endocrinology and Male Reproductive Biology**. CRC Press/Taylor & Francis. pp 115-165.

Alkafafy M. 2005. Glycohistochemical, immunohistochemical and ultrastructural studies of

the bovine epididymis. Dissertation, The Institute of Veterinary Anatomy II, Faculty of Veterinary Medicine, LMU, Munich, Germany.

Arrotéia KF, Garcia PV, Barbieri MF, Justino ML and Pereira LAV. 2012. The epididymis: embryology, structure, function and its role in fertilization and infertility In: Pereira LV (Ed.), **Embryology – Updates and Highlights on Classic Topics**. In-Tech, Available from: <http://www.intechopen.com/books/embryology-updates-and-highlightson-classic-topics/the-epididymis-embryology-structure-function-and-its-role-in-fertilization-and-infertility> and retrieved on 20th July, 2018.

Bacha WJ and Bacha LM. 2000. **Colour atlas of veterinary histology**, second ed. Lippincott, Williams and Wilkins, Philadelphia. pp. 203-219.

Calvo A, Pastor LM, Martinez E, Vazquez JM and Roca J. 1999. Age-related changes in the hamster epididymis. *Anat Rec.*, **256**: 335 – 346.

Chandler JA, Sinowatz F and Pierrepoint CG. 1981. The ultrastructure of dog epididymis. *Urol, Res.*, **9** (1): 33 - 44.

Cornwall GA. 2009. New insights into epididymal biology and function. *Hum Reprod Update*, **15** (2): 213 – 227.

Delhon G and von Lawzewitsch I. 1994. Ductus epididymidis compartments and morphology of epididymal spermatozoa in llamas. *Anat Histol Embryol.*, **23** (3): 217 - 225.

Elzoghby IMA, Sosa GA, Mona NAH and Manshawy AA. 2014. Postnatal development of the epididymis in the sheep. *Benha Vet Med J.*, **26** (1): 67 - 74.

Fayenuwo JO, Akande M, Taiwo AA, Adebayo AO, Saka JO, Lawal BO, Tiamiyu AK and Oyekan PO. 2003. *Guidelines for grasscutter rearing*. Technical Bulletin, IAR & T., Ibadan. pp. 38.

Flickinger CJ, Howards SS and English HF. 1978. Ultrastructural differences in efferent ducts and several regions of the epididymis of the hamster. *Am J Anat.*, **152** (4): 557 - 585.

Goswami SK, Sambyal RS, Singh Y, Nagpal SK. 1990. Regional histomorphology of the ampulla ductus deferentis of camel. *Ind J Anim Sci.*, **60**: 1043-1046.

Goyal HO and Williams CS. 1991. Regional differences in the morphology of the goat epididymis: A light microscopic and ultrastructural study. *Am J Anat.*, **190**: 349 – 69.

Goyal HO. 1985. Morphology of the bovine epididymis. *Am J Anat.*, **172** (2): 155 - 172.

Hamilton DW. 1975. Structure and function of the epithelium lining the ductuli efferentes, ductus epididymis, and ductus deferens in the rat. In: Greep RO and Astwood EB (Eds.), **Handbook of Physiology, Vol. 5: Male Reproductive System**. American Physiology Society, Washington, DC. pp 259 - 301.

Hermo L. 1995. Structural features and functions of principal cells of the intermediate zone of the epididymis of adult rats. *Anat Rec.*, **242**: 515 – 30.

Hermo L, Barin K and Oko R. 1998. Androgen binding protein secretion and endocytosis by principal cell in the adult rat epididymis and during postnatal development. *J Androl.*, **19**: 527 – 541.

Hermo L, Green H and Clermont Y. 1991. Golgiapparatus of epithelial principal cells of the epididymal initial segment of the rat: Structure, relationship with endoplasmic reticulum, and role in the formation of secretory vesicles. *Anat Rec.*, **229**: 159 – 76.

- Jones R, Hamilton DW and Fawcett DW. 1979. Morphology of the epithelium of the extratesticular rete testis, ductuli efferentes and ductus epididymidis of the adult male rabbit. *J Anat.*, **156**: 373 – 400.
- Kishore PVS, Geetha, R and Sabiha, H. 2012. Postnatal differentiation and regional histological variations in the ductus epididymis of rams. *Tamilnadu J Vet Anim Sci.*, **8 (3)**: 145 - 151.
- Kumari P. 2013. Gross, histomorphological and histochemical changes in testis, epididymis, vas, and seminal vesicles of developing (post-natal) kids of Black Bengal goats. (*Capra hircus*). Ph.D. thesis, West Bengal University of Animal and Fishery Sciences, India.
- Lasserre A, Barrozo R, Tezón JG, Miranda PV and Vazquez-Levin MH. 2001. Human epididymal proteins and sperm function during fertilization. *Biol Res.*, **34**: 165 – 78.
- Monadjem A, Taylor PJ, Denys C and Cotterill FP. 2015. **Rodents of sub-Saharan Africa: a biogeographic and taxonomic synthesis**, Walter de Gruyter GmbH, Berlin, Germany.
- Oke BO. 1982. Some studies on the reproductive organs of the African giant rat (*Cricetomys gambianus*, Waterhouse) during the climatic seasons at Ibadan. MSc. Thesis, Department of Veterinary Anatomy, University of Ibadan, Nigeria.
- Oke BO, Aire TA, Adeyemo O and Heath E. 1988. The structure of the epididymis of the giant rat (*Cricetomys gambianus*, Waterhouse): histological, histochemical and microstereological studies. *J Anat.*, **160**: 9 - 19.
- Oke BO, Aire TA, Adeyemo O and Heath E. 1989. The ultrastructure of the epididymis of the African giant rat (*Cricetomys gambianus*, Waterhouse). *J Anat.*, **165**: 75 - 89.
- Olude MA, Mustapha OA, Sonubi AC, Falade TE, Ogunbunmi TK, Adebayo AO and Akinloye AK. 2014. Morphometric study of the skull of the greater cane rat (*Thryonomys swinderianus*, Temminck). *Nig Vet J.*, **35 (3)**: 1026 – 1037.
- Olukole SG, Oyeyemi MO and Oke BO. 2009. Biometrical observations on the testes and epididymis of the domesticated adult African greater cane rat (*Thryonomys swinderianus*). *Eur J Anat.*, **13 (2)**: 71 - 75.
- Robaire R, Hinton BT and Orgebin-Crist MC. 2006. The epididymis. In *Physiology of Reproduction*, 3rd Edn., Knobil, E. and Neill, J. D., Eds. Elsevier, New York. pp. 1071 – 147.
- Ruhl S. 2001. Immunohistochemical localization of sperm adhesins in the testis and epididymis of the dog (*Canis familiaris*). Dissertation, Faculty of Veterinary Medicine, LMU, Munich, Germany.
- Sánchez B, Flores JM, Pizarro M and Garcia P. 1998. Histological and immunohistochemical study of the cat epididymis. *Anat Histol Embryol.*, **27 (2)**: 135 - 140.
- Shagufta B, Sharma K, Suri S and Devi J. 2012. Histochemical studies on the testis of adult Bakerwali goat (*Capra hircus*). *Ind J Vet Anat.*, **24 (1)**: 50 - 51.
- Soro D, Karamoko Y, Kimse M and Fantodji A. 2014. Study of basic haematological parameters: indicators of the general state and immune competence in the male grasscutter (*Thryonomys swinderianus*, Temminck, 1827) bred in captivity in Côte d'Ivoire. *J Anim Plant Sci.*, **22 (1)**: 3379 - 3387.
- Takano H. 1980. Qualitative and quantitative histology and histogenesis of the mouse epididymis, with special emphasis on the regional difference. *Acta Anat (Nippon).*, **55**: 575 - 587.
- Wrobel KH and Fallenbacher E. 1974. Histological and histochemical examinations on the epididymal epithelium of adult boars. *Breeding hyg.*, **9**: 20 – 31.
- Yanagimachi R, Kamiguchi Y, Mikamo K, Suzuki F and Yanagimachi H. 1985. Maturation of spermatozoa in the epididymis of the Chinese hamster. *Am J Anat.*, **172**: 317 - 330.
- Zayyed AE, Aly KH, Ibrahim IA and Abd El-maksoud FM. 2012. Morphological studies on the seasonal changes in the epididymal duct of the one-humped camel (*Camelus dromedarius*). *Vet Sci Dev.*, **2 (3)**: 7 - 14.

Jordan Journal of Biological Sciences

An International Peer – Reviewed Research Journal

Published by the Deanship of Scientific Research, The Hashemite University, Zarqa, Jordan



Name: الاسم:
 Specialty: التخصص:
 Address: العنوان:
 P.O. Box: صندوق البريد:
 City & Postal Code: المدينة: الرمز البريدي:
 Country: الدولة:
 Phone: رقم الهاتف:
 Fax No.: رقم الفاكس:
 E-mail: البريد الإلكتروني:
 Method of payment: طريقة الدفع:
 Amount Enclosed: المبلغ المرفق:
 Signature: التوقيع:
 Cheque should be paid to Deanship of Research and Graduate Studies – The Hashemite University.

I would like to subscribe to the Journal

For

- One year
 Two years
 Three years

One Year Subscription Rates

	Inside Jordan	Outside Jordan
Individuals	JD10	\$70
Students	JD5	\$35
Institutions	JD 20	\$90

Correspondence

Subscriptions and sales:

The Hashemite University
 P.O. Box 330127-Zarqa 13115 – Jordan
 Telephone: 00 962 5 3903333
 Fax no. : 0096253903349
 E. mail: jjbs@hu.edu.jo

المجلة الأردنية للعلوم الحياتية Jordan Journal of Biological Sciences (JJBS)

<http://jjbs.hu.edu.jo>

المجلة الأردنية للعلوم الحياتية: مجلة علمية عالمية محكمة ومفهرسة ومصنفة، تصدر عن الجامعة الهاشمية وبدعم من صندوق دعم البحث العلمي والإبتكار – وزارة التعليم العالي والبحث العلمي.

هيئة التحرير

رئيس التحرير

الأستاذ الدكتورة منار فايز عتوم
الجامعة الهاشمية، الزرقاء، الأردن

مساعد رئيس التحرير

الدكتور مهند عليان مساعدة
الجامعة الهاشمية، الزرقاء، الأردن

الأعضاء:

الأستاذ الدكتور جميل نمر اللحام
جامعة اليرموك

الاستاذ الدكتور زهير سامي عمرو
جامعة العلوم و التكنولوجيا الأردنية

الأستاذ الدكتورة حنان عيسى ملكاوي
جامعة اليرموك

الأستاذ الدكتور عبدالرحيم أحمد الحنيطي
الجامعة الأردنية

الاستاذ الدكتور خالد محمد خليفات
جامعة مؤتة

فريق الدعم:

المحرر اللغوي

الدكتور شادي نعامنة

تنفيذ وإخراج

م. مهند عقده

ترسل البحوث الى العنوان التالي:

رئيس تحرير المجلة الأردنية للعلوم الحياتية
الجامعة الهاشمية

ص.ب , 330127 , الزرقاء, 13115 , الأردن

هاتف: 0096253903333

E-mail: jjbs@hu.edu.jo, Website: www.jjbs.hu.edu.jo



المملكة الأردنية الهاشمية



المجلة الأردنية



للعلوم الحياتية

مجلة علمية عالمية محكمة

تصدر بدعم من صندوق دعم البحث العلمي و الابتكار



<http://jjbs.hu.edu.jo/>